VOL. 455 NOVEMBER 25, 1988

COMPLETE IN ONE ISSUE

AL OF

HROMATOGRAPHY

NATIONAL JOURNAL ON CHROMATOGRAPHY, ELECTROPHORESIS AND RELATED METHODS

EDITOR, Michael Lederer (Switzerland)

ASSOCIATE EDITORS, R. W. Frei (Amsterdam), R. W. Giese (Boston, MA), J. K. Haken (Kensington, N.S.W.), K. Macek (Prague), L. R. Snyder (Orinda, CA)

EDITOR, SYMPOSIUM VOLUMES, E. Heftmann (Orinda, CA)

EDITORIAL BOARD

W. A. Aue (Halifax)
V. G. Berezkin (Moscow)
V. Betina (Bratislava)
A. Bevenue (Belmont, CA)
P. Boček (Brno)
P. Boulanger (Lille)
A. A. Boulton (Saskatoon)
G. P. Cartoni (Rome)
S. Dilli (Kensington, N.S.W.)
L. Fishbein (Washington, DC)
A. Frigerio (Milan)
C. W. Gehrke (Columbia, MO)
E. Gil-Av (Rehovot)
G. Guiochon (Knoxville, TN)
I. M. Hais (Hradec Králové)
S. Hjertén (Uppsala)
E. C. Horning (Houston, TX)
Cs. Horváth (New Haven, CT)
J. F. K. Huber (Vienna)
A. T. James (Harrold)
J. Janák (Brno)
E. sz. Kováts (Lausanne)
K. A. Kraus (Oak Ridge, TN)
A. Liberti (Rome)
H. M. McNair (Blacksburg, VA)
Y. Marcus (Jerusalem)
G. B. Marini-Bettòlo (Rome)
A. J. P. Martin (Cambridge)
Č. Michalec (Prague)
R. Neher (Basel)
G. Nickless (Bristol)
N. A. Parris (Wilmington, DE)
R. L. Patience (Sunbury-on-Thames)
P. G. Righetti (Milan)
O. Samuelson (Göteborg)
R. Schwarzenbach (Dübendorf)
A. Zlatkis (Houston, TX)

EDITORS, BIBLIOGRAPHY SECTION

Z. Deyl (Prague), J. Janák (Brno), V. Schwarz (Prague), K. Macek (Prague)

ELSEVIER

JOURNAL OF CHROMATOGRAPHY

Scope. The *Journal of Chromatography* publishes papers on all aspects of chromatography, electrophoresis and related methods. Contributions consist mainly of research papers dealing with chromatographic theory, instrumental development and their applications. The section *Biomedical Applications*, which is under separate editorship, deals with the following aspects: developments in and applications of chromatographic and electrophoretic techniques related to clinical diagnosis or alterations during medical treatment; screening and profiling of body fluids or tissues with special reference to metabolic disorders; results from basic medical research with direct consequences in clinical practice; drug level monitoring and pharmacokinetic studies; clinical toxicology; analytical studies in occupational medicine.

Submission of Papers. Papers in English, French and German may be submitted, in three copies. Manuscripts should be submitted to: The Editor of *Journal of Chromatography*, P.O. Box 681, 1000 AR Amsterdam, The Netherlands, or to: The Editor of *Journal of Chromatography, Biomedical Applications*, P.O. Box 681, 1000 AR Amsterdam, The Netherlands. Review articles are invited or proposed by letter to the Editors. An outline of the proposed review should first be forwarded to the Editors for preliminary discussion prior to preparation. Submission of an article is understood to imply that the article is original and unpublished and is not being considered for publication elsewhere. For copyright regulations, see below.

Subscription Orders. Subscription orders should be sent to: Elsevier Science Publishers B.V., P.O. Box 211, 1000 AE Amsterdam, The Netherlands, Tel. 5803 911, Telex 18582 ESPA NL. The *Journal of Chromatography* and the *Biomedical Applications* section can be subscribed to separately.

Publication. The *Journal of Chromatography* (incl. *Biomedical Applications* and *Cumulative Author and Subject Indexes, Vols. 401–450*) has 37 volumes in 1988. The subscription prices for 1988 are:

J. Chromatogr. (incl. *Cum. Indexes, Vols. 401–450*) + *Biomed. Appl.* (Vols. 424–460):
Dfl. 6290.00 plus Dfl. 962.00 (p.p.h.) (total *ca.* US$ 3537.50)

J. Chromatogr. (incl. *Cum. Indexes, Vols. 401–450*) only (Vols. 435–460):
Dfl. 5070.00 plus Dfl. 676.00 (p.p.h.) (total *ca.* US$ 2803.00)

Biomed. Appl. only (Vols. 424–434):
Dfl. 2145.00 plus Dfl. 286.00 (p.p.h.) (total *ca.* US$ 1185.75).

Our p.p.h. (postage, package and handling) charge includes surface delivery of all issues, except to subscribers in Argentina, Australia, Brasil, Canada, China, Hong Kong, India, Israel, Malaysia, Mexico, New Zealand, Pakistan, Singapore, South Africa, South Korea, Taiwan, Thailand and the U.S.A. who receive all issues by air delivery (S.A.L. — Surface Air Lifted) at no extra cost. For Japan, air delivery requires 50% additional charge; for all other countries airmail and S.A.L. charges are available upon request. Back volumes of the *Journal of Chromatography* (Vols. 1 through 423) are available at Dfl. 230.00 (plus postage). Claims for missing issues will be honoured, free of charge, within three months after publication of the issue. Customers in the U.S.A. and Canada wishing information on this and other Elsevier journals, please contact Journal Information Center, Elsevier Science Publishing Co. Inc., 655 Avenue of the Americas, New York, NY 10010. Tel. (212) 989-5800.

Abstracts/Contents Lists published in Analytical Abstracts, ASCA, Biochemical Abstracts, Biological Abstracts, Chemical Abstracts, Chemical Titles, Chromatography Abstracts, Current Contents/Physical, Chemical & Earth Sciences, Current Contents/Life Sciences, Deep-Sea Research/Part B: Oceanographic Literature Review, Excerpta Medica, Index Medicus, Mass Spectrometry Bulletin, PASCAL-CNRS, Referativnyi Zhurnal and Science Citation Index.

See inside back cover for Publication Schedule, Information for Authors and information on Advertisements.

© ELSEVIER SCIENCE PUBLISHERS B.V. — 1988

0021-9673/88/$03.50

All rights reserved. No part of this publication may be reproduced, stored in a retrieval system or transmitted in any form or by any means, electronic, mechanical, photocopying, recording or otherwise, without the prior written permission of the publisher, Elsevier Science Publishers B.V., P.O. Box 330, 1000 AH Amsterdam, The Netherlands.

Upon acceptance of an article by the journal, the author(s) will be asked to transfer copyright of the article to the publisher. The transfer will ensure the widest possible dissemination of information.

Submission of an article for publication entails the authors' irrevocable and exclusive authorization of the publisher to collect any sums or considerations for copying or reproduction payable by third parties (as mentioned in article 17 paragraph 2 of the Dutch Copyright Act of 1912 and the Royal Decree of June 20, 1974 (S. 351) pursuant to article 16 b of the Dutch Copyright Act of 1912) and/or to act in or out of Court in connection therewith.

Special regulations for readers in the U.S.A. This journal has been registered with the Copyright Clearance Center, Inc. Consent is given for copying of articles for personal or internal use, or for the personal use of specific clients. This consent is given on the condition that the copier pays through the Center the per-copy fee stated in the code on the first page of each article for copying beyond that permitted by Sections 107 or 108 of the U.S. Copyright Law. The appropriate fee should be forwarded with a copy of the first page of the article to the Copyright Clearance Center, Inc., 27 Congress Street, Salem, MA 01970, U.S.A. If no code appears in an article, the author has not given broad consent to copy and permission to copy must be obtained directly from the author. All articles published prior to 1980 may be copied for a per-copy fee of US$ 2.25, also payable through the Center. This consent does not extend to other kinds of copying, such as for general distribution, resale, advertising and promotion purposes, or for creating new collective works. Special written permission must be obtained from the publisher for such copying.

No responsibility is assumed by the Publisher for any injury and/or damage to persons or property as a matter of products liability, negligence or otherwise, or from any use or operation of any methods, products, instructions or ideas contained in the materials herein. Because of rapid advances in the medical sciences, the Publisher recommends that independent verification of diagnoses and drug dosages should be made.

Although all advertising material is expected to conform to ethical (medical) standards, inclusion in this publication does not constitute a guarantee or endorsement of the quality or value of such product or of the claims made of it by its manufacturer.

Printed in The Netherlands

CONTENTS

(Abstracts/Contents Lists published in Analytical Abstracts, ASCA, Biochemical Abstracts, Biological Abstracts, Chemical Abstracts, Chemical Titles, Chromatography Abstracts, Current Contents/Physical, Chemical & Earth Sciences, Current Contents/Life Sciences, Deep Sea Research/Part B: Oceanographic Literature Review, Excerpta Medica, Index Medicus, Mass Spectrometry Bulletin, PASCAL-CNRS, Referativnyi Zhurnal and Science Citation Index)

Resolution of colloidal latex aggregates by sedimentation field-flow fractionation
by H. K. Jones, B. N. Barman and J. C. Giddings (Salt Lake City, UT, U.S.A.) (Received August 18th, 1988) 1

Consecutive gradients in chromatography. Gradients under sub- and supercritical conditions including composition gradients and multiple gradients
by B. Gemmel, F. P. Schmitz and E. Klesper (Aachen, F.R.G.) (Received July 26th, 1988) 17

Retention behaviour of polycyclic aromatic hydrocarbons in supercritical fluid chromatography on various chemically bonded stationary phases with carbon dioxide as a mobile phase
by K. Jinno and S. Niimi (Toyohashi, Japan) (Received July 13th, 1988) 29

Determination of partition coefficients by headspace gas chromatography
by W. J. Jones, M. J. Egoville, E. O. Strolle and E. S. Dellamonica (Wyndmoor, PA, U.S.A.) (Received July 27th, 1988) 45

Vapor-pressure measurement of complex hydrocarbon mixtures by headspace gas chromatography
by J. E. Woodrow and J. N. Seiber (Davis, CA, U.S.A.) (Received July 14th, 1988) . . . 53

Determination of the solubility of vapours in polymers by automated headspace gas chromatography
by K. Schoene, J. Steinhanses and A. König (Schmallenberg-Grafschaft, F.R.G.) (Received May 16th, 1988) 67

Retention reproducibility of basic drugs in high-performance liquid chromatography on a silica column with a methanol–ammonium nitrate eluent. Batch-to-batch reproducibility of the stationary phase
by R. M. Smith, T. G. Hurdley and J. P. Westlake (Loughborough, U.K.) and R. Gill and M. D. Osselton (Reading, U.K.) (Received August 23rd, 1988) 77

Ultrasound driven synthesis of reversed-phase stationary phases for liquid chromatography using 4-dimethylaminopyridine as acid-acceptor
by K. B. Sentell, K. W. Barnes and J. G. Dorsey (Gainesville, FL, U.S.A.) (Received July 21st, 1988) 95

Gas phase silylation, a rapid method for preparation of high-performance liquid chromatography supports
by P. Wikström, C. F. Mandenius and P.-O. Larsson (Lund, Sweden) (Received May 17th, 1988) 105

Degradation and analysis of polyoxyethylene monoalkyl ethers in the presence of acetyl chloride
by J. Szymanowski (Poznań, Poland) and P. Kusz, E. Dziwiński and Cz. Latocha (Kędzierzyn-Koźle, Poland) (Received July 11th, 1988) 119

Chemical degradation and analysis of polyoxyethylene glycols and ethylene oxide–α-butylene oxide block copolymers
by J. Szymanowski (Poznań, Poland) and P. Kusz and E. Dziwiński (Kędzierzyn-Koźle, Poland) (Received June 16th, 1988) 131

Flavor characterization of dentifrices using equilibrium headspace gas chromatography
by R. S. Robinson, E. A. Tavss, J. Santalucia and D. L. Carroll (Piscataway, NJ, U.S.A.) (Received May 25th, 1988) 143

(Continued overleaf)

26 APR 2531

Cross-axis synchronous flow-through coil planet centrifuge for large-scale preparative counter-current chromatography. III. Performance of large-bore coils in slow planetary motion
by Y. Ito (Bethesda, MD, U.S.A.) and T.-Y. Zhang (Beijing, China) (Received June 29th, 1988) 151

Identification of organophosphorus insecticides and their hydrolysis products by liquid chromatography in combination with UV and thermospray–mass spectrometric detection
by A. Farran, J. De Pablo and D. Barceló (Barcelona, Spain) (Received July 18th, 1988) . 163

Adaptation d'une méthode d'analyse des acides aminés, par chromatographie liquide haute performance, dans les sèves xylémiques
par P. Brunet, B. Sarrobert et N. Paris-Pireyre (Montpellier, France) (Reçu le 26 juillet 1988) 173

Resolution of diastereomers of N,N,N′,N′-tetrakis(2-hydroxypropyl)ethylenediamine (Quadrol) by reversed-phase high-performance liquid chromatography
by J. A. Fulton, H. K. Pokharna, M. J. Dunphy and D. J. Smith (Akron, OH, U.S.A.) (Received June 15th, 1988) 183

Purification of diethylenetriamine-N,N,N′,N″-tetraacetic acid-N″-propionic acid using anion-exchange displacement chromatography
by D. J. Sawyer, J. E. Powell and H. R. Burkholder (Ames, IA, U.S.A.) (Received August 4th, 1988) 193

Design and applications of biomimetic anthraquinone dyes. II. The interaction of C.I. Reactive Blue 2 analogues bearing terminal ring modifications with horse liver alcohol dehydrogenase
by S. J. Burton (Cambridge, U.K.), C. V. Stead (Manchester, U.K.) and C. R. Lowe (Cambridge, U.K.) (Received July 25th, 1988) 201

Resolution of the intermediates of *de novo* purine biosynthesis by ion-pair reversed-phase high-performance liquid chromatography
by R. G. Hards and D. Patterson (Denver, CO, U.S.A.) (Received July 20th, 1988) . . . 217

Purification of lentil lectins using preparative electrophoresis
by P. Wenger, A. Heydt, N. B. Egen, T. D. Long and M. Bier (Tucson, AZ, U.S.A.) (Received July 5th, 1988) 225

Determination of phenols by liquid chromatography using reductive electrochemical detection via precolumn derivatization
by C.-Y. Li and M. W. Kemp (Greenville, NC, U.S.A.) (Received June 6th, 1988) 241

Determination of phosphate and phosphite in plant material by gas chromatography–mass spectrometry and ion chromatography
by R. H. Smillie and B. Grant (Parkville, Australia) and R. L. Cribbes (Melbourne, Australia) (Received July 14th, 1988) 253

Retention and heats of adsorption of hydrocarbons and aliphatic alcohols on cellulose
by L. I. Dernovaya and Yu. A. Eltekov (Moscow, U.S.S.R.) (Received August 11th, 1988) 263

Liquid chromatographic determination of alliin in garlic and garlic products
by E. Mochizuki and A. Nakayama (Kofu, Japan), Y. Kitada (Nara, Japan), K. Saito (Saitama, Japan) and H. Nakazawa, S. Suzuki and M. Fujita (Tokyo, Japan) (Received August 9th, 1988) 271

Simultaneous high-performance liquid chromatographic determination of propoxyphene and acetaminophen in pharmaceutical preparations
by T. L. Ascah and B. T. Hunter (Bellefonte, PA, U.S.A.) (Received July 20th, 1988) . . 279

Purification of phosphofructokinase using transition-state analogue affinity chromatography
by S. P. J. Brooks and K. B. Storey (Ottawa, Canada) (Received August 1st, 1988) . . . 291

Notes

Damage to gas chromatographic columns caused by peroxides in liquid chromatographic eluents for coupled liquid chromatography–gas chromatography
by K. Grob (Zürich, Switzerland) and Z. Li (Chengdu, China) (Received August 18th, 1988) 297

Identification of alkylbenzenes up to C_{12} by capillary gas chromatography and combined gas chromatography–mass spectrometry. I. OV-101 as stationary phase
by E. Matisová, M. Rukríglová, J. Krupčík, E. Kovačičová and Š. Holotík (Bratislava, Czechoslovakia) (Received July 14th, 1988) 301

Effect of pH on the reaction of 2,4-dinitrophenylhydrazine with formaldehyde and acetaldehyde
by M. K. L. Bicking and W. M. Cooke (Columbus, OH, U.S.A.) and F. K. Kawahara and J. E. Longbottom (Cincinnati, OH, U.S.A.) (Received August 25th, 1988) 310

Use of mobile phase modifiers to alter retention and stereoselectivity on a bovine serum albumin high-performance liquid chromatographic chiral stationary phase
by I. W. Wainer and Y.-Q. Chu (Memphis, TN, U.S.A.) (Received August 9th, 1988) . . 316

Isothiocyanate as a liquid crystalline stationary phase in capillary gas chromatography for the separation of polyaromatic hydrocarbons
by J. Mazur, Z. Witkiewicz and R. Dąbrowski (Warsaw, Poland) (Received August 2nd, 1988) 323

Temperature programming in high-performance liquid chromatography
by S. U. Sheikh and J. C. Touchstone (Philadelphia, PA, U.S.A.) (Received July 22nd, 1988) 327

High-sensitivity laser-induced fluorescence–high-performance liquid chromatography studies of polyaromatic hydrocarbons using the argon ion laser–Yeung detector cell configuration
by M. C. Roach and M. D. Harmony (Lawrence, KS, U.S.A.) (Received August 2nd, 1988) 332

Simultaneous determination of thiols and corresponding disulphides in mixtures by high-performance liquid chromatography with polarographic detection using a Dual-Tast Analyser
by B. Dębowska, K. Samochocka, M. Przasnyski and D. Sybilska (Warsaw, Poland) (Received July 18th, 1988) 336

Separation of thiols on Spheron Ara activated with 2-nitrophenylhydrazonopropandinitrile ligand
by D. Podhradský and M. Antalík (Košice, Czechoslovakia) and E. Šturdík (Bratislava, Czechoslovakia) (Received August 9th, 1988) 344

Derivatisation of amines with O-acetylsalicyloyl chloride to enhance electrochemical detection in high-performance liquid chromatography
by R. M. Smith, A. Abdul Ghani, D. G. Haverty, G. S. Bament, A. Y. Chamsi and A. G. Fogg (Loughborough, U.K.) (Received July 25th, 1988) 349

Development of an high-performance liquid chromatographic method for the simultaneous analysis of the species involved in diethyl L-tartrate hydrolysis
by D. S. Kalonia and A. P. Simonelli (Storrs, CT, U.S.A.) (Received August 2nd, 1988) . 355

Simultaneous collection of the eluate from up to twenty liquid chromatographic columns by a minor modification to the fraction collector
by F. Marquard and O. Sonne (Aarhus, Denmark) (Received July 20th, 1988) 360

Measurement of methylated DNA purines by reversed-phase high-performance liquid chromatography and fluorimetric detection
by A. M. Tacchi-Bedford (London, U.K.) (Received August 30th, 1988) 364

Étude par chromatographie liquide haute performance des métabolites potentiels de la caféine. Comparaison de différentes techniques
par M. F. Vergnes, C. Grosset et J. Alary (La Tronche, France) (Reçu le 25 juillet 1988) . 369

Activity stain for polygalacturonase
by T. A. McKeon (Albany, CA, U.S.A.) (Received August 29th, 1988) 376

(Continued overleaf)

Indirect fluorimetric detection of non-electrolytes in thin-layer chromatography
by Y. Ma and E. S. Yeung (Ames, IA, U.S.A.) (Received June 15th, 1988) 382

Gas chromatographic determination of chloroacetamide herbicides in plants and soil
by A. Balinova (Sofia, Bulgaria) (Received June 15th, 1988) 391

Simultaneous separation and identification of carotenoids and chlorophylls in turf bermudagrass by high-performance liquid chromatography
by C. A. Bailey and B. H. Chen (College Station, TX, U.S.A.) (Received September 8th, 1988) 396

Separation of RNA and DNA by histone affinity high-performance liquid chromatography
by C. P. Holstege, M. J. Pickaart and L. L. Louters (Grand Rapids, MI, U.S.A.) (Received June 22nd, 1988) 401

Procyanidines galloylées du sarment de vigne (*Vitis vinifera*). Séparation et identification par chromatographie liquide haute performance et chromatographie en phase gazeuse
par M. Boukharta, M. Girardin et M. Metche (Vandoeuvre, France) (Reçu le 11 août 1988) 406

Determination of geniposide, gardenoside, geniposidic acid and genipin-1-β-gentiobioside in *Gardenia jasminoides* by high-performance liquid chromatography
by T. Oshima, K. Sagara and T. Yoshida (Saitama, Japan) and Y.-Y. Tong, G. Zhang and Y.-H. Chen (Beijing, China) (Received July 21st, 1988) 410

Quantitative high-performance liquid chromatographic determination of ampicillin embonate and amoxycillin embonate
by T. Saesmaa (Helsinki, Finland) (Received June 13th, 1988) 415

Application of amperometric detection to the high-performance liquid chromatographic determination of antipyrine and 4-aminoantipyrine in urine
by A. Burcinová, M. Tichý, V. Pacáková and K. Štulík (Prague, Czechoslovakia) (Received July 25th, 1988) 420

Liquid chromatographic determination of trace amounts of low-molecular-weight fatty acid vapours in industrial emissions
by K. Kuwata and S. Tanaka (Osaka, Japan) (Received July 4th, 1988) 425

High-performance liquid chromatographic determination of hinokitiol in cosmetics by the formation of difluoroborane compounds
by M. Endo, T. Mizutani and M. Matsumura (Osaka, Japan) and M. Moriyasu, M. Ichimaru, A. Kato and Y. Hashimoto (Hyogo, Japan) (Received June 23rd, 1988) 430

High-performance affinity chromatography of human progesterone receptor
by D. M. Boyle and L. A. van der Walt (Johannesburg, South Africa) (Received July 2nd, 1988) 434

Separation of some rodenticides and related compounds by thin-layer chromatography
by K. Opong-Mensah (Richmond, CA, U.S.A.) and W. R. Porter (North Chicago, IL, U.S.A.) (Received August 24th, 1988) 439

Book Reviews

Introduction to microscale high-performance liquid chromatography (edited by D. Ishii) 444

Quantitative gas chromatography for laboratory analyses and on-line process control (by G. Guiochon and C. L. Guillemin), reviewed by J. Janák 445

Author Index 446

In articles with more than one author, the name of the author to whom correspondence should be addressed is indicated in the article heading by a 6-pointed asterisk (*)

Automatic Methods of Analysis

by **M. VALCÁRCEL** *and* **M.D. LUQUE DE CASTRO,**
Department of Analytical Chemistry, University of Córdoba, Córdoba, Spain

(Techniques and Instrumentation in Analytical Chemistry, 9)

This new book gives a comprehensive overview of the state of the art of the automation of laboratory processes in analytical chemistry. The topics have been chosen according to such criteria as the degree of consolidation, scope of application and most promising trends.

The book begins with the basic principles behind the automation of laboratory processes, then describes automatic systems for sampling and sample treatment. In the second part the principal types of analysers are discussed: continuous, batch and robotic. The third part is devoted to the automation of analytical instrumentation: spectroscopic, electroanalytical and chromatographic techniques and titrators. The last part presents examples of the application of automation to clinical chemistry, environmental pollution monitoring and industrial process control.

The text is supplemented by 290 figures and 800 literature references. It is written primarily for those directly involved in laboratory work or responsible for industrial planning and control, research centres, etc. It will also be useful to analytical chemists wishing to update their knowledge in this area, and will be of especial interest to scientists directly related to environmental sciences or clinical chemistry.

CONTENTS:

1. Fundamentals of Laboratory Automation.
2. Computers in the Laboratory.
3. Automation of Sampling.
4. Automation in Sample Treatment.
5. Automatic Continuous Analysers: Air-Segmented Flow Analysers.
6. Automatic Continuous Analysers: Flow-Injection Analysis.
7. Automatic Continuous Analysers: Other Automatic Unsegmented Flow Methods.
8. Automatic Batch Analysers.
9. Robots in the Laboratory.
10. Automation of Analytical Instrumentation: Spectrometric Techniques.
11. Automation of Analytical Instrument ation: Electroanalytical Techniques.
12. Automation of Analytical Instrument ation: Chromatographic Techniques.
13. Automatic Titrators.
14. Automation in Clinical Chemistry.
15. Automation in Environmental Pollution Monitoring.
16. Process Analysers.

1988 xii + 560 pages
US$ 131.50 / Dfl.250.00
ISBN 0-444-43005-9

ELSEVIER SCIENCE PUBLISHERS

P.O. Box 211, 1000 AE Amsterdam, The Netherlands
P.O. Box 882, Madison Square Station, New York, NY 10159, USA

The ideal combination:

BOOK, SOFTWARE and DATABASE

BASIC GAS CHROMATOGRAPHY-MASS SPECTROMETRY: Principles and Techniques

F.W. Karasek *and* **R.E. Clement,**
Waterloo, Ont., Canada

The book opens with the principles of both GC and MS necessary to understand and deal with the data generated in GC/MS analyses.

The focus then turns to the particular requirements created by a direct combination of these two techniques into a single instrumentation system. The data generated and their use are covered in detail. The role of the computer and its specific software, especially in compound identification via mass spectral search techniques, receives special attention.

Representative applications and results obtained with GC/MS-computer techniques are presented, permitting extrapolation of specific applications to similar problems encountered by the reader. Instructional, informative and application-oriented, the material will be useful to a wide range of people.

Designed to be used independently, the book is admirably complemented when used in conjunction with the software.

1988 viii + 202 pages
US$ 79.00 / Dfl. 150.00
ISBN 0-444-42760-0

GAS CHROMATOGRAPHY-MASS SPECTROMETRY: A Knowledge Base

F.A. Settle, Jr. *and* **M.A. Pleva,**
Lexington, VA, USA

This electronic module, though an independent source of current information on GC/MS, can also be used as a helpful supplement to the book.

The module consists of a knowledge base and a retrieval program allowing the information to be presented in a user- friendly format. A number of special purpose files are included: an index, a glossary, and a list of keywords. The module is available for the IBM-PC and its compatibles as a set of three $5^1/_4$" diskettes, requiring 128K RAM memory and two disk drives.

It is useful as an introduction to the operation of instrument components, data systems and the interpretation of resulting data. It aids workers requiring GC/MS analysis in the fields of medicine, pharmacy, environmental and forensic science and helps to acquaint potential purchasers with the different types of equipment available, along with a guide to manufacturers and prices.

3 Diskettes + manual:
US$ 144.75 / Dfl. 275.00
ISBN 0-444-42761-9

A brochure giving full details is available from...

ELSEVIER SCIENCE PUBLISHERS

P.O. Box 211, 1000 AE Amsterdam, The Netherlands
P.O. Box 1663, Grand Central Station, New York, NY 10163, USA

JOURNAL OF CHROMATOGRAPHY

VOL. 455 (1988)

JOURNAL *of* CHROMATOGRAPHY

INTERNATIONAL JOURNAL ON CHROMATOGRAPHY,
ELECTROPHORESIS AND RELATED METHODS

EDITOR
MICHAEL LEDERER (Switzerland)

ASSOCIATE EDITORS
R. W. FREI (Amsterdam), R. W. GIESE (Boston, MA), J. K. HAKEN (Kensington, N.S.W.), K. MACEK (Prague), L. R. SNYDER (Orinda, CA)

EDITOR, SYMPOSIUM VOLUMES
E. HEFTMANN (Orinda, CA)

EDITORIAL BOARD

W. A. Aue (Halifax), V. G. Berezkin (Moscow), V. Betina (Bratislava), A. Bevenue (Belmont, CA), P. Boček (Brno), P. Boulanger (Lille), A. A. Boulton (Saskatoon), G. P. Cartoni (Rome), S. Dilli (Kensington, N.S.W.), L. Fishbein (Washington, DC), A. Frigerio (Milan), C. W. Gehrke (Columbia, MO), E. Gil-Av (Rehovot), G. Guiochon (Knoxville, TN), I. M. Hais (Hradec Králové), S. Hjertén (Uppsala), E. C. Horning (Houston, TX), Cs. Horváth (New Haven, CT), J. F. K. Huber (Vienna), A. T. James (Harrold), J. Janák (Brno), E. sz. Kováts (Lausanne), K. A. Kraus (Oak Ridge, TN), A. Liberti (Rome), H. M. McNair (Blacksburg, VA), Y. Marcus (Jerusalem), G. B. Marini-Bettòlo (Rome), A. J. P. Martin (Cambridge), Č. Michalec (Prague), R. Neher (Basel), G. Nickless (Bristol), N. A. Parris (Wilmington, DE), R. L. Patience (Sunbury-on-Thames), P. G. Righetti (Milan), O. Samuelson (Göteborg), R. Schwarzenbach (Dübendorf), A. Zlatkis (Houston, TX)

EDITORS, BIBLIOGRAPHY SECTION
Z. Deyl (Prague), J. Janák (Brno), V. Schwarz (Prague), K. Macek (Prague)

ELSEVIER
AMSTERDAM — OXFORD — NEW YORK — TOKYO

J. Chromatogr., Vol. 455 (1988)

© ELSEVIER SCIENCE PUBLISHERS B.V. — 1988

0021-9673/88/$03.50

All rights reserved. No part of this publication may be reproduced, stored in a retrieval system or transmitted in any form or by any means, electronic, mechanical, photocopying, recording or otherwise, without the prior written permission of the publisher, Elsevier Science Publishers B.V., P.O. Box 330, 1000 AH Amsterdam, The Netherlands.

Upon acceptance of an article by the journal, the author(s) will be asked to transfer copyright of the article to the publisher. The transfer will ensure the widest possible dissemination of information.

Submission of an article for publication entails the authors' irrevocable and exclusive authorization of the publisher to collect any sums or considerations for copying or reproduction payable by third parties (as mentioned in article 17 paragraph 2 of the Dutch Copyright Act of 1912 and the Royal Decree of June 20, 1974 (S. 351) pursuant to article 16 b of the Dutch Copyright Act of 1912) and/or to act in or out of Court in connection therewith.

Special regulations for readers in the U.S.A. This journal has been registered with the Copyright Clearance Center, Inc. Consent is given for copying of articles for personal or internal use, or for the personal use of specific clients. This consent is given on the condition that the copier pays through the Center the per-copy fee stated in the code on the first page of each article for copying beyond that permitted by Sections 107 or 108 of the U.S. Copyright Law. The appropriate fee should be forwarded with a copy of the first page of the article to the Copyright Clearance Center, Inc., 27 Congress Street, Salem, MA 01970, U.S.A. If no code appears in an article, the author has not given broad consent to copy and permission to copy must be obtained directly from the author. All articles published prior to 1980 may be copied for a per-copy fee of US$ 2.25, also payable through the Center. This consent does not extend to other kinds of copying, such as for general distribution, resale, advertising and promotion purposes, or for creating new collective works. Special written permission must be obtained from the publisher for such copying.

No responsibility is assumed by the Publisher for any injury and/or damage to persons or property as a matter of products liability, negligence or otherwise, or from any use or operation of any methods, products, instructions or ideas contained in the materials herein. Because of rapid advances in the medical sciences, the Publisher recommends that independent verification of diagnoses and drug dosages should be made.

Although all advertising material is expected to conform to ethical (medical) standards, inclusion in this publication does not constitute a guarantee or endorsement of the quality or value of such product or of the claims made of it by its manufacturer.

Printed in The Netherlands

Journal of Chromatography, 455 (1988) 1–15
Elsevier Science Publishers B.V., Amsterdam — Printed in The Netherlands

CHROM. 20 904

RESOLUTION OF COLLOIDAL LATEX AGGREGATES BY SEDIMENTATION FIELD-FLOW FRACTIONATION

HARLAN K. JONES*, BHAJENDRA N. BARMAN and J. CALVIN GIDDINGS*
Department of Chemistry, Henry Eyring Building, University of Utah, Salt Lake City, UT 84112 (U.S.A.)
(First received June 10th, 1988; revised manuscript received August 18th, 1988)

SUMMARY

The observation of a repetitive series of peaks while analyzing two different samples of poly(methyl methacrylate) colloidal latex spheres by sedimentation field-flow fractionation strongly suggests that part of the latex population has aggregated into doublets, triplets, and higher-order particle clusters. The aggregation hypothesis is confirmed for the two samples both by retention calculations and by electron microscopy. It is shown that the resolution of the latex clusters is influenced by flow velocity in a manner predicted by theory but that such resolution is limited by the polydispersities of the two latex samples. Polydispersity values are obtained using plate height *versus* flow velocity measurements and are shown to be consistent with the different resolution levels observed for the two colloids. A detailed analysis of the results shows that steric effects play an increasing role as cluster size increases. The steric role in this study is examined at some length.

INTRODUCTION

The separation of the components of complex colloidal materials is one of the most difficult challenges in separation science. Most chromatographic methods fail in the colloidal size range or, if operable, they perform poorly in terms of resolution, recovery, and reproducibility. Therefore it is desirable to examine alternate means that might solve important colloid separation and characterization problems encountered in working with biological, industrial, environmental, and geological materials.

The techniques of field-flow fractionation (FFF) appear to be well-suited to colloid analysis. The special subtechnique of sedimentation FFF is particularly effective in dealing with colloidal particles in the diameter range from 0.02 to 1 μm (up to 100 μm using the steric mode of operation). Not only is resolution high with the sedimentation subtechnique of FFF but separation occurs on the basis of differences in effective mass according to well-defined theoretical principles. The theoretical equations make it possible to calculate the properties of colloidal particles in terms of the elution characteristics observed for the particles in sedimentation FFF[1–3].

* Present address: Battelle PNL, Richland, WA 99352, U.S.A.

0021-9673/88/$03.50 © 1988 Elsevier Science Publishers B.V.

One of the most important colloidal processes, and one that is generally quite difficult to characterize, is the aggregation of single particles to form complexes made up of multiples of the individual particles. Aggregation is a common phenomenon for both natural and industrial colloids[4,5]. However, the resolving power of sedimentation FFF has not been fully focussed on the separation and characterization of colloidal aggregates. The clearest demonstration of the ability of sedimentation FFF to separate aggregated colloids was reported from this laboratory in 1980[6]: a complex biomaterial sample was shown to emerge as singlet, doublet, and higher-order aggregated viral rods.

Because of their uniformity, samples of latex microspheres appear to provide an ideal medium for the study of aggregation. However, these samples generally consist only of single particles; when aggregation is forced (*e.g.*, by freezing or adding salt), the single particles will generally clump together out-of-control, forming an unmanageable precipitate. Thus in our extensive studies with polystyrene latex standards we have not until recently observed simple aggregates consisting of two, three, or more particles. However, in some recent studies undertaken to characterize poly(methyl methacrylate) (PMMA) latex samples using sedimentation FFF, we immediately observed a series of peaks (see Fig. 1) suggestive of low order aggregation. In pursuing these studies we have found that sedimentation FFF provides extraordinary detail on both the aggregates and the aggregation process. While some of the details of these studies will be reported in the colloid literature, we will examine here the characteristics of sedimentation FFF that must be considered for the resolution of aggregated materials.

Normal sedimentation FFF obeys the basic principles originally formulated by Giddings *et al.*[7]; the favorable agreement between theory and experiment has been demonstrated many times for latex particles up to 1 μm diameter[1,3,7–11]. When the effective particle size exceeds *ca.* 1 μm (specifically when the particle radius becomes larger than the mean thickness of the steady-state particle layer), the steric limit of FFF is approached[12]. Unlike normal FFF where smaller particles elute before larger ones, steric FFF has an elution order similar to hydrodynamic chromatography[13] with larger particles eluting first. However, some steric effects become evident before this inversion in elution order occurs.

This study focuses on the ability of sedimentation FFF to resolve aggregated species, specifically singlet, doublet, and higher order PMMA aggregates. Electron microscopy is used in conjunction with this work to confirm the presence of separated aggregate species.

THEORY

The basic retention equation for normal FFF operation is given by[1–3,7]

$$R = 6\lambda[\coth(1/2\lambda) - 2\lambda] \tag{1}$$

where R is the retention ratio and λ is the dimensionless FFF retention parameter, a measure of the compression of the particle distribution against the channel wall by the field. If the sample is highly retained, in which case R and λ are small, R can be approximated by the simple form

$$R = 6\lambda \quad (\lambda \to 0) \tag{2}$$

In sedimentation FFF, the retention parameter λ is related to particle mass m by the expression

$$\lambda = \frac{kT}{mwG\Delta\rho/\rho_s} \tag{3}$$

where k is the Boltzmann constant, T is the absolute temperature of the carrier liquid, G is the centrifugal acceleration, w is the channel thickness, $\Delta\rho$ is the difference in density between the particle and carrier liquid, and ρ_s is the density of the sample particles. If the particles are spherical in shape, the retention parameter λ can be rewritten in terms of the particle diameter d

$$\lambda = \frac{6kT}{\pi\Delta\rho wGd^3} \tag{4}$$

From the experimental retention volume V_R, the retention ratio R is obtained by using

$$R = V_0/V_R \tag{5}$$

where V_0 is the retention volume of nonretained material, equal to the channel void volume. The measured value of R is then used either to calculate particle mass from eqns. 1 and 3 or particle diameter (in the case of spherical particles) from eqns. 1 and 4.

The transition from normal sedimentation FFF to steric FFF has been predicted by theory[14] and demonstrated by experiment[15]. However, an exact theory for particle retention in the steric FFF region has yet to be developed. Steric FFF can be thought of as the high-field large-particle limit of normal FFF. In steric FFF differences in particle size control the differential migration of the particles[12].

The retention equation when modified for the steric FFF mechanism takes the following form[14,16]

$$R = \frac{3\gamma d}{w} + 6\lambda \tag{6}$$

where γ is a dimensionless factor of order unity. The factor γ has been shown to be influenced by several experimental parameters such as flow-rate, field strength, and particle density[14,15].

The resolution R_s between two neighboring component peaks in FFF is defined in the same way as in chromatography

$$R_s = \frac{\Delta z}{4\sigma} \tag{7}$$

where Δz is the distance between the centers of gravity of the two peaks and σ is the average standard deviation of the peaks. Resolution can be related to the apparent number of theoretical plates N and the retention ratio R in the following way[17]

$$R_s = \frac{N^{1/2}}{4}\frac{\Delta R}{R} \tag{8}$$

where ΔR is the difference in the retention ratio of the two peaks. If the sample is well retained ($R < 0.5$ as $\lambda < 0.1$) then R is approximately inversely proportional to particle mass as shown by combining eqns. 2 and 3. For small $\Delta R/R$ values eqn. 8 can be expressed as

$$R_s = \frac{N^{1/2}}{4}\frac{\Delta m}{m} \tag{9}$$

where Δm is the mass difference between the particles in the two neighboring peaks and m is the mean particle mass.

When FFF is applied to particles distributed over a small but finite diameter range, the high selectivity of FFF causes the fractionation of the particles according to size and consequently increases the width of the particle peak. The plate height contribution of this "polydispersity" effect is designated as H_p. The apparent plate height H of the system can be approximated as the sum of H_p and the non-equilibrium term $C<v>$

$$H = H_p + C<v> \tag{10}$$

where $<v>$ is the mean linear flow velocity and C is a constant independent of $<v>$. Since $N = L/H$, where L is channel length, eqn. 9 becomes

$$R_s = \frac{1}{4}\left(\frac{L}{H_p + C<v>}\right)^{1/2}\frac{\Delta m}{m} \tag{11}$$

which shows that for finite polydispersity the value of R_s cannot be reduced below a fixed minimum level no matter how small the "true" system plate height $C<v>$. However, if H_p is negligible, R_s will vary inversely as $<v>^{1/2}$.

Particle size polydispersity is expressed here by the coefficient of variation, equal to the ratio of the standard deviation σ_d in particle size to the mean particle diameter d. The coefficient of variation of single (non-aggregated) latex particles can be determined by plotting the sedimentation FFF plate height for the first (singlet) peak *versus* the linear flow velocity $<v>$ of the carrier liquid. As shown by eqn. 10, the intercept of such a plot can be equated to the polydispersity contribution to plate height, H_p. The latter is related to σ_d/d by[7]

$$H_p = 9LS^2(\sigma_d/d)^2 \tag{12}$$

where S is the mass selectivity (which approaches unity for highly retained particles in sedimentation FFF[18]) and L is the length of the FFF channel.

EXPERIMENTAL

Two sedimentation FFF systems were used in this work. The basic apparatus for system I is a slightly modified version of the Model S101 sedimentation FFF instrument from FFFractionation (Salt Lake City, UT, U.S.A.). The apparatus was employed with a channel having tip-to-tip length $L = 94.2$ cm, thickness $w = 0.0254$ cm, and breadth $b = 1.40$ cm. The channel void volume V_0 measured as the elution volume (minus extrachannel volume) of a non-retained sodium benzoate peak was found to be 3.25 ml (slightly reduced from the normal 4.5 ml volume of the Model S101 system), a value used for all experimental retention ratio calculations. The accumulation (outer) wall was coated with a polyimide tape for inertness. The distance r_0 between the channel and axis of rotation is 15.5 cm.

The system II sedimentation FFF apparatus is similar to that reported in an earlier paper[19]. The apparatus has provisions for stream-splitting at the outlet end of the channel to enhance detector signal[20]. The channel dimensions are 90.5 cm length, 2.0 cm breadth, and 0.0254 cm thickness. The void volume is 4.5 ml. The channel is secured inside an aluminum rotor with a radius r_0 of 15.3 cm. The system accumulation wall has a highly polished Hastelloy C surface.

The flow stream for both systems was delivered by Gilson Minipuls 2 peristaltic pumps (Middleton, WI, U.S.A.). All experiments were carried out at a constant field strength of 61.6 g (600 rpm) for system II and 111.0 g (800 rpm) for system I. Altex Model 153 UV detectors from Beckman Instruments (Berkeley, CA, U.S.A.) filtered at 254 nm wavelength were used. The detector response was transcribed onto Houston Instrument strip chart recorders (Austin, TX, U.S.A.).

The standard carrier liquid was deionized, distilled water which was further purified by a Sybron/Barnstead Nanopure filtration system (Boston, MA, U.S.A.). For system II, 0.05% by wt. sodium dodecyl sulfate and 0.01% by wt. sodium azide, both from Sigma (St. Louis, MO, U.S.A.), were added to water. However, for system I a solution of 0.1% by vol. FL-70 detergent (Fisher Scientific, Pittsburgh, PA, U.S.A.) and 0.02% by wt. sodium azide was used.

Two PMMA latex samples were used in this work. One sample was supplied by Dr. T. Provder of The Glidden Company (Strongsville, OH, U.S.A.). The particle diameter of the latex spheres in this sample was given as 0.207 μm and the density as 1.214 g/ml. A second PMMA sample obtained from Seradyn (Indianapolis, IN, U.S.A.) was reported to have a single particle diameter of 0.230 μm and a particle density of 1.21 g/ml.

Concurrent with the sedimentation FFF work, scanning electron microscopy (SEM) was used to monitor the state of aggregation of the PMMA particles. Fractions of the PMMA sample were collected at predetermined elution volumes from the sedimentation FFF run. The fractions were then vacuum filtered onto 0.1 μm pore size Nuclepore filters (Pleasanton, CA, U.S.A.). The sample collected on the filter was then mounted on a standard SEM stub, gold coated with either a Technics Hummer III sputter coater (Alexandria, VA, U.S.A.) or a Vanton Vacuum Model Desk-I sputter coater (Cherry Hill, NJ, U.S.A.) and then observed either under a JEOL JSM35 scanning electron microscope (Tokyo, Japan) or a Hitachi S-450 scanning electron microscope (Tokyo, Japan).

RESULTS AND DISCUSSION

Representative fractograms of the two PMMA samples are shown in Fig. 1. These fractograms were obtained from sedimentation FFF system II with a carrier flow-rate of 0.80 ± 0.01 ml/min and a field strength of 61.6 *g*. The electron micrographs of these two PMMA samples are shown in Fig. 2. These micrographs show that the particle diameter is uniform whereas each fractogram in Fig. 1 displays a series of peaks that normally implies a non-uniformity in particle diameter. The logical explanation is that the first peak to elute represents (as we shall soon confirm) single latex particles. The second peak represents doublet particles, the third peak triplet clusters, and so on. Consistent with this explanation, clusters of various sizes are observed in the micrographs. The fractograms support the view that these are long-lived stable clusters rather than transient clusters formed during filtration for SEM sample analysis.

The resolution displayed in Fig. 1b is clearly better than that shown in Fig. 1a. Specifically, resolution values between singlet and doublet peaks are 1.43 and 1.20 for fractograms in Fig. 1a and b, respectively. The values which correspond to doublet and triplet peaks are 1.41 and 1.07. These differences in resolution can be attributed to the different polydispersities of the two samples of latex spheres. By combining the theory of band broadening and appropriate band-width measurements, the relevant polydispersities of the latex spheres can be ascertained.

Eqn. 10 shows that the polydispersity contribution to plate height H_p can be obtained as the intercept of a plot of plate height H *versus* flow velocity $<v>$. When data for the two single particle peaks studied here are plotted in this way, they yield straight lines as indicated in Fig. 3. The intercepts of the two lines differ substantially, indicating considerable differences in the two polydispersities.

Using the measured intercepts in conjunction with eqn. 12, the polydispersity (coefficient of variation) of the 0.207-μm latex spheres of Fig. 1a was found to be $(\sigma_d/d) = 0.040 \pm 0.012$, somewhat larger than the value $(\sigma_d/d) = 0.023 \pm 0.009$ determined for the 0.230-μm sample displayed in Fig. 1b. These results confirm that the fractograms of the respective PMMA samples shown in Fig. 1 differ in the resolution displayed primarily because of the differences in σ_d/d. Finite σ_d/d values not only interfere with apparent (not real) resolution but they put a limit on the maximum number of peaks that can be resolved.

Another important aspect of FFF theory is that the mean particle diameter d of a peak can be measured in terms of experimental retention volumes. This capability can be applied to the peaks in Fig. 1 to verify the assumed mechanism involving the aggregation of single particles. If the retention volumes of the first (singlet) peaks in Fig. 1 are measured and used in conjunction with eqns. 1, 4, and 5, the calculated particle diameters (using the reported densities of 1.21 g/ml) are 0.200 and 0.216 μm for Fig. 1a and b, respectively. These values are in good agreement with the reported diameters, 0.207 and 0.230 μm, respectively, and support the view that these peaks are composed of single latex beads.

We note that electron microscopy yields particle diameters of 0.200 ± 0.013 μm (measuring 133 particles) and 0.213 ± 0.013 μm (135 particles), respectively. The SEM calibration was performed using NBS standard SRM 1960 (9.89 μm) polystyrene beads[21].

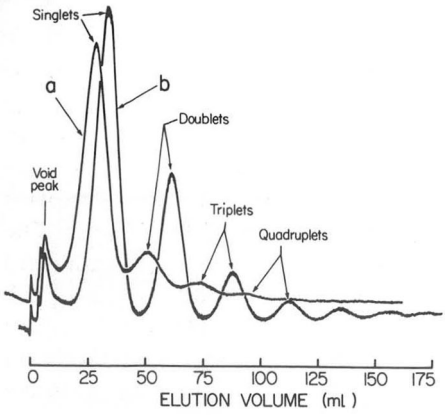

Fig. 1. Representative fractograms of aggregated PMMA latex samples obtained by system II at 61.6 *g* and a flow-rate of 0.80 ± 0.01 ml/min: (a) 0.207 μm PMMA aggregate series; (b) 0.230 μm PMMA aggregate series. Both samples were sonicated for about 30 min prior to runs.

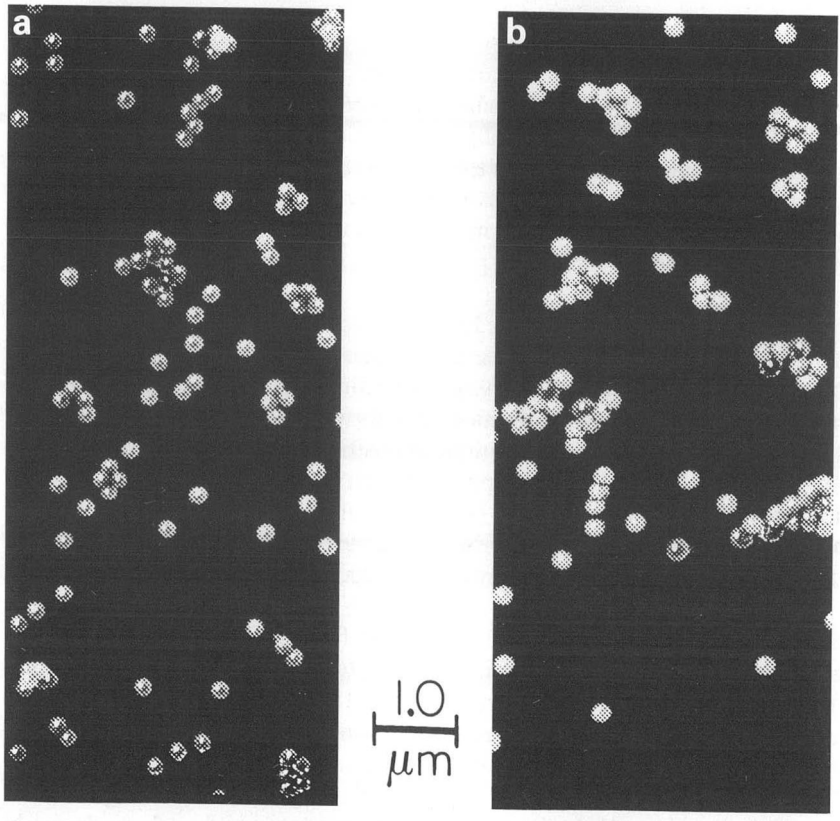

Fig. 2. Electron micrographs of (a) 0.207 μm and (b) 0.230 μm PMMA samples used to obtain fractograms in Figs. 1a and b, respectively.

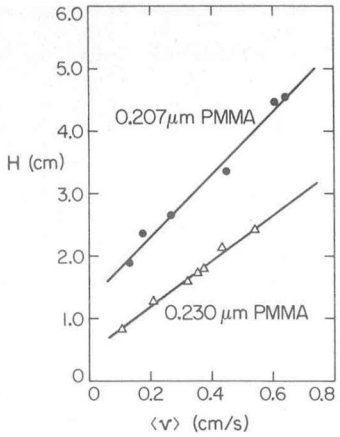

Fig. 3. Plate height H *versus* flow velocity $<v>$ plots for the singlet peaks of the two PMMA samples. Fractograms for plate height data were generated from system II at 61.6 g. Straight lines represent least squares fits: (a) 0.207 μm PMMA, $H = 1.30\ (\pm 0.12) + 5.01\ (\pm 0.29)\ <v>$; (b) 0.230 μm PMMA, $H = 0.435\ (\pm 0.065) + 3.364\ (\pm 0.057)\ <v>$.

The combination of eqns. 2, 3, and 5 shows that retention volume V_R is approximately proportional to particle mass. Thus singlets, doublets, triplets, and so on should appear as evenly spaced peaks along the elution volume axis. Fig. 1 is largely consistent with this conclusion but shows that the increment in V_R between successive peaks gradually falls off as V_R increases. Specifically, the retention volumes which correspond to the four successive peaks in Fig. 1a are 26.6, 51.4, 70.0 and 98.4 ml. Retention volumes for the six successive peaks of Fig. 1b are 32.9, 60.8, 87.7, 111.9, 134.2 and 155.2 ml.

Although the above calculations are highly supportive of the view that the peaks in Fig. 1 correspond to singlets, doublets, and higher order aggregates of the basic PMMA latex bead, a more absolute form of verification was obtained using electron microscopy. For this purpose narrow fractions or cuts were collected from the first five peaks of the nominal 0.207-μm PMMA sample at positions shown in Fig. 4. A fraction was also collected for the peak which appeared after the field was turned off. The individual fractions were then subjected to electron microscopy as described in the Experimental section. As expected, cut No. 1 yielded singlets, cut No. 2 yielded doublets, and so on. These results are shown in the electron micrographs displayed in Fig. 4.

Narrow fractions were also collected from the first six peaks of the 0.230-μm PMMA samples at positions shown in Fig. 5. We note that the difference in the two fractograms of 0.230 μm PMMA latex shown in Figs. 1b (system II) and 5 (system I) is due to the fact that Fig. 1b was obtained with a sonicated sample and Fig. 5 was obtained with the original sample. In the latter case the relative amount of higher order aggregated material is expected (and observed) to be high. The scanning electron micrographs of the fractions of the 0.230-μm sample indicated in Fig. 5 are shown in Fig. 6. The micrographs in Figs. 4 and 6 show that the resolution of different aggregate

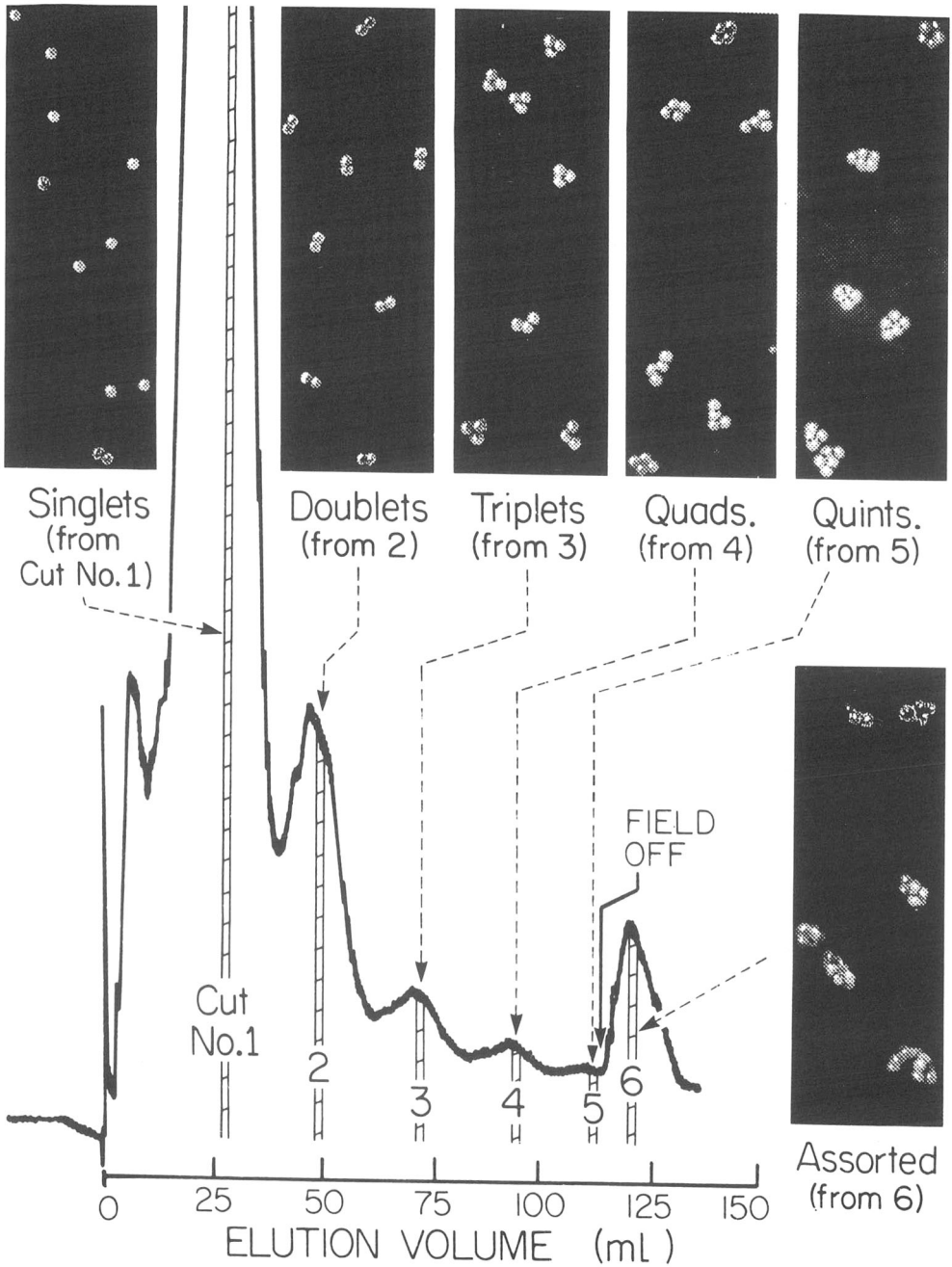

Fig. 4. Fractogram of 0.207 μm PMMA sample from which narrow fractions were cut. Inserted electron micrographs correspond to these fractions. Experimental conditions: sedimentation FFF system II was used at a field strength of 61.6 g and a flow-rate of 0.84 ml/min.

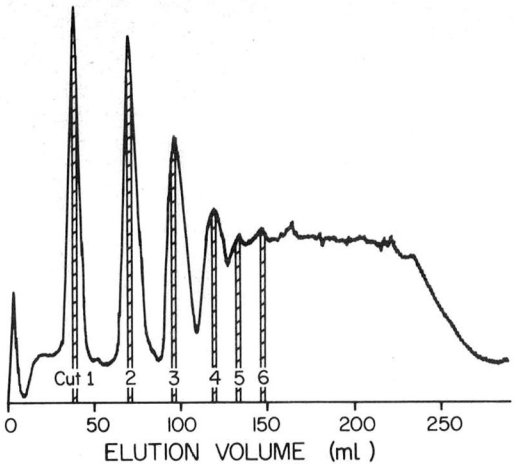

Fig. 5. Fractogram of 0.230 μm PMMA aggregate series from which six cuts were collected and prepared for SEM. Fractogram was obtained using system I and original sample. Experimental conditions: field strength 111 g, flow-rate 0.327 ml/min.

numbers is fairly complete, even for some cuts where the fractograms of Figs. 4 and 5 suggest incomplete resolution.

The micrographs in Figs. 4 and 6 show that the higher order PMMA aggregates vary considerably in shape. The assorted shapes co-elute in the same fraction but the different aggregation numbers do not, an observation confirming the theoretical conclusion (eqn. 3) that retention depends primarily on particle mass and density and not on shape.

Eqns. 10 and 11 show that sharper peaks and better resolution can be achieved by lowering the carrier liquid flow-rates in sedimentation FFF. This is consistent with previous observations[22]. Fig. 7, obtained using system I, shows the expected degradation of particle resolution with increasing flow-rate. A plot of R_s *versus* the relative mass difference $\Delta m/m$ for the singlet and doublet pair of peaks, the singlet and triplet pair, and the doublet and triplet peak pairs at the four flow-rates is shown in Fig. 8. This figure confirms the loss of resolution with increasing $<v>$. However, the resolution decrease is much less than predicted by the inverse $<v>^{1/2}$ dependence of eqn. 11 for $H_p = 0$, illustrating the important role played by polydispersity in peak resolution.

We note that the R_s values of Fig. 8 deviate from the linear dependence on $\Delta m/m$ suggested by eqn. 9. Closer analysis shows that strict linearity is not expected because of variations in N from one peak to another and the relatively large values of $\Delta m/m$.

The resolution of singlet/doublet PMMA particles illustrates the flexibility of sedimentation FFF in resolving aggregated from non-aggregated particles. Fig. 8 shows that an experimental field strength of 111 g (800 rpm) and a flow-rate of 0.327 ml/min yields $R_s = 2.38$, a value higher than needed. One can still achieve $R_s \approx 1.5$ for this pair at a flow-rate as high as 2.19 ml/min, this higher flow-rate increasing the speed of separation about seven-fold, down to *ca.* 30 min for elution of the doublet.

The average retention volume obtained for the first peak of each of the four

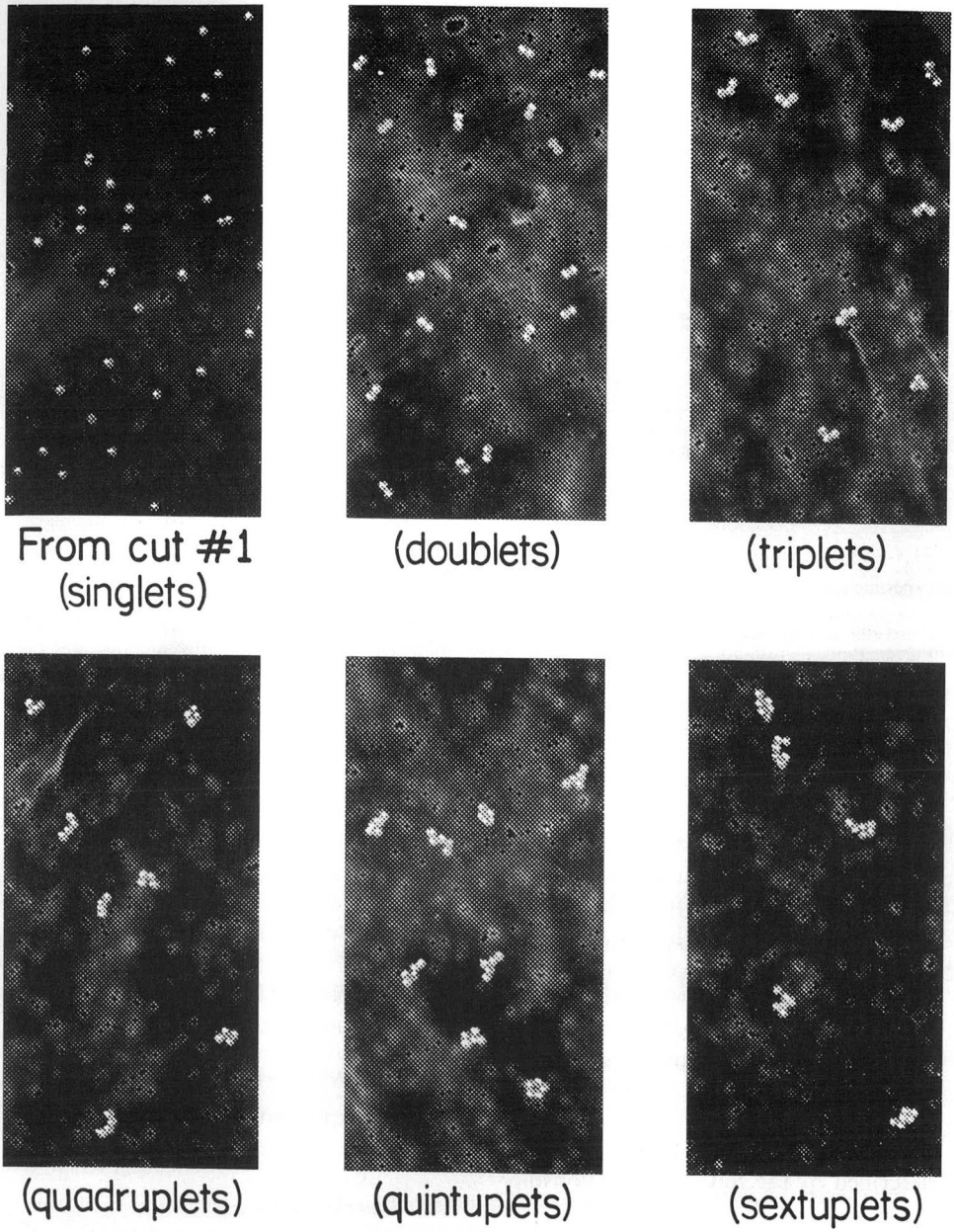

Fig. 6. Electron micrographs of cuts from the fractogram shown in Fig. 5.

fractograms in Fig. 7 is 40.2 $\pm$ 0.3 ml. This corresponds to a particle diameter of 0.213 μm, in excellent agreement with the value of 0.216 μm obtained for the first peak shown in the fractogram of Fig. 1b and also with the 0.213 μm value determined by SEM. The

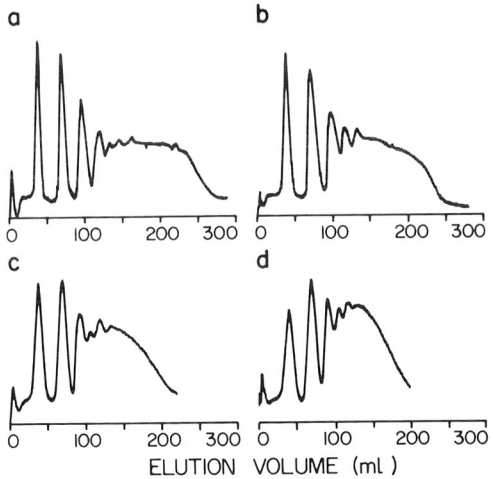

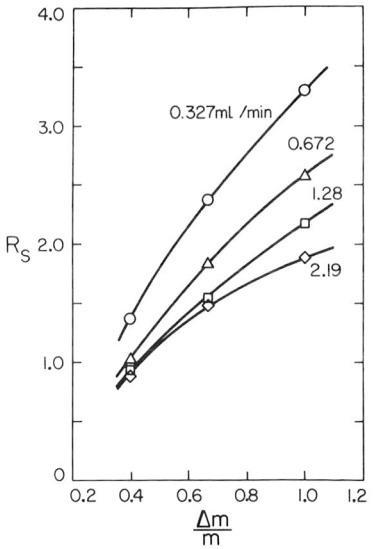

Fig. 7. Fractograms of 0.230 μm PMMA aggregate series obtained at 111.0 g using system I. The experimental flow-rates were varied as follows: (a) 0.327 ml/min, (b) 0.672 ml/min, (c) 1.28 ml/min, and (d) 2.19 ml/min.

Fig. 8. Plots of resolution, R_s, *versus* relative mass difference, $\Delta m/m$, at four different flow-rates (as indicated) for three pairs of peaks from the fractograms shown in Fig. 7. ($\Delta m/m = 0.4$ for doublet-triplet pair, 0.667 for singlet-doublet pair, and unity for singlet-triplet pair.)

close agreement in these results is noteworthy considering that two different sedimentation FFF systems were used under different experimental conditions.

A close inspection of the fractograms in Figs. 5 and 7 shows that there are some measurable departures from the predictions of eqns. 1–4 for the aggregated particles. As noted previously, the spacing between successive peaks in both of the figures decreases as one proceeds along the elution scale. In contrast, eqns. 2 and 3 predict a constant interval between peaks. Compounding this anomaly is the observation from Fig. 7 that the spacing between successive peaks (and thus the position of all peaks past the singlet) depends upon the flow-rate, again in contradiction to the theoretical equations.

The major features of these anomalies can be explained in terms of the steric effect. Thus if we combine eqns. 3, 5, and 6 we find that retention volume V_R is described by the following relationship

$$V_R = \frac{Bm}{1 + A\gamma md} \tag{13}$$

where A and B are constants. The term in the denominator containing A is the steric term which derives from the first term on the right of eqn. 6. If the steric term were negligible, A, for all practical purposes, would equal zero. In this limiting case the retention volume is predicted to increase in direct proportion to mass and therefore in

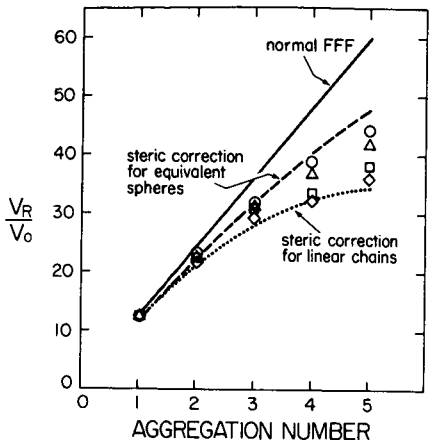

Fig. 9. Plot of V_R/V_0 *versus* aggregation number showing several theoretical lines. The upper line assumes normal FFF; the middle and lower lines incorporate steric corrections for spherical and straight chains geometries, respectively. (○) Flow-rate = 0.327 ml/min; (△) flow-rate = 0.672 ml/min; (□) flow-rate = 1.28 ml/min; (◇) flow-rate = 2.19 ml/min. Experimental points are obtained from fractograms given in Fig. 7.

direct proportion to aggregation number, which would lead to even spacing between all peaks. However, the A-containing term, which grows in proportion to both particle mass m and effective diameter d, increasingly erodes the ideal retention volume $V_R = Bm$ as particle size increases. Therefore the interval between successive peaks decreases as the aggregation number increases in conformity with experimental observations.

With regard to the velocity dependence of the peak spacing, we have known for some time that hydrodynamic lift forces serve to modulate the steric effect[23]. The practical consequence of this important factor is that parameter γ (which reflects lift force effects) increases with flow velocity $<v>$. Thus the steric term in eqn. 13 is increasingly magnified in effect as the flow velocity increases, leading to a velocity-dependent spacing between higher-order peaks as clearly observed in Fig. 7.

The velocity dependence of γ not only influences the distinguishable peaks of Fig. 7 but it also serves to shift the featureless signal on the right side of the fractograms, corresponding to the larger aggregates, to lower retention volumes with increasing flow-rate. It is very likely that the rather sudden dropoff of the signal on the far righthand side of the fractograms represents the steric transition or inversion point where steric FFF gains dominance over normal FFF[15].

The steric influence is further clarified in Fig. 9 which shows a plot of the ratio of retention volume V_R to void volume V_0 against the aggregation number. Along with the experimental data obtained at the various flow-rates, three theoretical curves (based on $d = 0.213$ μm) are shown. The upper curve corresponds to the operation of normal FFF without the intervention of the steric effect. The middle curve accounts for the steric effect under the assumption that $\gamma = 1$ and that the aggregate particles effectively coalesce into a spherical particle. The bottom curve is also based on the assumption that $\gamma = 1$, but the effective diameter d used in the steric term was given

a value at the opposite extreme, corresponding to the full length of a linear array of the aggregated latex spheres. We observe that the experimental points lie at some intermediate position between the bottom and middle line. The electron micrographs of Figs. 4 and 6 confirm that the aggregate clusters tend to be somewhat extended in space with little indication that the most compact cluster geometry is generally favored. Thus it is not surprising to see the experimental results drop well below the middle line of Fig. 9. However, since few of the observed clusters are maximally extended in a linear array geometry, the results would not be expected to approach the bottom curve of Fig. 9. Thus the intermediate range between these curves is consistent with expectation.

We note that steric effects, even for perfect spheres, are not yet subject to exact calculation; for geometrically complex bodies such as latex aggregates the magnitude of steric effects can only be predicted with considerable guesswork. Experiments of the kind reported here should eventually clarify the magnitude of such steric effects under diverse conditions.

CONCLUSIONS

The above study demonstrates that successive aggregates of small colloidal particles can be isolated from one another providing the particle size distribution is sufficiently narrow. Furthermore, the breadth of this distribution (the polydispersity) can be obtained using plots of plate height *versus* flow velocity. The conditions for such studies can be optimized on the basis of theory.

While all sedimentation FFF results are subject to some steric perturbations as particle size and mass increase, this effect is particularly severe in the present case because the particle aggregates assume rather extended structures of relatively large dimensions which serve to enhance the steric effect. Since it takes a linear array of only four of the 0.230-μm PMMA latex beads to generate a particle almost 1 μm in length, many of the larger clusters with aggregation numbers of 4, 5, 6, and beyond will have particles in this size range. Particles this large have long been known to have significant steric effects. These effects increase with flow velocity. We conclude that such steric effects must not only be accounted for in studies of particle aggregation but also in the study of other open dendritic type structures where the effective diameter is amplified out of proportion to the particle mass involved. A small amount of steric perturbation is observed even for the dimer particles (as reflected in the reduced peak spacing) which are less than 0.5 μm in length. We have observed steric perturbations under some conditions for spheres down to *ca.* 0.35 μm. It is likely that the steric effect is also responsible for the velocity-dependent anomalies observed by Kirkland *et al.*[10] in the study of needlelike and platelike particles whose longest dimensions were *ca.* 1 μm.

ACKNOWLEDGEMENT

This work was supported by grant DE-FG02-86ER60431 from the Department of Energy.

REFERENCES

1 J. C. Giddings, G. Karaiskakis, K. D. Caldwell and M. N. Myers, *J. Colloid Interface Sci.*, 92 (1983) 66.
2 J. C. Giddings, *Sep. Sci. Technol.*, 19 (1984) 831.
3 J. C. Giddings, K. D. Caldwell and H. K. Jones, in T. Provder (Editor), *Particle Size Distribution: Assessment and Characterization*, ACS Symposium Series No. 332, 1987, Ch. 15.
4 M. D. Summers and G. E. Smith, *Virology*, 84 (1978) 390.
5 F. Family and D. P. Landau (Editors), *Kinetics of Aggregation and Gelation*, North Holland, Amsterdam, 1984.
6 K. D. Caldwell, T. T. Nguyen, J. C. Giddings and H. M. Mazzone, *J. Virol. Methods*, 1 (1980) 241.
7 J. C. Giddings, F. J. F. Yang and M. N. Myers, *Anal. Chem.*, 46 (1974) 1917.
8 F. J. F. Yang, M. N. Myers and J. C. Giddings, *Anal. Chem.*, 46 (1974) 1924.
9 F. J. Yang, M. N. Myers and J. C. Giddings, *J. Colloid Interface Sci.*, 60 (1977) 574.
10 J. J. Kirkland, L. E. Schallinger and W. W. Yau, *Anal. Chem.*, 57 (1985) 2271.
11 J. Janca, D. Pribylova, K. Bouchal, V. Tyrackova and E. Zurkova, *J. Liq. Chromatogr.*, 9 (1986) 2059.
12 J. C. Giddings and M. N. Myers, *Sep. Sci. Technol.*, 13 (1978) 637.
13 H. Small, *J. Colloid Interface Sci.*, 48 (1974) 147.
14 M. N. Myers and J. C. Giddings, *Anal. Chem.*, 54 (1982) 2284.
15 S. Lee and J. C. Giddings, *Anal. Chem.*, in press.
16 T. Koch and J. C. Giddings, *Anal. Chem.*, 58 (1986) 994.
17 J. C. Giddings, *Dynamics of Chromatography: Part I, Principles and Theory*, Dekker, New York, 1965.
18 J. C. Giddings, *Pure Appl. Chem.*, 51 (1979) 1459.
19 H. K. Jones, K. Phelan, M. N. Myers and J. C. Giddings, *J. Colloid Interface Sci.*, 120 (1987) 140.
20 J. C. Giddings, *Anal. Chem.*, 57 (1985) 945.
21 S. Ratanathanawongs, private communication.
22 G. Karaiskakis, M. N. Myers, K. D. Caldwell and J. C. Giddings, *Anal. Chem.*, 53 (1981) 1314.
23 K. D. Caldwell, T. T. Nguyen, M. N. Myers and J. C. Giddings, *Sep. Sci. Technol.*, 14 (1979) 935.

Journal of Chromatography, 455 (1988) 17-27
Elsevier Science Publishers B.V., Amsterdam — Printed in The Netherlands

CHROM. 20 861

CONSECUTIVE GRADIENTS IN CHROMATOGRAPHY

GRADIENTS UNDER SUB- AND SUPERCRITICAL CONDITIONS INCLUDING COMPOSITION GRADIENTS AND MULTIPLE GRADIENTS

BERND GEMMEL, FRANZ P. SCHMITZ and ERNST KLESPER*
Lehrstuhl für Makromolekulare Chemie, RWTH Aachen, Worringerweg, D-5100 Aachen (F.R.G.)
(Received July 26th, 1988)

SUMMARY

Supercritical-fluid chromatography offers the possibility of using gradients of pressure, temperature or eluent composition, which allows the "tuning" of the chromatographic conditions to a specific separation. The gradients may be combined by using them either simultaneously or consecutively. Starting from the subcritical gaseous region, separations are presented in which two simultaneous and several consecutive gradients of the three individual gradient types have been combined. Thereby, the influence of the absolute levels and of the ramps of pressure, temperature and composition on the chromatographic performance is demonstrated. Possibilities for increasing or decreasing the speed of the chromatographic separations and increasing the resolution are demonstrated.

INTRODUCTION

In addition to the well established techniques of gas chromatography (GC) and liquid chromatography (LC), supercritical-fluid chromotagraphy (SFC) is being increasingly used as an alternative approach. By definition, a supercritical fluid used as the mobile phase in SFC is a medium that is above its critical temperature, T_c, and above its critical pressure, p_c, *i.e.*, which is a dense gas. The properties of such dense gases are intermediate between those of gases and liquids. Depending on the applied temperature and pressure, the behaviour can be more gas-like or more liquid-like.

The intermediate position of dense gases gives rise to a variety of gradient techniques that are useful for SFC. Similarly to GC, gradients of increasing temperature at, *e.g.*, constant density or pressure are applicable for enhancing solute transport through the separation column. Similarly to LC, gradients of eluent composition can be applied[1]. A unique property of SFC is that the density of the mobile phase and thereby its elution strength can be increased by means of a pressure gradient or by decreasing the temperature by a temperature gradient at constant pressure[2].

The sign (positive or negative) of the temperature gradient at constant pressure to be employed in SFC depends to some extent on the transport mechanism of the

0021-9673/88/$03.50 © 1988 Elsevier Science Publishers B.V.

analyte[3,4]. For instance, for analytes that have a high vapour pressure under vacuum, a positive temperature programme in the supercritical-fluid region will probably be more effective for elution than for analytes whose transport depends solely on solvation, given comparable solvation of the analytes by the dense gas. Moreover, multiple simultaneous gradients have been found to be useful for effecting high-resolution separations[1–3,5–9].

The intermediate position of SFC between GC and LC may be shown if a separation is started in the subcritical gaseous region and terminated under subcritical liquid conditions[10], as has been demonstrated by "circling" the critical point of the mobile phase under isocratic conditions by use of consecutive temperature and pressure programmes[11–13]. The interconnection between GC, SFC and LC was elaborated upon further in this study by using a series of consecutive gradients including composition gradients. In addition, the usefulness of combining consecutive and simultaneous gradients is demonstrated. Thereby, emphasis is placed on general features rather than on the optimal compromise between analysis time and resolution.

EXPERIMENTAL

The chromatographic equipment consisted of a Model 1084 B high-performance liquid chromatograph from Hewlett-Packard (Waldbronn, F.R.G.) modified for use in SFC as described previously[14], a Fractovap 4200 GC oven from Carlo Erba (Hofheim/Ts., F.R.G.) and a Tescom 26-3220-24-004 back-pressure valve from WSM (Eching, F.R.G.).

Temperature gradients were obtained using a Carlo Erba LT 430 temperature programmer. Pressure gradients were obtained by closing continuously the back-pressure valve. Gradients of eluent composition were programmed by means of the flow control device of the 1084 B instrument. The feed rate of the pumps was always 1 ml/min (liquid). UV detection was performed at 254 nm.

The stationary phase was LiChrosorb Si 100 (10μm), which was slurry packed into a stainless-steel column (25 cm × 4.5 mm I.D.) using a procedure described previously[10,15]. Before use the stationary phase was permanently modified by in-column treatment with 1,4-dioxane[15]. The mobile phase components (pentane and dioxane) were distilled and degassed before use.

The sample consisted of PS 800 polystyrene standard (from Pressure Chemical, distributed by Pfannenschmidt, Hamburg, F.R.G.) or an aromatic test mixture (naphthalene, anthracene, pyrene and chrysene) which was mixed with the PS 800. The sample solvent was hexane.

RESULTS

One advantage of SFC is the availability and usefulness of gradients of either pressure, temperature and eluent composition, which makes it possible to adjust precisely the chromatographic conditions to a given separation problem. Some of the possible combinations of the three gradients are discussed here.

In Fig. 1 a schematic outline of the first programme sequence is shown. It starts in the subcritical, low-pressure gaseous state with a temperature gradient (1), which leads to an end temperature above the critical temperature which is, however, still

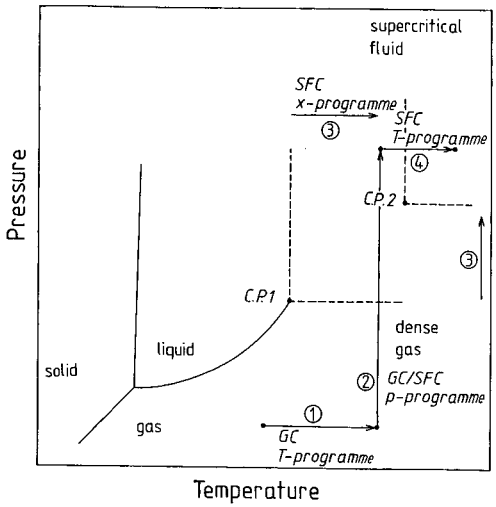

Fig. 1. Schematic representation of a sequence of consecutive gradients consisting of temperature, pressure and eluent composition gradients, the latter being superimposed by a simultaneous positive temperature gradient.

subcritical with respect to pressure. During this part of the programme sequence, elution is controlled predominantly by volatility, *i.e.*, by the vapour pressure of the analytes. Subsequently, a pressure gradient (2) is applied, leading to an end value above the critical pressure, *i.e.*, to the supercritical state. The increasing pressure causes an increase in mobile phase density, bringing about a more intense interaction between the mobile phase and the solutes and improved elution by way of solvation, a typical feature of SFC.

Finally, a composition gradient (*x* programme) (3) is applied after termination of the pressure gradient (2). By adding a component of higher solvating ability to the eluent, the retention is decreased owing to an increased interaction between the mobile phase and solute molecules, which depends on the chemical structure of the added component. The change in the mobile phase composition leads to a shift of the critical point of the mobile phase. This is indicated in Fig. 1 by the different positions of C.P. 1 (critical point for the initial mobile phase composition) and C.P. 2 (critical point for the mobile phase composition at the end of the composition programme). If the end temperature of programme 1 is below the critical temperature of the mobile phase at the end of the composition gradient (3), then the mobile phase will be a subcritical liquid at the end of the programme sequence. This effect is prevented, keeping the mobile phase in the supercritical state, if a temperature programme (4) is run simultaneously with the composition programme (3).

The separation of a polystyrene sample according to the gradient sequence in Fig. 1 is shown in Fig. 2. The pertinent chromatographic data are listed in Table I. Elution starts with a mobile phase of pentane–1,4-dioxane (95:5, v/v) at 10 bar and 190°C. The starting values were chosen as to achieve the elution of some of the low-molecular-weight oligomer species in the low-pressure gaseous state. During the first gradient, where the elution process is like that in GC, only the first two oligomers of the analyte mixture are eluted. Such a temperature gradient at a low pressure can

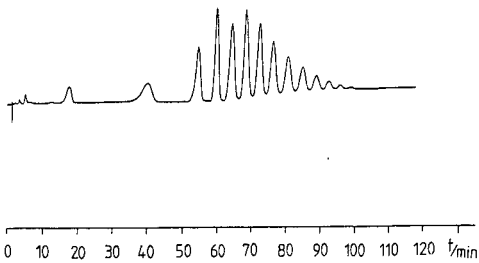

Fig. 2. Chromatographic separation according to the scheme in Fig. 1. Separation of PS 800. T_1 = 190–260°C; p = 10–70 bar; x = 5–60%. On the x programme is superimposed a temperature programme in two linear sections, T_2 = 260–290°C and T_3 = 290–300°C. For more detailed conditions see Table I and Experimental.

TABLE I

DATA FOR THE GRADIENTS UTILIZED TO OBTAIN THE CHROMATOGRAMS WITH PENTANE–1,4-DIOXANE AS THE MOBILE PHASE

T = Temperature (°C), either initial and final values or constant values; programming of T is linear with time. p = pressure at column exit (bar), either initial and final values or constant values; programming is linear. x = eluent composition. [% dioxane (v/v)], either initial and final values or constant values; programming is linear with respect to Q_B, where $Q_B = P_B/(1 - P_B)$ and P_B is the volume fraction of the mobile phase component B (1,4-dioxane). Hence the volume fraction itself is programmed non-linearly with time. t = time (min); all times are counted from the start of the chromatogram.

Chromatogram in Fig.	*T (°C)*	*p (bar)*	*x (% of second component)*	*t (min)*
2	190–260	10	5	0–30
	260	10–70	5	30–60
		70	5–60	60–140
	260–290	70		60–80
	290–300	70		80–140
4a	220–270	10–50	5	0–40
	270	50	5–60	40–120
4b	220–285	10–50	5	0–40
	285	50	5–60	40–120
4c	220–300	10–50	5	0–40
	300	50	5–60	40–120
6a	220–300	10–70	5	0–40
	300	70	5–60	40–120
6b	220–300	10–60	5	0–40
	300	60	5–60	40–120
6c	220–300	10–50	5	0–40
	300	50	5–60	40–120
8a	220–250	10–60	5	0–40
	250–300	60	5–60	40–120
8b	220–270	10–50	5	0–40
	270–300	50	5–60	40–120
9	180–260	10–60	5	0–40
		60	5–60	40–120
	260–290	60		40–60
	290–300	60		60–120

be of interest for the separation of samples that contain components with considerable vapour pressures, which are suitable for the GC mode.

During the subsequent pressure gradient (2), elution is greatly accelerated once a certain pressure level has been reached. If the chromatographic conditions are kept constant at the end of the pressure programme, exponentially increasing elution times would result for the remainder of the sample which has not yet been eluted, a typical feature of homologous series[16]. To compensate for this effect, a composition gradient (3) is applied subsequently. The temperature gradient (4) run in parallel with the composition gradient (3) keeps the mobile phase in the supercritical state despite the changing composition.

A different programme sequence is shown in Fig. 3. Here, the separation starts in the gaseous state at a temperature above the critical temperature of the eluent. A simultaneous (coupled) pressure–temperature (1) programme leads to the supercritical state. This yields a reasonably fast elution of the first components of the sample. Three different gradients, A, B, and C, are shown which all end at the same pressure but at different temperatures. The simultaneous p,T programmes are followed by a composition programme (2), in order to compensate for the increasing distances between the peaks of the higher members of the homologous series, this spreading occurring when the p,T programme has ended. During the composition programme a transition of the eluent from the supercritical to the subcritical gaseous state takes place for programmes B and C, whereas for programme A even a transition of the mobile phase from the gaseous to the liquid may occur. This is indicated when calculating the critical temperature of a pentane–1,4-dioxane mixture containing 60% (v/v) of dioxane[17].

The chromatograms corresponding to the scheme of gradients in Fig. 3 are shown in Fig. 4a–c. The numerical data for the gradients are given in Table I. Each of

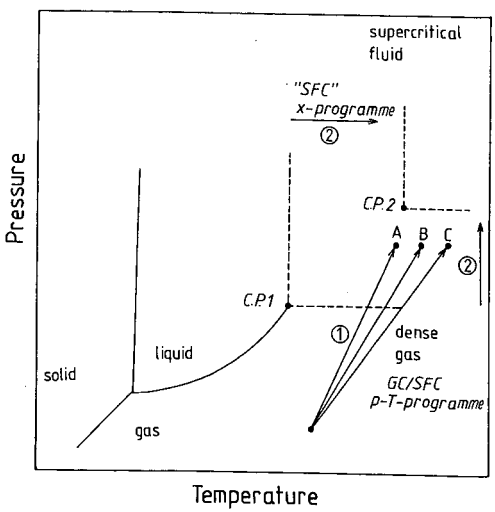

Fig. 3. Schematic representation of a sequence of gradients consisting of a simultaneous pressure–temperature programme (1) and a subsequent composition programme (2). Three gradient sequences have been run which differ in the end temperature of the simultaneous pressure–temperature programme A, B, and C.

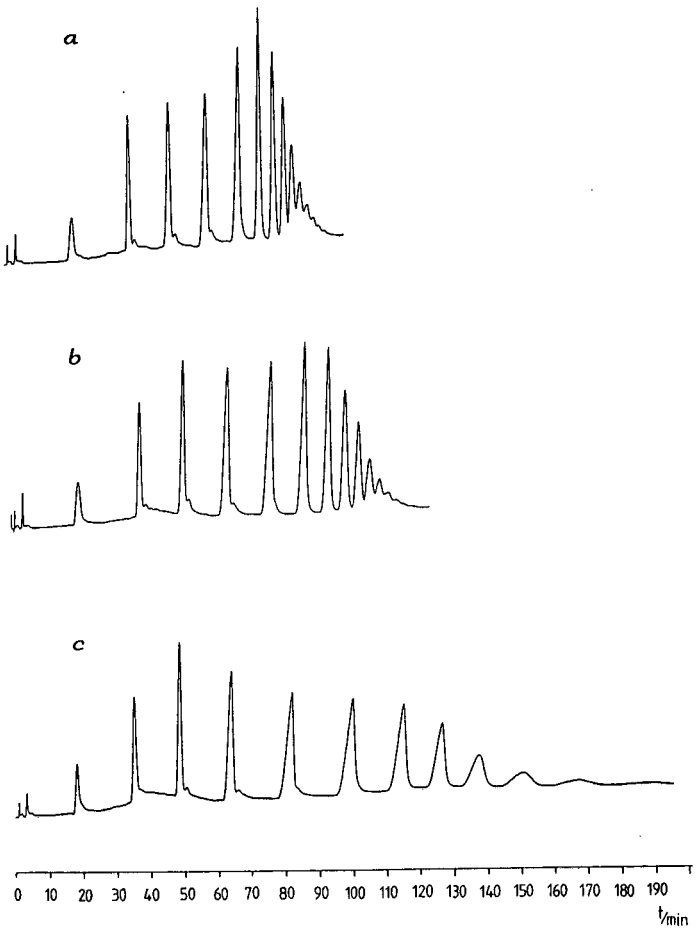

Fig. 4. Chromatographic separations according to the scheme in Fig. 3. Separation of PS 800. p = 10–50 bar; x = 5–60%. (a) T = 220–270°C; (b) T = 220–285°C; (c) T = 220–300°C. See Table I and Experimental.

the chromatograms follows the same pressure programme from 10 to 50 bar and the same composition programme from 5 to 60%. The ramp of the temperature gradients, however, increases from chromatogram a to c, ending at 270, 285 and 300°C, respectively, each starting at 220°C. During the simultaneous pressure–temperature gradients hardly any difference can be seen between the three chromatograms, three peaks appearing in each. The subsequent composition gradient speeds up the elution of the remaining less volatile and less soluble components. Because the same composition gradient has been used for the three p,T programmes, the effect of the end temperature of the p,T programme becomes obvious. Whereas at an end temperature of 270°C elution is very rapid and resolution is only moderate during the composition programme, elution is much retarded at 300°C and the resolution is improved. Comparing the number of peaks detectable in the three chromatograms, fifteen oligomeric species can be counted in Fig. 4a and b, whereas only twelve peaks and a much longer

analysis time are apparent in Fig. 4c. This retardation of elution at the higher temperature is due to the lower density of the mobile phase and, thereby, to the decreasing interaction between the analytes and the mobile phase. For chromatogram c, the interaction is even too weak to elute all components of the sample.

In the programme series in Figs. 3 and 4 it was the influence of temperature on the chromatographic separation that was discussed. In Fig. 5, a sequence of programmes is shown by means of which the effect of pressure can be demonstrated. Again the separation is started with a coupled pressure–temperature programme (1), this time ending at the same temperature but at three different end pressures (programmes A, B and C). After the end pressures have been reached, a composition gradient follows (2). For programmes A and B, the pressure and temperature are high enough to keep the eluent in the supercritical state during the whole range of the composition gradient. In C the conditions become subcritical during the composition gradient inasmuch as a pressure lower than the critical pressure leads to a subcritical dense gaseous state.

Fig. 6 shows the chromatograms corresponding to the scheme in Fig. 5. As seen in Table I, the temperature and composition programmes are the same for all three runs. The simultaneous pressure gradients, however, become steeper on going from c to a (Table I). The increased pressure ramp and level result in definite acceleration of elution going on from trace c to a. Whereas at the lowest pressure only twelve peaks are detected (c), there are fifteen peaks in the second chromatogram (b) and seventeen in the third (a). The steeper pressure gradient shows its influence at the beginning of the separation: the higher the pressure level, the faster is the elution of the first peaks. The subsequent composition gradient is matched well with the preceding p,T gradient in that the distances between the later peaks are kept approximately the same. For the composition gradient the effects of an increased pressure level are accelerated elution

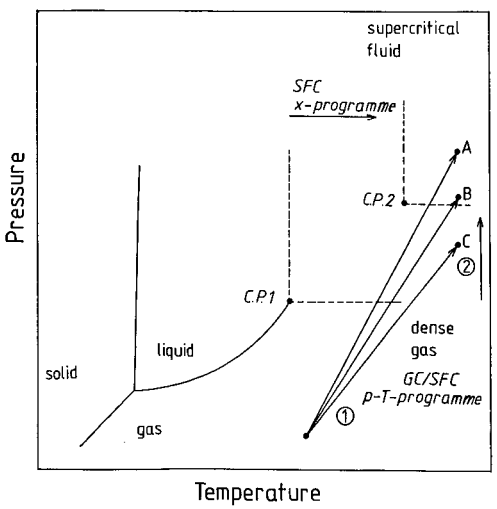

Fig. 5. Schematic representation of a sequence of gradients of simultaneous pressure–temperature programming (1) and subsequent composition programming (2) at different final pressures (A, B and C).

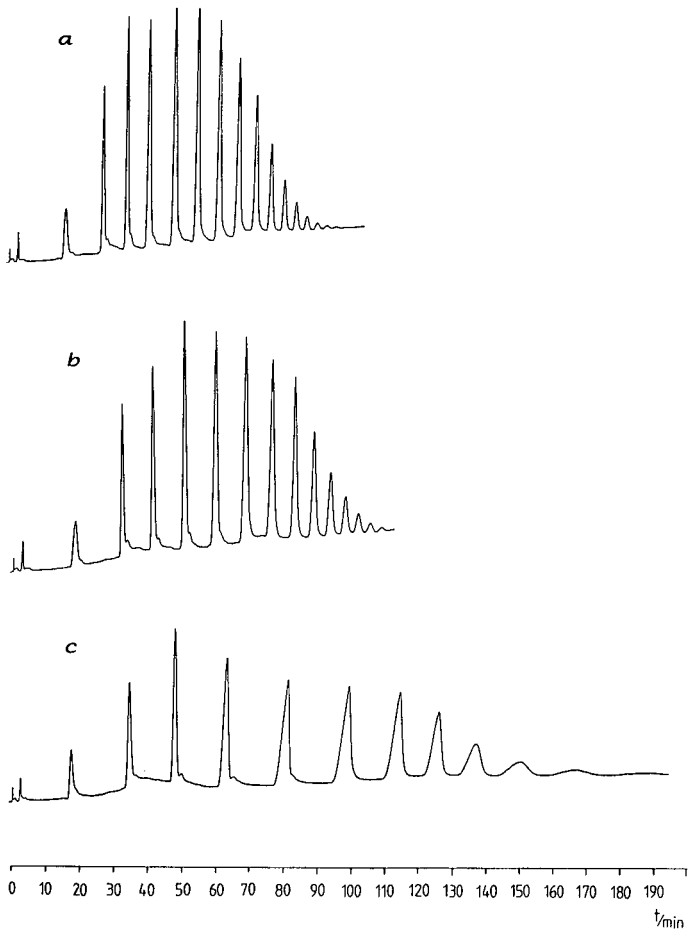

Fig. 6. Chromatographic separations according to the scheme in Fig. 5. Separation of PS 800. T = 220–300°C (a–c); x = 5–60% (a–c); p = (a) 10–70 bar, (b) 10–60 bar and (c) 10–50 bar. See Table I and Experimental.

and smaller peak widths. Hence, variation of the pressure level provides an effective means of optimizing the conditions for the composition gradient.

The scheme in Fig. 7 shows another possibility for working with coupled gradients. As in the two preceding series a pressure–temperature gradient is applied to proceed from the gaseous to the supercritical state, and then a composition gradient follows, the latter paralleled by a positive temperature gradient. The two programme sequences A and B can be regarded as a combination of the sequences shown in Figs. 1, 3 and 5. Combining the pressure and temperature gradients (p,T programme) corresponds to Figs. 3 and 5, and the final combination of a composition gradient with a temperature gradient (x,T programme) corresponds to Fig. 1. The two programme sequences shown in Fig. 7 differ in that for programme sequence A the mobile phase is supercritical during the entire x programme whereas a transition to

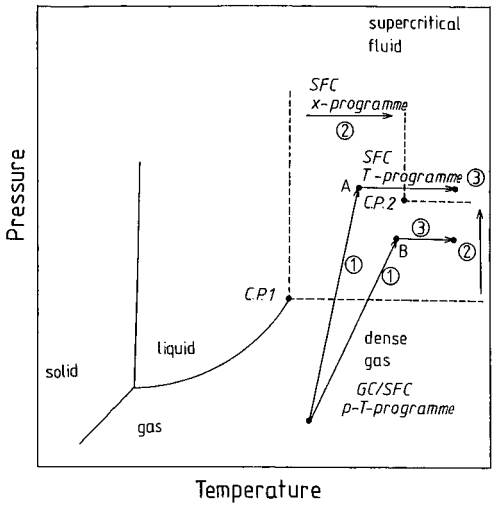

Fig. 7. Schematic representations of sequential programmes as in Figs. 3 and 5, except for combined composition (2)–temperature (3) programming.

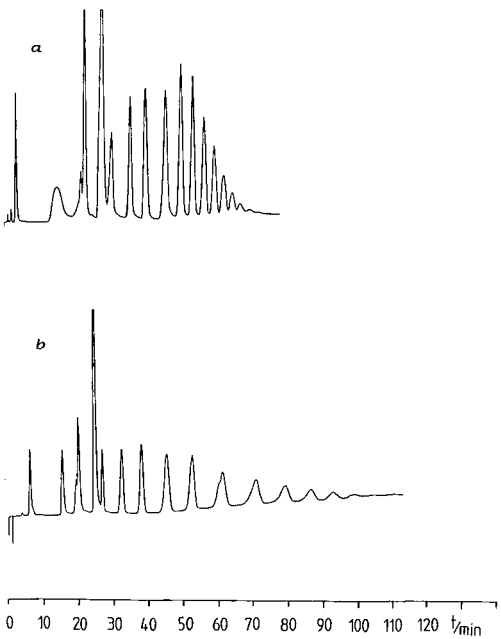

Fig. 8. Chromatographic separations according to the scheme in Fig. 7. (a) p = 10–60 bar, T_1 = 220–250°C, x = 5–60%, T_2 = 250–300°C; (b) p = 10–50 bar, T_1 = 220–270°C, x = 5–60%, T_2 = 270–300°C. Elution order: styrene oligomer with n = 1, naphthalene, anthracene, n = 2, pyrene, chrysene, n = 3 to n = 14. See Table I and Experimental.

the subcritical gaseous state occurs during the x programme in sequence B. The latter transition is due to the pressure being below p_c for part of the composition range of the binary mobile phase.

The chromatograms in Figs. 8 and 9, which were run according to the programming sequences in Fig. 7, show separations of a polystyrene sample to which a mixture of naphthalene, anthracene, pyrene and chrysene was added in order to give a larger number of volatile components in the sample. Fig. 8a shows a fast separation of the sample. As with the chromatogram in Fig. 8b, partial resolution of pyrene and the styrene oligomer species with $n = 2$ and also partial resolution of chrysene and the oligomer species with $n = 3$ are seen. Whereas fourteen oligomers can be detected in Fig. 8a, only twelve are resolved in Fig. 8b. The separation in Fig. 8b shows a significantly increased elution time in comparison with Fig. 8a, particularly in the second part of the chromatogram. This is caused by two effects acting in the same direction; the first is the lower pressure level compared with Fig. 8a, and the second is the more steeply ramped temperature gradient that takes the eluent more quickly to temperatures where lower density and slower elution prevail. During the whole separation the temperature level is higher in Fig. 8b than in Fig. 8a. The high temperature also brings about considerable peak broadening, the reason for which is not clear. Possibly isomeric species are partly separated, which makes the peaks look broader.

A similar effect of temperature is observed for the chromatograms in Figs. 6c and 8b. Compared with the chromatogram in Fig. 6, which was run with the same pressure programme, the same composition programme and to the same end temperature, elution is faster in Fig. 8b. This is due to the slower temperature increase in Fig. 8b, so that during the whole separation, except at the very end of the programme sequence, a lower temperature prevails.

Fig. 9 demonstrates a variation of the chromatogram in Fig. 8a. With the p and the x programmes being the same, the separation in Fig. 9 was started at a lower temperature (1) and the temperature gradient (3) was subdivided into two steps, a faster and a slower one (*cf.*, Table I). Based on previously published data for pentane–dioxane[17,18], this temperature gradient, which runs simultaneously with the composition programme (2), was chosen so as to match conditions of high resolution. Such combined x–T gradients have been reported to yield improved resolution compared with isothermal composition gradients[3,6,19]. In fact, a higher resolution is obtained towards the end of the chromatogram. However, the analysis time is longer and the peaks are broader. The broadening of the peaks may again be partly due to isomer separation.

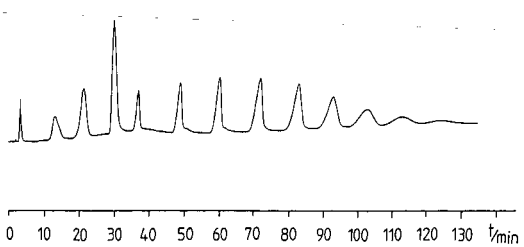

Fig. 9. Chromatographic separation according to the scheme in Fig. 7. p = 10–60 bar; T_1 = 180–260°C; x = 5–60%; T_2 = 260–290°C; T_3 = 290–300°C. See Table I and Experimental.

CONCLUSION

Chromatographic separations that utilize the p–T–x properties of supercritical fluids offer unique possibilities, *e.g.*, the option of applying gradients of pressure, temperature and eluent composition. As demonstrated here, SFC can be used as a link to either GC or LC, enabling the chromatographer both to extend and to interconnect the three techniques.

Consecutive and/or simultaneous gradients can be of value in order to "tune" chromatographic conditions to a given analytical problem. If a separation starts under subcritical gaseous conditions, volatile components of a given sample can be separated under high-resolution, GC-like conditions, followed by separation of the remainder of the sample with increasing temperature and pressure until supercritical conditions are reached. Thereby the temperature does not have to be raised as high as in high-temperature GC. Consecutively, composition gradients can be utilized to elute sample components of higher molar mass. The composition gradients may also be combined with simultaneous temperature gradients.

ACKNOWLEDGEMENT

Financial support by Arbeitsgemeinschaft Industrieller Forschungsvereinigungen (AIF) is gratefully acknowledged.

REFERENCES

1 F. P. Schmitz and E. Klesper, *J. Chromatogr.*, 388 (1987) 3.
2 E. Klesper and F. P. Schmitz, *J. Chromatogr.*, 402 (1987) 1.
3 F. P. Schmitz, D. Leyendecker, D. Leyendecker and B. Gemmel, *J. Chromatogr.*, 395 (1987) 111.
4 T. L. Chester and D. P. Innis, *J. High Resolut. Chromatogr. Chromatogr. Commun.*, 8 (1985) 561.
5 E. Klesper and W. Hartmann, *Eur. Polym. J.*, 14 (1978) 77.
6 D. Leyendecker, D. Leyendecker, F. P. Schmitz and E. Klesper, *J. High Resolut. Chromatogr. Chromatogr. Commun.*, 9 (1986) 525.
7 D. W. Later, E. R. Campbell and B. E. Richter, *J. High Resolut. Chromatogr. Chromatogr. Commun.*, 11 (1988) 65.
8 W. Gmür, J. O. Bosset and E. Plattner, *J. Chromatogr.*, 388 (1987) 335.
9 W. Gmür, J. O. Bosset and E. Plattner, *Mitt. Geb. Lebensmittelunters. Hyg.*, 78 (1987) 21.
10 F. P. Schmitz, H. Hilgers, B. Lorenschat and E. Klesper, *J. Chromatogr.*, 346 (1985) 69.
11 B. Gemmel, F. P. Schmitz and E. Klesper, *J. High Resolut. Chromatogr. Chromatogr. Commun.*, in press.
12 E. Klesper, *paper presented at the 29th Rocky Mountain Conference, Denver, CO, August 3rd, 1987.*
13 E. Klesper, *paper presented at the Supercritical Fluid Chromatography Symposium–87, Pittsburgh, PA, October 1st, 1987.*
14 F. P. Schmitz, H. Hilgers and E. Klesper, *J. Chromatogr.*, 267 (1983) 267.
15 F. P. Schmitz, D. Leyendecker and D. Leyendecker, *J. Chromatogr.*, 389 (1987) 245.
16 G. Glöckner, *Polymer Characterization by Liquid Chromatography (Journal of Chromatography Library*, Vol. 34), Elsevier, Amsterdam, 1987, pp. 310 and 311.
17 D. Leyendecker, D. Leyendecker, F. P. Schmitz and E. Klesper, *J. Chromatogr.*, 392 (1987) 101.
18 D. Leyendecker, F. P. Schmitz, D. Leyendecker and E. Klesper, *J. Chromatogr.*, 393 (1987) 155.
19 F. P. Schmitz and B. Gemmel, in M. Yoshioka, S. Parvez, T. Miyazaki and H. Parvez (Editors), *Progress in HPLC, Vol. 4, Supercritical Fluid Chromatography and Micro-HPLC*, VSP, Zeist, in press.

Journal of Chromatography, 455 (1988) 29–43
Elsevier Science Publishers B.V., Amsterdam — Printed in The Netherlands

CHROM. 20 834

RETENTION BEHAVIOUR OF POLYCYCLIC AROMATIC HYDROCARBONS IN SUPERCRITICAL FLUID CHROMATOGRAPHY ON VARIOUS CHEMICALLY BONDED STATIONARY PHASES WITH CARBON DIOXIDE AS A MOBILE PHASE

KIYOKATSU JINNO* and SAKAE NIIMI
School of Materials Science, Toyohashi University of Technology, Toyohashi 440 (Japan)
(First received June 15th, 1988; revised manuscript received July 13th, 1988)

SUMMARY

The retention behaviours of polycyclic aromatic hydrocarbons in supercritical fluid chromatography have been studied on various chemically bonded stationary phases with carbon dioxide as the mobile phase. The solute retention is mainly controlled by its molecular size as in liquid chromatography and its dipole moment also determines the elution order on silica and non-endcapped octadecylsilica phases. Phenyl bonded phases such as diphenyl and naphthylethyl show intermediate characters between silica and well covered octadecylsilicas.

INTRODUCTION

In recent years, the dependence of solute retention on column temperature and pressure in supercritical fluid chromatography (SFC) has been investigated by many researchers[1–8]. Schmitz *et al.*[9–11] reported the influence of the physical state of fluids on the retention and resolution of polycyclic aromatic hydrocarbons (PAHs) in SFC. We have also reported the retention characteristics of PAHs in SFC with carbon dioxide as the mobile phase and octadecylsilica as the stationary phase[12,13]. However, it is considered a big advantage of packed column SFC that a number of different types of stationary phases are available for liquid chromatography (LC) and one can use those stationary phases as the column materials.

In this communication, we report the retention behaviours of PAHs in packed column SFC using carbon dioxide as the mobile phase and different types of chemically bonded phases as the stationary phase, at changing mobile phase density and temperature.

EXPERIMENTAL

A Model BIP-I HPLC pump (Jasco, Tokyo, Japan) was used. The pump head was cooled by circulating cold methanol to deliver a fluid as the mobile phase to the analytical column. A Jasco Multi-320 UV photodiode array multichannel detector

0021-9673/88/$03.50 © 1988 Elsevier Science Publishers B.V.

TABLE I
STATIONARY PHASES USED

Index	*Column name*	*Particle diameter (μm)*	*Bonded phase*	*Size (mm)*
Sil	Jasco Finepack Sil	5	Silica	250 × 4.6 I.D.
P-ODS	Brownlee ODS-224	5	Polymeric C_{18}	220 × 4.6 I.D.
M-ODS	Brownlee OD-224	5	Monomeric C_{18}	220 × 4.6 I.D.
C_{18}	Jasco Finepack Sil C_{18}	5	Low polymeric (?)**	250 × 4.6 I.D.
Cap	Shiseido Capcell Pak C_{18}	5	Monomeric C_{18} bonded on silicone polymer	250 × 4.6 I.D.
Diol	Shimadzu Simpak Diol	5	Diol	150 × 4.6 I.D.*
DP	Supelco Sil LC-DP	5	Diphenyl	250 × 4.6 I.D.
NE	Naphthylethyl	5	Naphthylethyl	150 × 4.6 I.D.*

* Laboratory-packed.
** No endcapping.

with a detection cell that can withstand pressures up to 350 kg/cm^2 was used. It was controlled by a NEC PC-9801 VX 16-bit microcomputer (Nippon Electric, Tokyo, Japan). The column temperature was also controlled by the Jasco TU-100 system which was equipped with a manual backpressure regulator to control the column outlet pressure. The chromatographic columns used are summarized in Table I. P-ODS is polymeric ODS (octadecylsilica) and M-ODS is monomeric with endcapping. C_{18} is low polymeric without endcapping, and Cap is an unique ODS which has been bonded on silicone polymer coated on the base silica[14,15]. NE is a naphthylethyl bonded phase donated by N. Tanaka[16], Kyoto Institute of Technology, Kyoto, Japan. DP is a diphenyl bonded phase. Carbon dioxide was used as the mobile phase, at a flow-rate of 1 ml/min. It was pressurized by the pumping system between 100 and 300 kg/cm^2. The PAHs used as the sample probe are

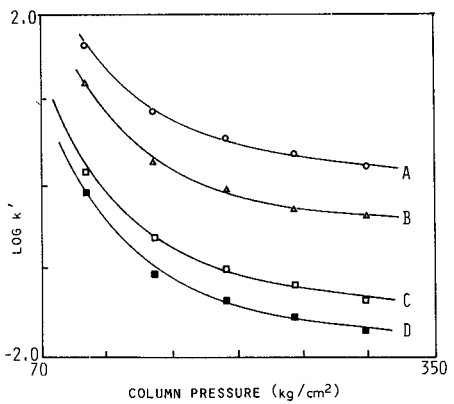

Fig. 1. Relationships between log k' of chrysene and column pressure on various stationary phases at 40°C: (A) P-ODS; (B) M-ODS; (C) Sil; (D) NE.

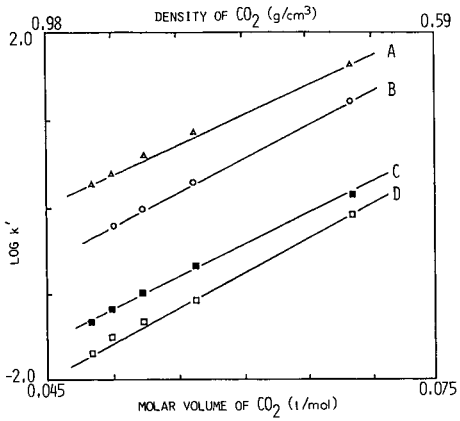

Fig. 2. Relationships between log k' of chrysene and the molar volume of carbon dioxide on various stationary phases at 40°C. Key as in Fig. 1.

commercially available. They were dissolved in dichloromethane which was used as the t_0 probe for capacity factor, k', calculations.

RESULTS AND DISCUSSION

The measured capacity factors of PAHs are summarized in Table II–IX. The retention is strongly dependent on the pressure and temperature of carbon dioxide. Chrysene was selected to demonstrate typical retention behaviours in SFC.

Fig. 1 shows the effect of column pressure on the retention at 40°C. It is apparent that increasing pressure decreases the retention, especially at lower pressures. This trend is the same as in Fig. 2, where the effect of the molar volume of carbon dioxide on the retention with various stationary phases is demonstrated. On increasing the molar

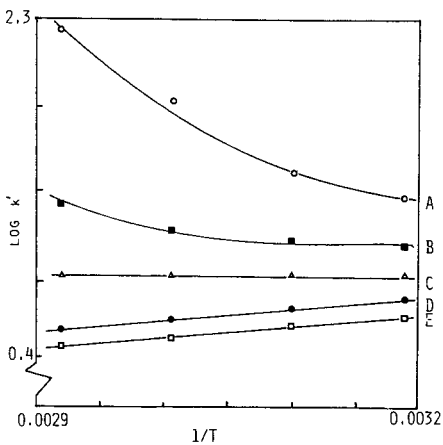

Fig. 3. Relationships between log k' of chrysene and the reciprocal column temperature ($1/T$) on the Cap column. Pressures (kg/cm²): (A) 100; (B) 150; (C) 200; (D) 250; (E) 300.

TABLE II
RETENTION DATA ON THE Sil COLUMN

Compound (PAH)	*P = 100* kg/cm²*	*P = 150 kg/cm²*				*P = 200 kg/cm²*			
	40°C	*40°C*	*50°C*	*60°C*	*70°C*	*40°C*	*50°C*	*60°C*	*70°C*
Naphthalene	1.022	0.512	0.604	0.814	1.176	0.366	0.399	0.464	0.565
Acenaphthylene	2.028	0.992	1.200	1.649	2.419	0.702	0.772	0.901	1.106
Acenaphthene	1.881	0.905	1.099	1.524	2.248	0.625	0.702	0.819	1.012
Fluorene	2.769	1.295	1.604	2.239	3.341	0.888	1.005	1.174	1.449
Phenanthrene	3.405	1.532	1.942	2.789	4.296	1.041	1.176	1.405	1.775
Anthracene	3.167	1.410	1.807	2.623	4.072	0.947	1.089	1.311	1.664
Fluoranthene	5.239	2.245	2.901	4.288	6.800	1.485	1.690	2.064	2.626
Pyrene	5.172	2.205	2.868	4.260	6.781	1.460	1.669	2.049	2.616
Benz[*a*]anthracene	8.750	3.352	4.556	7.188	12.075	2.121	2.493	3.153	4.116
Chrysene	9.294	3.580	4.840	7.613	12.765	2.265	2.648	3.339	4.353

* The data for 50, 60 and 70°C at 100 kg/cm² were not measured because of unstable conditions.

TABLE III
RETENTION DATA ON THE P-ODS COLUMN

Compound (PAH)	*P = 100* kg/cm²*	*P = 150 kg/cm²*				*P = 200 kg/cm²*			
	40°C	*40°C*	*50°C*	*60°C*	*70°C*	*40°C*	*50°C*	*60°C*	*70°C*
Naphthalene	1.872	0.996	1.150	1.327	1.779	0.775	0.805	0.851	0.898
Acenaphthylene	4.197	2.116	2.419	2.852	3.919	1.597	1.606	1.719	1.812
Acenaphthene	4.450	2.232	2.557	2.992	4.104	1.696	1.700	1.822	1.906
Fluorene	5.330	2.528	2.939	3.475	4.928	1.870	1.882	2.032	2.144
Phenanthrene	10.248	4.622	5.488	6.393	9.360	3.372	3.408	3.629	3.824
Anthracene	10.564	4.622	5.488	6.393	9.360	3.372	3.408	3.629	3.824
Fluoranthene	22.037	9.266	10.764	12.778	18.878	6.577	6.383	6.761	7.129
Pyrene	28.670	12.069	13.992	16.669	24.369	8.549	8.268	8.703	9.144
Benz[*a*]anthracene	53.197	20.189	23.390	29.097	44.239	13.652	12.909	13.546	14.344
Chrysene	60.986	23.210	26.622	33.027	49.919	15.636	14.672	15.278	16.090

* The data for 50, 60 and 70°C at 100 kg/cm² were not measured because of unstable conditions.

$P = 250\ kg/cm^2$				$P = 300\ kg/cm^2$			
40°C	*50°C*	*60°C*	*70°C*	*40°C*	*50°C*	*60°C*	*70°C*
0.300	0.301	0.338	0.385	0.260	0.248	0.274	0.303
0.573	0.578	0.657	0.739	0.490	0.477	0.535	0.572
0.506	0.523	0.590	0.668	0.426	0.426	0.469	0.513
0.710	0.744	0.837	0.942	0.588	0.612	0.670	0.714
0.826	0.860	0.987	1.125	0.690	0.691	0.772	0.842
0.753	0.789	0.913	1.054	0.628	0.632	0.716	0.785
1.170	1.215	1.408	1.615	0.976	0.960	1.081	1.182
1.150	1.198	1.392	1.610	0.964	0.946	1.070	1.180
1.616	1.736	2.042	2.390	1.302	1.337	1.525	1.685
1.730	1.843	2.168	2.530	1.402	1.418	1.612	1.783

$P = 250\ kg/cm^2$				$P = 300\ kg/cm^2$			
40°C	*50°C*	*60°C*	*70°C*	*40°C*	*50°C*	*60°C*	*70°C*
0.678	0.672	0.654	0.671	0.648	0.591	0.565	0.548
1.288	1.300	1.272	1.293	1.224	1.129	1.065	1.025
1.381	1.382	1.339	1.357	1.324	1.209	1.133	1.082
1.553	1.505	1.464	1.491	1.415	1.291	1.216	1.158
2.825	2.672	2.564	2.572	2.517	2.266	2.095	1.959
2.825	2.672	2.564	2.572	2.517	2.266	2.095	1.959
5.394	4.896	4.629	4.615	4.648	4.074	3.725	3.437
6.994	6.315	5.951	5.933	6.017	5.249	4.793	4.399
10.853	9.517	8.826	8.777	9.098	7.717	6.935	6.244
12.459	10.817	9.927	9.844	10.422	8.757	7.811	6.994

TABLE IV
RETENTION DATA ON THE M-ODS COLUMN

Compound (PAH)	*P = 100* kg/cm²*	*P = 150 kg/cm²*				*P = 200 kg/cm²*			
	40°C	*40°C*	*50°C*	*60°C*	*70°C*	*40°C*	*50°C*	*60°C*	*70°C*
Naphthalene	1.647	0.605	0.971	1.249	1.564	0.437	0.701	0.747	0.857
Acenaphthylene	3.480	1.347	1.871	2.466	3.167	0.973	1.292	1.398	1.624
Acenaphthene	3.887	1.510	2.062	2.704	3.449	1.100	1.432	1.536	1.760
Fluorene	4.430	1.675	2.265	3.040	3.978	1.157	1.516	1.650	1.926
Phenanthrene	7.891	2.868	3.787	5.154	6.802	2.046	2.461	2.682	3.132
Anthracene	7.891	2.868	3.787	5.154	6.802	2.046	2.461	2.682	3.132
Fluoranthene	13.765	5.379	6.871	9.490	12.740	3.743	4.279	4.664	5.461
Pyrene	19.330	6.778	8.562	11.794	15.744	4.747	5.325	5.772	6.729
Benz[*a*]anthracene	32.235	10.152	12.996	18.664	26.251	6.816	7.578	8.322	9.892
Chrysene	35.267	11.016	14.081	20.154	28.273	7.391	8.201	8.983	10.612

* The data for 50, 60 and 70°C at 100 kg/cm² were not measured because of unstable conditions.

TABLE V
RETENTION DATA ON THE C_{18} COLUMN

Compound (PAH)	*P = 100* kg/cm²*	*P = 150 kg/cm²*				*P = 200 kg/cm²*			
	40°C	*40°C*	*50°C*	*60°C*	*70°C*	*40°C*	*50°C*	*60°C*	*70°C*
Naphthalene	2.050	1.088	1.268	1.514	1.983	0.864	0.864	0.924	1.016
Acenaphthylene	4.241	2.105	2.545	3.117	4.220	1.604	1.636	1.777	1.992
Acenaphthene	4.451	2.210	2.661	3.226	4.325	1.690	1.720	1.841	2.047
Fluorene	5.541	2.589	3.208	4.028	5.579	1.949	1.998	2.207	2.479
Phenanthrene	8.493	3.768	4.732	5.983	8.508	2.751	2.861	3.144	3.581
Anthracene	8.241	3.768	4.732	5.983	8.508	2.751	2.861	3.144	3.581
Fluoranthene	15.527	6.555	8.370	10.916	15.958	4.658	4.811	5.434	6.251
Pyrene	17.804	7.669	9.545	12.458	18.220	5.329	5.488	6.215	7.120
Benz[*a*]anthracene	30.611	11.442	15.128	20.735	32.316	7.781	8.134	9.424	11.068
Chrysene	32. 776	12.280	16.201	22.170	34.396	8.302	8.694	10.056	11.770

* The data for 50, 60 and 70°C at 100 kg/cm² were not measured because of unstable conditions.

$P = 250\ kg/cm^2$				$P = 300\ kg/cm^2$			
40°C	*50°C*	*60°C*	*70°C*	*40°C*	*50°C*	*60°C*	*70°C*
0.373	0.581	0.600	0.610	0.343	0.506	0.556	0.491
0.803	1.047	1.077	1.123	0.731	0.902	1.041	0.879
0.935	1,171	1.187	1.209	0.820	1.003	1.130	0.952
0.950	1.209	1.239	1.281	0.855	1.027	1.160	0.985
1.634	1.932	1.974	2.041	1.456	1.620	1.748	1.548
1.634	1.932	1.974	2.041	1.456	1.620	1.748	1.548
2.910	3.286	3.323	3.425	2.569	2.719	2.814	2.545
3.677	4.068	4.097	4.202	3.240	3.372	3.438	3.127
5.100	5.587	5.629	5.842	4.406	4.522	4.550	4.203
5.552	6.030	6.074	6.387	4.760	4.869	4.873	4.491

$P = 250\ kg/cm^2$				$P = 300\ kg/cm^2$			
40°C	*50°C*	*60°C*	*70°C*	*40°C*	*50°C*	*60°C*	*70°C*
0.714	0.725	0.732	0.759	0.621	0.606	0.595	0.625
1.306	1.346	1.373	1.439	1.105	1.138	1.085	1.152
1.359	1.404	1.428	1.476	1.171	1.194	1.116	1.185
1.551	1.602	1.657	1.784	1.322	1.334	1.278	1.388
2.189	2.224	2.343	2.460	1.812	1.872	1.780	1.906
2.189	2.224	2.343	2.460	1.812	1.872	1.780	1.906
3.636	3.617	3.874	4.149	2.954	3.046	2.853	3.142
4.168	4.135	4.421	4.736	3.383	3.488	3.249	3.577
5.905	5.812	6.362	6.950	4.615	4.828	4.486	5.092
6.277	6.172	6.744	7.262	4.912	5.108	4.764	5.331

TABLE VI
RETENTION DATA ON THE Cap COLUMN

Compound (PAH)	*P = 100* kg/cm²*	*P = 150 kg/cm²*				*P = 200 kg/cm²*			
	40°C	*40°C*	*50°C*	*60°C*	*70°C*	*40°C*	*50°C*	*60°C*	*70°C*
Naphthalene	1.233	0.664	0.771	0.968	1.237	0.522	0.548	0.585	0.632
Acenaphthylene	2.476	1.225	1.458	1.881	2.452	0.941	0.991	1.064	1.164
Acenaphthene	2.789	1.396	1.643	2.105	3.724	1.078	1.120	1.195	1.295
Fluorene	3.036	1.433	1.737	2.288	3.039	1.081	1.144	1.243	1.368
Phenanthrene	5.374	2.403	2.946	3.912	5.254	1.775	1.871	2.038	2.237
Anthracene	5.473	2.403	2.946	3.912	5.254	1.775	1.871	2.038	2.237
Fluoranthene	10.273	4.248	5.266	7.021	10.053	3.031	3.192	3.479	3.830
Pyrene	13.258	5.440	6.717	8.842	12.208	3.872	4.039	4.374	4.784
Benz[*a*]anthracene	21.298	7.715	9.848	13.361	19.587	5.250	5.527	6.080	6.751
Chrysene	23.236	8.376	10.657	14.265	21.053	5.678	5.964	6.540	7.234

* The data for 50, 60 and 70°C at 100 kg/cm² were not measured because of unstable conditions.

TABLE VII
RETENTION DATA ON THE Diol COLUMN

Compound (PAH)	*P = 100* kg/cm²*	*P = 150 kg/cm²*				*P = 200 kg/cm²*			
	40°C	*40°C*	*50°C*	*60°C*	*70°C*	*40°C*	*50°C*	*60°C*	*70°C*
Naphthalene	0.945	0.436	0.532	0.689	1.000	0.325	0.349	0.403	0.473
Acenaphthylene	2.345	1.018	1.266	1.642	2.401	0.755	0.785	0.927	1.075
Acenaphthene	1.885	0.816	1.023	1.344	2.015	0.599	0.632	0.755	0.894
Fluorene	2.415	0.991	1.266	1.708	2.614	0.709	0.762	0.918	1.093
Phenanthrene	4.910	1.908	2.436	3.231	5.020	1.342	1.410	1.670	1.996
Anthracene	4.910	1.908	2.436	3.231	5.020	1.342	1.410	1.670	1.996
Fluoranthene	9.830	3.573	4.587	6.165	9.728	2.409	2.529	2.974	3.580
Pyrene	11.945	4.312	5.500	7.368	11.569	2.899	3.023	3.554	4.248
Benz[*a*]anthracene	19.870	6.330	8.394	11.750	19.510	4.021	4.268	5.137	6.314
Chrysene	22.480	7.151	9.431	13.118	21.644	4.540	4.778	5.721	6.991

* The data for 50, 60 and 70°C at 100 kg/cm² were not measured because of unstable conditions.

$P = 250\ kg/cm^2$				$P = 300\ kg/cm^2$			
40°C	*50°C*	*60°C*	*70°C*	*40°C*	*50°C*	*60°C*	*70°C*
0.453	0.454	0.463	0.488	0.405	0.406	0.393	0.398
0.792	0.795	0.827	0.862	0.701	0.702	0.677	0.691
0.898	0.904	0.934	0.970	0.807	0.800	0.767	0.780
0.909	0.904	0.943	0.994	0.788	0.792	0.767	0.783
1.447	1.448	1.513	1.578	1.261	1.245	1.208	1.226
1.447	1.448	1.513	1.578	1.261	1.245	1.208	1.226
2.436	2.413	2.502	2.596	2.090	2.034	1.975	1.991
3.099	3.038	3.125	3.240	2.655	2.562	2.483	2.481
4.082	3.997	4.140	4.338	3.424	3.301	3.185	3.208
4.412	4.306	4.448	4.644	3.698	3.551	3.421	3.430

$P = 250\ kg/cm^2$				$P = 300\ kg/cm^2$			
40°C	*50°C*	*60°C*	*70°C*	*40°C*	*50°C*	*60°C*	*70°C*
0.274	0.282	0.300	0.339	0.235	0.244	0.249	0.264
0.619	0.648	0.680	0.740	0.526	0.544	0.557	0.659
0.488	0.513	0.549	0.607	0.419	0.431	0.443	0.469
0.571	0.612	0.660	0.727	0.484	0.505	0.524	0.527
1.071	1.117	1.186	1.306	0.903	0.915	0.941	0.984
1.071	1.117	1.186	1.306	0.903	0.915	0.941	0.984
1.909	1.941	2.071	2.252	1.568	1.576	1.630	1.663
2.290	2.319	2.466	2.661	1.879	1.876	1.934	1.969
3.083	3.183	3.403	3.719	2.460	2.484	2.637	2.647
3.480	3.575	3.794	4.112	2.768	2.781	2.927	2.919

TABLE VIII
RETENTION DATA ON THE DP COLUMN

Compound (PAH)	*P = 100* kg/cm²*	*P = 150 kg/cm²*				*P = 200 kg/cm²*			
	40°C	*40°C*	*50°C*	*60°C*	*70°C*	*40°C*	*50°C*	*60°C*	*70°C*
Naphthalene	0.695	0.354	0.404	0.510	0.738	0.270	0.278	0.314	0.366
Acenaphthylene	1.329	0.625	0.745	0.949	1.415	0.472	0.500	0.551	0.660
Acenaphthene	1.352	0.634	0.752	0.965	1.433	0.482	0.511	0.562	0.670
Fluorene	1.601	0.717	0.866	1.122	1.734	0.533	0.571	0.636	0.767
Phenanthrene	2.456	1.041	1.271	1.676	2.634	0.760	0.818	0.935	1.113
Anthracene	2.456	1.041	1.271	1.676	2.635	0.760	0.818	0.935	1.113
Fluoranthene	4.020	1.578	1.952	2.673	4.277	1.125	1.213	1.418	1.693
Pyrene	4.537	1.767	2.210	2.974	4.762	1.260	1.358	1.579	1.887
Benz[*a*]anthracene	7.570	2.546	3.258	4.593	7.851	1.742	1.909	2.271	2.760
Chrysene	8.003	2.690	3.436	4.836	8.277	1.839	2.008	2.404	2.909

* The data for 50, 60 and 70°C at 100 kg/cm² were not measured because of unstable conditions.

TABLE IX
RETENTION DATA ON THE NE COLUMN

Compound (PAH)	*P = 100* kg/cm²*	*P = 150 kg/cm²*				*P = 200 kg/cm²*			
	40°C	*40°C*	*50°C*	*60°C*	*70°C*	*40°C*	*50°C*	*60°C*	*70°C*
Naphthalene	0.390	0.173	0.228	0.305	0.460	0.128	0.150	0.169	0.197
Acenaphthylene	0.814	0.327	0.435	0.593	0.928	0.249	0.270	0.310	0.373
Acenaphthene	0.915	0.354	0.482	0.661	1.033	0.268	0.301	0.343	0.399
Fluorene	1.113	0.425	0.575	0.785	1.270	0.315	0.350	0.408	0.477
Phenanthrene	1.825	0.655	0.886	1.237	2.040	0.482	0.531	0.610	0.725
Anthracene	1.876	0.655	0.886	1.237	2.105	0.482	0.531	0.610	0.725
Fluoranthene	3.260	1.075	1.456	2.102	3.612	0.763	0.850	0.991	1.186
Pyrene	3.712	1.217	1.653	2.378	4.112	0.856	0.951	1.113	1.337
Benz[*a*]anthracene	6.740	1.951	2.731	4.040	7.408	1.335	1.482	1.746	2.130
Chrysene	7.186	2.071	2.881	4.277	7.816	1.412	1.562	1.840	2.238

* The data for 50, 60 and 70°C at 100 kg/cm² were not measured because of unstable conditons.

$P = 250\ kg/cm^2$				$P = 300\ kg/cm^2$			
40°C	*50°C*	*60°C*	*70°C*	*40°C*	*50°C*	*60°C*	*70°C*
0.226	0.230	0.244	0.271	0.206	0.202	0.208	0.216
0.392	0.402	0.416	0.472	0.354	0.347	0.360	0.372
0.401	0.410	0.420	0.475	0.363	0.354	0.365	0.375
0.439	0.449	0.467	0.539	0.390	0.385	0.402	0.414
0.620	0.642	0.658	0.764	0.546	0.542	0.565	0.583
0.620	0.642	0.658	0.764	0.546	0.542	0.565	0.583
0.910	0.943	0.958	1.128	0.785	0.782	0.822	0.847
1.021	1.052	1.066	1.257	0.875	0.874	0.918	0.942
1.377	1.433	1.457	1.755	1.161	1.162	1.232	1.266
1.446	1.509	1.531	1.848	1.222	1.221	1.295	1.335

$P = 250\ kg/cm^2$				$P = 300\ kg/cm^2$			
40°C	*50°C*	*60°C*	*70°C*	*40°C*	*50°C*	*60°C*	*70°C*
0.106	0.118	0.126	0.140	0.097	0.100	0.100	0.104
0.198	0.220	0.230	0.252	0.181	0.178	0.188	0.193
0.223	0.240	0.247	0.270	0.195	0.199	0.200	0.209
0.253	0.276	0.293	0.320	0.225	0.221	0.235	0.241
0.388	0.415	0.431	0.473	0.329	0.331	0.342	0.357
0.388	0.415	0.431	0.473	0.329	0.331	0.342	0.357
0.615	0.646	0.690	0.743	0.513	0.523	0.538	0.554
0.689	0.724	0.778	0.838	0.574	0.580	0.600	0.622
1.040	1.102	1.192	1.270	0.859	0.858	0.892	0.924
1.099	1.154	1.251	1.329	0.903	0.897	0.931	0.964

TABLE X
ELUTION ORDER OF ACENAPHTHENE–FLUORENE AND ACENAPHTHYLENE WITH VARIOUS COLUMNS UNDER VARIOUS SFC CONDITIONS

Column	*Elution order*
Sil	Acenaphthene, acenaphthylene, fluorene
P-ODS	Acenaphthylene, acenaphthene, fluorene
M-ODS	Acenaphthylene, acenaphthene, fluorene
Cap	Acenaphthylene, acenaphthene, fluorene
C_{18}	Acenaphthylene, acenaphthene, fluorene
DP	Acenaphthylene, acenaphthene, fluorene
NE	Acenaphthylene, acenaphthene, fluorene

volume, the retention increases linearly. This means that density is the important factor in the retention, as is generally the case in SFC.

In Fig. 3, Van 't Hoff plots are shown for chrysene. As is typical in SFC, at lower pressures the retention increases with increasing temperature but at higher pressures the opposite occurs.

The retention mechanism for PAHs in SFC is dependent on the following situations:

(1) isothermal situation: the retention is dependent on the change in density of the mobile phase, increasing density leading to decreased retention

(2) isobaric situation: the retention is dependent on the pressure of the mobile phase, at lower pressures, increasing temperature, *viz.*, decreasing density results in increased retention, *ie.*, the retention is controlled by the solute solubility. At higher pressures, increasing temperature results in decreased retention, *i.e.*, the retention is controlled by the volatility of the solute.

The details of the retention behaviours of PAHs were evaluated from the data summarized in Tables II–IX. Roughly, the solute elution is controlled by its size. However, the elution orders sometimes changed depending on the conditions and the separation systems. The typical solute groups which showed changes in the elution order depending on the separation conditions are acenaphthene–acenaphthylene–

TABLE XI
ELUTION ORDER OF THREE PAHs ON THE Diol COLUMN UNDER VARIOUS SFC CONDITIONS
A = Acenaphthene, fluorene, acenaphthylene; C = acenaphtene, acenaphthylene, fluorene; E = acenapthene–fluorene, acenaphthylene.

P (kg/cm²)	*T (°C)*			
	40	*50*	*60*	*70*
100	C	–	–	–
150	A	E	C	C
200	A	A	A	C
250	A	A	A	A
300	A	A	A	A

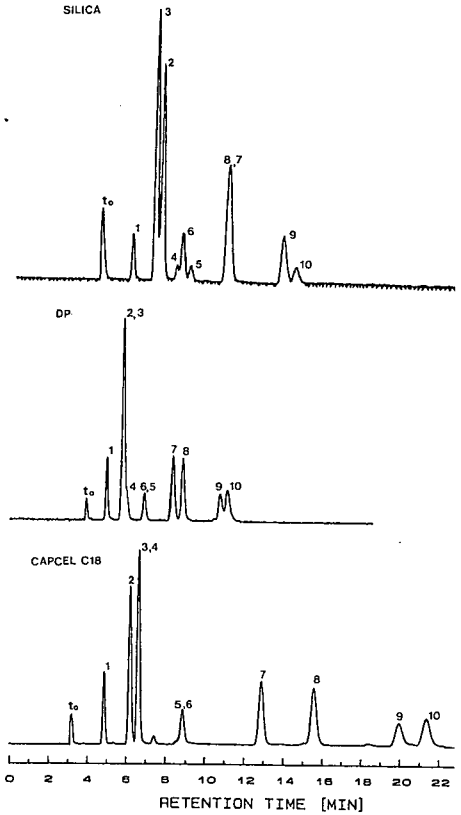

Fig. 4. SFC chromatograms of ten PAHs at 200 kg/cm^2 and 40°C with UV detection at 225 nm. Peak: 1 = naphthalene; 2 = acenaphthylene; 3 = acenaphthene; 4 = fluorene; 5 = phenanthrene; 6 = anthracene; 7 = fluoranthene; 8 = pyrene; 9 = benz[*a*]anthracene; 10 = chrysene.

TABLE XII
VALUES OF THE MOLECULAR POLARIZABILITY AND DIPOLE MOMENT OF PAHs

Compound	*Polarizability*	*Dipole moment, D*
Naphthalene	17.48	0.003
Acenaphthylene	22.34*	0.258
Acenaphthene	20.61	0.084
Fluorene	21.69	0.099
Anthracene	25.93	0.005
Phenanthrene	24.70	0.038
Fluoranthene	28.35	0.210
Pyrene	29.34	0.028
Benz[*a*]anthracene	32.86	0.062
Chrysene	33.06	0.004

* Calculated.

TABLE XIII

RELATIONSHIPS BETWEEN k', POLARIZABILITY AND DIPOLE MOMENT ON VARIOUS PHASES

$\log k' = a\,\alpha + b\,\mu^2 + c$ where α is the molecular polarizability and μ is the dipole moment.

Column	*a*	*b*	*c*	*Correlation coefficient (r^2)*
Sil	0.050	12.589	−1.226	0.984
C_{18}	0.061	8.982	−1.125	0.993
NE	0.061	7.738	−1.892	0.994
DP	0.052	6.000	−1.423	0.993
P-ODS	0.073	3.734	−1.450	0.993
M-ODS	0.064	5.051	−1.351	0.990
Cap	0.061	4.912	−1.353	0.987

fluorene, phenanthrene–anthracene and fluoranthene–pyrene. Table X shows those elution orders on various stationary phases except Diol under SFC conditions. On Sil, the elution orders of several PAHs as mentioned above are different from those on other ODS phases. An interesting case is found on the Diol column as shown in Table XI. The elution order of fluorene and acenaphthylene changes between the molar volumes of 0.0607 and 0.665 l/mol. These elution order changes were also found in LC separations[17].

In Fig. 4, typical separations are demonstrated on Sil, DP and Cap columns. The elution order differences are clearly seen for three groups of PAHs. To explain this, the molecular polarizability and dipole moments of particular PAHs should be considered. In Table XII such values are summarized. The dipole moment of the PAHs can explain the elution orders on various stationary phases. On the Sil column, the solutes wich have relatively large dipole moments were eluted later than their counter solutes, *i.e.*, acenaphthylene, phenanthrene and fluoranthene. On C_{18} and DP, similar but weaker trends are seen for those solutes. Therefore, multiregression analysis has been performed for the data sets using molecular polarizability and dipole moments as the parameters[18]. The results are shown in Table XIII. The retention of PAHs with various phases in SFC can be explained by this treatment as shown in the table. On Sil, the contribution of the dipole moment to the retenton is very large, and also on C_{18} which has not been endcapped the contribution of the dipole moment is also larger than on other phases. Therefore, the behaviour can be explained by the interaction of the solute with remaining silanol groups on the stationary phase surface. On NE and DP, resonance structures of the bonded phases influence the dipole–dipole interaction. On Cap, P-ODS and M-ODS, the reason why the contribution of dipole moments to the retention is small can be explained by the small number of residual silanol groups.

In conclusion, the retention of PAHs on various chemically bonded phases in carbon dioxide SFC can be controlled mainly by their sizes and dipole moments under fixed conditions; also their solublity and volatility contribute to the overall retention at various pressures and temperatures.

ACKNOWLEDGEMENTS

The authors thank M. Kuwajima for his assistance during this work. This work has been partially supported by a Grant-in-Aid for special project (Grant No. 62217010) from the Ministry of Education of Japan.

REFERENCES

1 M. Novotný, W. Bertsch and A. Zlatkis, *J. Chromatogr.*, 61 (1971) 17.
2 T. H. Couw and R. E. Jentoft, *J. Chromatogr.*, 68 (1972) 303.
3 U. Wassen and G. M. Schneider, *Chromatographia*, 8 (1975) 274.
4 J. E. Conaway, J. A. Graham and L. B. Rogers, *J. Chromatogr. Sci.*, 16 (1978) 102.
5 D. R. Gere, R. Board and D. McManigill, *Anal. Chem.*, 54 (1982) 736.
6 T. L. Chester and D. P. Innis, *J. High Resolut. Chromatogr. Chromatogr. Commun.*, 8 (1985) 561.
7 P. Mourier, P. Sassiat, M. Caude and R. Rosset, *J. Chromatogr.*, 353 (1986) 61.
8 C. M. White and R. K. Houek, *J. High Resolut. Chromatogr. Chromatogr. Commun.*, 9 (1986) 4.
9 F. P. Schmitz, D. Leyendecker and E. Klesper, *Ber. Bunsenges. Phys. Chem.*, 88 (1984) 912.
10 D. Leyendecker, D. Leyendecker, F. P. Schmitz and E. Klesper, *J. Chromatogr.*, 371 (1986) 93.
11 D. Leyendecker, D. Leyendecker, F. R. Schmitz and E. Klesper, *J. High Resolut. Chromatogr. Chromatogr. Commun.*, 9 (1986) 566.
12 K. Jinno, M. Saito, T. Hondo and M. Senda, *Chromatographia*, 21 (1986) 219.
13 K. Jinno and M. Kuwajima, *Chromatographia.*, 23 (1987) 629.
14 Y. Ohtsu, H. Fukui, T. Kanda, K. Nakamura, M. Nakano, O. Nakata and Y. Fujiyama, *Chromatographia*, 24 (1987) 380.
15 Y. Ohtsu, O. Shirota, T. Ogawa, I. Tanaka, T. Ohta, O. Nakata and Y. Fujiyama, *Chromatographia*, 24 (1987) 351.
16 N. Tanaka, Y. Tokuda, K. Iwakuchi and M. Araki, *J. Chromatogr.*, 239 (1983) 761.
17 H. Lamparczyk, M. Atomura and K. Jinno, *Chromatographia*, 23 (1987) 752.
18 R. Kaliszan, *The Quantitative Structure-Chromatographic Retention Relationships*, Wiley–Interscience, New York, 1987, pp. 176–190.

Journal of Chromatography, 455 (1988) 45–51
Elsevier Science Publishers B.V., Amsterdam — Printed in The Netherlands

CHROM. 20 890

DETERMINATION OF PARTITION COEFFICIENTS BY HEADSPACE GAS CHROMATOGRAPHY

WILLIAM J. JONES*, MARY JO EGOVILLE, EUGENE O. STROLLE* and EDWARD S. DELLAMONICA*

U.S. Department of Agriculture, ARS, Eastern Regional Research Center, 600 E. Mermaid Lane, Wyndmoor, PA 19118 (U.S.A.)

(First received October 12th, 1987; revised manuscript received July 27th, 1988)

SUMMARY

Air–water partition coefficients of ethyl acetate are determined by analysis of the headspace vapor from a closed system containing ethyl acetate and sodium chloride solutions of various concentrations. Knowing the amount of ethyl acetate in the headspace, it is possible to calculate the partition coefficient. This paper describes a simple method of determining these values without gas injection valves or other specialized equipment. The values obtained are within 7% of previously published values.

INTRODUCTION

Research was conducted to model an absorption freezing vapor compression process to determine the loss of volatile flavor components. This process concentrates aqueous solutions, such as fruit juices, by freezing water in the process stream[1]. Cooling is provided by evaporating water at the triple point and the resulting water vapor is absorbed in a sodium solution of 15 to 20% (w/v) which is controlled at 0°C. This solution also absorbs volatile flavor components. To design a suitable essence recovery system, it was necessary to determine the extent of the absorption of essence in the sodium chloride solution. A static headspace technique appeared suitable to simulate the equilibrium conditions of the air–water partitioning process. Other researchers[2] have demonstrated that the concentration of volatile components in the liquid and vapor phases could be determined. These researchers used direct injection to determine the concentration of the volatile compound in the liquid phase, while a gas sampling loop was used to measure the concentration of compounds in the vapor. In this paper, we show that a headspace method using syringe injection and ethyl acetate as a model compound provided a rapid measure of the partition coefficient. With this technique, it is not necessary to inject the liquid phase, thereby avoiding contamination of the injector and the analytical column. In addition we show the differences between

* Retired.

PTFE bottles and glass bottles for the equilibration container. The method should be adaptable to other organic compounds.

REAGENTS AND MATERIALS*

Ethyl acetate, distilled in glass, was obtained from Burdick and Jackson Labs. (Muskegon, MI, U.S.A.) sodium chloride from J. T. Baker (Phillipsburg, NJ, U.S.A.), the chromatographic column (15% Carbowax 20 M, 80/100 Chromosorb W AW) from Supelco (Bellefonte, Pa, U.S.A.), the glass serum bottles from Kimble (Neutraglass, 120 ml), the PTFE bottles from Nalgene (125 ml) and the PTFE faced silicone septa from Pierce (Rockford, IL, U.S.A.). The caps for the PTFE bottles were drilled to allow a needle to penerate the septum between the bottle and the cap.

Apparatus

Analyses were conducted with a Varian Model 3700 gas chromatograph with a flame ionization detector set at 200°C and with the range set at 10^{-11} A/mV. The chromatographic column used was a 12 ft. long, 1/8 in. outside diameter stainless-steel column packed with 15% Carbowax 20 M, 80/100 Chromosorb W AW. Operating conditions were as follows: Column temperature, 100°C; injection port, 200°C; helium carrier gas flow-rate, 15 ml/min. A Spectra-Physics 4270 integrator was used to integrate peak areas. A Unimetrics 1-ml gas--tight syringe was used for headspace sampling. A Hamilton 10-μl syringe was used for injecting the standard solutions.

Procedure

Static headspace concentrations were measured by sampling 1.00 ml of vapor from a 125-ml glass serum bottle or a 139-ml PTFE bottle containing 50.0 ml of sodium chloride (0 to 20%) solution, and varying amounts of ethyl acetate (0.42 to 6.26 mg). The glass bottles were sealed with rubber septa and the PTFE bottles were sealed with PTFE faced silicone septa. These vessels were immersed to the neck in a constant temperature bath at 0°C ($\pm$0.1°C), and allowed to equilibrate for 24 h before sampling. Standards were prepared by weighing ethyl acetate into a volumetric flask and diluting to volume with water. Volumes of 5 μl of each of the standards were injected into the gas chromatograph using a Hamilton 10-μl syringe.

Calculations

The concentration of ethyl acetate in the vapor was determined by using an external standard method. The partition coefficients were calculated with the following equations

$$K_p = M_v/M_l \tag{1}$$

where: K_p = partition coefficient; M_v = molar concentration of ethyl acetate in the vapor, mol/l; M_l = molar concentration of ethyl acetate in the liquid, mol/l.

The concentration in the vapor phase was determined by comparison of the

* Reference to brand or firm name does not constitute endorsement by the U.S. Department of Agriculture over others of a similar nature not mentioned.

headspace peak areas to the peak areas read from the standard curve. The concentration in the liquid phase was calculated from the difference between the amount of ethyl acetate in the vpor phase and the amount of ethyl acetate added.

RESULTS AND DISCUSSION

The standard curve of ethyl acetate exhibited a linear response with a correlation coefficient of 0.9934. Amounts of ethyl acetate measured ranged from 98 to 477 ng. The injection precision of the standard was 2.8% relative standard deviation (RSD).

Other researchers[3] had found that carryover in the syringe used to sample the headspace vapor was significant. We found carryover to be less than 0.1% when the plunger was removed between injections. Figs. 1 and 2 are plots of total ethyl acetate in the system *versus* peak area of the vapor injection. The linearity at each level of sodium chloride shows that the vapor phase concentration is a fixed percentage of the total ethyl acetate at each sodium chloride level. In Fig. 1 each line exhibits a positive x-intercept, due to adsorption of ethyl acetate onto the walls of the glass serum bottle[2]. Adsorption should be constant if the number of active sites on the silica surface is constant. Because each plot has approximately the same x-intercept, the number of active sites for the brand of serum bottle we used appears constant. In contrast, Fig. 2 shows no significant x-intercept indicating that there is no adsorption onto the PTFE bottle wall. This can be explained by the lack of absorption sites on the PTFE.

Fig. 3 shows a plot of the partition coefficient calculated from the raw data obtained in glass bottles. The partition coefficient was not constant at different levels of ethyl acetate. This indicates that adsorption to the serum bottle wall was significant and the data must be corrected if glass bottles are used. By subtracting an amount equal to the x-intercept from each concentration of ethyl acetate as shown in Table I,

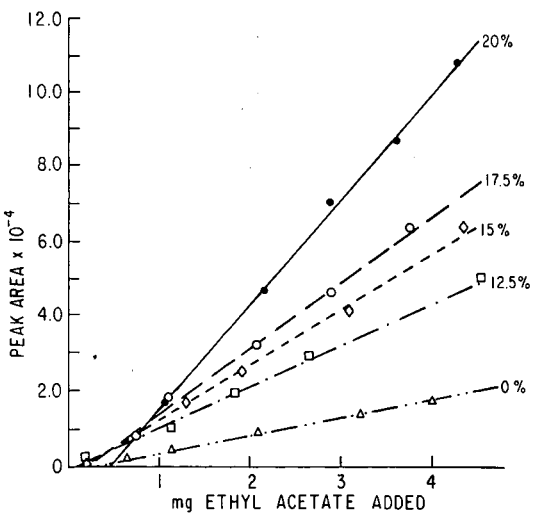

Fig. 1. Peak area response *versus* total amount of ethyl acetate in system at various concentrations of sodium chloride in glass bottles. One milliliter headspace vapor injected. Temperature of system controlled at 0°C (±0.1°C).

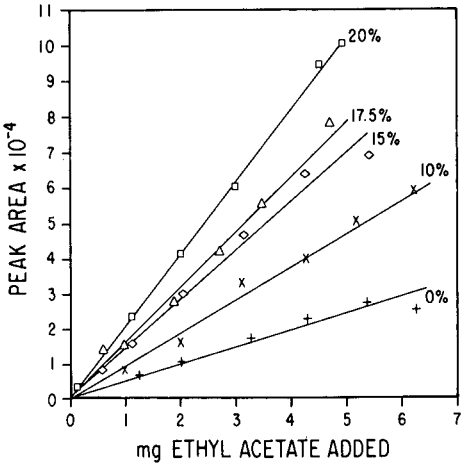

Fig. 2. Peak area response *versus* total amount of ethyl acetate in system at various concentrations of sodium chloride in PTFE bottles. One milliliter headspace vapor injected. Temperature of system controlled at 0°C (±0.1°C).

and recalculating the partition coefficients, the plots graphed in Fig. 4 are obtained. The slopes of the lines on this graph can be shown to be not statistically different than zero by a comparison of the regression coefficient to significant values of the regression coefficient at the 95% confidence level. The near zero slopes of these lines

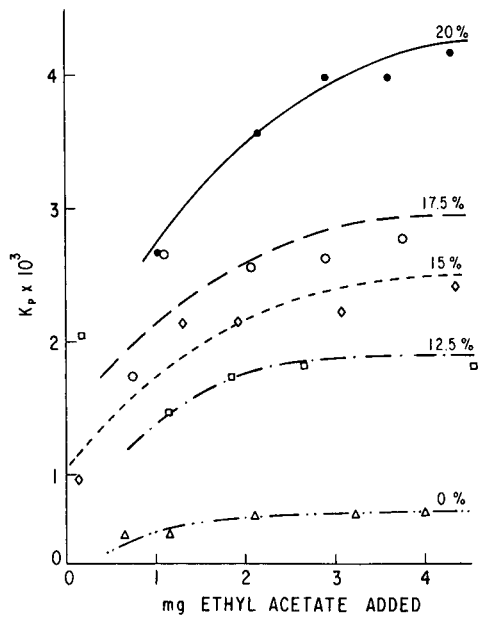

Fig. 3. Uncorrected partition coefficient *versus* total amount of ethyl acetate in system in glass bottles. Partition coefficients at different concentrations of sodium chloride were calculated from uncorrected data.

TABLE I

CORRECTIONS APPLIED TO GLASS CONTAINERS

Sodium chloride concentration (%, w/v)	*Correction (x-intercept) (mg ethyl acetate)*
20.0	−0.4597
17.5	−0.2257
15.0	−0.1741
12.5	−0.0893
0.0	−0.2341

demonstrates that the concentration of ethyl acetate has no effect on the partition coefficient. It can also be seen that the higher concentrations of sodium chloride produce a "salting-out" effect which drives the ethyl acetate out of the liquid phase into the vapor phase thus increasing the partition coefficient at higher levels of sodium chloride.

Fig. 5 shows a plot of the partition coefficient calculated from the raw data obtained in PTFE bottles. The slopes of these lines are not statistically different from zero at the 95% confidence level. Because no correction is necessary for adsorption, as is required when using glass bottles, PTFE appears to be more suitable as a container for gas samples than glass. Fig. 6 shows the variation of the natural logarithm of the

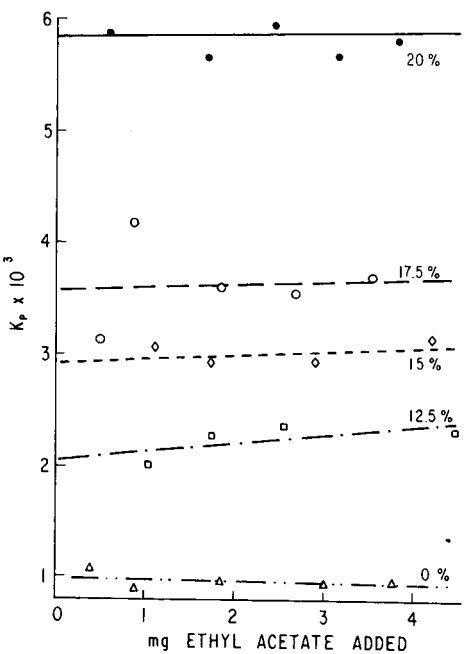

Fig. 4. Corrected partition coefficient *versus* total amount of ethyl acetate in system in glass bottles. Partition coefficients at different concentrations of sodium chloride were calculated from corrected data. The correction was applied to eliminate the effect due to adsorption of ethyl acetate onto the walls of the serum bottle.

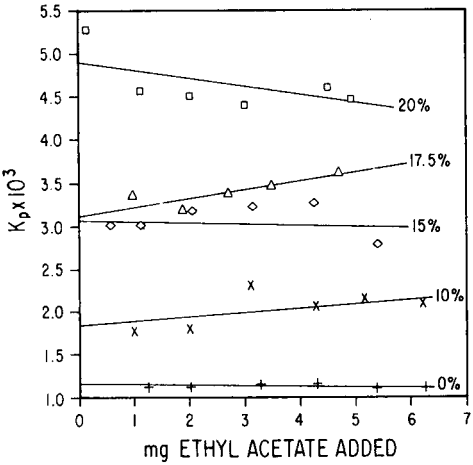

Fig. 5. Partition coefficient *versus* total amount of ethyl acetate in system in PTFE bottles. Raw data was used to calculate partition coefficients.

partition coefficient with respect to the concentration of sodium chloride in the liquid in glass and in PTFE bottles. This graph shows a linear correlation and can be used to predict the partition coefficient at various levels of sodium chloride solution at 0°C.

To check the accuracy of this method, the partition coefficient of ethyl acetate was determined at 25°C in distilled water to compare the values to previously published data. The partition coefficient obtained in glass bottles equalled $7.44 \cdot 10^{-3}$, compared to $6.94 \cdot 10^{-3}$, the value obtained by Kieckbusch and King[4] under the same conditions. The two methods show a difference of 6.95%. The partition coefficient obtained in PTFE bottles equalled $6.55 \cdot 10^{-3}$, a difference of 5.78%.

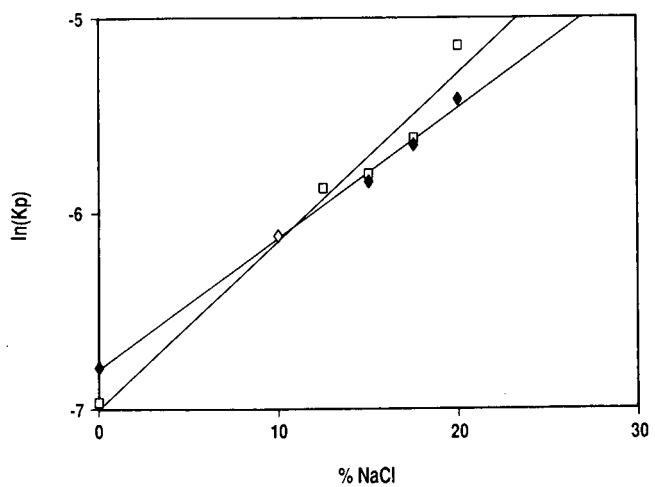

Fig. 6. Natural logarithm of the partition coefficient *versus* concentration of sodium chloride in the liquid. □ = Glass corrected; ◆ = PTFE.

The most serious problem using glass bottles is the need to apply a correction to account for the adsorption of ethyl acetate onto the walls of the serum bottle. Because brands vary, each new lot would require re-determination of the correction factor. We have shown this effect can be reduced or eliminated by using PTFE bottles which are relatively inert with respect to adsorption.

This method offers a rapid means of determining the partition coefficient of ethyl acetate with a minimum of specialized equipment and should be readily adaptable to other organic compounds. It could also be used to determine the total amount of a component in a closed system once the partition coefficient is determined for that system with the condition that the vapor and liquid volumes are accurately known. The activity coefficient can also be calculated once the partition coefficient is found.

REFERENCES

1 S. S. Deshpande, H. R. Bolin and D. K. Salunkhe, *Food Technol.*, May (1982) 68.
2 R. G. Buttery, S. C. Ling and D. G. Guadagni, *J. Agric. Food Chem.*, 17 (1969) 385.
3 T. G. Kieckbusch and C. J. King, *J. Chromatogr. Sci.*, 17 (1979) 273.
4 T. G. Kieckbusch and C. J. King, *J. Agric. Food Chem.*, 27 (1979) 504.

Journal of Chromatography, 455 (1988) 53–65
Elsevier Science Publishers B.V., Amsterdam — Printed in The Netherlands

CHROM. 20 835

VAPOR-PRESSURE MEASUREMENT OF COMPLEX HYDROCARBON MIXTURES BY HEADSPACE GAS CHROMATOGRAPHY

JAMES E. WOODROW and JAMES N. SEIBER*
Department of Environmental Toxicology, University of California, Davis, CA 95616 (U.S.A.)
(First received May 6th, 1988; revised manuscript received July 14th, 1988)

SUMMARY

Headspace gas chromatography was used to measure the vapor pressures of single *n*-alkane hydrocarbons and their binary, ternary and quaternary mixtures at various temperatures in the range 38–107°C. In addition, diesel fuel, gasoline and crude oil vapor pressures were measured at 38 and 70°C. The microprocessor-controlled headspace gas chromatograph automatically thermostated the samples contained in septum-sealed glass vials to equilibrate the vapor and liquid for a pre-set period of time (usually 60 min), pressurized the vials to a pre-set pressure (at least 138 kPa gauge) by inserting a hollow needle through the septum, and sampled the vapor for a pre-set period of time (0.01 min) by allowing the pressure in the vial to drive an aliquot of the vapor (*ca.* 9 μl) through the needle and onto the analytical column. Using this technique, single *n*-alkane hydrocarbon vapor pressures, measured by totally vaporizing μl aliquots in the vials, agreed, on the average, to within 1% with calculated values based on hydrocarbon properties. Likewise, measured total vapor pressures of the binary, ternary, and quaternary mixtures compared well with calculated values, assuming ideal behavior for the mixtures, and the measured vapor pressures of diesel fuel, gasoline, and several crude oils showed good precision and accuracy.

INTRODUCTION

Evaporation of constituents of petroleum mixtures may contribute reactive hydrocarbons to the atmosphere. In order to assess the potential for evaporation from fuels and crude oil compositions, a test method for vapor pressure is required. The vapor pressure of a hydrocarbon mixture represents the sum of contributions from its hydrocarbon and related organic constituents —disproportionately so for the more volatile constituents. Methods that rely on measurement of total pressure within a sealed container (*e.g.*, the Reid vapor pressure method[1]) will also include contributions from dissolved air and water in crude oil, for example, and require at least equilibration of the container with water before a vapor-pressure measurement can be made. In order to separate the contributions of organic from inorganic constituents, an approach is needed whereby the organic constituents only are

0021-9673/88/$03.50 © 1988 Elsevier Science Publishers B.V.

measured and the results then combined to calculate total vapor pressure for the organic fraction of the crude.

Of the methods available for vapor pressure determination —isoteniscope[2], Knudsen effusion[3,4], gas saturation[5,6], and gas chromatographic (GC) techniques[7]— GC offers advantages in terms of speed, solute sample size, purity, and stability requirements. Furthermore, vapor-density determination through headspace sampling and GC analysis affords the best approach for complex hydrocarbon mixtures. The principles and application of headspace sampling for GC analysis have been extensively reviewed[8–13]. A solid or liquid sample (single component or mixture) is placed in a glass container sealed with an inert septum which can be later punctured with a syringe needle. The container is then maintained at a constant temperature until vapor–liquid equilibration occurs. An aliquot of the headspace is then withdrawn with a syringe and injected into a gas chromatograph. The analyte concentration in the headspace can be determined by calibration of the gas chromatograph with suitable standards yielding, in the present case, the vapor density from which vapor pressure may be determined.

The technique of manipulation can vary from a manual syringe removal of headspace via the container septum and then injection of the contents on the gas chromatograph column to fairly sophisticated automated techniques accomplishing basically the same purpose. In this report, we describe a procedure which employed an automated headspace sampler and analysis system, with the goal of developing a relatively fast and accurate method for determining vapor pressures of complex mixtures, such as fuels and crude oils. The procedure was validated using single *n*-alkanes, their simple mixtures and diesel fuel, as a model petroleum mixture.

EXPERIMENTAL

Equipment

Analysis was accomplished using the Perkin-Elmer (Norwalk, CT, U.S.A.) Model HS-100 headspace sampler coupled to the Model Sigma 2000 gas chromatograph (flame ionization detector) and Model LCI-100 laboratory integrator. The gas chromatograph was equipped with a 30 m × 0.25 mm I.D. fused-silica open tubular (FSOT) column coated with phase-bonded silicone oil (DB-1; J&W Scientific, Rancho Cordova, CA, U.S.A.).

Materials

The glass headspace vials (22 ml), Teflon®-coated butyl rubber septa, aluminum caps, and vial cap crimping tool were supplied by Perkin-Elmer. The crimping tool was lubricated with fluoro-Glide (Chemplast, Wayne, NJ, U.S.A.) film bonding lubricant. Pure (at least 99+%) *n*-alkane hydrocarbons (Aldrich, Milwaukee, WI, U.S.A.), pentane through hexadecane, were used as received, diesel fuel and gasoline were obtained from local fueling stations, and crude oil samples were obtained from the McKittrick oil field near Bakersfield, CA, U.S.A. All bottled gases (hydrogen, helium, nitrogen), except compressed air, were at least 99.995% pure (Liquid Carbonic, Chicago, IL, U.S.A.). Glass syringes (μl), with fixed needles, were obtained from Hamilton (Reno, NV, U.S.A.).

Methods

The FSOT column was placed in the gas chromatograph oven, one end was connected to the detector and the other was directly connected without a splitter to the end of the transfer line containing a section of wide-bore (0.32 mm) FSOT column coated with phase-bonded silicone oil (DB-1). The headspace vials were sealed with the crimping tool by alternating between rotating the vial and squeezing the tool; if the vial cap could be moved, the crimping tool was applied again. Before use, the crimping tool was sprayed with a fluorocarbon lubricant to make sure the cap was properly crimped and the septum not wrinkled.

Into a series of separate, sealed vials were injected, using fixed-needle syringes at ambient temperature, increasing μl amounts of the hydrocarbon series pentane through hexadecane. The samples were thermostated at various temperatures in the range 38–107°C for 15 min prior to sampling. Binary (hexane–decane), ternary (hexane–decane–dodecane), and quaternary (hexane–decane–dodecane–hexadecane) mixtures and a seven-component mixture (hexane through dodecane) were prepared in bulk and aliquots were transferred to the vials using pipettes followed by immediate sealing of the vials. The mixtures were thermostated at temperatures in the range 38–107°C for 60 min prior to sampling. The binary and ternary mixtures consisted of approximately equimolar amounts of the constituents, the quaternary mixture consisted of about 10 mol% hexane and 30 mol% of each of the other constituents, and the seven-component mixture consisted of less than 10 mol% of each of the components in a matrix of hexadecane at greater than 50 mol%. Aliquots of diesel fuel were transferred to the vials using pipettes followed by immediate sealing of the vials. The fuel samples were thermostated at 38 and 70°C for 60 min prior to sampling. For all of the mixtures, the vials were filled to different extents to give vapor volume-to-liquid volume (V/L) ratios of 4:1 (4.4 ml), 2:1 (7.3 ml), and 1:1 (11.0 ml). After vapor–liquid equilibration, the vial septa were punctured by the instrument using a hollow sampling needle, the internal pressure of each vial was raised to at least 138 kPa gauge with helium, and the vapor sampled for 0.01 min (*ca.* 9 μl vapor). In most cases, the transfer line temperature was set at 150°C, and the column oven was operated isothermally at 50, 80, 110 or 130°C and was also temperature programmed (2°C/min, 5°C/min) beginning at 40°C and ending in the range 80–130°C, depending on the type of sample.

RESULTS AND DISCUSSION

Analysis using headspace sampling and GC requires thermodynamic equilibrium between a condensed phase (liquid or solid) and its vapor phase in a sealed container so that aliquots of the vapor can be removed for quantitative GC analysis. For a liquid mixture in equilibrium with its vapor in a sealed container, GC response of a component in the vapor is proportional to the vapor density:

$$A_i = c_i(n_i/V)$$

where A_i = GC response of component i, c_i = a calibration factor, n_i = number of moles in the vapor, and V = volume of the vapor space. Furthermore, since

$$(n_i/V)RT = P_i$$

then

$$A_i(RT) = c_iP_i$$

where P_i = the partial pressure of component i in the vapor, R = the gas constant, and T = the absolute temperature. Therefore, measuring the GC response implies measuring the partial pressure if the calibration factor is known. The calibration factor has a specific value for each component in the mixture and depends on the characteristics of the detector used. However, a complex hydrocarbon mixture can be represented by a relatively small number of n-alkane reference standards[14,15] and the properties of the standards can be attributed to the mixture. Also, GC detector response can be calibrated with these standards by relating GC response to vapor density. The form of the relationship would be

$$A_r = a_r + b_r(n_r/V)$$

where the constants a_r and b_r are the intercept and slope, respectively, and r stands for reference. The slope is actually a calibration factor and if detector response is linear ($a_r = 0$), this expression will have the form

$$A_r = b_r(n_r/V)$$

which is essentially the same as

$$A_i = c_i(n_i/V)$$

A_i then becomes a summation of GC responses for a series of components represented by a single n-alkane reference standard. Then, the partial pressure corresponding to each subsection is obtained from

$$P_i = (n_i/V)RT$$

where $(n_i/V) = A_i/(b_rM_r)$ and M_r = the molecular weight of the reference standard representing the subsection, and total pressure (P_t) of the mixture from

$$P_t = \sum P_i$$

The equation for partial pressure is the ideal gas equation. No correction for real gas behavior was necessary since total pressure in the sealed vials remained below about 304 kPa, above which gases become non-ideal[16].

A major objective of this study was the development of a method for headspace GC analysis of the vapor phase of equilibrated complex hydrocarbon mixtures, such as fuels and crude oils. Using individual pure hydrocarbons and their simple mixtures to validate the method, calculation of vapor pressure of these complex mixtures could then be done using the analytical results. Obviously of critical importance in accomplishing the objectives was the analytical instrumentation, which needed to be

able to handle a large number of samples at one time, individually thermostat the samples, and achieve acceptable reproducibility through automatic control. A commercial programmable multisampling system composed of a pneumatically operated injection system, a thermostated carousel for up to 15 sample vials, and an electronically controlled sample magazine was employed. Sampling was based on a pneumatic-balanced pressure principle which avoids the disadvantages associated with gas syringes, such as change of partial pressures of the volatiles due to reduced pressure in the syringe. The system allowed pressurization of the sample vial to any pressure independent of the column head pressure. Thus, the operator was able to control the sample size, a feature that would be especially useful for low-volatility substances. In a typical operation, the septum of the thermostated sample was pierced by the hollow sampling needle, the vial was pressurized, and then an aliquot of the headspace was injected onto the FSOT column using the vial pressure as the driving force[10].

Instrument conditions

Relating response to hydrocarbon amount (μl *vs.* GC response) up through vapor saturation in the headspace vial resulted in a sigmoid curve for hexane at 38°C (Fig. 1A). This shape was less pronounced for heptane and octane (Fig. 1C, D) and the phenomenon was not observed for decane. The sigmoid shape was eliminated entirely for hexane by inserting a section of wide-bore (0.32 mm) FSOT into the transfer line (Fig. 1B). The presence of a wide-bore insert also served to improve compound peak resolution, a result to be expected from reducing the dead volume of the transfer line.

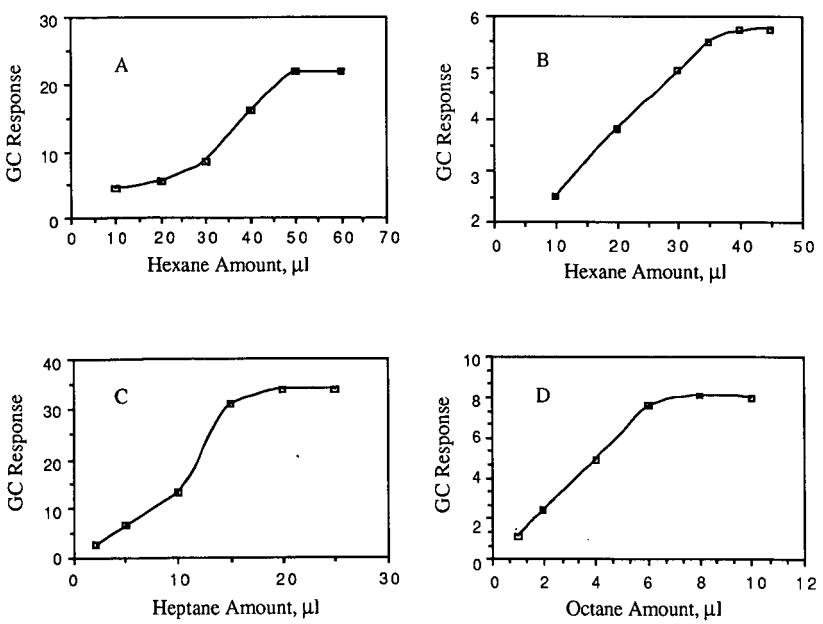

Fig. 1. Isothermal (50°C) gas chromatographic responses of hexane (A, B), heptane (C), and octane (D). Only hexane (B) had transfer line insert.

TABLE I

GC RESPONSE VARIATION FOR TOLUENE AT 38°C AND THREE TRANSFER LINE TEMPERATURES

V/L = Vapor volume-to-liquid volume ratio.

V/L	*GC Area ($\times 10^7$), average ($\pm$ relative S.D., $n = 3$)*		
	Transfer line temperature (°C)		
	68	*100*	*150*
4:1	2.99 (±2.6%)	3.76 (±0.9%)	4.13 (±1.8%)
1:1	2.74 (±1.3%)	3.49 (±0.6%)	4.10 (±1.9%)

All vapor pressure determinations for single hydrocarbons, their simple mixtures, and petroleum mixtures were made with a wide-bore insert in the transfer line.

Another important consideration was the transfer line temperature. Instrument default temperature was 30°C above the sample temperature. However, average differences in instrument response for V/L = 4:1 and 1:1 (single hydrocarbons and mixtures) were always significant. Using toluene as a model[17], transfer line temperature was set at 68, 100 and 150°C for a sample temperature of 38°C. When the transfer line temperature was increased (starting at 68°C), absolute response increased for both V/L = 4:1 and 1:1, but their differences at 100 and 150°C were 7.6% (significant) and 0.9% (not significant), respectively (Table I). Precision was 0.6–0.9% (100°C) and 1.8–1.9% (150°C). It may be important that toluene GC response for V/L = 4:1 and 1:1 did not begin to agree until the transfer line temperature was increased to above the boiling point of toluene (110.6°C). All vapor pressure determinations for single hydrocarbons and the mixtures were made with the transfer line temperature set at 150°C. It was possible to set the temperature at a higher value; however, the time

TABLE II

VAPOR PRESSURES OF PURE HYDROCARBONS AT THREE TEMPERATURES

ND = Not determined (either vapor density was below detection limit or it was too high for accurate measurement and safety).

Hydrocarbon	*Vapor pressure ± S.D. ($n \geq 3$) (kPa)*					
	38°C		*70°C*		*107°C*	
	Experimental	*Calculated**	*Experimental*	*Calculated**	*Experimental*	*Calculated**
Hexane	34.00 ± 0.63	34.19	103.91 ± 0.53	104.69	ND	291.44
Decane	0.43 ± 0.01	0.43	2.50 ± 0.05	2.52	12.45 ± 0.12	12.48
Dodecane	ND	0.05	0.42 ± 0.005	0.42	2.75 ± 0.01	2.78
Hexadecane	ND	0.0009	ND	0.01	0.15 ± 0.02	0.16

* Calculated using the Harlacher equation: $\ln P = A + B/T + C \ln T + DP/T^2$, where P is pressure, T is temperature and A, B, C and D are constants taken from ref. 16.

required for the instrument to become ready to process samples increased dramatically, and in some cases the instrument failed to become ready at all. This might have been due in part to the close proximity of the hot transfer line to the cooler sample set. The microprocessor controlling the instrument would not process the samples until the operator-set temperatures were reached; the microprocessor could not be overridden or by-passed.

Single hydrocarbons

The capabilities of the technique were partly evaluated by determining accuracy and precision through measurement, with replication, of the vapor pressures of a series of pure *n*-alkane hydrocarbons (hexane, decane, dodecane and hexadecane) at 38, 70 and 107°C. The results are summarized in Table II, which also includes vapor pressure values calculated using the Harlacher equation[16]. Agreement between experimental and calculated values was good. Differences ranged from about 0.3 to 5.7% at 38°C, from about 0.6 to 1.3% at 70°C, and from about 0.2 to 4.2% at 107°C. Precision of the average values fell in the ranges ±1.6–1.9% at 38°C, ±0.5–2.0% at 70°C, and ±0.2–9.6% at 107°C. The high values for the two ranges at 107°C were due primarily to the difficulty in accurately measuring small volumes of hexadecane (*ca.* 0.3 μl injected into sealed vials for vapor saturation). Vapor pressures were not measured for all compounds at all temperatures because of either the inability to measure very small volumes of the low volatility hydrocarbons (0.10 μl for dodecane and 0.002 μl for hexadecane at 38°C and 0.03 μl for hexadecane at 70°C for vapor saturation) or the chance of saturating the GC detector and generating unsafe pressures in the vials with the more volatile hydrocarbons, especially at 107°C.

Varying vial V/L, using the neat hydrocarbons, did not significantly affect instrument response for samples at 43°C (Table III). However, at 72 and 107°C, all differences between V/L = 4:1 and 1:1 were significant. The greatest differences between V/L = 4:1 and 1:1 were exhibited by dodecane and hexadecane, in part because their boiling points were, respectively, about 76 and 137°C greater than the transfer line temperature (see Table I). In spite of this, their use as standards for

TABLE III

GAS CHROMATOGRAPHIC RESPONSE OF PURE HYDROCARBONS

V/L	*Temp. (°C)*	*GC Response (× 10³), average (± relative S.D., n = 3)*			
		Hexane	*Decane*	*Dodecane*	*Hexadecane*
4:1	38	13.36 (±0.59%)	1.04 (±5.52%)	–	–
2:1		13.32 (±0.79%)	0.99 (±5.56%)	–	–
1:1		13.38 (±1.59%)	0.96 (±6.10%)	–	–
4:1	72	–	10.82 (±1.25%)	2.46 (±1.50%)	–
2:1		–	10.45 (±0.92%)	2.26 (±0.53%)	–
1:1		–	9.50 (±2.54%)	1.97 (±1.54%)	–
4:1	107	–	–	5.34 (±2.10%)	0.43 (±1.10%)
2:1		–	–	5.04 (±1.43%)	0.36 (±3.82%)
1:1		–	–	4.69 (±1.59%)	0.25 (±2.41%)

TABLE IV

GAS CHROMATOGRAPHIC RESPONSE OF MIXTURES OF PURE HYDROCARBONS AT 43, 72 AND 107°C

Mixture type	*Temp. (°C)*	*V/L*	*GC Response (× 10²), average (± relative S.D., n = 3)*			
			Hexane	*Decane*	*Dodecane*	*Hexadecane*
Binary*	43	4:1	87.58 (±2.42%)	9.76 (±5.53%)	–	–
		2:1	82.87 (±7.22%)	9.73 (±2.27%)	–	–
		1:1	86.82 (±6.08%)	8.92 (±5.71%)	–	–
Ternary*		4:1	138.38 (±1.85%)	8.39 (±2.45%)	1.72 (±6.42%)	–
		2:1	138.38 (±0.08%)	7.22 (±17.32%)	1.33 (±9.34%)	–
		1:1	140.64 (±0.54%)	6.37 (±1.78%)	1.07 (±2.93%)	–
Quaternary**		4:1	129.31 (±0.11%)	6.01 (±7.67%)	0.95 (±8.55%)	–
		2:1	129.46 (±0.003%)	6.05 (±6.41%)	0.96 (±6.06%)	–
		1:1	125.81 (±2.67%)	5.62 (±1.71%)	0.80 (±6.74%)	–
Binary*	72	4:1	382.20 (±7.86%)	45.00 (±3.86%)	–	–
		2:1	403.60 (±0.74%)	42.10 (±2.98%)	–	–
		1:1	395.50 (±3.39%)	45.20 (±3.07%)	–	–
Ternary*		4:1	359.97 (±4.84%)	28.70 (±1.26%)	9.07 (±7.69%)	–
		2:1	340.15 (±1.27%)	29.12 (±4.87%)	8.10 (±9.71%)	–
		1:1	345.14 (±0.90%)	28.90 (±1.92%)	9.28 (±5.93%)	–
Quaternary**		4:1	143.20 (±0.72%)	14.90 (±3.29%)	4.82 (±2.84%)	–
		2:1	144.98 (±0.43%)	15.28 (±2.83%)	4.91 (±1.65%)	–
		1:1	146.55 (±0.55%)	14.45 (±0.76%)	4.72 (±3.00%)	–
Quaternary**	107	4:1	328.81 (±0.94%)	65.24 (±3.39%)	28.97 (±3.53%)	6.96 (±1.66%)
		2:1	337.41 (±1.29%)	68.92 (±1.68%)	30.66 (±0.95%)	6.56 (±2.73%)
		1:1	340.99 (±1.55%)	65.54 (±8.29%)	29.45 (±7.10%)	5.49 (±14.61%)

* Equimolar.

** Hexane at 0.1 mole fraction, all other components (decane, dodecane and hexadecane) at 0.3 mole fraction. Response for hexadecane was below the detection limit at 43 and 72°C.

complex mixtures, such as fuels and crude oils, would not present a problem since their retention times would place them in regions of mixture chromatograms that would represent small fractions of the total equilibrated vapor for fuels and crude oils. Precision of triplicate determinations varied from ±0.53 to ±6.10%, with an average of ±2.27% for 18 sets of triplicate determinations.

Simple mixtures

For the mixtures of the *n*-alkane hydrocarbons at 43, 72, and 107°C, average precision was ±4.66, ±3.18, and ±3.98% for 24, 24, and 12 determinations, respectively (Table IV). Relative responses at V/L = 4:1 and 1:1 were significantly different in only 5 cases out of 20 listed. In some of the cases where differences were significant, percent difference was small (2–4%). Variability in precision from sample to sample can be due to inconsistency in instrument operation and/or to some problem in not always making a good seal with the Teflon-lined septa. The effects of variability on the quality of the data may be minimized by adequate replication. We used

TABLE V

VAPOR PRESSURES OF MIXTURES OF PURE HYDROCARBONS

Temp. (°C)	*Type*	*V/L*	*Partial pressure (kPa)*				*Total pressure (kPa)*	
			Hexane	*Decane*	*Dodecane*	*Hexadecane*	*Experimental*	*Calculated**
43	Binary	4:1	18.52	0.29	–	–	18.81	20.95
		2:1	19.79	0.29	–	–	20.08	
		1:1	18.11	0.26	–	–	18.37	
	Ternary	4:1	13.03	0.25	0.04	–	13.32	14.10
		2:1	13.03	0.22	0.03	–	13.28	
		1:1	13.31	0.19	0.02	–	13.52	
	Quaternary**	4:1	3.86	0.18	0.02	–	4.06	4.34
		2:1	3.86	0.18	0.02	–	4.06	
		1:1	3.75	0.17	0.01	–	3.93	
72	Binary	4:1	47.90	1.19	–	–	49.09	56.90
		2:1	54.14	1.11	–	–	55.25	
		1:1	51.77	1.20	–	–	52.97	
	Ternary	4:1	41.48	0.75	0.25	–	42.48	38.37
		2:1	35.74	0.76	0.22	–	36.72	
		1:1	37.19	0.76	0.26	–	38.21	
	Quaternary**	4:1	10.50	0.50	0.13	–	11.13	12.11
		2:1	10.65	0.51	0.13	–	11.29	
		1:1	10.78	0.48	0.13	–	11.39	
107	Quaternary***	4:1	28.29	2.64	0.82	0.12	31.87	33.76
		2:1	29.06	2.81	0.88	0.12	32.87	
		1:1	29.38	2.66	0.83	0.10	32.97	

* Activity coefficient assumed to be unity.
** Hexadecane response below the detection limit.
*** Temperature too high for binary and ternary mixtures.

a minimum of three replicates per sample type; when outliers occurred in a data set, we repeated the analyses.

Accuracy depends on having reliable reference data. As a first approximation, we assumed that the mixtures of the pure *n*-alkanes were essentially ideal (*i.e.*, component activity coefficient equal to unity). This approximation was supported by the Scatchard–Hildebrand solution theory[18] and the UNIFAC method[16], both of which allow one to calculate component activity coefficient after making certain assumptions. In either case, component activity coefficients for the simple mixtures were calculated to be near unity. This allowed us then to determine component vapor density from standard injections of the hydrocarbons used to make up the mixtures. Assuming ideal behavior, average difference between experimental total mixture vapor pressure and calculated total vapor pressure was about 6% (Table V). Average precision for vapor pressure determinations was $\pm 3\%$. For the mixture where component mole fraction was less than 0.1, difference between predicted and experimental total vapor pressures was about 5% (Table VI). Furthermore, average

TABLE VI

COMPONENT PARTIAL PRESSURES OF PURE HYDROCARBONS IN A SEVEN-COMPONENT MIX AT 72°C

The hydrocarbons were blended in a matrix of hexadecane.

V/L	*Partial pressure (kPa)**							*Total pressure (kPa)*
	Hexane	*Heptane*	*Octane*	*Nonane*	*Decane*	*Undecane*	*Dodecane*	
4:1	9.43	3.33	1.38	0.38	0.16	0.08	0.03	14.79
2:1	9.42	3.34	1.45	0.40	0.19	0.08	0.03	14.91
1:1	9.46	3.04	1.18	0.38	0.21	0.08	0.03	14.38

* Predicted component partial pressures were as follows (all values in kPa): hexane: 10.03; heptane: 3.47; octane 1.24; nonane: 0.45; decane: 0.17; undecane: 0.06; dodecane: 0.02. Total vapor pressure = 15.44 kPa.

precision was about ±2%. These differences between predicted and experimental vapor pressures reflected not only instrument operation, but also variability in the preparation of the mixtures; the latter were prepared in bulk and aliquots were pipetted into the headspace vials.

Complex mixtures

Aliquots of diesel fuel were pipetted into the headspace vials at various *V/L* ratios and chromatograms at sample temperatures of 38 and 70°C were developed. The GC trace was divided into 6 and 7 subsections (38 and 70°C, respectively), each approximately centered about the retention time of a pure hydrocarbon standard. This is illustrated in Fig. 2 which shows a gas chromatogram of a vapor sample of diesel fuel at 38°C and retention times (from injection) for a series of *n*-alkane reference standards (pentane through decane), each of which represents one of the six subsections (1–6).

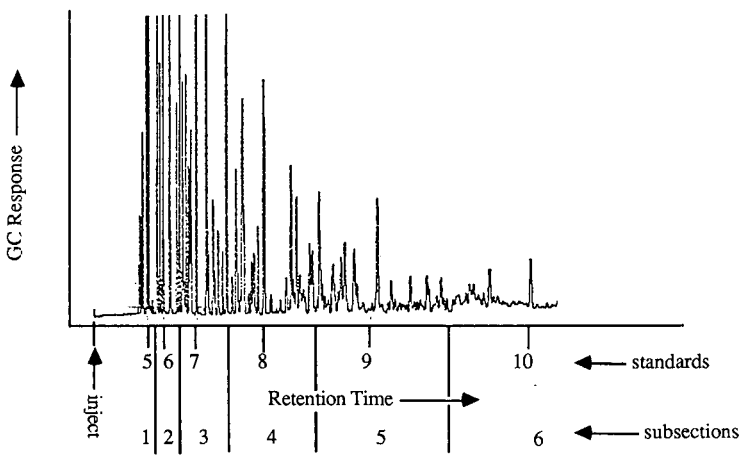

Fig. 2. Gas chromatogram of diesel fuel with standard retentions (C_5–C_{10}). Column: 40°C (5 min), 2°C/min to 80°C.

TABLE VII

VAPOR PRESSURE OF DIESEL FUEL BY HEADSPACE GAS CHROMATOGRAPHY AT TWO TEMPERATURES

Temperature (°C)	*V/L*	*Vapor pressure (kPa) (average ± S.D., n = 3)**
38	4:1	1.13 ± 0.03
	1:1	1.14 ± 0.01
70	4:1	3.83 ± 0.08
	1:1	3.92 ± 0.03

* Typical values at 38°C fall in the range 1.03–1.38 kPa, depending on the season.

Standard curves were generated for each hydrocarbon reference by injecting into sealed headspace vials increasing μl amounts, giving vapor densities below saturation. Then, each standard curve was used to calculate the vapor density for each subsection of the complex chromatogram, yielding subsection partial pressures.

Table VII lists the average total vapor pressures for diesel fuel at the two test temperatures. Vapor pressure was determined from the summed subsection partial pressures, which were derived from the ideal gas law using the subsection vapor density based on the calibration curve of each subsection hydrocarbon standard. The values for V/L = 4:1 and 1:1 had precisions of ± 2 and $\pm 1\%$, respectively. Agreement between the values at V/L = 4:1 and 1:1 were within 1–2% (38°C) and 2–3% (70°C). However, the differences were not significant at the 95% confidence level.

Further evaluation of the method using light fuels and crude oils is currently in progress. Table VIII lists a few preliminary results for gasoline, light, medium-light and heavy crude oils at 38°C and V/L = 4:1. Included are results obtained using the Reid method[1], which measures vapor pressures of petroleum mixtures equilibrated in sealed metal cylinders, equipped with mechanical pressure gauges, at V/L = 4:1. Compared to the average Reid vapor pressures, gasoline and light and medium-light crudes differed by -2.2, -6, and -19%, respectively. Average precision for these mixtures using headspace GC was about $\pm 1\%$, while the Reid values exhibited precisions of $\pm 1\%$ (gasoline), $\pm 5\%$ (light crude), and $\pm 38\%$ (medium-light crude). Results for the heavy crude indicate that the headspace GC method is capable of measuring vapor pressures of low-volatility mixtures; the Reid method is not able to do this.

TABLE VIII

VAPOR PRESSURE OF GASOLINE AND THREE CRUDE OILS AT 38°C

Mixture (at V/L = 4:1)	*Vapor pressure (kPa) (average ± S.D., n = 3)*	
	Headspace GC	*Reid method*
Gasoline	58.86 ± 0.76	60.17 ± 0.41
Light crude	26.05 ± 0.14	26.91 ± 1.38
Medium-light crude	2.96 ± 0.07	3.65 ± 1.38
Heavy crude	0.04 ± 0.01	–

CONCLUSIONS

With headspace GC, it is possible to measure relatively quickly equilibrium (saturation) vapor pressures of pure *n*-alkanes and of simple and complex mixtures. In the latter case, it is not necessary to know the precise composition of the mixture, but the mixture can be approximated with reference standards the GC retention times of which span the chromatogram of the mixture. A significant aspect of the headspace GC technique is microprocessor control of the critical steps in the analysis, promising precise and accurate measurements: (1) sample thermostating; (2) vial pressurization; and (3) headspace sampling and injection. Furthermore, microprocessor control would allow around-the-clock operation for high sample through-put (*ca.* 50–100/day).

The method, as presented here, had good precision and accuracy at all experimental temperatures. Furthermore, increasing the number of components in the synthetic mixtures seemed to give better behaved solutions, where all component partial pressures were close to the predicted values. This implies that the method would work well with complex petroleum mixtures, which was demonstrated to be the case in this study using diesel fuel as a model petroleum mixture and for some samples of gasoline and crude oil. In a current study, the method is being used to measure vapor pressures of fuels (*e.g.*, gasoline and jet fuel), syncrude, and light, medium and heavy crude oils at several temperatures and V/L ratios for further evaluation. These applications will be the subject of a separate report.

ACKNOWLEDGEMENTS

We gratefully acknowledge the technical assistance of J. Sagebiel. We also thank J. Paskind, R. Grant, J. Courtis and H. Metzger, all with the California Air Resources Board, and R. Farnham, Western Oil and Gas Association, for their assistance and helpful suggestions. This study was supported by the California Air Resources Board under Contract A6-178-32 and presented in part at the *192nd National Meeting of the American Chemical Society (ENVR 68), Anaheim, CA, U.S.A., September 7–12, 1986.* The statements and conclusions in this report are those of the contractor and not necessarily those of the California Air Resources Board. The mention of commercial products, their source or their use in connection with material reported herein is not to be construed as either an actual or implied endorsement of such products.

REFERENCES

1 *American Society for Testing and Materials Annual Book of Standards*, American Society for Testing and Materials, Philadelphia, PA, 1973, p. 198.
2 *American Society for Testing and Materials Annual Book of Standards, Part 24*, American Society for Testing and Materials, Philadelphia, PA, 1978, p. 740.
3 G. W. Thomson, in A. Weissberger (Editor), *Technique of Organic Chemistry*, Vol. I, Part I, Interscience, New York, 3rd ed., 1959, Ch. IX, p. 401.
4 G. W. Thomson and D. R. Douslin, in A. Weissberger and B. W. Rossiter (Editors), *Techniques of Chemistry*, Vol. I, Part I, Wiley-Interscience, New York, 1971, Ch. II, p. 23.
5 W. F. Spencer and M. M. Cliath, *Environ. Sci. Technol.*, 3 (1969) 670.
6 W. F. Spencer and M. M. Cliath, *Residue Rev.*, 85 (1983) 57.
7 Y.-H. Kim, J. E. Woodrow and J. N. Seiber, *J. Chromatogr.*, 314 (1984) 37.
8 H. Hachenberg and A. P. Schmidt, *Gas Chromatographic Headspace Analysis*, Wiley, New York, 1977.

9 B. Kolb (Editor), *Applied Headspace Gas Chromatography*, Heyden, Philadelphia, PA, 1980.
10 B. V. Ioffe and A. G. Vitenberg, *Head-Space Analysis and Related Methods in Gas Chromatography*, Wiley, New York, 1984.
11 J. Drozd and J. Novák, *J. Chromatogr.*, 165 (1979) 141.
12 M. E. McNally and R. L. Grob, *Am. Lab.*, January (1985) 20.
13 M. E. McNally and R. L. Grob, *Am. Lab.*, February (1985) 107.
14 F. T. Eggertsen, N. R. Nygard and L. D. Nickoley, *Anal. Chem.*, 52 (1980) 2069.
15 J. E. Woodrow, J. N. Seiber and Y.-H. Kim, *Environ. Sci. Technol.*, 20 (1986) 783.
16 R. C. Reid, J. M. Prausnitz and T. K. Sherwood, *The Properties of Gases and Liquids*, McGraw-Hill, New York, 3rd ed., 1977.
17 B. Kolb, Bodenseewerk Perkin-Elmer, Überlingen, private communication, 1986.
18 J. M. Prausnitz, *Molecular Thermodynamics of Fluid-Phase Equilibria*, Prentice-Hall, Englewood, NJ, 1969, p. 269.

Journal of Chromatography, 455 (1988) 67–75
Elsevier Science Publishers B.V., Amsterdam — Printed in The Netherlands

CHROM. 20 831

DETERMINATION OF THE SOLUBILITY OF VAPOURS IN POLYMERS BY AUTOMATED HEADSPACE GAS CHROMATOGRAPHY

K. SCHOENE*, J. STEINHANSES and A. KÖNIG
Fraunhofer Institute for Environmental Chemistry and Ecotoxicology, D-5948 Schmallenberg-Grafschaft (F.R.G.)
(Received May 16th, 1988)

SUMMARY

An experimental procedure is described for measuring sorption equilibria between polymers and condensable vapours at temperatures above 40°C by headspace gas chromatography. From the results, the solubility coefficients, S, for 20°C were derived. Sorption isotherms and S values were determined for the systems polyethylene–bis(2-chloroethyl) sulphide, polyethylene–2-methoxyethanol, polyethylene–2-methoxyethyl acetate, FFAP–(Carbowax 20M–2-nitroterephthalic acid)–bis(2-chloroethyl) sulphide and Tenax TA–tetrachloroethene. From the sorption isotherms, it appears that in the polyethylene and FFAP systems merely absorption occurs (positive deviation from Henry's law), whereas with Tenax both adsorption and absorption take place.

INTRODUCTION

Headspace gas chromatography (HSGC) is a well known analytical application, in addition to a convenient technique for measuring vapour pressures and related physicochemical parameters[1,2]. In previous papers, we reported the determination of adsorption isotherms for hazardous chemicals[3] and Henry's law constants of aqueous solutions[4] by HSGC. It is now convenient to use this technique also for measuring the sorption–desorption equilibria between vapours and polymer matrices.

The need for information about the solubility of vapours in polymers arose in our laboratory from different routes of investigations, dealing with the permeation of vapours through polyethylene foils and the application limits of sorbent tubes for air sampling purposes. In both cases the solubility coefficient, $S = c_p/c_g$, where c_p and c_g are the equilibrium concentrations in the polymer and in the gas phase, respectively, is one of the important parameters governing the dynamic process. The HSGC technique provides an easy access to this interesting parameter so that it seemed worthwile to describe the general procedure and the results for some typical examples.

0021-9673/88/$03.50 © 1988 Elsevier Science Publishers B.V.

TABLE I

HSGC CONDITIONS

Solute	*Carrier gas (helium) (bar)*	*Equilibr. time (min)*	*Sampl. pressure (bar)*	*Sampl. time (min)*	*Transfer temp. (°C)*	*Column temp. (°C)*	*Retention time (min)*
2-Methoxyethanol	0.4	120	1.5	1.2	120	80	2.58
2-Methoxyethyl acetate	0.4	120	1.5	1.2	120	80	3.87
Tetrachloroethene	0.4	120	1.5	3.0	120	75	3.48
Bis(2-chloroethyl) sulphide	0.85	180	2.2	3.0	150	110	4.75

EXPERIMENTAL

Materials and equipment

2-Methoxyethanol (99.9%), 2-methoxyethyl acetate (98%) and tetrachloroethene (99.9%) were obtained from Aldrich (Steinheim, F.R.G.), bis(2-chloroethyl) sulphide (97.5%) from Atlanta (Heidelberg, F.R.G.). Sorbent materials obtained from Macherey & Nagel (Düren, F.R.G.) were Tenax TA (60–80 mesh) and FFAP (Carbowax 20M–2-nitroterephthalic acid), 23.5% on Chromosorb W AW DMCS (60–80 mesh) (abbreviated as FFAPCHR), and polyethylene foil of thickness 73.1 μm and density 1.004 g/cm^3 was obtained from Wolff (Walsrode, F.R.G.).

The experiments were performed using the automatic HSGC instrument HS 100 from Bodenseewerk Perkin-Elmer (Überlingen, F.R.G.), equipped with a "Megabore" column (WCOT quartz, 30 m × 0.53 mm, DB-5, 1.5 μm). The test vials ("HS-flasks", 22.28 cm^3) were sealed with PTFE-coated septa from butyl rubber. The lowest operating temperature of the HS 100 is about 40°C. Sorption measurements were carried out with the following combinations: bis(2-chloroethyl) sulphide–FFAPCHR (system I); bis(2-chloroethyl) sulphide–polyethylene (II); 2-methoxyethyl acetate–polyethylene (III); 2-methoxyethanol–polyethylene (IV) and tetrachloroethene–Tenax (V).

Procedure

The HSGC system was calibrated in the usual way[5] by analyzing HS-flasks, thermostatted at 80°C and containing different amounts of the test substances (without sorbent). The test substances were dissolved in isooctane; the stock solutions were made up such that the aliquots introduced into the HS-flask would be vaporized completely at 80°C. The appropriate equilibration time was evaluated by analyzing series of HS-flasks, containing sorbent and test substances, after different times of storage at 41.5°C. With increasing storage time, the detector signals decreased to a minimum value, which then remained constant upon prolonged storage. The time which was necessary to achieve this minimum gas concentration in the headspace (corresponding to maximum uptake by the polymer) is given as the "equilibration time" in Table I.

For the determination of the sorption equilibria, known amounts of sorbent and pure test substance, m, were introduced into the HS flask in such a way that the liquid did not touch the solid material. After sealing and thermostatting at 41.5, 50.8 or 60.5°C for the respective equilibration time, the headspace analysis was done. From the calibration graph, the amount, m_g, of gaseous test substance in the headspace was derived, which, upon subtraction from m, yielded the amount, m_p, present in or at the sorbent. From the sorbents, the following amounts were applied: 5–100 mg FFAPCHR, 20–30 mg Tenax and 43.9 mg (= 6 cm^2) of the polyethylene foil. The respective ranges of the test substances were: 0.5–2 mg bis(2-chloroethyl) sulphide, 2-methoxyethyl acetate and 2-methoxyethanol and 0.5–6.5 mg tetrachloroethene. The test substances were injected by a dead volume-free syringe (Hamilton 7005).

For converting the mass m_g into the respective gas concentration, c_g, via the ideal gas law, the actual volume of the headspace must be known, *i.e.*, the volume of the HS-flask (22.28 cm^3) minus the volume of the sorbent. The latter were calculated from the densities, as determined by a "volumenometer"[6]: Tenax, 1.2 ± 0.1 g/cm^3; FFAPCHR, 1.75 ± 0.2 g/cm^3.

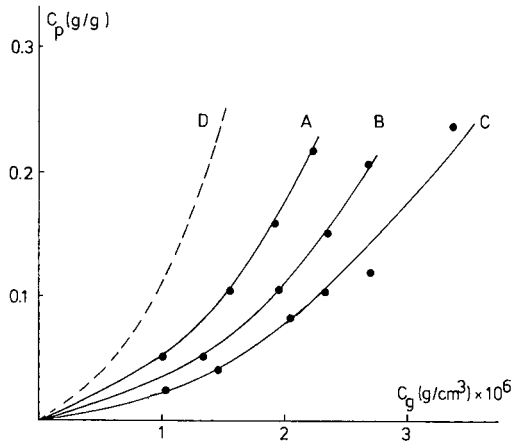

Fig. 1. Sorption isotherms of system I, bis(2-chloroethyl) sulphide–FFAPCHR, as measured at 41.5 (A), 50.8 (B), 60.5°C (C) and as calculated at 20.0°C (D); c_p = grams sorbed per gram pure FFAP.

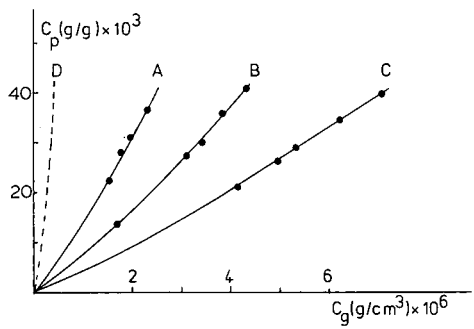

Fig. 2. Sorption isotherms of system II, bis(2-chloroethyl) sulphide–polyethylene, as measured at 41.5 (A), 50.8 (B), 60.5°C (C) and as calculated at 20.0°C (D).

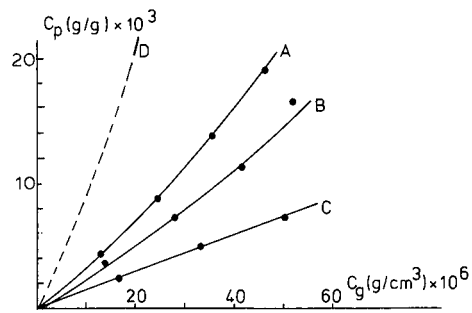

Fig. 3. Sorption isotherms of system III, 2-methoxyethyl acetate–polyethylene, as measured at 41.5 (A), 50.8 (B), 60.5°C (C) and as calculated at 20.0°C (D).

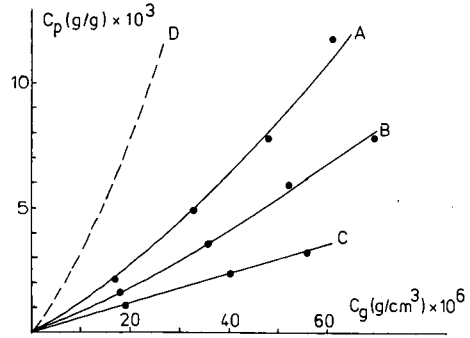

Fig. 4. Sorption isotherms of system IV, 2-methoxyethanol–polyethylene, as measured at 41.5 (A), 50.8 (B), 60.5°C (C) and as calculated at 20.0°C (D).

RESULTS AND DISCUSSION

Figs. 1–5 show the sorption isotherms obtained at the three experimental temperatures and, as dashed lines, the isotherms as calculated for 20°C.

In the systems I–IV (Figs. 1–4) the solubility coefficient, $S = c_p/c_g$ (cm^3), increases with increasing c_g. As has been shown by other authors[7–9], this behaviour can be described by

$$\log S = ac_g + \log S_0 \tag{1}$$

From c_p and c_g (Figs. 1–4) the individual solubility coefficients, S, were calculated and subjected to linear regression according to eqn. 1. The results are given in Table II. As a typical example a plot of log S *vs.* c_g for system I is shown in Fig. 6. The respective data are related to the 23.5% portion of pure FFAP; separate measurements revealed

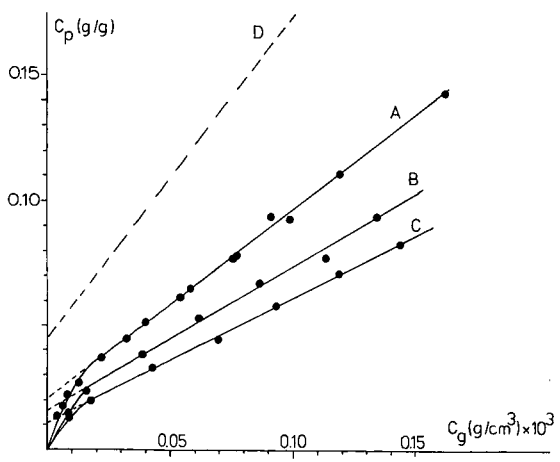

Fig. 5. Sorption isotherms of system V, tetrachloroethene–Tenax, as measured at 41.5 (A), 50.8 (B) and 60.5°C (C); from the linear parts of curves A–C the corresponding line D for 20.0°C was calculated.

TABLE II

LINEAR REGRESSION DATA FOR EQN. 1

$\log S = ac_g + \log S_0$ (cm^3/g)

Temp. (°C)	*System**											
	I			*II*			*III*			*IV*		
	$a \cdot 10^{-5}$	$\log S_0$**	*r*	$a \cdot 10^{-4}$	$\log S_0$	*r*	$a \cdot 10^{-3}$	$\log S_0$	*r*	$a \cdot 10^{-3}$	$\log S_0$	*r*
41.5	2.64	4.40	0.998	4.12	4.11	0.89	3.37	2.46	0.990	4.05	2.03	0.98
50.8	2.20	4.29	0.999	2.81	3.86	0.97	2.15	2.37	0.81	2.03	1.92	0.93
60.5	1.94	4.17	0.98	1.42	3.65	0.95	0.00	2.16		0.00	1.75	
20.0***	3.46	4.70		7.60	4.70		7.18	2.87		9.33	2.39	

* I = Bis(chloroethyl) sulphide–FFAPCHR; II = bis(chloroethyl) sulphide–polyethylene; III = 2-methoxyethyl acetate–polyethylene; IV = 2-methoxyethanol–polyethylene.

** S and S_0 in cm^3 per g pure FFAP.

*** Calculated using eqns. 2 and 3.

TABLE III

LINEAR REGRESSION DATA FOR EQNS. 2 AND 3, S_0 AND S_c CALCULATED AT 20°C AND THE SLOPE, a^{20}, OF EQN. 1 FOR 20°C

System	*Eqn. 2*				*Eqn. 3*			*Eqn. 1 for 20°C*	
	$a' \cdot 10^{-3}$	b'	*r*	$\log S_0^{20}$	c ($g/cm^3 \cdot 10^6$)	$a'' \cdot 10^{-3}$	b''	$\log S_c^{20}$	a^{20}
I*	1.27	0.384	0.999	4.70	1	1.65	−0.570	5.05	$3.03 \cdot 10^5$
II	2.54	−3.96	0.998	4.70	4	3.13	−5.69	5.00	$7.60 \cdot 10^4$
III	1.68	−2.87	0.98	2.87	40	2.43	−5.13	3.16	$7.18 \cdot 10^3$
IV	1.53	−2.82	0.97	2.39	40	2.43	−5.51	2.76	$9.33 \cdot 10^3$

* Related to the content in pure FFAP.

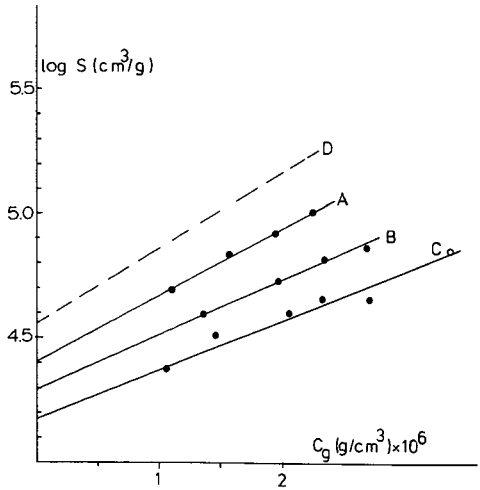

Fig. 6. Logarithm of the solubility coefficient, S, as a function of the equilibrium gas concentration, c_g, according to eqn. 1, for System I, as measured at 41.5 (A), 50.8 (B), 60.5°C (C) and as calculated at 20.0°C (D). The S values are related to the content in pure FFAP.

that the Chromosorb carrier made a negligible contribution to the sorptive capacity.

The temperature dependence of the solubility over small ranges of temperature can be represented by Arrhenius-type equations[7–9]:

$$\log S_0 = a' \cdot 1/T + b' \tag{2}$$

$$\log S_c = a'' \cdot 1/T + b'' \tag{3}$$

In Table III, the linear regression data for the four systems are given, using throughout the respective S_0 from Table II and, additionally, one appropriate S_c within the experimental range of c_g. Fig. 7 shows as an example the graph obtained for system

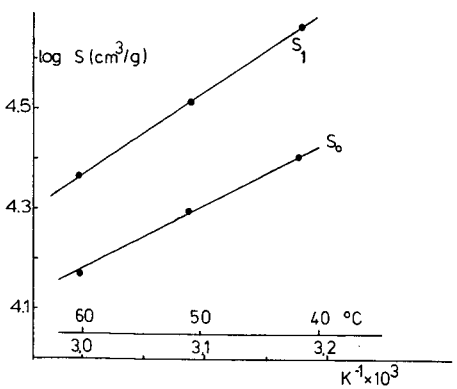

Fig. 7. Temperature dependence of the solubility coefficients at the equilibrium gas concentrations $c_g = 0$ (S_0) and $c_g = 1 \cdot 10^{-6}$ g/cm³ (S_1), as calculated for system I according to eqn. 1.

TABLE IV

LINEAR REGRESSION DATA OF EQN. 5 FOR SYSTEM V

Temp. (°C)	S (cm^3/g)	α ($g/g \cdot 10^2$)	r
41.5	759	2.07	0.998
50.8	575	1.58	0.997
60.5	495	1.14	0.999

I with S_0, *i.e.*, S for $c_g = 0$ and S_c for $c_g = 1\ \mu g/cm^3$ (indicated in Fig. 7 as S_1). These S_c values were calculated by inserting $c_g = 1 \cdot 10^{-6}$ g/cm^3 into each of the respective regression equations 1 for the three experimental temperatures. Linear regression according to eqn. 3 resulted in the values of a'' and b'' given in Table III, from which log S_c^{20} was calculated.

Hence, with log S_0^{20} and S_c^{20} two values of eqn. 1 for 20°C are obtained, which allow a plot of the dashed line D in Fig. 6 (assuming eqn. 1 to be valid also at 20°C), according to:

$$\log S_c^{20} = a^{20} c_g + \log S_0^{20} \tag{4}$$

The respective data are included in Table III. From these, using the relationship $c_p = S_c c_g$, the dashed curve D in Fig. 1 was constructed. The curves D in Figs. 2–4 were obtained in the same way.

The isotherms found for system V, Tenax–tetrachloroethene, exhibit a biphasic shape: at low c_g, c_p ascends like an adsorption-type isotherm whereas at higher vapour concentrations, so far as were measured, the sorption behaviour follows Henry's law according to:

$$c_p = S c_g + \alpha \tag{5}$$

The parameters S and α, resulting from linear regression, are given in Table IV. From these data, the temperature dependences of S and α are:

$$\log S = 1024 \cdot 1/T - 0.383 \qquad (r = 0.990) \tag{6}$$

$$\log \alpha = 1426 \cdot 1/T - 6.211 \qquad (r = 0.998) \tag{7}$$

With eqns. 6 and 7 the linear regression parameters according to eqn. 5 for 20°C were calculated (included in Table IV), from which line D in Fig. 5 was constructed.

The positive deviation from Henry's law in systems I–IV may either be a consequence of structural changes in the polymer matrix or result from the fact that the solute–solute interactions are stronger than those between the solute and the polymer[10]. Negative deviation from Henry's law as in system V represents "initial sorption on some kind of specific sites"[10]. The value of α gives an estimate of this initial sorptive capacity, which was found to be in a similar range also with other compounds. This behaviour of Tenax, favouring sorption at low gas concentrations, will be the subject of further studies.

REFERENCES

1 H. Hachenberg and A. P. Schmidt, *Gas Chromatographic Headspace Analysis*, Heyden, London, Philadelphia, Rheine, 1977.
2 B. Kolb, *Applied Headspace Chromatography*, Heyden, London, Philadelphia, Rheine, 1980.
3 K. Schoene, J. Steinhanses and U. Wienand, *J. Colloid Interface Sci.*, 91 (1983) 595.
4 K. Schoene and J. Steinhanses, *Fresenius' Z. Anal. Chem.*, 321 (1985) 538.
5 K. Schoene, W. Böhmer and J. Steinhanses, *Fresenius' Z. Anal. Chem.*, 319 (1984) 903.
6 D. Hochrainer and M. Spiekermann, in preparation.
7 C. E. Rogers, V. Stannett and M. Swarc, *J. Polym. Sci.*, 45 (1960) 61.
8 N. N. Li and R. B. Long, *Am. Ind. Chem. Eng. J.*, 15 (1969) 73.
9 A. S. Michaels and H. J. Bixler, *J. Polym. Sci.*, 50 (1961) 393.
10 C. E. Rogers, in J. Comin (Editor), *Polymer Permeability*, Elsevier Applied Science Publ., London, New York, 1986, p. 31.

Journal of Chromatography, 455 (1988) 77–93
Elsevier Science Publishers B.V., Amsterdam — Printed in The Netherlands

CHROM. 20 920

RETENTION REPRODUCIBILITY OF BASIC DRUGS IN HIGH-PERFORMANCE LIQUID CHROMATOGRAPHY ON A SILICA COLUMN WITH A METHANOL–AMMONIUM NITRATE ELUENT

BATCH-TO-BATCH REPRODUCIBILITY OF THE STATIONARY PHASE

ROGER M. SMITH*, TONY G. HURDLEY and JAMES P. WESTLAKE
Department of Chemistry, Loughborough University of Technology, Loughborough, Leics. LE11 3TU (U.K.)
and
RICHARD GILL and M. DAVID OSSELTON
Central Research Establishment, Home Office Forensic Science Service, Aldermaston, Reading, Berks. RG7 4PN (U.K.)
(First received June 9th, 1988; revised manuscript received August 23rd, 1988)

SUMMARY

The effect of changing the brand and batches of the silica stationary phase used with a methanol–aqueous ammonium nitrate eluent for the high-performance liquid chromatographic separation of basic drugs has been studied. Considerable care had to be taken to obtain a reproducible eluent and the effect of small changes in the concentration of the ammonia solution were examined closely. Large differences in both the capacity factor and relative capacity factors were found for separations on columns packed with four different brands of silica. Significant differences were also observed with columns containing eighteen different batches of Spherisorb S5W, which had been manufactured over a period of several years.

INTRODUCTION

Although high-performance liquid chromatography (HPLC) is a very reliable technique for analytical work, intra- and interlaboratory reproducibility of separations can be very poor. With care, reproducible conditions of eluent composition and temperature can be maintained but different commercial brands of packing material or different batches of the same brand can cause variations in overall retention times and selectivities. Over the past few years manufacturers have improved batch-to-batch reproducibility but occasional changes, often unannounced, in the manufacturing processes have caused some abrupt changes to the chromatographic behaviour of packing materials[1,2]. Differences between brands of reversed-phase column packings are often large, because of differences in the chemistry of the bonding reactions and the degree of end-capping. There can also be differences in the underlying silica material.

As part of a series of studies aimed at investigating the reproducibility of retentions in the HPLC analysis of drugs, the separations of barbiturates[3], local anaesthetics[4] and thiazide diuretics[5] on ODS-Hypersil and other brands of octadecyl bonded silica have been compared. There were considerable differences between different brands but the results on different batches of ODS-Hypersil were very reproducible.

These studies have now been extended to a detailed examination of basic drug separations on silica columns using a methanol–aqueous ammonium nitrate eluent[6]. The effects on the capacity factors and relative capacity factors caused by small changes in the eluent composition and the operating conditions have been examined on a single batch of Spherisorb S5W silica. These studies showed that for consistent results it was necessary to carefully control the composition of the eluent (in particular the pH and the ionic strength) and the column temperature. The reproducibility of the retentions observed on four columns prepared from the same batch of silica suggested that, with care, reliable results could be obtained. This method was then examined in a collaborative study using the same single batch of silica[7]. The results, showed that, as expected from an earlier study on ODS-silica, relative capacity factors gave much better reproducibility than capacity factors. However, the variations were still much greater than in the study within a single laboratory and it was considered that probable causes were differences in the column temperatures and in the concentration of the ammonia solutions used to prepare the eluent. Further confirmation of the interlaboratory variation has also come from a more recent international collaborative study of the same system[8].

In the present paper, the effects of different brands of column material have been studied and differences were noted between batches of a single brand of silica. In order to test the long term reproducibility of the separation, a single column was then examined in order to assess the influence on the separation of small changes in the concentration of the ammonia solution with time due to evaporation. These results were compared with the effect of making deliberate large changes in the proportion of ammonia. These studies enabled the expected range of results for a single batch of silica under controlled conditions to be established, which was then compared with the batch-to-batch variation within a single brand of silica.

In a previous report, in which this type of HPLC system was used, it was noted that retentions on different brands of silica packing material were markedly different[9]. Similar variations between analyses on different brands of silica have also been observed with a related eluent system based on the use of methanolic perchloric acid[10] but different batches of the same brand were found to give very similar retentions for a large number of compounds[11].

EXPERIMENTAL

Chemicals and standards

Ammonium nitrate was analytical reagent-grade, methanol was HPLC-grade, and ammonia was 0.880 laboratory grade from FSA Laboratory Supplies (Loughborough, U.K.). Samples of basic drugs were from the reference collection of the Central Research Establishment, Home Office Forensic Science Service.

HPLC equipment

HPLC separations were carried out using a Pye Unicam Model 4020 pump and an Altex Model 153 fixed-wavelength detector (254 nm). The samples (5μl) were injected using a 7125 Rheodyne valve onto a Shandon column (25 cm × 5 mm I.D.) packed with silica. The eluent was pumped at 2 ml min^{-1} and was passed through a pre-column, which was installed between the pump and the injection valve, packed with silica. The pre-column and the analytical column were maintained at 30°C in a circulating water bath. The eluent consisted of methanol–aqueous ammonium nitrate buffer (9:1, v/v) and the buffer was prepared by mixing 0.880 concentrated ammonia (90 ml), ammonium nitrate (27 g) and water (900 ml). The retention times were determined using a Hewlett Packard Model 3390 integrator. The column void volume (t_0) was determined using an injection of sodium nitrate (30.0 mg ml^{-1}) in methanol–water (9:1, v/v). At the end of each working day the column was flushed with methanol–water (9:1, v/v).

Silica column packing materials

Spherisorb S5W, 5-μm (Numerous batches, see Table IV), was obtained from Phase Separations (Queensferry, U.K.); Hypersil, 5-μm, from Shandon Southern Products (Runcorn, U.K.); Partisil, 10-μm, from Whatman (Maidstone U.K.); LiChrosorb, 5-μm, from Merck (Darmstadt, F.R.G.).

In each case the material was slurry packed, using methanol to disperse the silica. Shandon Southern columns (250 × 5 mm I.D.) were used. Each column was equilibrated with eluent before use until consistent retention results were obtained.

Standard test solutions of basic drugs

Eight test solutions were made up as mixtures, each including protriptyline hydrochloride as an internal standard, in ethanol–water (90:10, v/v) with concentrations (0.02–8 mg ml^{-1}) chosen to give a similar detector response for each drug[6]: (A) Caffeine, imipramine hydrochloride, morphine hydrochloride, methylamphetamine hydrochloride and protriptyline hydrochloride. (B) Cocaine hydrochloride, phentermine, ephedrine and protriptyline hydrochloride. (C) Diazepam, propranolol, nortriptyline hydrochloride and protriptyline hydrochloride. (D) Amitriptyline hydrochloride, prolintane hydrochloride, phenylephrine bitartrate and protriptyline hydrochloride. (E) Nitrazepam, chlorpromazine hydrochloride, pipazethate hydrochloride and protriptyline hydrochloride. (F) Dextropropoxyphene hydrochloride, amphetamine sulphate, pholcodine and protriptyline hydrochloride. (G) Papaverine, dipipanone hydrochloride, codeine phosphate, methdilazine hydrochloride and protriptyline hydrochloride. (H) Procaine hydrochloride, promazine, ethoheptazine citrate, protriptyline hydrochloride and strychnine.

Simplified test mixture

For much of the work a simplified test procedure was developed involving eight test drugs and requiring the injection of four solutions. The detailed composition of these solutions are [concentrations in mg ml^{-1} in ethanol–water (90:10)]: (A) Dipipanone hydrochloride (0.40), prolintane hydrochloride (1.24), protriptyline hydrochloride (0.15) and strychnine (0.07). (B) Promazine (0.006), phenylephrine bitartrate (1.44) and protriptyline hydrochloride (0.15). (C) Codeine phosphate (1.07), ephe-

drine (2.25) and protriptyline hydrochloride (0.15). (D) Sodium nitrate [30 mg ml^{-1} in methanol–water (90:10)].

Calculations

All the retention times were measured in duplicate and the capacity factors were calculated as $k' = (t_r - t_O)/t_O$. Relative capacity factors were calculated as k'/k'_P, where k'_P is the capacity factor for the protriptyline present as an internal standard in each test solution.

Principal components analysis

Multivariant principal components analyses on the covariance matrix were carried out using the GENSTAT programs Version 4.03 on a Honeywell Multics computer at Loughborough University.

RESULTS AND DISCUSSION

In order to reduce the total number of packing materials in use in U.K. forensic science laboratories, thus allowing rapid transfer of methods between different laboratories, all work involving silica columns has been adapted to use Spherisorb S5W. Furthermore all laboratories were supplied from a single batch of this packing material and this material was used in the previous investigation of the effect of altering the eluent[6] and in the interlaboratory collaborative study[7].

In the present study on the separation of basic drugs it was important to determine if the results obtained with Spherisorb S5W silica would differ greatly if other brands of packing material were used and to consider whether consistent results might be obtained on subsequent batches of Spherisorb S5W once the present stocks are exhausted.

In the preceding studies on the reproducibility of retentions with the present HPLC system, it was found that relative capacity factors compared to an internal standard gave more reproducible results than capacity factors[6]. The latter are very dependent on the value determined for the column void volume whereas relative methods are virtually independent of this measurement. This study also showed that if the aqueous buffer solution was prepared by taking a specified mass of ammonium nitrate and a fixed volume of concentrated ammonia, the pH of the solution was very reproducible. Repeated analyses on four columns prepared over a short period from the same batch of Spherisorb silica gave very consistent results[6]. As no bonding reactions are involved in the production of silica packings it was expected that these materials might be more uniform in their selectivity than alkyl bonded silica columns, although the overall retention times might alter due to differences in surface area and pore size.

Different brands of packings material

Different brands of silica differ in particle shape (spherical or irregular), pore size, and the pH and chemistry of their surface[12,13]. In some studies, these differences appeared to have little effect on the retention properties and only minor variations between brands have been reported[14]. To determine if these factors would affect the retentions and selectivity of the basic drug separation, four different brands of silica

were tested, two with spherical (Hypersil and Spherisorb) and two with irregular particles (LiChrosorb and Partisil). The results are presented in the order of elution on Spherisorb S5W (Table I). The differences in the capacity factors of the drugs were often large and the order of elution differed between materials. The results on one column material could not therefore be easily compared directly with results on another material.

If the relative capacity factors were calculated using protriptyline as the internal standard, the results for many of the analytes were very similar on the four columns suggesting that the differences were mainly in their overall retention power (Table I). However, significant differences were still present for a number of compounds, in particular dipipanone, prolintane, codeine, pipazethate, phenylephrine and strych-

TABLE I

REPRODUCIBILITY OF CAPACITY FACTORS AND RELATIVE CAPACITY FACTORS OF BASIC DRUGS ON DIFFERENT BRANDS OF SILICA PACKING MATERIAL

Eluent, methanol–ammonium nitrate (90:10); temperature 30°C. Column packing materials: Sph, Spherisorb S5W (batch No. 2752 mean value from four columns[6]); Hyp, Hypersil, 5-μm; Part, Partisil, 10-μm; Lich, LiChrosorb, 5-μm.

Compound	*Capacity factors*				*Relative capacity factors (× 100)*			
	Sph	*Hyp*	*Part*	*Lich*	*Sph*	*Hyp*	*Part*	*Lich*
Diazepam	0.02	0.03	0.03	0.03	1.3	2.3	1.7	1.5
Nitrazepam	0.02	0.03	0.03	0.03	1.3	2.3	1.7	1.5
Papaverine	0.06	0.04	0.05	0.04	2.6	3.1	2.9	1.9
Dextropropoxyphene	0.09	0.05	0.06	0.06	4.5	3.8	3.4	2.9
Caffeine	0.10	0.08	0.14	0.14	5.0	6.1	8.0	6.8
Cocaine	0.11	0.07	0.09	0.10	6.0	5.4	5.1	4.9
Procaine	0.17	0.11	0.16	0.20	8.8	8.5	9.1	9.7
Amitriptyline	0.39	0.27	0.37	0.44	19.9	20.8	21.1	21.4
Chlorpromazine	0.44	0.30	0.40	0.48	22.4	23.1	22.9	23.3
Propranolol	0.44	0.27	0.37	0.43	22.5	20.8	21.1	20.9
Dipipanone	0.45	0.21	0.19	0.25	22.9	16.2	10.9	12.1
Imipramine	0.60	0.43	0.57	0.66	31.1	33.1	32.6	32.0
Phentermine	0.61	0.40	0.55	0.64	31.4	30.8	31.4	31.1
Amphetamine	0.69	0.47	0.66	0.77	35.6	36.1	37.7	37.4
Promazine	0.75	0.53	0.70	0.85	38.5	40.8	40.0	41.3
Codeine	0.91	0.67	0.94	1.07	46.6	51.5	53.7	51.9
Prolintane	0.93	0.55	0.58	0.73	47.7	42.3	33.1	35.4
Morphine	0.96	0.71	1.02	1.15	49.7	54.6	58.3	55.8
Pipazethate	1.07	0.69	0.75	0.89	54.9	53.1	42.9	43.2
Nortriptyline	1.19	0.81	1.12	1.30	60.9	62.3	64.0	63.1
Ethoheptazine	1.19	0.86	1.16	1.36	61.1	66.1	66.3	66.0
Pholcodine	1.23	0.88	1.25	1.40	63.4	67.7	71.4	68.0
Phenylephrine	1.24	0.87	1.37	1.52	63.8	66.9	78.3	73.6
Methdilazine	1.32	0.95	1.25	1.45	67.9	73.1	71.4	70.4
Ephedrine	1.35	0.93	1.31	1.50	69.5	71.5	74.9	72,8
Methylamphetamine	1.54	1.06	1.47	1.69	79.1	81.5	84.0	82.0
Protriptyline	1.94	1.30	1.75	2.06	100.0	100.0	100.0	100.0
Strychnine	2.71	1.88	2.26	2.55	139.5	144.6	129.1	123.8

nine. In most of these cases, the two columns packed with irregular silica (Partisil and LiChrosorb) gave lower relative capacity factors than the spherical silica materials (Hypersil and Spherisorb). Codeine and particularly phenylephrine, both of which contain phenolic groups, which will be ionised in the eluent, showed an opposite behaviour. In their study on the characterization of silicas, Engelhardt and Müller[12] found that aqueous suspensions of the irregular materials, Partisil and LiChrosorb, had pH values of 7.2 and 7.8 while the spherical materials, Spherisorb and Hypersil, had pH values of 9.0 and 9.5. Comparable experimental values were obtained with the present packing materials on initial suspension in water; Partisil, 6.72; LiChrosorb, 7.64; Hypersil, 8.96 and Spherisorb (batch 2752), 9.59. As these values are similar to the pH of the eluent, 9.39, and to the pK_a values of the compounds which appear to be sensitive to the different silicas, it suggests that small differences in the degree of ionisation of the silica surface or the degree of interaction with the analytes may cause these effects. Except for codeine, these anomalous compounds had also shown unusual behavior on changing the pH or ionic strength of the eluent with a single Spherisorb column[6].

Thus to obtain comparable results in interlaboratory studies or for the establishment of a database of retention values it will be necessary to standardise on a single brand of packing material.

Comparison of different batches of Spherisorb S5W

Consistent retentions were obtained in the first part of the present study with different columns packed with the same batch of Spherisorb S5W[6] and it was initially anticipated that different batches would also be very similar. However, when results on Spherisorb S5W batch No. 2752, which had been used as the standard material in U.K. forensic science laboratories and was used in the preceding paper[6], were compared with results on a column prepared from Spherisorb S5W batch No. 4488, the capacity factors (Fig. 1) and relative capacity factors of some test compounds were markedly different. The previous study had shown that no systematic changes in overall retention or selectivity occurred with the use of the HPLC columns over many weeks and thus it appears that we are dealing with permanent differences in the chromatographic properties in the silicas. Although for many compounds the relative capacity factors, which should be independent of overall changes in retention properties, on the new batch of Spherisorb were very similar, much larger values were obtained for prolintane (62.1 compared to 47.7), pipazethate (66.3 compared to 54.9) and strychnine (155.8 compared to 139.5) but a lower value was found for phenylephrine (58.5 compared to 63.4). Except for strychnine these are compounds which have previously been found to be particularly sensitive to changes in the separation conditions[6] and are also sensitive to different brands of column material (Table I).

To ensure that the observed differences between these two batches were not isolated phenomena, the variation in retention on a further eight batches of Spherisorb silica manufactured over a period of years were compared (Table II). As with earlier work large variations were observed for drugs with very short retentions ($k' < 0.4$) but these are primarily due to the errors of measuring small values. For the more strongly retained compounds ($k' > 0.4$), the coefficients of variation (C.V.) for the capacity factors on these columns were much larger (8–23%) than the C.V. values for the same compounds on columns prepared from a single batch (1–3%)[6]. The relative

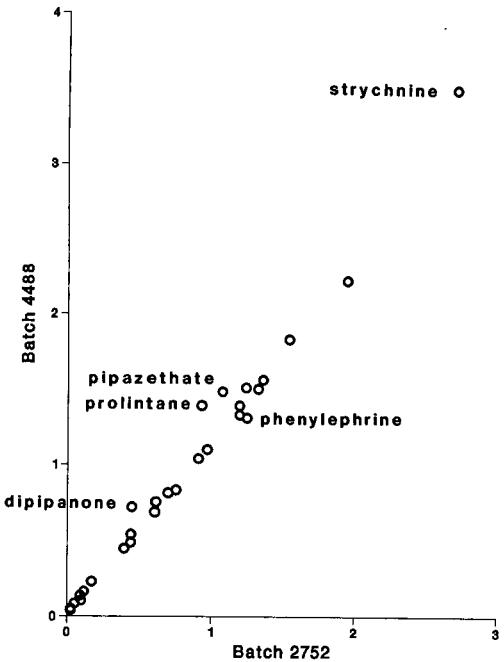

Fig. 1. Comparison of capacity factors for basic drugs on two batches of Spherisorb S5W (Nos. 2752 and 4488). Anomalous compounds labelled.

capacity factors should compensate for any changes due to the overall retentive capacity of the columns and for most of the basic drugs the variations were much smaller (Table II). However, a number of compounds, dipipanone, pipazethate, phenylephrine, prolintane and strychnine, still showed particularily large C.V. values (4–15%). These are the same compounds which were anomalous in the initial comparison of two batches (Fig. 1). In some cases the differences between the different batches of Spherisorb S5W were sufficiently large to cause changes in elution order involving these anomalous drugs. The pH of aqueous suspensions of the Spherisorb batches were measured and compared but although the initial values varied from pH 9.19 to 9.70 no correlation was found between these results and the retention properties. Clearly, the results obtained on one batch could not be used for identification purposes on a different batch even if expressed as relative capacity factors.

It therefore appears that certain compounds and probably certain functional groups are particularly sensitive to the differences between different brands and batches of silica packing material and also to changes in the mobile phase. Thus these compounds could be potentially useful in the characterisation and testing of silica materials for reproducibility. It was desirable to identify a few compounds which show particularly characteristic retention variations and which could be used as marker compounds to simplify testing procedures. The relative factors for all 28 compounds on all ten batches were therefore examined using a multivariant principal components analysis in order to identify which compounds contributed most significantly to the overall variance between the batches.

TABLE II

REPRODUCIBILITY OF CAPACITY FACTORS AND RELATIVE CAPACITY FACTORS OF BASIC DRUGS DETERMINED ON TEN DIFFERENT BATCHES OF SPHERISORB S5W

Based on columns prepared from ten different batches of packing material. Eluent, methanol-aqueous ammonium nitrate (90:10); temperature, 30°C. S.D. = Standard deviation.

Compound	*Capacity factors*			*Relative capacity factors (× 100)*		
	Mean	*S.D.*	*C.V. (%)*	*Mean*	*S.D.*	*C.V. (%)*
Diazepam	0.03	0.01	33.0	1.6	0.3	18.7
Nitrazepam	0.03	0.01	33.0	1.5	0.4	26.7
Papaverine	0.06	0.01	16.7	2.9	0.5	17.4
Caffeine	0.10	0.01	10.0	4.7	0.3	6.4
Dextropropoxyphene	0.11	0.02	18.2	5.6	1.0	17.9
Cocaine	0.14	0.02	14.3	6.4	0.6	9.3
Procaine	0.19	0.03	15.8	9.1	0.5	5.5
Amitriptyline	0.42	0.04	9.5	19.9	0.4	2.0
Chlorpromazine	0.46	0.04	8.7	22.0	0.5	2.2
Propranolol	0.49	0.06	12.2	23.0	0.8	3.4
Dipipanone	0.59	0.14	23.7	27.5	4.2	15.3
Imipramine	0.66	0.06	9.1	31.0	0.5	1.6
Phentermine	0.69	0.08	11.6	32.6	0.8	2.4
Amphetamine	0.76	0.08	10.5	36.1	0.3	0.8
Promazine	0.80	0.06	7.5	37.9	1.0	2.6
Codeine	0.98	0.09	9.2	46.3	1.1	2.3
Morphine	1.05	0.09	8.6	49.4	1.2	2.4
Prolintane	1.16	0.22	19.0	54.3	5.9	10.8
Pipazethate	1.26	0.20	15.9	59.4	4.5	7.6
Nortriptyline	1.28	0.11	8.6	60.5	0.8	1.3
Phenylephrine	1.29	0.10	7.7	61.3	2.6	4.2
Ethoheptazine	1.30	0.13	10.0	61.6	1.2	1.9
Pholcodine	1.37	0.15	10.9	64.7	1.8	2.7
Methdilazine	1.41	0.14	10.0	67.4	1.4	2.1
Ephedrine	1.47	0.14	9.5	69.6	0.7	1.0
Methylamphetamine	1.70	0.18	10.6	80.6	0.9	1.1
Protriptyline	2.12	0.20	9.4	100.0	–	–
Strychnine	3.11	0.42	13.5	146.5	7.0	4.8

Because overall differences in the retention capacity of columns contribute to the values of capacity factors, the relative capacity factors were chosen as the more usefull comparison for changes in selectivity. A plot of the loading factors from the principal components analysis showed that the loadings for most of the compounds in the first two components were very small and they were clustered near the origin. However, the five anomalous compounds (dipipanone, prolintane, pipazethate, phenylephrine and strychnine) identified earlier showed much larger loadings and could be identified as being primarily responsible for the variance between columns (Fig. 2). In the contributions to the first principal component the weighting of phenylephrine (+0.18) was of the opposite sign to the other anomalous compounds, dipipanone (−0.36), pipazethate (−0.39), prolintane (−0.52) and strychnine (−0.60). All the other test compounds had loadings in the first component of less than ± 0.12. As the

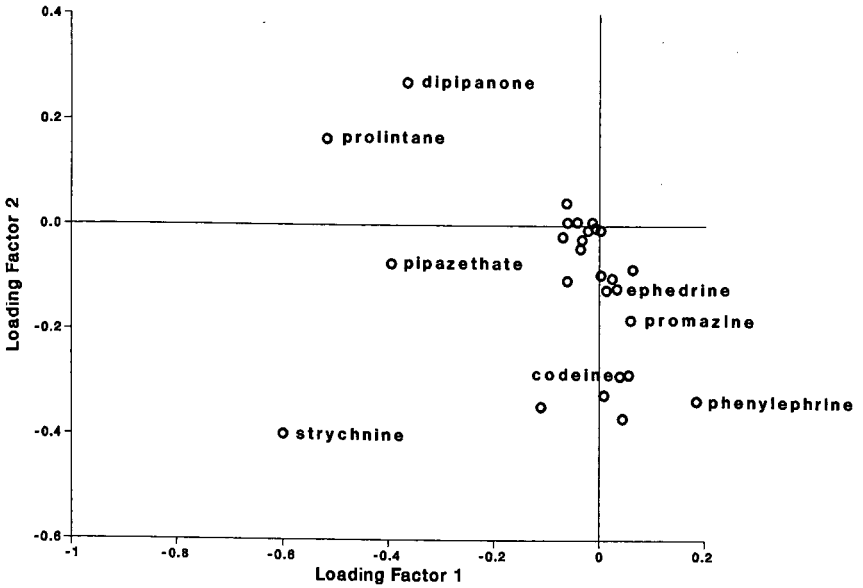

Fig. 2. Loading plot of basic drugs in principal components analysis of relative capacity factors of 27 basic drugs on ten batches on Spherisorb S5W.

first principal component accounted for almost all the variance (88.8%) in the retention of the basic drugs, it appeared that the differences between columns were primarily due to a single cause. In most cases the same anomalous compounds also contributed significantly to the second principal component.

All these columns were nominally the same material and would have satisfied the conventional quality control criteria applied by the manufacturer. It thus appears that the current HPLC system involving the separation of the basic drugs is a more severe test for silica columns than the tests which are usually used for quality control which generally involve normal phase separations. This difference probably arises because the mode of separation of the drugs involves ion-exchange and ion-pair interactions[7].

Selection of a simplified test mixture

In order to extend this study further and examine a wider range of different Spherisorb batches a small group of eight test drugs was selected as characteristic of the original sample set, based upon the results of the principal components analysis. Dipipanone, prolintane and strychnine were chosen as compounds whose retentions were apparently sensitive to changes in the packing material. Because the effect on phenylephrine was in the opposite direction it was also included along with codeine which had shown a large difference in the comparison of different silica brands (Table I). Two compounds, ephedrine and promazine, were included as typical compounds which were largely unaffected by differences in the batches. A set of four new simplified test mixtures was prepared and protriptyline was included in each mixture as an internal standard for the determination of relative capacity factors (see experimental). All the test compounds were well retained and thus not susceptible to small variations in the measurement of the column void volume.

Effect of ammonia concentrations on separation and selectivity

In order to ensure that the differences that were observed between batches were significant, it was necessary to determine the expected range of the results from a single batch over the period of the study as a consequence of small differences in the preparation of the eluent. In particular, it was desirable to estimate the possible effects that would be caused by the loss of ammonia from the stock bottle by evaporation and by deliberate changes in the ammonia concentration such as might be found between bottles from different sources. Although in the previous study it had been found the eluent pH was unaffected by small changes in the ammonia concentration[6], there was concern that the consequential changes in the ionic strength might also alter the selectivity. Also with reference to the interlaboratory study[7], it was concluded that differences in the nominal concentration of ammonia used in the different laboratories could have been a significant factor (together with differences in column temperature) in the greater variations in relative retention that were observed. As the separations observed for many of the original test mixture compounds were unaffected by changes in conditions, the simplified test mixtures were used to monitor the separation.

A single column of Spherisorb S5W (batch No. 2752) was studied over a period of four months. For each separation the eluent was prepared from the same stock bottle of 0.880 concentrated ammonia. The ammonia concentration was determined by titration and dropped from 17.1 to 16.5 *M* during the experiment. A sample of the original solution of concentrated ammonia kept in a sealed bottle showed no loss over this period. A series of nine sets of separations were carried out using the standard conditions over the study period. The relative capacity factors were very consistent and were comparable to those obtained in the repeated runs on a single column on successive days[6]. The standard deviations (Table III) were much smaller than those found in the interlaboratory study[7].

TABLE III

REPRODUCIBILITY OF CAPACITY FACTORS AND RELATIVE CAPACITY FACTORS OF BASIC DRUGS DETERMINED IN REPLICATE SEPARATIONS ON A SINGLE BATCH OF SPHERISORB S5W

Based on single column prepared from Spherisorb S5W batch No. 2752. Eluent, methanol-aqueous ammonium nitrate (90:10); temperature, 30°C. Results are based on nine separations carried over a period of four months.

Compound	*Capacity factors*			*Relative capacity factors (× 100)*		
	Mean	*S.D.*	*C.V. (%)*	*Mean*	*S.D.*	*C.V. (%)*
Dipipanone	0.37	0.02	5.4	20.3	0.8	3.9
Promazine	0.71	0.02	4.2	38.8	1.3	3.4
Codeine	0.88	0.03	3.4	48.2	1.5	3.1
Prolintane	0.88	0.02	2.3	48.2	1.0	2.1
Phenylephrine	1.17	0.04	3.4	64.0	1.5	2.3
Ephedrine	1.28	0.04	3.1	70.1	1.3	1.9
Protriptyline	1.83	0.04	2.2	100.0	–	–
Strychnine	2.65	0.06	2.3	144.4	1.9	1.3

In addition runs were studied in which the ammonia concentration was deliberately increased to 160, 180 and 200% or decreased to 90, 80 and 60% of the specified value (Table IV). The 90% and 80% runs were repeated in triplicate and their variations were similar to those observed using the standard eluent. These larger changes in the eluent had marked effects on the separation and the capacity factors and relative capacity factors increased or decreased correspondingly for the sensitive test compounds. This confirmed that the separation can be very dependent on the ammonia concentration, which would be difficult to control in interlaboratory comparisons. It has lead us to undertake a subsequent examination of alternative eluent compositions with different non-volatile buffer components[15].

Spherisorb comparisons

The retention values for components of the simplified test mixtures on nine further batches of Spherisorb were determined in duplicate. In each case the difference between the replicates was within the range which had been determined for batch No. 2752. The mean capacity factors were combined with the corresponding results from the individual batches examined previously (Table V) and the relative capacity factors were compared (Table VI). These results were then examined using principal components analysis. Almost all of the variance in the relative capacity factors on the different columns was expressed by the first and second principal components (Table VII). The loading factors of the test components were similar to those obtained for the analysis of the original ten batches. The major contributor to the variance (represented by the largest latent vector) was strychnine (0.829). As expected the contributions of ephedrine, codeine and promazine, were very small (latent vectors 0.017, 0.075 and 0.031, respectively) confirming that, relative to an internal standard, little variation had occurred between the different batches. The sensitive compounds (strychnine, prolintane and dipipanone) all showed significant contributions to the variance with the same sign of weighting suggesting a similar interaction. Phenylephrine showed a smaller contribution but with the opposite sign.

The scores for each batch (sum of latent vectors multiplied by the individual deviation for each test compound) for the first and second principal components were plotted (Fig. 3). It was noticeable that there was a progression from the older to the newer batches and the three oldest batches 876, 1290 and 1540 were markedly different from more recent batches. The standard batch (No. 2752) occupied an intermediate position quite different from batch No. 4488 discussed earlier (Fig. 1). Subsequently, the manufacturers have confirmed that this intermediate batch (No. 2752) was produced at a time when a major change occurred in the silica source used for the production of Spherisorb and some minor changes were noted in their own internal quality test[16]. The correlation between the position and the date of manufacture is not as clear with the later batches, except that the batches up to No. 4488 seemed to be bunched separately from those produced later, 5026 to 5615, with the exception of batch No. 5493. Although the majority of the later batches appeared to be grouped in one area, the differences between batches can be sufficiently large to cause inversion of the elution order for some drugs, *e.g.* prolintane and phenylephrine (Table VI).

It was of interest to try to identify common or specific features of the anomalous compounds. Phenylephrine contains a phenolic group, pK_a 8.9, and would therefore be expected to be anionic under the separation conditions so its unique behav-

TABLE IV

EFFECT OF DIFFERENT AMMONIA CONCENTRATIONS ON THE RETENTION OF BASIC DRUGS ON A SINGLE BATCH OF SPHERISORB S5W

Based on single column prepared from Spherisorb S5W batch No. 2752. Standard eluent, methanol–aqueous ammonium nitrate (90:10); temperature, 30°C. Number of runs examined are indicated in parentheses.

Compound	*Capacity factors*							*Relative capacity factors (× 100)*						
	% ammonia relative to standard eluent							*% ammonia relative to standard eluent*						
	60(1)	*80(3)*	*90(3)*	*100*(9)*	*160(1)*	*180(1)*	*200(1)*	*60(1)*	*80(3)*	*90(3)*	*100*(9)*	*160(1)*	*180(1)*	*200(1)*
Dipipanone	0.66	0.45	0.43	0.37	0.24	0.21	0.21	32.2	23.3	22.4	20.3	14.1	13.1	13.7
Promazine	1.01	0.78	0.77	0.71	0.53	0.48	0.63	49.3	40.4	40.1	38.8	31.2	30.0	41.2
Codeine	1.13	0.98	0.96	0.88	0.71	0.67	0.45	55.1	50.8	50.0	48.2	41.8	41.9	29.4
Prolintane	1.29	1.00	0.97	0.88	0.66	0.60	0.52	62.9	51.8	50.5	48.2	38.8	37.5	34.0
Phenylephrine	1.37	1.24	1.25	1.17	1.05	0.99	1.02	66.8	64.2	65.1	64.0	61.8	61.9	66.7
Ephedrine	1.56	1.39	1.37	1.28	1.13	1.07	0.97	76.1	72.0	71.4	70.0	66.5	66.9	63.4
Protriptyline	2.05	1.93	1.92	1.83	1.70	1.60	1.53	100.0	100.0	100.0	100.0	100.0	100.0	100.0
Strychnine	3.64	2.95	2.86	2.65	2.00	1.84	1.72	177.6	152.8	149.0	144.4	117.6	115.0	112.4

* Values from Table III.

TABLE V

CAPACITY FACTORS OF SELECTED BASIC DRUGS ON 18 DIFFERENT BATCHES OF SPHERISORB S5W

Eluent, methanol–aqueous ammonium nitrate (90:10); temperature, 30°C.

Compound	*Capacity factors*																	
	Batch numbers																	
	876	*1290*	*1540*	*2396*	*2579*	*2683*	*2752**	*3112*	*3248*	*3882*	*4488*	*5026*	*5106*	*5115*	*5116*	*5123*	*5493*	*5615*
Dipipanone	0.19	0.36	0.40	0.58	0.64	0.63	0.37	0.68	0.73	0.69	0.72	0.47	0.43	0.49	0.42	0.46	0.80	0.51
Promazine	0.54	0.71	0.68	0.85	0.86	0.79	0.71	0.85	0.86	0.81	0.83	0.79	0.77	0.80	0.76	0.81	0.87	0.77
Codeine	0.67	0.86	0.82	1.03	1.07	0.97	0.88	1.04	1.05	0.99	1.04	1.00	0.98	1.02	0.96	1.02	1.10	0.97
Prolintane	0.53	0.81	0.83	1.16	1.29	1.24	0.88	1.28	1.38	1.30	1.39	1.08	1.03	1.10	1.01	1.10	1.50	1.09
Phenylephrine	1.01	1.13	1.14	1.37	1.41	1.27	1.17	1.41	1.35	1.30	1.31	1.28	1.25	1.30	1.21	1.29	1.45	1.22
Ephedrine	1.04	1.25	1.24	1.54	1.55	1.50	1.28	1.59	1.61	1.51	1.56	1.40	1.36	1.42	1.34	1.41	1.67	1.38
Protriptyline**	1.47	1.79	1.78	2.19	2.25	2.17	1.83	2.28	2.33	2.18	2.24	1.94	1.89	1.96	1.88	1.96	2.39	1.95
Strychnine	1.74	2.45	2.42	3.19	3.49	3.21	2.65	3.36	3.48	3.28	3.49	3.10	3.02	3.21	2.90	3.14	3.82	3.12

* Mean values from Table III.

** Values taken from injection of test mixture H (batch Nos. 1290–2683 and 3112–4488) and mean value of the three simplified test mixtures (batch Nos. 876, 2752 and 5026–5615).

TABLE VI

RELATIVE CAPACITY FACTORS OF SELECTED BASIC DRUGS ON 18 DIFFERENT BATCHES OF SPHERISORB S5W

Eluent, methanol–aqueous ammonium nitrate (90:10); temperature, 30°C. Relative to protriptyline internal standard in each sample mixture.

Compound	*Relative capacity factors (× 100)*																	
	Batch numbers																	
	876	*1290*	*1540*	*2396*	*2579*	*2683*	*2752**	*3112*	*3248*	*3882*	*4488*	*5026*	*5106*	*5115*	*5116*	*5123*	*5493*	*5615*
Dipipanone	12.9	20.1	22.5	26.5	28.4	29.0	20.3	29.8	31.3	31.6	32.1	24.2	22.8	25.0	22.3	23.5	33.5	26.1
Promazine	36.7	39.7	38.2	38.7	38.2	36.4	38.8	37.3	36.9	37.2	37.1	40.7	40.7	40.8	40.4	41.3	36.4	39.5
Codeine	45.6	48.0	46.1	47.0	47.6	44.7	48.2	45.6	45.1	45.4	46.4	51.5	51.9	52.0	51.1	52.0	46.0	49.7
Prolintane	36.0	45.3	46.6	53.0	57.3	57.1	48.2	56.1	59.2	59.6	62.1	55.7	54.5	56.1	53.7	56.1	62.8	55.9
Phenylephrine	68.7	63.1	64.0	62.6	62.7	58.5	64.0	61.8	57.9	59.6	58.5	66.0	66.1	66.3	64.4	65.8	60.7	62.6
Ephedrine	70.7	69.8	69.7	70.3	68.9	69.1	70.0	69.7	69.1	69.3	69.6	72.2	72.0	72.4	71.3	71.9	69.9	70.8
Strychnine	119.0	136.9	136.0	145.7	155.1	147.9	144.4	147.4	149.4	150.5	155.8	159.8	159.8	163.8	154.3	160.2	159.8	160.0

* Mean values from Table III.

TABLE VII

WEIGHTING OF LATENT VECTORS IN PRINCIPAL COMPONENTS ANALYSIS OF RELATIVE CAPACITY FACTORS OF EIGHT TEST DRUG COMPOUNDS ON 18 DIFFERENT BATCHES OF SPHERISORB S5W

Eluent, methanol–aqueous ammonium nitrate (90:10). All remaining vectors had weightings of less than 0.7%.

Compound	*Vector 1 weighting 80.2%*	*Vector 2 weighting 18.6%*
Dipipanone	0.290	0.553
Promazine	0.031	−0.238
Codeine	0.075	−0.385
Prolintane	0.462	0.364
Phenylephrine	−0.084	−0.420
Ephedrine	0.017	−0.160
Strychnine	0.829	−0.393

iour is not unexpected. The three tertiary amines strychnine (pK_a = 8.0), dipipanone (pK_a = 8.5) and prolintane (pK_a unreported but estimated about 8.5) have relatively low pK_a values compared to the pH of the mobile phase (9.39) and would be only slightly ionised compared to many of the more basic amines such as methylamphetamine (pK_a = 10.1). The effects appear therefore to be complex and possibly due to

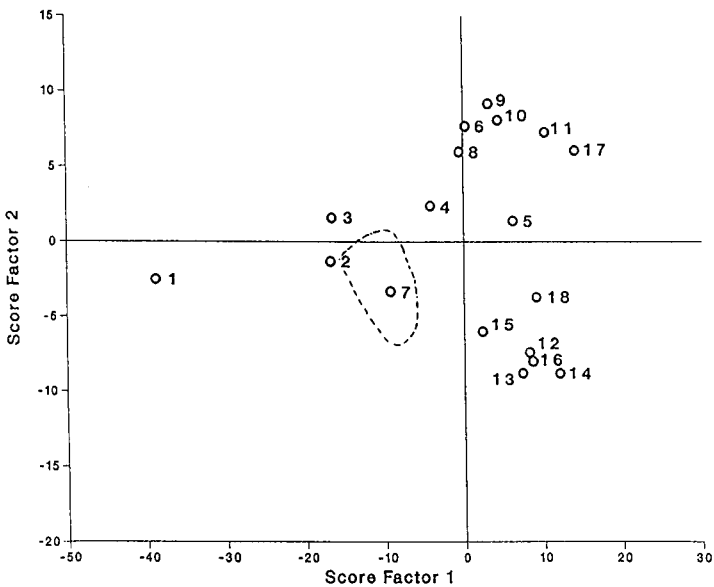

Fig. 3. Comparison of first two principal component scores for relative capacity factors of eight test drugs (dipipanone, promazine, codeine, prolintane, phenylephrine, ephedrine, protriptyline and strychnine) on 18 different batches of Spherisorb S5W: 1, No. 876; 2, No. 1290; 3, No. 1540; 4, No. 2396; 5, No. 2579; 6, No. 2683; 7, No. 2752; 8, No. 3112; 9, No. 3248; 10, No. 3882; 11, No. 4488; 12, No. 5026; 13, No. 5106; 14, No. 5115; 15, No. 5116; 16, No. 5123; 17, No. 5493; 18, No. 5615.

small changes in the steric environment of the basic groups and their interaction with the reactive sites on the silica surface. An attempt had been made previously to examine the separation of similar drugs on silica using a methanol–perchloric eluent but no relationship could be identified between the structures and the changes with eluent composition[9].

In order to compare the reproducibility of the retentions on a single batch with those on different batches the loading factors and mean values from the principal components analysis can be used to calculate the principal component scores for the replicate runs on batch No. 2752 over the four month period and the effects of deliberately changing the ammonia concentration. If these results are plotted on the same axes as the results for the different batches it can be seen that the interbatch results (Fig. 4 and indicated by the dotted line on Fig. 3) confirm that the differences between batches are greater than the variation expected within one batch. Thus, if the conditions are closely controlled real differences in batches can be identified. These results contrast with those obtained in an international collaborative trial in which the variations between columns packed from one batch of silica were as great as the variations between batches[8] although, as already indicated above, the variations in this case may arise from different temperatures and ammonia concentrations.

Similarly if the results from the separations conducted with different ammonia concentrations are plotted the significant effects of the large changes in the ammonia concentration can be seen. The positions on the plot of the three other brands of

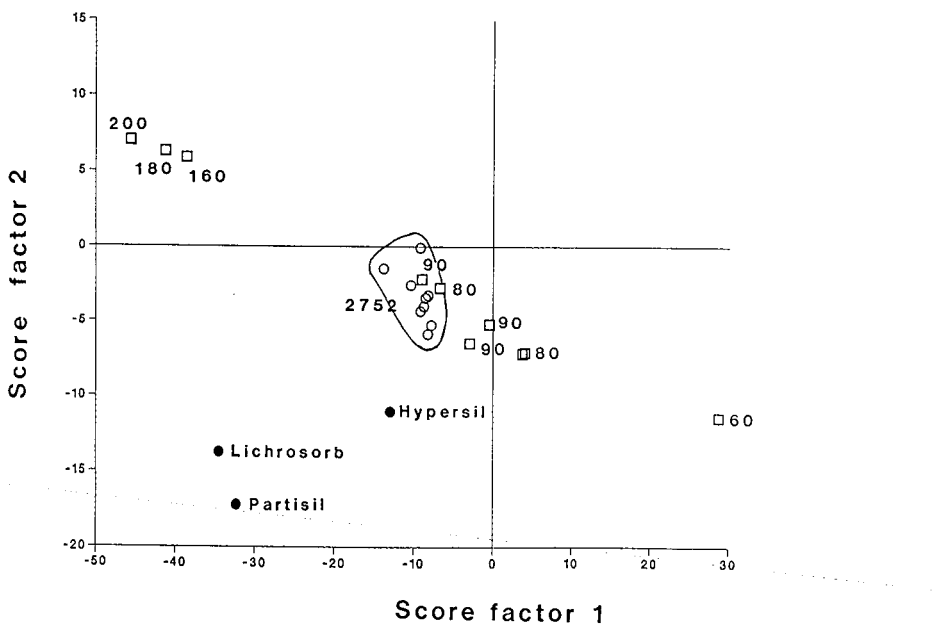

Fig. 4. Calculated first two principal component scores for changes in the conditions of the separation of the simplified test mixtures based on relative capacity factors for seven test drugs (dipipanone, promazine, codeine, prolintane, phenylephrine, ephedrine and strychnine) compared to protriptyline: ○, replicate separations on a single batch of Spherisorb S5W (batch No. 2752); □, different ammonia concentrations as indicated; other brands of silica (●); H, Hypersil; L, LiChrosorb; P, Partisil.

stationary phase can be calculated and, as expected, these are markedly different (Fig. 4).

CONCLUSIONS

With the present HPLC system for basic drugs the large differences in the retention properties of different commercial brands of silica mean that for reproducible results to be obtained in interlaboratory studies each laboratory must standardise on the same brand of packing material. However, the retention properties of several basic drugs have been shown to vary on different batches of a single brand of silica. Consequently standardisation should involve ideally a single batch of packing material. This may be possible within one organisation, as has been achieved in U.K. forensic science laboratories, but poses severe limitations on the generation of retention databases for more general use. The results have shown that batches manufactured over a short period of time can show significant variations and the matching of batches as old materials are used up and replaced by new ones can only be accomplished through trial and error. As yet no simple method can be used to predict which column materials will give similar results.

Subsequently a number of these batches were used in an international collaborative study but the interlaboratory variation obscured any differences between batches confirming that although the ammonia concentration and temperature can be controlled within one laboratory, when different labororatories are involved, the variations can be too large. Work is therefore in progress to devise an alternative mobile phase to increase the robustness of the assay and temperature control would appear to be essential.

ACKNOWLEDGEMENTS

We wish to thank the Science and Engineering Research Council for a CASE studentship to T.G.H. and Phase Separations Ltd. for samples of Spherisorb S5W and for background information.

REFERENCES

1 P. A. Bristow and P. N. Brittain, *Anal. Chem.*, 52 (1981) 1045A.
2 G. S. Murkitt, R. M. Lee and R. D. McDowall, *Anal. Proc.*, 21 (1984) 246.
3 R. M. Smith, T. G. Hurdley, R. Gill and A. C. Moffat, *Chromatographia*, 19 (1984) 407.
4 R. M. Smith, T. G. Hurdley, R. Gill and A. C. Moffat, *J. Chromatogr.*, 355 (1986) 75.
5 R. M. Smith, G. A. Murilla, T. G. Hurdley, R. Gill and A. C. Moffat, *J. Chromatogr.*, 351 (1986) 259.
6 R. M. Smith, T. G. Hurdley, R. Gill and M. D. Osselton, *J. Chromatogr.*, 398 (1987) 73.
7 R. Gill, M. D. Osselton, R. M. Smith and T. G. Hurdley, *J. Chromatogr.*, 386 (1987) 65,
8 R. Gill, M. D. Osselton, R. M. Smith and T. G. Hurdley, *J. Pharm. Biomed. Anal.*, in press.
9 B. Law, R. Gill and A. C. Moffat, *J. Chromatogr.*, 301 (1984) 165.
10 R. J. Flanagan and I. Jane, *J. Chromatogr.*, 323 (1985) 173.
11 I. Jane, A. McKinnon and R. J. Flanagan, *J. Chromatogr.*, 323 (1985) 191.
12 H. Engelhardt and H. Müller, *J. Chromatogr.*, 218 (1981) 395.
13 G. B. Cox and R. W. Stout, *J. Chromatogr.*, 384 (1987) 315.
14 P. Helboe, *J. Chromatogr.*, 245 (1982) 229.
15 R. M. Smith, J. P. Westlake, R. Gill and D. M. Osselton, in preparation.
16 Phase Separations Ltd., personal communication.

Journal of Chromatography, 455 (1988) 95–104
Elsevier Science Publishers B.V., Amsterdam — Printed in The Netherlands

CHROM. 20 913

ULTRASOUND DRIVEN SYNTHESIS OF REVERSED-PHASE STATIONARY PHASES FOR LIQUID CHROMATOGRAPHY USING 4-DIMETHYLAMINOPYRIDINE AS ACID-ACCEPTOR*

KAREN B. SENTELL, KAREN W. BARNES** and JOHN G. DORSEY*
Department of Chemistry, University of Florida, Gainesville, FL 32611 (U.S.A.)
(First received March 29th, 1988; revised manuscript received July 21st, 1988)

SUMMARY

A reproducible new method for synthesizing high density monomeric reversed-phase chromatographic packings based on the use of ultrasonic waves as the driving force for the bonding reaction is presented. The use of ultrasound has two distinct advantages over traditional reflux methods. It provides a reaction driving force that is independent of temperature; in addition, the power of the ultrasonic driving force can be varied using a variable-power ultrasonic probe. The use of a novel acid-acceptor, 4-dimethylaminopyridine, is also recommended in the bonding reaction due to its ease of use and the resulting high bonding densities.

INTRODUCTION

Reversed-phase bonded silicas are the most popular packings used in high-performance liquid chromatography (HPLC). Although the role of the mobile phase in chromatographic retention and selectivity has been extensively investigated, that of the stationary phase has been less studied and as a result the effect of the stationary phase on these chromatographic properties is not yet fully understood. One reason for this dearth of knowledge is the lack of precise and reliable methods for determining bonded phase characteristics such as the density, homogeneity and topographical distribution of the bonded alkyl ligands and the residual hydroxyl groups on the support surface. These properties are a direct consequence of the bulk silica medium and the reagent and reaction conditions for the silanization process[1]. In order to obtain reversed-phase packings with reproducible surface characteristics, the silanization reaction conditions must be painstakingly controlled. Sander and Wise[2] have extensively reviewed the preparation of bonded chromatographic stationary phases.

In the preparation of reversed-phase packings, one objective is the modification of as many surface hydroxyl groups on the silica as possible, especially the highly acidic isolated silanols. These residual isolated silanol groups have been shown to be the main

* Dedicated to Professor T. W. Gilbert on the occasion of his retirement.

** Present address: Shulton Research Division, American Cyanamid, 697 Route 46, Clifton, NJ 07015, U.S.A.

0021-9673/88/$03.50 © 1988 Elsevier Science Publishers B.V.

cause of tailing of chromatographic peaks for basic compounds, of mechanical instability for the packing and of low sample capacity for the column[3,4]. Because of their greater reactivity, di- or tri-functional silanes are sometimes favored over monoreactive silanes, although their use may result in a more complex bonded phase surface. There are a number of possibilities for reaction sites. The silane may simply anchor at two (or three) silica surface sites and yield only a single layer of surface coverage. More likely however, one or more of the leaving groups on the silane will hydrolyze and then react with other leaving groups to form a polymeric network extending out from the silica surface. This polymerization reaction may occur in solution before bonding to the silica surface, after the silane has been bonded to the surface or both. Both the extent of crosslinking and the amount of silane bonded to the surface are very sensitive to the reaction conditions. Sander and Wise[5] have shown that polymeric phases can be made reproducibly; using a single lot of silica and carefully controlling the water content in the reaction mixture, they reported the preparation of four phases with a relative standard deviation (R.S.D.) of only 0.96% in surface coverage. While the polymeric phases do result in a higher carbon content, or more bonded "mass", they are still not free from the secondary interaction of solutes with residual hydroxyl sites. While the silica surface may be totally protected, hydroxyl sites will often occur on the "last" silanes in the polymeric network from hydrolysis of the leaving groups.

Monomeric stationary phases have the advantage of providing a very well defined, single layer of coverage of the silica surface. They also generally exhibit superior column performance to polymeric phases due to their faster solute mass transfer kinetics[6,7]. Commercially available monomeric octadecyl columns have lower bonding densities than polymeric columns, with typical values of 2.5–3.0 μmol/m^2. The bonding reaction for octadecyldimethylchlorosilane, the most commonly used monoreactive silane, is depicted in Fig. 1.

The chromatographic advantages of higher bonded phase surface coverage are severalfold. First, the shielding prevents solute access to the surface and thus minimizes retention due to adsorption on the silica. Second, shielding protects against base hydrolysis of the silica, increasing the stability of the stationary phase. Also, the molecular organization of densely bonded phases more closely resembles that of biomembranes, and may have application as a model system. Increased bonding density may lead to higher chromatographic selectivity; there is some evidence that the improved selectivity for certain compounds offered by polymeric phases is simply a function of the bonding density[5,8–11]. The investigation of selectivity behavior for high density monomeric phases has been difficult because of the limitations imposed by the synthetic methodology; although the average value for the surface hydroxyl concentration of amorphous silica is 8 μmol/m^2 (ref. 12), in practice octadecyl monomeric bonded phase coverages attained under reflux conditions are limited to about 3 μmol/m^2 (refs. 12–15).

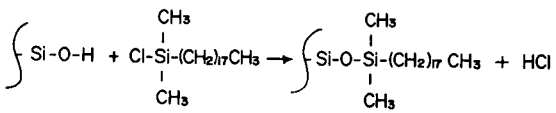

Fig. 1. Bonding reaction for monomeric octadecyl reversed-phase packings.

Jones[16,17] has determined that large excesses of the silanizing reagent, the presence of an acid-acceptor, predrying of the reaction solvent, performing the reactions under an inert gas atmosphere and the use of chlorinated as opposed to hydrocarbon reaction solvents are statistically significant variables which optimize the synthesis of monomeric stationary phases. Kinkel and Unger[1] have studied the roles of the solvent and the base in these monofuctional bonding reactions and have found their choice to be crucial. When alkylhalosilanes are reacted with silica, a base is added to serve as the acid-acceptor, binding the haloacid formed during the reaction and driving the equilibrium to the product side. In addition, the base favorably affects the kinetics of the silanization reaction. Mechanistic studies of these types of reactions[18] have shown that two molecules of base attack one molecule of silane, activating the Si–X bond such that a reactive intermediate and a hydrohalide are formed. Formation of this reactive intermediate greatly increases the kinetics of the bonding reaction; indeed, the addition of the acid-acceptor results in approximately 90% of the total conversion taking place within the first hour of the reaction[1]. In their study, Kinkel and Unger[1] found that the two most effective acid-acceptors for organohalosilanes were imidazole and 2,6-lutidine and that methylene chloride and N,N-dimethylformamide were the most effective solvents for the bonding reaction.

Many organic reactions have been shown to be enhanced by ultrasound[19–24] and reviews of the ultrasonification process and its synthetic applications have recently appeared[25,26]. Boudjouk and Han[27] have shown that in the presence of ultrasonic waves both alkyl and aryl chlorosilanes could be coupled over lithium wire; without ultrasonification, this reaction occurred to no appreciable extent. Reactions at solid–liquid interfaces are also particularly enhanced by ultrasound[19,24]. It is then reasonable to assume that reversed-phase bonding reactions might be facilitated under ultrasonification. The use of ultrasound has two distinct advantages over traditional reflux methods. The ultrasonic waves serve as a driving force which is independent of temperature, allowing reaction temperatures to be varied over any desired range. Secondly, the power of the ultrasonic driving force can be varied by using a variable-power ultrasonic probe.

We have investigated the effect of ultrasound on the silane bonding reaction; the effects of subambient and superambient temperatures on the ultrasonic reaction were also studied. The use of a novel base, 4-dimethylaminopyridine, was investigated as the acid-acceptor.

EXPERIMENTAL

Reagents

All organic solvents used were supplied by Fisher Scientific (Fairlawn, NJ, U.S.A.). Water was deionized, passed through a Barnstead (Boston, MA, U.S.A.) purification system and filtered through a 0.45-μm Nylon 66 membrane (Rainin, Woburn, MA, U.S.A.). The methanol used was HPLC grade; the methylene chloride and diethyl ether were reagent grade. Methylene chloride was dried by stirring over phosphorus pentoxide (Fisher Scientific) for 24 h, followed by distillation under a dry nitrogen atmosphere.

Dimethyloctadecylchlorosilane and trimethylchlorosilane (99.9%) were used as received from Petrarch Systems (Bristol, PA, U.S.A.). The 2,6-lutidine (Sigma, St.

Louis, MO, U.S.A.) was stirred for 24 h over barium oxide (Fisher Scientific) prior to distillation under dry nitrogen atmosphere; 4-dimethylaminopyridine (4-DMAP; Nepera, Harriman, NY, U.S.A.) was oven dried at 80°C for 24 h before use.

The 20–30 μm chromatographic silica was from a single lot of Davisil (W. R. Grace, Baltimore, MD, U.S.A.) synthetic amorphous silica with an average pore diameter of 147 Å and an absolute surface area (S_{BET}, as measured by BET analysis) of 300 m^2/g. The 10-μm Davisil had identical chemical and physical properties to the larger diameter silica. Unless noted otherwise the 20–30 μm silica was used in the bonding reactions. As recommended by Snyder and Kirkland[13] both silicas were acid leached in 0.1 *M* nitric acid at 90°C for 24 h in order to fully hydroxylate the surface and to remove any metal contaminants remaining from the manufacturing process. They were then washed thoroughly with water until all traces of the nitric acid had been removed and dried under vacuum at 240°C for 24 h prior to use in order to remove physically adsorbed water from the surface[28].

Silane bonding reaction

It is essential that the silane bonding reaction be carried out under scrupulously dry conditions in order to prevent the water-initiated dimerization of the silane reagent. Immediately prior to use, presilanized glassware was oven dried at 125°C for at least 4 h in order to remove trace moisture and allowed to cool in a dry box under nitrogen atmosphere. The reagents were mixed together in the dry box and the reaction flasks kept under dry nitrogen atmosphere at all times. Based on Kinkel and Unger's[1] estimation of a maximum of five micromoles of reactive hydroxyl sites per square meter of silica surface, a two-fold excess of the silane reagent was added. A four-fold excess of the base (2,6-lutidine or 4-DMAP) was added both to serve as an acid-acceptor for the hydrogen chloride produced in the reaction and to act as a reactive intermediate at the silica–solution interface. Dry methylene chloride was used as the reaction solvent, using a ratio of 10 ml of methylene chloride per gram of base silica.

The reaction flasks were sonicated by immersion to the flask neck in an ultrasonic cleaning bath (Bransonic model B-2200R-1, Branson Cleaning Equipment, Shelton, CT, U.S.A.) with a power rating of 100 W and a frequency of 55 kHz. Stirring of the reagents within the flasks was accomplished by rotating a magnetic bar submerged in the bath adjacent to the reaction flask, resulting in the corresponding rotation of a magnetic stirring bar within the flask. Temperature control of the reaction vessel immersed in the ultrasonic bath was accomplished by passing a thermostatted solution of ethylene glycol and water through coiled copper tubing lining the inner perimeter of the bath, thereby maintaining a constant temperature bath. The solution was thermostatted by an Endocal or Exacal water bath (Neslab Instruments, Portsmouth, NH, U.S.A.). Refluxed reactions were carried out at 50°C using an oil bath and magnetic stirrer. Control reactions were carried out by stirring the reaction mixture at room temperature. Reactions were carried out for 24 h (as recommended by Kinkel and Unger[1]) unless otherwise noted.

Once the reaction time was complete, each bonded phase product was washed three times with each solvent using the rinse sequence methylene chloride, methanol, methanol–water (50/50, v/v), methanol and diethyl ether. After the ether was allowed to evaporate from the product, the derivatized silica was dried under vacuum at 125°C

for 16–24 h in order to ensure that any adsorbed organic residue from the synthetic procedure was removed. (Caution: It is imperative that the ether be completely evaporated from the product prior to drying the product in the vacuum oven in order to avoid a possible explosion.) Products were analyzed by in-house elemental analysis performed at least in duplicate for each sample. Reliability of the elemental analysis was confirmed by repeated submission of a standard packing material over a two year period; for 66 measurements the resultant absolute standard deviaton was $\pm$ 0.20% carbon.

RESULTS AND DISCUSSION

Synthesis using ultrasonic waves

The first reported use of ultrasound in organic chemistry was in 1938, but it was not until the late 1970's that ultrasound was used to speed reactions in non-aqueous media[19,20]. Ultrasonic radiation can be introduced to the reaction medium either by immersion of the reaction vessel into the liquid of a common laboratory ultrasonic cleaning bath or by introducton of an ultrasonic generating probe directly into the reaction medium. Ultrasonic frequencies span the range of 20 kHz to 10 MHz, with associated acoustic wavelengths of 7.6 to 0.015 cm. Therefore sonochemistry cannot be accounted for in terms of direct coupling of the acoustic field with chemical species on a molecular level[24]. However, the effects of ultrasound can be attributed to three different phenomena. The variation of sonic pressure causes the rapid movement (oscillation) of fluids, subjecting them to compression and rarefaction. Negative pressure in the rarefaction region gives rise to cavitation, the formation and collapse of microbubbles. The violent implosion of these microbubbles generates powerful shock waves with a considerable energy output[19,20,24]. Pressures in the kilobar range and temperatures of 2000–3000°C have been estimated in the region of the collapsing bubble for time periods in the nanosecond range[29]. The third contributing phenomenon is microstreaming, where a large amount of vibrational energy is put into small volumes with little heating[19]. The extremes of temperature and pressure generated by ultrasonic waves cause the generation of free radicals and ions, the dispersion of chemical layers and the promotion of intimate contact between reactants. Emulsification of immiscible liquids and enhanced mass transfer at solid–liquid interfaces are secondary effects of ultrasonification. All of these effects can contribute to the promotion of chemical reactions[19,24].

Effect of ultrasound on bonding reaction

The surface coverage should be expressed as the number of silane molecules attached to the surface, usually as micromoles of bonded silane molecules per square meter of silica surface, taking into account the increase in weight of the silica after the bonding reaction. These surface coverages are calculated from the percentage of carbon as obtained from elemental analysis of the bonded phase[14]. This calculation for monochlorosilanes (the most commonly used monoreactive reagents) can be expressed by

$$\alpha = \frac{\%C \cdot 10^6}{12.011\ n_c S[100 - (\%C/12.011 n_c)(M - 36.5)]} \quad (1)$$

where α is the surface coverage (μmol/m^2); %C is grams carbon per 100 grams bonded silica, as obtained from elemental analysis; n_c is the number of carbon atoms per mole silane; M is the molecular weight of the silane; and S is the surface area of the native silica in m^2/g. Care must be taken in describing the surface structure of polymeric phases. As the polymerization reaction proceeds, it is possible for a reactive silane molecule to anchor at a point more distant from the silica surface. As the degree of polymerization is almost never known, their surface density numbers should be viewed only as a rough indication of true chain density. Sander and Wise[5] state that "the use of surface coverage values to calculate interchain distances is probably not justified for polymeric phases."

Early experiments at ambient temperatures using ultrasound as the driving force and 2,6-lutidine as the acid-acceptor yielded phases of comparable bonding density to those prepared by traditional reflux methods. Lowering the temperature of the reaction and increasing the reaction time gave only a slight improvement in bonding density. The results of these experiments are included in Table I, which will be discussed in detail later.

4-Dimethylaminopyridine as acid-acceptor

There are advantages in the use of 4-DMAP as the acid-acceptor. The presence of the dimethylamino group should serve to make this base better at forming a reactive intermediate with the silane than 2,6-lutidine. In addition it has a relatively high melting point (108–110°C) which allows it to be oven-dried rather than necessitating distillation to remove adsorbed water. The odor of 4-DMAP is also quite mild in comparison to that of 2,6-lutidine.

The first set of experiments using 4-DMAP as the acid-acceptor was performed using methylene chloride as the solvent and dimethyloctadecylchlorosilane as the reactive silane. The reaction mixture was refluxed and stirred at 50.0°C for 24 h. The bonded phase product had an average bonding density ($\pm$ the range for two trials) of

TABLE I

COMPARISON OF SILICA OCTADECYL BONDING DENSITIES.

Reaction conditions are further described in the text.

Reaction conditions	*Temperature (°C)*	*Reaction time (h)*	*C_{18} Bonding density (μmol/m^2)*	
			4-DMAP	*2,6-Lutidine*
Refluxed	50.0	24	3.44	2.82
Ultrasound	28.0	24	–	2.71
Ultrasound	31.0	24	3.35	–
Ultrasound	8.5	101	–	2.84
Ultrasound	4.0	97	3.24	–
Ultrasound	3.0	144	3.60	–
Stirred Only	3.0	144	3.48	–
Refluxed	50.0	144	3.44	–
Ultrasound*	3.0	205	4.07	–
Stirred Only*	3.0	205	3.41	–

* These reactions were performed on 10 μm silica; all others performed on 20–30 μm silica.

3.44 ± 0.02 μmol/m^2, much higher than that achieved in our previous syntheses using 2,6-lutidine (2.82 ± 0.02 μmol/m^2). This bonding density is also greater than that accomplished by Kinkel and Unger[1] (3.34 μmol/m^2) under reflux conditions using methylene chloride and 2,6-lutidine. This is especially significant because the silane in our experiments was used as received from a commercial source; Kinkel and Unger[1] synthesized and then distilled their silane under reduced pressure in order to obtain a reactive silane of the utmost purity. Silane purity has been shown to be a very important factor in obtaining high bonding densities[1]. Additionally, the silica used by Kinkel and Unger[1] had a pore diameter of 250 Å as compared to the 147 Å pore diameter silica used in our work. Sands *et al.*[30] have shown that octadecyl bonding density increases by at least 0.25 μmol/m^2 for every 50 Å increase in pore diameter for pore diameters up to 250 Å.

The second set of experiments using 4-DMAP as the acid-acceptor was run with the same reagents as described above; the reaction mixture was immersed in the ultrasonic bath and stirred at a temperature of 31.0°C for 24 h. The average bonding density of the resultant bonded phases (± the range for two trials) was 3.35 ± 0.05 μmol/m^2, again much higher than we achieved under similar circumstances using 2,6-lutidine as the acid-acceptor (2.71 ± 0.01 μmol/m^2).

At low temperatures bonding density might be enhanced due to increased order (decreased entropy) in a lower temperature system. It is here that the ultrasound reactions are most unique, as they allow the temperature of the reaction to be controlled independently of the ultrasonic driving force. Additionally, low reaction temperatures have been found to enhance reaction yields for ultrasonically catalyzed chemical reactions. One explanation for this phenomenon is that low temperatures cause the vapor pressures of the reactants to be decreased, enabling increased efficiency of ultrasonically produced cavitation[19,20,24]. In order to overcome the slower kinetics expected at lower temperatures, reaction times were increased beyond the usual 24 h time period.

A low temperature ultrasound reaction was carried out under the same conditions as above, with a reaction temperature of 4.0°C for a duration of 97 h. For the two trials, an average bonding density of 3.24 ± 0.01 μmol/m^2 was obtained. A second set of low temperature ultrasound reactions was performed under analogous conditions with a reaction temperature of 3.0°C for 144 h; the average ± the range for the set was 3.60 ± 0.01 μmol/m^2. A third set of low temperature reactions was performed on the 10-μm silica at identical conditions as the second except that the reaction time was lengthened to 205 h. The resultant bonded phase had a much higher bonding density than achieved in any of our previous attempts; the average ± the range was 4.07 ± 0.02 μmol/m^2.

To ensure that the high bonding densities accomplished in these low temperature experiments were a result of the ultrasonic driving force as well as the lengthy reaction time, three control reactions were carried out. In the first, the reaction was performed exactly as the second set above (at 3.0°C for 144 h with stirring) except that the reaction flask was *not* sonicated. In the second, the reaction was stirred for 144 h, but the reaction mixture was refluxed at 50.0°C rather than sonicated. Additionally, a reaction with the 10-μm silica was performed exactly as the third set above (at 3.0°C for 205 h with stirring) except without sonification. From duplicate elemental analyses of each of these materials, the average bonding density (± the range) for the silica stirred (but

not sonicated) at 3.0°C for 144 h was 3.48 ± 0.00 μmol/m^2; that for the silica refluxed and stirred at 50.0°C for 144 h was 3.44 ± 0.03 μmol/m^2, a result virtually identical to that achieved for a 24 h reaction time under refluxed conditions (3.44 ± 0.02 μmol/m^2). The average bonding density (± the range) for the 10-μm silica stirred (but not sonicated) at 3.0°C for 205 h was 3.41 ± 0.02 μmol/m^2. Since the absolute error in the elemental analysis is ± 0.20% carbon, which corresponds to ± 0.03 μmol/m^2 for these octadecyl packings, the differences in bonding density between the materials refluxed at 50.0°C or stirred at 3.0°C for 144 h and the silica which was sonicated at 3.0°C for 144 h (3.60 μmol/m^2) is statistically both real and significant. For the 205 h reaction at 3.0°C with 10 μm silica there is an unequivocal difference between the sonicated (4.07 μmol/m^2) and non-sonicated silica (3.41 μmol/m^2). It should also be emphasized that at these high bonding densities, each small incremental increase in bonding density becomes increasingly harder to accomplish as the maximum attainable bonding density (when steric constraints are considered) is approached. Therefore it can be concluded that subambient ultrasound reactions utilizing 4-DMAP as the acid-acceptor are especially efficacious for synthesizing stationary phases with very high alkyl bonding densities.

In order to investigate the effect of superambient temperatures on the ultrasonic bonding reaction, two types of experiment were performed. In the first, the reaction was carried out by stirring with the same reagents as previously described for a reaction time of 24 h and with the ultrasonic bath maintained at a temperature of 50.0°C. For two trials, the average ± the range was 3.34 ± 0.04 μmol/m^2, virtually identical to that achieved under ambient ultrasonic conditions (3.35 ± 0.05 μmol/m^2). In the second experiment, the reagents were stirred and sonicated at 31.0°C for one hour and then refluxed and stirred at 50.0°C for an additional 23 h, to investigate if the preliminary sonication of the reagents would permit greater accessibility of the reactive silane to silanols located deep within the silica pores. The resulting bonding density (for two trials) of 3.42 ± 0.03 μmol/m^2 is comparable to that achieved under reflux conditions alone (3.44 ± 0.02 μmol/m^2). These results indicate that silica bonding reactions performed in an ultrasonic bath are not affected by superambient temperatures; this is in contrast to those performed at subambient temperatures, which were found to give an increasing yield as the temperature was decreased.

Experiments were also carried out on the 20–30 μm silica in the ultrasonic bath at 28.0°C for 24 h and at 3.0°C for 144 h using trimethylchlorosilane (TMCS) as the reactive silane, 4-DMAP as the base and methylene chloride as the reaction solvent. TMCS is a much smaller molecule than the octadecyl silane and therefore should approximate the maximum bonding density obtainable in these reactions when steric hindrance is minimized. The average bonding density achieved at 28.0°C in 24 h for the two trials was 3.51 ± 0.01 μmol/m^2; that accomplished at 3.0°C in 144 h was 4.25 ± 0.07 μmol/m^2. These experiments show that TMCS bonding densities show a marked increase under subambient ultrasound conditions and that octadecyl densities can approach TMCS ones under these conditions. The results of the 4-DMAP experiments, as summarized in Table I, demonstrate that it is indeed a superior acid-acceptor to 2,6-lutidine for reversed-phase bonding reactions.

CONCLUSIONS

Ultrasonic syntheses performed at subambient temperatures using 4-DMAP as the acid-acceptor have proven to be effective for the production of stationary phases with much higher alkyl bonding densities than are found in commercial packings. Based on our observations from both scanning electron micrographs and column packing experiments, there has been no evidence of silica fracturing by the ultrasound process. Ongoing investigations of these ultrasonic reactions in terms of temperature, acoustic power and the starting silica material will hopefully provide other novel synthetic methods for reversed-phase packings. We are also currently investigating the chromatographic behavior of these ultrasonically produced stationary phases as compared to those prepared using traditional reflux techniques. We have already shown that these high density monomeric stationary phases exhibit enhanced selectivity for isomeric polyaromatic hydrocarbons[11]. The use of 4-DMAP as the acid-acceptor is recommended due to its ease of use and the resulting high bonding densities. The small ranges of the bonding density for duplicate syntheses show that reversed-phase packings with reproducible bonding densities can be synthesized by these methods.

ACKNOWLEDGEMENTS

The authors thank Dr. John Gerdes for suggesting the use of 4-DMAP in the bonding reaction and Nepera, Inc. for supplying samples of the 4-DMAP. K.B.S. is grateful for support from an ACS Analytical Division fellowship sponsored by the Procter and Gamble Company. The authors are grateful for support of this work by NIH GM33382.

The contents of this manuscript are the subject of a United States patent application.

REFERENCES

1 J. N. Kinkel and K. K. Unger, *J. Chromatogr.*, 316 (1984) 193.
2 L. C. Sander and S. A. Wise, *CRC Crit. Rev. Anal. Chem.*, 18 (1987) 299.
3 J. Köhler, D. B. Chase, R. D. Farlee, A. J. Vega and J. J. Kirkland, *J. Chromatogr.*, 352 (1986) 275.
4 J. Köhler and J. J. Kirkland, *J. Chromatogr.*, 385 (1987) 125.
5 L. C. Sander and S. A. Wise, *Anal. Chem.*, 56 (1984) 504.
6 N. H. C. Cooke and K. Olsen, *J. Chromatogr. Sci.*, 18 (1980) 512.
7 L. C. Sander and S. A. Wise, *Anal. Chem.*, 59 (1987) 2309.
8 L. C. Sander and S. A. Wise, *J. Chromatogr.*, 316 (1984) 163.
9 S. A. Wise and L. C. Sander, *J. High Resolut. Chromatogr. Chromatogr. Commun.*, 8 (1985) 248.
10 S. A. Wise and W. E. May, *Anal. Chem.*, 55 (1983) 1479.
11 K. B. Sentell and J. G. Dorsey, *J. Chromatogr.*, (1988) in press.
12 W. Cheng and M. McCown, *J. Chromatogr.*, 318 (1985) 173.
13 L. R. Snyder and J. J. Kirkland, *Introduction to Liquid Chromatography*, Wiley-Interscience, New York, 2nd ed., 1979, Ch. 7.
14 G. E. Berendsen and L. de Galan, *J. Liq. Chromatogr.*, 1 (1978) 561.
15 G. E. Berendsen, K. A. Pikaart and L. de Galan, *J. Liq. Chromatogr.*, 3 (1980) 1437.
16 K. Jones, *J. Chromatogr.*, 392 (1987) 1.
17 K. Jones, *J. Chromatogr.*, 392 (1987) 11.
18 R. J. P. Corriu and C. Guerin, *J. Organomet. Chem.*, 198 (1980) 231.
19 D. Bremner, *Chem. Br.*, 22 (1986) 633.

20 P. Boudjouk, *J. Chem. Educ.*, 63 (1986) 427.
21 B.-H. Han and P. Boudjouk, *Organometallics*, 2 (1983) 769.
22 S. Clough, E. Goldman, S. Williams and B. George, *J. Chem. Educ.*, 63 (1986) 176.
23 B.-H. Han and P. Boudjouk, *J. Org. Chem.*, 47 (1982) 751.
24 K. S. Suslick, *Mod. Synth. Methods*, 4 (1986) 1.
25 J. P. Lorimer and T. J. Mason, *Chem. Soc. Rev.*, 16 (1987) 239.
26 J. Lindley and T. J. Mason, *Chem. Soc. Rev.*, 16 (1987) 275.
27 P. Boudjouk and B.-H. Han, *Tetrahedron Lett.*, 22 (1981) 3813.
28 K. K. Unger, *Porous Silica*, Elsevier, New York, 1979, Ch. 3.
29 C. Sehgal, R. G. Sutherland and R. E. Verral, *J. Phys. Chem.*, 84 (1980) 396.
30 B. W. Sands, Y. S. Kim and J. L. Bass, *J. Chromatogr.*, 360 (1986) 353.

Journal of Chromatography, 455 (1988) 105–117
Elsevier Science Publishers B.V., Amsterdam — Printed in The Netherlands

CHROM. 20 823

GAS PHASE SILYLATION, A RAPID METHOD FOR PREPARATION OF HIGH-PERFORMANCE LIQUID CHROMATOGRAPHY SUPPORTS

PER WIKSTRÖM*, CARL FREDRIK MANDENIUS and PER-OLOF LARSSON
Department of Pure & Applied Biochemistry, Chemical Center, University of Lund, P.O. Box 124, S-221 00 Lund (Sweden)

(First received October 19th, 1987; revised manuscript received May 17th, 1988)

SUMMARY

A new method for preparing chromatographic supports is described. Porous silica was treated with gaseous silanes and gaseous triethylamine at high temperature and reduced pressure. The silylation procedure was rapid and gave supports with a covalently bound monolayer of aminopropyl- or epoxysilane. Diol silica prepared by gas phase silylation was compared with diol silica prepared in the aqueous or organic phase (toluene). Seven proteins were chromatographed and the protein recovery, plate number and peak asymmetry were calculated. Silica prepared by the gas phase silylation method showed improved performance. The separation of carbohydrates on aminopropylsilica and the isolation of lactate dehydrogenase with nicotinamide–adenine dinucleotide–silica, prepared from gas phase silylated diol silica, are described.

INTRODUCTION

Chromatographic supports of inorganic origin, such as silica and controlled pore glass, are usually surface modified with various reagents, for example, alkylsilanes. The silylation procedures applied are usually carried out in organic solvents in the presence of a catalyst such as triethylamine, or in aqueous solution. The procedures often require long reaction times and laborious handling, *e.g.*, drying of solvents, sometimes taking more than 24 h per preparation. Thus, simplification of the procedures is well justified in order to facilitate production of silylated chromatographic supports especially on a larger scale.

Vapour deposition for surface coating for protection of, *e.g.*, painted surfaces, plastics and metal containers, with silane compounds has successfully been employed. Alkylsilanes have been vapour deposited on silicon wafers and on particles by using deposition from condensed silane vapour[1], in condensed thin films[2] or in the gas phase at reduced pressure[3–5]. Attractive features of vapour deposition silylation are the small amount of solvent used and the ease with which monomeric layers are obtained. It has been reported in these studies that the alkyloxysilane reaction requires a reaction time of 12–20 h at elevated temperature. This is longer compared to that in silylation

0021-9673/88/$03.50 © 1988 Elsevier Science Publishers B.V.

methods performed in organic solvents or in aqueous media, and can partially be explained by the absence of the triethylamine catalyst which is used in the solvent methods.

In the present study we have employed a combination of the advantageous properties of vapour deposition (no solvents, monolayer formation) and organic phase/aqueous phase silylation (catalysed reaction) in a new method for preparation of supports for high-performance liquid chromatography (HPLC). This method involves gas phase silylation at reduced pressure and the presence of triethylamine as a catalyst. The silylation reaction is completed within 1–2 h and the total time for the preparation is less than 3 h.

MATERIALS AND METHODS

Materials

LiChrospher Si 300, Si 100, LiChroprep Si 100 and LiChrosorb 100 were obtained from E. Merck (Darmstadt, F.R.G.), 3-Glycidoxypropyltrimethoxysilane (Z-6040) from Dow Corning (Seneffe, Belgium). 3-Aminopropyltriethoxysilane, catalase (bovine liver), lysozyme (chicken egg white), haemoglobin (beef blood), ovalbumin and pepsin (porcine stomach mucosa) were obtained from Sigma (St. Louis, MO, U.S.A.), tresyl chloride (2,2,2-trifluoroethanesulphonyl chloride) from Fluka (Buchs, Switzerland). The nicotinamide–adenine dinucleotide (NAD) analogue, N^6-[N-(2-ami-noethyl)carbamoylmethyl]-NAD, was synthesized according to a previously described method[6].

Gas phase silylation (procedure 1)

Silica was evenly spread in a glass container at the bottom of a heated alumina reactor (Fig. 1). The silica was dried for 1 h at 100–160°C under reduced pressure (< 2 mmHg) using a vacuum pump. Epoxy- or aminosilane was injected with a syringe through a membrane at the top of the reactor. The silylation reaction proceeded for 1–20 h, at a constant temperature in the range 100–160°C. Any excess of silane vapour was finally evacuated from the reactor and the silica cooled to room temperature. In the case of epoxysilylation, coinjection of triethylamine (catalyst) was sometimes carried out.

Gas phase silylation with intermittent hydrolysis of remaining alkoxy groups (procedure 2; recommended procedure)

LiChrospher Si 300 (1.6 g) was placed in the same reactor as above and dried for 1 h at 160°C under reduced pressure using a vacuum pump. Epoxysilane (0.5 ml) and triethylamine (0.25 ml) were injected with a syringe and the reaction was carried out for 1 h at 160°C. Unreacted epoxysilane was removed *in vacuo*. The silica was then removed from the reactor and placed in a test-tube. Water was added and the test-tube placed in a water-bath at 90°C for 15 min (to hydrolyse the remaining methoxy groups). Using a sintered glass funnel, the silica was washed with acetone and again placed in the reactor and dried. The silylation procedure was then repeated.

Aqueous phase silylation

LiChrospher Si 300 (2.0 g) was silylated according to a previously described

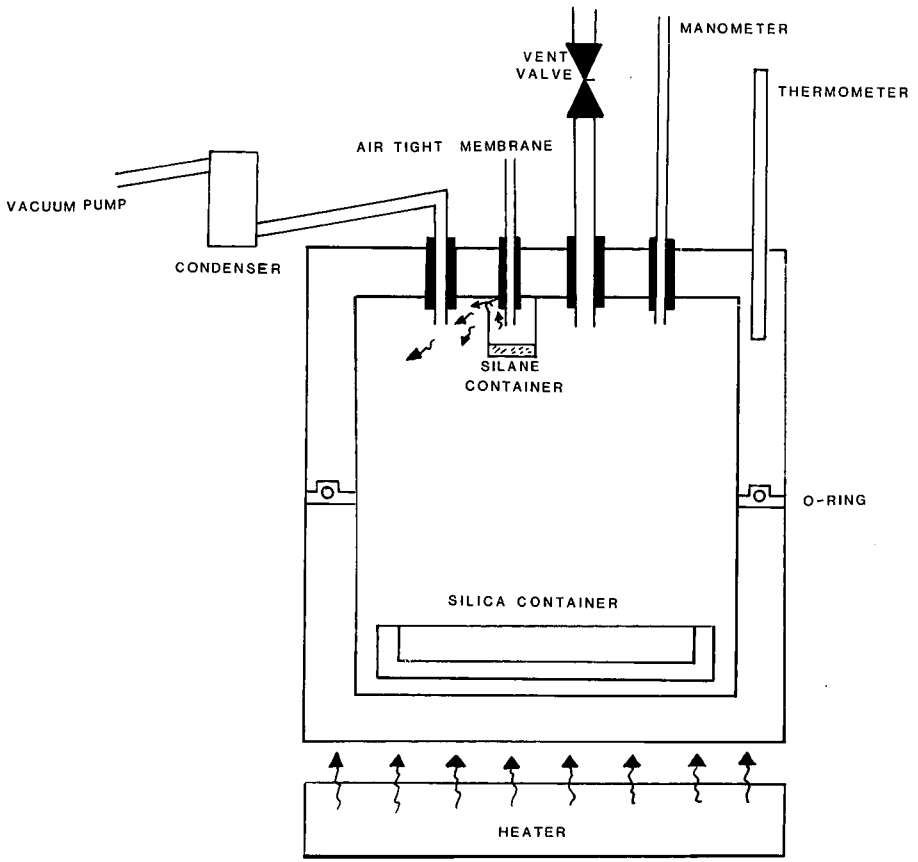

Fig. 1. A cross-section of the silylation apparatus.

method[7]. The silica was stirred for 5 h at 90°C in 10 ml 0.1 *M* sodium acetate, pH 5.5, containing 0.4 ml 3-glycidoxypropyltrimethoxysilane. The silica was subsequently washed with 0.1 *M* sodium acetate, pH 5.5 and water.

Organic phase silylation (epoxysilane)

LiChrospher Si 300 (1.8 g) was dried *in vacuo* for 4 h at 160°C. Toluene (300 ml, sodium dried) was added to the silica followed by 1.1 ml epoxysilane and 100 µl of the catalyst, triethylamine. The slurry was stirred and refluxed under dry nitrogen for 12 h. When the silylation reaction was complete, the amino silica was filtered off and washed extensively with dry toluene, and acetone[8].

Organic phase silylation (aminosilane)

LiChrosorb Si 100 (1.3 g) was dried overnight at 160°C. Toluene (300 ml, sodium dried) was added to the silica followed by 3 ml 3-aminopropyltriethoxysilane. The slurry was stirred and refluxed for 12 h. When the silylation reaction was complete, the slurry was filtered off and washed extensively with dry toluene and acetone[8].

Preparation of diol silica

Epoxysilica was converted into diol silica by suspending the silica in water acidified to pH 2.3 with sulphuric acid and stirred at 90°C for 3 h.

Preparation of NAD-bound silica

The diol silica (LiChrospher Si 300, 1 g) was activated with tresyl chloride, according to a published procedure[9]. For 1 g of dry diol silica, 8 ml of dry acetone, 0.2 ml of pyridine and 0.1 ml of tresyl chloride were used. The slurry was thoroughly mixed and allowed to react on a rocking table for 15 min. The activated silica was washed with 100 ml of acetone, acetone–5 m*M* hydrochloric acid (70:30, 50:50 and 30:70), 5 m*M* hydrochloric acid and 0.2 *M* sodium bicarbonate buffer pH 7.5. The silica gel was then suspended in 8 ml of the same buffer containing 20 mg of N^6-[N-(2-amino-ethyl)carbamoylmethyl]-NAD. The slurry was placed in a sealed test-tube and allowed to react at room temperature for 1 h. Unreacted tresyl groups were then blocked with 0.2 *M* 2-mercaptoethanol pH 7.5, overnight.

Functional group analysis of modified silica

The epoxy group content was determined by reaction with sodium thiosulphate and titration of released hydroxide ions[10]. The amino group content was determined from the picric acid ion-pairing capacity according to Alpert and Regnier[11]. Methyl red dye adsorption was used to give a qualitative measure of the remaining exposed silanol groups on the silica surface[12].

Enzyme assay

Lactate dehydrogenase activity was monitored by the oxidation of NADH at 340 nm and 21°C using puruvate as the substrate. The enzyme was added to an end volume of 3.1 ml, containing 0.21 m*M* NADH and 1.0 m*M* sodium pyruvate in 0.05 *M* sodium phosphate buffer, pH 7.0.

Packing of columns

All columns used were standard HPLC columns with compression fittings. They were packed using the slurry technique[13].

Chromatographic conditions

HPLC equipment from LKB (Bromma, Sweden) was used. Samples (20 μl) were injected in triplicate and emerging proteins were monitored at 280 nm. The data scatter (retention times, peak heights, peak widths) was in all cases within 5%.

RESULTS AND DISCUSSION

Gas phase silylation procedure

The general outline of the gas phase silylation procedure developed here was straightforward: porous silica was placed in a vacuum chamber (Fig. 1) and heated for 1 h to remove any adsorbed water. While maintaining the vacuum, the silane was injected into the chamber, where it vaporized and reacted with the silica. The procedure normally involved coinjection of triethylamine, which catalyzed the silylation reaction, as will be discussed further. Silylation was complete after 1 h at 160°C.

TABLE I

EPOXY- AND AMINOSILANE ADSORPTION ON LICHROSPHER Si 100

Gas phase silylation was carried out as described in Materials and Methods (Procedure 1). Epoxy groups were determined via reaction with sodium thiosulphate and the amino groups were detected by the picric acid ion-pairing capacity method.

Temperature (°C)	*Epoxysilane (μmol/g silica)*	*Aminosilane (μmol/g silica)*
100	530	425
120	640	560
135	550	590
150	490	580

In gas phase silylation, silane is initially deposited on the silica surface and later covalently bound[4], The deposition of epoxy- and aminosilane on LiChrospher Si 100 at temperatures ranging from 100 to 150°C is detailed in Table I. Although the data show some scatter, no temperature effect is seen. The deposition of silane is thus considered to be independent of temperature in the range investigated. Assuming a surface concentration of available silane binding sites of 2 μmol/m^2 silica would result in 500 μmol bound silane per gram for a LiChrospher Si 100 preparation[14,15]. Thus the data in Table I are consistent with the formation of a monolayer at all temperatures investigated, meaning that the transport rate of silane to the surface is sufficient. However, investigation of the stability of the silica indicated insufficient anchoring of the monolayer to the silica surface. For example, washing of the treated beads for 30 min at pH 2 and 70°C resulted in a significant loss of silanes according to the methyl red test. The release of silanes generates free silanol groups, which adsorb methyl red, leading to a coloured silica preparation. Clearly, the deposited silane monolayer must be firmly bound to its support if the gas phase silylation is to be considered a viable procedure.

In previous works concerning gas phase silylation, covalent binding was

TABLE II

EFFECT OF TRIETHYLAMINE (TEA) AND TEMPERATURE ON COVALENT ATTACHMENT OF EPOXYSILANE

Gas phase silylation was carried out as described in Materials and Methods (procedure 1). The silylated silica was treated with acidified water pH 2 for 30 min at 70°C, washed, dried and finally subjected to the methyl red test.

Silica	*Amount (mg)*	*Silane (μl)*	*TEA (μl)*	*Temp. (°C)*	*Time (h)*	*Methyl red colouring*
LiChroprep 100	200	200	–	160	1	Strong
LiChroprep 100	200	200	50	100	1	Strong
LiChroprep 100	200	200	50	100	5	Weak
LiChrosorb 100	200	200	50	100	20	Weak
LiChrosorb 100	200	200	50	160	1	None
LiChrospher 300	1200	1000	500	160	1	None

achieved by increasing the reaction time to 12–24 h[2–4]. We suggest an alternative procedure based on silylation in the presence of the catalyst triethylamine for 1–3 h.

Table II shows the catalytic effect of triethylamine on the silylation reaction. In the presence of triethylamine, silylation occurs at 100°C although the reaction is not complete after 20 h. However, as indicated by Table II, increasing the temperature increases the reaction rate such that silylation of silica of pore size 100 Å and surface area of 250 m^2 at 160°C is complete within 1 h. If the catalyst triethylamine is excluded, insufficient reaction takes place even at 160°C.

Gas phase silylation in the presence of triethylamine has been carried out many times according to the protocols given in Materials and Methods. We have found the protocols reliable, and to give very consistent results.

Chromatographic performance of gas phase silylated silica

In order to characterize the performance of gas phase silylated silica and its general usefulness in comparison to silica produced with other methods, a number of chromatographic tests were carried out. Wide pore (300 Å) silica supports, primarily related to chromatography of proteins which should neither be excluded nor retained by an ideally coated support, were employed. The tests involved recovery studies, plate number calculations and peak asymmetry measurements.

Protein recovery. Protein recovery was chosen as a sensitive measure of anomalies on the silica surface, especially residual unsilylated areas. Seven well characterized proteins with widely different isoelectric points and molecular weights were selected (Table III) as a representative group. To enhance the sensitivity of the test, the amount of proteins injected on the columns was small, 5 μg. Four columns (50 mm × 4.6 mm) were used, packed with diol silica prepared by aqueous silylation, organic phase silylation (toluene), gas phase silylation or by a modified gas phase silylation which involved a second silylation after removal of the methoxy groups introduced in the first silylation step (Procedure 2).

TABLE III

RECOVERY OF PROTEINS FROM DIOL SILICA PREPARED BY DIFFERENT METHODS

The proteins were chromatographed on the diol silica columns and the recoveries calculated from the peaks obtained. Column: 50 mm × 4.6 mm I.D. Temperature: 20°C. Detection: UV, 280 nm. Sample: 0.25 mg/ml injected with a 20-μl loop (5 μg protein). Buffer: 0.05 *M* phosphate buffer pH 7.0 containing 0.1 *M* sodium chloride; flow-rate, 1 ml/min.

Compound	*pI*	*MW (kilodaltons)*	*Recovery (%) after silylation in*			
			Aqueous phase	*Organic phase*	*Gas phase procedure 1*	*Gas phase procedure 2*
Pepsin	2.9	33.0	76	59	75	79
Ovalbumin	4.7	45.0	94	86	94	95
Albumin	5.1	67.0	91	59	70	83
Haemoglobin	7.0	16.0	91	2	45	67
Catalase	8.0	240.0	68	46	54	62
Trypsinogen	9,3	24.0	71	42	59	67
Lysozyme	10.5	14.3	94	6	72	97
Mean value			84	42	67	79

TABLE IV

SILANE SURFACE CONCENTRATION

The silane surface concentration was determined by elemental analysis of carbon.

Method	*Surface concentration (μmol of silane per m²)*
Organic phase	2.8
Aqueous phase	5.8
Gas phase (Procedure 1)	3.2
Gas phase (Procedure 2)	3.7

The recovery varied considerably depending on the protein as well as the silylation method used (Table III). Water-free toluene silylation gave, for all proteins investigated, lower recovery than the other methods. In the case of, for example, lysozyme a particularly low recovery (0.6%) was obtained for the organic phase silylated material. This may be at least partially explained by a strong interaction between the highly positively charged protein and the negative charges of the remaining silanol groups on the silica surface. Other types of interactions, *e.g.*, hydrogen bonds, have also been suggested to take part in irreversible protein adsorption on silica[16].

On the other hand, aqueous phase silylated silica gave a very good recovery of lysozyme (94%), indicating a more complete coating and shielding of any remaining silanol groups. The good recovery accords with the carbon content data in Table IV, where aqueous phase silylated silica is shown to have about twice the carbon content compared to organic phase silylated material. The silane concentration of 5.8 μmol/m^2 obtained for aqueous phase silylation indicates a silica surface covered by more than a monolayer. Clearly, such a multilayer cover would provide a more efficient shielding of silanol groups.

As is also shown in Table III, gas phase silylation gives a fair recovery of 72% for lysozyme, suggesting only a limited amount of non-specific adsorption sites on the silica surface. An even better recovery (97%) was achieved using a silica prepared by the modified gas phase silylation procedure (Procedure 2). The initial gas phase silylation product was treated with water (to hydrolyze unreacted methoxy groups), dried at 160°C and subjected to a second silylation. Additional silanes were thereby bound as indicated in Table IV. The recovery properties of the silica were thereby improved for lysozyme as well as for other proteins to the level of recovery obtained using silica silylated with the aqueous phase method. There may be several explanations for the beneficial effects of a second silylation. The process may result in "end capping" of remaining silanol groups. Another possible explanation would be a more complete engagement of silane-derived silanol groups in the second silylation step.

Table V also gives the k' values obtained, calculated from $k' = (V_e - V_0)/V$ where V_e is the elution volume for the substance under study and V_0 the elution volume for a non-retarded, non-excluded substance (potassium nitrate). Ideally, the k' values for larger molecules like proteins should all be zero or slightly negative for an inert support based on medium pore (300 Å) silica, indicating the absence of attractive

TABLE V

k' VALUES ON DIOL SILICA PREPARED BY DIFFERENT METHODS

k' was calculated by $k' = (V_e - V_0)/V_0$, where V_0 is the elution volume for a non-retarded non-excluded substance (potassium nitrate). Chromatographic conditions as in Table III.

Compound	k'			
	Aqueous phase	*Organic phase*	*Gas phase procedure 1*	*Gas phase procedure 2*
Pepsin	−0.02	0.01	−0.02	−0.04
Ovalbumin	−0.12	−0.10	−0.11	−0.13
Albumin	−0.13	0.45	−0.07	−0.10
Haemoglobin	−0.05		0.11	−0.05
Catalase	−0.08	−0.01	−0.04	−0.08
Trypsinogen	−0.07	0.15	0.03	−0.06
Lysozyme	0.13		2.4	0.14

forces and the presence of a slight size-exclusion effect. However, as is clear from the recovery discussion above, several support–protein combinations behaved far from ideally. This is also reflected in the k' values that in several cases are well above zero. As expected, low recovery often co-varies with high k' values, with some exceptions. For example, lysozyme is fairly strongly retained on gas phase (Procedure 1) silica ($k' = 2.4$) but the recovery is still high (72%). Trypsinogen on the other hand is hardly retained ($k' = 0.03$) but the recovery is lower (59%). The discrepancy probably reflects that several types of binding sites are present on the silica.

Plate number calculations. The number of theoretical plates was calculated for

TABLE VI

PLATE NUMBER FOR DIOL SILICA PREPARED BY DIFFERENT METHODS

Chromatographic conditions as in Table III. The plate number was calculated as described by Kirkland and Snyder[17].

Compound	*Silylation in*			
	Aqueous phase	*Organic phase*	*Gas phase procedure 1*	*Gas phase procedure 2*
Pepsin	3400	2800	4000	4200
Ovalbumin	2300	4200	6900	5700
Albumin	2400	310	2700	2600
Haemoglobin	2600	–	1000	4000
Catalase	1400	2200	2600	1700
Trypsinogen	7500	800	3000	8500
Lysozyme	4200	–	600	4100
Mean value	3400	2100	3000	4400
Nitrate	8600	9500	8700	7500

seven proteins chromatographed on four types of diol silica columns (Table VI). Significant differences between the different types of silica were seen.

The aqueous phase silylation gave high plate numbers for most of the proteins, the average for the seven proteins being 3400 plates/m. A low plate number was observed only for catalase. This very large protein may require a lower flow-rate for satisfactory performance.

The organic phase silylated silica gave somewhat heterogeneous results. Due to heavy adsorption, thus low recovery, the values for lysozyme and haemoglobin could not be calculated. The remaining proteins had plate numbers ranging from 310 (serum albumin) to about 4200 (ovalbumin).

Diol silica prepared by the standard gas phase silylation procedure showed intermediate plate numbers with the exception of lysozyme and haemoglobin. However, the use of twice silylated material improved the plate number considerably, for lysozyme ten times and four times for haemoglobin. This material also showed the highest average plate number of all the preparations, 4400.

Peak asymmetry. Protein peaks are often not "well behaved", *i.e.*, they show considerable tailing and other deviations from the ideal Gaussian distribution. For high resolution work, narrow (high plate number) and symmetric peak (asymmetry factor close to unity) are required. A closer examination of the peak shapes obtained by the gas phase silylated material was therefore considered appropriate. A comparison of asymmetry factors is given in Table VII[17]. The same trend occurs as for the plate numbers described in Table VI, *i.e.*, the best results are obtained with gas phase silylated silica and aqueous phase silylated silica.

The peaks of lysozyme and trypsinogen generated on the four silica preparations are shown in Fig. 2a and b. The amount of protein injected was the same for all columns. Trypsinogen (Fig. 2b) behaves fairly well on all columns. Fig. 2b shows the appearance of lysozyme peaks. Note that the very small peak obtained on silica silylated in the organic phase is due to heavy adsorption onto the silica. Also note the

TABLE VII

PEAK ASYMMETRY FACTORS ON DIOL SILICA PREPARED BY DIFFERENT METHODS

Chromatographic conditions as in Table III. Peak asymmetry factors were calculated as described by Kirkland and Snyder[17].

Compound	*Silylation in*			
	Aqueous phase	*Organic phase*	*Gas phase procedure 1*	*Gas phase procedure 2*
Pepsin	2.2	3.2	3.0	2.6
Ovalbumin	2.2	2.7	1.4	2.4
Albumin	1.4	3.5	2.3	2.2
Haemoglobin	2.7	–	4.1	2.7
Catalase	1.8	2.5	1.8	1.5
Trypsinogen	2.2	5.2	3.1	2.2
Lysozyme	5.5	–	5.0	3.4
Mean value	2.6	3.4	3.0	2.4

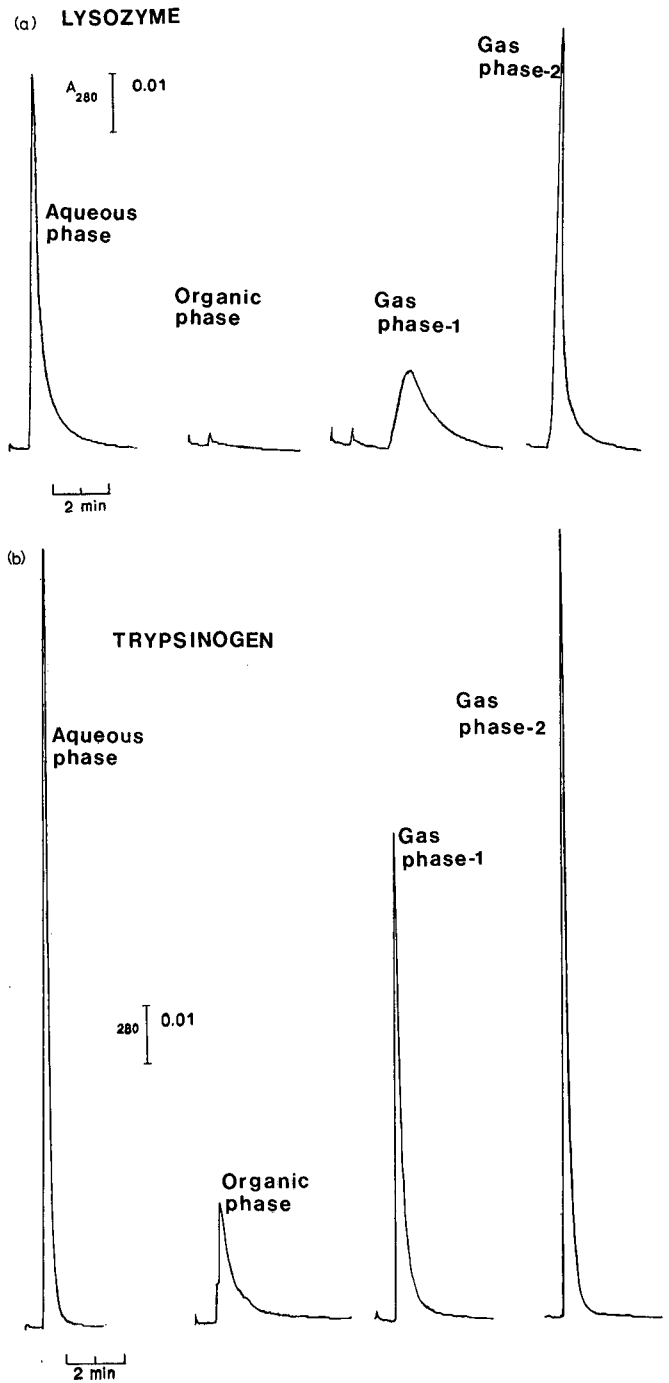

Fig. 2. A comparison of the chromatograms obtained for lysozyme (a) and trypsinogen (b) using silica prepared by the four silylation methods. The buffer used was 0.05 *M* sodium phosphate, 0.1 *M* sodium chloride, pH 7.0. The protein concentration was 5 μg per 20-μl sample and the flow-rate was 1.0 ml/min.

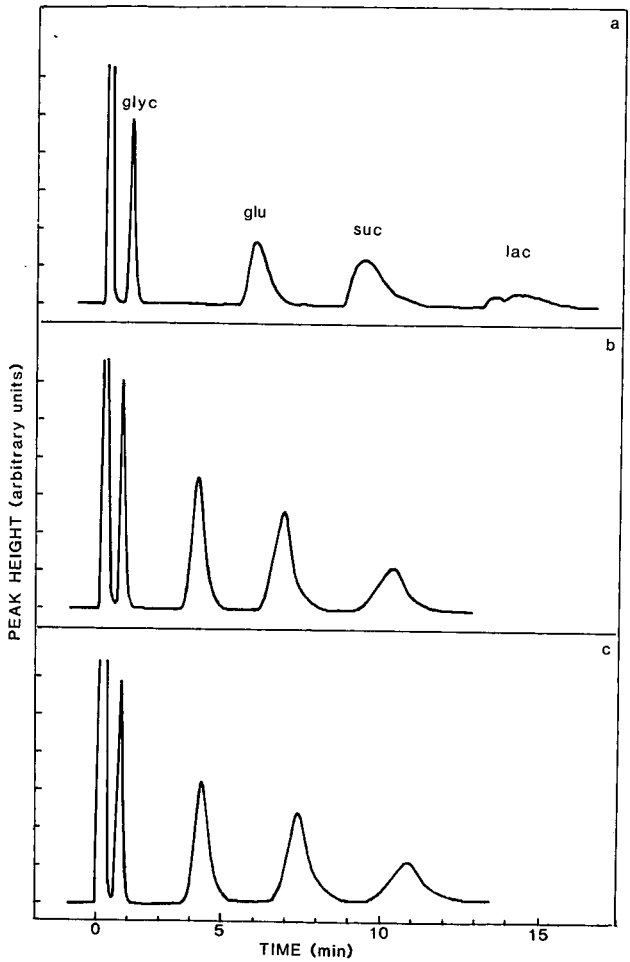

Fig. 3. A comparison of the chromatograms obtained for glycerol (8 mg/ml) glucose, sucrose and lactose (each 25 mg/ml) dissolved in water–acetonitrile (20:80). The injection volume was 20 μl and the flow-rate was 1.0 ml/min.

improvement in the peak shape when going from standard gas phase silylated material (Procedure 1) to twice silylated gas phase material (Procedure 2).

Applications

Fig. 3 shows the separation profiles for a test mixture of glucose, sucrose, lactose and glycerol on aminopropylsilica prepared by three different methods. The three columns readily separate the mixture into its components. However, a closer look reveals that the gas phase silylated silica (Procedure 1) gave the best result, with regard to peak height and peak shape. The relative plate numbers are given in Table VIII.

In another application, gas phase silylated silica was used for chromatography of lactate dehydrogenase using an affinity chromatography column. The affinity column

TABLE VIII

RELATIVE PLATE NUMBERS FOR AMINOPROPYLSILICA

Chromatographic conditions as in Fig. 3. The plate numbers were calculated as described by Kirkland and Snyder[17].

Compound	*Silylation in*		
	Undried organic phase	*Dried organic phase*	*Gas phase procedure 1*
Glycerol	1.11	1.02	1.0
Glucose	0.82	0.92	1.0
Sucrose	0.57	0.88	1.0
Lactose	0.38	0.86	1.0

was prepared by coupling an NAD analogue to tresyl chloride activated diol silica[18]. Lactate dehydrogenase was eluted using 5 m*M* NADH and the enzyme activity of the eluate was monitored. On loading 0.20 mg of enzyme, a recovery of 99% was obtained using the above procedure.

CONCLUSION

This work has demonstrated (1) that silanes can be covalently bound to silica in a much shorter reaction time when the silylation is done in the gas phase in the presence of a catalyst, and (2) that the silica material obtained shows a significantly improved chromatographic performance compared with materials derived from previously described methods.

An additional advantage of special relevance for large scale preparation of derivatized silica is the fact that the gas phase procedure will give a defined product even when the reagents are of varying quality. For instance, the gas phase procedure will allow only unpolymerized silanes to react with the silica support. Also the absence of solvents should be of importance when preparing derivatized supports in large amounts.

ACKNOWLEDGEMENT

The authors thank Perstorp Biolytica AB (Lund, Sweden) for valuable support.

REFERENCES

1 I. Haller, *J. Am. Chem. Soc.*, 100 (1978) 8050–8055.
2 K. K. Unger, N. Becker and P. Roumeliotis, *J. Chromatogr.*, 125 (1976) 115–127.
3 U. Jönsson, G. Olofsson, M. Malmquist and I. Rönnberg, *Thin Solid Films*, 124 (1985) 117–123.
4 F. Buzek and J. Rathousky, *J. Colloid Interface Sci.*, 79 (1981) 47–55.
5 C. F. Mandenius, K. Mosbach, S. Welin and I. Lundström, *Anal. Biochem.*, 157 (1986) 154.
6 M. Lindberg, P.-O. Larsson and K. Mosbach, *Eur. J. Biochem.*, 40 (1973) 187.
7 R. E. Walters, *J. Chromatogr.*, 249 (1982) 19–28.
8 P.-O. Larsson, M. Glad, L. Hansson, M. O. Månsson, S. Ohlsson and K. Mosbach, *Adv. Chromatogr. (N.Y.)*, 21 (1983) 41.

9 K. Nilsson and K. Mosbach, *Biochem. Biophys. Res. Commun.*, 102 (1981) 449–457.
10 R. Axen, H. Drevin and J. Carlsson, *Acta Chem. Scand., Ser. B*, 29 (1975) 471.
11 A. J. Alpert and F. E. Regnier, *J. Chromatogr.*, 185 (1979) 375–392.
12 I. Shapiro and I. M. Kolthoff, *J. Am. Chem. Soc.*, 72 (1950) 776.
13 P. A. Bristow, P. N. Brittain, C. M. Riley and B. F. Williamson, *J. Chromatogr.*, 131 (1977) 57.
14 K. K. Unger, *Porous Silica*, Elsevier, Amsterdam, 1979, p. 284.
15 A. K. Roy and S. Roy, in I. M. Chaiken, M. Wilchek and I. Parikh (Editors), *Affinity Chromatography and Biological Recognition*, Academic Press, New York, 1983, p. 257.
16 I. Lundström, *Prog. Colloid Polym. Sci.*, 70 (1985) 76.
17 J. J. Kirkland and L. R. Snyder, *Introduction to Modern Liquid Chromatography*, Wiley, Chichester, 1979.
18 P. Wikström and P.-O. Larsson, *J. Chromatogr.*, 388 (1987) 123.

Journal of Chromatography, 455 (1988) 119–129
Elsevier Science Publishers B.V., Amsterdam — Printed in The Netherlands

CHROM. 20 827

DEGRADATION AND ANALYSIS OF POLYOXYETHYLENE MONOALKYL ETHERS IN THE PRESENCE OF ACETYL CHLORIDE

J. SZYMANOWSKI*
Technical University of Poznań, Institute of Chemical Technology and Engineering, Pl. M. Sklodowskiej-Curie 2, 60-965 Poznań (Poland)
and
P. KUSZ, E. DZIWIŃSKI and Cz. LATOCHA
Institute of Heavy Organic Synthesis "Blachownia", 47-225 Kędzierzyn-Koźle-7 (Poland)
(First received March 22nd, 1988; revised manuscript received July 11th, 1988)

SUMMARY

Degradation of model polyoxyethylene glycol monoalkyl ethers in the presence of an excess of acetyl chloride was studied. The degradation products were identified by gas chromatography–mass spectrometry. It was found that degradation is complete at 250°C after 2 h, and this method of degradation can be used to determine the average degree of ethoxylation with high precision and accuracy. The degrees of ethoxylation determined were equal to the actual ones.

INTRODUCTION

Polyoxyethylene glycol monoalkyl ethers obtained in the reaction of different alcohols with ethylene oxide are complex polydisperse mixtures containing different homologues with increasing numbers of oxyethylene groups. Also present are polyoxyethylene glycols formed as by-products in the reaction:

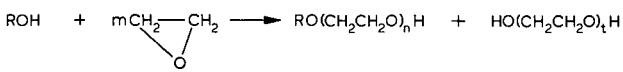

The direct gas chromatographic (GC) analysis of such products is possible after converting them into trimethylsilyl, acetyl or other volatile derivatives, but only if they contain homologues having less than 16 or 17 oxyethylene groups[1].

Commercial products are obtained from mixtures of different alcohols and their compositions are usually very complex. It is usually impossible to separate all components of such commercial non-ionic surfactants. As they contain long polyoxyethylene chains or as they are obtained from commercial alcohols containing several components, the average degree of ethoxylation cannot be determined directly by GC. It is necessary to degrade the polyoxyethylene chain and to determine the

0021-9673/88/$03.50 © 1988 Elsevier Science Publishers B.V.

contents of the different degradation products. Several methods for degradation have been employed but the results obtained were not completely satisfactory[2,3].

Fission of oxyethylene groups is usually carried out according to the procedure proposed by Siggia *et al.*[4] and adopted by the American Society for Testing and Materials and by the Commision International d'Analyse of the Comite' International des Derives Tensio-Actifs as standards D 2959-71, ANSI/ASTM D2959-74, ISO 2270-1972 (E). In this method hydroiodic acid is used and the overall reactions may be summarized as

$$R(OCH_2CH_2)_nOH \xrightarrow{HI} RI + n\,ICH_2CH_2I + (n+1)H_2O$$

followed by

$$ICH_2CH_2I \xrightarrow{HI} I_2 + CH_3CH_2I$$

or

$$ICH_2CH_2I \rightarrow I_2 + CH_2{=}CH_2$$

The following reaction is also possible:

$$CH_2{=}CH_2 + HI \rightarrow CH_3CH_2I$$

Taking this into account, alkyl iodides and alkenes are not determined but the iodine content is estimated by titration with standard sodium thiosulphate solution. As a blank analysis is concurrently done, the content of ethylene oxide can be precisely determined with the reproducibility per individual analyst being within 1.5% of the average value.

However, as discussed by Cross[2], this method is not universal and cannot be used for the analysis of surfactants having polymeric chains of oxypropylene, either alone or as a copolymer with oxyethylene. Some problems also occur with the analysis of oxyethylated fatty amines and alkylphenols.

When an unknown product is analyzed the structure of the hydrophobe, which can be and usually is quite a complicated mixture, must also be determined. Hoyt *et al.*[5,6] proposed a complicated procedure, in which, after titration of the liberated iodine with sodium thiosulphate, the alkyl iodides were extracted from the resultant solution into hexane and separated by means of GC. Another portion of the same extract was trimethylsilanized and the overall composition of the mixture was deduced from the combined results.

However, the presence of free iodine can result in a free radical attack upon the alkyl iodide leading to its further conversion. Cross[2] suggests "to resist using the products of the oxyethylene estimation experiments for hydrophobe examination and to perform a second fission in which hypophosphorous acid has been added to reduce any iodine back to hydrogen iodide". In such a case the analysis must be done twice. We decided to look for a fission method which can be used to determine in one

procedure both the content of the polyoxyethylene chain and the structure of the components forming the hydrophobic part of non-ionic surfactants.

The method of Waszeciak and Nadeau[7] was selected for further studies because it seemed to us that the reaction with acetyl chloride has potential for further development. Cross[2] came to the same conclusion: "Its simplicity, the lack of need for special glassware or lengthy heating periods, the quantitative nature, plus the fact that (in the case of oxyethylates) a single product is obtained which is amenable to flame ionization or electron capture detection all point to this technique being thoroughly worthy of further investigation".

The aim of this work is to study the degradation of some model polyoxyethylene glycol monoalkyl ethers in the presence of acetyl chloride and the application of this method to the determination of the average degree of alcohol ethoxylation.

EXPERIMENTAL

Model trioxyethylene glycol monodecyl ether (TGMDE), $C_{10}H_{21}O(CH_2CH_2O)_3H$, of purity > 94% as determined by GC, and polyoxyethylene glycol monododecyl ethers (PGMDE), $C_{12}H_{25}O(CH_2CH_2O)_nH$, having an average degree of ethoxylation equal to 7, were used for degradation. Acetyl chloride, puriss. p.a. (Fluka, Buchs, Switzerland) was used as an acylation and degradation agent.

A sample (0.010–0.015 g) of polyoxyethylene glycol monoalkyl ethers was weighed into a reaction vial (Nimonic 80, Mettler Instr.) of capacity 0.5 cm^3. Acetyl chloride (200 μl) was then added and the reaction mixture was heated under pressure at 250°C for 2 h. The cooled post-reaction mixture was diluted in benzene or ethylene dichloride (1:1, v/v) and analyzed by GC.

A gas chromatograph (Perkin-Elmer, Model 900) with a flame ionization detector was used. The separation was carried out in stainless-steel columns: I, 0.4 m × 2.7 mm I.D. packed with 1% Dexsil 400 on Chromosorb G AW DMCS (80–100 mesh); II, 1.8 m × 2.7 mm I.D. packed with 3% OV-17 on Chromosorb G AW DMCS (60–80 mesh); III, 1.6 m × 2.7 mm I.D. packed with 12% Carbowax 20M-TPA on Chromosorb W AW DMCS (80–100 mesh). Argon was used as the carrier gas at 30 cm^3/min. The temperature of column I was 130°C for 1 min and then raised to 360°C at 6°C/min. The temperatures of the injector and the detector were 380°C. The temperature of column II was 120°C for 4 min, and then raised to 300°C at 6°C/min. The temperatures of the injector and the detector were 300 and 320°C, respectively. The temperature of column III was 100°C for 1 min, and then raised to 220°C at 5°C/min. The temperatures of the injector and the detector were 250°C.

The average degree of ethoxylation, α in the direct analysis was calculated according to

$$\alpha = \frac{M_H \sum_{i=1}^{j} \frac{44\, n_i x_i}{M_i}}{44 \sum_{i=1}^{j} \frac{x_i M_H}{M_i}} \qquad (1)$$

where M_H denotes the average molecular mass of the alcohols used to obtain the polyoxyethylene glycol monoalkyl ethers, M_i the molecular mass of the "i" homologue of the polyoxyethylene monoalkyl ethers, n_i the number of oxyethylene groups in this homologue and x_i the content of this homologue calculated from the surface areas of the separated peaks, assuming the correction factors to be 1. After degradation, α was calculated from

$$\alpha = \frac{\sum_{i=1}^{n} \frac{A_i K_i}{M_i}}{\sum_{j=1}^{m} \frac{A_j' K_j'}{M_j'}} \qquad (2)$$

where M_i and M_j' denote the molecular masses of components "i" and "j" formed from the polyoxyethylene chain and hydrophobic alkyl, respectively, A_i and A_j' are the surface areas of the corresponding peaks and K_i and K_j' their correction factors, calculated according to the method of Sternberg *et al.*[8] using the concept of the effective number of carbon atoms.

The separated components were identified by means of a mass spectrometer coupled to a gas chromatograph (GC–MS 2091; KLB, Bromma, Sweden). The chromatographic column and separation conditions were the same as in the GC analysis; column III was used. An ionization energy of 70 eV and an ion-source temperature of 250°C were employed.

Acetates of polyoxyethylene glycol monoalkyl ethers used in the direct analyses were obtained by esterification of their samples (0.1–0.2 g) with acetyl chloride (2 cm^3) at 50–60°C for 15 min. After cooling, hydrogen chloride, acetic acid and an excess of acetyl chloride were evaporated in a stream of dry nitrogen. Then, benzene (1 cm^3) was added and acetates were analyzed.

A thermoanalyzer TA-2 (Mettler Instr., Greifensee, Switzerland) was used. Samples (0.02–0.03 g) of polyoxyethylene glycol monododecyl ethers and of mixtures with acetyl chloride or trifluoroacetic anhydride (1:20, w/w) were placed in a platinum crucible with a perforated lid, capacity 0.5 cm^3, and heated to 500°C at a rate of 10°C/min. Argon was used as an inert gas.

RESULTS AND DISCUSSION

Fig. 1 shows the results of thermogravimetric–differential thermogravimetric analysis (TGA–DTG) of polyoxyethylene glycol monododecyl ethers (PGMDEs) and their acetates and trifluoroacetates in the presence of an excess of acetyl chloride or trifluoroacetic anhydride (1:20, w/w). Acetyl chloride promotes this degradation which commences below 200°C. At 250°C the degradation products do not contain initial homologues of PGMDE (Fig. 2). Before degradation, PGMDE contains homologues at least up to one having 17 oxyethylene units (12/17). Unreacted dodecyl alcohol (12/0) is also present. All 18 homologues of PGMDE are well separated but small peaks of polyglycols which should be eluted between the main peaks[1] are not

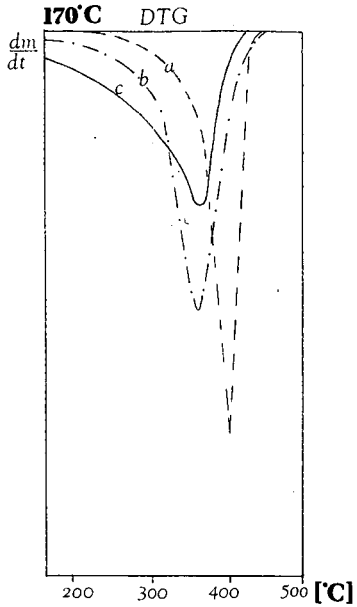

Fig. 1. Thermogravimetric analysis of the polyoxyethylene glycol monododecyl ethers: (a) PGME; (b) PGMDE–trifluoroacetic anhydride (1:20, w/w); (c) PGMDE–acetyl chloride (1:20, w/w).

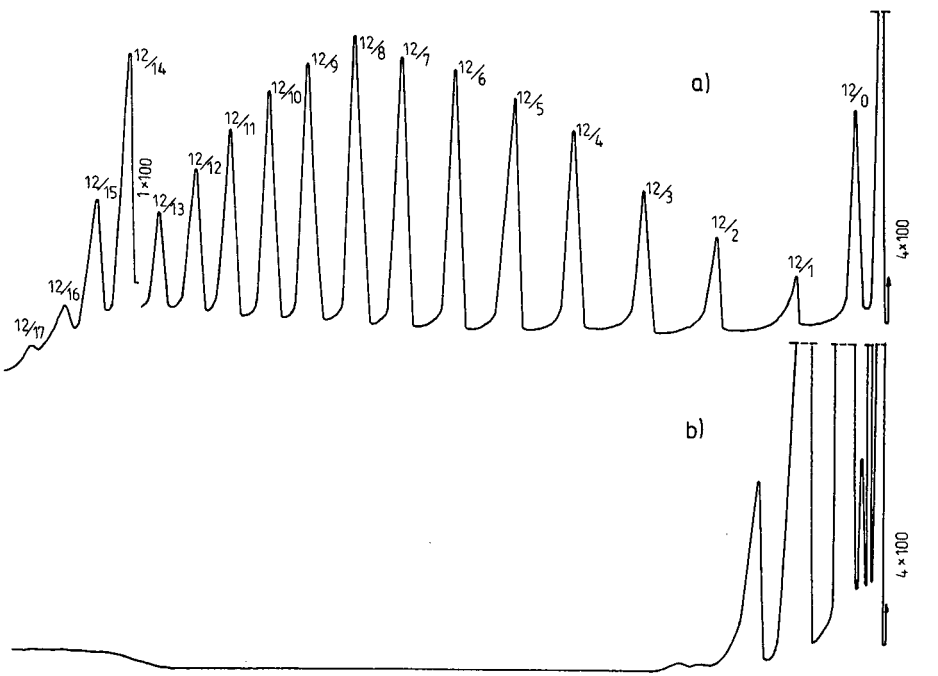

Fig. 2. Chromatogram of the polyoxyethylene glycol monododecyl ethers: (a) before degradation and (b) after degradation with acetyl chloride. Degradation conditions: 250°C; 2 h. Column I, analytical conditions as in Experimental.

observed under our chromatographic conditions. After degradation all these peaks disappear, and new ones at short retention times are observed. However these new components formed during degradation are not separated on column I in which Dexsil 400 was used as the liquid phase. A much better separation was obtained on column II packed with Chromosorb G AW DMCS impregnated with silicone resin OV-17 (sum of the first McReynolds constants, $\sum_{1}^{5} \Delta I = 884$), often used for the analysis of non-ionic surfactants having polyoxyethylene chains. However, this separation was also not complete. The best separation was achieved on column III packed with Chromosorb W AW DMCS impregnated with highly polar Carbowax 20M-TPA ($\sum_{1}^{5} \Delta I = 2318$). Thus column III was used to separate and identify degradation products by means of GC–mass spectrometry (MS).

Some degradation products are the same as those identified previously in degradation products of polyoxyethylene glycols. Their mass spectra are quite similar

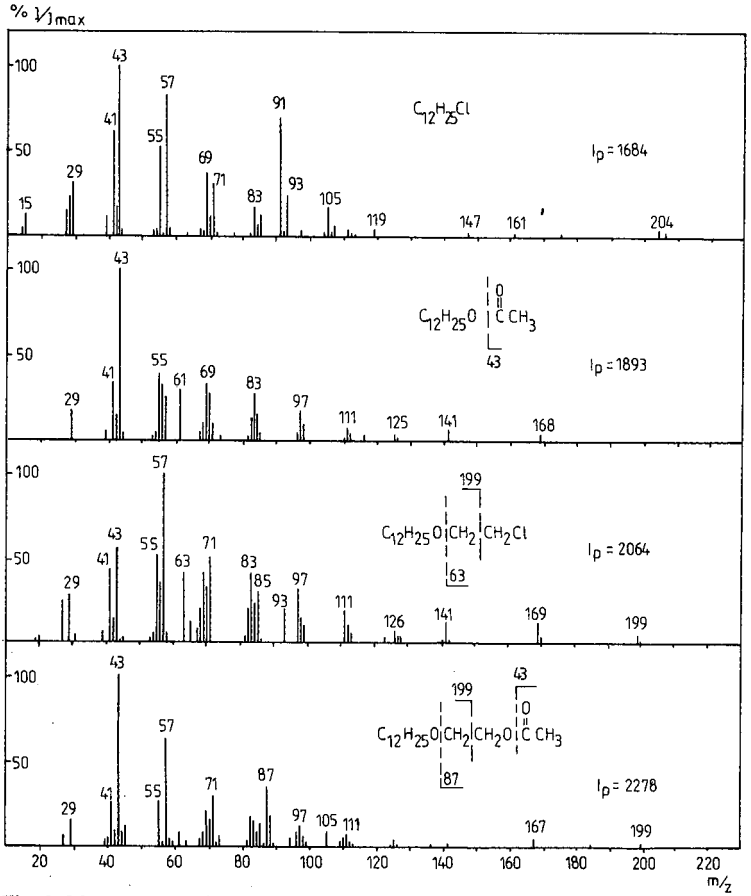

Fig. 3. Mass spectra of the separated components of the degradation products.

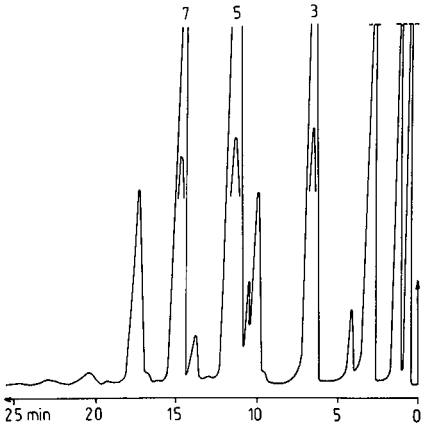

Fig. 4. Chromatogram of the polyoxyethylene glycol monododecyl ethers after degadation with acetyl chloride. Column II, analytical conditions as in Experimental. Peak identification as in Table I.

to those reported previously[9]. The highest intensity is observed at $m/z = 43$, characteristic for $[CH_3CO]^+$, formed by loss of an acetyl group. Other much lower intensity lines are observed as a result of the intramolecular splitting of the polyoxyethylene chain. Thus, the degradation of the polyoxyethylene chain in polyoxyethylene glycol monoalkyl ethers is similar to that of polyoxyethylene glycols[9]. Dodecyl chloride, cyclododecane, dodecyl acetate, 1-dodecyl-2-chloroethyl ether and 3-oxapentadecyl acetate are formed from the hydrophobic dodecyl group. The dodecyl group splits in a typical way between successive methylene groups, giving ions with molecular masses differing by 14.

The presence of chlorine atoms in some compounds is demonstrated by the characteristic ratio of isotopic line intensities. The presence of 1-chlorododecane, dodecyl acetate, cyclododecane, 1,2-dichloroethane and dioxy- and trioxyethylene

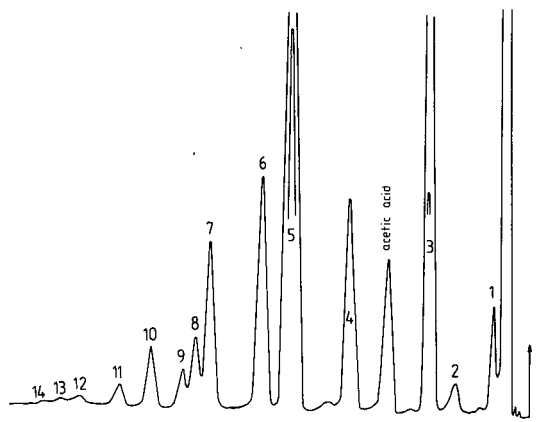

Fig. 5. Chromatogram of the polyoxyethylene glycol monododecyl ethers after degradation with acetyl chloride. Column III, analytical conditions as in Experimental. For peak identification see Table I.

TABLE I

PRODUCTS OF DEGRADATION OF THE POLYOXYETHYLENE GLYCOL MONODODECYL ETHERS ON CARBOWAX 20M-TPA

Peak	*Compound*	*Formula*	*Retention index, I*	*Correction factor*	*Content (%, w/w)*
1	1,2-Dichloroethane	$ClCH_2CH_2Cl$	1065	1.21	4.76
2	Cyclododecane	$CH_2(CH_2)_{10}CH_2$	1236	0.35	0.82
3	2-Chloroethyl acetate	$CH_3COOCH_2CH_2Cl$	1318	1.00	38.51
4	Bis(2-chloroethyl) ether	$ClCH_2CH_2OCH_2CH_2Cl$	1536	1.11	14.70
5	1-Chlorododecane	$CH_3(CH_2)_{10}CH_2Cl$	1684	0.37	14.90
6	5-Chloro-3-oxapentyl acetate	$CH_3COOCH_2CH_2OCH_2CH_2Cl$	1757	0.98	12.11
7	Dodecyl acetate	$CH_3COOC_{12}H_{25}$	1893	0.38	3.67
8	1,8-Dichloro-3,6-dioxaoctane	$ClCH_2CH_2OCH_2CH_2OCH_2CH_2Cl$	1935	1.07	4.80
9	Dioxyethylene glycol diacetate	$CH_3COOCH_2CH_2OCH_2CH_2OOCCH_3$	1970	0.91	1.79
10	1-Dodecyl-2-chloroethyl ether	$ClCH_2CH_2OC_{12}H_{25}$	2064	0.41	1.54
11	8-Chloro-3,6-dioxaoctyl acetate	$CH_3COOCH_2CH_2OCH_2CH_2OCH_2CH_2Cl$	2157	0.98	1.40
12	3-Oxapentadecyl acetate	$CH_3COOCH_2CH_2OC_{12}H_{25}$	2278	0.42	0.30
13	1,12-Dichloro-3,6,9-trioxaundecane	$ClCH_2CH_2OCH_2CH_2OCH_2CH_2OCH_2CH_2Cl$	2330	1.04	0.54
14	Trioxyethylene glycol diacetate	$CH_3COOCH_2CH_2OCH_2CH_2OCH_2CH_2OOCCH_3$	2375	0.92	0.16

TABLE II

PRODUCTS OF DEGRADATION OF TRIOXYETHYLENE GLYCOL MONODECYL ETHER ON CARBOWAX 20M-TPA

Compound	*Formula*	*Retention index, I*	*Correction factor*	*Content (%, w/w)*
Cyclodecane	$CH_2(CH_2)_8CH_2$	1076	0.30	5.81
2-Chloroethyl acetate	$CH_3COOCH_2CH_2Cl$	1318	1.00	51.03
1-Chlorodecane	$CH_3(CH_2)_8CH_2Cl$	1470	0.38	19.24
Bis(2-chloroethyl) ether	$ClCH_2CH_2OCH_2CH_2Cl$	1536	1.11	6.53
Decyl acetate	$CH_3COOC_{10}H_{21}$	1684	0.40	6.40
5-Chloro-3-oxapentyl acetate	$CH_3COOCH_2CH_2OCH_2CH_2Cl$	1757	0.98	6.61
1-Decyl-2-chloroethyl ether	$ClCH_2CH_2OC_{10}H_{21}$	1838	0.44	2.78
1,8-Dichloro-3,6-dioxaoctane	$ClCH_2CH_2OCH_2CH_2OCH_2CH_2Cl$	1935	1.07	0.42
Dioxaethylene glycol diacetate	$CH_3COOCH_2CH_2OCH_2CH_2OOCCH_3$	1970	0.91	0.38
3-Oxatridecyl acetate	$CH_3COOCH_2CH_2OC_{10}H_{21}$	2068	0.45	0.38
8-Chloro-3,6-dioxaoctyl acetate	$CH_3COOCH_2CH_2OCH_2CH_2OCH_2CH_2Cl$	2157	0.98	0.42

glycol diacetates was also supported by comparison with the retention times of these compounds.

The mass spectra of the components separated are presented in Fig. 3. Those reported in our previous work[9] and obtained from the polyoxyethylene chain are omitted. Their formulae, retention indices, correction factors and contents are given in Table I. The numbers of the compounds given are the same as in the chromatograms in Figs. 4 and 5.

Quite similar degradation was observed when the model trioxyethylene glycol monodecyl ether (TGMDE), $H(OCH_2CH_2)_3OC_{10}H_{21}$, was used. Similar components were identified in the degradation products and their formulae and contents are given in Table II.

The results obtained demonstrate that the degradation of polyoxyethylene glycol monoalkyl ethers in the presence of an excess of acetyl chloride is complete at 250°C after 2 h. 2-Chloroethyl acetate formed from the polyoxyethylene chain and alkyl chloride obtained from the hydrophobic alkyl are the main products. Thus, the degradation proceeds in agreement with the Underwood reaction[10]:

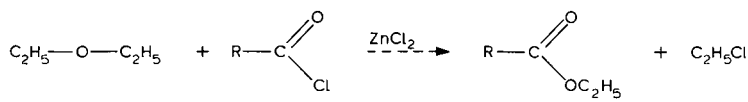

Acetic acid is formed from acetyl chloride and can be neglected.

The most significant drawback of this degradation is the number of compounds formed. Several components must be identified and their contents determined taking

TABLE III

AVERAGE DEGREE OF ETHOXYLATION OF POLYOXYETHYLENE GLYCOL MONOALKYL ETHERS

Ether	*Parameter*	*Direct analysis*	*After degradation*	
			Internal standardization method eqn. 2	*Internal standard method*
TGMED	Ethoxylation	2.69	3.06	2.89
	degree	2.75	2.91	2.88
	(individual results)	2.58	2.96	3.00
		2.69	3.13	2.79
		2.78	3.16	2.87
	Average	2.70	3.04	2.89
	Standard deviation, s_r	0.0284	0.0353	0.0260
	Confidence limits ($\alpha = 0.05$)	$\pm$0.10	$\pm$0.15	$\pm$0.10
PGMDE	Ethoxylation degree	5.70	7.20	6.30
	(individual results)	5.32	6.90	6.54
		5.28	7.07	6.30
		5.45	6.80	6.53
		5.41	7.05	6.76
	Average	5.43	7.00	6.49
	Standard deviation, s_r	0.0303	0.0223	0.0298
	Confidence limits ($\alpha = 0.05$)	$\pm$0.23	$\pm$0.22	$\pm$0.27

into account their correction factors, which can influence the precision and accuracy of the qualitative analysis.

Average degrees of ethoxylation determined by the direct analysis of polyoxyethylene glycol monoalkyl ethers and after their degradation, together with a statistical assessment of the results obtained, are given in Table III. The precision of the measurements is good and similar for both products considered and for both methods of analysis. However, the accuracy of the two methods is different. Higher ethoxylation degrees were obtained after degradation, even for trioxyethylene glycol monodecyl ether. In the case of polyoxyethylene glycol monododecyl ethers having an average degree of ethoxylation of 7, calculated from the amount of ethylene oxide used for the synthesis, the direct analysis gives a value of 5.43, about 22% lower than the actual one. This means that some homologues of PGDME having long polyoxyethylene chains are not completely eluted from the column during chromatographic analysis. For products having average ethoxylation degrees higher than 7 this diifference would be even more significant.

A very good agreement is observed between the ethoxylation degree determined after degradation by the method of internal standardization using eqn. 2 and the actual ones calculated from the masses of reagents used during the syntheses of polyoxyethylene glycol monoalkyl ethers, *i.e.*, 3.04 and 3.0 for TGMDE and 7.00 and 7.0 for PGMDE, respectively. This demonstates the complete degradation of polyoxyethylene glycol monoalkyl ethers and complete elution of all degradation products from the chromatographic column. Thus, the degradation of polyoxyethylene glycol monoalkyl ethers in the presence of an excess of acetyl choride can be used to

determine the average degree of ethoxylation with high precision and accuracy. The values determined using an internal standard (last column of Table III) are somewhat lower, *i.e.*, *ca.* 3.7 and 7.3% for TGMDE and PGMDE, respectively.

CONCLUSIONS

Degradation of polyoxyethylene glycol monoalkyl ethers in the presence of an excess of acetyl chloride is complete at 250°C after 2 h. 2-Chloroethyl acetate formed from the polyoxyethylene chain and alkyl chloride obtained from the hydrophobic alkyl are the main products. This degradation can be used to determine the average degree of ethoxylation with high precision and accuracy. The values obtained by means of the internal standardization are strictly the same as the actual ones. This confirms the complete degradation of polyoxyethylene glycol monoalkyl ethers and complete elution of all degradation products from the chromatographic column.

The most significant drawback of the degradation of polyoxyethylene glycol monoalkyl ethers in the presence of acetyl chloride is the number of compounds formed. They must all be identified and their contents quantitated. However, GC–MS need not be used because the polyoxyethelene chains are degraded to the same products which can be identified from their retention indices.

REFERENCES

1 J. Szymanowski, H. Szewczyk and A. Atamańczuk, *Tenside Deterg.*, 21 (1984) 139.
2 J. Cross (Editor), in *Nonionic Surfactants. Chemical Analysis*, Marcel Dekker, New York, 1987, pp. 137, 169.
3 J. Szymanowski, P. Kusz and H. Szewczyk, *Pollena-Tluszcze, Srodki Piorące, Kosmetyki*, 30 (1986) 201.
4 S. Siggia, A. C. Starke, J. J. Garis and C. K. Stahl, *Anal. Chem.*, 30 (1958) 115.
5 E. L. Sones, J. L. Hoyt and A. J. Sooter, *J. Am. Oil Chem. Soc.*, 56 (1979) 689.
6 J. L. Hoyt, E. L. Sones and A. J. Sooter, *J. Am. Oil Chem. Soc.*, 56 (1979) 701.
7 P. Waszeciak and H. G. Nadeau, *Anal. Chem.*, 36 (1964) 764.
8 J. C. Sternberg, W. S. Gallaway and D. T. L. Jones, in N. Brenner, J. E. Callen and H. D. Weiss (Editors), *Gas Chromatography*, Academic Press, New York, 1962, p. 231.
9 J. Szymanowski, P. Kusz and E. Dziwiński, *J. Chromatogr.*, 131.
10 H. Underwood, *J. Am. Chem. Soc.*, 52 (1930) 387.

Journal of Chromatography, 455 (1988) 131–141
Elsevier Science Publishers B.V., Amsterdam — Printed in The Netherlands

CHROM. 20 843

CHEMICAL DEGRADATION AND ANALYSIS OF POLYOXYETHYLENE GLYCOLS AND ETHYLENE OXIDE–α-BUTYLENE OXIDE BLOCK COPOLYMERS

J. SZYMANOWSKI*

Technical University of Poznań, Institute of Chemical Technology and Engineering, Pl. M. Sklodowskiej-Curie 2, 60-965 Poznań (Poland)

and

P. KUSZ and E. DZIWIŃSKI

Institute of Heavy Organic Synthesis "Blachownia", 47-225 Kędzierzyn-Koźle-7 (Poland)

(First received January 29th, 1988; revised manuscript received June 16th, 1988)

SUMMARY

The chemical degradation of polyoxyethylene glycols and block copolymers of ethylene oxide and α-butylene oxide by means of acetyl chloride in the presence of iron(III) chloride was investigated and used to determine with satisfactory precision and accuracy the content of polyoxyethylene groups in model and commercial products. The degradation products were identified by gas chromatography–mass spectrometry.

INTRODUCTION

Non-ionic surfactants having polyoxyethylene chains are complex mixtures containing homologues having different numbers of oxyethylene units, usually they also contain different homologues of polyoxyethylene glycols which are formed as by-products during the synthesis of surfactants:

$$RXH + (n+m)CH_2—CH_2 \longrightarrow RX(CH_2CH_2O)_nH + HO(CH_2CH_2O)_mH$$

where X = O, C_6H_5O, S, COO, etc.

Gas–liquid chromatography of such polydisperse mixtures is limited to products containing less than 20 oxyethylene groups[1] in the least volatile homologue as a result of the too low volatility and thermal degradation of homologues having higher molecular masses. Hence direct analysis cannot be used for commercial products that contain more oxyalkylene units in some higher homologues present in polydisperse mixtures to be analysed. In such an event chemical or thermal degradation could be used to determine the average contents of polyoxyethylene chains and/or the average degree of ethoxylation. However, results published up to now are not satisfactory[2].

0021-9673/88/$03.50 © 1988 Elsevier Science Publishers B.V.

TABLE I

METHODS FOR DEGRADATION OF NON-IONIC SURFACTANTS HAVING POLYOXYETHYLENE CHAINS

Degradation agent	*Degradation conditions*	*Main degradation products*	*Chromatographic column filling*	*Ref.*
HCl	6 *M* HCl, 140–200°C, 10–20 h	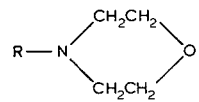	PEG 4000 on Embacel-AW	3
HBr	40–50% HBr in CH_3COOH, 150°C, 2–3 h	$BrCH_2CH_2Br$, RBr	PEGA on G-Cel-AW	4
			Apiezon L on Chromosorb W	5
			Apiezon L on Universal Q	6
			OV-210 on silanized Chromosorb W	7
			OV-1 on Chromosorb W AW DMCS	8
HI	HI or HI–85% H_3PO_4, 150–160°C, 1 h	I_2*	–	9, 10
p-$CH_3C_6H_4SO_2OOCCH_3$	120°C, 0.5–2 h	Acetates	FFAP on Uniport Q	11, 12
H_3PO_4	85% H_3PO_4, 100°C	Aldehydes, olefins	–	13, 14
CH_3COCl	CH_3COCl–$FeCl_3$, 20–25°C	$ClCH_2CH_2Cl$, acetates	DC-550 on Chromosorb W	15
Thermal degradation	360–650°C, 0.5–2 h	Low-boiling hydrocarbons	DC-200 silicone oil	16
Thermal degradation –H_3PO_4	2% solution in H_3PO_4, 300–400°C, 0.5–1 h	Aldehydes, olefins	Citroflex on Chromosorb W	17
	500–600°C, few seconds	Aldehydes, olefins, Dioxane	Porapak Q	18–21

* Determined by titration with $Na_2S_2O_3$.

Different methods for the degradation of the polyoxyethylene chains in various types of non-ionic surfactants have been proposed[3–21] (Table I). Usually different acids or their derivatives were used, *e.g.*, HCl, HBr, HI, H_3PO_4, CH_3COCl and mixed anhydrides of carboxylic and sulphonic acids. Non-catalysed and catalysed thermal degradations have also been considered[16–21]. However, the degradation products are usually complex mixtures containing several different components and their compositions can vary with the degradation conditions, the type of surfactants degraded and the length of the polyoxyethylene chain. Moreover, high-boiling resins and tars are often formed, especially during the degradation of polyoxyethylene alkylphenols and alcohols by means of hydrobromic acid, which is very inconvenient for manual operations. With hydroiodic acid low-boiling products are formed which are inconvenient for chromatographic analysis. As a result, iodine is usually determined by titration with sodium thiosulphate. Non-catalysed and catalysed pyrolyses are very unselective methods and, as they give several very volatile degradation products, they are very inconvenient for quantitative analysis. Mixed anhydrides appear to be convenient degradation reagents but they must be prepared according to the methods described by Karger and Mazur[22–25]. Acetyl chloride is easily accessible and convenient to use. The degradation products obtained can be easily separated and determined.

The aim of this work was to identify the products of the degradation of polyoxyalkylene glycol and to use this chemical degradation to determine the contents of oxyethylene groups in model and commercial polyoxyethylene glycols and in block copolymers of ethylene oxide and α-butylene oxide. It was decided to continue the work of Waszeciak and Nadeau[15], who degraded polyoxyethylene glycols by means of acetyl chloride in the presence of different inorganic salts. It seemed to us that such a method could be used to degrade different types of non-ionic surfactants. The degradation products were identified by gas chromatography–mass spectrometry (GC–MS).

EXPERIMENTAL

Model trioxyethylene glycol, $HO(CH_2CH_2O)_3H$ (P.P.H. POCh, Gliwice, Poland), polyoxyethylene glycols PEG-200 (ICSO, "Blachownia", Kędzierzyn-Koźle, Poland) and Carbowax 1500 (LOBA-Chemie, Vienna, Austria), and block copolymers of ethylene oxide and α-butylene oxide, BE 1500-44[26] and BEB 2000-44[27], where 1500 and 2000 denote the average molecular weights and 44 the content of the polyoxyethylene chains calculated from the mass of reacted ethylene oxide, were used:

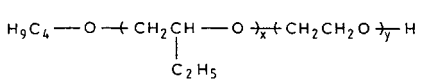

BE

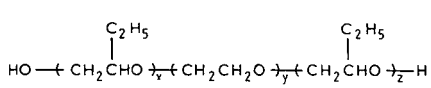

BEB

Samples of polyoxyethylene glycol or block copolymer (0.05 g) and *n*-hexadecane (0.01–0.02 g) used as an internal standard were weighed into reaction vials (Supelco, Bellefonte, PA, U.S.A.) of 5 cm^3 capacity and anhydrous iron(III) chloride (0.04–0.05 g) and acetyl chloride (0.7–1 cm^3) were added. The vials were shaken to obtain a clear solution and heated at 150°C for 0.5 h. After cooling, the degradation products were diluted with dichloromethane (1:1, v/v) and analysed.

A Perkin-Elmer Model 900 gas chromatograph with a flame ionization detector was used. The separation was carried out in a stainless-steel column (1.8 m × 2.7 mm I.D.) packed with Chromosorb W AW DMCS (80–100 mesh) coated with 12% Carbowax 20M–TPA. Argon was used as the carrier gas at a flow-rate of 30 cm^3/min. The temperatures of the injector and the detector were 250°C. The column temperature was 100°C for 1 min, then raised to 220°C at 5°C/min. The contents of the separated components were determinated from their peak areas and the peak area of the internal standard using appropriate correction factors, which were calculated according to the method proposed by Sternberg *et al*[28].

The identification of the separated components was carried out by means of a mass spectrometer coupled to a gas chromatograph (GC–MS 2091 LKB, Bromma, Sweden). The chromatographic column and the separation conditions were the same as in the GC analysis. The mass spectra were taken at the tops of the chromatographic peaks. An ionization energy of 70 eV and an ion-source temperature of 250°C were employed.

A gas chromatograph (Model 400, MERA-ELWRO, Wrocław, Poland) with a thermal conductivity detector was used to determine the water contents of the polyoxyethylene glycols. A stainless-steel column (1.2 m × 4 mm I.D.) filled with Chromosorb 101 (80–100 mesh) was used. Hydrogen was used as the carrier gas at a flow-rate of 25 cm^3/min. The temperature of the injector and the detector were 250°C. The column temperature was 100°C for 1 min, then raised to 200°C at 4°C/min. Anhydrous acetone or ethyl methyl ketone were used as an internal standard and anhydrous ethanol as a solvent.

RESULTS AND DISCUSSION

The purity of model trioxyethylene glycol, as determined by direct analysis of its diacetate, was 94.95%. Small peaks of ethylene glycol, dioxyethylene glycol and tetraoxyethylene glycol were also observed but their contents were only 0.39, 3.09 and 1.57%, respectively. PEG 200 polyoxyethylene glycol contained successive homologues up to hexaoxyethylene glycol. Carbowax 1500 contained much higher homologues and hence it was impossible to analyse it directly.

Typical chromatograms of degradation products obtained without a catalyst and in the presence of iron(III) chloride are shown in Figs. 1 and 2 and the mass spectra of the main separated components obtained by polyoxyethylene glycol degradation are given in Fig. 3. The structures and retention indices of the separated compounds are presented in Tables II and III. Retention indices are also given on the chromatograms.

The chromatograms obtained demonstrate that much deeper degradation was achieved when iron(III) chloride was used as a catalyst, and the chromatograms obtained for the degradation of trioxyethylene glycol were similar to those obtained

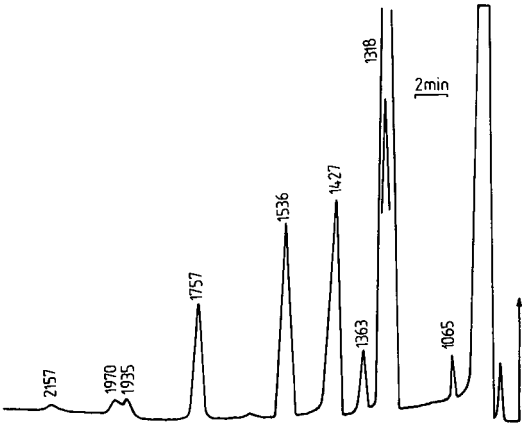

Fig. 1. Chromatogram of the degradation products of PEG-200 polyoxyethylene glycol (degradation without catalyst). Column and analytical conditions as in Experimental. For peak identification see Table II.

for Carbowax 1500. 2-Chloroethyl acetate was the main degradation product and its content was 96.33 and 96,68%, respectively, for trioxyethylene glycol and Carbowax 1500 degradation when acetic acid and γ-pyrone derivatives were not taken into consideration. Acetic acid is formed by the hydrolysis of acetyl chloride whereas γ-pyrones are formed by the reaction of acetyl chloride with acetic acid in the presence of a mineral acid[29]. Acetyl chloride and ion(III) chloride (15:1, m/m) were heated at 150°C for 0.5 h; a chromatogram of the reaction products is shown in Fig. 4 and mass spectra of the separated components together with their formulae are given in Fig. 5. Four different derivatives of γ-pyrone were identified by comparison of their mass spectra with those given in the literature[30]. Their retention indices were 2035, 2107,

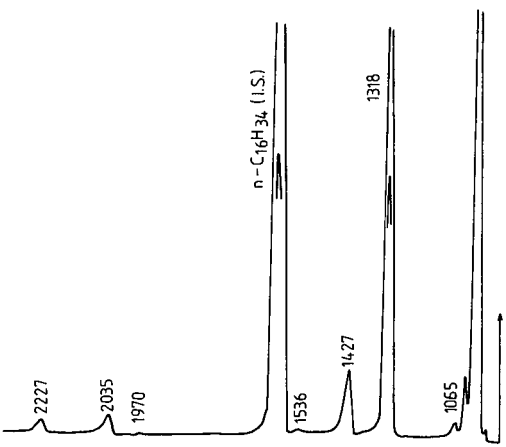

Fig. 2. Chromatogram of the degradation products of Carbowax 1500 [iron(III) chloride as a catalyst]. Column and analytical conditions as in Fig. 1. For peak identification see Table III.

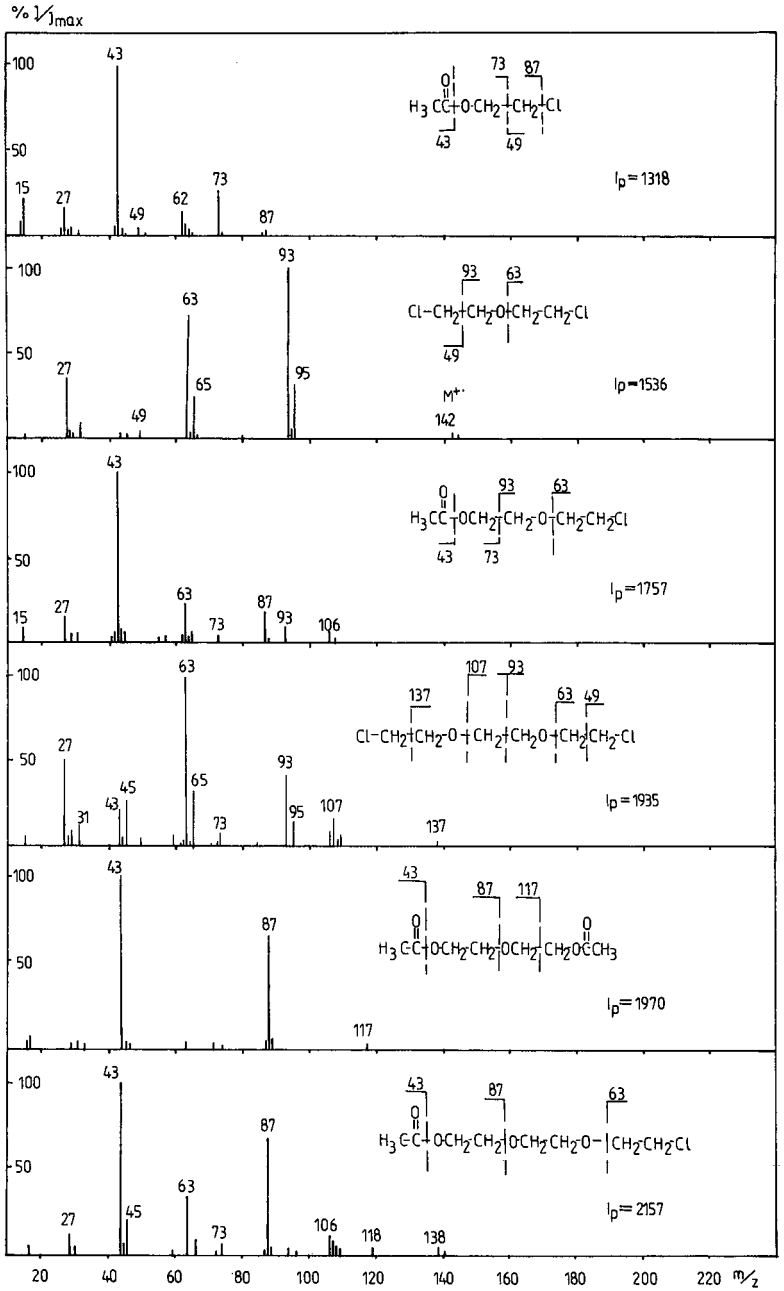

Fig. 3. Mass spectra of the separated components obtained by degradation of polyoxyethylene glycols.

2227 and 2405 and their contents in the products of the degradation of polyoxyethylene glycols did not exceed 5%. Hence γ-pyrone derivatives and acetic acid can be neglected. As a result, the content by weight of oxyethylene groups in the polyoxy-

TABLE II

DEGRADATION PRODUCTS: POLYOXYETHYLENE GLYCOL PEG 200, DEGRADATION WITHOUT A CATALYST

Component	*Formula*	*Retention index*
1,2-Dichloroethane	$ClCH_2CH_2Cl$	1065
2-Chloroethyl acetate	$ClCH_2CH_2OOCCH_3$	1318
Unknown	–	1363
Acetic acid	CH_3COOH	1427
Bis(2-chloroethyl) ether	$ClCH_2CH_2OCH_2CH_2Cl$	1536
5-Chloro-3-oxapentyl acetate	$ClCH_2CH_2OCH_2CH_2OOCCH_3$	1757
1,8-Dichloro-3,6-dioxaoctane	$ClCH_2CH_2OCH_2CH_2OCH_2CH_2Cl$	1935
Dioxyethylene glycol diacetate	$CH_2COOCH_2CH_2OCH_2CH_2OOCCH_3$	1970
8-Chloro-3,6-dioxaoctyl acetate	$ClCH_2CH_2OCH_2CH_2OCH_2CH_2OOCCH_3$	2157

TABLE III

DEGRADATION PRODUCTS: TRIOXYETHYLENE GLYCOL, CARBOWAX 1500, IRON(III) CHLORIDE AS CATALYST

Retention index (I_p)	*Component*
1065	1,2-Dichloroethane
1318	2-Chloroethyl acetate
14.27	Acetic acid
1536	Bis(2-chloroethyl) ether
1600	*n*-Hexadecane (I.S.)*
1970	Dioxyethylene glycol diacetate
2035	}
2227	} γ-Pyrone derivatives

* Internal standard.

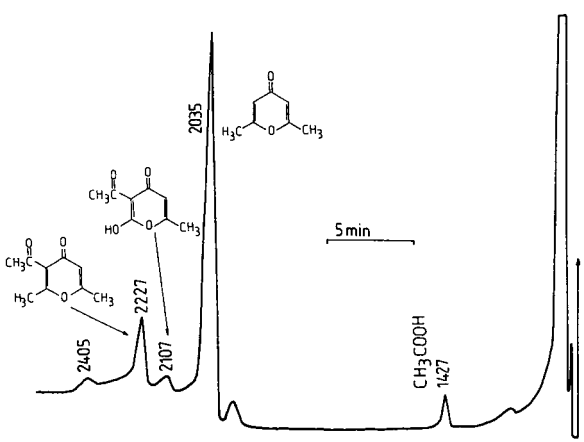

Fig. 4. Chromatogram of the products obtained by reaction of acetyl chloride with iron(III) chloride at 150°C.

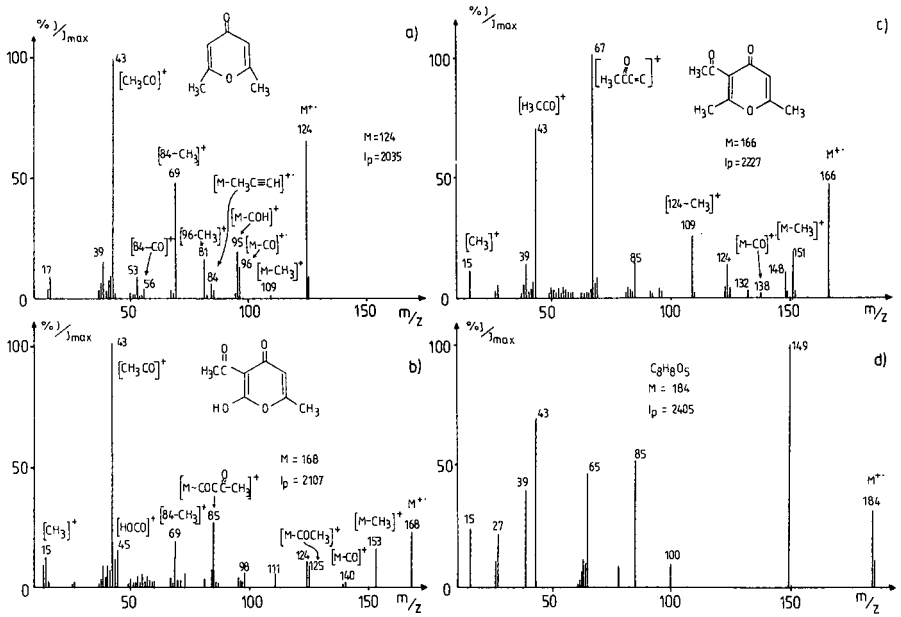

Fig. 5. Mass spectra of the separated γ-pyrone derivatives: (a) 2,6-dimethyl-γ-pyrone; (b) 2-hydroxy-3-acetyl-6-methyl-γ-pyrone; (c) 2,6-dimethyl-3-acetyl-γ-pyrone; (d) $C_8H_8O_5$.

ethylene glycols studied can be determined easily and precisely from the peak areas of the degradation products, mainly 2-chloroethyl acetate and *n*-hexadecane used as the internal standard. Such a determination is also possible when degradation is carried out without a catalyst. However, owing to incomplete degradation and the presence of products with higher molecular masses a larger number of separated components must be taken into consideration and the accuracy and precision of analysis are lower.

The data in Table IV demonstrate good agreement between the determined masses of polyoxyethylene glycols and those taken for analysis when the water contents (9.25% in trioxyethylene glycol and 1.65% in Carbowax 1500), determined separately by gas–solid chromatography were taken into consideration. The determined masses of polyoxyethylene glycols are only *ca.* 2.5–3.5% lower than the actual values. The confidence limits for a significance level of 0.05 are ±0.0017 g. Hence GC can be used to determine the contents of polyoxyethylene groups in commercial polyoxyethylene glycols.

TABLE IV

DETERMINED MASSES OF POLYOXYETHYLENE GLYCOLS

Glycol	*Glycol mass (g) (a)*	*Determined mass (g) (b)*	*Confidence limits (g) (α = 0.05)*	$\frac{b}{a} \cdot 100\ (\%)$
Trioxyethylene glycol	0.0412	0.0398	±0.0017	96.60
Carbowax 1500	0.1040	0.1013	±0.0017	97.40

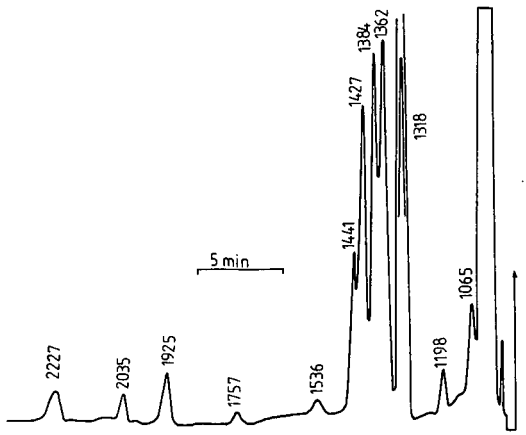

Fig. 6. Chromatogram of the degradation products of BEB 2000-44 block copolymer. Column and analytical conditions as in Fig. 1. For peak identification see Table VI.

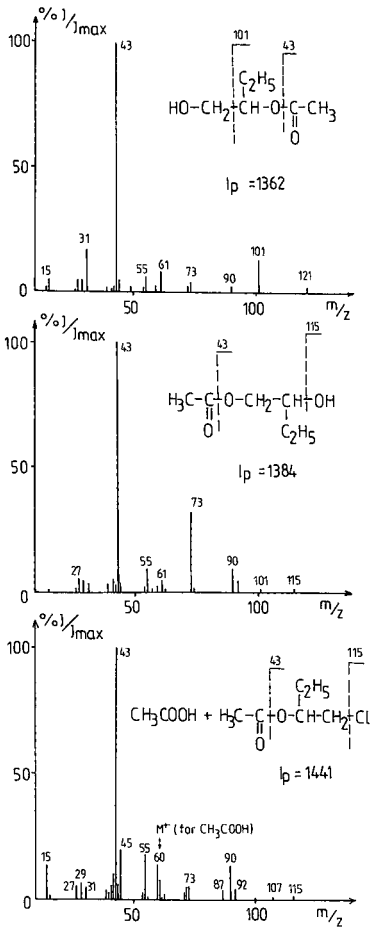

Fig. 7. Mass spectra of the degradation products obtained from polyoxybutylene chains.

TABLE V

COMPOSITION OF THE DEGRADATION PRODUCTS OF BE 1500-44 BLOCK COPOLYMER

*Group of products**	*Component*	*Retention index (I_p)*	*Average content (mol-%)*	*Confidence limits (α = 0.05)*	*Oxyethylene group content (wt.-%) (α = 0.05)*
I	1,2-Dichloroethane	1065	3.71	±2.35	44.13 ± 1.36
	2-Chloroethyl acetate	1318	51.53	±2.23	
	Bis(2-chloroethyl) ether	1536	0.08	±0.33	
	5-Chloro-3-oxapentyl acetate	1757	0.32	±0.29	
II	1,2-Dichlorobutane	1198	5.15	±1.36	
	2-(Hydroxymethyl)-propyl acetate	1362	12.36	±0.81	
	2-Hydroxybutyl acetate	1384	12.96	±0.97	
	2-(Chloromethyl)-propyl acetate	1441	9.78	±1.52	
	Bis(2-chlorobutyl) ether	1925	3.30	±0.73	

* I and II denote the products obtained from polyoxyethylene and polyoxybutylene chains, respectively.

A typical chromatogram of the products of the degradation of BEB block copolymer (Fig. 6) is more complex than the previous chromatograms as a result of degradation of the central polyoxyethylene chain and both terminal polyoxybutylene chains. Similar chromatograms were obtained for BE block copolymer. The mass spectra, although they do not contain molecular ions, give information about the structures of the separated components (Fig. 7). The retention indices of the separated components are in agreement with values obtained for commercially available

TABLE VI

COMPOSITION OF THE DEGRADATION PRODUCTS OF BEB 2000-44 BLOCK COPOLYMER

*Group of products**	*Component*	*Retention index (I_p)*	*Average content (mol-%)*	*Confidence limits (α = 0,05)*	*Oxyethylene group content (wt.-%) (α = 0.05)*
I	1,2-Dichloroethane	1065	6.68	±1.01	43.46 ± 2.14
	2-Chloroethyl acetate	1318	47.56	±1.64	
	Bis(2-chloroethyl) ether	1536	0.82	±0.45	
	5-Chloro-3-oxapentyl acetate	1757	0.64	±0.47	
II	1,2-Dichlorobutane	1198	2.73	±0.56	
	2-(Hydroxymethyl)-propyl acetate	1362	17.04	±0.61	
	2-Hydroxybutyl acetate	1384	15.34	±2.23	
	2-(Chloromethyl)propyl acetate	1441	7.07	±0.23	
	Bis(2-chlorobutyl) ether	1925	2.06	±0.87	

* I and II denote the products obtained from polyoxyethylene and polyoxybutylene chains, respectively.

standards. The separated components and their structures together with a statistical assessment of the results obtained, calculated from five independent analyses, are given in Tables V and VI. The results demonstrate a satisfactory precision. The calculated contents of polyoxyethylene chains (44.13 ± 1.36% and 43.46 ± 2.14% for BE and BEB block copolymers, respectively) are in agreement with the initial analytical data (44%).

CONCLUSIONS

Polyoxyethylene glycols and block copolymers of ethylene oxide and α-butylene oxide can be degraded to simple compounds by reaction with acetyl chloride at 150°C for 0.5 h in the presence of iron(III) chloride as catalyst. 2-Chloroethyl acetate is the main product (*ca.* 96%) of degradation of the polyoxyethylene chain. Degradation of polyoxybutylene chains is much more complex and several products are formed in similar amounts. The contents of successive degradation products can be determined by GC using an internal standard method. They can be further used to calculate with good precision and accuracy the mass and/or the content of polyoxyethylene groups.

REFERENCES

1 J. Szymanowski, A. Voelkel and H. Szewczyk, *J. Chromatogr.*, 360 (1986) 43.
2 J. Szymanowski, P. Kusz and H. Swewczyk, *Pollena-Tluszcze, Środki Piorąe, Kosmetyki*, 30 (1986) 201.
3 J. Jainz, K. Künzler and W. Kupfer, *Fette Seifen Anstrichm.*, 72 (1970) 793.
4 A Mathias and N. Mellor, *Anal. Chem.*, 38 (1966) 472.
5 J. B. Stead and A. H. Hindley, *J. Chromatogr.*, 42 (1969) 470.
6 I. I. Kaduji and J. B. Stead, *Analyst (London)*, 101 (1976) 728.
7 B. G. Luke, *J. Chromatogr.*, 84 (1973) 43.
8 C. Slagt, J. M. H. Daemen, W. Dankelman and W. A. Sipman, *Fresenius' Z. Anal. Chem.*, 264 (1973) 401.
9 K. Obruba, E. Kučerova and M. Jureček, *Microchim. Ichnoanal. Acta*, 1 (1964) 44.
10 K. Bey, *Fette Seifen Anstrichm.*, 64 (1962) 900.
11 K. Tsuji and K. Konishi, *J. Am. Oil Chem. Soc.*, 51 (1974) 55.
12 K. Tsuji and K. Konishi, *J. Am. Oil Chem. Soc.*, 52 (1975) 106.
13 M. J. Rosen, *Anal. Chem.*, 27 (1955) 787.
14 J. D. Knight and R. House, *J. Am. Oil Chem. Soc.*, 36 (1959) 195.
15 P. Waszeciak and H. G. Nadeau, *Anal. Chem.*, 36 (1964) 764.
16 E. W. Neumann and H. G. Nadeau, *Anal. Chem.*, 35 (1963) 1454.
17 R. N. Mokeeva and Ya. Carfin, *Plast. Massy*, 3 (1970) 52.
18 I. Zéman, L. Novák, L. Mitter, J. Steklá and O. Holendová, *J. Chromatogr.*, 119 (1976) 581.
19 R. Denig, *Tenside Deterg.*, 10 (1973) 59.
20 R. Denig, *Fette Seifen Anstrichm.*, 76 (1974) 412.
21 R. Denig in R. Bock (Editor), *Analytiker Taschenbuch*, Vol. 8, Springer, Berlin, Heidelberg, 1983, pp. 220–261.
22 M. H. Karger and Y. Mazur, *J. Am. Chem. Soc.*, 90 (1968) 3878.
23 M. H. Karger and Y. Mazur, *J. Org. Chem.*, 36 (1971) 528.
24 M. H. Karger and Y. Mazur, *J. Org. Chem.*, 36 (1971) 532.
25 M. H. Karger and Y. Mazur, *J. Org. Chem.*, 36 (1971) 540.
26 J. Myszkiwski, J. Symanowski, W. Goc and K. Alejski, *Tenside Deterg.*, 19 (1982) 7.
27 J. Szymanowski, J. Myszkowski, K. Prochaska and K. Szafraniak, *Tenside Deterg.*, 19 (1982) 11.
28 J. C. Sternberg, W. S. Gallaway and D. T. L. Jones, in N. Brenner, J. E. Callen and H. D. Weiss (Editors), *Gas Chromatography*, Acacemic Press, New York, 1962, p. 231.
29 *Beilsteins Handbuch der Organische Chemie*, Springer, Berlin, 1934, Vol. XVII, p. 152; 1952, Vol. XVII, EII, p. 315.
30 Q. N. Porter and J. Baldas, *Mass Spectrometry of Heterocyclic Compounds*, Wiley-Interscience, New York, 1971, p. 144.

Journal of Chromatography, 455 (1988) 143–149
Elsevier Science Publishers B.V., Amsterdam — Printed in The Netherlands

CHROM. 20 844

FLAVOR CHARACTERIZATION OF DENTIFRICES USING EQUILIBRIUM HEADSPACE GAS CHROMATOGRAPHY

R. S. ROBINSON, E. A. TAVSS*, J. SANTALUCIA and D. L. CARROLL
Research and Development Division, Colgate-Palmolive Company, 909 River Road, Piscataway, NJ 08854 (U.S.A.)
(Received May 25th, 1988)

SUMMARY

Equilibrium headspace gas chromatography was used to measure quantity and composition of flavor released from dentifrices into the headspace of sealed vials. Dentifrice formulations varying in composition were analyzed for volatile flavor components after thermodynamic equilibrium between the gas (headspace air) and liquid phase (dentifrice) was established. Comparison of dentifrice formulations allowed for determination of the effect of individual components on flavor binding. This information is useful to formulators, since knowing the extent of the effect of dentifrice components on flavor release allows the formulator to intelligently modify the dentifrice components/flavor. This technique is advantageous over the previously reported kinetic procedure in that the results of equilibrium headspace gas chromatography are not complicated by the effect of varied viscosity.

INTRODUCTION

Flavor is the most important factor affecting human perception of dentifrice taste. Flavor oil has been demonstrated to bind to dentifrices to various extents[1], thereby affecting taste. An instrumental procedure whereby the degree of binding of flavor oil to the dentifrice could be quantitatively measured, would be of benefit to the formulator. With this knowledge the dentifrice and/or flavor oil could be modified to achieve a desired degree of flavor binding, thereby optimizing the dentifrice taste.

Due to the composition of dentifrices, *i.e.*, volatile flavor components within a matrix of non-volatile organic and inorganic materials, headspace gas chromatography (GC) was the appropriate method of analysis. Similar applications utilize headspace analysis such as the determination of trace organic substances in water and sewage[2,3]; ethanol and other compounds of toxicological interest in biological samples[4–7]; residual monomers in polymers[8]; bacterial metabolites[9]; and flavors in foods and beverages[10–13].

One headspace method[11] which approached the goal suffered from the fact that the measurements were made prior to attaining equilibrium. In this kinetic technique, the rate of diffusion of flavor from the dentrifrice core to the surface, which varies

0021-9673/88/$03.50 © 1988 Elsevier Science Publishers B.V.

inversely with viscosity, becomes an important contributing factor, especially since dentifrices vary significantly in rheological properties. A procedure was required in which the complicating effect of viscosity was not a factor. This was accomplished by developing a quantitative instrumental method in which the flavor released was measured at equilibrium.

EXPERIMENTAL

Instrumental headspace

A Perkin-Elmer Sigma 2000 gas chromatograph equipped with an HS-100 automated headspace sampler and a flame ionization detector (Perkin-Elmer, Norwalk, CT, U.S.A.) was used throughout this work. The dentifrices were laboratory batch samples, typically containing the following ingredients: dicalcium phosphate dihydrate, water, glycerin, sodium lauryl (dodecyl) sulfate (SDS), cellulose gum, flavor, sodium monofluorophosphate, sodium benzoate, tetrasodium pyrophosphate and sodium saccharin. The flavor was a spearmint/peppermint blend containing excess menthol and carvone, plus anethole. A 140-mg amount (approximately 0.10 ml) of dentifrice was dispensed into a 22-ml headspace vial (Perkin-Elmer) and weighed to the nearest 0.0001 g. The vial was hermetically sealed by crimping an aluminum cap containing an aluminum-coated silicone rubber septum (Perkin-Elmer) onto the vial. The sealed vial was placed into the sample carriage of the HS-100 headspace sampler which was programmed to maintain each vial at 40°C for 5–7 h, achieving equilibrium of the contents. An aliquot of the headspace was then automatically injected onto a Supelcowax 10 bonded-phase fused-silica capillary column, 30 m × 0.32 mm with a 0.25 -μm film thickness (Supelco, Bellefonte, PA, U.S.A.). The carrier gas was helium; the flow-rate was 5 ml/min; the split ratio was 20:1 and the column was held at 50°C for 2 min, then programmed to 150°C at a rate of 10°C/min. Use of the HS-100 automated headspace sampler allowed for unattended analysis of up to 100 samples. The chromatograms were processed by an LCI-100 computing integrator (Perkin-Elmer). Analysis of each dentifrice was replicated six times.

Instrumental viscosity

Relative viscosity measurements of the dentifrices varying in gum concentration were made with a Brookfield (Stoughton, MA, U.S.A.) digital viscometer model RVTD. Measurements were made directly in the dentifrice tube, two per sample.

RESULTS

Four sets of flavored dentifrices were tested in this study. A representative equilibrium headspace gas chromatogram of a flavored dentifrice is shown in Fig. 1. The first set of dentifrices contained six concentrations of a detergent, SDS. Table I shows the effect of increasing the SDS concentration on flavor released into headspace. As the SDS concentration increased from 0.3 to 1.8%, the equilibrium headspace flavor decreased by 35%.

The degree of binding of flavor in a dentifrice to β-cyclodextrin was determined (Table II). A flavor–β-cyclodextrin complex was prepared and added to the dentifrice in place of flavor oil. The β-cyclodextrin significantly decreased the amount of flavor

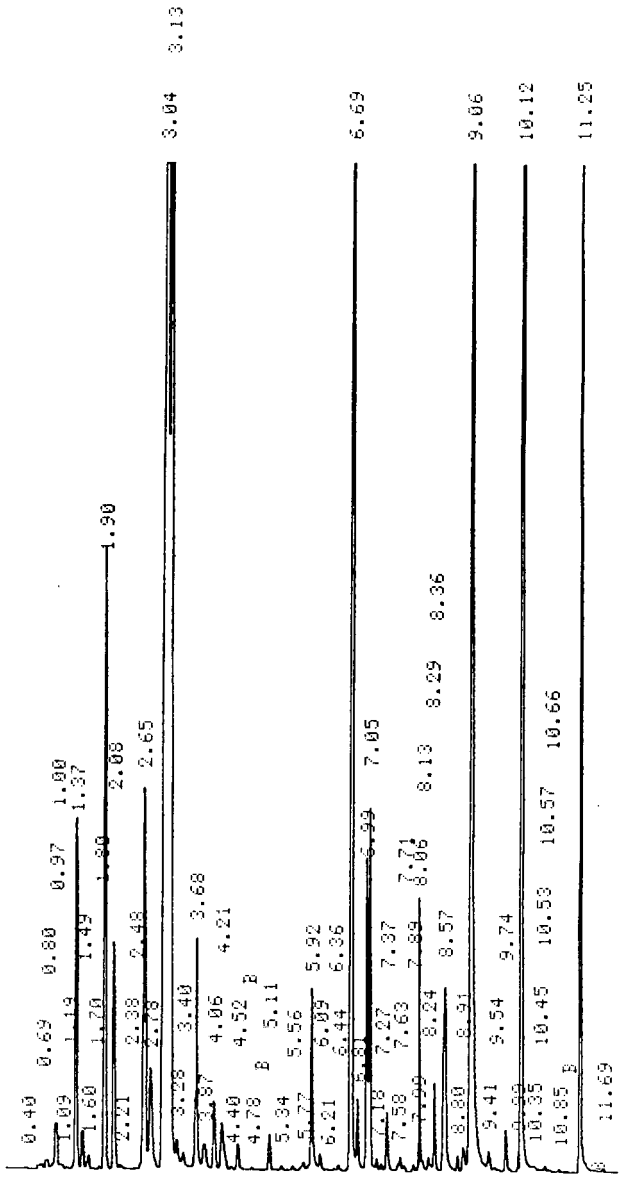

Fig. 1. Equilibrium headspace gas chromatogram of a flavored dentifrice. (Numbers indicate retention times in min.)

released into headspace, demonstrating the binding of flavor to β-cyclodextrin within the dentifrice. Also, the reproducibility of this method is exhibited by the coefficient of variation values of less than 3% for six replicate analyses per sample.

A series of dentifrices with eight different levels of flavor from 0 to 3.0% were tested by equilibrium headspace GC (Fig. 2, Table III). Results showed a strong

TABLE I

EFFECT OF DETERGENT (SDS) CONCENTRATION ON EQUILIBRIUM HEADSPACE FLAVOR

SDS Concentration (%)	*Total area (GC units)**	
	Mean ± standard error of the mean (n = 6)	*Coefficient of variation (%)*
0.3	17.14 ± 0.318	1.86
0.6	16.71 ± 0.082	0.49
0.9	16.55 ± 0.061	0.37
1.2	14.89 ± 0.237	1.59
1.5	12.30 ± 0.331	2.69
1.8	11.14 ± 0.073	0.66

* Electronic integrator counts (relative to component concentration).

TABLE II

EFFECT OF β-CYCLODEXTRIN ON EQUILIBRIUM HEADSPACE FLAVOR

Sample	*Total area (GC units)*	
	Mean ± standard error of the mean (n = 6)	*Coefficient of variation (%)*
Control	6.32 ± 0.159	2.52
Flavor + β-cyclodextrin	3.53 ± 0.057	1.61
1.2 × flavor + β-cyclodextrin	4.30 ± 0.049	1.14
1.5 × flavor + β-cyclodextrin	4.24 ± 0.049	1.16

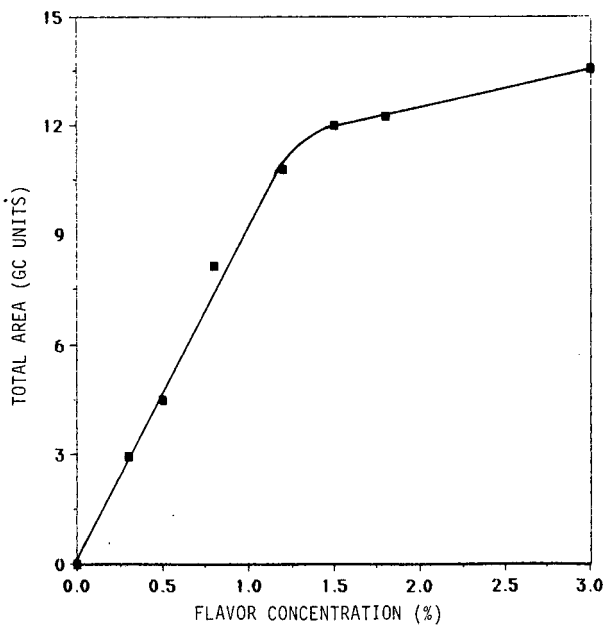

Fig. 2. Equilibrium headspace of dentifrices varying in flavor concentration.

TABLE III

EFFECT OF DENTIFRICE FLAVOR CONCENTRATION ON EQUILIBRIUM HEADSPACE FLAVOR

Sample (% flavor)	*Total area (GC units)*	
	Mean ± standard error of the mean (n = 6)	*Coefficient of variation (%)*
0	0 ± 0	0
0.3	2.95 ± 0.041	1.39
0.5	4.48 ± 0.094	2.10
0.8	8.17 ± 0.294	3.60
1.2	10.79 ± 0.302	2.90
1.5	12.01 ± 0.196	1.63
1.8	12.27 ± 0.098	0.80
3.0	13.54 ± 0.229	1.69

positive linear relationship between flavor concentration and headspace flavor from 0 to 1.2% (linear regression correlation coefficient = 0.998). Above 1.2% flavor, the flavor release continued to rise, but at a lower slope.

The fourth set of dentifrices tested contained six different concentrations of carboxymethyl (CM) cellulose thickening gum (from 0.3 to 2.0%). Table IV summarizes the results of this study, showing a 13.0% decrease in flavor release as the CM-cellulose concentration increased. Measurements by a Brookfield digital viscometer showed an increase of over two orders of magnitude in the viscosity of the dentifrices from 0.3 to 2.0% CM-cellulose (Fig. 3). Analysis of these dentifrices by kinetic headspace GC[1] resulted in a 28% decrease in released flavor over this range.

DISCUSSION

This analysis on four sets of dentifrices provides a simple, reproducible method for determining absolute effects of dentifrice compositional differences on flavor released into headspace, independent of viscosity. Analysis of flavor released into head-

TABLE IV

EFFECT OF CM-CELLULOSE CONCENTRATION ON EQUILIBRIUM HEADSPACE FLAVOR

Sample (% cellulose)	*Total area (GC units)*	
	Mean ± standard error of the mean (n = 6)	*Coefficient of variation (%)*
0.3	7.95 ± 0.176	2.21
0.5	7.83 ± 0.159	2.03
0.9	7.81 ± 0.216	2.77
1.3	7.55 ± 0.196	2.60
1.7	7.37 ± 0.094	1.28
2.0	6.91 ± 0.118	1.71

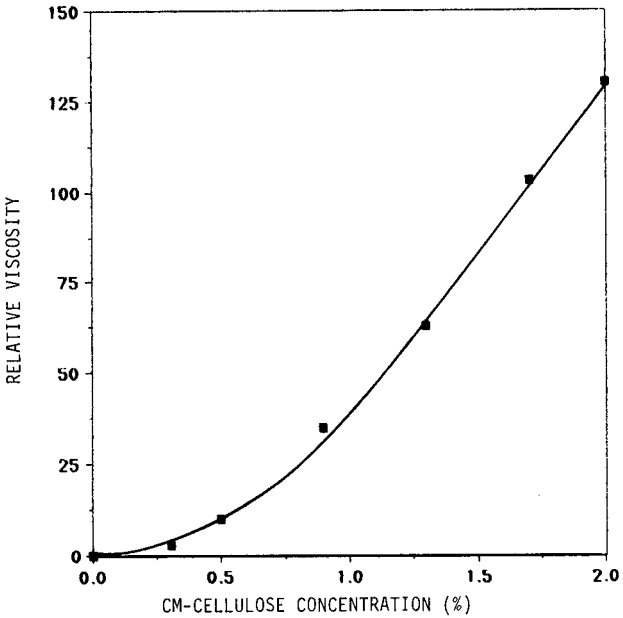

Fig. 3. Viscosity of dentifrices varying in CM-cellulose concentration.

space after thermodynamic equilibrium is attained reveals the binding affinity of a dentifrice component for flavor. Excellent reproducibility is illustrated by the low coefficient of variation data.

It was of interest to investigate the effect of SDS on flavor release in a dentifrice. SDS serves to form foam in a dentifrice, as well as to help dissolve the flavor oil. The results (Table I) demonstrated that the SDS has a rather substantial effect of complexing the dentifrice flavor, retarding its release. This is probably caused by the flavor oil being trapped in SDS micelles.

A complexing agent, β-cyclodextrin, was investigated for its ability to bind flavors as clathrates. The results (Table II) prove that it was effective.

The measured relationship (Fig. 2) found between flavor concentration and equilibrium headspace areas (within practical range) allows for quantitative modification of flavor levels in dentifrices to match desired flavor release.

The equilibrium CM-cellulose study (Table IV), when combined with the corresponding kinetic CM-cellulose study[1], allows for determination of the contribution of viscosity to flavor release. Since the equilibrium results are independent of viscosity, the 13% decrease found by equilibrium headspace GC is due to an interaction between CM-cellulose and flavor which inhibits flavor release. The 28% decrease found by kinetic headspace GC is a combination of two factors: a 13% decrease caused by the flavor–CM-cellulose interaction and a 15% decrease due to viscosity inhibiting the flavor migration from dentifrice to headspace.

Equilibrium headspace GC is of great value in analyzing large numbers of dentifrice formulations to determine the effect of dentifrice processing and formula-

tion changes on flavor. The results of these studies should be very useful to formulators, since knowing the effect of components such as SDS on flavor release would allow for corrections in detergent level, and flavor concentration and/or composition to be made.

REFERENCES

1 E. A. Tavss, S. G. Wiet, R. S. Robinson, J. Santalucia and D. L. Carroll, *J. Chromatogr.*, 438 (1988) 273.
2 A. G. Vitenberg, I. L. Butaeva, L. M. Kunznetsova and M. D. Inshakov, *Anal. Chem.*, 49 (1977) 128.
3 J. Drozd, J. Novák and J. A. Rijks, *J. Chromatogr.*, 158 (1978) 471.
4 N. C. Jain and R. H. Cravey, *J. Chromatogr. Sci.*, 10 (1972) 263.
5 R. H. Cravey and N. C. Jain, *J. Chromatogr. Sci.*, 12 (1974) 209.
6 H. Hachenberg and A. P. Schmidt, *Gas Chromatographic Headspace Analysis*, Heyden, London, 1977, p. 125.
7 B. Kolb, *J. Chromatogr.*, 122 (1976) 553.
8 R. J. Steichen, *Anal. Chem.*, 48 (1976) 1398.
9 J. M. Zechman, S. Aldinger and J. N. Labows, Jr., *J. Chromatogr.*, 277 (1986) 49.
10 P. L. Wylie, *Chromatographia*, 21 (1986) 251.
11 A. J. Nunez and H. Maarse, *Chromatographia*, 21 (1986) 44.
12 W. Wellnitz-Ruen, G. A. Reineccius and E. L. Thomas, *J. Agric. Food Chem.*, 30 (1982) 512.
13 G. Takeska and W. Jennings, *J. Chromatogr. Sci.*, 22 (1984) 177.

Journal of Chromatography, 455 (1988) 151–162
Elsevier Science Publishers B.V., Amsterdam — Printed in The Netherlands

CHROM. 20 857

CROSS-AXIS SYNCHRONOUS FLOW-THROUGH COIL PLANET CENTRIFUGE FOR LARGE-SCALE PREPARATIVE COUNTER-CURRENT CHROMATOGRAPHY

III. PERFORMANCE OF LARGE-BORE COILS IN SLOW PLANETARY MOTION

YOICHIRO ITO*

Laboratory of Technical Development, National Heart, Lung, and Blood Institute, National Institutes of Health, Building 10, Room 5D-12, Bethesda, MD 20892 (U.S.A.)

and

TIAN-YOU ZHANG

Beijing Institute of New Technology Application, Beijing (China)

(Received June 29th, 1988)

SUMMARY

A preparative capability of the present cross-axis synchronous flow-through coil planet centrifuge was demonstrated with 0.5 cm I.D. multilayer coils. Results of the model studies with short coils indicated that the optimal separations are obtained at low revolutional speeds of 100–200 rpm in both central and lateral coil positions. Preparative separations were successfully performed on 2.5–10 g quantities of test samples in a pair of multilayer coils connected in series with a total capacity of 2.5 l. The sample loading capacity will be scaled up in several folds by increasing the column width.

INTRODUCTION

In the foregoing articles (Parts I[1] and II[2]), the capability of the cross-axis synchronous flow-through coil planet centrifuge (X-axis CPC) has been demonstrated in preparative counter-current chromatography (CCC) of dinitrophenyl (DNP)-amino acids and dipeptides with paired multilayer coils of 2.6 mm I.D. rotated at 450–500 rpm. The use of relatively high centrifugal force field (*ca.* 50 *g*), however, limits the use of longer columns for further scaling up the sample loading capacity of the system due to mechanical strain of the planetary centrifuge system. This problem may be solved by utilizing a large-bore separation column which shifts the optimal revolutional speed down to a few hundred rpm range and, therefore, permits safe operation of a much larger separation column.

The present paper describes preliminary studies on performance of a large-bore column of 5 mm I.D. Model studies were performed with single-layer short coils to

0021-9673/88/$03.50 © 1988 Elsevier Science Publishers B.V.

investigate both retention of the stationary phase and partition efficiency for determination of the optimal operational conditions. The preparative capability of the present method was demonstrated on multigram separations of test samples with paired multilayer coils with a total capacity of 2.5 l.

EXPERIMENTAL

Apparatus

The present studies were performed with the X-axis CPC with a 20-cm revolutional radius which has been used in the previous studies. The design of the apparatus is described in detail in Part I[1].

Two types of coiled columns were tested: short coils for model studies on retention of the stationary phase and partition efficiency, and a pair of multilayer coils for preparative-scale separations. The short coil was prepared from a 4.2 m length of 5.5 mm I.D. fluorinated ethylene propylene (FEP) tubing (Galtek Corporation, Jonathan Industrial Center, Chaska, MN, U.S.A.) by winding it onto a holder hub of 15 cm diameter to form a single-layer coil. The coil was mounted on the holder at two locations, at the center of the holder ($l = 0$ cm) and at 9 cm on the left of the center ($l = -9$ cm). The total capacity of the short coil measured about 110 ml. Each multilayer coil was prepared from 5 mm I.D. polytetrafluoroethylene (PTFE) tubing (Zeus Industrial Products, Raritan, NJ, U.S.A.) by winding it onto a spool-shaped holder measuring 5 cm in width between the flanges and 10 cm in hub diameter. It consisted of 13 layers with 9–10 coils in each layer (total 120 coils) with a capacity of

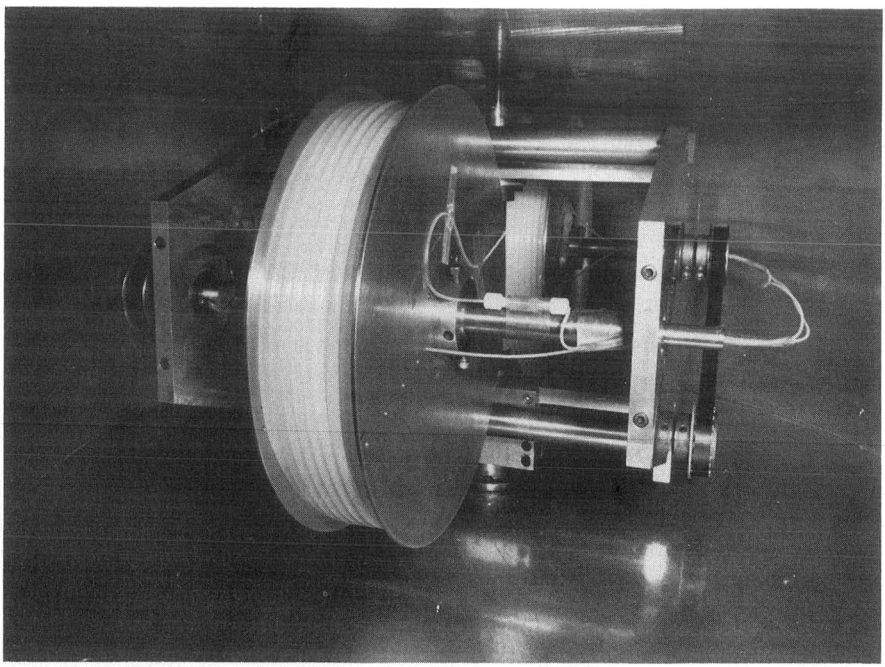

Fig. 1. Photograph of the X-axis CPC equipped with a pair of multilayer coils in the central position.

about 1250 ml. Two identical multilayer coils were connected in series and symmetrically mounted on the rotary frame to provide stable balance of the centrifuge system as shown in Fig. 1.

The thick-wall FEP tubing used for the short coil is transparent and resists flattening on coiling and, therefore, is ideal for model studies, whereas much lighter, less expensive PTFE tubing is more suitable in the practical use for fabrication of a long multilayer coil.

Reagents

Two-phase solvent systems were prepared from chloroform, *n*-butanol (both were glass-distilled chromatographic grade from Burdick & Jackson Labs., Muskegon, MI, U.S.A.); acetic acid (reagent grade from J. T. Baker, Phillipsburg, NJ, U.S.A.); 1 *M* hydrochloric acid (reagent grade from Sigma, St. Louis, MO, U.S.A.); and distilled water. The following compounds were used for test samples (all reagent grade from Sigma): N^{δ}-2,4-DNP-L-ornithine (DNP-orn), N-2,4-DNP-L-aspartic acid (DNP-asp), N-2,4-DNP-DL-glutamic acid (DNP-glu), N,N-di(2,4-DNP)-L-cystine [diDNP-$(cys)_2$], N-2,4-DNP-β-alanine (DNP-β-ala), N-2,4-DNP-L-alanine (DNP-ala), N-2,4-DNP-L-proline (DNP-pro), N-2,4-DNP-L-leucine (DNP-leu), L-valyl-L-tyrosine (val-tyr), L-leucyl-L-tyrosine (leu-tyr) and L-tryptophyl-L-tyrosine (trp-tyr).

Preparation of two-phase solvent systems and sample solutions

Two different solvent systems were used: chloroform–acetic acid–0.1 *M* hydrochloric acid (2:2:1, v/v/v) for DNP-amino acid separations and *n*-butanol–acetic acid–water (4:1:5, v/v/v) for dipeptide separations. Each solvent system was thoroughly equilibrated in a separatory funnel at room temperature and the two phases separated shortly before use.

Sample solutions for DNP-amino acid separations were prepared as follows: For the preliminary studies with short coils, equal quantities of DNP-glu and DNP-ala were dissolved in the upper aqueous phase to make the concentration of each component 0.5 g%, and 0.5 ml of the sample solution was loaded in each experiment. For the large-scale preparative chromatography in the multilayer coils, mixtures of five DNP-amino acids with a total weight of 10 g were dissolved in 100 ml of the solvent mixture: The sample solution for the run with the upper phase mobile contained 1 g of DNP-orn, 2 g of DNP-asp, 2 g of DNP-glu, 1 g of diDNP-$(cys)_2$, and 4 g of DNP-ala, while that with the lower phase mobile contained 1 g of DNP-leu, 2 g of DNP-pro, 2 g of DNP-β-ala, 1 g of diDNP-$(cys)_2$, and 4 g of DNP-glu.

For the preliminary separations in short coils, the peptides were dissolved in the lower aqueous phase to make concentrations of val-tyr and trp-tyr 1 g% and 0.3 g%, respectively, and 0.5 ml of this solution were used for each run. For the preparative separations in the multilayer coils, 1 g of val-tyr, 1 g of leu-tyr, and 0.5 g of trp-tyr were dissolved in 200 ml of the solvent mixture.

Model studies on stationary phase retention and partition efficiency in short coils

Experiments were performed according to the procedure described in Part II[2]. For each experiment, the coil was first completely filled with the stationary phase. This was followed by injection of sample solution through the sample port. Then, the mobile phase was eluted through the coil at 120 ml/h while the apparatus was rotated

at the desired rpm value. The effluent from the outlet of the coil was continuously monitored with an LKB Uvicord S at 278 nm and fractionated into test tubes with an LKB fraction collector for later analysis. After the two peaks were eluted from the coil, the apparatus was stopped and the retention of the stationary phase was measured by collecting the column contents into a graduated cylinder. This was done by connecting the inlet of the column to a pressured nitrogen line, while the coil was slowly rotated at 100 to 200 rpm in a direction to make the outlet of the coil the head to facilitate emptying the column contents. The measurements were performed at various rpms, ranging from 0 to 300, using both the upper and the lower phases as the mobile phase in the central (l = 0 cm) and the lateral (l = −9 cm) coil positions.

As described in the foregoing articles (Parts I and II), performance of laterally mounted coils is affected by three factors, *i.e.*, the Archimedean screw effect represented by head-tail elution mode, planetary motion P_I or P_{II} (see Table I), and inward-outward elution mode. All possible combinations were examined at moderate revolutional speeds of 100 to 200 rpm to select the favorable experimental conditions which were further investigated at a broader range of revolutional speeds. The selected experimental conditions are summarized in Table I.

Preparative separations with paired multilayer coils

Preparative separations were performed with a pair of multilayer coils connected in series and mounted on the center of the holder shaft (l = 0 cm), using the optimal experimental conditions determined by the preliminary model studies with short coils. The experiment was initiated by filling the entire column with the stationary phase. Air trapped in the column can be easily eliminated by rotating the column slowly in a direction to make the outlet of the column the head while pumping the stationary

TABLE I

SUMMARY OF EXPERIMENTAL CONDITIONS IN MODEL STUDIES WITH SHORT COILS

Coil position	*Mobile phase*	*Head-tail elution mode*	*Planetary motion**	*Inward or outward elution mode (handedness)***
Center (l = 0 cm)	Upper phase	head→tail		
	Lower phase	tail→head		
Lateral (l = −9 cm)	Upper phase	head→tail	P_I	O (L)
	Upper phase	head→tail	P_I	I (R)
	Upper phase	head→tail	P_{II}	O (R)
	Upper phase	head→tail	P_{II}	I (L)
	Lower phase	tail→head	P_I	O (L)
	Lower phase	tail→head	P_I	I (R)
	Lower phase	tail→head	P_{II}	O (R)
	Lower phase	tail→head	P_{II}	I (L)

* Planetary motion: P_I: 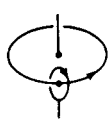 ; P_{II}: 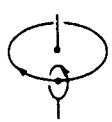

** I = Inward elution; O = outward elution; L = left-handed; R = right-handed.

phase. During this filling process, stationary phase flowing from the outlet of the column can be recycled by adding it back to the reservoir, if desired. After completion of this procedure, sample solution was injected through the sample port. Then, the mobile phase was pumped into the coil in a proper elution mode at a flow-rate of 120 ml/h while the apparatus was rotated at the optimal revolutional speed. The effluent from the outlet of the column was continuously monitored with an LKB Uvicord S at 278 nm and then fractionated with an LKB fraction collector. After all peaks were eluted, the apparatus was stopped, and the column contents were pumped out by pressured nitrogen as described earlier. An aliquot of fractions was mixed with methanol and absorbance was determined with a Zeiss Model PM6 spectrophotometer: DNP-amino acids were analyzed at 430 nm and dipeptides at 280 nm as in the preliminary studies.

RESULTS AND DISCUSSION

Retention of stationary phase and partition efficiency in short coils

Fig. 2 illustrates a set of phase retention diagrams obtained from chloroform–acetic acid–0.1 *M* hydrochloric acid (2:2:1) (top) and *n*-butanol–acetic acid–water (4:1:5) (bottom) each with the upper (left) and the lower (right) phases used as the mobile phase. In each diagram, percent retention of the stationary phase relative to the total column capacity is plotted against the applied revolutional speed from 0 to 300 rpm. The data obtained from three different experimental conditions —the central coil position, and the lateral coil position with planetary motions P_I and P_{II}— are drawn with different symbols as indicated in the figure. The retention of over 50% is

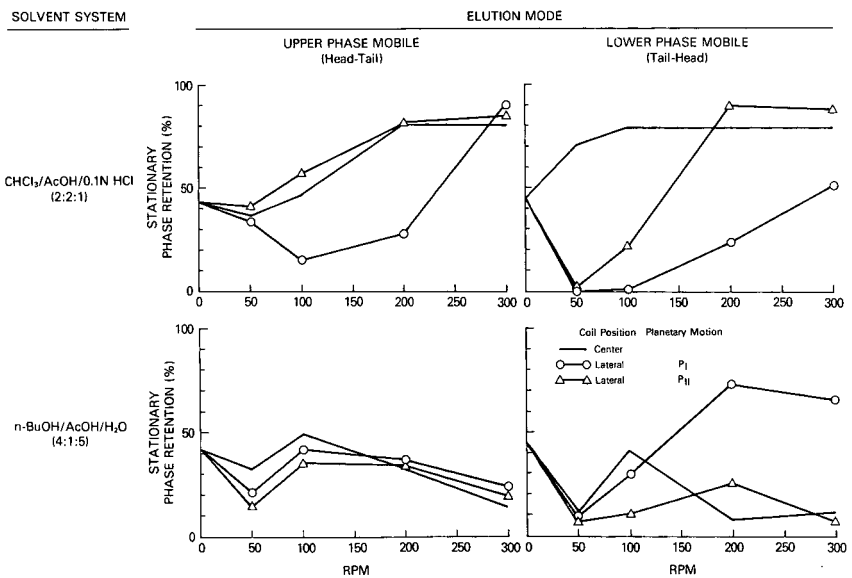

Fig. 2. Retention of stationary phase in short coils in the central and lateral positions. AcOH = Acetic acid; n-BuOH = *n*-butanol.

considered satisfactory, but over 30% may also be used for separation, if carryover of the stationary phase is minimum.

At 0 rpm, all groups yield similar retention at 40 to 45% simply by the effect of gravity. At a slow rotation of 50 rpm, most of the retention curves drop appreciably, some approaching the 0% line. Further increase of the revolutional speed to 100–200 rpm, however, results in a sharp increase of retention in all groups. Increasing the revolution above 200 rpm produces contrasted results between the two solvent systems: The retention of the chloroform phase system either continues to rise or forms a plateau, whereas that of the *n*-butanol phase system tends to decline.

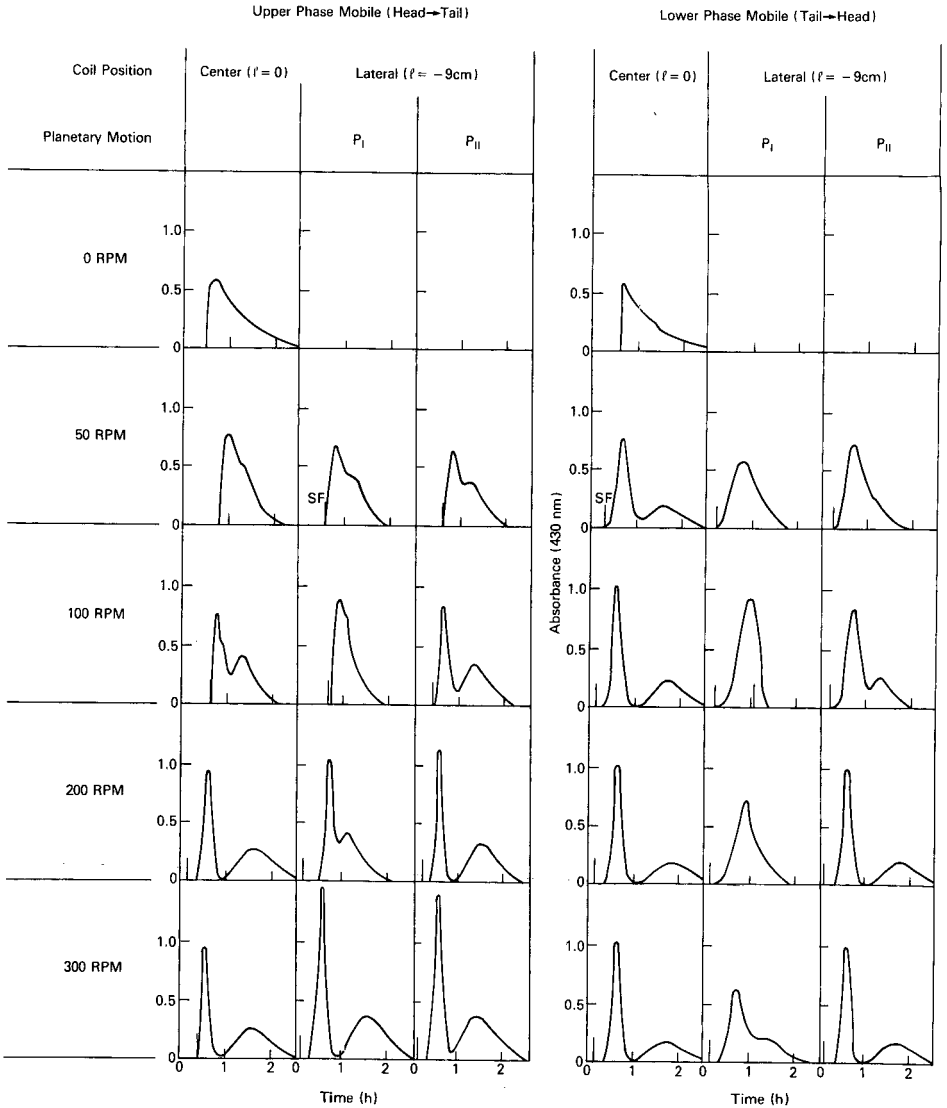

Fig. 3. Effects of revolutional speed, column position and planetary motion on DNP-amino acid separation.

The retention curves obtained from the central coil position are quite different from those obtained from the lateral coil position. Furthermore, retention curves obtained from the lateral coil position at the two planetary motions, P_I and P_{II}, are mostly very different from each other: In the chloroform phase system, P_{II} yields higher retention than P_I, whereas in the *n*-butanol phase system this relationship is reversed, P_I

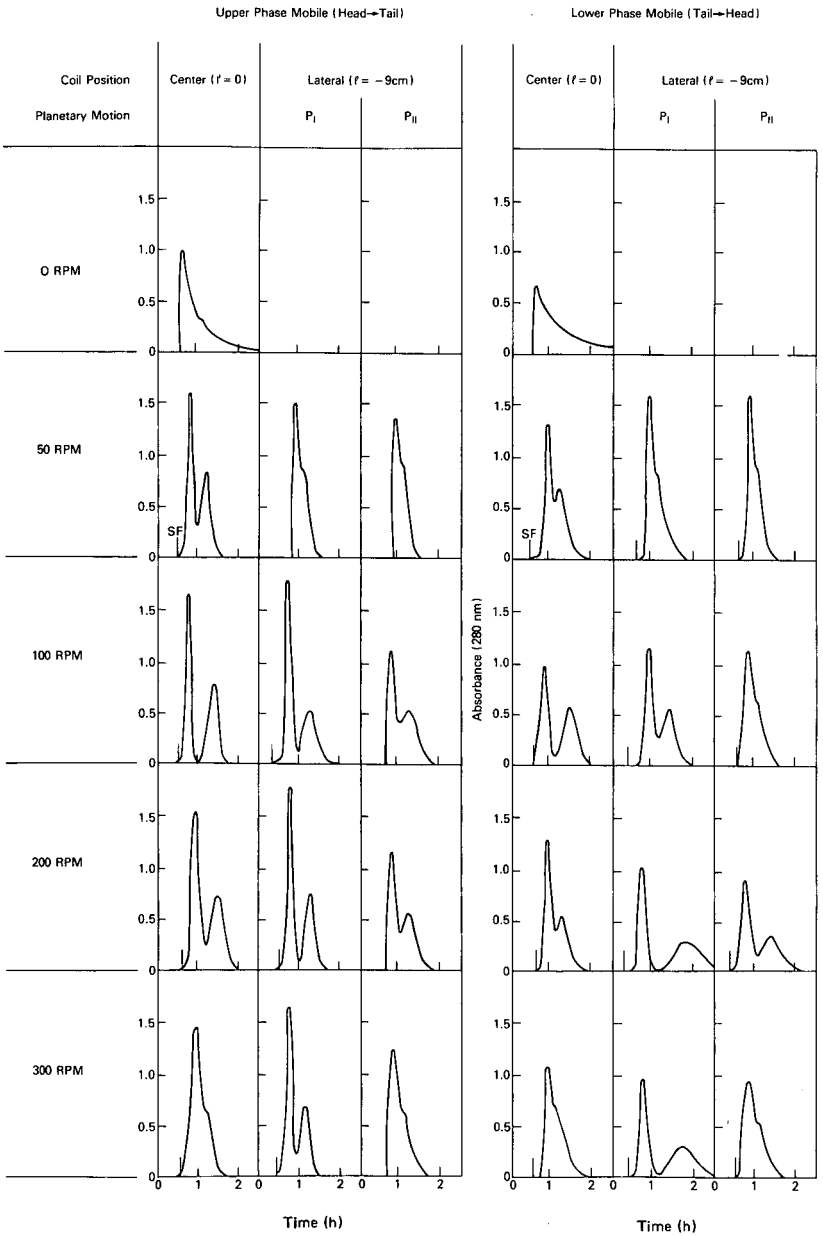

Fig. 4. Effects of revolutional speed, column position and planetary motion on dipeptide separation.

yielding better retention than P_{II}. Overall results indicated that satisfactory retention is available at relatively low revolutional speeds from 100 to 200 rpm in all groups.

Fig. 3 shows a set of chromatograms of DNP-amino acids obtained with a two-phase solvent system composed of chloroform–acetic acid–0.1 *M* hydrochloric

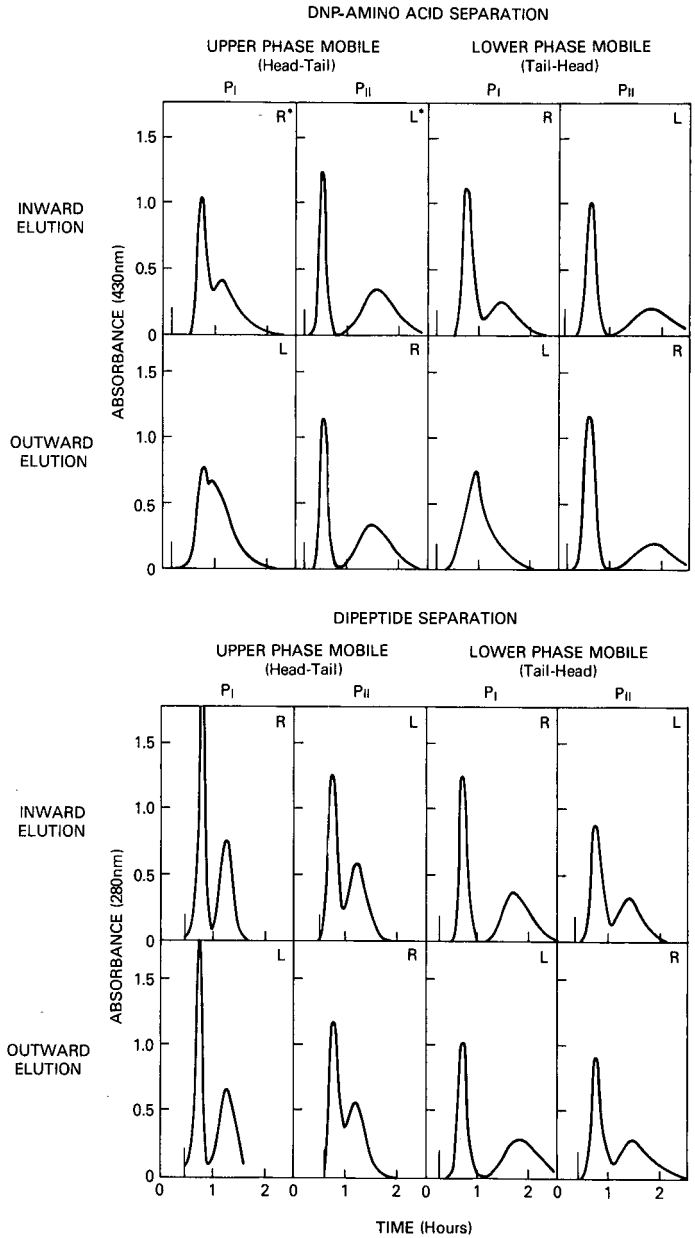

Fig. 5. Effects of inward or outward elution mode and planetary motion on partition efficiency.

acid (2:2:1) by using the upper (left panel) and the lower (right panel) phases as the mobile phase. These chromatograms are arranged according to the coil positions (top) and the applied revolutional speeds ranging from 0 to 300 rpm (left). Partition efficiency of each chromatogram is easily estimated from the degree of peak resolution by observing the height of the trough between the two peaks.

In the central coil position ($l = 0$ cm) (left column in each panel), the partition efficiency sharply increases with revolution up to 100–200 rpm where the two peaks are completely resolved. Further increase of revolutional speed to 300 rpm shows little improvement in peak resolution. In the lateral coil position ($l = -9$ cm), two planetary motions, P_I and P_{II}, yield quite different results: P_{II} produces high peak resolutions quite similar to those obtained from the central coil position, while P_I gives much lower peak resolutions, especially when the lower phase is mobile (right panel).

Fig. 4 shows a set of chromatograms of dipeptides obtained with a two-phase solvent system composed of *n*-butanol–acetic acid–water (4:1:5). The chromatograms are arranged according to the format used in the foregoing DNP-amino acid separations. In the central coil position, partition efficiency rose with the increased revolution up to 100 rpm where the peak resolution becomes maximum. Further increase of revolutional speed results in decline of partition efficiency in both mobile phase groups. In the lateral coil position, planetary motion P_I produces similar results, yielding the highest peak resolution at 200 rpm, while planetary motion P_{II} gives much lower peak resolution.

Effect of the inward or outward elution mode on the partition efficiency was investigated with right-handed (R) and left-handed (L) coils mounted in the lateral position ($l = -9$ cm). Fig. 5 shows a set of chromatograms of the test samples obtained at the optimum revolutional speeds, *i.e.*, 200 rpm for DNP-amino acid separations (upper panel) and 100 rpm for dipeptide separations (lower panel). In both samples, chromatograms obtained from the inward and outward elution modes under the otherwise identical experimental conditions are quite similar to each other compared with those obtained from a given inward or outward elution mode at the two different planetary motions, P_I and P_{II}. These results clearly indicate that the mode of planetary motion produces much more profound effects on partition efficiency than the inward/outward elution mode.

The fact that the inward-outward elution mode produces no significant effect on the partition efficiency gives an important implication for the use of multilayer coils in the lateral location on the holder. The multilayer coil used in CCC consists of multiple coiled layers in which running direction of the coil along the axis of the holder reverses in each neighbouring layers. For example, if the first layer runs outward from the right toward the left, then the second layer runs inward from the left toward the right, and so forth. Thus, under a given experimental condition, each neighbouring coiled layer is subjected to opposite inward/outward elution modes, while other conditions such as the head-tail elution mode and planetary motion remain the same. Consequently, the above results ensure the efficient use of the multilayer coils in the lateral position provided that other experimental conditions are properly selected.

Preparative separations with paired multilayer coils

Capability of the present CCC system was demonstated on multigram separations of test samples with a pair of long multilayer coils with a total capacity of about

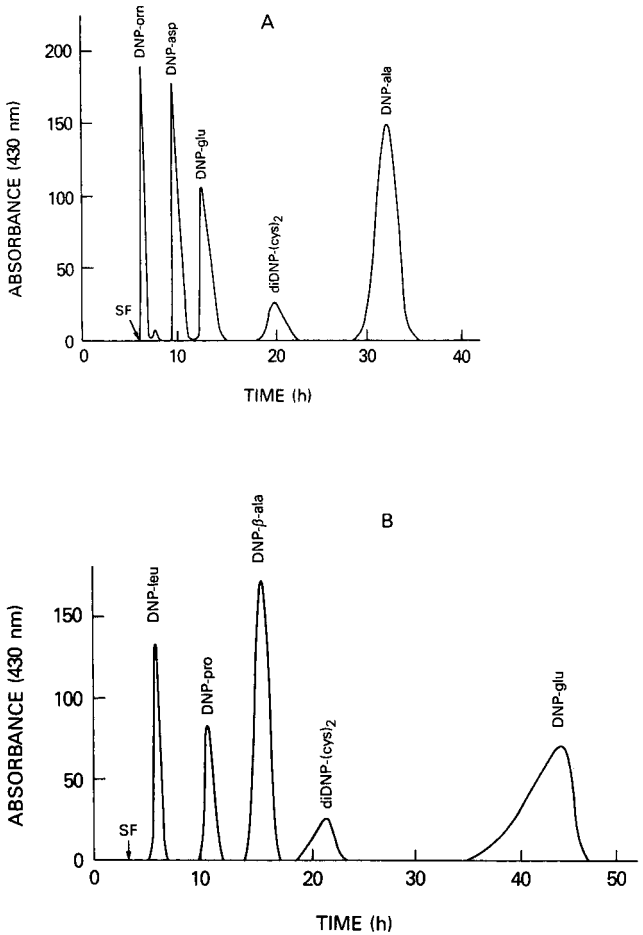

Fig. 6. Preparative separations of DNP-amino acids. Conditions: apparatus, X-axis CPC, 20 cm radius; column, paired multilayer coils, 5 mm I.D., 2.5 l capacity, β = 0.25–0.6, central position; sample, DNP-amino acids, 10 g; solvent system, chloroform–acetic acid–0.1 *M* hydrochloric acid (2:2:1); mobile phase, upper aqueous phase (A) or lower non-aqueous phase (B); elution mode, head→tail (A) or tail→head (B); flow-rate, 120 ml/min; revolution, 200 rpm, P_I (A) or P_{II} (B); retention, 67% (A) or 84% (B). SF = Solvent front, β = ratio of the coil radius to the radius of revolution.

2.5 l. The separations were performed under the optimal operational conditions determined in the preliminary model studies with short coils.

Fig. 6 shows chromatograms of DNP-amino acids with a solvent system composed of chloroform–acetic acid–0.1 *M* hydrochloric acid (2:2:1) using the upper (Fig. 6A) and the lower (Fig. 6B) phases as the mobile phase. In each separation, a total of 10 g quantity samples was completely resolved into discrete peaks in 35 to 50 h. Partition efficiencies computed according to the conventional gas chromatographic formula, $N = (4t_R/W)^2$ (N denotes the partition efficiency expressed in terms of theoretical plate number, t_R the retention time of the peak maximum and W the peak width expressed in the same unit as t_R), range from 400 to 1000 theoretical plates.

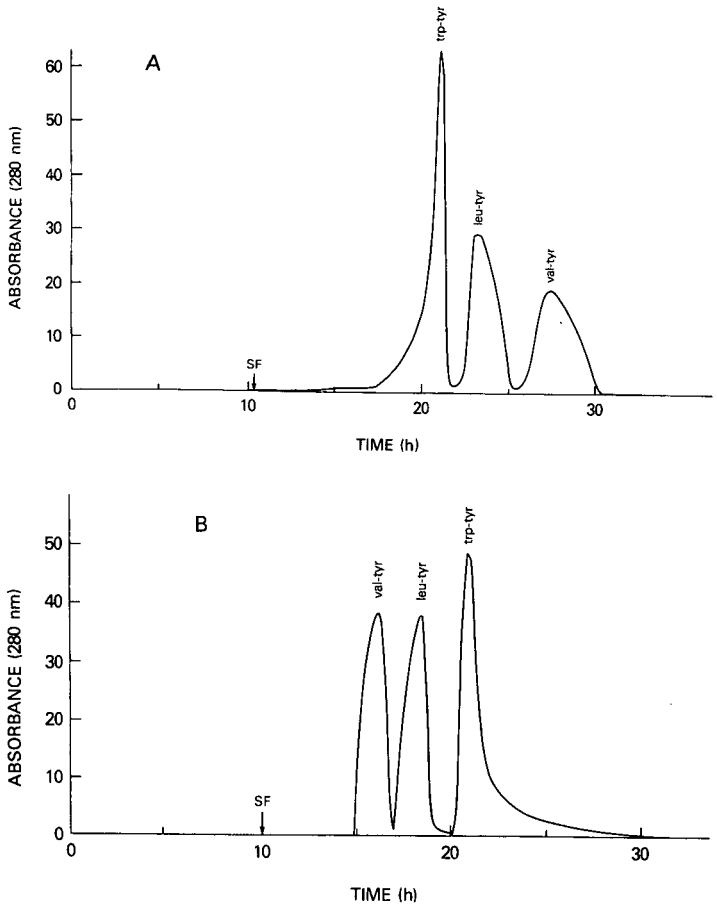

Fig. 7. Preparative separations of dipeptides. Conditions: apparatus, column and flow-rate as in Fig. 6; sample, dipeptides, 2.5 g; solvent system, *n*-butanol–acetic acid–water (4:1:5); mobile phase, upper non-aqueous phase (A) or lower aqueous phase (B); elution mode, head→tail (A) or tail→head (B), revolution, 100 rpm, P_I (A) or P_{II} (B); retention, 27% (A) or 33% (B).

Fig. 7 similarly illustrates chromatograms of dipeptides obtained with a two-phase solvent system composed of *n*-butanol–acetic acid–water (4:1:5) using the upper (Fig. 7A) and the lower (Fig. 7B) phases as the mobile phase. Non-linear isotherm of the peptides in the present solvent system produced skewed peaks, especially in trp-tyr, in both chromatograms. Nevertheless, all three components were fairly well resolved in 30 h.

The above results successfully demonstrate an excellent preparative capability of the present X-axis CPC equipped with 5 mm I.D. multilayer coils in the central coil position ($l = 0$ cm) at low revolutional speeds of 100–200 rpm. As indicated by the results obtained from the model studies with short coils, the lateral coil position ($l = -9$ cm) can also produce similar results at the same revolutional speed under the proper mode of planetary motion (see Figs. 3 and 4). This clearly indicates that the

column capacity, hence the sample loading capacity, of the present system can be increased in several folds simply by extending the width of the multilayer coils toward one side of the holder shaft. The results of present studies also strongly suggest that the use of large-bore coils would further decrease the optimal revolutional speed below 100 rpm, as in the case of the slowly rotating coil assembly reported earlier[3,4], thus facilitating the use of huge capacity multilayer coils for industrial-scale separations.

REFERENCES

1 Y. Ito and T.-Y. Zhang, *J. Chromatogr.*, 449 (1988) 135.
2 Y. Ito and T.-Y. Zhang, *J. Chromatogr.*, 449 (1988) 153.
3 Y. Ito and R. Bhatnagar, *J. Liq. Chromatogr.*, 7 (1984) 257.
4 Y. Ito, *J. Liq. Chromatogr.*, 11 (1988) 1.

Journal of Chromatography, 455 (1988) 163–172
Elsevier Science Publishers B.V., Amsterdam — Printed in The Netherlands

CHROM. 20 868

IDENTIFICATION OF ORGANOPHOSPHORUS INSECTICIDES AND THEIR HYDROLYSIS PRODUCTS BY LIQUID CHROMATOGRAPHY IN COMBINATION WITH UV AND THERMOSPRAY–MASS SPECTROMETRIC DETECTION

A. FARRAN and J. DE PABLO
Department of Chemical Engineering, ETSEIB, Diagonal 647, 08028 Barcelona (Spain)
and
D. BARCELÓ*
Environmental Chemistry Department, CID-CSIC, c/Jorge Girona Salgado, 18-26, 08034 Barcelona (Spain)
(First received May 16th, 1988; revised manuscript received July 18th, 1988)

SUMMARY

Liquid chromatography with ultraviolet detection (LC–UV) and positive and negative ion mode (PI and NI, respectively) thermospray LC–mass spectrometry (LC–MS) were used for the analysis of the organophosphorus pesticides azinphos-methyl, diazinon and parathion-methyl and their corresponding breakdown products obtained after basic hydrolysis (pH 7–11). LC analysis was performed in the reversed-phase mode using methanol–water (80:20) or methanol–water (70:30) + 0.1 *M* ammonium acetate for LC–UV or LC–MS, respectively. By employing NI thermospray LC–MS the identification of *p*-nitrophenol, showing the $[2M-H]^-$ ion as the base peak, was feasible and confirmed the LC–UV chromatogram at 220 nm. When the PI mode was used, $[M+NH_4]^+$ and $[M+H]^+$ions were obtained as base peaks for azinphos-methyl and diazinon, respectively. The degradation rates varied from diazinon, which showed no degradation during a period of ten days, to azinphos-methyl and parathion-methyl, for which degradation occured rapidily when the pH was increased from 7 to 11.

INTRODUCTION

Organophosphorus pesticides are of interest owing to their wide use in agriculture and, in some instances, their high mammalian toxicity[1]. Their low persistency is known and hydrolysis can easily occur, either enzymatically as in organisms[2], or microbially in soils[3] or biotically and abiotically as in freshwaters and estuarine waters[4]. Further, the biodegradation rates in waters are dependent on the microbial community biomass and activity, chlorophyll, pH and total organic carbon[4].

Organophosphorus pesticides and their corresponding metabolites are currently analysed by capillary gas chromatography (GC) with thermionic[5,6] or flame photo-

0021-9673/88/$03.50 © 1988 Elsevier Science Publishers B.V.

metric detection[7]. Mass spectrometric (MS) detection has been frequently employed in combination with capillary GC in the electron impact[8,9] or in the positive chemical ionization mode with methane [9–11], isobutane[12] and ammonia[10] or in the negative chemical ionization mode with methane[11,13], methane–oxygen[11] and dichloromethane[14]. However, organophosphorus pesticides which are thermally labile, such as trichlorfon[7,8], or polar such as parathion[5] and malathion[15], are difficult to analyse by GC. More problems arise when analysing organophosphorus pesticide breakdown products. In such instances even chemical derivatization is needed, *e.g.*, with *p*-nitrophenol, a metabolite of parathion obtained under basic hydrolysis, which is usually derivatized with pentafluorobenzyl bromide and subsequently analysed by GC with electron-capture detection[16].

Because of these problems, the analysis of organophosphorus pesticides and their corresponding metabolites has been carried out by liquid chromatography (LC) using either UV[17], reductive amperometric[18], selective thermionic[19] or MS detectors, employing either direct liquid introduction[20–22], moving belt[23] or thermospray interfaces[24–26]. Recently, even the applicability of supercritical fluid chromatography (SFC)–MS[27] and tandem mass spectrometry (MS–MS)[28] has been reported.

In the work described here LC–UV and LC–MS with a thermospray (TSP) interface have been applied to the analysis of the organophosphorus pesticides parathion-methyl, diazinon and azinphos-methyl and their corresponding breakdown products obtained under basic hydrolysis. Solutions of the decomposed analytes at pH 7–11 were directly injected into the LC system with UV detection at 220 nm and MS detection. The results demonstrated the utility of both positive ion (PI) and negative ion (NI) TSP LC–MS, as reported previously for a group of chlorophenols and herbicides[29]

EXPERIMENTAL

Materials

HPLC-grade water and methanol (Carlo Erba, Milan, Italy) were passed through a 0.45-μm filter from Scharlau (Barcelona, Spain) before use. Analytical-reagent grade ammonium acetate was obtained from Panreac, Montplet & Esteban (Montcada i Reixach, Barcelona, Spain), azinphos-methyl and diazinon from Polyscience (Niles, IL, U.S.A.) and parathion-methyl and *p*-nitrophenol from Dr. Su. I. Ehrenstorfer (Augsburg, F.R.G.).

Chromatographic system

Eluent delivery was provided either by two Model 510 high-pressure pumps, coupled with Model 680 automated gradient controller (Waters Chromatography Division, Milipore, Milford, MA, U.S.A.) and a Model 7125 injection valve with a 20-μl loop from Rheodyne (Cotati, CA, U.S.A.) or by a Spectra-Physics (San José, CA, U.S.A.) Model SP-8700 solvent delivery unit with an SP-8440 UV–VIS detector and an SP-4270 integrator (San José, CA, U.S.A.). Stainless-steel columns of dimensions (30 × 0.40 cm I.D. (Tracer Analítica, Barcelona, Spain) and 12 × 0.4 cm I.D. packed with 10-μm particle diameter Spherisorb ODS-2 (Merck, Darmstadt, F.R.G.) and Nucleosil C_{18} (Knauer, Bad Homburg, F.R.G.), respectively, were used.

Mass spectrometer

A Hewlett–Packard (Palo Alto, CA, U.S.A.) Model 5988A TSP LC–MS quadrupole mass spectrometer and a Hewlett-Packard Model 35741B instrument for data acquisition and processing were employed. The TSP temperatures were: stem 107°C, tip 178°C, vapour 194°C and ion source 264°C with the filament on. In all the experiments the filament-on mode of the TSP was used, in which conventional positive and negative chemical ionization can be carried out by using the vaporized mobile phase as the chemical ionization reagent gas. In essence, the vaporized mobile phase acts as a moderating gas to produce a high population of thermal-energy electrons which can be captured by the sample molecules. The TSP interface works at its highest sensitivity with at least 10% aqueous and with a sufficient concentration of ionizing additive, generally 0.1 *M* ammonium acetate. During the TSP vaporization process, interaction between the solvent and the volatile ionizing additive provides a soft ionization process, usually with little fragmentation of the primary ions[24–26].

RESULTS AND DISCUSSION

Degradation studies by LC with UV detection

The hydrolysis of the three model organophosphorus pesticides was studied by adjusting the pH of the standard aqueous solutions with ammonia and keeping the temperature at 20°C. Three different pHs, 7, 9 and 11, were considered for the hydro-

TABLE I

DEGRADATION OF PARATHION-METHYL, AZINPHOS-METHYL AND DIAZINON AT DIFFERENT pH AS A FUNCTION OF TIME

Temperature: 20°C. Results given are concentrations (mg/l) for an initial concentration of each pesticide of 100 mg/l.

Pesticide	*Time (h)*	*pH*		
		7	*9*	*11*
Parathion-methyl	2	100	98	95
	4	100	95	87
	6	100	93	77
	24	100	91	76
	48	100	86	63
	72	95	75	46
	144	88	55	27
	336	87	32	10
Azinphos-methyl	1	100	97	88
	4	100	78	47
	6	100	68	26
	48	100	55	0.1
	144	100	49	ND*
	216	100	40	ND*
Diazinon	240	No degradation observed		

* ND = Not detected.

lysis studies. This last value was used to simulate an analytical procedure for removing organophosphorus pesticides from polluted wastewater and the other two pH values are more similar to those found in natural waters[4].

The degradation of pesticides and the appearance of metabolites were followed by LC–UV. The Results obtained at different pH values and times are given in Table I. No degradation was observed for diazinon at any basic pH during ten days, whereas parathion–methyl and azinphos-methyl commenced to degrade considerably, to the extent of 14% and 45%, respectively, after 48 h at pH 9. These values agree in principle with the half-lifes reported for these pesticides[1], diazinon showing the longest half-life of the three compounds.

The corresponding LC–UV chromatograms of the three pesticides after degradation at pH 11 for 48 h are shown in Fig. 1. Parathion-methyl and azinphos-methyl showed one and three metabolites, respectively, before the peak of the compound, whereas for diazinon no metabolite was observed.

Thermospray LC–MS of organophosphorus pesticides and metabolites

By employing LC–MS the characterization of the investigated pesticides was confirmed and some metabolites could be identified. Similarly to GC–MS when using ammonia as reagent gas[10], azinphos-methyl showed an $[M+NH_4]^+$ ion as the base peak, as can be seen in Fig. 2. Degraded solutions of azinphos-methyl were also analysed. Fig. 3A shows a typical PI TSP LC–MS trace of a degraded solution of azinphos-methyl with an increase in the baseline noise at retention times from 2 to 6 min. The mass spectrum of this baseline noise showed an intense fragment at m/z = 141, which does not correspond to the reagent gas spectrum. This fragment ion can presumably be attributed to $[(CH_3O)_2PSO]^+$, corresponding to the functional group of the pesticide after a sulphur–oxygen exchange and obtained after hydrolysis.

The favoured formation of $[M+NH_4]^+$ ion as the base peak for organophosphorus pesticides in PI TSP LC–MS[23–25] indicates that such compounds exhibit proton affinities slightly lower than that for ammonia (858 kJ/mol)[30]. An exception is diazinon (see Fig. 2) with a pyrimidinyl group in its structure, yielding higher proton affinity values than ammonia and so ensuring the formation of $[M+H]^+$ ion as the base peak. Other fragments corresponding to adduct ions between $[M-FG]^+$, where FG = $(C_2H_5O)_2PSO$, and the reagent gas adduct ions such as $[M-FG+NH_4]^+$, $[M-FG+(CH_3OH)NH_4]^+$ and $[M-FG+(CH_3COO)NH_4]^+$, with relative intensities of 50%, 30% and 50%, respectively, were also obtained. With diazinon no degradation peaks or fragments were observed in either LC–UV and LC–MS.

Fig. 4 shows the NI TSP LC–MS spectrum of parathion-methyl which shows an $[M-R]^-$ ion as the base peak, as previously reported for other organophosphorus pesticides[26]. The stability of this fragment may be explained by its quinone-like structure, which can easily delocalize the unpaired electron in the negative ion radical, as in NCI GC–MS[13]. Such a fragment ion, characteristic of organophosphorus pesticides, has already been observed in direct liquid introduction LC–MS but with much lower intensity (*ca.* 4%)[21]. Other fragments observed for parathion-methyl are at m/z = 183, which may correspond to $[(CH_3O)_2PS + CH_3COO - H]^-$, and at m/z = 198 and 277, from the *p*-nitrophenol structure of the parathion-methyl. The NI TSP LC–MS spectrum of *p*-nitrophenol, the main hydrolysis product of parathion-methyl, it is also shown in Fig. 4. The base peak corresponds to $[2M-H]^-$, which is

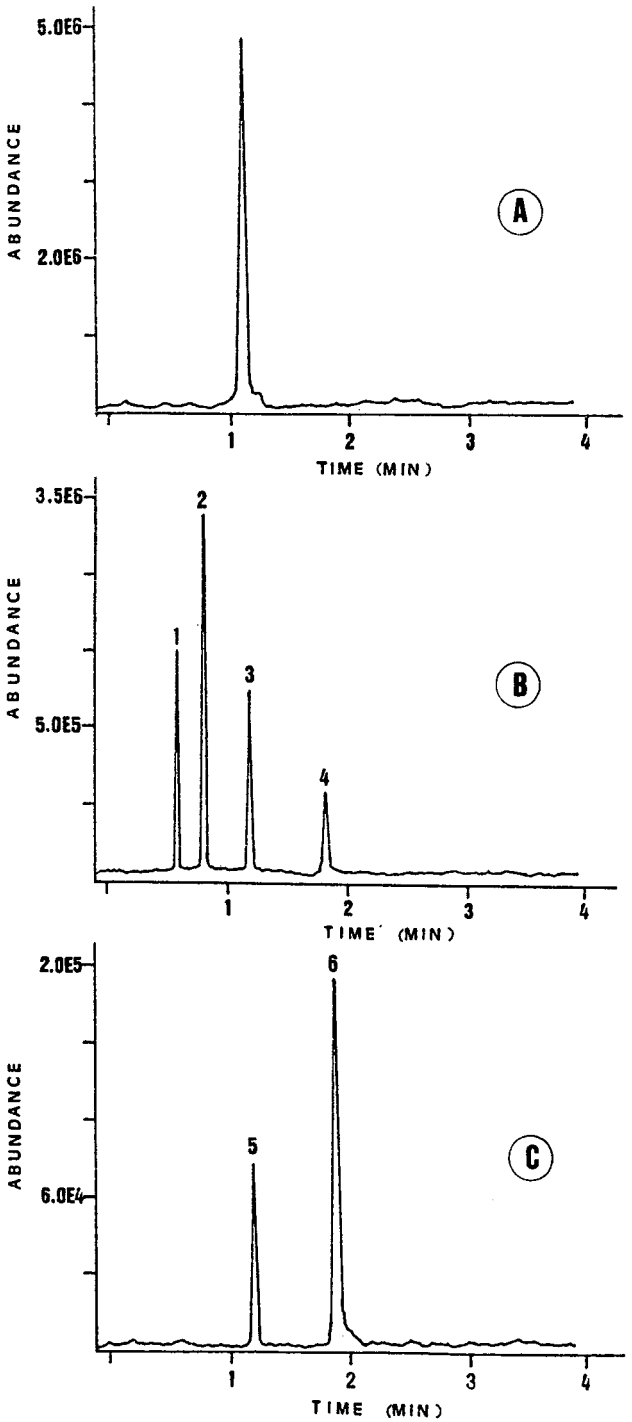

Fig. 1. LC trace with UV absorbance at 220 nm of solutions containing 100 ppm of each component after 48 h at pH 11: (A) diazinon: (B) azinphos-methyl (peak 4); and (C) *p*-nitrophenol (peak 5) and parathion-methyl (peak 6). Peaks 1, 2 and 3 are unknown breakdown products of azinphos-methyl. Column packing, 10-μm Nucleosil C_{18}; mobile phase, methanol–water (80:20) at a flow-rate of 1 ml/min; loop volume, 10 μl.

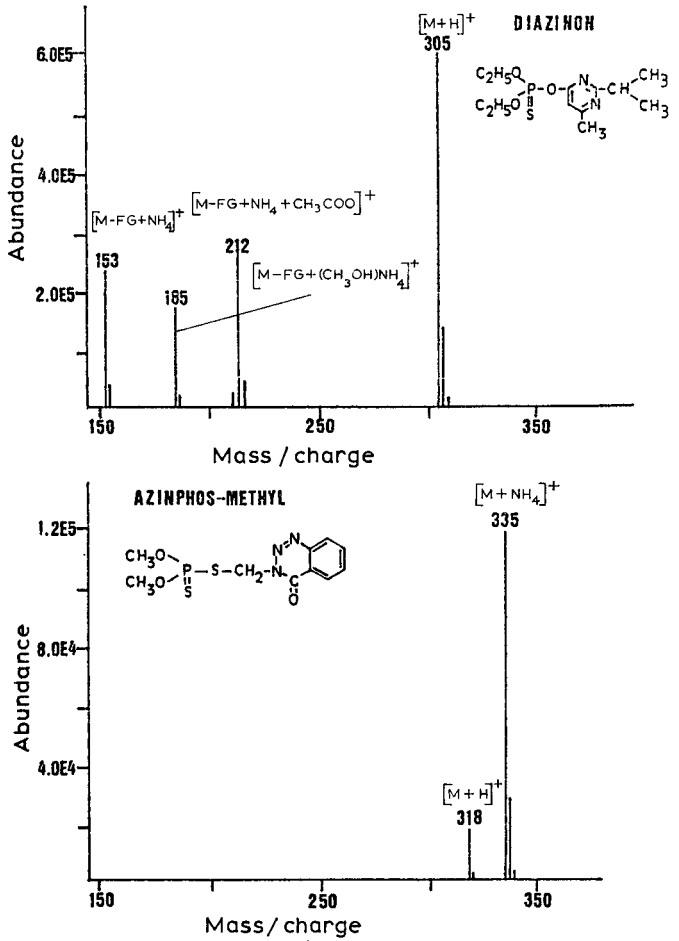

Fig. 2. Direct flow injection PI TSP MS spectra of diazinon and azinphos-methyl. Carrier stream, methanol–water (70:30) + 0.1 *M* ammonium acetate; flow-rate 1 ml/min; injection, 1 μg of each compound.

due to the fact that *p*-nitrophenol, similarly to chlorophenols[29] and nitrohydroxy polycyclic aromatic compounds[31], has a gas-phase acidity value much lower than 1464 kJ/mol, indicating stronger acidity than acetic acid, and hence acetate should deprotonate it. The high intensity of $[2M-H]^-$ has been attributed to the aromatic moiety containing electron-attracting nitro groups which stabilize the $[2M-H]^-$ ion by electron delocalization. The $[M-H]^-$ ions was not observed for *p*-nitrophenol, similarly to 2,4-dichlorophenol[29], owing to the relatively high scan values (above $m/z = 140$) required[25].

In PI TSP LC–MS no detection occurred when 200 ng of *p*-nitrophenol where injected under conditions similar to those above, whereas for parathion-methyl better sensitivities were obtained by employing PI TSP LC–MS, as generally occurs for organophosphorus pesticides[25,26]. In order to obtain the necessary information

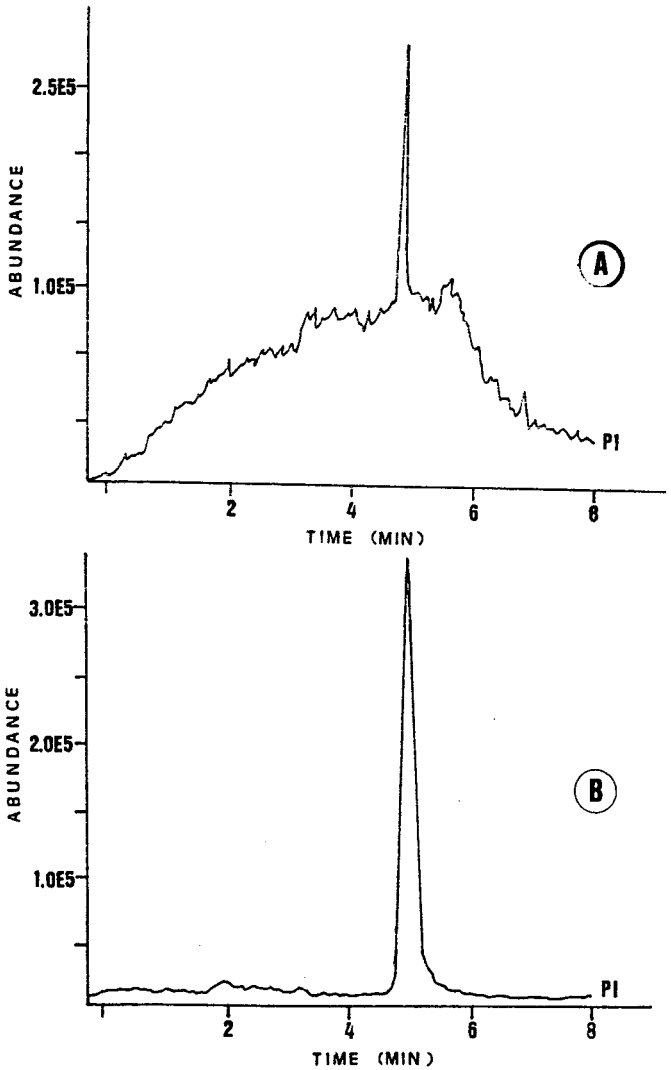

Fig. 3. Reconstructed ion chromatograms in PI TSP LC–MS of (A) 250 ppm of degraded solution of azinphos-methyl at pH 11 after 6 h and (B) 250 ppm of azinphos-methyl standard solution. Column packing, 10-μm Spherisorb ODS-2; mobile phase, methanol–water (70:30) + 0.1 *M* ammonium acetate at a flow-rate of 1 ml/min; loop volume, 20 μl.

about the formation of *p*-nitrophenol, a metabolite of parathion-methyl, NI TSP LC–MS was used as shown in Fig. 5, where chromatograms of a standard and a degraded solution of parathion-methyl are shown. The detection limit in NI TSP LC–MS for *p*-nitrophenol was at the low nanogram level (0.5 ng) whereas for parathion-methyl it was about 500 ng, using full scan conditions in both cases. The lower detection limit for *p*-nitrophenol is due to the fact that the molecular anion obtained as the base peak for *p*-nitrophenol, $[2M-H]^-$, is more stable than the corresponding base peak for parathion-methyl, $[M-R]^-$.

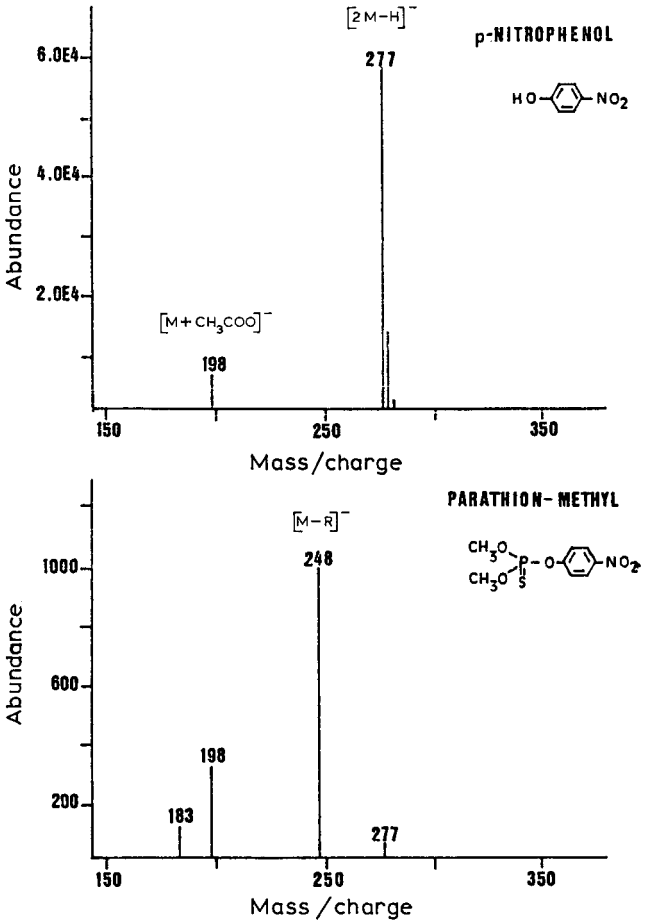

Fig. 4. Direct flow injection NI TSP MS spectra of *p*-nitrophenol and parathion-methyl. Conditions as in Fig. 2.

CONCLUSIONS

The combination of LC with UV detection at 220 nm and PI and NI TSP LC–MS allowed the unequivocal identification of azinphos-methyl, diazinon, parathion-methyl and the main breakdown product of parathion-methyl, *p*-nitrophenol, obtained after induced basic hydrolysis. Different behaviours were observed for the organophopshorus pesticides. Thus, for diazinon no degradation of solutions containing 100 ppm at pH 7–11 occurred after 10 days, whereas for azinphos-methyl and parathion-methyl 50% and 15% degradation, respectively, occurred after 4 h for solutions containing similar concentrations of pesticide and of similar pH. Possible degradation products of azinphos-methyl could be observed in the LC–UV chromatogram at 220 nm whereas in LC–MS no other peaks appeared. This fact can be attributed either to bad ionization of the degradation products or to the relatively

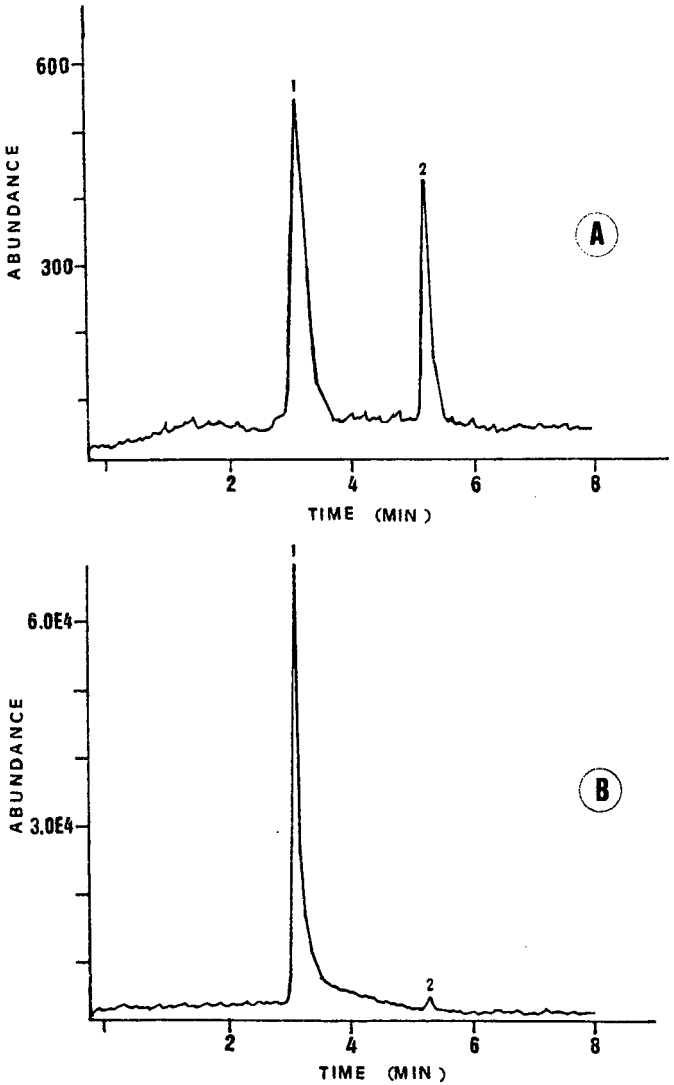

Fig. 5. Reconstructed ion chromatograms in NI TSP LC–MS of (A) 500 ppm of degraded solution of parathion-methyl (peak 2) at pH 11 after 6; peak 1 was identified as *p*-nitrophenol; (B) 2000 ppm of a standard solution containing *p*-nitrophenol (peak 1) and parathion-methyl (peak 2). Other experimental conditions as in Fig. 3.

high scan values (up to $m/z = 140$) which will not allow fragment ions to be detected below this value. The baseline noise showed a fragment ion at $m/z = 141$, probably attributable to $[(CH_3O)_2PSO]^+$.

Future developments will include the use of other organophosphorus pesticides as model compounds in order to study the formation of metabolites induced by hydrolysis by comparison with results in real environmental situations. Such model

compounds will be chosen in order to yield metabolites that can easily be measured by LC as an alternative to GC methods that require derivatization; *e.g.*, 2,4,5-trichlorophenol, the main metabolite of the organophosphorus pesticides ronnel and tetrachlorvinphos, can be analysed by LC–UV at 230 nm and NI LC–MS[28].

ACKNOWLEDGEMENTS

Financial support was provided by the Polytechnical University of Catalunya (U.P.C.) and the Consejo Superior de Investigaciones Científicas (C.S.I.C.). M[a].G. Martrat was the recipient of a scholarship from Comissió Interdepartamental de Recerca i Innovació Tecnológica (Generalitat de Catalunya) and assisted in the experimental work. R. Alonso (C.S.I.C.) is thanked for technical assistance.

REFERENCES

1 M. Eto, *Organophosphorus Pesticides: Organic and Biological Chemistry*, CRC Press, Boca Raton, FL, 1979, pp. 58 and 180.
2 C. Fest en K. J. Schmidt, *The Chemistry of Organophosphorus Pesticides*, Springer-Verlag, Berlin, 1982, p. 257.
3 K. D. Racke and J. R. Coats, *J. Agric. Food Chem.*, 36 (1988) 193.
4 P. H. Pritchard, C. R. Cripe, W. W. Walker, J. C. Spain and A. W. Bourquin, *Chemosphere*, 16 (1987) 1509.
5 L. Zenon-Roland, R. Agneessens, P. Nanginot and H. Jacobs, *J. High Resolut. Chromatogr. Chromatogr. Commun.*, 7 (1984) 480.
6 J. Kjølholt, *J. Chromatogr.*, 325 (1985) 231.
7 S. M. Prinsloo and P.R. De Beer, *J. Assoc. Off. Anal. Chem.*, 68 (1985) 1100.
8 J. P. G. Wilkins, A. R. C. Hill and D. F. Lee, *Analyst (London)*, 110 (1985) 1045.
9 A. K. Singh, D. W. Hewetson, K. C. Jordon and M. Ashraf, *J. Chromatogr.*, 369 (1986) 83.
10 R. L. Holmstead and J. E. Casida, *J. Assoc. Off. Anal. Chem.*, 57 (1974) 1050.
11 K. L. Busch, M. M. Bursey, J. R. Hass and G. W. Sovocool, *Appl. Spectrosc.*, 32 (1978) 388.
12 H.J. Stan, *Fresenius Z. Anal. Chem.*, 287 (1977) 104.
13 H. J. Stan and G. Kellner, *Biomed. Mass Spectrom.*, 9 (1982) 483.
14 R. C. Dougherty and J. D. Wander, *Biomed. Mass Spectrom.*, 7 (1980) 401.
15 I. M. Haniff and R. H. Zienius, *J. Chromatogr.*, 264 (1983) 33.
16 J. F. Lawrence, *Int. J. Environ. Anal. Chem.*, 29 (1987) 289.
17 A. Farran and J. De Pablo, *Int. J. Environ. Anal. Chem.*, 30 (1987) 59.
18 G. J. Clark, R. R. Goodin and J. W. Smiley *Anal. Chem.*, 57 (1985) 2223.
19 J. C. Gluckman, D. Barceló, G. J. de Jong, R. W. Frei, F. A. Maris and U. A. Th. Brinkman, *J. Chromatogr.*, 367 (1986) 35.
20 C. E. Parker, C. A. Haney and J. R. Hass, *J. Chromatogr.*, 237 (1982) 233.
21 C. E. Parker, C. A. Haney, D. J. Harvan and J. R. Hass, *J. Chromatogr.*, 242 (1982) 77.
22 D. Barceló, F. A. Maris, R. B. Geerdink, R. W. Frei, G. J. De Jong, and U. A. Th. Brinkman, *J. Chromatogr.*, 394 (1987) 65.
23 K. D. White, Z. Min, W. C. Brumley, R. T. Krause and J. A. Sphon, *J. Assoc. Off. Anal. Chem.*, 66 (1983) 1385.
24 R. D. Voyksner and C. A. Haney, *Anal. Chem.*, 57 (1985) 991.
25 D. Barceló, *LC, GC, Mag. Liq. Gas Chromatogr.*, 6 (1988) 324.
26 D. Barceló, *Biomed. Environ. Mass Spectrom.*, in press.
27 H. T. Kalinoski and R. D. Smith, *Anal. Chem.*, 60 (1988) 529.
28 J. A. G. Roach and D. Andrzejewski, in J. D. Rosen (Editor), *Applications of New Mass Spectrometry Techniques in Pesticide Chemistry*, Wiley, New York, 1987, p. 187.
29 D. Barceló, *Chromatographia*, 25 (1988) 295.
30 A. G. Harrison, *Chemical Ionization Mass Spectrometry*, CRC Press, Boca Raton, FL 1983, pp. 33–38.
31 J. M. Bayona, D. Barceló and J. Albaigés, *Biomed. Environ. Mass Spectrom.*, (1988) in press.

Journal of Chromatography, 455 (1988) 173–182
Elsevier Science Publishers B.V., Amsterdam — Printed in The Netherlands

CHROM. 20 871

ADAPTATION D'UNE MÉTHODE D'ANALYSE DES ACIDES AMINÉS, PAR CHROMATOGRAPHIE LIQUIDE HAUTE PERFORMANCE, DANS LES SÈVES XYLÉMIQUES

PHILIPPE BRUNET, BRUNO SARROBERT et NICOLE PARIS-PIREYRE*
Laboratoire de Physiologie Végétale, Université des Sciences et Techniques du Languedoc, Place E. Bataillon, 34060 Montpellier Cedex (France)
(Reçu le 26 juillet 1988)

SUMMARY

Modified procedure for the high-performance liquid chromatographic analysis of amino acids in xylem sap.

Pre-column *o*-phthaldialdehyde derivatization followed by high-performance liquid chromatography was used for the determination of amino acids in xylem sap. The pre-column derivatization conditions have been reviewed. To reduce analysis time and to improve peak separation, the solvent composition and the gradient programme were modified. The amino acids of tomato xylem sap were identified using α-aminobutyric acid as internal standard. The reproducibility of this new method was tested and its field of application is discussed.

INTRODUCTION

L'extraordinaire développement de l'analyse par chromatographie liquide haute performance (HPLC) a permis depuis quelques années son application dans les domaines les plus divers[1], dont celui de l'analyse des acides aminés, où elle a supplanté la chromatographie échangeuse d'ions avec marquage à la ninhydrine. Si, en ce qui concerne l'analyse des liquides biologiques (sérum, plasma et urine)[2], ou celle des produits alimentaires[3], les analyses par HPLC avec pré-dérivatisation sont arrivées à un stade de routine, à notre connaissance aucun travail n'a été fait au niveau de l'analyse des liquides végétaux, et en particulier de la sève xylémique. En effet, l'application de cette technique peut dégager des perspectives de recherche intéressantes pour l'identification des produits azotés transportés dans la sève xylémique[4].

Partant de la méthode décrite par Turnell et Cooper[5] pour l'urine et le sérum, et adaptée par Barbe[6] pour l'hémolymphe des écrevisses, nous avons étudié certaines modifications susceptibles de la rendre simple et efficace pour le dosage des acides aminés dans les sèves.

0021-9673/88/$03.50 © 1988 Elsevier Science Publishers B.V.

MATÉRIEL ET MÉTHODES

Instrumentation

L'appareil d'HPLC utilisé est un Varian LC 5000, équipé d'un Fluorimètre Varian No. 4300202. Un intégrateur Varian 4270 est utilisé pour le tracé des chromatogrammes et le calcul des concentrations. La chromatographie est réalisée sur une colonne Varian RP-18 ODS (5 μm), de dimension 150 × 4,6 mm I.D., munie d'une pré-colonne.

Réactifs

Tous les acides aminés ont été obtenus auprès de Sigma (St. Louis, MO, U.S.A.), sauf l'hydroxyisoleucine qui a été isolée par Sauvaire *et al.*[7] sur des graines de fenugrec. Les amines synthétiques proviennent du Laboratoire de Chimie Organique de l'USTL.

Les produits nécessaires à la dérivatisation: *o*-phthaldialdehyde (OPA), mercaptoéthanol, réactif iodo-acétique (RIA), acide borique et hydroxyde de sodium, ont été fournis par Merck (Darmstadt, F.R.G.) comme le propioniate de sodium et le diméthylsulfoxyde (DMSO). Le méthanol et l'acétonitrile proviennent de chez BDH. (Poole, U.K.).

Nous utilisons de l'eau bidistillée et désionisée sur un appareil Waters. Les solvants sont filtrés sur filtres Millipore (Millipore, Bedford, MA, U.S.A.) HVLP de 0,45 μm.

Conditions chromatographiques

Pour l'HPLC: flux, 1,6 ml min^{-1}; pression maximum, 330 atm; volume d'injection, 10 μl. Pour l'intégrateur: atténuation, AT (voir figures); vitesse de déroulement du papier, CS = 0,5 cm min^{-1}; pics marqueurs, PM = 1; rapport hauteur/largeur pics, PW = 1; auto-zéro, AZ = 1. Méthode de calcul, MN = 0 pour les essais.

Le temps de réaction de l'OPA a été fixé à 1 min et la sensibilité du fluorimètre à 50.

Le gradient d'élution est obtenu par le mélange de deux solvants selon les conditions fixées par Turnell et Cooper[5]. Solvant A: eau–propionate de sodium–acétonitrile (72:20:8, v/v). Solvant B: eau–acétonitrile–méthanol–diméthylsulfoxyde (42:30:25:3, v/v).

Prélèvements des sèves xylémiques

Les sèves xylémiques sont récoltées à partir de plantes de tomate (*Lycopersicon esculentum* Mill.) selon la technique décrite par Lahkdari[8]. Pour les analyses nous utilisons un mélange de sèves provenant de plantes ayant poussé dans les mêmes conditions culturales.

RÉSULTATS

Détermination des conditions de dérivatisation à partir d'une solution étalon

L'analyse des acides aminés dans les sèves pose deux problèmes: (i) les volumes exsudés sont faibles (10–500 μl en une heure selon les conditions de cultures) et (ii) la concentration totale en acides aminés est faible (1 μmol ml^{-1}) d'où la recherche de

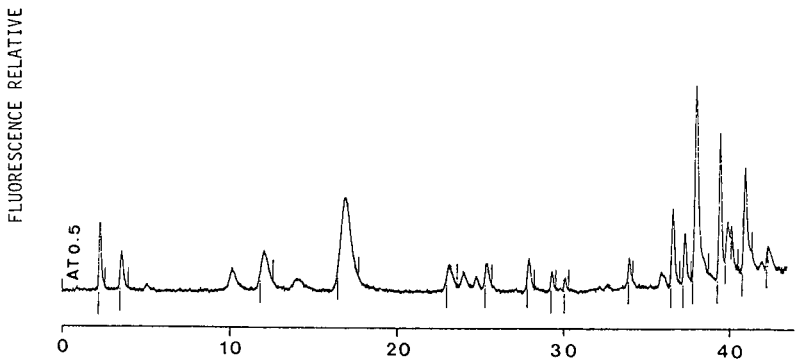

Fig. 1. Profil d'élution d'acides aminés d'un mélange de sèves xylémiques de tomate (méthode de Turnell et Cooper[5]).

conditions de dérivatisation permettant une concentration maximale de l'échantillon de sève.

Les volumes préconisés par Barbe[6] (20 µl échantillon, 100 µl RIA, 100 µl OPA) sont difficilements utilisables pour l'étude quantitative des sèves celles-ci étant trop diluées. En effet, la Fig. 1 nous montre que si l'identification est possible, la surface des aires trop petite rend le calcul des concentrations peu fiables. D'autre part, il faut aussi tenir compte de l'ajout d'une solution de standard interne nécessaire aux calculs des concentrations par l'intégrateur. Nous avons donc testé les mélanges du Tableau I.

L'examen des chromatogrammes obtenus (Fig. 2) à partir des différents mélanges montre que l'on peut faire baisser la quantité d'échantillon jusqu'à 10 µl et celle des réactifs jusqu'à 25 µl sans nuire à la qualité de l'analyse (Fig. 2c). Les chromatogrammes d, e et f prennent en compte le volume du standard interne remplacé ici par de l'eau. On voit que les résultats obtenus sont comparables quel que soit le mélange utilisé. Pour nos expériences nous retenons le mélange e qui correspond au facteur de dilution le plus faible.

TABLEAU I

COMPOSITION DES DIFFÉRENTS MÉLANGES TESTÉS

Mélange	*Solution étalon (µl)*	*Standard* interne (µl)*	*RIA/OPA (µl)*	*Volume total (µl)*	*Facteur dilution (µl)*
a	20	–	100/100	220	11
b	20	–	50/50	120	6
c	10	–	25/25	60	6
d	20	10	50/50	130	6,5
e	20	10	35/35	100	5
f	10	10	25/25	70	7

* Dans ces expériences, de l'eau remplace le standard interne.

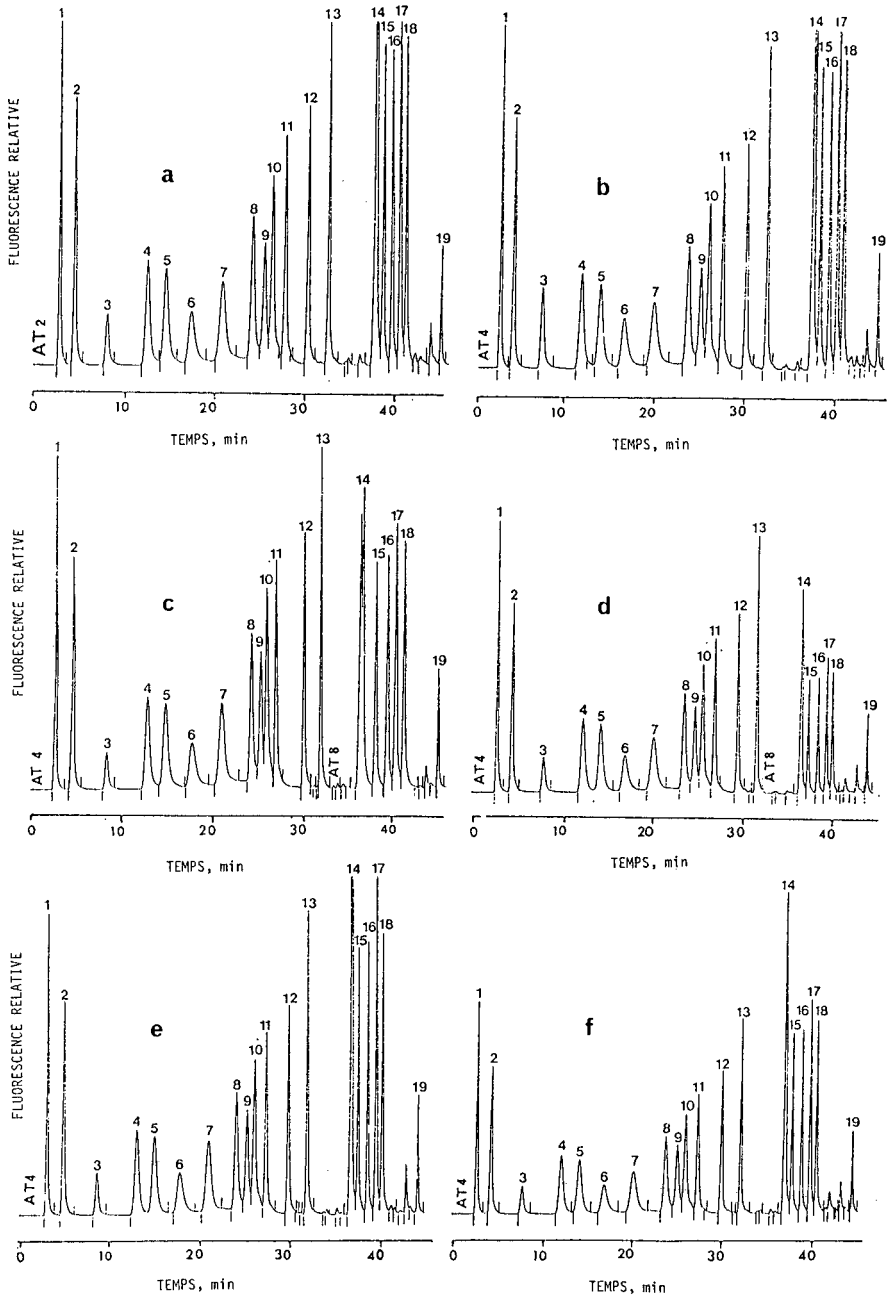

Fig. 2. Influence du facteur de dilution sur les chromatogrammes d'une solution étalon d'acides aminés. La composition des mélanges et les facteurs de dilution sont donnés sur le Tableau I, 1 = Asp; 2 = Glu; 3 = Cys; 4 = Asn; 5 = Ser; 6 = His; 7 = Gln; 8 = Hser; 9 = Gly; 10 = Thr; 11 = Arg; 12 = Ala; 13 = Tyr; 14 = Val/Met; 15 = Try; 16 = Phe; 17 = Ileu; 18 = Leu; 19 = Lys.

TABLEAU II

DIFFÉRENCES DE TEMPS D'ÉLUTION ENTRE Val/Met ET Leu EN FONCTION DE LA COMPOSITION DU SOLVANT B

ACN = Acétonitrile.

Composition	*H_2O (%)*	*ACN (%)*	*Méthanol (%)*	*DMSO (%)*	*Δt (min)*
B_0	42	30	25	3	2,85
B_1	22	40	35	3	1,93
B_2	36,5	17,4	43,5	2,6	3,17
B_3	42	20	35	3	3,84
B_4	0	0	100	0	2,01

Amélioration des conditions d'analyse

Nous avons étudié deux paramètres: (i) la séparation à l'intérieur du dernier groupe de pics (Val/Met→Leu) et (ii) la durée totale de l'analyse.

Séparation du dernier groupe. Nous avons modifié la composition du solvant B, majoritaire à ce moment de l'analyse, en faisant varier la proportion des divers constituants. Le critère de séparation sera la différence de temps d'élution entre le pic Val/Met et celui de Leu.

Le Tableau II montre que c'est le mélange B_3 qui offre la meilleure séparation.

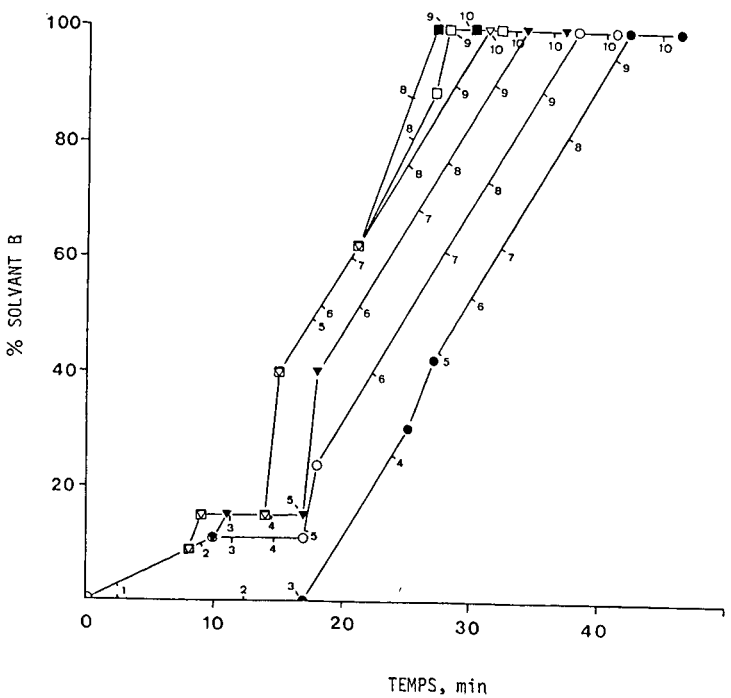

Fig. 3. Évolution des temps d'élution de certains acides aminés en fonction des différents gradients: GR 0^5 (●); GR 1 (○); GR 2 (▼); GR 3 (▽); GR 4 (□); GR 5 (■). 1 = Asp; 2 = Asn; 3 = His; 4 = Hser; 5 = Arg; 6 = Ala; 7 = Tyr; 8 = Val/Met; 9 = Leu; 10 = Lys.

Par contre une trop grande proportion d'acétonitrile (B_1) ou à l'opposé de méthanol (B_4) produit des séparations médiocres, et aucun de ces mélanges ne séparent le couple Val/Met d'une manière satisfaisante.

Réduction de la Durée de l'Analyse. Elle doit satisfaire à deux contraintes: (i) réduire les espaces entre certains groupes de pics et (ii) conserver une distance entre pics garantissant une bonne séparation à l'intérieur d'un même groupe.

La Fig. 3 montre qu'au début les pics sont très espacés, de même qu'entre Arg et le couple Val/Met, ainsi qu'entre Leu et Lys. La première étape consiste donc à supprimer le plateau du gradient de Turnell et Cooper[5] (GR 0) entre 0 et 17 min, et faire débuter le gradient de solvant B au temps $t = 0$ (GR 1). La réduction de la distance entre Hser, Gly, Thr, Arg et Ala, se fait grâce à une augmentation rapide de la quantité de solvant B (GR 2 et GR 3), alors que la séparation entre Asn, Ser, His, Gln est maintenue par la conservation du plateau. La réduction de la distance entre Tyr et Val/Met n'a pas été possible. L'accroissement du gradient en fin d'analyse (GR 5) rend la séparation entre Val/Met, Try, Phe, Ileu, Leu, peu satisfaisante. Par contre un passage à 100% de sovant B après l'élution de Phe, permet un rapprochement non négligeable du pic de Lys. C'est le cas du gradient 4 (GR 4) que nous retenons pour la suite de nos travaux.

Élaboration d'une solution d'étalon adaptée aux sèves

Identification des acides aminés présents dans les sèves xylèmiques de tomate. Partant des travaux de White et al.[9] sur les sèves de tomates, et de travaux sur les acides aminés libres de tissus végétaux[3,10,11] nous avons pu identifier les acides aminés présents dans les sèves (Fig. 4). Cette identification a été confirmée par des "piquâges" individuels dans le mélange de sèves. Afin de se rapprocher des concentrations présentes dans les sèves, nous avons dilué par 20 les concentrations définies par Barbe[6].

Choix du standard interne. L'utilisation de la prédérivatisation à l'OPA impose l'apport d'un standard interne (SI) lors du mélange des réactifs afin de corriger les variations dûes aux pipetages et au temps de réaction avec l'OPA.

Celui-ci devra donc satisfaire à plusieurs conditions: (a) être absolument étranger à l'échantillon; (b) être stable dans le temps; (c) bien réagir avec l'OPA pour la détection; (d) avoir un pic d'élution net et bien séparé des autres pics.

Nous en avons testés de trois types: (i) d'origine spécifiquement animale; (ii) de synthèse par voie chimique; (iii) d'origine végétable spécifique de certains végétaux.

Le Tableau III montre que seul l'acide α-amino butyrique (Aaba) peut être retenu comme standard interne. Bidlingmeyer *et al.*[3] l'utilisent comme standard interne pour l'analyse de produits alimentaires d'origine végétale. Cependant White *et al.*[9] en ont trouvé des traces dans des sèves de tomates cultivées en présence de fortes concentrations en zinc. Mais ce n'est pas le cas dans nos échantillons (Fig. 4). Aussi pour plus de sécurité nous avons préféré nous assurer de son absence avant l'analyse d'un nouvel échantillon.

La solution d'étalons ainsi mise au point avec le standard interne donne la Fig. 5.

Mise au point des paramètres d'intégration

Les travaux de James[12] n'étant pas directement applicables à notre système d'analyse, nous donnons le détail du processus de programmation de l'intégrateur.

Sur l'intégrateur Varian 4270 les calculs à l'aide du standard interne utilisent la

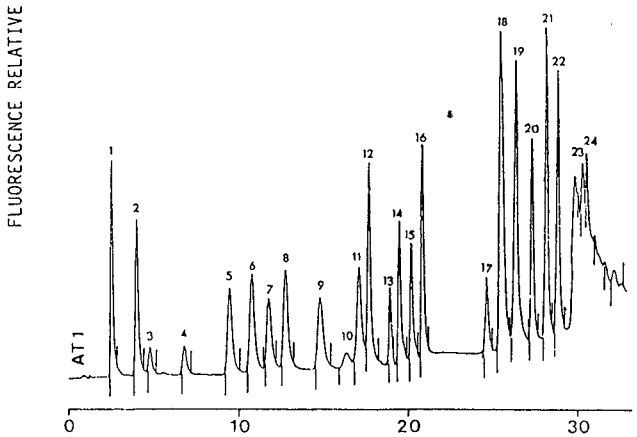

Fig. 4. Chromatogramme et identification des acides aminés d'un mélange de sèves xylémiques de tomate. 1 = Asp; 2 = Glu; 3 = Hcys; 4 = Cys; 5 = Asn; 6 = Ser; 7 = His; 8 = Gln; 9 = Hser; 10 = Gly; 11 = Thr; 12 = Arg; 13 = Bala; 14 = Ala; 15 = Gaba; 16 = Tyr; 17 = Eta; 18 = Val/Met; 19 = Try; 20 = Phe; 21 = Ileu; 22 = Leu; 23 = Orn; 24 = Lys.

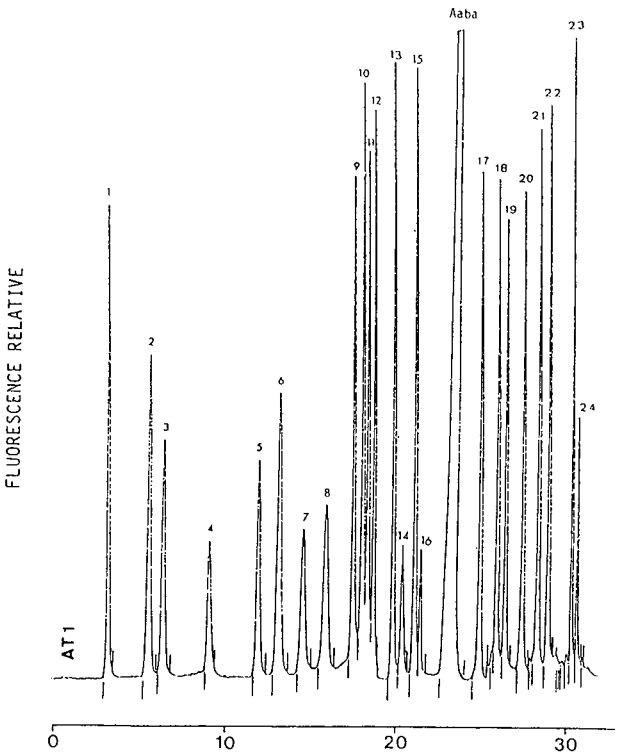

Fig. 5. Chromatogramme de la solution étalon définitive avec le standard interne (Aaba). 1–24 Comme pour la Fig. 4.

TABLEAU III

IDENTIFICATION DES ACIDES AMINÉS PRÉSENTS DANS LES SÈVES XYLÉMIQUES DE TOMATE

t_R (min)	Nom	Présent dans les sèves	Retenu dans l'étalon	t_R (min)	Nom	Présent dans les sèves	Retenu dans l'étalon
2,66	Asp	oui	oui	19,43	Ala	oui	oui
4,21	Glu	oui	oui	20,22	Gaba	oui	oui
5,06	Hcys	oui	oui	20,74	Tyr	oui	oui
7,08	Cys	oui	oui	22,75	Aaba	non	non
9,74	Asn	oui	oui	24,31	Eta	oui	oui
10,99	Ser	oui	oui	25,31	Val/Met	oui	oui
11,23	His	oui	oui	25,95	Try	oui	oui
12,87	Gln	oui	oui	26,26	Phe	oui	oui
14,90	Hser	oui	oui	27,78	Ileu	oui	oui
16,40	Gly	oui	oui	28,44	Leu	oui	oui
17,13	Thr	oui	oui	30,50	Orn	oui	oui
17,64	Arg	oui	oui	30,83	Lys	oui	oui
19,01	Bala	oui	oui				

méthode 2 (MN = 2). La notice de l'intégrateur recommande un rapport de surface de 10 pour le standard interne par rapport aux autres pics. Nous avons estimé cela trop élevé, et la concentration du standard interne dans la solution mère a été fixée à 250 nmol ml^{-1} ce qui donne une quantité injectée de 0.25 nmol (IS AMT) pour un volume de 0,01 ml (SAM AMT) et un facteur de dilution de la solution initiale de 5 (scale factor). Rappelons que lors de la programmation des concentrations des différents acides aminés de la solution étalon, il faut tenir compte de cette dilution; pour un acide aminé présent à 25 nmol ml^{-1} dans la solution, on programme une concentration de 5 nmol ml^{-1} (CC = 5).

Le point délicat est l'évaluation des temps de rétention pour la programmation des fenêtres d'identification. Par défaut, l'intégrateur programme une fenêtre de $\pm 10\%$. Si cela donne une fenêtre assez large en fin d'analyse, au début elle est trop étroite, d'où des erreurs possibles sur les premiers pics. Le moyen le plus sûr de les éviter est de procéder à deux injections à "blanc" avant la programmation, afin de tenir compte de la variation des temps de rétention, faible mais suffisante pour introduire une erreur d'identification.

Comme nous avons conçu notre étalon de façon à avoir des concentrations en acides aminés voisines de celles des échantillons, nous sommes dans un domaine où la réponse du détecteur varie linéairement avec la concentration. Nous programmons donc NV = 1. Nous avons opté pour trois injections de calibration car deux sont insuffisantes pour la précision du calcul des R.F. (responses factors) par l'intégrateur, et quatre n'accroissent pas la précision de manière notable et font perdre du temps. Pour l'analyse des échantillons de sèves, deux analyses suffisent. Pour d'autres produits plus complexes, une troisième peut être envisagée. En programmant AC = 2 après la calibration, on obtient une étude statistique pour chaque échantillon. Enfin, entre deux calibrations, nous estimons que l'on peut traiter six échantillons soit douze analyses. Bien que l'analyse ne dépasse pas 32 min, il faut compter injecter toutes les 35 min, 3 min étant nécessaires pour assurer la stabilisation de la colonne avec le solvant A.

TABLEAU IV

VÉRIFICATION STATISTIQUE DES NOUVELLES CONDITIONS D'ANALYSE

Average: moyenne de deux injections; R.S.D. (%): déviation standard relative; %Dev./Eta.: pourcentage de déviation par rapport à l'étalon.

File entry	*Average (nmol ml^{-1})*	*R.S.D. (%)*	*%Dev./Eta.*	*File entry*	*Average (nmol ml^{-1})*	*R.S.D. (%)*	*%Dev./Eta.*
Asp	24,98	1,883	0,08	Ala	25,807	8,261	3,228
Glu	25,383	14,212	1,532	Gaba	126,657	10,874	0,525
Hcys	125,553	2,781	0,442	Tyr	25,742	1,611	2,968
Cys	52,463	2,161	4,93	Aaba (IS)	0	0	0
Asn	25,029	1,268	0,116	Eta	125,663	1,872	0,53
Ser	24,824	2,711	0,704	Val/Met	24,087	5,745	3,652
His	24,511	3,052	1,956	Try	25,467	1,53	1,868
Gln	25,047	0,865	0,188	Phe	25,419	0,978	1,676
Hser	25,091	1,072	0,364	Ileu	25,811	0,707	3,244
Thr	24,636	3,193	1,456	Leu	25,691	0,597	2,76
Gly	25,274	0,336	1,096	Orn	126,093	1,741	0,874
Arg	25,471	0,002	1,884	Lys	25,416	9,9	1,664
Bala	125,768	1,336	0,614				

Vérification

Celle-ci consiste à pratiquer trois injections de calibration, puis deux injections d'analyses pour la même solution d'étalon. Le Tableau IV nous indique que, d'une part à l'intérieur d'une même série d'analyses le pourcentage de déviation relative [R.S.D. (%)] varie de 0,02% (Arg) à 14,21% (Glu), ce qui est analogue à la fourchette donnée par Turnell et Cooper[5]; d'autre part le pourcentage de déviation par rapport à la solution étalon (%Dev./Eta.) ne dépasse pas 4%, ce qui est conforme au seuil communément admis.

DISCUSSION

Nous venons de démontrer que les modifications que nous avons apportées à la méthode décrite par Turnell et Cooper[5] ne nuisent pas à sa précision et améliorent le rendement et la qualité des analyses. Cependant, certaines imperfections demeurent.

(1) Nous n'avons pas réussi à séparer le complexe Val–Met, de même que nous n'avons pas éliminé les résidus de nature inconnue qui perturbent la fin de l'analyse sur les échantillons de sève.

(2) l'Emploi de la pré-dérivatisation à l'OPA peut aussi être discuté. En effet, l'OPA ne permet pas la détection des amines secondaires, que rend possible la pré-dérivatisation avec du 9-fluoroénylméthyloxycarbonyl chloride (FMOC)[13] ou avec du phénylisothiocyanate (PITC)[14]. Cependant tous deux présentent le désavantage de nécessiter un processus de pré-dérivatisation complexe et long qui rend délicate l'automatisation du système. En outre le PITC est moins sensible que l'OPA[15] alors que le FMOC ne permet pas une bonne détection de Cys, His et Try[2]. Sur certains de nos échantillons nous avons utilisé une pré-dérivatisation au FMOC pour doser seulement la proline. Outre les inconvénients déjà cités, la quantité d'échantillon nécessaire à l'analyse, 100 μl, rend ce système peu pratique pour l'analyse des sèves dont les volumes récoltés sont souvent inférieurs à 100 μl. Nous le recommandons seulement pour des échantillons où le dosage des amines secondaires est inévitable.

(3) Certains complexes acides aminés–OPA ne sont pas stables dans le temps[15], mais les conditions d'analyses que nous venons de définir étant invariables d'une analyse à l'autre, cela ne pose pas de problème.

CONCLUSION

Ce travail a montré que la méthode d'analyse que nous venons de décrire possède les qualités nécessaires pour le dosage des acides aminés dans les sèves. Le temps relativement court, la reproductibilité des analyses et le faible volume d'échantillon requis, permettent d'envisager son utilisation de manière routinière et sur des produits autres que les sèves. Dans notre laboratoire, nous avons déjà obtenu des résultats sur le dosage des acides aminés libres des algues et nous travaillons actuellement afin de l'adapter à l'analyse de produits alimentaires comme des farines de soja.

RÉSUMÉ

Dans le but de doser les acides aminés présents dans les sèves xylémiques, nous avons adapté une méthode d'analyse par HPLC utilisant la pré-dérivatisation à l'*o*-phthaldialdehyde. Les conditions de pré-dérivatisation ont été discutées. Afin de réduire le temps d'analyse et d'améliorer la séparation entre les pics, nous avons modifié la composition du solvant et le gradient d'élution. Nous avons identifié les acides aminés de la sève xylémique de tomate en utilisant l'acide α-aminobutyrique comme standard interne. La reproductibilité de cette nouvelle méthode a été testée et son champ d'applications discuté.

REMERCIEMENTS

Nous remercions Messieurs Lautier et Ristérucci pour leurs conseils avisés et les moyens matériels qu'ils nous ont procurés.

BIBLIOGRAPHIE

1 M. Eslami, J. D. Stuart et K. A. Cohen, *J. Chromatogr.*, 411 (1987) 121.
2 P. Fürst, H. G. Godel et T. A. Gräser, dans H. Kalasz et L. S. Ettre (Editors), *Chromatography '85*, Akadémiai Kiado, Budapest, 1986, p. 29.
3 B. A. Bidlingmeyer, S. A. Cohen, T. L. Tarvin et B. Frost, *J. Assoc. Off. Anal. Chem.*, 70 (1987) 241.
4 A. Oaks et B. Hirel, *Ann. Rev. Plant Physiol.*, 36 (1985) 345.
5 D. C. Turnell et J. D. H. Cooper, *Clin. Chem.*, 28 (1982) 527.
6 L. Barbe, *These de 3e Cycle*, Université des Sciences et Techniques du Languedoc, Montpellier, 1984.
7 Y. Sauvaire, P. Girardon, J. C. Baccou et M. Ristérucci, *Phytochemistry*, 23 (1984) 479.
8 F. Lakhdari, *Diplôme de Doctorat*, Université des Sciences et Techniques du Languedoc, Montpellier, 1986.
9 M. C. White, A. M. Decker et R. L. Chaney, *Plant Physiol.*, 67 (1981) 292.
10 G. F. Soldatini et A. Giannini, *Agrochimica*, 29 (1985) 74.
11 W. M. Pulich, Jr., *Plant Physiol.*, 80 (1986) 283.
12 L. B. James, *J. Chromatogr.*, 410 (1987) 176.
13 S. Einarsson, *J. Chromatogr.*, 348 (1985) 213.
14 P. Edman et A. Henschen, dans S. B. Needleman (Editor), *Determination in Protein Sequence Analysis*, Springer-Verlag, Berlin, 2nd ed., 1975, p. 232.
15 G. Ogden et P. Földi, *Amino Acid Analysis: An Overview of Current Methods*, Vol. 5, LKB-Biochrom, Cambridge, 1987.

Journal of Chromatography, 455 (1988) 183–192
Elsevier Science Publishers B.V., Amsterdam — Printed in The Netherlands

CHROM. 20 877

RESOLUTION OF DIASTEREOMERS OF N,N,N′,N′-TETRAKIS(2-HYDROXYPROPYL)ETHYLENEDIAMINE (QUADROL) BY REVERSED-PHASE HIGH-PERFORMANCE LIQUID CHROMATOGRAPHY

J. A. FULTON, H. K. POKHARNA, M. J. DUNPHY and D. J. SMITH*
Department of Chemistry, The University of Akron, Akron, OH 44325 (U.S.A.)
(Received June 15th, 1988)

SUMMARY

Quadrol, N,N,N′,N′-tetrakis(2-hydroxypropyl)ethylenediamine, has been recently observed to display biological activity. It is an immunostimulant and has been implicated as a potentially useful agent in accelerated wound healing. Quadrol exists as a mixture of four unique diastereomers, each of which may, upon further investigation, display differences in biological activity. This paper describes an high-performance liquid chromatographic procedure (both analytical and prep) for the separation of the Quadrol diastereomers. Gas–liquid chromatograpy and NMR data are presented which corroborate the high-performance liquid chromatographic results. This procedure may be used to obtain pure Quadrol diastereomers, to monitor the progress of Quadrol synthesis from propylene oxide and ethylenediamine or to develop a quantitative assay for Quadrol diastereomers.

INTRODUCTION

Quadrol, N,N,N′,N′-tetrakis(2-hydroxypropyl)ethylenediamine (Fig. 1), is a viscous, colorless liquid possessing four chiral carbon atoms. It has been used as a metal complexing agent[1–3], a polar base in buffers for automatic protein sequencing[4] and as a crosslinking agent and catalyst in the synthesis of urethane foams[5]. Quadrol, as a mixture of diastereomers, was recently reported to possess immunological activity. *In vitro* macrophage stimulation was observerd as an increase in spreading and

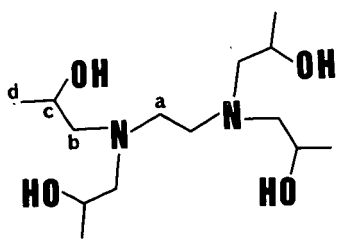

Fig. 1. Structure of Quadrol [N,N,N′,N′-tetrakis(2-hydroxypropyl)ethylenediamine]. The carbon atoms producing unique signals in the ^{13}C NMR spectrum are labeled a, b, c, and d.

0021-9673/88/$03.50 © 1988 Elsevier Science Publishers B.V.

phagocytosis [6,7]. In addition, wound healing experiments involving normal and diabetic mice[8] have demonstrated that Quadrol (as a mixture of isomers) accelerates collagen deposition in wound sites, and thus may be useful as a promoter of the wound healing process. Quadrol has also been incorporated into a hydrogel polymer[9] for potential use in wound dressings.

The development of a suitable high-performance liquid chromatographic (HPLC) procedure was initiated to monitor the progress of the reaction between propylene oxide and ethylenediamine to form Quadrol and to assess the purity of the final product. In the process, we noted that pure Quadrol consistently produced a multiplet of peaks. After verifying the absence of contaminants in our material, we hypothesized that the chromatographic system was resolving diastereomers of Quadrol. Resolution of diastereomers by HPLC has been observed for various other compounds[10–13]. The possibility exists that one of the diastereomers of Quadrol could be more biologically active than the others. Therefore, a procedure which allows one to separate and potentially assay individual isomers could be a valuable tool in the study of the biochemical mechanism of Quadrol's action. This paper describes the development of a method to separate the diastereomers of Quadrol by reversed-phase HPLC with electrochemical detection. Each of the diastereomer peaks is identified by analyzing mixtures of synthetic Quadrol diastereomers. The HPLC results are corroborated with data from ^{13}C NMR and gas–liquid chromatographic (GLC) analyses.

MATERIALS AND METHODS

Chemicals

Reagent-grade perchloric acid, acetic acid, sodium hydroxide, potassium hydroxide, sodium sulfate, methanol, ethanol, anhydrous diethyl ether, methylene chloride and HPLC-grade methanol were purchased from Fisher (Cleveland, OH, U.S.A.). N,N,N′,N′-Tetrakis(2-hydroxypropyl)ethylenediamine, ethylenediamine, propylene oxide and *S*-propylene oxide were obtained from Aldrich (Milwaukee, WI, U.S.A.). Octyl sodium sulfate was purchased from Eastman Kodak (Rochester, NY, U.S.A.).

Synthesis

Preparation of N-2-hydroxypropylethylenediamine (mono), N,N′-bis(2-hydroxypropyl)ethylenediamine (diol) and N,N,N′-tris(2-hydroxypropyl)ethylenediamine (triol). Mono, diol and triol were each prepared by appropriate stoichiometric addition of propylene oxide to ethylenediamine followed by either crystallization or fractional distillation purification according to the methods of Plucinski *et al.*[14] and Smith and Patel[9].

Preparation of N,N,N′,N′-tetrakis(2-hydroxypropyl)ethylenediamine (Quadrol). In a typical preparation of Quadrol, propylene oxide (2.0 g, 34.4 mmol) was added to a solution of ethylenediamine (0.2 g, 3.4 mmol) in 2 ml of 50% ethanol. The reaction mixture was contained in a three-necked flask with an attached dry ice condenser and maintained at 90°C for 6 h. After concentration *in vacuo*, the resultant oil was dissolved in diethyl ether and dried over anhydrous sodium sulfate. Filtration

and concentration *in vacuo* produced a colorless oil (0.9 g) in 90% yield. Further purification, if necessary, was accomplished by fractional distillation at 175°C at 0.8 mmHg or by recrystallization of the perchlorate salt of Quadrol from methanol.

Preparation of N,N,N',N'-tetrakis([2S]-2-hydroxypropyl)ethylenediamine (SSSS-Quadrol), Syn 1. *S*-Propylene oxide (2.0 g, 34.4 mmol) was added to ethylenediamine (0.2 g, 3.4 mmol) in accordance with the procedure outlined for the synthesis of Quadrol. After the removal of the diethyl ether, a white crystalline product, *SSSS*-Quadrol (m.p. 43.5°C; $[\alpha]_D^{25} = +171$, $c = 0.035$, $CHCl_3$), was obtained (0.8 g) in 80% yield.

Preparation of a mixture of SSSS-Quadrol and N,N,N'-tris([2S]-2-hydroxypropyl -N'-([2R]-2-hydroxypropyl)ethylenediamine [SSSR-Quadrol], Syn 2. *S*-Propylene oxide (1.0 g, 17.2 mmol) was added to N-2-hydroxypropyl-ethylenediamine (mono) (0.5 g, 4.3 mmol) following the procedure outlined for the synthesis of Quadrol. After purification, a colorless oil, *SSSS*- and *SSSR*-Quadrol, was obtained (1.2 g) in 95% yield.

Preparation of a mixture of SSSS-Quadrol, SSSR-Quadrol, and N,N'-bis ([2S]-2-hydroxypropyl) -N,N'-bis(2R]-2-hydroxyproplyl)ethylenediamine (SRSR-Quadrol), Syn 3. N,N'-Bis([2*S*]-2-hydroxypropyl) ethylenediamine (*SS*-diol) was first prepared by reacting *S*-propylene oxide (1.0 g, 17.2 mmol) with ethylenediamine (0.5 g, 8.5 mmol) according to the procedure of Smith and Patel[9]. The *SS*-diol was obtained as a white crystalline solid (0.3 g, 20% yield). *SS*-Diol (0.3 g, 1.7 mmol) was added to propylene oxide (1.0 g, 17.2 mmol), and the reaction was then processed according to the procedure for the synthesis of Quadrol. The product, a colorless oil (0.4 g), *SSSS*-, *SSSR*- and *SRSR*-Quadrol, was obtained in 82% yield.

Purification and extraction of Quadrol

Quadrol perchlorate was prepared by a modification of the method of Rorabacher and co-workers[15,16]. Typically, 50 ml of a 10% (w/v) solution of Quadrol in methanol was mixed with 5 ml of 70% perchloric acid, and the salt was precipitated by adding 25 ml of anhydrous diethyl ether. The Quadrol perchlorate was purified by several recrystallizations from methanol. An aqueous solution of the salt was injected onto the HPLC column, and the typical peak pattern for the diastereomers of Quadrol was observed. During preparative HPLC experiments, Quadrol diastereomers were recovered from the mobile phase by a simple extraction procedure. After rotary evaporation to remove methanol, the mobile phase was adjusted to pH 13 with potassium hydroxide and extracted with dichloromethane. Typically, Quadrol was recovered in greater than 90% yield after evaporation of the solvent. The purity of the extracted Quadrol (as a mixture or as a pure diatereomer) was assessed by NMR and GLC analyses in addition to reinjection on the HPLC column.

Gas chromatography

GLC analyses were performed using an HP 5890 gas chromatograph (Hewlett-Packard, Avondale, PA, U.S.A.) equipped with a flame ionization detector and a 6 ft. silanized glass column packed with 3% SP-2100 DB on 100–120 Supelcoport (Supel-

co, Bellefonte, PA, U.S.A.). The injector and detector were maintained at 300°C. Carrier gas (helium) flow was 30 ml/min at the analyses oven temperature of 230°C. Typically, 5 μl of an ethanolic solution of sample (0.5 mg/ml) was injected. Chromatograms were plotted on a strip-chart recorder.

Nuclear magnetic resonance spectrometry

The ^{1}H and ^{13}C NMR spectra were measured on a Varian XL-300 NMR operating at 300 MHz. The instrument was locked onto the $^{2}HCI_3$ solvent triplet as a reference for the ^{13}C NMR spectra, and the center peak was set at 77 ppm. The samples were dissolved in 1 ml of deuterated chloroform and analyzed in 5-mm high-resolution NMR tubes.

High-performance liquid chromatography

The HPLC system consisted of a Model 590 pump, a Model 710B WISP autosampler, a lambda-max 481 variable-wavelength UV detector and a Model 730 data module (Waters Assoc., Milford, MA, U.S.A.). Manual injections were done using a 50-μl Hamilton syringe and an in-line Rheodyne Model 7125 injector valve, both purchased from Supelco. Column eluent was monitored with an amperometric detector (e.c. monitor) from LDC/Milton Roy (Riviera Beach, FL, U.S.A.). As little as 2 nmol of Quadrol could be detected at a range setting of 2 nA/V, however, most analyses were performed at 10 nA/V. Quadrol was detectable at a voltage setting of +0.90 or higher, the optimum voltage being +1.00. The diastereomers of Quadrol were separated using a 15 cm × 3.9 mm I.D. Nova-Pak® C_{18} column (4 μm packing) from Waters Assoc. A precolumn (5 cm × 4.6 mm I.D.) containing 40 μm Pelligard® C_{18} packing (Supelco) was placed in-line just prior to the analytical column.

The primary mobile phase was composed of methanol–0.1 *M* acetate buffer (pH 5.5 with 3 m*M* octyl sodium sulfate) (2:8, v/v). Variations of this mixture were prepared when studying the effects of octyl sodium sulfate, methanol and pH on isomer resolution. The mobile phase was purged with helium prior to use. The mobile phase flow-rate was 1.0 ml/min which typically produced a column back-pressure of 1800 p.s.i. (124 bar). In most cases, 10 μl of aqueous solutions of Quadrol samples (typically 0.1 mg/ml) were injected.

Recovery of eluted Quadrol diastereomers

To obtain samples of each of the Quadrol diastereomers appearing in the HPLC chromatogram, the analytical column was replaced with a 25 cm × 10 mm I.D. RSil® C_{18} preparative column with 10 um packing (Alltech Assoc., Deerfield, IL, U.S.A.). The primary mobile phase was used at a flow-rate of 4.0 ml/min (back-pressure 800 p.s.i., 55 bar). The column was loaded with 25 mg of Quadrol, and fractions were collected every minute between 50 and 140 min after injection. Fractions collected from six separate injections were then pooled according to their diastereomeric content.

RESULTS AND DISCUSSION

The method used to synthesize Quadrol involves sequential attachment of 2-hydroxypropyl groups (from propylene oxide) to the two nitrogens of ethylenedi-

amine. Consequently, the diol and triol compounds, precursors to Quadrol, must typically be removed from the desired Quadrol product. We originally sought to develop an HPLC method capable of separating diol, triol and Quadrol in order to assess the purity of synthesized Quadrol. A reversed-phase column (C_{18}) and mobile phase consisting of methanol–acetate buffer (pH 5.5 with 0.5 m*M* octyl sodium sulfate (2:8 v/v) were used initially. Quadrol absorbs UV light poorly in the range of wavelengths useful with the mobile phase. Therefore, because of the presence of oxidizable groups on Quadrol, we chose to use electrochemical detection (ED). The first analyses generated interesting results. Commercially pure and our own synthesized Quadrol both produced a triplet of peaks eluting at 10.9, 11.7, and 13.3 min. Pure diol eluted as one peak at 4.8 min., and purified triol generated two peaks with retention times of 11.2 and 12.5 min. After eliminating the possibility of impurities (by several recrystallizations and GLC analysis), we hypothesized that diastereomers of triol and Quadrol were being resolved. Efforts were then focused upon verifying this assumption relative to Quadrol.

Quadrol has four chiral centers and thus may exist as a mixture of 8 diastereomeric pairs of enantiomers. However, because Quadrol has a center of symmetry, four of the isomers (*SSSR, RSSS, SSRS,* and *SRSS*) are actually identical. In addition, the *SRSR* and *SRRS* isomers are equivalent due to intramolecular rotations. Therefore, four diastereomeric structures (*SSRR, SSSR, SSSS,* and *SRSR* or the corresponding enantiomers) could possibly be resolved by a suitable chromatographic system. Assuming that a given mixture is not artificially enriched in any particular isomer, the diastereomers should exist in a 1:4:1:2 ratio respectively. A chromatogram from a typical HPLC analysis of pure Quadrol, with optimized mobile phase and ED, is shown in Fig. 2. Peak asignments are as follows: (1) *SSRR*, (2) *SSSR*, (3) *SSSS* and (4) *SRSR*. By averaging the areas of individual diastereomer peaks from numerous HPLC analyses of pure Quadrol samples, a ratio of 1.2:3.9:0.8:2 was obtained. This reasonably approximates the predicted ratios.

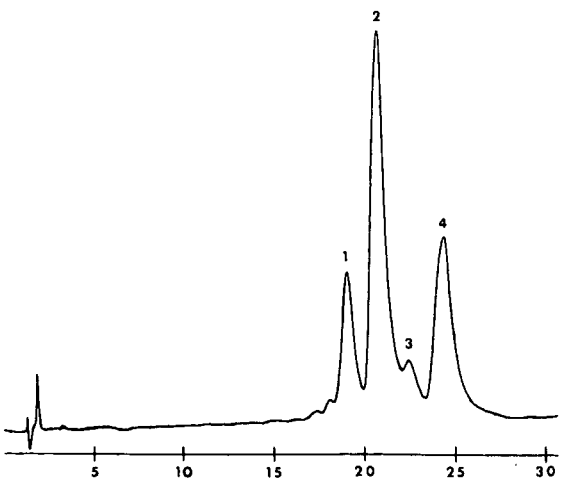

Fig. 2. HPLC chromatogram of Quadrol diastereomers separated on a 15 cm × 3.9 mm I.D. Nova-Pak® C_{18} column. The chart speed was 0.5 cm/min and the mobile phase was methanol and 0.1 *M* acetate buffer (pH 5.5) with 3m*M* octyl sodium sulfate (2:8, v/v). The mobile phase flow-rate was 1.0 ml/min.

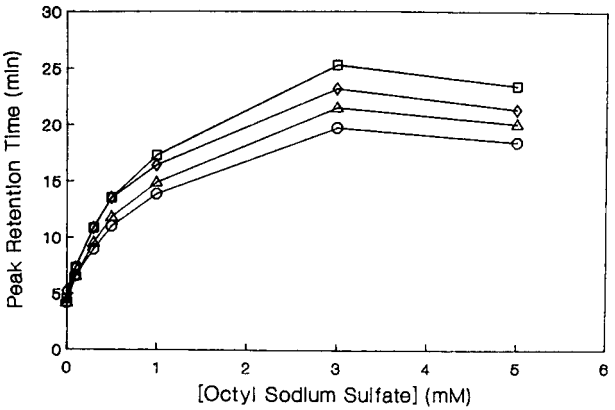

Fig. 3. Variation of Quadrol diastereomer retention times as a function of OSS concentration in the mobile phase. The Quadrol isomers are labeled as follows: (○) peak 1 (*SSRR*); (△) peak 2 (*SSSR*); (◇) peak 3 (*SSSS*); and (□) peak 4 (*SRSR*).

Because the initial mobile phase produced only free peaks for Quadrol, conditions were manipulated in order to optimize the separation of the four expected diastereomers. We investigated the effects of mobile phase pH, ion-pairing reagent, octyl sodium sulfate, concentration and methanol content on peak resolution and retention time. First, the octyl sodium sulfate concentration was varied from 0 to 5 m*M* with all other conditions as stated previously. The results, shown in Fig. 3, indicate that solute retention time increases with the concentration of octyl sodium sulfate. This was expected since Quadrol is a cation at pH 5.5 and should pair strong-

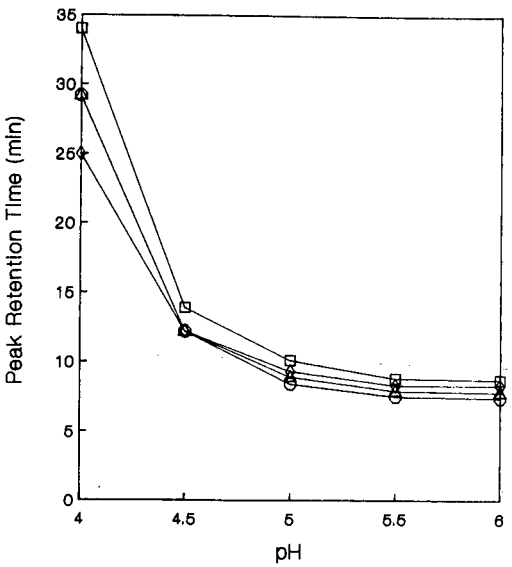

Fig. 4. Variation of Quadrol diastereomer retention times as a function of mobile phase acetate buffer pH. The Quadrol isomers are labeled as follows: (○) peak 1 (*SSRR*); (△) peak 2 (*SSSR*); (◇) peak 3 (*SSSS*); and (□) peak 4 (*SRSR*).

ly with octyl sodium sulfate. The effect on Quadrol retention time plateaus at 3 m*M* octyl sodium sulfate. The association of this type of leveling effect with ion-pair reagents has been reported[17]. Most importantly, however, a fourth peak appears in the Quadrol chromatogram when the concentration of octyl sodium sulfate is at least 1 m*M*. The best resolution of the four peaks was observed using 3 m*M* octyl sodium sulfate, and thus, this concentration was used in all subsequent analyses. The results from variation of buffer pH are shown in Fig. 4. As the mobile phase pH is increased from 4 to 6, solute retention times decrease, with peak 3 (the *SSSS* isomer) most drastically affected. The dicationic form of Quadrol, as a mixture of isomers, has two ionizable quarternary ammonium groups with pK_a values of 4.36 and 9.04 respectively[18]. The increased elution rate is probably due to diminishing Quadrol–octyl sodium sulfate interaction as the more acidic of the two ammonium groups ionizes and loses charge with the increasing pH. Apparently, intramolecular pertubations caused by individual isomer stereochemistry are affecting the pK_a values of the isomers. This might, to some extent, account for the greater sensitivity of the *SSSS* isomer to alterations in pH. The best diastereomer separation was observed at or above pH 5.5. Altering the methanol content of the mobile phase above or below 20% resulted in no particular advantage. Therefore, the mobile phase indicated in the legend of Fig. 2 was considered optimal for the separation of the diastereomers of Quadrol.

In order to verify that the peaks observed during the HPLC analysis corresponded to particular Quadrol diastereomers, preparative HPLC was employed (as indicated in the experimental section) to collect sufficient amounts of each eluting diastereomer to perform GLC and NMR analyses. Up to 20 mg of each individual eluting compound could be obtained after fractions were pooled and extracted. When any one of the four eluted compounds was re-injected onto the analytical column, the peak with the retention time corresponding to the particular diastereomer injected was observed, though minor contamination with the other diastereomers frequently occurred.

When commercial or synthesized Quadrol (as a mixture of diastereomers) is dissolved in ethanol and analyzed by isothermal GLC, one peak is observed over the temperature range from 140 to 250°C. At 230°C, the Quadrol elutes at 1.9 min, and the peak obtained is sharp and symmetrical. Each of the individual compounds obtained from the prep HPLC procedure also eluted at 1.9 min. when subjected to the same GLC analysis. Diol and triol both eluted in less than 1 min, and neither was observed in any of the purified Quadrol solutions.

The proton NMR spectrum of each diastereomer obtained from the preparative HPLC procedure matched the spectrum of pure Quadrol and thus provided additional evidence that each HPLC peak corresponds to a Quadrol structure. The ^{13}C NMR analysis of each isolated isomer displayed important chemical shift differences. The ^{13}C NMR spectrum of purified Quadrol (as a mixture of diastereomers) is shown in Fig. 5. The chemical shift regions of the spectrum are identified with letters (a,b,c,d) corresponding to the carbon atom labeling scheme in Fig. 1. When a particular isomer (1,2,3 or 4), isolated by preparative HPLC, was subjected to ^{13}C NMR analysis, a single set of absorption peaks was greatly enhanced. The peaks in each region of the spectrum are numbered (1,2,3,4) to correspond with the Quadrol diastereomers in Fig. 2.

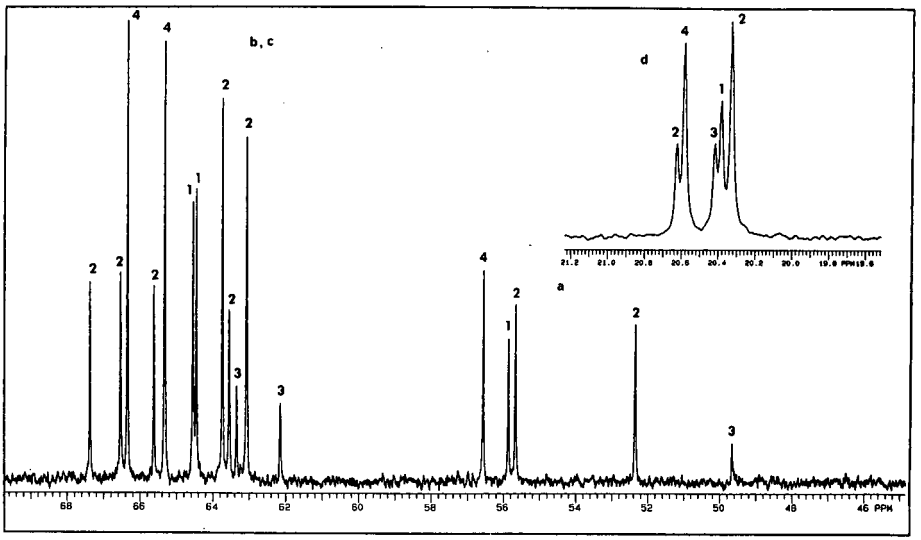

Fig. 5. ^{13}C NMR spectrum of purified Quadrol (as a mixture of diastereomers) in C^2HDCCL_3. Spectrum regions labeled a, b, c, and d correspond to the chemical shifts of the Quadrol carbon atoms as shown in Fig. 1. The individual peaks in the ^{13}C NMR spectrum are numbered to correspond to the particular Quadrol diastereomers as shown in Fig. 2.

TABLE I

CHEMICAL SHIFTS IN THE ^{13}C NMR SPECTRA OF QUADROL DIASTEREOMERS

Listed below are the 300-MHz ^{13}C NMR chemical shifts (ppm) for the synthesized diastereomers (Syn 1 = *SSSS*-Quadrol; Syn 2 = *SSSS*- and *SSSR*-Quadrol; Syn 3 = *SSSS*-, *SSSR*- and *SRSR*-Quadrol) and those obtained from preparative HPLC (peaks 1–4). The chemical shift values (δ) are listed for Quadrol carbon atoms a, and b and c as in Fig. 1.

Chemical shift	*Quadrol*	*Syn 1*	*Syn 2*	*Syn 3*	*Peak 1*	*Peak 2*	*Peak 3*	*Peak 4*
δ_a	49.7	49.7	49.7	49.7		Trace	49.8	
(ppm)	52.4		52.4	52.4		52.5		
	55.7		55.8	55.8		55.8		
	55.9				56.1	Trace		
	56.6			56.7		Trace		56.9
$\delta_{b \text{ and } c}$	62.2	62.3	62.3	62.3		Trace	62.4	Trace
(ppm)	63.1		63.2	63.2		63.2		
	63.4	63.3	63.3	63.4		Trace	63.5	Trace
	63.6		63.6	63.6		63.7		
	63.7		63.7	63.8		63.8		
	64.5				64.6	Trace		
	64.6				64.9	Trace		
	65.3			65.4		Trace		65.5
	65.6		65.6	65.7		65.7		
	66.4			66.4		Trace		65.5
	66.5		66.6	66.6		66.6		
	67.4		67.4	67.4		67.5		

In order to provide final verification that the peaks in the HPLC chromatogram were indeed diastereomers of Quadrol, we proceeded to synthesize the isomers. The *SSSS*-Quadrol isomer was prepared and isolated as a pure substance (Syn-1), however, the other isomers were obtained in specific mixtures. Syn-2 resulted in a mixture of the *SSSS* and *SSSR* isomers, and the mixture obtained from Syn-3 included the *SSSS*, *SSSR* and *SRSR* Quadrol isomers. The proton NMR spectra of the *SSSS* isomer and the two mixtures matched the spectrum of Quadrol, and GLC analysis (using conditions previously described) of each produced a single peak eluting at 1.9 min. HPLC analysis of the synthesized materials generated the predicted results. The *SSSS* isomer eluted as a single peak at 22.9 min, the Syn-2 product appeared as two peaks eluting at 21.3 min (*SSSR*) and at 22.9 min (*SSSS*), and the Syn-3 product mixture produced three peaks with retention times of 21.3 min (*SSSR*), 22.9 min (*SSSS*) and 24.7 min (*SRSR*). Thus, the peak eluting at 19.1 min is apparently the *SSRR* isomer [N,N-bis([2*S*]-2-hydroxypropyl)-N′,N′-bis-([2*R*]-2-hydroxypropyl)-ethylenediamine]. The results from ^{13}C NMR analysis of these compounds, provided in Table I, correspond with those obtained by HPLC. By comparing the NMR and HPLC for Syn-1, Syn-2 and Syn-3 products, the identity of each peak in the Quadrol HPLC chromatogram (Fig. 2) was established.

This paper describes a simple HPLC procedure (analytical and preparative) for the separation of the diastereomers of Quadrol. In addition, we have provided evidence from GLC, proton NMR and ^{13}C NMR analyses that the peaks appearing in the HPLC chromatogram correspond to the four predicted Quadrol diastereomers. Recent work in our laboratory indicates that Quadrol is an immunostimulant and may be useful in some biological applications. It is possible that a particular stereoisomer may possess greater biological activity than others, and therefore this separation and isolation method can be used to provide the isomer samples needed to further our studies or any other work involving the diastereomers of Quadrol, including the development of quantitative assays for each isomer.

ACKNOWLEDGEMENT

This work was supported in part by the American Diabetes Association.

REFERENCES

1 L. Pike and J. H. Yoe, *Anal. Chim. Acta*, 31 (1964) 318.
2 J. L. Hall, F. R. Jones, C. E. Delchamps and C. W. McWilliams, *J. Am. Chem. Soc.*, 79 (1957) 3361.
3 M. Orama, H. Saarinen and L. Kaila, *Finn. Chem. Lett.*, 6 (1979) 182.
4 G. S. Begg, B. H. Leslie and F. J. Morgan, *Anal. Biochem.*, 138 (1984) 30.
5 R. B. Kennedy, R. J. Fricke and P. J. Crehan, *U.S. Pat.*, 4 515 638 (1985).
6 M. V. Bhide, S. Patel, E. C. Rowland and D. J. Smith, *J. Immunopharmacol.*, 7 (1985) 303.
7 M. V. Bhide and D. J. Smith, *Immunopharmacol. Immunotoxicol.*, 9 (1978) 129.
8 M. V. Bhide, M. J. Dunphy, N. Mirkopulos and D. J. Smith, *Immunopharmacol. Immunotoxicol.*, submitted for publication.
9 D. J. Smith and S. Patel, *J. Polym. Sci., Polym. Lett. Ed.*, 23 (1985) 633.
10 A. Van Schepdael, E. Roets, J. Hoogmartens and H. Vanderhaeghe, *J. Chromatogr.*, 370 (1986) 149.
11 S. M. Gaines and J. L. Bada, *J. Chromatogr.*, 389 (1978) 219.
12 G. W. Mihaly, K. M. Hyman, R. A. Smallwood and K. J. Hardy, *J. Chromatogr.*, 415 (1978) 177.
13 P. J. Soine and W. H. Soine, *J. Chromatogr.*, 422 (1978) 309.

14 J. Plucinski, H. Prystasz and F. Pawul, *Chem. Stosow.*, 25 (1981) 195.
15 D. B. Rorabacher, T. S. Turan, J. A. Defever and W. G. Nickels, *Inorg. Chem.*, 8 (1969) 1498.
16 D. B. Rorabacher and D. B. Moss, *Inorg. Chem.*, 9 (1970) 1314.
17 A. Bartha, H. A. H. Billiet, L. de Galan and G. Vigh, *J. Chromatogr.*, 291 (1984) 91.
18 J. L. Hall, *Proc. W. Va. Acad. Sci.*, 35 (1963) 104.

Journal of Chromatography, 455 (1988) 193–200
Elsevier Science Publishers B.V., Amsterdam — Printed in The Netherlands

CHROM. 20 888

PURIFICATION OF DIETHYLENETRIAMINE-N,N,N′,N″-TETRAACETIC ACID-N″-PROPIONIC ACID USING ANION-EXCHANGE DISPLACEMENT CHROMATOGRAPHY

DOUGLAS J. SAWYER*,*
Department of Chemistry, Iowa State University, Ames, IA 50011-3020 (U.S.A.)
and
JACK E. POWELL and HARVEY R. BURKHOLDER
Ames Laboratory, U.S. Department of Energy, and Department of Chemistry, Iowa State University, Ames, IA 50011-3020 (U.S.A.)
(Received August 4th, 1988)

SUMMARY

The synthesis, purification and characterization of dietylenetriamine-N,N,N′,N″-tetraacetic acid-N″-propionic acid are reported. The purification is achieved using anion-exchange displacement chromatography.

INTRODUCTION

A new chelating agent, diethylenetriamine-N,N,N′,N″-tetraacetic acid-N″-propionic acid (DTTAP), has been successfully prepared in our laboratory. This new chelating agent shows promise as a ligand that can assist in the successful separation of trivalent actinides from the trivalent lanthanides[1]. A successful Ln–An separation is necessary for the effective disposal of high-level radioactive wastes that contain the transuranic actinides.

The synthesis of DTTAP, has been carried out in two steps. In each step, good separation of the reaction products was achieved using ion displacement chromatography. In the first experiment, cation-exchange displacement chromatography was used to isolate pure diethylenetrianic-N-propionic acid. Anion-exchange displacement chromatography was used to isolate pure DTTAP in the second separation.

Few examples of anion-exchange displacement chromatography have been reported in the literature. In 1952, Partridge and Brimley[2] reported the use of this technique for the separation of several mixtures of amino acids. This work illustrates the tremendous value of this technique for resolving mixtures of aminocarboxylic acids possessing very similar pK_a values. Peterson and Torres[3] and Peterson[4] have reported the use of carboxymethyldextrans as spacers and displacers in anion-exchange displacement chromatography. In these reports, dextran was carboxymethylated to varying degrees with chloroacetate. The derivatives containing the largest number of carboxylate groups (*ca.* 400) were used as displacers, and the intermediately

* Present address: Department of Chemistry, Arizona State University, Tempe, AZ 85287, U.S.A.

0021-9673/88/$03.50 © 1988 Elsevier Science Publishers B.V.

substituted derivatives were used as spacers in an anion-exchange separation of various proteins. Gueron *et al.*[5] reported the separation of mixtures of acrylic and methacrylic acids using anion-exchange displacement chromatography. In 1968, Coleman and Gilbert[6] showed that chromium(III) thiocyanate complexes can also be separated using this technique.

After reviewing the work of Peterson[3] and Partridge and Brimley[2], it is not surprising that anion-exchange displacement chromatography is the most successful method of separation for the purification of this new polyaminopolycarboxylate.

EXPERIMENTAL

Materials

All chemicals were of reagent-grade. Deionized water in this laboratory was prepared by passing condensed steam through a mixed bed of cation- and anion-exchange resins.

^{13}C NMR

All ^{13}C NMR spectra were recorded on a Nicolet 300 MHz Fourier transform NMR spectrometer. The chemical shifts are reported relative to a dioxane standard (66.5 ppm).

Elemental analyses

All elemental analyses were performed by Desert Analytics, Tucson, AZ, U.S.A. Analyses were performed using a Perkin-Elmer 240C elemental analyzer.

Mass spectrometry

The mass spectral analysis was performed using a Kratos-MS-50 mass spectrometer.

Procedure

Step 1. One mole of 3-chloropropionic acid (108.5 g) was dissolved in a minimum of deionized water and neutralized slowly with one mole of sodium hydroxide in an ice-water bath. This solution was reacted with 3 moles of diethylenetriamine at 50°C, with magnetic stirring. The pH was kept between 8 and 10 with periodic additions of sodium hydroxide. After 24 h, the reaction solution was adjusted to pH 2 with concentrated sulfuric acid. The desired intermediate diethylenetriamine-N-propionic acid was isolated by cation-exchange displacement chromatography.

Step 2. A concentrated aqueous solution containing 0.232 moles of the mono-propionic acid intermediate was prepared and neutralized to pH 8 with sodium hydroxide. This solution was reacted with an aqueous solution containing 1.02 moles of chloroacetate at 50°C with magnetic stirring. The pH was kept between 8 and 10 by periodic additions of sodium hydroxide. After $2\frac{1}{2}$ h, the pH was adjusted to pH 2 with concentrated hydrochloric acid. The desired product, DTTAP, was then isolated by anion-exchange displacement chromatography.

Isolation of intermediate

Pure diethylenetriamine-N-propionic acid was isolated from the other products

of Step 1, by cation-exchange displacement chromatography. The mixture was first placed onto a 48 in. × 2 in. diameter column containing approximately 4.5 moles of Dowex 50-X8 cation-exchange resin capacity, 40–50 mesh, in the H^+ form. The mixture was then rinsed with deionized water to remove any highly acidic species. The mixture was then displaced with 0.1 *M* aqueous ammonia solution along the 2-in. diameter column and then, along two 48 in. × 1 in. diameter columns, each containing approximately 1.1 moles of Dowex 50W-X8 cation-exchange resin capacity in the H^+ form. The flow-rate of the displacing ammonia solution was a slow 2.5 ml/min. Ammonia was a convenient displacing molecule, as it did not displace unreacted diethylenetriamine. After several days, the lightly colored band reached the bottom of the third column.

Thirty-four fractions were collected over a period of three days. Each sample contained 200–250 ml of solution. Samples 1–30 (pH 9.32–9.41) were combined after they were each found to contain the pure end-substituted monopropionate by ^{13}C NMR spectroscopy. Samples 31–34 were found to contain the middle-substituted monopropionate by ^{13}C NMR spectroscopy.

Isolation of final product

The reaction mixture from Step 2 was first displaced through a series of two cation-exchange columns in an effort to separate the polyaminopolycarboxylate products from the other substances (*i.e.* Na^+, $Cl\text{–}CH_2COO^-$). The columns used were 48 in. × 2 in. Dowex 50-X8 (H^+ form) and 48 in. × 1 in. Dowex 50W-X8 (H^+ form). The displacer was 0.15 *M* ammonia at a flow-rate of 3 ml/min.

All fractions from the above displacement within pH 2–6 were combined and the products were further separated by anion-exchange displacement chromatography.

The mixture was displaced through a series of six 48 in. × 1 in. diameter columns, each containing approximately 1.1 moles of Dowex-2 anion-exchange resin capacity in the OH^- form. The columns were regenerated with a filtered solution containing 1 *M* barium hydroxide and 1 *M* potassium hydroxide. The carbonate-free solution was protected with an Ascarite trap. The presence of carbonate must be avoided, otherwise carbon dioxide bubbles will form on the column when the pH becomes acidic. The light colored band was displaced with 0.10 *M* hydrochloric acid solution at a flow-rate of 2 ml/min. Sixteen fractions were collected having pH 1–3. Samples 8–12 were found, using ^{13}C NMR spectroscopy, to contain the major reaction product in high purity.

RESULTS AND DISCUSSION

^{13}C NMR

The proton-decoupled ^{13}C NMR spectrum of diethylenetriamine-N-propionic acid in shown in Fig. 1. The chemical shifts of the seven observed peaks are listed in Table I.

The end-substituted product is the only product of Step 1 that would give a proton-decoupled ^{13}C NMR spectrum containing seven lines. Peaks 1 and 7 from Table 1 have been assigned to the carbons labeled 1 and 7 in the formula. The five remaining peaks occur in the region expected for the five remaining carbon atoms, each adjacent to an amine and to a methylene group[7].

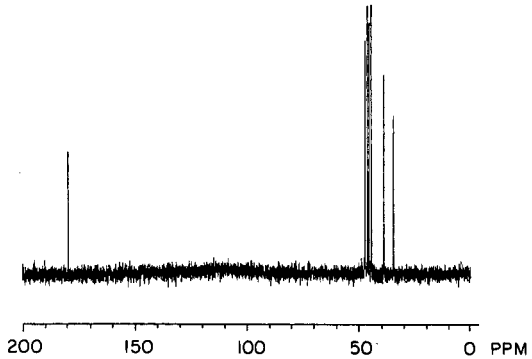

Fig. 1. Proton-decoupled ^{13}C NMR spectrum of diethylenetriamine-N-propionic acid.

The proton-decoupled ^{13}C NMR spectrum of diethylenetriamine-N′-propionic acid is shown in Fig. 2. The chemical shifts of the five observed lines are listed in Table II.

Five lines are expected in the ^{13}C NMR spectrum of this compound. All lines of this spectrum have been assigned based on their relative intensities and the expected relative chemical shifts of the carbon atoms in this compound[7]. The assignments are indicated by the numbering of the carbon atoms in the formula, which corresponds to the numbered peaks in Table II. The spectrum of this middle-substituted product contains lines of minor intensity corresponding to the end-substituted propionate, indicating an incomplete separation of the two isomers.

The proton-decoupled ^{13}C NMR spectrum of the final product, DTTAP, is shown in Fig. 3. The chemical shifts of the thirteen observed lines are listed in Table III. The peaks observed at 169.5 ppm and 56.21 ppm have been assigned to the carbons labeled 3 and 5, respectively. These two peaks are of double intensity compared to the others and are undoubtedly a result of the two equivalent acetate groups. The peak at 169.22 ppm is assigned to the carboxylic acid of the propionate group, as this carbon is expected to resonate upfield relative to the other carboxylic acid carbons. The peaks at

TABLE I

CHEMICAL SHIFTS OBSERVED IN THE ^{13}C NMR SPECTRUM OF DIETHYLENETRIAMINE-N-PROPIONIC ACID

$NH_2CH_2CH_2NHCH_2CH_2NHCH_2\overset{7}{C}H_2\overset{1}{C}OOH$

Peak	*Chemical shift (ppm)*
1	179.4
2	47.2
3	46.2
4	45.5
5	44.5
6	38.7
7	34.5

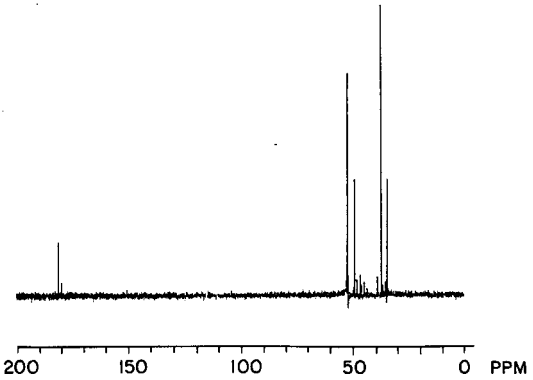

Fig. 2. Proton-decoupled ^{13}C NMR spectrum of diethylenetriamine-N'-propionic acid.

173.8 ppm and 173.7 ppm have been assigned to the carboxylic acid carbons labeled 1 or 2 in Figure 4. Distinguishing which of these nearly coincident peaks belongs to which of these carbonyl carbons is not possible without further experimentation. The peak at 28.2 ppm has been assigned to the carbon atom labeled "13" on the structure in Table III. The remaining seven peaks are currently unassigned. The chemical shifts of these peaks are, however, in the range one would expect for the remaining seven carbon atoms of DTTAP.

Elemental analyses

Diethylenetriamine-N-propionic acid was isolated as the trihydrochloride. Found: %C = 29.79, %H = 7.28, %N = 14.77, %Cl = 36.38; calculated for $C_7H_{20}N_3O_2Cl_3$: %C = 29.53, %H = 7.03, %N = 14.76, %Cl = 37.43; yield = 50% (pure compound).

DTTAP was isolated as the monohydrate from ethanol solution, mp = 159–162°C. Found: %C = 42.09, %H = 6.13, %N = 9.44; calculated for $C_{15}H_{25}N_3O_{10} \cdot H_2O$: %C = 42.35, %H = 6.35, %N = 9.88; yield = 2% (pure compound) based on original chloropropionic acid.

TABLE II

CHEMICAL SHIFTS OBSERVED IN THE ^{13}C NMR SPECTRUM OF DIETHYLENETRIAMINE-N'-PROPIONIC ACID

$HOOC\overset{1}{C}H_2\overset{5}{C}H_2\overset{3}{N}(\overset{4}{C}H_2\overset{2}{C}H_2NH_2)_2$

Peak	*Chemical shift (ppm)*
1	181.0
2	51.8
3	48.8
4	36.9
5	34.1

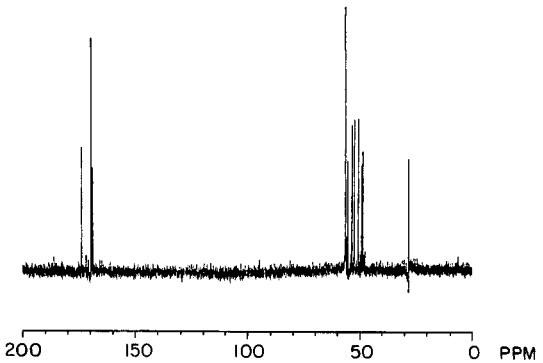

Fig. 3. ^{13}C NMR spectrum of DTTAP.

Titration data

Two equal-volume aliquots of aqueous DTTAP were titrated with standard base. The bare acid was titrated in the first experiment. The acid was titrated in the presence of one equivalent of Sm(III) in the second experiment. The ratio of equivalence point volumes for the two experiments is 3.0:5.0, indicating that five protons are released upon complexation[8].

TABLE III

^{13}C NMR CHEMICAL SHIFTS OF DTTAP

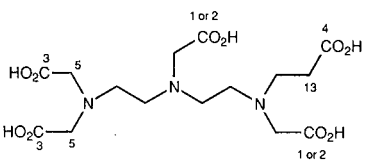

Peak	*Shift (ppm)*
1	173.78
2	173.71
3	169.54
4	169.22
5	56.21
6	55.31
7	53.43
8	52.31
9	52.27
10	50.54
11	48.88
12	48.50
13	28.17

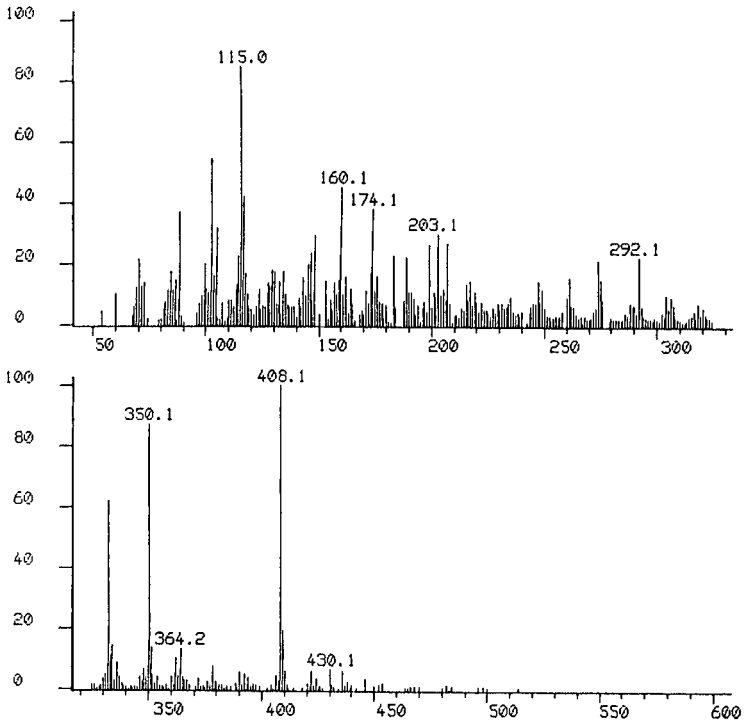

Fig. 4. Mass spectrum of DTTAP. Molecular formula DTTAP: $C_{15}H_{25}N_3O_{10}$; molecular weight: 407.1 a.m.u.

Mass spectrometry

The fast-atom-bombardment mass spectrum of DTTAP, in a glycerol–water matrix, was taken. The matrix subtracted mass spectrum can be seen in Fig. 4. The M+1 peak observed at 408.1 (*m/z*) provides further convincing evidence that the desired DTTAP has been formed. Other major peaks in the mass spectrum are due to fragments of the original DTTAP molecule. The peak at 115 (mass/charge) is probably due to a species formed by glycerol (mol. wt. = 92.1 a.m.u.) and sodium (mol. wt. = 22.99 a.m.u.)[9,10].

CONCLUSIONS

Diethylenetriamine-N-propionic acid and DTTAP have been prepared and purified for the first time. The 4:1 end to middle ratio of replaceable protons contributes to the observed dominance of the end-substituted product over the middle-substituted product in Step 1.

^{13}C NMR spectra for three compounds are reported for the first time. These spectra, along with the other evidence, allow for the unambiguous characterizaton of these compounds.

This work illustrates the value of ^{13}C NMR spectroscopy as a characterization tool for compounds of this type. The ^{1}H NMR spectra of these polyaminocarboxylates are often difficult to interpret. Unresolved multiplets are often observed, and the

isolation of the pure compounds in the absence of water or hydrochloric acid has not been achieved. Elemental analysis provides useful information, but is not an adequate characterization technique by itself. It is especially inadequate for characterizing products of a reaction where isomers are possible. The unambiguous characterization and evaluation of the purity of these compounds is accomplished when ^{13}C NMR spectroscopy is used.

Although cation-exchange displacement chromatography was successfully used to isolate the intermediate of the synthesis, this technique proved unsuccessful when used to isolate DTTAP. The impurities present in the second step are believed to be incompletely substituted tri- and tetra-carboxylic acids. DTTAP was isolated from these impurities using anion-exchang displacement chromatography.

The infrequent use of anion-exchange displacement chromatography is surprising. This work and the few examples that can be found in the literature illustrate that this technique deserves wider application for the preparative-scale separation of anionic species.

ACKNOWLEDGEMENTS

This work was supported by the Department of Chemistry, Iowa State University, and was performed at Ames Laboratory. Ames Laboratory is operated for the U.S. Department of Energy by Iowa State University under contract No. W-7405-ENG-82.

REFERENCES

1 D. J. Sawyer, *Ph. D. Dissertation*, Iowa State University, Ames, IA, 1988.
2 S. M. Partridge and R. C. Brimley, *Biochem. J.*, 51 (1952) 628–39.
3 E. A. Peterson and A. R. Torres, *J. Biochem. Biophys. Methods*, 1 (1979) 349–60.
4 E. A. Peterson, *Anal. Biochem.*, 90 (1978) 767–84.
5 A. Gueron, J.-P. Lefevre, M. Caude and R. Rosset, *Analusis*, 4 (1) (1976) 12–15.
6 J. S. Coleman and G. L. Gilbert, *J. Chromatogr.*, 34 (1968) 289–91.
7 G. C. Levy and G. L. Nelson, *Carbon-13 Nuclear Magnetic Resonance for Orgaic Chemists*, Wiley, New York, 1972.
8 D. G. Peters, J. M. Hayes and G. M. Hieftje, *Chemical Separations and Measurements*, Saunders, Philadelphia, PA, 3rd ed., 1974.
9 S. A. Martin, C. E. Costello and K. Blemann, *Anal. Chem.*, 54 (1982) 2362.
10 M. Barber, R. S. Bordoli, G. J. Eliott, D. Sedgwick and A. N. Tyler, *Anal. Chem.*, 54 (4) (1982) 645A.

Journal of Chromatography, 455 (1988) 201–216
Elsevier Science Publishers B.V., Amsterdam — Printed in The Netherlands

CHROM. 20 829

DESIGN AND APPLICATIONS OF BIOMIMETIC ANTHRAQUINONE DYES

II. THE INTERACTION OF C.I. REACTIVE BLUE 2 ANALOGUES BEARING TERMINAL RING MODIFICATIONS WITH HORSE LIVER ALCOHOL DEHYDROGENASE

STEVEN J. BURTON
Institute of Biotechnology, University of Cambridge, Downing Street, Cambridge CB2 3EF (U.K.)
C. VIVIAN STEAD*
Research Department, Imperial Chemical Industries plc, Organics Division, P.O. Box 42, Blackley, Manchester M9 3DA (U.K.)
and
CHRISTOPHER R. LOWE*
Institute of Biotechnology, University of Cambridge, Downing Street, Cambridge CB2 3EF (U.K.)
(First received June 9th, 1988; revised manuscript received July 25th, 1988)

SUMMARY

A number of terminal ring analogues of the anthraquinone dye C.I. Reactive Blue 2 were synthesised and characterised. The interaction of these dye analogues with horse liver alcohol dehydrogenase was investigated by difference spectroscopy and analytical affinity chromatography. Studies by difference spectroscopy showed that anionic terminal ring substituents or an unsubstituted phenyl ring promoted tight binding of the dye to the enzyme, whereas neutral or cationic terminal ring substituents reduced the affinity of the dye. Terminal ring analogues of C.I. Reactive Blue 2 with *ortho*- or *meta*-orientated groups were bound more tightly than those with *para*-orientated substituents. The observed differences in the affinity of the dye analogues towards horse liver alcohol dehydrogenase could be accounted for by proposing that the terminal ring of C.I. Reactive Blue 2 is bound in a relatively apolar pocket lateral to the principal coenzyme binding site and located in the catalytic domain of the enzyme. The 2900-fold difference in affinity between the C.I. Reactive Blue 2 analogues and horse liver alcohol dehydrogenase in solution was not translated into significant differences in chromatographic behaviour when the dyes were immobilised to beaded agarose. However, an *ortho*-orientated sulphonate substituent promoted exceptionally tight binding of the enzyme to the immobilised dye. Immobilisation of the dye analogues via the reactive chlorotriazine was identified as the most likely explanation for the relatively minor influence of the terminal ring substituent of the immobilised dye on enzyme binding.

* Present address: Dyestuffs Consultancy Service, 187 Victoria Avenue East, Blackley, Manchester M9 2HW, U.K.

0021-9673/88/$03.50 © 1988 Elsevier Science Publishers B.V.

INTRODUCTION

Immobilised textile dyes are being used increasingly for protein purification[1–4]. The low cost of reactive dyes coupled with their ease of immobilisation and resistance to chemical and biological degradation, has led to dye adsorbents that are invariably less expensive and more stable than those based on natural biological ligands[1–2]. Furthermore, textile dyes have been shown to interact with a large number of seemingly unrelated proteins[5–7], in some cases, with remarkable degrees of specificity[8–10].

To date, however, almost all studies have been performed with commercially available textile dyes. The selectivity of these affinity ligands could, in principle, be improved by designing synthetic dyestuffs which mimic the structure and binding of natural biological ligands. Such "biomimetic" dyes should not only display high specificity for the target protein, but also retain most of the advantages of the commercial dyes. As a first step towards designing entirely novel dyes, the interaction between analogues of C.I. Reactive Blue 2 and horse liver alcohol dehydrogenase was investigated. The structure of this enzyme has been studied extensively[11–13] and its interaction with dyes has been established by X-ray crystallography[14] and affinity labelling[15]. The dye binds to the NAD^+-binding site with the anthraquinone, diaminobenzene sulphonate and triazine rings apparently adopting similar positions with respect to the adenine, adenyl-ribose and pyrophosphate groups of NAD^+. In contrast, the terminal aminobenzene sulphonate ring of the dye is bound in a lateral cleft not normally occupied by NAD^+, being some 10Å distant from the nicotinamide binding site[14]. It was deemed likely, therefore, that the interaction between C.I. Reactive Blue 2 and horse liver alcohol dehydrogenase could be improved by selective modification of the terminal ring moiety of the dye. Previous work has shown that even relatively minor modifications to the structure of reactive dyes may markedly influence their capacity to bind proteins[8]. Consequently, it was expected that alterations to the charge, hydrophobicity and spatial arrangement of substituents on the terminal ring of C.I. Reactive Blue 2 would lead to dye analogues with altered specificity and affinity for horse liver alcohol dehydrogenase. Thus, a number of terminal ring analogues of C.I. Reactive Blue 2 have been synthesised and their interaction with the enzyme investigated in free solution and by analytical affinity chromatography[16]. This report demonstrates that modification of the terminal ring moiety of C.I. Reactive Blue 2 influences protein binding in a manner entirely consistent with the postulated interaction between the dye and horse liver alcohol dehydrogenase.

EXPERIMENTAL

Chemicals

Bromamine acid (1-amino-4-bromoanthraquinone-2-sulphonic acid), 2,5-diaminobenzenesulphonic acid, cyanuric chloride (2,4,6-trichloro-*s*-triazine) and the terminal ring forming groups *o*-, *m*- and *p*-aminobenzenesulphonic acid, *o*-, *m*- and *p*-aminobenzoic acid, *p*-aminobenzylphosphonic acid, *m*-aminobenzamide, *m*-aminobenzylalcohol and *m*- and *p*-aminobenzenetrimethylammonium chloride were supplied by ICI Organics Division. Dried acetone and 1,6-diaminohexane were obtained from Fisons (Loughborough, U.K.), whilst 1,1'- carbonyldiimidazole (CDI) was pur-

chased from Sigma (Poole, U.K.). Horse liver alcohol dehydrogenase [alcohol: NAD^+ oxidoreductase: E.C.1.1.1.1. (2.7 U mg^{-1})] and the coenzymes NAD^+ (free acid, grade 1) and NADH (disodium salt; grades I and II) were from Boehringer (Lewes, U.K.). Sepharose 4B was obtained from Pharmacia Biotechnology (Uppsala, Sweden). All other reagents and solvents were of analytical grade and were obtained from U.K. suppliers.

Synthesis of terminal ring analogues of C.I. Reactive Blue 2

The terminal ring analogues of C.I. Reactive Blue 2 were synthesised, characterised and purified according to previously published procedures[17].

Molecular models

A single subunit α-carbon model of horse liver alcohol dehydrogenase (scale 1 cm = 1 Å) was constructed from a kit of parts supplied by Shapely Models (Milton Keynes, U.K.). The model was built according to the method of Fletterick and Matela[18] using atomic coordinates stored in the Brookhaven Protein Data Bank. Models of NAD^+ and C.I. Reactive Blue 2 analogues (scale 1 cm = 1 Å) were constructed from components purchased from Labquip (Reading, U.K.).

Difference spectral titration

The dissociation constants (K_d) of the analogues of C.I. Reactive Blue 2 with horse liver dehydrogenase were determined by difference spectral titration at 25°C. A stock solution (approximately 1 mg ml^{-1}) of enzyme (clarified by filtration through a 0.45 μm pore size filter) in tricine–sodium hydroxide buffer, pH 8.5 (0.1 *M*) was prepared and the subunit concentration determined from the absorbance at 280 nm using an extinction coefficient of 0.455 ml mg^{-1} cm^{-1} and a subunit M_r of 40 000[19,20]. A solution of stock enzyme (5.0–12.5 μ*M* subunits; 1 ml) in tricine–sodium hydroxide buffer, pH 8.5 (0.1 *M*) was added to a black-walled silica cuvette (10 mm pathlength) and placed in the sample beam of a Perkin-Elmer Lambda 5 spectrophotometer. Tricine–sodium hydroxide buffer, pH 8.5 (0.1 *M*; 1 ml) was placed in a similar cuvette in the reference beam. A background-absorbance correction was performed between 850–500 nm, whereupon identical aliquots (2–10 μl) of purified dye solution (0.5–1.0 m*M*) were added to both cells and the difference absorption spectrum recorded after each pair of additions.

The maximum difference absorption ($\Delta A_{\lambda,max}$) was obtained either directly from the titration results, or calculated from a double reciprocal plot of dye concentration against difference absorbance (ΔA_λ) using linear regression analysis. A difference extinction coefficient ($\Delta\varepsilon_\lambda$) was calculated, from which the concentration of enzyme–dye complex ([ED]) formed with each dye addition could be estimated. The K_d was calculated using non-linear regression analysis[21] (with bi-square weighting) by fitting values of total dye concentration ($[D_T]$) and [ED] to the expression:

$$[ED] = \frac{[E_T]\,([D_T] - [ED])}{K_d + ([D_T] - [ED])}$$

where $[E_T]$ is the total enzyme subunit concentration and $[D_T]$ is the total dye concentration.

Synthesis of 6-aminohexyl derivatives of C.I. Reactive Blue 2 analogues

To a stirred solution of 1,6-diaminohexane (12.5 mmol) in water (20 ml) was added a solution of purified dye (1.25 mmol) in water (30 ml) and the temperature increased to 60°C. Stirring was continued for 3 h and the reaction followed by analytical thin-layer chromatography (TLC)[17] using a propan-2-ol–ammonia–water (7:2:1, v/v/v) solvent. Sodium chloride solution (3%, w/v) was added and the mixture allowed to cool. The pH was reduced to 1.0 by the addition of hydrochloric acid and the product precipitate filtered off, washed with hydrochloric acid (1 *M*, 100 ml), acetone (50 ml) and dried under vacuum. Typically, yields of 90–95% were achieved by this procedure.

Immobilisation of 6-aminohexyl C.I. Reactive Blue 2 analogues to Sepharose 4B

Sepharose 4B was activated with CDI[22] to facilitate the immobilisation of 6-aminohexyl C.I. Reactive Blue 2 analogues. Exhaustively washed Sepharose 4B (3 g moist weight) was washed sequentially with water–acetone (2:1, v/v; 20 ml), water–acetone (1:2, v/v; 20 ml), acetone (20 ml) and dried acetone (50 ml). The gel was resuspended in dried acetone (5 ml) to which CDI (0.06–0.12 g) was added and the mixture agitated for 15 min at 20–25°C. The activated gel was washed with dried acetone (100 ml) and used immediately.

A solution of 6-aminohexyl dye (0.25 mmol) in dimethyl sulphoxide (DMSO)–water (50%, v/v; 8 ml) was adjusted to pH 10.0 with 2 *M* sodium carbonate solution, whereupon CDI-activated Sepharose 4B (3 g) was added. The mixture was tumbled overnight (4°C) and washed sequentially with water (200 ml), sodium chloride solution (1 *M*, 100 ml), water (100 ml), DMSO solution (50% v/v; 20 ml) and water (200 ml). Dyed gels were stored in sodium azide solution (0.02% w/w; 4°C) until required.

Determination of immobilised dye concentration

Dyed Sepharose (30 mg moist weight) was hydrolysed (60°C; 5 min) following the addition of hydrochloric acid (5 *M*; 0.6 ml). The hydrolysate was neutralised by the addition of sodium hydroxide (10 *M*; 0.3 ml) and potassium phosphate buffer, pH 7.6 (1 *M*; 2.1 ml). The absorbance (620 nm; 25°C) of the hydrolysate was read against a Sepharose 4B blank treated in an identical manner. Molar extinction coefficients of purified 6-aminohexyl dyes were determined (620 nm; 25°C) from dye solutions (20 μM) made up in a medium identical to that of the hydrolysed gel. Immobilised dye concentrations were calculated as μmol dye per g moist weight gel.

Affinity chromatography of horse liver alcohol dehydrogenase on immobilised C.I. Reactive Blue 2 analogues

The interaction of horse liver alcohol dehydrogenase with C.I. Reactive Blue 2 analogues immobilised to Sepharose 4B was determined by analytical affinity chromatography at 4°C. A linear gradient of NADH was used to displace adsorbed horse liver alcohol dehydrogenase, the eluting concentration of the coenzyme being taken as a measure of the affinity of the enzyme for the immobilised dye.

Glass minicolums (0.5 × 10 cm) packed with adsorbent (1.0 g moist weight)

were equilibrated with 4-(2-hydroxyethyl)-1-piperazineethanesulphonic acid (HEPES)–sodium hydroxide buffer, pH 7.5 (20 m*M*) at a flow-rate of 30 ml $h^{-1}cm^{-2}$. Horse liver alcohol dehydrogenase (10 mg ml^{-1}) was dialysed overnight against 2000 vol. equilibration buffer and 200 μl of the dialysed enzyme (approximately 3 units) run into the gel bed. The sample was incubated with the adsorbent (10 min) by halting the buffer flow, following which the gel bed was washed with equilibration buffer (6 ml) and adsorbed enzyme eluted with a linear NADH (grade II) gradient (20 ml; 0–0.5 m*M*). Fractions (1 ml) were collected and samples (20 μl) assayed for enzyme activity.

Alcohol dehydrogenase was assayed by following the reduction of NAD^+ at 340 nm (25°C). In a total volume of 1 ml were: glycine (180 μmol)–sodium pyrophosphate (61 μmol) buffer, pH 9.0; semicarbazide (73 μmol); ethanol, 99.7% (v/v) (0.56 mmol); reduced glutathione (10 μmol) and NAD^+ (1.8 μmol). The molar extinction coefficient of NADH at 340 nm was taken to be 6220 l mol^{-1} cm^{-1}.

RESULTS

A series of analogues of C.I. Reactive Blue 2 were synthesised which bore anionic, cationic, neutral and hydrophobic groups substituted at various positions (*ortho*, *meta* or *para*) on the terminal aminobenzene ring of the dye (Fig. 1). These analogues were synthesised by a method similar to that for the parent dye[16,17]. The desired terminal ring structure was achieved by reacting the blue dichlorotriazinyl precursor of C.I. Reactive Blue 2 with the relevant substituted arylamine.

The reactive dyes used in this study were extensively purified as minor impurities in reactive dye preparations are known to interact with proteins[23,24]. C.I. Reactive Blue 2 analogues with terminal ring modifications were purified by Sephadex LH-20 column chromatography[17]. A 60:40 (v/v) methanol–water solvent was used for dyes possessing anionic and neutral terminal ring substituents, whereas less soluble dyes bearing cationic trimethylammonium groups were chromatographed in a 50:50 (v/v) methanol–water solvent. The degree of purification of the dyes was assessed by both analytical TLC and high-performance liquid chromatography (HPLC) as described previously[17]. Greater resolution of dyes with cationic terminal ring substituents was achieved by TLC using a solvent system comprising butanone–ammonia–water (3:4:3, v/v/v) rather than the butan-1-ol–propan-2-ol–ethylacetate–water (2:4:1:3, v/v/v) system used for anionic and neutral dyes. In all cases, the puri-

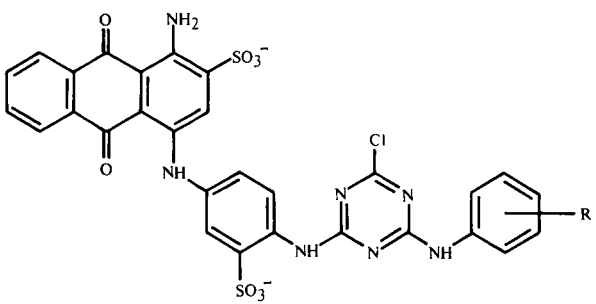

Fig. 1. The structure of C.I. Reactive Blue 2 analogues with terminal ring modifications.

TABLE I

SPECTRAL DATA DETERMINED FOR TERMINAL RING ANALOGUES OF C.I. REACTIVE BLUE 2

*C.I. Reactive Blue 2 Analogue**	*Terminal ring substituent (R)*	M_r *(sodium salt)*	λ_{max}** *(nm)*	ε_{620}** *(l mol^{-1} cm^{-1})*
I	*ortho*-SO_3^-	839.5	617	12 600
II	*meta*-SO_3^-	839.5	620	11 100
III	*para*-SO_3^-	839.5	624	11 000
IV	*ortho*-COO^-	803.5	618	10 600
V	*meta*-COO^-	803.5	624	11 100
VI	*para*-COO^-	803.5	624	10 300
VII	*para*-$CH_2PO_3H^-$	853.5	626	11 200
VIII	*meta*-CH_2OH	767.5	620	9800
IX	*meta*-$CONH_2$	780.5	616	9700
X	-H	737.5	618	9000
XI	*meta*-$N^+(CH_3)_3Cl^-$	831.0	624	7500
XII	*para*-$N^+(CH_3)_3Cl^-$	831.0	617	9000

* See Fig. 1.

** Data obtained from 100 μM aqueous solutions.

fied dyes chromatographed as single blue bands and were estimated by peak integrations from HPLC to be 96% pure, with the majority having a purity >99%.

The spectral properties of the C.I. Reactive Blue 2 analogues with terminal ring modifications were determined from 100 μM aqueous solutions of purified dye (Table I). A characteristic broad absorption peak with a λ_{max} centred around 620 nm was observed for all dye analogues. The molar extinction coefficients at 620 nm (ε_{620}) were found to be in the range of 7500–12 600 l mol^{-1} cm^{-1}, even though all of the dyes possessed the same chromogen. This phenomenon is likely to be due to dye stacking, since the relatively hydrophobic dye molecules aggregate in aqueous solution in a concentration-dependent manner. The degree of dye stacking (as determined by ε_{620}) appeared to be dependent upon the overall anionic charge carried by the dye and thus the solubility of the dye. Dyes with anionic terminal ring substituents (Table I: I–VII; net charge −3) exhibited notably higher molar extinction coefficients than dyes with neutral (Table I: VIII–X) or cationic (Table I: XI–XII) terminal ring substituents which possessed net charges of −2 and −1, respectively. Plots of dye concentration against A_{620} (not shown) suggested that dyes with neutral and cationic terminal ring substituents exhibited a greater deviation from Beer's law compared to dyes with anionic terminal ring functions.

The 1,4-diaminoanthraquinone chromophore of C.I. Reactive Blue 2 exhibits marked spectral changes upon interacting with ligand binding sites of proteins [25,26]. Thus, the binding of free C.I. Reactive Blue 2 analogues to horse liver alcohol dehydrogenase was readily assessed by difference spectroscopy in the 500–850 mm region. Fig. 2 shows a typical example in which the dye displayed difference spectra composed of multiple peaks, from which the most prominent peak (typically in the region 650–670 nm) was used to calculate the K_d. Peak heights were measured either relative to a zero-absorbance reference point (usually 850 nm) or an isosbestic point. The practice of measuring one peak height relative to that of another was not fol-

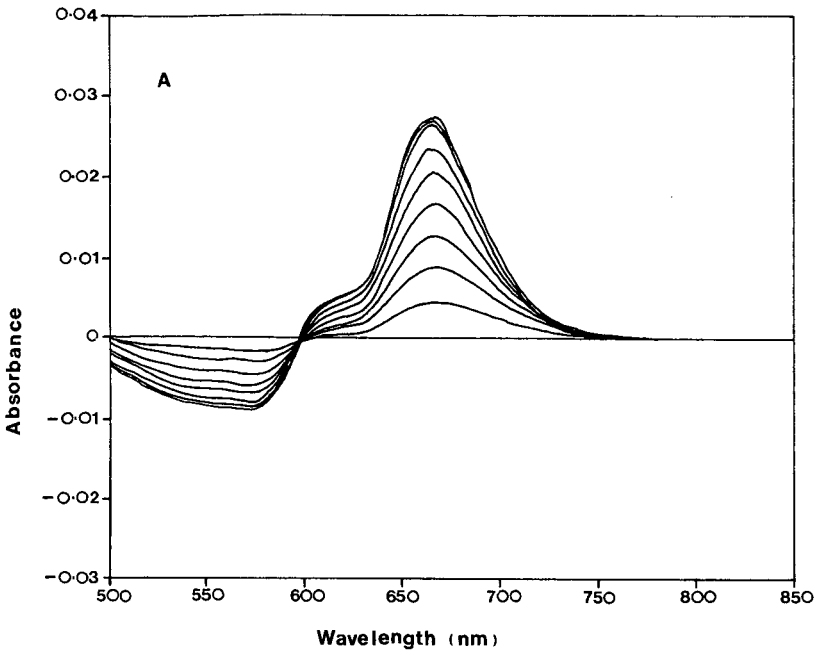

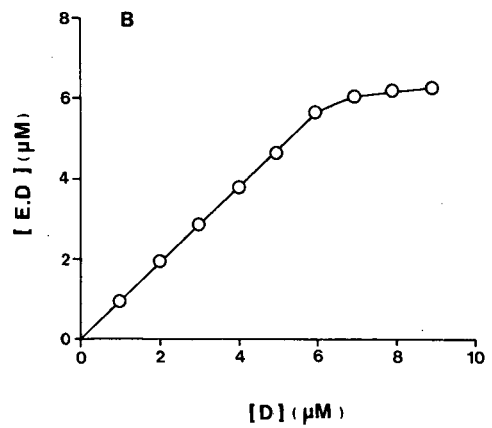

Fig. 2. Titration of horse liver alcohol dehydrogenase with V. A solution of enzyme (6.25 μmol subunits) in 1 ml tricine–sodium hydroxide buffer, pH 8.5 (0.1 *M*) and a buffer reference were titrated with 2 μl aliquots of V (0.5 m*M*) and the difference absorption spectrum recorded at 25°C following each pair of additions (A). A $\Delta\varepsilon_{666}$ of 4200 l · mol^{-1} cm^{-1} was calculated, from which the concentration of enzyme–dye complex formed with each pair of dye additions could be estimated (B).

lowed since peaks were occasionally observed to increase in intensity in a disproportionate manner. Non-linear regression analysis was used to calculate K_d values from spectral data since previously reported methods[25] proved unreliable for tightly bound dyes. Furthermore, the higher dye concentrations required for K_d determinations of the lower affinity dyes often gave higher than expected ΔA_λ values, particularly at

TABLE II

SPECTRAL DIFFERENCE TITRATION OF HORSE LIVER ALCOHOL DEHYDROGENASE WITH C.I. REACTIVE BLUE 2 ANALOGUES

*C.I. Reactive Blue 2 analogue**	λ_{max}*** *(nm)*	$\Delta\varepsilon_\lambda$ *($l\ mol^{-1}\ cm^{-1}$)*	K_d *(μM)*
I	672	5400	0.42 ± 0.05
II	656	4800	1.60 ± 0.08
III	668	5100	9.30 ± 1.60
IV	674	3800	0.20 ± 0.04
V	666	4200	0.06 ± 0.02
VI	660	4500	5.90 ± 0.10
VII	660	4500	10.5 ± 1.90
VIII	664	7000	4.50 ± 0.15
IX	660	6500	5.70 ± 0.20
X	654	4000	0.19 ± 0.04
XI	720	–	–
XII	700	3900	172 ± 5.00
XIII	676	5000	3.00 ± 0.10
XIV	668	6400	6.40 ± 0.50

* See Fig. 1.

** Mean value determined for the major difference absorption peak.

dye concentrations above 60 μM. This effect was probably attributable to non-specific dye–protein interaction which is known to occur at high dye:protein ratios[27]. Thus, K_d values were only calculated from data obtained at dye concentrations below 60 μM.

C.I. Reactive Blue 2 analogues bearing carboxylate terminal ring substituents (Table I: IV, V) displayed higher affinities for horse liver alcohol dehydrogenase than dyes with more bulky sulphonate (Table I: I–III) or methylphosphonate (Table I: VII) groups at equivalent positions on the terminal ring (Table II). Furthermore, dyes with *para*-orientated anionic groups were bound with a reduced affinity compared to dyes with equivalent *ortho*- or *meta*-orientated anionic groups. Thus, of the C.I. Reactive Blue 2 analogues containing anionic terminal ring groups, dye VII (*p*-methylphosphonate substituent) exhibited the lowest affinity (K_d = 10.5 μM) whereas dye V (*m*-carboxylate substituent) had the highest affinity (K_d = 0.06 μM). Dyes with *meta*-orientated anionic groups (II, V) were bound more tightly than dyes with *meta*-orientated neutral hydrophilic terminal ring substituents (VIII, IX). For example, exchange of a *m*-aminobenzoate terminal ring (dye V) for a *m*-aminobenzamide terminal ring (dye IX), resulted in a decrease in binding energy equivalent to 11.3 kJ mol^{-1}. This observation suggests that electrostatic interaction is important for the binding of the terminal ring of C.I. Reactive Blue 2 to horse liver alcohol dehydrogenase.

The introduction of a cationic trimethylammonium substituent on the terminal ring produced a marked decrease in affinity for the enzyme. Thus, dye XII (*p*-trimethylammonium substituent) exhibited the lowest affinity of all the C.I. Reactive Blue 2 analogues investigated (K_d = 172 μM). The K_d of dye XI (*m*-trimethylammonium substituent) could not be estimated with any accuracy due to interferences caused by dye stacking.

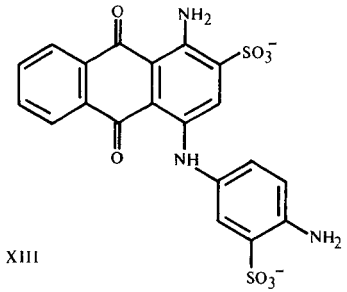

XIII

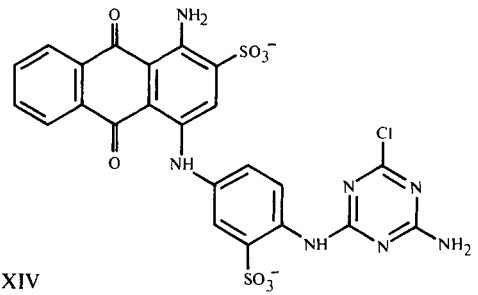

XIV

Fig. 3. The structure of C.I. Reactive Blue 2 intermediate compounds XIII and XIV.

A terminal ring devoid of substituent groups (dye X) facilitated tight dye binding (K_d = 0.19 μM). Thus, with the exception of *ortho*- and *meta*-orientated carboxyl groups, the addition of substituent groups to an otherwise unsubstituted phenyl ring lowers the affinity of the dye for the enzyme binding site. This observation would suggest that hydrophobic interaction and steric hindrance also influence the binding of the terminal ring of C.I. Reactive Blue 2 to horse liver alcohol dehydrogenase.

The affinity for the enzyme of two partial structures of C.I. Reactive Blue 2 were also determined. The purified chromophoric base compound (Fig. 3, XIII), 1-amino-4-(4′-amino-3′-sulphoanilino)-anthraquinone-2-sulphonic acid[17], exhibited a comparatively high affinity for the enzyme (K_d = 3.0 μM). This compound is also bound avidly by other C.I. Reactive Blue 2 binding proteins, particularly dehydrogenases, where it is thought to mimic the binding of the adenosine monophosphate (AMP) moiety of NADH[23].

The purified intermediate (Fig. 3, XIV), 1-amino-4-[4′-(2″-chloro-4″-amino-*s*-triazin-6″-ylamino)-3′-sulphoanilino]-anthraquinone-2-sulphonic acid (synthesised by reacting the dichlorotriazinyl precursor compound[17] with ammonia at 20–25°C) was bound with a slightly reduced affinity (K_d = 6.4 μM) compared to dye XIII. Thus, the introduction of a 2-chloro-4-amino-*s*-triazine group onto dye XIII lowers its affinity for horse liver alcohol dehydrogenase by 1.9 kJ mol^{-1}. The addition of a terminal arylamine ring to XIV had a variable effect on the overall affinity of the dye for the enzyme. In general, the addition of a substituted terminal phenyl ring increased the affinity of the dye for the enzyme. However, the introduction of phenyl

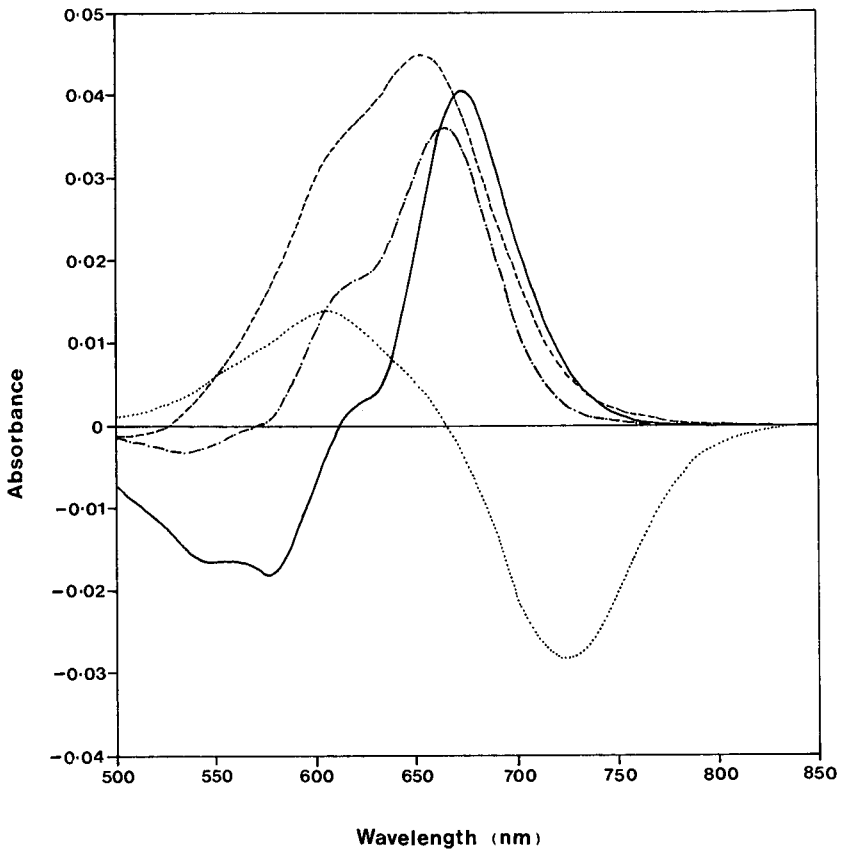

Fig. 4. Difference spectra profiles of C.I. Reactive Blue 2 analogues bound to horse liver alcohol dehydrogenase. Sample solutions contained in 1 ml total volume: tricine–sodium hydroxide buffer, pH 8.5 (99 μmol); enzyme (0.5 mg; 12.5 nmol) and 10 nmol of the C.I. Reactive Blue 2 analogues I (——), II (· – · – ·), X (– – –) and XI (·····). Difference spectra were recorded against a tricine–sodium hydroxide buffer, pH 8.5 (0.1 *M*, 1 ml) blank (25°C), containing dye (10 nmol).

rings bearing bulky *para*-orientated substituents (dyes III, VII and XII) lowered the affinity of the dyes.

The shape of the difference spectra generated when analogues of C.I. Reactive Blue 2 were bound to horse liver alcohol dehydrogenase was influenced by the structure of the terminal ring of the dye (Fig. 4). From a study of the spectral properties of Cibacron Blue F3G-A (dye I) in ionic and apolar solution, Subramanian[26] suggested that a negative difference peak at 585 nm is characteristic of electrostatic dye–protein interaction, whereas a positive peak shoulder at 610 nm and a slight negative peak below 550 nm are characteristic of hydrophobic interaction. On the basis of these observations it may be inferred that the anthraquinone chromogen of I is located in a largely electrostatic environment, whilst that of II is located in a more hydrophobic environment. Thus, alterations to the terminal ring of C.I. Reactive Blue 2 may well influence the binding conformation of the whole dye molecule. The difference spec-

trum observed for XI bore no resemblance to spectra obtained for other C.I. Reactive Blue 2 analogues, since a positive peak at 608 nm and a strong negative peak at 720 nm was observed (Fig. 4). The paradoxical difference spectrum observed for XI, a relatively insoluble dye, was probably due to dye aggregation phenomena, rather than the mode in which the anthraquinone chromophore was bound to the enzyme.

The binding of C.I. Reactive Blue 2 analogues to horse liver alcohol dehydrogenase was competitive with coenzyme binding, since the addition of NADH (grade 1) to enzyme–dye mixtures reduced the intensity of the difference spectrum. The concentration of NADH required to displace 50% of a bound dye was proportional to the affinity of the dye for the enzyme.

The affinity of horse liver alcohol dehydrogenase for immobilised analogues of C.I. Reactive Blue 2 was assessed by analytical affinity chromatography. Dyes were immobilised to beaded agarose by a 1,6-diaminohexane spacer arm to promote optimal protein–ligand interaction (Fig. 5). Adsorbent performance was compared at an immobilised dye concentration of approximately 2.0 μmol g^{-1} moist weight gel, achieved by adjusting the concentration of CDI used in the matrix activation step. The molar extinction coefficients observed for purified 6-aminohexyl dyes in hydrolysed gel media were approximately 14% lower than those obtained for the unsubstituted dyes in distilled water. This reduced extinction was probably due to stacking of the 6-aminohexyl dyes in strongly ionic solutions, and highlights the need to consider such effects when determining the concentrations of reactive dyes in free solution by spectral methods.

With the exception of dye I, the affinity of horse liver alcohol dehydrogenase for the immobilised dyes (as determined by the concentration of NADH required for elution, see Table III) paralleled the affinity of the enzyme for the dye in free solution (Table II). Thus, immobilised dyes V and X bound the enzyme more tightly than dyes III and VII. Furthermore, immobilised dyes XI and XII merely retarded the enzyme, which was eluted prior to the application of the linear NADH gradient. However, the apparent differences in affinity to the immobilised dyes for horse liver alcohol dehydrogenase were less than expected from the $2.9 \cdot 10^3$-fold difference in affinity displayed by the dyes in free solution (Table II). This suggested that the method of dye immobilisation to the matrix sterically hindered dye binding to the enzyme and thus obfuscated intrinsic differences in affinity of the soluble dyes. Not surprisingly, therefore, dye analogues coupled directly to beaded agarose via the chlorotriazine

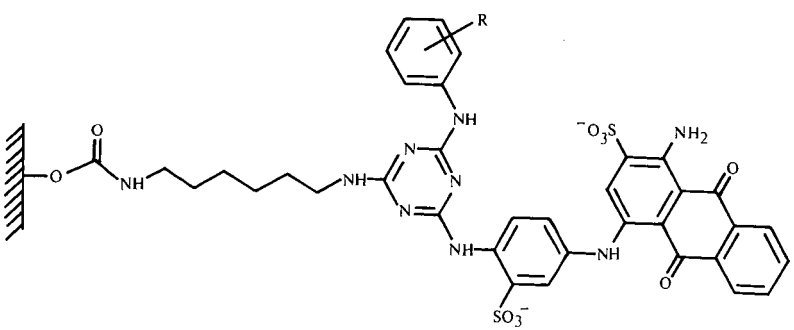

Fig. 5. The structure of 6-aminohexyl-C.I. Reactive Blue 2 analogues coupled to CDI-activated agarose.

TABLE III

AFFINITY CHROMATOGRAPHY OF HORSE LIVER ALCOHOL DEHYDROGENASE ON C.I. REACTIVE BLUE 2 ANALOGUES COUPLED TO SEPHAROSE 4B WITH A 1,6-DIAMINOHEXANE SPACER ARM (4°C; pH 7.5)

C.I. Reactive Blue 2 analogue	*Immobilised dye concentration (μmol g^{-1} moist weight)*	*[NADH] required for elution*	*Activity recovered (%)*
I	2.2	245	54
II	2.1	78	100
III	2.2	73	90
IV	2.1	81	87
V	1.8	90	80
VI	2.1	80	83
VII	1.9	78	83
VIII	2.3	83	78
X	1.9	89	83
XI	2.2	0	81
XII	2.3	0	84

ring[2] behaved similarly, with very little difference in enzyme binding behaviour being observed between the various analogues (data not shown).

The *ortho*-sulphonate isomer of C.I. Reactive Blue 2 (I) bound horse liver alcohol dehydrogenase considerably more tightly than other C.I. Reactive Blue 2 analogues with higher affinities in free solution. A substantial amount of enzyme was still bound to the column at the end of the elution gradient. An alternative elution strategy (0–1.0 *M* potassium chloride gradient) was employed to determine whether immobi-

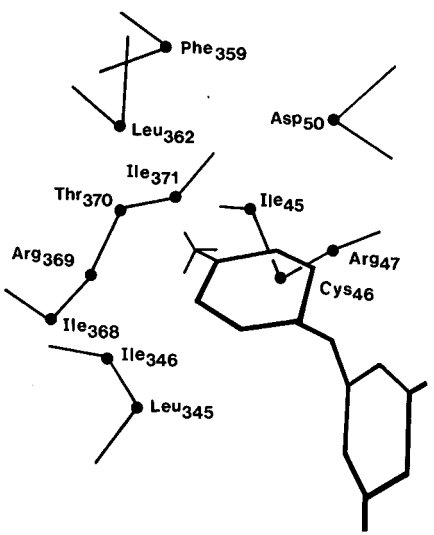

Fig. 6. Structure of the putative C.I. Reactive Blue 2 terminal ring binding site of horse liver alcohol dehydrogenase.

lised dye I displayed a genuinely high affinity for the enzyme or was merely binding non-competitively with respect to NADH. The concentration of potassium chloride required to elute the enzyme from immobilised dye I (0.25 *M*) was notably higher than the concentration required for elution from immobilised dye V (0.16 *M*). This observation suggested that immobilised dye I had a higher affinity for horse liver alcohol dehydrogenase than would have been predicted from the performance of other C.I. Reactive Blue 2 analogues.

DISCUSSION

Crystallographic studies reveal that the terminal phenyl ring of C.I. Reactive Blue 2 is bound by horse liver alcohol dehydrogenase in a region not normally associated with coenzyme binding[14]. From information given by Biellmann *et al.*[14] and deductions made from constructed molecular models, the terminal ring binding site is composed of residues which are located in the catalytic domain of the enzyme. The majority of the residues (Ile_{45}, Leu_{345}, Ile_{346}, Phe_{359}, Leu_{363}, Ile_{368} and Ile_{371}) are apolar. Of the remaining residues, two are cationic (Arg_{47} and Arg_{369}), two are polar (Thr_{370} and Cys_{46}) and one is anionic (Asp_{50}), with the latter being located at the top of the putative binding pocket. The molecular architecture of this site (Fig. 6) can entirely account for the observed affinity of the various C.I. Reactive Blue 2 analogues.

The preponderance of hydrophobic residues in the terminal ring binding site will favour the binding of predominantly hydrophobic species. Thus, dye X was bound more tightly than most C.I. Reactive Blue 2 analogues with hydrophilic groups attached to the terminal phenyl ring (Table II). The two juxtaposed arginine residues (Arg_{47} and Arg_{369}) will encourage the entry of anionic species into the pocket. Thus, dyes bearing acidic groups (I–VII) displayed a much higher affinity for the enzyme compared to dyes with basic groups on the terminal phenyl ring (XI, XII). Dyes bearing terminal rings substituted with carboxylates had higher affinities than dyes possessing sulphonate residues at equivalent positions on the terminal ring. These differences in affinity may be attributed to the smaller size of the carboxyl group relative to the sulphonate group, thereby permitting entry into a relatively narrow pocket, and the smaller hydration shell of a carboxylic acid. A small hydration shell on an anionic terminal ring substituent will promote electrostatic interaction with the cationic arginine residues which line the pocket and will also facilitate hydrophobic interaction by reducing the number of water molecules in the vicinity of the pocket. The tight binding of V is therefore attributable to the optimal hydrophobic and electrostatic interaction between the terminal ring of the dye and its binding site. This conclusion may be significant, since reactive textile dyes invariably rely on sulphonate as opposed to carboxylate groups for solvation. The observation that *para*-orientated terminal ring substituents do not bind as tightly as equivalent *ortho*- and *meta*- substituents may be explained by steric hindrance, since the interchain distance between residues at the bottom of the terminal ring binding pocket (Gly_{44} and Ile_{371}) is only 4.2 Å. *Para*-orientated anionic groups are also unfavourably positioned for interaction with Arg_{47}. The low affinity of XII is thus readily accounted for by unfavourable steric and charge interactions created by the *p*-trimethylammonium cation.

The difference spectra generated on binding C.I. Reactive Blue 2 analogues to horse liver alcohol dehydrogenase suggested that the environment of the anthraquinone chromophore was influenced by the structure of the terminal phenyl ring. The position of anionic groups on the terminal ring may favour interaction with one of the two arginine residues which line the pocket. Such an event may indirectly influence the binding of the anthraquinone moiety of the dye to the adenine binding pocket of the enzyme. Furthermore, by analogy to the binding of NAD^+ to horse liver alcohol dehydrogenase[13], a change in enzyme conformation might also be triggered by the binding of C.I. Reactive Blue 2 analogues, in a manner dependent upon the nature and orientation of the terminal ring substituent. This hypothesis is supported by studies of Cibacron Blue F3G-A binding to glutamine synthetase[28], where the difference spectrum generated upon dye binding was shown to be influenced by the conformational state of the enzyme. The form of the observed difference spectrum may be explained by the bound chromophore interacting with different residues within the adenosine binding crevice of horse liver alcohol dehydrogenase. A hydrophobic type difference spectrum (as observed for II, see Fig. 4) was probably due to strong interaction of the anthraquinone region of the dye with hydrophobic residues such as Phe_{198}. The electrostatic type difference spectrum (as observed for I) is probably the result of a preferred interaction between the anthraquinone-2-sulphonate group and Arg_{271}.

C.I. Reactive Blue 2 analogue I differs from the other analogues in that the terminal ring of the dye is not rotationally mobile due to the presence of an *ortho*-orientated sulphonic acid group. This feature of I may account for the tight binding of the immobilised dye to the enzyme during chromatography. The hindrance to free rotation of the terminal sulphonated phenyl ring of I will be increased by immobilisation of the dye through the triazine ring. Thus, the immobilised dye may be locked into a position which is highly favourable for binding the enzyme. The orientation of the terminal phenyl ring sulphonate group had a marked effect on the affinity of the dye for horse liver alcohol dehydrogenase.

Differences in affinity of C.I. Reactive Blue 2 isomers towards proteins such as dopamine-β-monooxygenase have also been reported[29]. However, on the basis of our work, claims that the *meta*-sulphonate isomer of C.I. Reactive Blue 2 is not an inhibitor of horse liver alcohol dehydrogenase[14] must be discounted. Thus, care must be exercised in selecting affinity adsorbents composed of immobilised C.I. Reactive Blue 2, since commercial dye preparations are known to be heterogeneous[17] and different isomeric forms of the dye may exhibit entirely unexpected chromatographic properties.

Although large differences in affinity towards horse liver alcohol dehydrogenase were displayed by C.I. Reactive Blue 2 analogues in free solution, this was not apparent in the majority of cases when the dyes were immobilised. This observation suggests that the method of immobilisation used does not allow the terminal ring of the dye to interact fully with the enzyme. The weak binding of XIV relative to XIII (Table II) suggests that the triazine ring does not contribute significantly to dye binding. Immobilisation of the dye by the triazine ring may worsen its already weak binding to render this part of the molecule redundant in enzyme binding. This hypothesis is supported by crystallographic data which suggest that the triazinyl chlorine atom of C.I. Reactive Blue 2 bound to horse liver alcohol dehydrogenase is directed towards

the active site of the enzyme[14]. It is highly improbable that the triazine ring adopts a similar orientation when immobilised to a solid support matrix due to severe steric hindrance. Thus, although the anthraquinone and terminal ring regions of the dye contribute to enzyme binding in free solution, it is unlikely that this situation exists when the dye is immobilised. Under the latter circumstances, protein binding is apparently dominated by the anthraquinone ring region.

The effectiveness of the blue chromogen of C.I. Reactive Blue 2 in binding proteins has been amply demonstrated[30–32]. This region of the dye has a particularly high affinity for adenine nucleotide binding proteins, where it frequently mimics the binding of AMP[6,23,33]. The general nature of the hydrophobic/electrostatic interaction of proteins with the anthraquinone region of the dye may account for the wide variety of unrelated proteins which are bound by the immobilised dye. It might be anticipated therefore, that immobilisation of C.I. Reactive Blue 2 analogues by the anthraquinone ring will reduce non-specific dye–protein interaction and allow the terminal ring of the immobilised dye to interact more fully with its complementary binding site. The true effect of modifications to the terminal ring of C.I. Reactive Blue 2 on protein purification by affinity chromatography may then be more readily observed.

REFERENCES

1 C. R. Lowe, in A. Wiseman (Editor), *Topics in Enzyme and Fermentation Biotechnology*, Vol. 9, Ellis Horwood, Chichester, pp. 78–161.
2 C. R. Lowe and J. C. Pearson, *Methods Enzymol.*, 104 (1984) 97–113.
3 F. Quadri, *Trends Biotechnol.*, 3 (1985) 7–12.
4 G. Birkenmeier, G. Kopperschlager and G. Johansson, *Biomed. Chromatogr.*, 1 (1986) 64–77.
5 P. D. G. Dean and D. H. Watson, *J. Chromatogr.*, 165 (1979) 301–319.
6 G. Kopperslager, H.-J. Bohme and E. Hoffman, in A. Fiechter (Editor), *Advances in Biochemical Engineering*, Vol. 25, Springer Verlag, Berlin–Heidelberg, 1982, pp. 101–138.
7 L. A. Haff and R. L. Easterday, in F. Eckstein and P. V. Sundaram (Editors), *Theory and Practice in Affinity Chromatography*, Academic Press, New York, NY, 1978, pp. 23–44.
8 J. C. Pearson, S. J. Burton and C. R. Lowe, *Anal. Biochem.*, 158 (1986) 383–389.
9 J. E. C. McArdell, T. Atkinson and C. J. Bruton, *Eur. J. Biochem.*, 125 (1982) 361–366.
10 P. Hughes, R. F. Sherwood and C. R. Lowe, *Eur. J. Biochem.*, 144 (1984) 135–142.
11 H. Eklund, B. Nordstrom, E. Zeppezauer, G. Soderlund, I. Ohlsson, T. Bowie, B.-O. Soderberg, O. Tapia and C.-I. Branden, *J. Mol. Biol.*, 102 (1976) 27–59.
12 H. Eklund, J.-P. Samama, L. Wallen, C. I. Branden, A. Akeson and T. A. Jones, *J. Mol. Biol.*, 146 (1981) 561–587.
13 H. Eklund, J.-P. Samama and T. A. Jones, *Biochemistry*, 23 (1984) 5982–5996.
14 J.-F. Biellman, J.-P. Samama, C.-I. Branden and H. Eklund, *Eur. J. Biochem.*, 102 (1979) 107–110.
15 D. A. P. Small, C. R. Lowe, A. Atkinson and C. J. Bruton, *Eur. J. Biochem.*, 128 (1982) 119–123.
16 C. R. Lowe, S. J. Burton, J. C. Pearson, Y. D. Clonis and C. V. Stead, *J. Chromatogr.*, 376 (1986) 121–130.
17 S. J. Burton, S. B. McLoughlin, C. V. Stead and C. R. Lowe, *J. Chromatogr.*, 435 (1988) 127–137.
18 R. J. Fletterick and R. Matela, *Biopolymers*, 21 (1982) 999–1003.
19 D. J. Cannon and R. H. McKay, *Biochem. Biophys. Res. Commun.*, 35 (1969) 403–409.
20 H. Jornvall, *Eur. J. Biochem.*, 16 (1970) 25–40.
21 R. G. Duggleby, *Anal. Biochem.*, 110 (1981) 9–18.
22 G. S. Bethel, J. S. Ayers, W. S. Hancock and M. T. W. Hearn, *J. Biol. Chem.*, 254 (1979) 2572–2574.
23 R. S. Beissner and F. B. Rudolph, *J. Chromatogr.*, 161 (1978) 127–135.
24 B. H. Weber, K. Willeford, J. G. Moe and D. Piszkiewicz, *Biochem. Biophys. Res. Commun.*, 86 (1979) 252–258.

25 S. T. Thompson and E. Stellwagen, *Proc. Natl. Acad. Sci USA*, 73 (1976) 361–365.
26 S. Subramanian, *Arch. Biochem. Biophys.*, 216 (1982) 116–125.
27 O. Bertrand, S. Cochet, Y. Kroviarski, A. Truskolaski and P. Boivin, *J. Chromatogr.*, 346 (1985) 111–124.
28 M. M. Federici, P. B. Chock and E. R. Stadtman, *Biochemistry*, 24 (1985) 647–660.
29 T. Skoteland, *Biochem. Biophys. Acta*, 659 (1981) 312-325.
30 L. Bornmann and B. Hess, *Z. Naturfortsch.*, 32 (1977) 756–759.
31 R. S. Beissner and F. B. Rudolph, *Arch. Biochem. Biophys.*, 189 (1978) 76–80.
32 D. Charytonowicz, M. Konieczny and A. D. Ingolt, *Arch. Immunol. Ther. Exp.*, 32 (1984) 247–251.
33 Y. D. Clonis and C. R. Lowe, *Biochem. J.*, 191 (1980) 247–251.

Journal of Chromatography, 455 (1988) 217–224
Elsevier Science Publishers B.V., Amsterdam — Printed in The Netherlands

CHROM. 20 832

RESOLUTION OF THE INTERMEDIATES OF *DE NOVO* PURINE BIOSYNTHESIS BY ION-PAIR REVERSED-PHASE HIGH-PERFORMANCE LIQUID CHROMATOGRAPHY

ROBERT G. HARDS* and DAVID PATTERSON
Eleanor Roosevelt Institute for Cancer Research, 1899 Gaylord Street, Denver, CO 80206 (U.S.A.)
(First received March 25th, 1988; revised manuscript received July 20th, 1988)

SUMMARY

An ion-pair reversed-phase high-performance liquid chromotographic procedure capable of resolving twelve of the fourteen intermediates of *de novo* purine biosynthesis is presented. The method utilizes isocratic elution and detection by ultraviolet light absorption. Separation of all twelve intermediates can be achieved in 90 min.

INTRODUCTION

A simple, single chromatographic separation for the intermediates of *de novo* purine biosynthesis has not been documented until now. While various methodologies have been established to isolate one[1–3] or at best two or three[4–6] of the intermediates no one system was directly applicable to the entire pathway. Resolution of the greatest number of intermediates was accomplished by the methods of Patterson and co-workers[7–10], which were not without certain drawbacks. The methods involved incorporation of radioactive precursors into the intermediates, extraction of the labelled cells, separation of the compounds by TLC*, visualization by autoradiography

* The following abbreviations are used: ADP = adenosine 5′-diphosphate; Ade = adenine; AICAR = 5′-aminoimidazole-4-carboxamide ribonucleotide; AICR = 5′-aminoimidazole-4-carboxylate ribonucleotide; AIR = 5′-aminoimidazole ribonucleotide; AMP = adenosine 5′-monophosphate; AMPS = adenylosuccinic acid; ATP = adenosine 5′-triphosphate; CHO = Chinese hamster ovary; DBAP = dibutyl ammonium phosphate; EDTA = ethylenediaminetetraacetic acid; F12 = Ham's F12 culture media; FAICAR = 5′-formaminoimidazole-4′-carboxamide ribonucleotide; FC = fetal bovine serum; FCM = macromolecular fraction of fetal bovine serum; FGAM = N-formylglycinamidine ribonucleotide; FGAR = N-formylglycinamide ribonucleotide; FH = tetrahydrofolate; GAR = glycinamide ribonucleotide; glu = glutamic acid; gluNH$_2$ = glutamine; GMP = guanosine 5′-monophosphate; HEPES = N-2-hydroxyethylpiperazine-N′-2-ethanesulfonic acid; HPLC = high-performance liquid chromatography; IMP = inosine 5′-monophosphate; NADP = nicotinamide–adenine dinucleotide phosphate, oxidized; NADPH = nicotinamide–adenine dinucleotide phosphate, reduced; PEI = polyethyleneimine; P_i = inorganic phosphate; PRA = phosphoribosylamine; PRPP = 5′-phosphoribosyl-1-pyrophosphate; SAICAR = 5′-aminoimidazole-4-N-succinocarboxamide ribonucleotide; TLC = thin layer chromatography; XMP = xanthosine 5′-monophosphate.

0021-9673/88/$03.50 © 1988 Elsevier Science Publishers B.V.

and finally removal of the compounds from the TLC matrix. The procedures are time consuming, prone to loss of material and require radioactive labelling of the compounds. The method described in this paper utilizes an ion-pair reversed-phase HPLC system employing isocratic elution and detection by ultraviolet light absorption, thereby eliminating the need to remove the compounds of interest from the matrix after detection and the requirement that the intermediates be radioactively tagged.

Because of the large number of compounds that will absorb ultraviolet light in the range used for detection in the system described, "clean" samples are required for analysis. A method for the preparation of such samples is presented.

MATERIALS AND METHODS

Chemicals

The following chemicals were purchased from Sigma: AMP, GMP, XMP, IMP, AMPS and AICAR. The mobile phase components DBAP and acetonitrile were obtained from Aldrich and Burdick & Jackson Labs., respectively. Methanol and ethanol were purchased from Fisher Chemical. All chemicals were of the highest quality available. Chemically synthesized GAR was kindly provided by Dr. S. Benkovic of the Pennsylvania State University.

HPLC separation of purine intermediates

Separation of the intermediates of *de novo* purine biosynthesis was accomplished using a 30 cm × 3.9 mm μBondapak C^{18} reverse phase HPLC column (Waters Assoc.) coupled to a 5 cm × 4.6 mm guard column of Bondapak C_{18}/Corasil (Waters Assoc.). The isocratic mobile phase consisted of the ion-pairing buffer 5 m*M* DBAP, pH 6, plus 1% or 3% acetonitrile. The mobile phase was delivered by a Waters M6000A pump at a flow-rate of 1 ml/min. Eluting compounds were detected by a Model 440 absorbance detector with a 254-nm wavelength filter (Waters Assoc.) connected to a Waters Model 730 DATA module and/or a Model GM770 variable-wavelength detector (Schoeffel) set at 210 mm connected to an Omniscribe recorder (Houston Instruments). In some experiments a Flow One Beta radioactive detector (Radiomatic Instruments) set to measure ^{14}C and connected to a dot matrix printer was used to monitor eluting compounds.

For anion-exchange HPLC a 25 cm × 4.6 mm Partisil-10 SAX column (Whatman, Inc.) was employed, connected to a 5 cm × 4.6 mm guard column packed with pellicular anion exchanger (Whatman). The solvent, 20 m*M* ammonium phosphate, pH 4.2, plus 1% acetonitrile was delivered by a Waters M6000A pump at a flow-rate of 2 ml/min. Detection of the compounds was achieved using the two UV-absorbance systems described above.

Preparation of intermediates

The intermediates of *de novo* purine biosynthesis were obtained from mutant CHO cells defective in one or more steps of the pathway[7,10] using a modification of the procedure described previously[7]. Cells were grown on plastic tissue culture plates (Lux Science Corp.) in F12 (Flow Labs.) plus 8% FC and 0.1 m*M* glycine for 24 to 36 h at 37°C. Cells were harvested prior to confluence by brief trypsinization which was stopped by the addition of 5% FCM. The cells were harvested by centrifugation,

washed three times with F12 minus hypoxanthine and glutamine plus 8% FCM and 20 m*M* HEPES, pH 7.5, and then resuspended in F12 minus hypoxanthine plus 8% FCM, 2 m*M* glutamine, 0.1 m*M* glycine and 20 m*M* HEPES, pH 7.5, at approximately $5 \cdot 10^6$ cells/ml. For the Ade-G cell line which accumulates FGAR and FGAM, 10 μCi/ml of [^{14}C]formate (50 mCi/nmol, New England Nuclear) was added for some experiments. The cells were incubated at 37°C with shaking for 2 h, chilled, washed twice with ice-cold F12 minus hypoxanthine and the intermediates extracted with ice-cold 80% ethanol for 30 min at 4°C with gentle agitation. Cells were pelleted by centrifugation and the supernatant applied to a Sep-Pak silica column (Waters Assoc.). The column was washed with 4 ml of absolute methanol and the compounds of interest eluted with 10 ml of distilled/deionized water. The sample was quickly frozen, lyophilized to dryness, resuspended in 1 ml of 100 m*M* ammonium acetate, pH 8.8, and applied to a 6.5 cm × 0.7 cm column of Affigel 601 (boronate gel, Bio-Rad Labs.). The column was washed with 14 ml of 100 m*M* ammonium acetate, pH 8.8, and the purine intermediates then eluted with 20 m*M* acetic acid (10 ml, of which the first two were discarded). The sample was quickly frozen, lyophilized to dryness and resuspended in a minimum volume of 5 m*M* DBAP, pH 6, plus 1% or 3% acetonitrile. Immediately prior to HPLC analysis the samples were centrifuged at 13 000 *g* for 5 min and the supernatant injected.

Methods of peak identification

Detection of diazotizable aromatic amines and preparation of derivatives of such compounds were carried out using the procedure of Bratton and Marshall[11] as modified by Flaks and Lukens[12,13].

Enzyme assays of FGAR amidotransferase and AIR synthetase were run as previously described[14]. Briefly [^{14}C]FGAR or [^{14}C]FGAM, isolated using ion-pair reversed-phase HPLC was incubated with CHO-K1 extract in the presence of 50 m*M* HEPES, pH 7, 10 m*M* magnesium chloride, 100 m*M* potassium chloride, 0.1 m*M* EDTA and 2 m*M* ATP in a total volume of 100 ml. For the FGAR amidotransferase assay 5 m*M* glutamine was also present. After incubation for 15 min at 37°C the reactions were stopped by the addition of 100 ml of ice-cold ethanol. Following centrifugation to remove protein, aliquots of the supernatants were spotted on PEI-cellulose TLC plates which were then developed in 0.35 *M* lithium chloride, air dried and placed on X-ray film (Kodak). Radioactive spots were identified by their R_F values.

Ultraviolet and visible absorption spectra of various compounds were obtained using a Beckman DU-50 spectrophotometer equipped with an Epson RX-80 printer.

Identification of the purine intermediate FAICAR involved its conversion to IMP or AICAR. These chemical reactions were accomplished using the procedures of Lukens and Flaks[13].

RESULTS AND DISCUSSION

Purine auxotrophs isolated and characterized by Patterson and co-workers[7–10] were used as the sources for twelve intermediates of *de novo* purine biosynthesis resolved by the ion-pair reversed-phase HPLC system described in this communication (Fig. 1). The retention time for each intermediate and the method(s) used to

confirm its identity are listed in Table I. A description of the cell lines used and the intermediates isolated from each is given below.

Ade-E cells were found to accumulate a compound that eluted at 3.5 min. This compound failed to absorb ultraviolet light above 230 nm and co-eluted with chemically produced GAR when analysed with either ion-par reversed-phase or anion-exchange HPLC. The peak was therefore identified as GAR.

Ade-G cells were found to significantly accumulate two peaks, FGAM and FGAR, which eluted at 4.5 and 10.7 min, respectively (Fig. 2). The peaks were identified by their co-elution with [^{14}C]FGAM and [^{14}C]FGAR that had been prepared and characterized by TLC[14]. In addition, intermediate accumulation with Ade-G cells was carried out in the presence of [^{14}C]formate. The putative FGAM and FGAR were isolated by ion-pair reversed-phase HPLC and subsequently used as

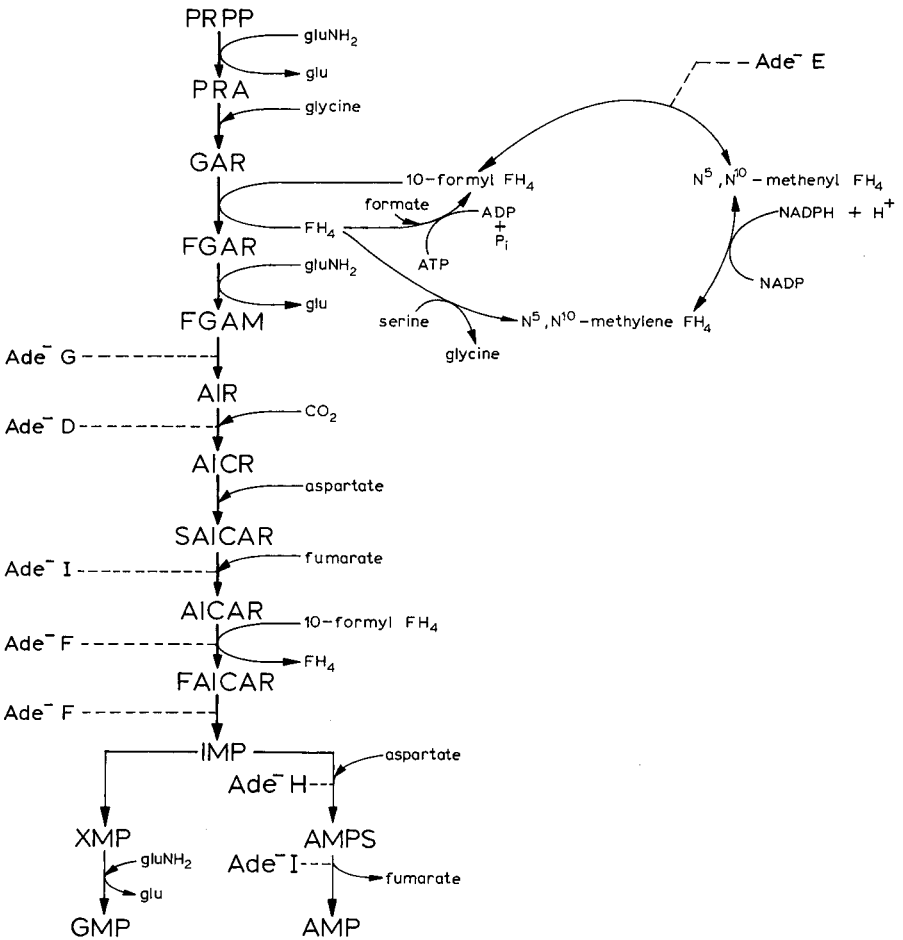

Fig. 1. A simplified representation of purine biosynthesis indicating intermediates and CHO mutant cell lines discussed in text.

TABLE I

RETENTION TIMES OF INTERMEDIATES OF *DE NOVO* PURINE BIOSYNTHESIS USING ION-PAIR REVERSED-PHASE HPLC

Methods of peak identity confirmation: 1 = co-elution with known compound using ion-pair reversed-phase HPLC; 2 = co-elution with known compound using anion-exchange HPLC; 3 = characteristic positive reaction for diazotizable aromatic amine; 4 = comparison of absorption spectrum to known compound; 5 = use as substrate in enzyme assay; 6 = chemical conversion of compound.

Compound	*Retention time (min)*		*Method of peak identity confirmation*
	1% CH_3CN	*3% CH_3CN*	
GAR	3.5		1
FGAM	4.5		1, 5
AIR	5.0	4.5	3
FGAR	10.7		1, 5
AICAR	24.3		1, 2, 3, 4
GMP	31.6	12.0	1, 2, 4
IMP	33.4	13.0	1, 2, 4
SAICAR	42.8	15.9	4, 5
FAICAR	48.7		4, 6
XMP	50.8	18.0	1, 2, 4
AMP	72.1	23.4	1, 2, 4
AMPS		90.6	1, 2, 4

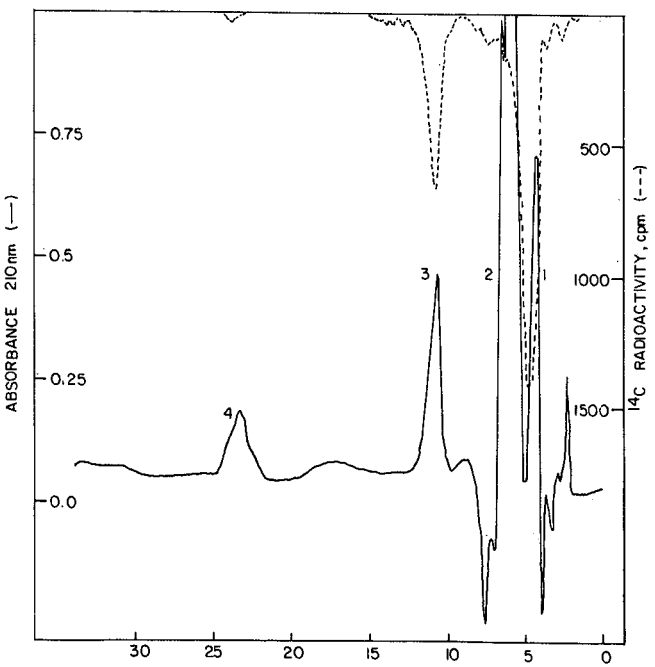

Fig. 2. Simultaneous UV and radioactivity detection of ion-pair reversed-phase HPLC separation of intermediates accumulated by Ade-G cells. Mobile phase: 5 m*M* DBAP, pH 6, plus 1% acetonitrile. Peaks: 1 = FGAM; 2 = acetate; 3 = FGAR; 4 = unknown. Slight offset of radioactive peaks due to time required for flow between detectors.

substrates in AIR synthetase and FGAR amidotransferase assays. The products obtained confirmed the peak assignments.

Ion-pair reversed-phase HPLC analysis of Ade-D cell extract revealed only a single significant peak which eluted at 5.0 min. The compound did not absorb UV light above 230 nm and when tested for the presence of a diazotizable aromatic amine produced an orange coloured compound (absorption maximum of 500 nm). This is a definitive test for the compound AIR.

Extract from Ade-F cells showed a large peak eluting at 24.3 min as well as a less pronounced peak eluting at 48.7 min. The first peak exhibited a UV absorbance spectrum identical to that of commercially produced AICAR, co-eluted with commercially produced AICAR when run on either ion-pair reversed-phase or anion-exchange HPLC and gave a positive reaction when tested for diazotizable aromatic amines with an absorption maximum of 540 nm. The compound eluting at 24.3 min was thus identified as AICAR. The second compound, retention time 48.7 min, had an absorbance maximum at 264 nm. When treated with 0.1 *M* sodium hydroxide for 20 min at 38°C, this compound was converted to another that eluted at 34.0 min and co-eluted with IMP. Treatment in 0.2 *M* sulfuric acid for 3 min at 100°C converted the 48.7-min peak to a compound that co-eluted with AICAR at 25.0 min. These results confirm the identity of the peak eluting at 48.7 min as FAICAR.

In addition to the compounds discussed above the purine auxotrophs grown in hypoxanthine deficient medium were found to accumulate low levels of AMP, IMP, GMP and XMP. These minor peaks were identified by comparison to commercially available compounds with respect to UV absorbance spectra and co-elution on ion-pair reversed-phase and anion-exchange HPLC.

The final purine auxotroph studied was Ade-I and resolution of the accumulated compounds required a slight modification of the chromatographic protocol. Due to the affinity exhibited by one of the accumulated products for the column matrix it was necessary to increase the acetonitrile concentration to 3%. Three major peaks at 4.5, 15.9 and 90.6 min were observed (Fig. 3). The earliest eluting peak failed to exhibit an absorption spectrum above 230 nm and when tested for diazotizable aromatic amines gave a positive result with a maximum absorbance of 500 nm. Thus the peak at 4.5 min would seem to be AIR. The compound eluting at 15.9 min showed an absorption maximum at 267 nm and gave a positive reaction for diazotizable aromatic amines only when tested at 4°C in the presence of 10 *M* sulfuric acid. These results confirm the peak's identity as SAICAR. When run on the ion-pair reversed-phase column with a mobile phase of 1% acetonitrile SAICAR was found to have a retention time of 42.8 min. The compound eluting at 90.6 min was identified as AMPS by comparison to the commercially prepared compound. Not only were the absorption spectra identical but the biologically and commercially prepared compounds co-eluted when run on either an ion-pair reversed-phase or anion-exchange column. In addition to these major accumulations minor peaks corresponding to IMP, GMP, XMP and AMP were also observed and identified as discussed previously.

As expected analyses of extracts from a non-mutant CHO cell line did not indicate accumulation of any intermediates of *de novo* purine biosynthesis. The largest peak observed eluted at approximately 6 min with both 1% and 3% acetonitrile and was identified as acetate. Minor peaks were detected at later elution times

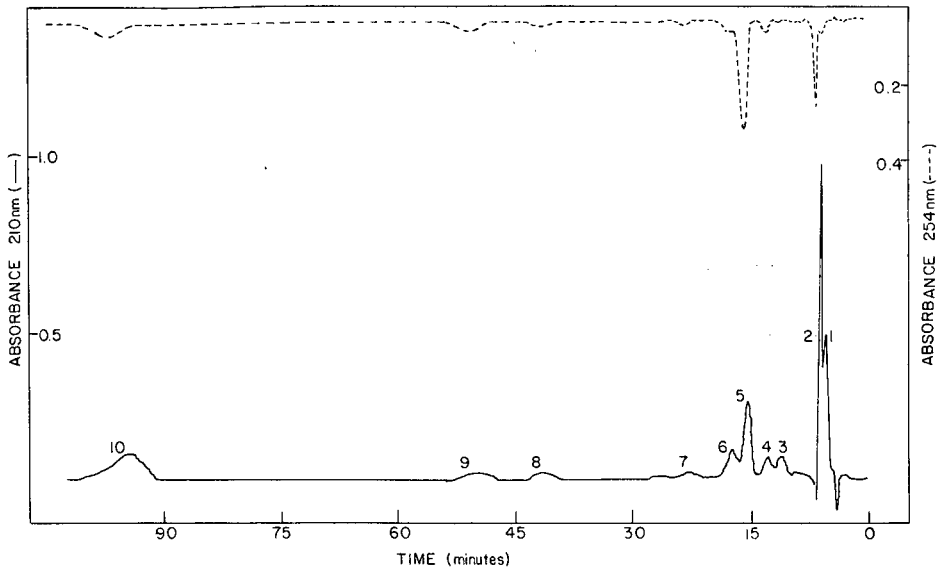

Fig. 3. Ion-pair reversed-phase HPLC separation of intermediates accumulated by Ade-I with UV detection at 210 and 254 nm. Mobile phase: 5 m*M* DBAP, pH 6, plus 3% acetonitrile. Peaks: 1 = AIR; 2 = acetate; 3 = IMP; 4 = GMP; 5 = SAICAR; 6 = XMP; 7 = AMP; 8, 9 = unknown; 10 = AMPS. Slight offset of peaks detected at 254 nm due to time required for flow between the two detectors.

and were shown to correspond to AMP, IMP, GMP and XMP. These compounds which are also observed in analyses of the mutant cell lines grown in hypoxanthine deficient media, are likely components of the normal equilibrium between the cells' nucleoside mono-, di- and triphosphate pools. Levels of the minor peaks were approximately equal in mutant and non-mutant lines.

Two intermediates of the *de novo* purine biosynthetic pathway were not resolved using the system described. The first, PRA, is known to be very unstable[15,16] with a half life of 33 to 35 s at 37°C and pH 7.5. Such a high degree of instability makes it impossible to biologically prepare this compound and isolate it. Failure to resolve the second compound, AICR, is also probably due to a stability problem. Mutants of *Salmonella typhimurium* likely defective in the conversion of AICR to SAICAR do not accumulate AICR but its decarboxylation product AIR[17]. An identical situation seems to have occurred with the Ade-I auxotroph which accumulates SAICAR and AIR, the two intermediates that bracket AICR. It is most probable that the AIR present in Ade-I extract is due to breakdown of AICR. Attempts to minimize this breakdown during the described procedure were to no avail.

The single methodology for the separation of the intermediates of *de novo* purine biosynthesis presented here will be valuable in the study of the pathway be it in regards to regulation by intermediate metabolites or end products[5,18], identification of defective enzyme activities in clinical[2,19–23] or laboratory[1,7,9,24] situations or determining the sites of action for potential therapeutic agents[7,19,25,26]. The methodology described can also be used, in conjunction with available mutants that accumulate the intermediates, as a preparative tool to yield biologically active substrates for

the enzymes of the pathway. While the system described does not require radioactive tagging for detection, if labelled intermediates are required it is a simple matter to include labelled precursors during the 2-h incubation period during which accumulation occurs. The labelled intermediates generated may still be detected using ultraviolet light absorption or by radioactivity if so desired.

ACKNOWLEDGEMENTS

This is contribution No. 931 of the Eleanor Roosevelt Institute for Cancer Research. This work was supported in part by grant AG00029 from the National Institutes of Health. R.G.H. was a recipient of a National Down Syndrome Society Scholar Award during the course of these investigations.

REFERENCES

1 J. Bal and N. J. Pieniązek, *J. Chromatogr.*, 169 (1979) 474.
2 P. K. De Bree, S. K. Wadman, M. Duran and H. Fabery De Jonge, *Clin. Chim. Acta*, 156 (1986) 279.
3 Y. Sidi and B. S. Mitchell, *J. Clin. Invest.*, 76 (1988) 2416.
4 B. M. Torrello, M. A. Paz and P. M. Gallop, *Mech. Ageing Devel.*, 19 (1982) 147.
5 R. L. Sabina, D. Patterson and E. W. Holmes, *J. Biol. Chem.*, 260 (1988) 6107.
6 E. G. E. Jahngen and E. F. Rossomando, *Anal. Biochem.*, 137 (1984) 493.
7 D. Patterson, *Som. Cell Genet.*, 1 (1975) 91.
8 M. Irwin, D. C. Oates and D. Patterson, *Som. Cell Genet.*, 2 (1979) 203.
9 D. Patterson, in M. Gottesman (Editor), *Molecular Cell Genetics*, Wiley, New York, 1985, p. 268.
10 A. S. Tu and D. Patterson, *Biochem. Genet.*, 15 (1977) 195.
11 A. C. Bratton and E. K. Marshall, *J. Biol. Chem.*, 128 (1939) 537.
12 J. G. Flaks and L. Lukens, *Methods Enzymol.*, 6 (1963) 52.
13 L. Lukens and J. G. Flaks, *Methods Enzymol.*, 6 (1963) 671.
14 S. Henikoff, M. A. Keene, J. S. Sloan, J. Bleskan, R. Hards and D. Patterson, *Proc. Natl. Acad. Sci. USA*, 83 (1986) 720.
15 D. P. Nierlich and B. Magasanik, *J. Biol. Chem.*, 240 (1965) 366.
16 Y. S. Cheng, M. Murray, F. Schendel, J. Otvos, S. Werhli and J. Stubbe, *Adv. Enzyme Regul.*, 26 (1987) 319.
17 C. A. Westby and J. S. Gots, *J. Biol. Chem.*, 244 (1969) 2095.
18 D. P. Nierlich and B. Magasanik, *J. Biol. Chem.*, 240 (1965) 358.
19 P. K. Laikind, J. E. Seegmiller and H. E. Gruber, *Anal. Biochem.*, 156 (1986) 81.
20 G. Van Den Berghe and J. Jaeken, *J. Pediatr.*, 19 (1985) 780.
21 J. Jaeken and G. Van Den Berghe, *Lancet*, ii (1984) 1058.
22 N. C. Kar and C. M. Dearson, *Muscle Nerve*, 4 (1981) 174.
23 R. A. Roesel, P. L. Hartlage, P. R. Blankenship and C. K. Ho, *Am. J. Hum. Genet.*, 39 (1986) A19.
24 R. A. Woods and I. E. Jackson, *Biochem. Biophys. Res. Commun.*, 53 (1973) 787.
25 M. K. Spassova, K. Ch. Grancharov and E. V. Golovinsky, *Int. J. Biochem.*, 16 (1984) 1091.
26 K. Ch. Grancharov, G. A. Gorneva, M. K. Spassova and J. P. Mladenova, *Int. J. Biochem.*, 17 (1985) 619.

Journal of Chromatography, 455 (1988) 225–239
Elsevier Science Publishers B.V., Amsterdam — Printed in The Netherlands

CHROM. 20 833

PURIFICATION OF LENTIL LECTINS USING PREPARATIVE ELECTROPHORESIS

PIERRE WENGER, ARIANE HEYDT, NED B. EGEN, TERRY D. LONG and MILAN BIER*
Center for Separation Science, University of Arizona, Bldg. 20, Tucson, AZ 85721 (U.S.A.)
(First received March 29th, 1988; revised manuscript received July 5th, 1988)

SUMMARY

Electrophoresis presents an interesting alternative to chromatography for the purification of biological compounds. To document the performance of three preparative electrophoresis apparatus currently available, they were applied to the purification of lectins from lentil seeds which contain two isolectins usually purified by chromatography. Purification by electrophoresis consists of first isolating a mixture of the two isolectins and then separating them. For the first step, either of two free-flow electrophoresis apparatus were employed: the Elphor VaP 22, using field step electrophoresis and the Biostream using zone electrophoresis. To optimize the process, the Biostream was modified to a recycling mode. This required repositioning one dialysis membrane which separates an electrode from the separation chamber. This allowed the lentil extract to be desalted by electrodialysis directly in the apparatus prior to fractionation. A high concentration of lectins was collected at the cathode and acidic proteins were collected at the anode. The bulk of the extract was recycled until the whole volume was processed. In a second step the isolectins were separated by recycling isoelectric focusing in the recycling isoelectric focusing apparatus. The present work clearly demonstrates that electrophoretic methods provide lectins with higher purity than chromatographically purified commercial products.

INTRODUCTION

The seeds of many plants contain proteins called hemagglutinins or lectins. Lectins have been extensively studied for their many interesting properties[1], as they bind specific sugars and agglutinate red blood cells of many animal species. They have also been used to purify glycoproteins. Lectins extracted from the plant seeds are usually purified by chromatography[2–4]. Lentil seeds contain two isolectins LcH-A and LcH-B, differing in charge[3] and isoelectric points (p*I* of LcH-A = 8.15, p*I* of LcH-B = 8.65)[5]. They form a complex[6] which appears in isoelectric focusing gels as a middle band (p*I* 8.45). Each lectin has a molecular weight of 49 kDa and consists of two identical polypeptides. For lentil lectin purification Howard *et al.*[3] used two chromatographic steps: (i) a DEAE cellulose column for the purification of the mix-

0021-9673/88/$03.50 © 1988 Elsevier Science Publishers B.V.

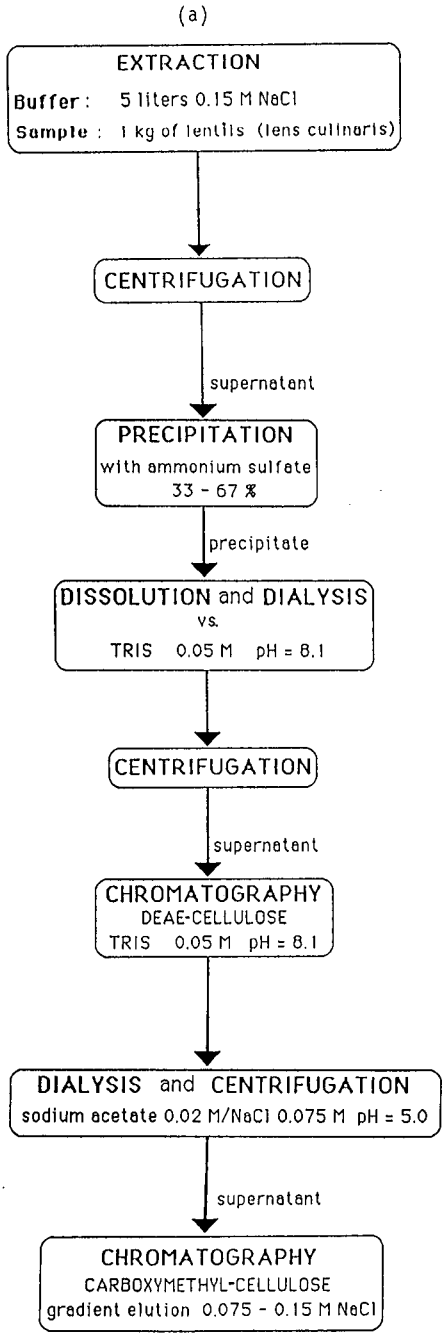
(a)
EXTRACTION
Buffer : 5 liters 0.15 M NaCl
Sample : 1 kg of lentils (lens culinaris)
CENTRIFUGATION
supernatant
PRECIPITATION
with ammonium sulfate
33 - 67 %
precipitate
DISSOLUTION and DIALYSIS
vs.
TRIS 0.05 M pH = 8.1
CENTRIFUGATION
supernatant
CHROMATOGRAPHY
DEAE-CELLULOSE
TRIS 0.05 M pH = 8.1
DIALYSIS and CENTRIFUGATION
sodium acetate 0.02 M/NaCl 0.075 M pH = 5.0
supernatant
CHROMATOGRAPHY
CARBOXYMETHYL-CELLULOSE
gradient elution 0.075 - 0.15 M NaCl

Fig. 1.

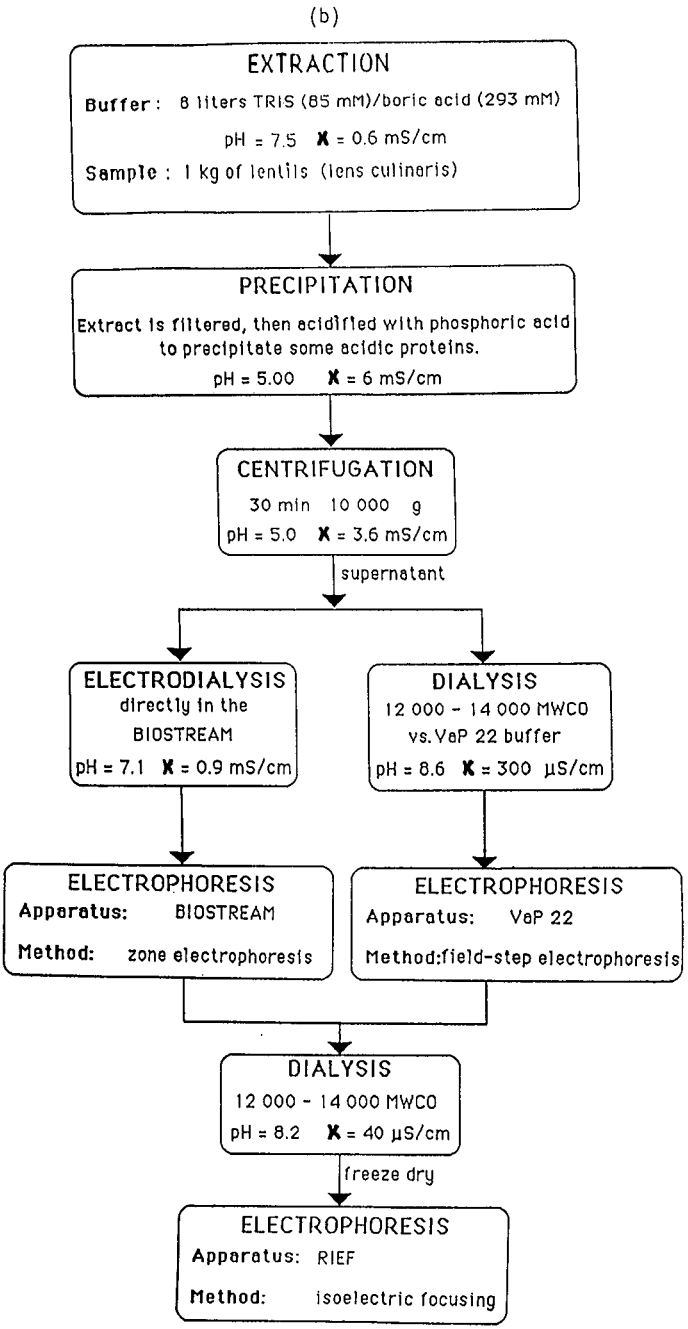

Fig. 1. Schematic representation of lectin purification. (a) Chromatography according to ref. 3; (b) electrophoresis. MWCO = Molecular weight cut-off.

ture of LcH-A and LcH-B and, (ii) a carboxymethyl cellulose column for the separation of the two isolectins. This work shows that the chromatographic steps can be replaced by electrophoretic methods (Fig. 1). The fact that the lectins are the most basic proteins in the extract is clearly an advantage in electrophoretic purification.

Several companies furnish commercial preparative electrophoresis apparatus, three of which were used in this work: the Elphor VaP 22[7], the Biostream[8] and the recycling isoelectric focusing (RIEF) developed at our center[9]. These apparatus differ in throughput, field of applications and operating principles. Free-flow electrophoresis can be operated in several modes: zone electrophoresis (ZE), isoelectric focusing (IEF), isotachophoresis (ITP) and field step electrophoresis (FSE)[10]. An advantage of electrophoresis is its ability to concentrate the sample during purification. For this purpose, FSE and IEF were used in the Elphor VaP 22 and in the RIEF, respectively, while zone electrophoresis was used in the Biostream. Usually ZE dilutes the sample, but our modification of the Biostream to a recycling mode allowed the simultaneous purification and concentration. The isolation and separation of lentil lectins provided a suitable means for comparing these devices. The isolation of a mixture of the two isolectins was accomplished using either the Elphor VaP 22 by FSE or the Biostream by recycling ZE. The separation of isolectins LcH-A and LcH-B was carried out by IEF in a narrow pH profile using the RIEF instrument. The lectins were analyzed by UV absorption at 280 nm, agglutination activity and analytical polyacrylamide gel isoelectric focusing (PAGIEF) and compared to commercially available material. Performance of the instruments was assessed in terms of throughput and purity.

EXPERIMENTAL

Materials

Ampholine carrier ampholytes for preparative and analytical IEF were purchased from LKB Produkter (Pleasant Hill, CA, U.S.A.), acrylamide, Bis, N,N,N′,N′-tetramethylethylethylenediamine (TEMED), ammonium persulfate and urea from BioRad (Richmond, CA, U.S.A.), β-alanine, Coomassie Brilliant Blue G-250, 5-aminopentanoic acid (EACA), Gly-Gly, imidazol, morpholinoethanesulfonic acid (MES) and Tris from Serva (Westbury, NY, U.S.A.), lentils (lens culinaris) from a local food store, LcH-B from ICN ImmunoBiologicals (Lisle, IL, U.S.A.), Lectin from Sigma (St. Louis, MO, U.S.A.), and Vector Labs. (Burlingame, CA, U.S.A.) and reagents for color silver stain from Pierce (Rockford, IL, U.S.A.). All other chemicals were reagent grade.

Lectin extraction

Dried lentils were soaked overnight at 4°C in a Tris (9 g/l)–boric acid (18 g/l) buffer, pH 7.4 and conductivity of 0.6 mS/cm (1 kg lentil seeds in 2.4 l buffer). The seeds were then homogenized in a Waring blender with 1.6 l of the buffer, for 5 min. This suspension was stirred for 1 h at room temperature and then filtered through a nylon screen with 0.5 mm pores. The retentate was washed twice with 2 l portions of buffer and the filtrates were pooled. This filtrate contained 43 g total dry lentil solid/l. It was titrated to pH 5.0 with phosphoric acid (85%, w/v) which precipitated some acidic proteins. The solution was stored overnight at 4°C and then centrifuged at 13 000 *g* for 30 min. A clear solution with a conductivity of 3.6 mS/cm was obtained

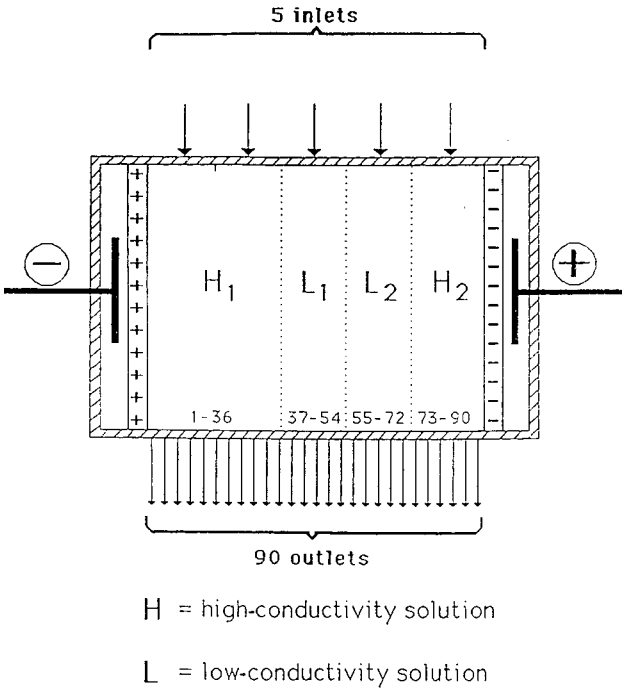

Fig. 2. Elphor VaP 22 principle for field step electrophoresis showing the arrangement of the various buffers. H1 = Catholyte; H2 = anolyte; L1, L2 = sample zones.

and contained 15 g total dry solid/l. The solution was then desalted by electrodialysis or dialysis before electrophoresis.

Electrophoretic apparatus and experimental methods

FSE in the Elphor VaP 22. The Elphor VaP 22 is a continuous free-flow apparatus from Bender & Hobein (Munich, F.R.G.) in which solutions flow between two parallel glass plates. The electrical field is applied perpendicularly to the liquid flow. The solutions are introduced at the top of the chamber through five inlet tubes. Charged proteins are deflected by the electrical field and are collected at the bottom through 90 outlet tubes (Fig. 2). The dimensions of the separation chamber are 100 × 500 × 0.5 mm[7]. This apparatus can be used for ZE, IEF, ITP and FSE[11–13].

For FSE[14,15] the electrolyte system schematically illustrated in Fig. 2 was used. Two solutions of low conductivity (K), one containing the sample, were bracketed between an anolyte and a catholyte of at least 20 times higher conductivity, forming a stepwise conductivity profile. Charged proteins in the sample area migrate electrophoretically until they reach the high conductivity boundary, where their velocity decreases due to the lower electric potential. Thus, they are concentrated at the conductivity interfaces. Two variants of this principle were employed.

Recycling zone electrophoresis in the Biostream. The Biostream is a continuous free-flow apparatus developed at the Harwell Laboratory of the United Kingdom Atomic Energy Authority and commercialized by CJB Developments (Portsmouth,

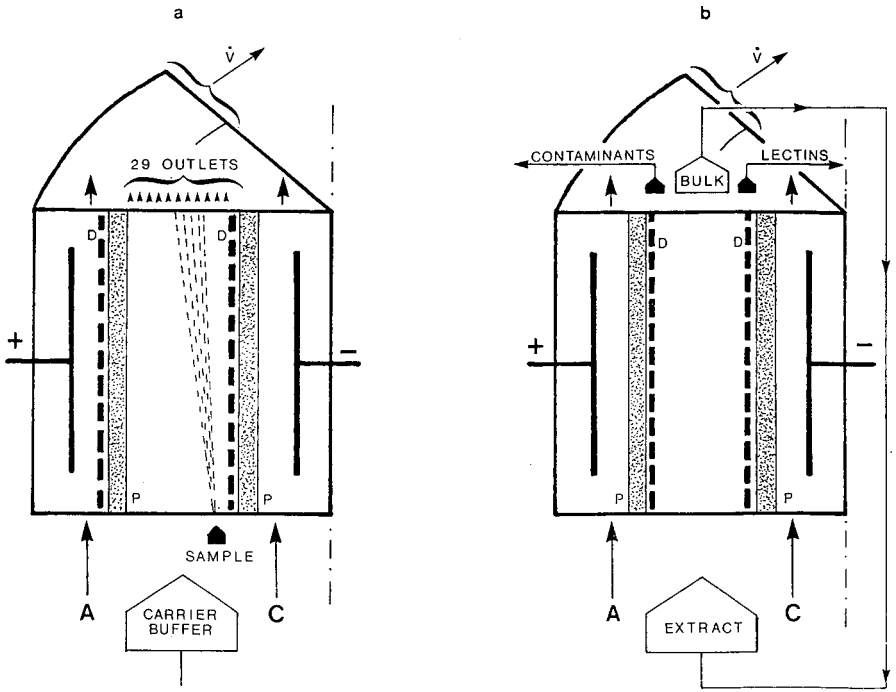

Fig. 3. Schematic representation of the Biostream illustrating the position of the dialysis membranes and the flow paths for (a) the usual configuration as designed by the manufacturer and (b) the recycling mode where lectins and contaminants are continuously withdrawn. A = Anolyte; C = catholyte; D = dialysis membrane.

U.K.). In this machine the electrophoretic separation takes place radially in an annulus between two concentric cylindrical electrodes. The chamber is 1 m in length and 3 mm in thickness. To stabilize the laminar flow, the outer cylinder rotates at 150 rpm during electrophoresis[8]. The samples are collected through 29 outlet tubes at the top of the chamber. The separation chamber is separated from the two electrode compartments by dialysis membranes supported by rigid cylindrical porous spacers. In the usual configuration of the Biostream these membranes are stretched over the external surface of the spacers. The boundaries of the separation chamber are then a dialysis membrane at the inner cylinder (cathode) and a porous material at the outer cylinder (anode). A carrier buffer flows through the chamber from the bottom to the top. The sample is introduced separately through a narrow slit at the bottom of the inner cylinder (Fig. 3a). The separation conditions have to be selected to prevent proteins from reaching and penetrating the outer porous spacer. To avoid this problem, a dialyzing membrane was streched over the inside of the outer spacer (Fig. 3b). As a result, proteins can migrate towards both membranes. The advantages are that the sample solution functions as the carrier buffer and the most acidic and basic fractions are concentrated at the membranes. This is achieved by recycling the sample through the chamber and continuously drawing off proteins that concentrate at the inner and outer membranes. In addition, this allows the use of the Biostream as an

electrodialyzer for preliminary desalting: the solution is recycled until the correct pH and conductivity are reached. For the present work, the fractions closest to the cathode containing pure lectins were collected. The anodic fractions containing acidic proteins were discarded to avoid their accumulation in the chamber. The middle fractions were recycled until the whole was processed. This method is called recycling zone electrophoresis.

Isoelectric focusing in the RIEF apparatus. In the RIEF-apparatus, developed in our laboratory and commercialized by Ionics (Watertown, MA, U.S.A.) the protein and carrier ampholyte solution to be focused is recirculated through a multicompartment apparatus with the ten subcompartments, separated by nylon screens (pore size 6 μm)[9]. The electrical field is applied perpendicularly to the screens and generates the pH profile by focusing of carrier ampholytes[16]. Proteins migrate through the screen separators until they reach a compartment with the pH of their isoelectric point[17,18].

Analysis

The pH and K values of all fractions were measured and the lectins quantified by A280 and agglutinating activity. In addition, analytical IEF gels were utilized as a measure of purity.

Activity tests. The activity of lectins was measured on microtiter plates by serial dilutions of 25 μl of sample with 25 μl phosphate buffer–saline (PBS) (0.05 *M* sodium phosphate–0.15 *M* sodium chloride, pH 7.0)[1,19], added to 25 μl of a 4% rabbit red

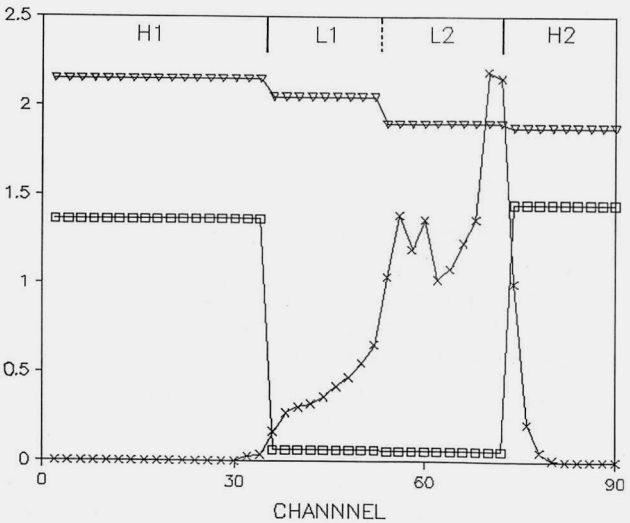

Fig. 4. Lectin purification in the Elphor VaP 22 with sample introduction through L1. The initial pH (▽) and conductivity (□) profiles are shown together with the absorbance measurements at 280 nm (×). Buffer system: catholyte H1: 0.05 *M* phosphate buffer (pH = 8.6, K = 6880 μS/cm); sample L1: lentil extract, dialyzed, in 0.1 *M* imidazole–0.1 *M* EACA (pH = 8.2, K = 314 μS/cm); L2: 0.1 *M* imidazole–0.1 *M* Gly-Gly (pH = 7.6, K = 280 μS/cm); anolyte H2: 0.05 *M* phosphate buffer (pH = 7.5, K = 7200 μS/cm). Separation conditions: current, 125 mA; voltage, 519 V; residence time, 4.7 min; flow-rate per inlet, 65 ml. (Actual pH = pH × 0.25. Actual K = K × 0.0002.)

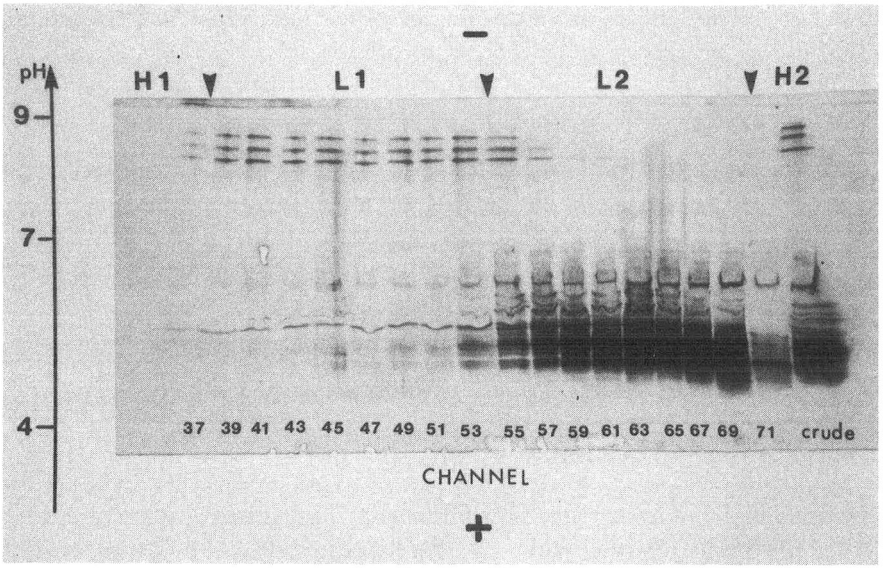

Fig. 5. Silver stained PAGIEF analysis of selected fractions from the experiment of Fig. 4 showing the distribution of proteins along the electrophoresis chamber. The three bands in the basic region are the two isolectins LcH-A (pH 8.15), LcH-B (p*I* 8.65) and a complex of the two forms (p*I* 8.45).

blood cell suspension (40 μl of packed red blood cells diluted to 100 μl with PBS). The highest agglutinating dilution is reported as the activity titer of the solution.

Analytical IEF gel. Native PAGIEF was performed as previously described[20]. Proteins were visualized by Coomassie Blue or silver staining[21,22].

RESULTS AND DISCUSSION

Purification of the lectin mixture

FSE in the Elphor VaP 22. Two different systems of field step electrophoresis were utilized for the lectin purification.

(i) The dialyzed lentil extract was introduced at the cathodic side of the sample area Fig. 4, (L1). Figs. 4 and 5 show the results when the crude extract was dialyzed and adjusted to pH 8.2 with imidazole–EACA. At this pH the lectins are virtually immobile in the sample area L1 and exit the chamber almost without deflection. The acidic proteins of the extract migrate from the L1 area into the low conductivity buffer L2 (imidazole–Gly-Gly, pH 7.6). Lectins which reached L2, reversed direction and returned to the L1–L2 boundary. The acidic proteins at pH 7.6 migrated in the direction of the anode and concentrated at the L2–H2 boundary. In comparison to the initial solution (activity titer: 128) with this method the lectins were purified but not concentrated (activity titer: 64)

(ii) The extract was introduced into the anodic side of the sample area (L2) at an acidic pH, forcing the lectins to the cathode. Figs. 6 and 7 show the results obtained when the crude extract was dialyzed and adjusted to pH 5.99 with EACA – Gly-Gly. This pH was 2.5 pH units below the p*I* of the lectins. When the lectins reached L1 the

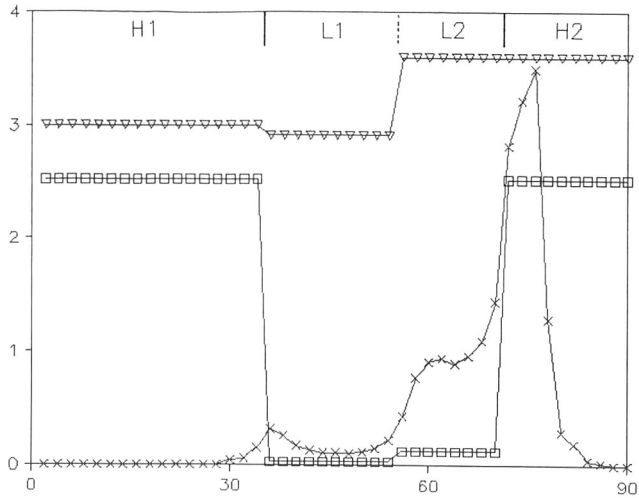

Fig. 6. Lectin purification in the Elphor VaP 22 with introduction of the sample through L2. The pH (▽) and conductivity (□) profiles are shown together with the absorbance measurements at 280 nm (×). Buffer system: catholyte H1: 0.05 *M* phosphate buffer (pH = 5.0, K = 6300 μS/cm); sample L1: 0.1 *M* MES/0.1 *M* β-alanine (pH = 4.85, K = 70 μS/cm); L2 : lentil extract, dialyzed, in 0.1 *M* EACA–0.1 *M* Gly-Gly (pH = 5.99, K = 303 μS/cm); anolyte H2: 0.05 *M* phosphate buffer (pH = 6.0, K = 5800 μS/cm). Separation conditions: current, 200–150 mA; voltage, 1100–1400 V; residence time, 4.6 min. (Actual pH = pH × 0.6. Actual K = K × 0.0004.)

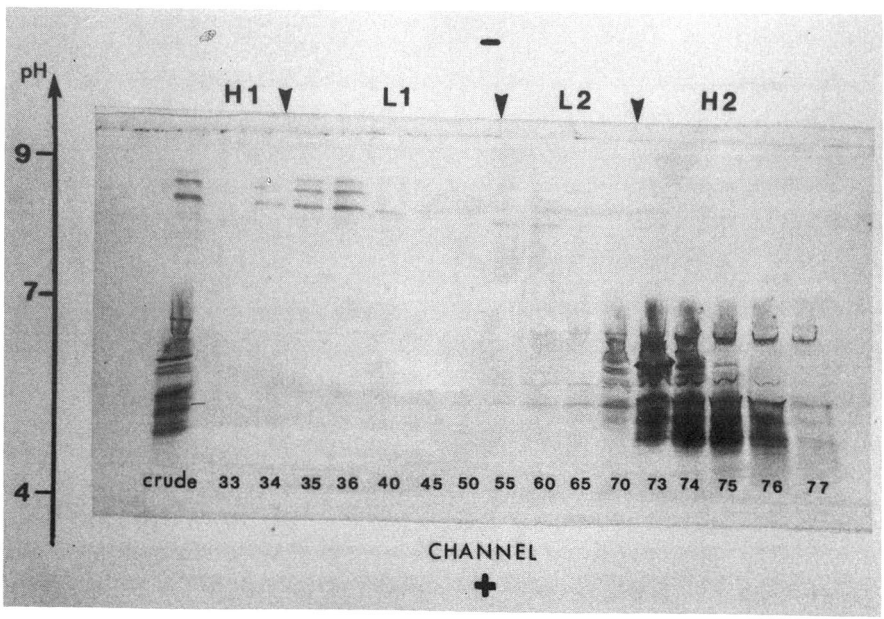

Fig. 7. Silver stained PAGIEF analysis of selected fractions from the experiment of Fig. 6. The activity titers were 128 for the crude extract, 16, 64, 128, 128, 32, 16, 32, 32, 8, 4, 8, 2, 0, 0, 0 for the respective fractions.

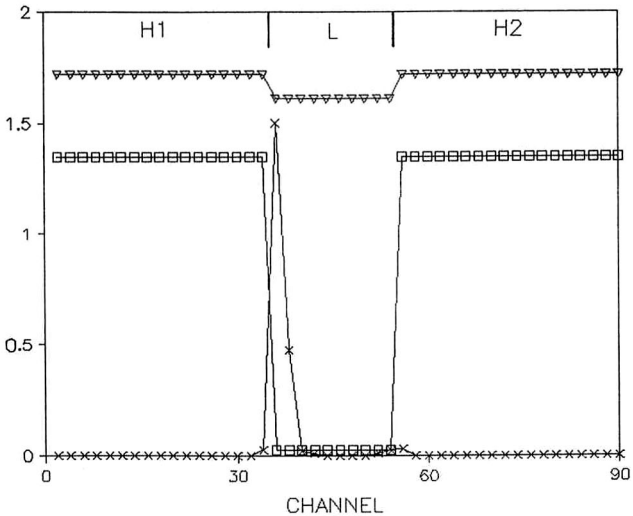

Fig. 8. Lectin concentration by field step electrophoresis in the Elphor VaP 22. The initial pH (▽) and conductivity (□) profiles are shown together with the absorbance measurements at 280 nm (×). Buffer system: catholyte H1: acetic acid–sodium hydroxide (pH = 4.91, K = 6700 μS/cm); sample L: fraction 33–41 of Fig. 6 (pH = 4.6, K = 127 μS/cm); anolyte H2: acetic acid–sodium hydroxide (pH = 4.91, K = 6700 μS/cm). Separation conditions: current, 175 mA; voltage, 630 V; residence time, 3.0 min; flow-rate per inlet, 100 ml/h. (Actual pH = pH × 0.35. Actual K = K × 0.002.)

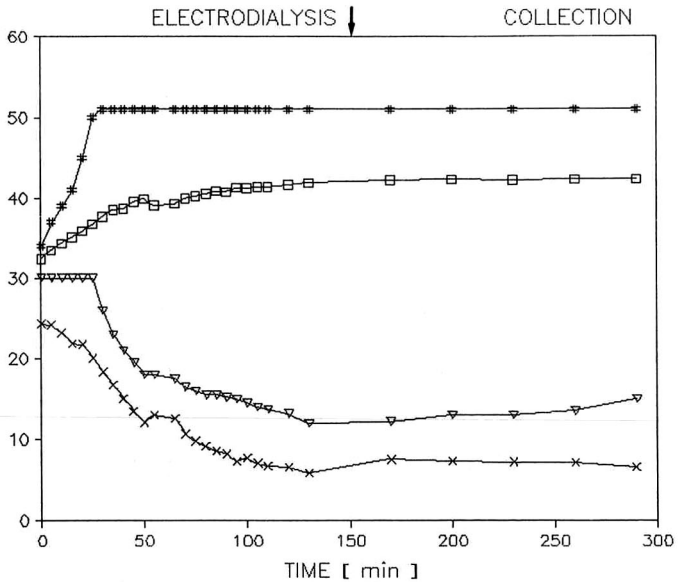

Fig. 9. Temporal variation of voltage (#), current (▽), pH (□) and conductivity (×) of the bulk fluid during electrodialysis and collection of 5 l of lentil extract (pH = 5.0, K = 5.8 mS/cm) using the Biostream in the recycling mode. Electrolyte system: catholyte: boric acid (2 g/l)–sodium hydroxide (pH = 8.0, K = 3.3 mS/cm, flow-rate = 150 ml/min); anolyte: tris (2 g/l)–sodium hydroxide (pH = 5.0, K = 5.0 mS/cm, flow-rate = 150 ml/ min). (Actual pH = pH × 6. Actual K = K × 6.8.)

lower pH of this buffer (MES–β-alanine, pH 4.85) they were accelerated to the field step between L1 and H1. Most acidic proteins stayed in L2 or migrated to H2 (Fig. 7). In this experiment 65 ml/h of dialyzed crude extract with a total protein concentration of 3.3 g/l containing 0.3 g/l of lectins (activity titer 128) were processed. After electrophoresis, lectin activity was detected in fractions 32–74, but only fractions 32–54 contained pure lectins. The recovery rate in fractions 32–54 was 80 ml/h of 0.16 mg/ml or 13 mg lectin/h. In comparison to Fig. 5 it is shown that these lectins have the same activity as the initial solution (activity titer 128). However the specific activity (ratio between activity titer and total protein concentration in g/l shows a 20-fold enrichment (ratio between final and initial specific activity). Fractions 55–74 with 6 mg of lectins and all acidic proteins were discarded. The recovery was 68%.

In a second step, a normal field step system was used to concentrate the purified fractions. The fractions 33–41 (Fig. 7) with the highest lectin concentration were pooled producing 32 ml of lectin solution with 0.2 g/l (activity titer 128) representing 35% of the lectin in the starting material. This solution was introduced at pH 4.6 directly between two high conductivity solutions (Fig. 8), with a flow-rate of 100 ml/h (20 mg lectins/h). The lectins concentrated in only five fractions (35–39), with 80% (16 mg/h) in fraction 36 and 37, seven times concentrated (c = 1.4 g/l, activity titer 1024). The solution was concentrated but not enriched (same specific activity). In summary 16 mg of lectins were produced in 4 h: 3 h for the first step to produce 100 ml of initial pure material which concentrated in 1 h during the second step.

Recycling zone electrophoresis in the Biostream. Five liters of crude extract (4 g total protein/l, activity titer 128, pH 5.0, K = 3.6 mS/cm) were electrodialyzed for 2½ h to pH of 7.02 and K 0.8 mS/cm. The final current was 10 A, the final voltage, 50 V (Fig. 9). The extract was recycled at 1 l/h through the chamber. The distribution of lectins across the chamber (29 fractions) at this state is shown in Fig. 10. Then fraction 1, containing pure lectins, was collected at 210 ml/h. The contaminants were removed from fraction 29, at the same flow-rate. The activity titers of these fractions was 512 and 128 respectively. The total protein concentration of fraction 1 was 1.3 g/l, determined by dry solid weight after dialysis against water. Fig. 11 presents a comparison of the purity obtained with the Biostream to commercial lentil lectins purified by chromatography.

This purification by recycling ZE was performed as a batch process. Thus, the concentration of collected lectins decreased with time (for example from 2.2 tot 0.55 g/l). The extract was processed for 5 h in the Biostream. After this time, the lectin concentration in fraction 1 decreased to 1.3 g/l, similar to that obtained with the VaP 22. During this time, 1 l of lectins solution (1.3 g/l) was produced, representing an average of 250 mg of lectins/h and a yield of 56%. This represents an about 60 times higher processing rate than with the VaP 22 with a comparable recovery and enrichment.

Separation of LcH-A and LcH-B by isoelectric focusing in the RIEF

To separate the two lectins, (p*I* difference of 0.5 pH units), two sequential RIEF steps were performed (Fig. 12).

(i) A volume of 270 ml of lectin solution, prepurified in the Biostream (1.8 g total protein/l, activity titer 256), was processed for 3 h with 2% (w/v) carrier ampholytes (pH 8–9.5). In this step the last traces of salt and contaminants, which disturb

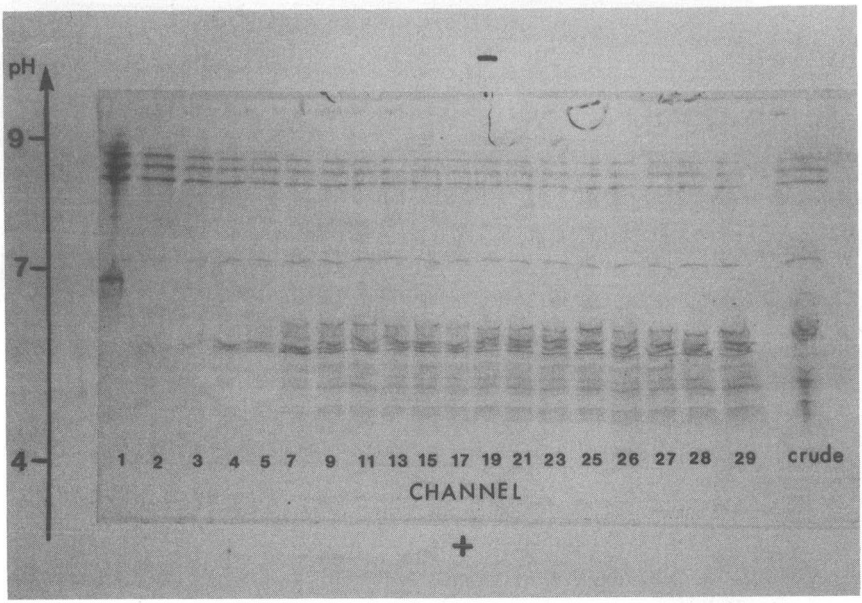

Fig. 10. PAGIEF analysis (stained with Coomassie Blue) showing the distribution of proteins in the 29 Biostream fractions at the beginning of collection. Fraction numbers start at the cathode.

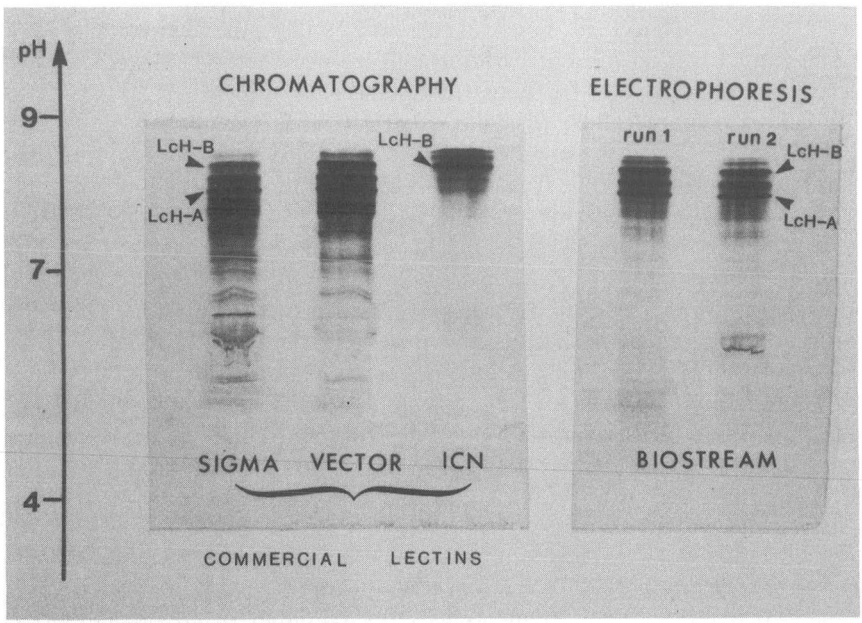

Fig. 11. Silver stained PAGIEF analysis of commercially available lentil lectins from Sigma (No. L-5800, lot 114F-9670), Vector (No. L-1040, lot 50607) and ICN ImmunoBiologicals (No. 79-135-1, lot LB 17-02) in comparison to the Biostream purified product (fraction 1 of two different runs). The ICN product contains LcH-B only, whereas all other samples contain two lectins. Volumes 15 μl of each sample (5 mg/ml) were applied.

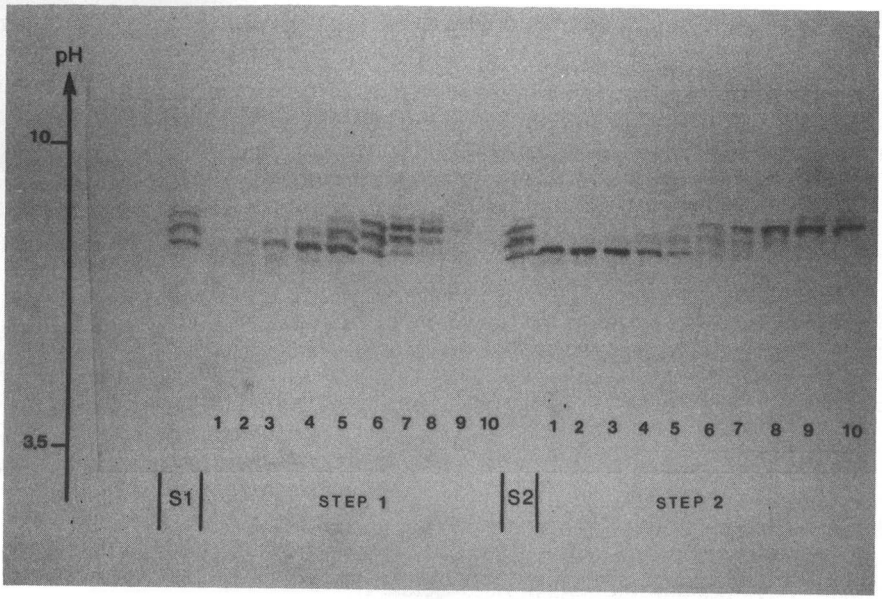

Fig. 12. Distribution of lectins in the ten RIEF compartments for two consecutive runs analyzed by Coomassie Blue stained PAGIEF. For step 1 the inital and final current were 200 and 130 mA respectively and the voltage changed from 340 to 680 V. The corresponding current values for step 2 were 102 and 55 mA at a constant voltage of 700 V.

the linear profile, were removed. Lectins were collected in fractions 5, 6, 7. The pooled fractions had a total protein concentration of 2.4 g/l and an activity titer of 1024 representing a 3 fold enrichment.

(ii) The pooled fractions 5, 6, 7 (72 ml) were diluted to 150 ml and 27 g of urea (3 *M*) were added to dissociate the complex of the two isolectins. This solution, which had a total protein concentration of 1.2 g/l and an activity titer of 512, was focused for 4 h. In this step the two lectins were separated. The highest concentration of LcH-A was recovered from fraction 2 (15 ml): concentration of 1.7 g/l, activity titer of 512. The highest concentration of LcH-B was recovered from fraction 9 (15 ml): concentration of 1.5 g/l, activity titer of 512.

The specific activity is similar in the initial and final solution indicating 3 *M* urea does not deactivate the lectins. In two steps and a total of 7 h 60 mg of each pure isolectin were produced with the RIEF.

CONCLUSION

The present work was intended to compare the use of several electrophoretic instruments for protein purification. Lectins were chosen as a model protein because of their low cost, ready availability and because they have been purified by ion exchange and affinity chromatography. This permits a comparison of electrophoresis to chromatography.

To integrate preparative electrophoretic methods into a purification scheme some important parameters must be considered: (i) Only solutions of low conductiv-

ities can be applied. For biological mixtures, usually, a dialysis or electrodialysis step is a prerequisite. (ii) To obtain the best separation conditions (pH, K) the buffers must be well defined. The choice depends on the type of electrophoretic method and the sample. (iii) In some cases, preliminary purification of the crude extract may be required, especially when the contaminant concentration is high relative to the active compound. In the present work a precipitation was performed before electrophoresis.

Three electrophoretic methods were used successfully to purify lentil lectins. None of the methods were optimized for this specific task, but further optimization is surely possible. Under the condition presented, the Elphor VaP 22 processed 4 mg of lectins/h. However this instrument permits a 10-fold scale-up. The Biostream, designed for large scale processing, usually results in high dilution of the purified sample. The modification of the Biostream described in this paper avoided the dilution and 200 mg/h of lectins were processed in 5–20 l batches of extract.

The RIEF was used as a polishing step to remove the last traces of acidic contaminants and to produce lectins with the highest purity. Lectins, which were prepurified in the Biostream were further enriched 3-fold in the RIEF. In a second RIEF step, the two isolectins were resolved. The small p*I* difference between the two isolectins necessitates the use of a more narrow pH gradient in the second run, which was obtained by pooling the appropriate lectins fractions from the first step. The formation of the complex between the two lectins was avoided by using urea. RIEF favorably competed with affinity chromatography to separate LcH-A and LcH-B.

ACKNOWLEDGEMENTS

The generous loan of both the Biostream and the Elphor VaP 22 apparatus by CJB Developments and Bender & Hobein respectively is gratefully acknowledged. The authors would like to thank the Swiss National Foundation for Scientific Research, the German Research Foundation (DFG) and NASA (NAGW-693) for their financial support of this work.

REFERENCES

1 H. Lis and N. Sharon, in A. Marcus (Editor), *Biochemistry of Plants*, Vol. 6, Academic Press, New York, 1981, Ch. 10, p. 371.
2 I. K. Howard and H. J. Sage, *Biochemistry*, 8 (1969) 2436.
3 I. K. Howard, H. J. Sage and M. D. Stein, *J. Biol. Chem.*, 246 (1971) 1590.
4 S. Toyoshima, T. Osawa and A. Tonomura, *Biochim. Biophys. Acta*, 221 (1970) 514.
5 *Calibration Kits for pI Determinations using Isoelectric Focusing*, Pharmacia Fine Chemicals AB, Uppsala, 1981.
6 L. Hagel and G. Johansson, Paper presented at the *7th International Symposium on HPLC of Proteins, Peptides and Polynucleotides, Washington, DC, November 2–4, 1987*, Paper No. 722.
7 *Owners Manual for Free-Flow Electrophoresis*, Bender & Hobein, Münich, 1983.
8 P. Mattock, G. F. Aitchison and A. R. Thomson, *Sep. Purif. Methods*, 9 (1980) 1.
9 M. Bier, N. B. Egen, T. T. Allgyer, G. E. Twitty and R. A. Mosher, in E. Gross and J. Meienhofer (Editors), *Peptides: Structure and Biological Function*, Pierce, Rockford, IL, 1979, p. 79.
10 M. Bier, N. B. Egen, G. E. Twitty, R. A. Mosher and W. Thormann, in C. J. King and J. D. Navratil (Editors), *Chemical Separations, Vol. 1*, Litarvan Literature, Denver, CO, 1986, p. 133.
11 H. Wagner and W. Speer, *J. Chromatogr.*, 157 (1978) 259.
12 H. Wagner and V. Mang, in F. M. Everaerts (Editor), *Analytical Isotachophoresis*, Elsevier, Amsterdam, 1981, p. 41.

13 H. Wagner, V. Mang, R. Kessler, A. Heydt and R. Manzoni, in H. Hirai (Editor), *Electrophoresis '83*, Walter de Gruyter, Berlin, 1984, p. 283.
14 A. Heydt, H. Wagner and H. L. Paul, *J. Virolog. Methods*, 19 (1988) 13–22.
15 H. Wagner and R. Kessler, *GIT Labor-Med.*, 7 (1984) 30.
16 P. G. Righetti, *Isoelectric Focusing: Theory, Methodology and Applications*, Elsevier, Amsterdam, 1983.
17 N. B. Egen, F. E. Russell, D. W. Sammons, R. C. Humphreys, A. L. Guan and F. S. Markland Jr., *Toxicon*, 25 (1987) 1189.
18 T. L. Nagabhushan, B. Sharma and P. P. Trotta, *Electrophoresis*, 7 (1986) 552.
19 H. J. Sage and J. J. Vasquez, *J. Biol. Chem.*, 242 (1967) 120.
20 F. E. Russel and N. B. Egen, *Toxicon*, 22 (1984) 653.
21 R. W. Blakesley and J. A. Boezi, *Anal. Biochem.*, 82 (1977) 580.
22 C. Merril, D. Goldman, S. A. Sedman and M. H. Ebert, *Science (Washington, D.C.)*, 211 (1981) 1437.

Journal of Chromatography, 455 (1988) 241–251
Elsevier Science Publishers B.V., Amsterdam — Printed in The Netherlands

CHROM. 20 842

DETERMINATION OF PHENOLS BY LIQUID CHROMATOGRAPHY USING REDUCTIVE ELECTROCHEMICAL DETECTION VIA PRE-COLUMN DERIVATIZATION

CHIA-YU LI* and MARK W. KEMP

Department of Chemistry, College of Arts and Sciences, East Carolina University, Greenville, NC 27858 (U.S.A.)

(First received November 10th, 1987, revised manuscript received June 6th, 1988)

SUMMARY

A reductive amperometric detection method has been developed for the high-performance liquid chromatographic determination of phenols in aqueous samples. The phenols were derivatized to form the corresponding quinoneimines employing the 4-aminoantipyrine reaction prior to reversed-phase chromatographic separations. In contrast to the conventional oxidative detection of phenols with a high applied potential of over +0.95 V, a low potential of −0.20 V *vs.* Ag/AgCl was used successfully to detect the derivatized phenols with a glassy carbon electrode. The principal advantage of this method is that oxygen removal from the mobile phase is not required. This is because the applied potential is so low that oxygen reduction is not detectable at this potential. A linear dynamic range of concentrations between 10^{-7} *M* and 10^{-4} *M* was observed for some selected phenols.

INTRODUCTION

In the last few years, a wide variety of methods has been developed for the analysis of phenols in environmental and clinical samples at trace levels. Some of these new developments include chromatography[1–15], mass spectrometry[16,17], and flow-injection analysis[18]. The once popular colorimetry method of using 4-aminoantipyrine (4-AAP) to form colored derivatives with phenols[19] is now largely replaced by these new instrumentation methods. However, the classical 4-AAP reaction has been used successfully by Gasparič *et al.*[20,21] for derivatizing the phenols followed by paper and thin-layer chromatography analysis. More recently, the 4-AAP method was modified by Norwitz and Keliher[22] for the spectrophotometric determination of phenol after steam distillation of sample. The 4-AAP reaction was the basis for high-performance liquid chromatographic (HPLC) post-column derivatization with absorption detection at 470 or at 509 nm[12]. Ten priority pollutant phenols were quantified by Bigley and Grob[12] at ppm levels after solid phase extraction prior to reversed-phase separation with gradient elution[12]. Their method required a preconcentration step, which helped to enhance the sensitivity of detection.

For phenols of extremely low concentration, liquid chromatography with

0021-9673/88/$03.50 © 1988 Elsevier Science Publishers B.V.

electrochemical detection (LC–ED) seems to be the method of choice. Using a glassy carbon thin-layer transducer, Shoup and Mayer[6] reported a detection limit of phenols in aqueous environmental samples at parts-per-trillion levels. Roston and Kissinger[5] used both single and dual-electrode transducers to identify nanomole quantities of phenolic constituents in alcoholic beverages. Detection of nanogram to picogram levels of phenolic compounds has been reported using a carbon-polyethylene electrode[2] and a graphite composite electrode[3,7]. Confirmation of chlorophenols in urine samples at ppb* levels has been accomplished using LC–ED detection[4]. More recently, MacCrehan and Brown-Thomas[15] developed an LC–ED method for phenols and naphthols in unrefined petroleum products. They reported detection limits of 100 ng/g of crude oil or below.

All previous LC–ED work of phenols employed an oxidation potential of around +0.95 V *vs.* Ag/AgCl or higher. In this investigation, we describe a scheme of determining derivatized phenols using a reductive LC–ED detection with a low applied potential of only −0.2 V *vs.* Ag/AgCl. The procedure of derivatizing the phenols, which is based on the 4-AAP reaction, was adopted from that used by Gasparič *et al.*[20,21] with slight modification.

In reductive LC–ED, dissolved oxygen in both mobile phase and sample solutions exhibits serious interferences at negative applied potentials[23]. The reduction of oxygen starts around −0.5 V *vs.* Ag/AgCl at a glassy carbon electrode, but around −0.1 V at a mercury-coated gold electrode. At −0.2 V no detectable oxygen reduction is observed on a glassy carbon electrode. Therefore, oxygen removal from the mobile phase by means of exhaustive degassing is not required if a glassy carbon electrode is used. Because of its relatively high oxygen overpotential, lower cost, and ready availability, the glassy carbon electrode was thus selected over mercury in this work.

The precolumn derivatization reaction of phenols used in this work can be shown as follows:

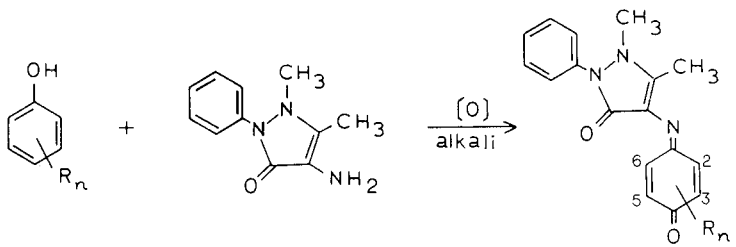

where R_n groups are substituents derived from the starting phenols. In a previous paper[24], we have reported the electrochemistry and HPLC behavior of 11 synthetically prepared quinoneimine dyes. The dye prepared from the unsubstituted phenol was named N-antipyryl-*p*-benzoquinoneimine (ABQI) and those prepared from the substituted phenols as the derivatives of ABQI. For example, *m*-cresol gives 2-methyl-ABQI; and *o*-chlorophenol gives 3-chloro-ABQI, etc. The structures of these quinoneimines proposed here were based on the NMR studies by Jones and Johnson[25] and the chromatographic investigations by Gasparič *et al.*[20,21]. Generally speaking, the reaction is positive only when the monohydric phenols have a free *para* position or

* Throughout the article the American billion (10^9) is meant.

with halogen, carboxyl, alkoxyl, or sulfonic acid group substituted at the *para* position.

EXPERIMENTAL

Apparatus

The LC system consisted of a Model 396 Instrument miniPump (Laboratory Data Control/Milton Roy, Riviera Beach, FL, U.S.A.), a Rheodyne Model 7010 valve injector with a 10-μl sample loop (Rheodyne, Cotati, CA, U.S.A.), a BAS TL-5A glassy carbon thin-layer cell, and a BAS LC-4B amperometric detector (Bioanalytical Systems, West Lafayette, IN, U.S.A.). All reversed-phase separations were carried out using either a Zorbax ODS column (DuPont, Wilmington, DE, U.S.A.) or an Econosphere C_{18} column (Alltech, Deerfield, IL, U.S.A.), both with 5-μm packing and a dimension of 15 cm $\times$ 4.6 mm I.D. The pressure was monitored with a Solfrunt pressure gauge. Coiled stainless-steel tubings (0.04 in. I.D.) were used between the pump and the precolumn, which was packed with 62 mesh silica gel. Capillary stainless-steel tubings (0.007 in. I.D.) were used between the precolumn and the valve injector and between the valve injector and the analytical column. Capillary PTFE connecting tube from Bioanalytical Systems, was used between the analytical column and the thin-layer transducer. All chromatograms were recorded on a Fisher Series 5000 Recordall strip chart recorder (Fisher Scientific, Pittsburgh, PA, U.S.A.), and peak integrations were done using an SP4270 chromatography integrator (Spectra-Physics, San Jose, CA, U.S.A.). Cyclic voltammetry experiments were run on a Bioanalytical Systems BAS-100A electrochemical analyzer.

Reagents

The phenols used in this investigation were purchased either from Fisher Scientific, Aldrich (Milwaukee, WI, U.S.A.) or from Eastman-Kodak (Rochester, NY, U.S.A.). All other chemicals, including 4-aminoantipyrine, were ACS Certified grade and were received from Fisher Scientific. The methanol used in the mobile phase was HPLC grade. The water was either HPLC grade or prepared in house by pumping distilled water through a NANOpure-A 4-holder system (Sybron/Barnsted, Boston, MA, U.S.A.). The mobile phase was filtered through a 0.8-μm polycarbonate membrane before use.

Analytical methodology

All phenols were derivatized via the 4-AAP method to form the corresponding quinoneimine dyes prior to the chromatographic runs. The scheme involved pipetting 25 ml of aqueous phenol samples, 1 ml of 0.1 *M* carbonate buffer of pH 10, 5 ml of 0.025 *M* of 4-AAP, and 1 ml of 0.060 *M* potassium ferricyanide into a 250-ml separatory funnel. After shaking the mixture for a few minutes, the resulting red quinoneimines were extracted by two aliquots of chloroform of 5-ml each into a small round bottom flask. The chloroform extract was then dried using a rotary evaporator. The dried sample was dissolved in methanol, quantitatively transferred into a 10-ml volumetric flask, and diluted to volume with methanol. The reconstituted solution was then chromatographed. All runs were carried out at room temperature in an air-conditioned laboratory. The glassy carbon electrode was resurfaced at least once

per week using alumina abrasives and soft polishing cloth followed by cleaning in an ultrasonic cleaner.

RESULTS AND DISCUSSION

The cyclic voltammograms of the synthetically prepared ABQI and the derivatized phenol obtained from the chloroform extract are compared in Fig. 1a and b. Both exhibit a cathodic wave near -0.2 V *vs.* Ag/AgCl and an anodic wave near $+0.1$ V. The analytically pure crystalline ABQI (m.p. 162°C) was prepared by following the literature procedure[25]. The red ABQI crystals were dissolved in the HPLC mobile phase prior to the voltammetric experiments. The chloroform extract was prepared by derivatizing the unsubstituted phenol after the procedure outlined in the *Analytical methodology* section and was reconstituted with the HPLC mobile phase for the voltammetric experiments. The results clearly demonstrate that the reconstituted chloroform extract did contain the expected ABQI, which has been formed from the unsubstituted phenol via derivatization. Similarly, the voltammograms of the derivatized *m*-cresol and *o*-chlorophenol (Fig. 1c and d) also exhibit the characteristic cathodic peak between -0.1 and -0.4 V and the anodic peak near $+0.1$ V. The electrode reactions of all ABQIs involve a single 2e, $2H^+$ step in a manner similar to that of the *p*-benzoquinoneimine–*p*-aminophenol redox couple[24,26].

In all cases, the anodic peaks of the derivatized phenols merge partially with a large background wave. By comparing with Fig. 1e, this background wave is attributed to 4-AAP, which we suspect was partially extracted into the chloroform layer. The voltammogram of 4-AAP clearly shows that there is no observable cathodic peak even at a potential as negative as -1.00 V. As a consequence, no chromatographic peak corresponding to 4-AAP was found; therefore, it does not interfere with LC–ED analysis.

Chloroform was chosen here as the extracting solvent because it has been used successfully by previous workers to extract the ABQI dyes formed in the antipyrine reaction[20,21]. It has high extraction efficiency and the extracts were found to be very stable, a real advantage for storing and preparing sample solutions prior to the chromatographic runs.

Effect of the amount of reagents

To determine how the yield of ABQI in the chloroform extract is affected by the quantities of 4-AAP and phenol used in the derivatization reaction, a study similar to the work by Ettinger *et al.*[27] was undertaken. In this study, the amounts of phenol (25.00 ml of $4.00 \cdot 10^{-5}$ *M*), carbonate buffer, and potassium ferricyanide were kept constant during the reaction while varying the amounts of 4-AAP. The sample preparation procedure was the same as outlined in the *Analytical methodology* section. The chloroform extract was chromatographed at an applied potential of -0.200 V *vs.* Ag/AgCl. The results are shown in Fig. 2. It can be seen that the peak heights (also peak areas, not shown in figure) reach a plateau value when the mole ratio of 4-AAP *versus* phenol exceeds approximately 10:1. In other words, the results have proven that phenol is the limiting reagent in the derivatization reaction as long as 4-AAP exists in large excess. No attempts were made to investigate the effect of the amount of oxidant on the yield of ABQI since Ettinger has already shown that the ferricyanide

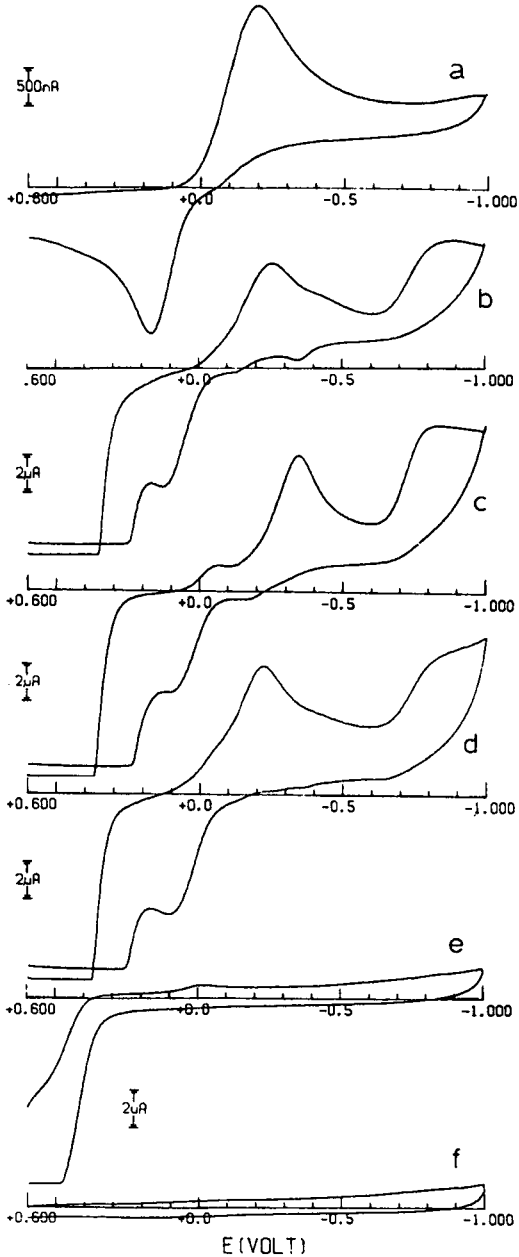

Fig. 1. Cyclic voltammograms of (a) synthetically prepared ABQI; (b) derivatized phenol; (c) derivatized *m*-cresol; (d) derivatized *o*-chlorophenol; (e) 4-aminoantipyrine and (f) background. Sample concentration: $2.00 \cdot 10^{-4}$ *M* each. Solvent: methanol–phosphate buffer (pH 5) (48:52). Working electrode: glassy carbon. Reference electrode: Ag/AgCl. Scan rate: 0.100 V/s.

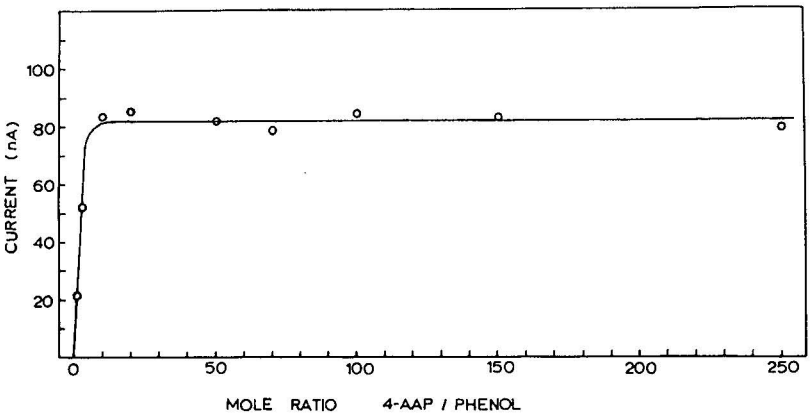

Fig. 2. Effect of the amount of 4-AAP reagent on the peak current of derivatized phenol.

concentration is not critical[27]. The reaction time of all trials during the derivatization step was less than five minutes at room temperature.

Chromatographic behavior

To determine the optimum applied potential for LC–ED of derivatized phenols, their hydrodynamic voltammograms were determined. All phenols (25.00 ml of $5.00 \cdot 10^{-5}$ *M*) were derivatized and extracted in the same manner as outlined in the *Analytical methodology* section. The methanol reconstituted chloroform extracts were chromatographed at different applied potentials. The resulting normalized hydrodynamic voltammograms are shown in Fig. 3. All derivatized phenols except thymol reached the limiting current at a potential less than -0.30 V. For reasons unknown, the derivatized thymol behave very sluggishly on the glassy carbon electrode.

From the hydrodynamic voltammograms, it seems that an applied potential of -0.40 V should be chosen for all derivatives studied. However, a potential of -0.20 V was selected instead as the optimum value. The rationale for choosing this value is that at this potential the currents due to impurities and oxygen in the mobile phase are negligibly small, thus exhaustive degassing of the mobile phase is not required. At this potential, the observed currents of all derivatized phenols except thymol have reached between 63% and 97% of their limiting values. Therefore, this low value does not seriously jeopardize the sensitivity. Another advantage is that a low applied potential also gives better selectivity[28]. Furthermore, a low applied potential usually results in lower background currents and faster decay to the steady background value. For example, we observed that using an applied potential of -0.20 V, it took less than 6 min for the cell current to decay to a steady value of about 0.7 nA as soon as the cell was switched on. On the contrary, it took more than 40 min for the cell current to decay to a much higher steady value of 3 nA at $+0.6$ V and more than 1 h to reach a steady value of 6.5 nA at $+0.8$ V.

The chromatographic data of individually derivatized phenols are summarized in Table I. Using a mobile phase of methanol–water (48:52) containing 0.04 *M* potassium chloride and 0.01 *M* phosphate buffer of pH 5, all derivatized phenols

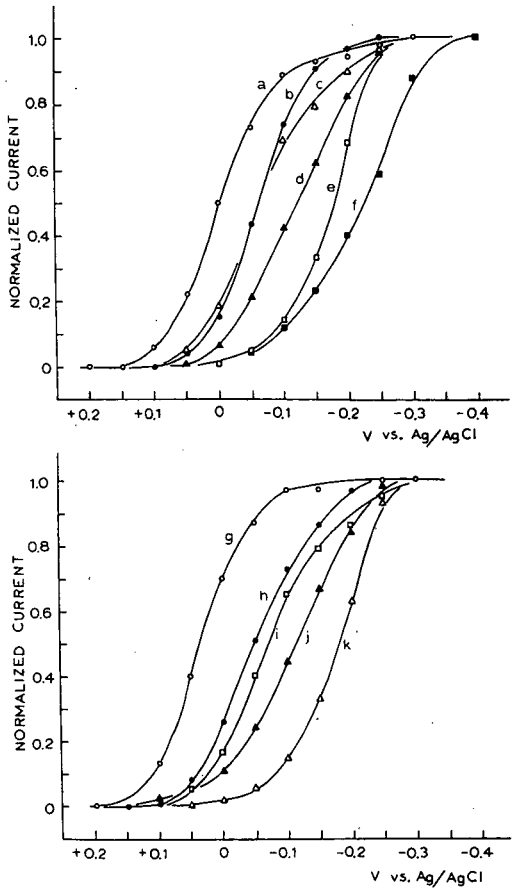

Fig. 3. Normalized hydrodynamic voltammograms of derivatized phenols. (a) Phenol; (b) *m*-chlorophenol; (c) 2,3-dimethylphenol; (d) guaiacol; (e) 2,5-dichlorophenol; (f) thymol; (g) *o*-chlorophenol; (h) 2,4,6-trichlorophenol; (i) 2,5-dimethylphenol; (j) *m*-cresol; (k) 2,3-dichlorophenol.

were eluted within 45 min on a C_{18} reversed-phase column. It should be noted that in addition to the listed phenols, *o*-nitro-, *p*-nitrophenol, and 4-hexylresorcinol were also tested, but they failed to give identifiable peaks. Fig. 4 shows the separation of a mixture of 11 derivatized phenols at an applied potential of -0.20 V using the same mobile phase. The aqueous phenol mixture containing $1.00 \cdot 10^{-5}$ *M* each was derivatized in the same manner as the individual phenols. It can be seen that eight derivatized phenols are eluted within 30 min, but severe overlap occurs for the di-and tri-substituted chlorophenols. No attempts were made to develop a better separation scheme to resolve these peaks.

Four phenols representing different substituent groups were selected to test the linear dynamic response. All original phenol solutions before derivatization were prepared in the range of 10^{-7} *M* to 10^{-4} *M*, which corresponds to 25 ppb to 13 ppm depending on the identity of the phenols. The results are summarized in Table II. The day-to-day reproducibility is good. For a period of 48 h, the peak height changes for

TABLE I

CHROMATOGRAPHIC DATA OF DERIVATIZED PHENOLS

Mobile phase: methanol–water containing 0.04 *M* potassium chloride, 0.01 *M* phosphate buffer (pH 5) (48:52).

Compound	*k'*
Phenol	6.1
Guaiacol	6.8
o-Cresol	9.9
m-Cresol	12.3
o-Chlorophenol	14.3
m-Chlorophenol	17.7
2,5-Dimethylphenol	20.9
2,3-Dimethylphenol	23.5
2,4,6-Trichlorophenol	36.2
2,5-Dichlorophenol	37.3
2,3-Dichlorophenol	37.9
Thymol	54.1

unsubstituted phenol were on the average less than 1%, but higher (*ca.* 7%) for other phenols with longer retention times. Better reproducibility can be achieved if the electrode is frequently polished and the mobile phase composition is kept constant. Excellent linear relationships (correlation coefficients >0.99) were found for the four phenols studied between $3 \cdot 10^{-7}$ *M* to $1 \cdot 10^{-4}$ *M*, a more than 300-fold variation in concentration. The dynamic range reported here was the range arbitrary chosen and studied. Our previous work[24] has shown that ABQI at a $1 \cdot 10^{-7}$ *M* level can still be

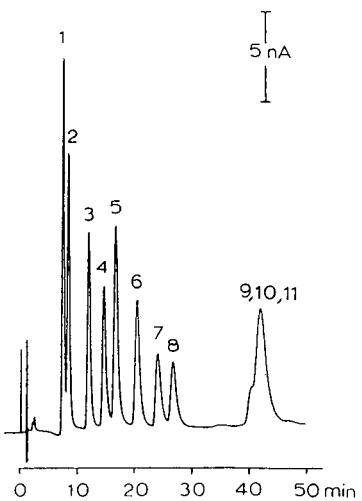

Fig. 4. Chromatogram of a mixture of derivatized phenols ($1.00 \cdot 10^{-5}$ *M* each) on a C_{18} column. 1 = Phenol; 2 = guaiacol; 3 = *o*-cresol; 4 = *m*-cresol; 5 = *o*-chlorophenol; 6 = *m*-chlorophenol; 7 = 2,5-dimethylphenol; 8 = 2,3-dimethylphenol; 9 = 2,4,6-trichlorophenol; 10 = 2,5-dichlorophenol; 11 = 2,3-dichlorophenol. Mobile phase; methanol–phosphate buffer (pH 5) (48:52). Flow-rate: 1.5 ml/min. $E_{applied} = -0.200$ V *vs.* Ag/AgCl on a glassy carbon electrode.

TABLE II
LINEAR REGRESSION ANALYSIS OF DERIVATIZED PHENOLS

Compound	*Range** *(ng)*	*Corr. Coef.*	*Regression Line** (slope ± S.D.)*	*Sensitivity*** (nA/μM)*	*R.S.D.§ peak ht.*
Phenol	0.26– 86	0.9978	1.098 ± 0.042	2.23	0.41
Guaiacol	0.37–124	0.9976	1.078 ± 0.043	1.87	0.85
o-Cresol	0.32–108	0.9999	1.030 ± 0.048	1.23	1.7
o-Chlorophenol	0.39–129	0.9920	1.050 ± 0.077	1.92	0.36

* Amount of derivatized phenols injected using a 10 μl sample valve. Calculated from each original phenol concentration by assuming 100% conversion to the corresponding ABQIs.

** Calculated from log current *vs.* log concentration plots.

*** Obtained from the slope of current *vs.* concentration plots.

§ Relative standard deviation calculated from at least four repetitive injections at each original phenol sample concentration of 10^{-5} *M*.

detected with ease. It is conceivable that the dynamic range could be improved at least three-fold, but vigorous testing at such low levels has not been attempted.

All four log peak currents *versus* log concentration calibration plots give a slope of nearly unity (Table II). This is an excellent indication that the observed current is, indeed, proportional to concentration. It should be noted that initial attempt of using technical-grade commercial *o*-chlorophenol to establish a calibration curve gave poorer linear response than the other three phenols. An excellent response was obtained after it was purified by drying *o*-chlorophenol over potassium sulfate followed by distillation. From the results of regression analysis in Table II, it can be seen that the sensitivity of this technique follows the order: phenol > *o*-chlorophenol > guaiacol > *o*-cresol. It is interesting to note that *o*-chlorophenol has higher sensitivity than either *o*-cresol or guaiacol despite its longer retention time. This observation is probably due to the fact that at −0.2 V, *o*-chlorophenol, being highly reversible at the glassy carbon electrode, has already reached its limiting current value; while *o*-cresol and guaiacol have only reached 85% and 83% of their maximum heights, respectively.

For unsubstituted phenol, the detection limit (based on a signal-to-noise ratio, S/N of 2) of this technique is estimated to be around $4 \cdot 10^{-8}$ *M*, which corresponds to 34 pg per injection if a 10-μl sample loop is used. It should be mentioned that direct injections of chloroform extract without reconstitution with methanol were also tried. Unfortunately, chloroform is also electroactive at −0.2 V; and it coelutes with the derivatized phenol using a mobile phase of methanol–water (48:52) (with phosphate buffer). A more polar mobile phase such as methanol–water (46:54) was needed to make chloroform to elute just prior to the phenol peak. The disadvantage is, of course, longer retention times are required for phenol samples.

The application of the reductive LC–ED detection is demonstrated with a waste water sample as shown in Fig. 5. The sample was obtained from a local waste water treatment plant. The silt and sludge in the sample were allowed to settle overnight, and the liquid portion of the sample was then filtered several times. No other pretreatment was performed. The filtered sample was then treated and chromatographed following the same procedure as described in the Analytical methodology section. The

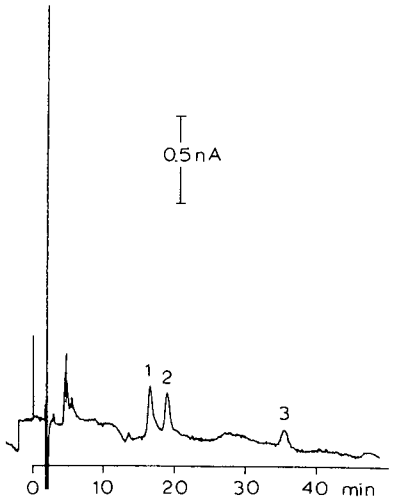

Fig. 5. Chromatogram of a waste water sample. Mobile phase: methanol–phosphate buffer (pH 5) (50:50). 1 = Phenol; 2 = guaiacol; 3 = *o*-chlorophenol. Flow-rate: 1.0 ml/min. $E_{applied} = -0.200$ V *vs.* Ag/AgCl on a glassy carbon electrode.

separation was performed on a 15 cm × 4.6 mm I.D. ODS column using a mobile phase of methanol–phosphate buffer (50:50) and a slower flow-rate of 1 ml/min. The sample was found to contain low levels of phenol (78 ppb), guaiacol (137 ppb), and *o*-chlorophenol (30 ppb). The small ill-defined peak between guaiacol and *o*-chlorophenol and peaks eluted after *o*-chlorophenol were not identified. It is interesting to note that the phenol levels detected in our sample are in the same order of magnitude as reported previously in the waste water samples of other regions of the country by LC–ED oxidative detection[2].

CONCLUSION

The chromatographic method described above has demonstrated that it is feasible to determine ppb levels of phenols via derivatization using low-potential (−0.2 V) reductive amperometric detection without exhaustive oxygen removal. Low potential detection has additional advantages, including lower background currents and potentially less interferences; because not many compounds are electroactive at −0.2 V. The conversion of phenols into quinoneimines (ABQIs) is rather straightforward and rapid. The precolumn derivatization procedure involves only two simple operations: mixing reagents in a separatory funnel at room temperature followed by extraction with chloroform and reconstitution of chloroform extract with methanol. The major drawback of the precolumn derivatization technique is, of course, the limitation of the 4-AAP reaction, which gives negative tests to certain *para*-substituted phenols and nitrophenols.

ACKNOWLEDGEMENTS

This work was supported in part by a grant from the East Carolina University Research/Creative Activity Committee. We thank Mr. Akovete Agbodjan for running some of the tests.

REFERENCES

1 T. Hanai, *CRC Handbook of Chromatography: Phenols and Organic Acids, Vol. I*, CRC Press, Boca Raton, FL, 1982.
2 D. N. Armentrout, J. D. McLean and M. W. Long, *Anal. Chem.*, 51 (1979) 1039.
3 D. E. Weisshaar, D. E. Tallman and J. L. Anderson, *Anal. Chem.*, 53 (1981) 1809.
4 E. M. Lores, T. R. Edgerton and R. F. Moseman, *J. Chromatogr. Sci.*, 19 (1981) 466.
5 D. A. Roston and P. T. Kissinger, *Anal. Chem.*, 53 (1981) 1695.
6 R. E. Shoup and G. S. Mayer, *Anal. Chem.*, 54 (1982) 1164.
7 M. H. Shah and I. L. Honigberg, *Anal. Lett.*, 16 (1983) 1149.
8 K. P. Naikwadi, S. Rokushika and H. Hatano, *Anal. Chem.*, 56 (1984) 1525.
9 M. K. Conditt and R. E. Sievers, *Anal. Chem.*, 56 (1984) 2620.
10 W. E. Schaltenbrand and S. P. Coburn, *Clin. Chem.*, 31 (1985) 2042.
11 K. Otsuka, S. Terabe and T. Ando, *J. Chromatogr.*, 348 (1985) 39.
12 F. P. Bigley and R. L. Grob, *J. Chromatogr.*, 350 (1985) 407.
13 F. Mangani, A. Fabbri, G. Crescentini and F. Bruner, *Anal. Chem.*, 58 (1986) 3261.
14 C. A. Chang and Q. Wu, *Anal. Chim. Acta*, 189 (1986) 293.
15 W. A. MacCrehan and J. M. Brown-Thomas, *Anal. Chem.*, 59 (1987) 477.
16 D. F. Hunt, J. Shabanowitz, T. M. Harvey and M. Coates, *Anal. Chem.*, 57 (1985) 525.
17 M. V. Buchanan, *Anal. Chem.*, 56 (1984) 546.
18 A. Trojanek and S. Bruckenstein, *Anal. Chem.*, 58 (1986) 983.
19 L. C. Thomas and G. J. Chamberlin, *Colorimetric Chemical Analytical Methods*, The Tintometer Ltd., Salisbury, 9th ed., 1980, p. 61.
20 J. Gasparič, D. Svobodová and A. Matysová, *J. Chromatogr.*, 88 (1974) 364.
21 J. Gasparič and D. Svobodová, *J. Chromatogr.*, 153 (1978) 153.
22 G. Norwitz and P. N. Keliher, *Anal. Chim. Acta*, 144 (1982) 273.
23 W. Jacobs, *Curr. Sep.*, 4 (1982) 45.
24 C. Li, E. Whalen and P. Hodges, *Am. Lab. (Fairfield, Conn.)*, 15 (1983) 36.
25 P. F. Jones and K. E. Johnson, *Can. J. Chem.*, 51 (1973) 2860.
26 R. N. Adams, *Electrochemistry at Solid Electrodes*, Marcel Dekker, New York, 1969, p. 336.
27 M. B. Ettinger, C. C. Ruchhoft and R. J. Lishka, *Anal. Chem.*, 23 (1951) 1783.
28 P. T. Kissinger, *Anal. Chem.*, 49 (1977) 448A.

Journal of Chromatography, 455 (1988) 253–261
Elsevier Science Publishers B.V., Amsterdam — Printed in The Netherlands

CHROM. 20 866

DETERMINATION OF PHOSPHATE AND PHOSPHITE IN PLANT MATERIAL BY GAS CHROMATOGRAPHY–MASS SPECTROMETRY AND ION CHROMATOGRAPHY

R. H. SMILLIE* and B. GRANT
Russell Grimwade School of Biochemistry, Melbourne University, Parkville, Victoria 3052 (Australia)
and
R. L. CRIBBES
Research and Development Laboratory, Albright & Wilson (Australia) Ltd., Melbourne, Victoria (Australia)
(First received March 9th, 1988; revised manuscript received July 14th, 1988)

SUMMARY

A method is described for the rapid and simultaneous detection of phosphate and phosphite in samples of plant material as small as 10 mg fresh weight. Samples are extracted into formic acid–isopropanol, clarified by the addition of chloroform and partially purified by sequential passage through cation- and anion-exchange resins. The analytes can then be separated directly by single-column anion-exchange chromatography using a conductivity detector. Alternatively they can be separated by capillary gas chromatography after the formation of *tert.*-butyldimethylsilyl esters. Recoveries of 95% or better were achieved, estimated both by the addition of ^{32}P or by mass addition. The lower limit of detection was 100 ng using ion chromatography and 100 pg with mass spectrometry.

INTRODUCTION

Phosphorous acid and its salts (phosphites) exhibit activity against a number of species of fungi of the order Peronosporales[1]. In Australia, phosphite is currently being used as a treatment against *Phytophthora cinnamomi* infection of avocado trees, and appears to be as least as effective as Phosetyl-Al[2,3]. It is under development as a treatment against other fungal pathogens. The development of phosphite as an antifungal agent has imposed a demand for an effective, yet simple mean of analysis of this compound in a wide variety of plant tissues destined for human consumption. In addition, investigation of the mode of action of phosphite requires a method which allows the analysis of both phosphite and phosphate in small amounts of plant and fungal tissues.

Methods for the analysis of phosphite and phosphate by gas chromatography (GC) following derivatization with diazomethane, trimethylsilane (TMS) and *tert.*-butyldimethylsilane (t-BDMS) have been reported[4–6], together with adaptations which allowed the analysis of phosphite in plant material[7,8]. However, unless rigorous

0021-9673/88/$03.50 © 1988 Elsevier Science Publishers B.V.

(and often complex) procedures were followed, these methods suffered from limited and variable recovery of phosphite[8]. Phosphate and phosphite have also been separated by anion-exchange liquid chromatography[9], and ion chromatography systems, incorporating a high-resolution anion-exchange column and conductivity detector, have been used to separate and quantify phosphorus salts[10,11]. In this paper we report a procedure for the analysis of phosphite and phosphate in a wide variety of plant material. It offers higher recoveries and higher sensitivities than methods currently available, and yet is simple to use. It offers the choice of detection by ion chromatography or, after derivatization, by GC and mass spectrometry (MS). The high recovery and high sensitivity of the method allow it to be applied to samples of plant tissue as small as 10 mg fresh weight.

EXPERIMENTAL

Materials

All solutions used in this work were prepared using water which had been purified using a Waters Millipore Milli-Q® system. Silylation reagents were obtained from Pierce (Rockford, IL, U.S.A.), phosphorous acid from Albright & Wilson (Australia), and phosphoric acid from BDH (Australia). Samples of both phosphoric acid and phosphorous acid were shown to be better than 99% pure by ^{31}P NMR spectrometry. All other chemicals were of analytical-reagent grade. The ^{32}P-labelled phosphate and phosphite were obtained from the Australian Atomic Energy Commission (Lucas Heights, Australia). The [^{32}P]phosphite was checked for radio-isotopic purity by paper electrophoresis[12] prior to use. Plant material was obtained from either the local markets, or in the case of phosphite-treated material, from field trials conducted to determine phosphite efficacy.

Methods

Sample preparation. Plant material was frozen at −20°C until required. Freeze drying was found to give unsatisfactory recoveries of phosphite from some avocado tissues and was not used. Seeds were initially ground to a flour in a small coffee mill, prior to homogenization. Plant material to be extracted (routinely 100 mg) was homogenized with one volume of 1 *M* formic acid (analytical-reagent grade). The homogenate was then centrifuged (10 000 *g*, 5 min) and the clarified supernatant transferred to a 2.5-ml plastic microfuge tube. The residue was re-extracted with 1 ml isopropanol, centrifuged again, and the supernatant added to the original extract, together with 200 μl chloroform and the combined cloroform–isopropanol extract shaken and centrifuged (10 000 *g*, 5 min). Fatty tissues, such as avocado fruit, required slightly more chloroform and 300 μl was added in these analyses. On centrifugation, two liquid phases separated, together with a precipitate at the interface. The lower (chloroform) layer and the precipitate were discarded.

The upper layer which contained the phosphite and phosphate was removed and re-extracted with chloroform to remove residual isopropanol before further purification. It was then passed through a cation-exchange column [1 ml strong cation exchanger (SCX) Bond-Elut cartridges, Analytichem International, H^+ form] to remove cations and protonated amino acids. Cartridges were regenerated and reused

several times, according to manufacturers instructions. This was followed by a strong anion-exchange step. The strong anion exchanger (SAX) (Bio-Rad AG 1-X8, 200–400 mesh, Cl^- form) was converted to the OH^- form by washing with 2 ml 1 *M* sodium hydroxide, followed by 2 ml water, prior to use. The prepared SAX (300 μl) was then added to a 1-ml disposable syringe, and washed with 500 μl of distilled water. The sample (1 ml) was loaded onto the column and washed with a further 1 ml of distilled water. The sample containing phosphite was then eluted in 2 ml of 1 *M* hydrochloric acid freshly prepared from constant boiling hydrochloric acid.

After freeze drying, the sample was redissolved in water for analysis by ion chromatography, or derivatized for analysis by GC. To achieve maximum recovery with the lowest amounts of material it was essential to process the samples as soon as possible after elution from the SAX column.

Recovery of phosphate and phosphite in the extraction procedure was calculated using samples of fruits augmented with 0.5 μCi [^{32}P]phosphate or phosphite per sample, added at the time of homogenization. Sub-samples (100 μl) were withdrawn and the ^{32}P counted in 10 ml of scintillant[13] using an LKB 1215 liquid scintillation counter (Window 120-212).

Ion chromatography. Samples were injected using a Rheodyne fixed-volume loop (routinely 100 μl) onto a Hamilton PRP-X100 10-cm SAX column, and eluted with 100 m*M* succinic acid, pH 2.75, at a flow-rate of 4 ml/min. The eluent was monitored using a conductivity detector (Milton Roy ConductoMonitor III) and the data processed using a Milton Roy data acquisition system. Subsequent work showed that an SGE (Australia) 100GL4-SAX-8/5 SAX column was equally effective in the separation of phosphate and phosphite from other anions present in the extract.

Standards of phosphate and phosphite were prepared in the plant extract under investigation. It was essential that fresh standards be prepared daily.

Gas chromatography–mass spectrometry. An aliquot (50–100 μl) of the sample containing the analytes was placed into a Pasteur pipette which had previously had one end sealed, and was dried under vacuum. Pyridine (50 μl) and N-methyl-*tert.*-butyl-dimethylsilyl-trifluoroacetamide (MTBSTFA, Pierce) (100 μl) were then added and the tube sealed. Derivatization was complete within 4 h at room temperature.

Separation was carried out using a Hewlett-Packard 5880 gas chromatograph. Injections (3 μl) of the preparation were made using a split/splitless injection, with the injector port at 200°C. The SGE (Australia) BP1 column, 12.5 m × 0.3 mm, was held at 100°C for 4 min then increased to 200°C at 10°C/min. Phosphite and phosphate t-BDMS derivatives were eluted as separate peaks, and were detected using a Finnigan 700 ion trap detector scanning from 50 to 450 *m/z*. Mass recoveries were determined by addition of pure phosphoric and phosphorous acids to the samples at the extraction stage.

Comparison of gas chromatography detectors. Sample detection thresholds were determined for two GC detectors and the Finnigan ion trap. Serial 1/10 dilutions of phosphite were prepared and derivatized as described. The samples were detected using a Hewlett-Packard flame ionization detector and nitrogen/phosphorus specific thermionic detector.

RESULTS

Recovery of added phosphite in the extraction step and following preparation and detection by ion chromatography and GC–MS was found to be better than 95% (Table I). Similar values were obtained using ion chromatography with preparations of leaf and stem tissues from lupin, tobacco, and subterranean clover, and from chick pea seeds. Recovery of [^{32}P]phosphate was better than 99%, and ranged between 95 and 105% using IC.

Ion chromatography

Separation by ion chromatography and detection by conductivity allowed the detection of 100 ng phosphite at concentrations as low as 1 ppm (using a 100-μl injection) (Table II). This is equal to 10 ppm in a 10-mg fresh weight sample. The phosphite was clearly separated from phosphate and from other peaks in the extract (Fig. 1). The chloride peak, which followed the phosphite peak, did not interfere with the integration of that peak. Standards of phosphite gave linear responses over two orders of magnitude (Fig. 2). It was noted however that the slopes of the standard curves differed from one type of plant tissue to another, and from standards prepared in water or dilute acid. The lack of linearity at the lowest concentrations appears to be due to oxidation of phosphite to phosphate during sample preparation and was also observed in material analyzed by GC (Fig. 2).

Gas chromatography

Phosphate and phosphite as the t-BDMS derivatives were separated by GC and detected using flame ionization detection, nitrogen/phophorus detection and ion trap. Of the four solvents for derivatization (tetrahydrofuran, dimethyl formamide, acetonitrile and pyridine) investigated, pyridine gave a consistently higher yield of derivatives of both analytes in the presence of plant extract. Derivatization of standards was complete within 1 h at room temperature, but plant material required

TABLE I

RECOVERY OF PHOSPHITE MASS AND RADIOACTIVITY

Phosphite (10 ppm wet weight) containing 10^5 dpm ^{32}P was added to the fruit homogenates. Recovery of ^{32}P after sample extraction and preparation, and after derivatization and analysis by GC–MS or ion chromatography are shown. Data are the means of duplicate analyses. Phosphate recoveries were shown to be better than 99% using [^{32}P]phosphate, (10 ppm, 10^5 dpm per sample), and to range between 95 and 105% mass recoveries in ion chromatography. Mass recoveries of phosphate using GC–MS were not determined. ND = Not determined.

Fruit	*Recovery of ^{32}P (%)*	*Recovery by GC–MS (%)*	*Recovery by ion chromatography (%)*
Apple	98	ND	94
Avocado	105	98	100
Grape	97	ND	110
Orange	99	ND	100
Pawpaw	98	ND	ND
Tomato	97	95	102

TABLE II
DETECTION LIMITS FOR PHOSPHITE USING VARIOUS ANALYTICAL METHODS

Method	*Preparation concentration*	*Injection volume (μl)*	*Detection limit (ng)*	*Ref.*
Packed column GC–flame ionization detection (t-BDMS)	Solid	–	4.0	12
Capillary column GC–flame ionization detection (t-BDMS)	4 μg/g fresh wt.	1	2.0	14
Adogen, packed column GC–flame ionization detection (TMS)	0.1 μg/ml	1	2.5	16
Ion chromatography–conductance detection	1.0 μg/ml	100	100	This work
Capillary column GC–flame ionization detection (t-BDMS)	3.0 μg/ml	3	3.0	This work
Capillary column GC–nitrogen/ phosphorus detection (t-BDMS)	1.0 μg/ml	1	0.3	This work
Capillary column GC–ion trap (t-BDMS)	0.1 μg/ml	3	0.1	This work

longer (4 h at room temperature or 70°C for 1 h). Derivatizations with BSTFA to yield the trimethylsilyl ester were tested but did not give as reproducible recoveries as the t-BDMS esters.

The detection limit using flame ionization detection (3 ng) was of the same magnitude as reported by others (Table II). The nitrogen/phosphorus specific

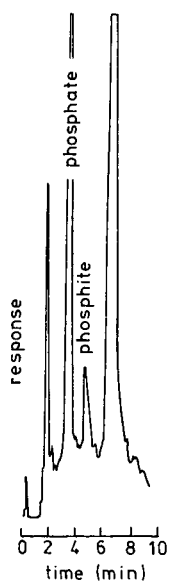

Fig. 1. Sample ion chromatogram of added phosphite (10 ppm) and endogenous phosphate in an extracted avocado preparation separated using an SAX column and detected by conductivity. The large peak eluting after the posphite peak is chloride.

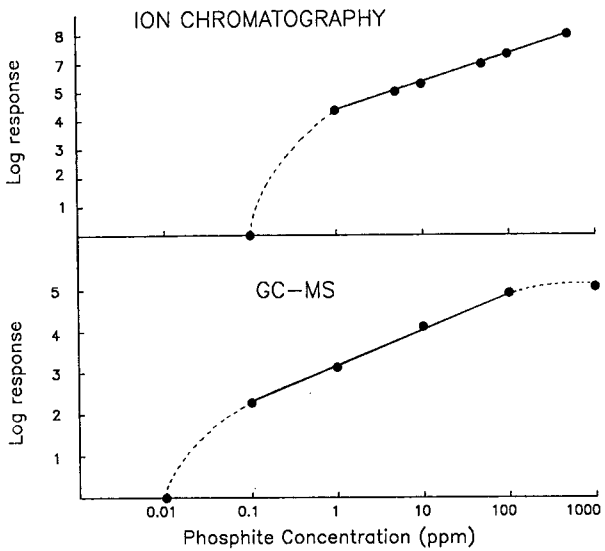

Fig. 2. Detection response of phosphite by (bottom) GC–ion trap as the t-BDMS derivative and (top) ion chromatography using a conductivity detector.

thermionic detector, while more sensitive to phosphorus-containing materials, was found to offer little practial advantage because of the increased background from derivatization reagents which contain nitrogen (Fig. 3). Furthermore, these detectors are subject to gradual loss of sensitivity as the silyl derivatization reagents react with and progressively inactivate the rubidium coat on the bead.

The ion trap detector (full scan mode) was an order of magnitude more sensitive than flame ionization or nitrogen/phosphorus detection, and was linear over three orders of magnitude (Fig. 2). Assuming complete linearity of response it is theoretically possible to detect 10 pg of phosphite at 0.01 ppm concentration using the ion-selective mode (*m/z* 256) where the phosphite derivative is seen as a single peak on a flat baseline (Fig. 4). However, detection at these low levels was not achieved due to loss of linearity at the lowest concentration range, and in practice 0.1 ppm in a 1-μl

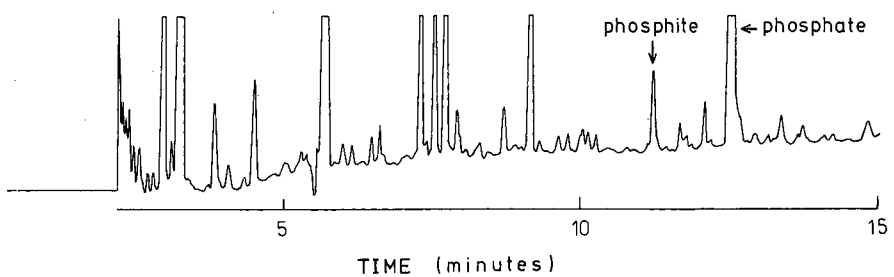

Fig. 3. Capillary gas chromatogram of added phosphite, 10 ppm in avocado tissue extract (3 μl injection of t-BDMS phosphite ester), detected using nitrogen/phosphorus specific thermionic detector. A high background from reagent peaks is evident. The phosphate in this sample originated from endogenous material in the fruit.

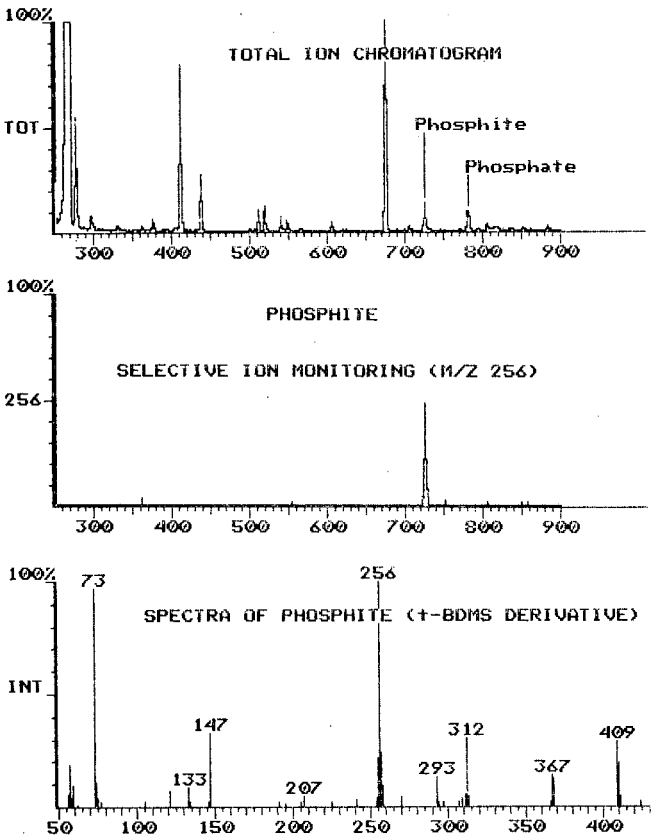

Fig. 4. Total ion chromatogram, showing phosphate and phosphite standards, prepared in water (t-BDMS derivatives, each 1.0 ng); single-ion (*m/z* 256) chromatogram of phosphite t-BDMS derivative; mass spectrum of phosphite t-BDMS derivative.

TABLE III

PHOSPHATE AND PHOSPHITE CONCENTRATIONS IN AVOCADO FRUITS

Avocado fruit were harvested from three trees. The control tree was infected with *Phytophthora cinnamomi*, and had not been treated with phosphorous acid; T-1 and T-2 were trees which were infected and which had been injected with a neutralized solution of potassium phosphite (T-1: 10%, w/v; T-2: 20%, w/v) according to the method of Pegg *et al.*[2], six months prior to harvest of fruit. $n = 6$ for each group.

	Concentration (μg/g fresh weight)	
	Phosphate	*Phosphite*
Control	600 ± 147	Not detected
T-1	1406 ± 184	78 ± 32
T-2	1523 ± 360	28 ± 14

sample (10 pg) was found to be the lower operating limit. This allows the analysis of phosphite or phosphate at 1 ppm in a 10 mg fresh weight sample. While we did not compare capillary with packed columns, reference to the literature suggests that the differences in detection limits between the two are negligible (Table II).

The method described in the foregoing was applied to the analysis of phosphite and phosphate in plants which had been treated with phosphite. Lupin leaves and stems, sub-clover stems, tobacco leaves, chick peas and seedlings drenched with phosphite were analyzed, using the ion chromatography separation. Phosphite was readily detected in the extracts in concentratons which ranged from 20 to more than 120 μg/g fresh weight. Avocado fruits, taken from three separate trees in a trial to determine the efficacy of the phosphite treatment were also analyzed with the results shown in Table III. Fruit from trees which had been treated with phosphite contained residual levels of phosphite which were readily detectable (28 and 78 μg/g fresh weight) while no phosphite was detected in fruits from untreated trees.

DISCUSSION

The method described here offers a means of determining phosphite and phosphate in a wide variety of plant species and tissues. The extraction and preparation lends itself to analysis by either ion chromatography or by GC and can be applied to samples as small as 10 mg fresh weight containing as little as 100 ng (ion chromatography) or 100 pg (GC–MS) phosphate or phosphite. Recoveries of both ions were typically better than 95%. Although we were initially concerned only with phosphite detection, the discovery that the concentration of phosphate present determine in part the efficacy of phosphite assimilation by some fungi[14], has meant that simultaneous measurement of the two anions is important in applications related to the mode of phosphite action as a fungicide.

The isopropanol–chloroform extraction removes both high-molecular-weight compounds and non-polar compounds such as phenols, while maintaining analyte concentration. The extraction, precipitation and cation-exchange chromatography steps are fast and allow a minimum of ten samples to be manually processed daily. The solid-phase anion-exchange step, although more time consuming, is simpler than the HPLC purification described by Saindrenan *et al.*[8]. Where larger numbers of samples are to be analyzed the commercialy prepared anion-exchange columns (*e.g.* Bond Elut International®) can be used

We examined the feasibility of using the liquid anion exchanger Adogen 646 (Aldrich) as a simpler means of analyte purification. This material has been reported as being suitable for extraction and subsequent derivatization of phosphate from water[15]. While Adogen 646 gave excellent recovery of phosphite from aqueous samples it gave consistently poor recoveries (1–10%) of phosphite from plant extracts and for this reason was discarded. Ion chromatography on anion-exchange columns coupled with conductivity detection provided the resolution and sensitivity needed (1–100 ppm) for analysis of phosphite residues in food stuffs and for measurement of gross phosphite distribution within plants. The anion-exchange step and the subsequent freeze drying may be omitted for ion chromatography analysis, although this may result in higher background and reduced column life with some types of plant material. The detection of phosphite in several of the fruits tested required minor

modification to the eluent strength to achieve optimum resolution of co-eluting peaks. We emphasis the necessity of preparing fresh standards in the extract under analysis if the maximum accuracy is required. The variations in slope found in the different matrices are presumably the result of other anions co-eluting with the phosphite peak in the ion chromatographic separation but the identity of these compounds was not established. Common plant anions such as chloride (retention time 6.4 min), oxalate (retention time 11 min) and sulphate (retention time >15 min) all eluted at positions removed from the analyte peaks. However it is essential to have reference plant material known to be phosphite free when ion chromatographic analysis is to be used exclusively.

Where only small samples of tissue are available and where the phosphite concentratons are low, the GS–MS analysis system is clearly the method of choice allowing analysis of phosphite in thin sections of stem or leaf and in xylem and phloem exudate. The problem of loss of phosphite at very low levels remains unsolved. However, since in practice we have found that in the tissues of phosphite-treated plants the concentrations of phosphite in tissues ranged from 5–500 ppm, and in fruits and seeds from 20–1200 ppm, analysis of extremely low levels of phosphite has not been required in this application.

ACKNOWLEDGEMENTS

We thank Albright & Wilson (Australia) Ltd. for supporting this project and Frances Seretis of Albright & Wilson for technical assistance. We also acknowledge the generosity of Professor J. S. Waid of the Microbiology Department, La Trobe University for access to GC–MS equipment. Dr. K. Pegg of the Queensland Department of Primary Industries kindly supplied the avocados.

REFERENCES

1 M. E. Fenn and M. D. Coffey, *Phytopathology*, 75 (1985) 1064.
2 K. G. Pegg, A. W. Whiley, J. B. Saranah and W. Glass, *Aust. Plant Pathol.*, 14 (1985) 25.
3 M. F. Piccone, A.W. Whiley and K. E. Pegg, *Aust. Horticulture*, May (1987) 5.
4 C. J. Hardy, *J. Chromatogr.*, 13 (1964) 372.
5 W. C. Butts and W. T. Rainey, *Anal. Chem.*, 43 (1971) 538.
6 T. P. Mawhinney, *J. Chromatogr.*, 257 (1983) 37.
7 J. J. Bezuidenhout, L. Korsten and J. M. Kotez, *8th Yearbook*, South African Avocado Growers Association, Tzaneen, 1985, p. 100.
8 P. Saindrenan, G. Darakis and G. Bompeix, *J. Chromatogr.*, 347 (1985) 267.
9 F. H. Pollard, D. E. Rodger, M. T. Rothwell and G. Nickles, *J. Chromatogr.*, 9 (1962) 227.
10 D. T. Gjerde and J. S. Fritz (Eitors), *Ion Chromatography*, Hüthig, Heidelberg, 1987.
11 D. S. Ryder, *J. Chromatogr.*, 354 (1986) 438.
12 M. Halman and L. Kugel, *J. Inorg. Nucl. Chem.*, 25 (1963) 1343.
13 H. Fock, *Chromatographia*, 9 (1976) 99.
14 J. M. Griffith, unpublished results.
15 D. R. Mathews, W. D. Shults and M. R. Guerin, *Anal. Chem.*, 43 (1971) 1582.

Journal of Chromatography, 455 (1988) 263–269
Elsevier Science Publishers B.V., Amsterdam — Printed in The Netherlands

CHROM 20 898

RETENTION AND HEATS OF ADSORPTION OF HYDROCARBONS AND ALIPHATIC ALCOHOLS ON CELLULOSE

L. I. DERNOVAYA and Yu. A. ELTEKOV*
Institute of Physical Chemistry, the USSR Academy of Sciences, Moscow 117915 (U.S.S.R.)
(First received October 12th, 1987; revised manuscript received August 11th, 1988)

SUMMARY

The interaction of methanol, ethanol, *n*-propanol, *n*-butanol, *n*-hexane, *n*-octane, *n*-nonane, *n*-decane, benzene, toluene and ethylbenzene molecules with the surface of microspherical cellulose beads has been studied by gas chromatography. The retention volumes and their dependences on the temperature and molecular parameters of the adsorbate have been determined. The initial differential heats of adsorption have been calculated. The character of interaction of these organic substances has been shown to be determined by the electronic and geometric structures of the molecules.

INTRODUCTION

Polymeric organic sorbents, including those based on polysaccharides, are widely used in liquid column and planar chromatography. Therefore, the macroporous microspherical cellulose (MC), synthesized and studied at the Institute of Macromolecular Chemistry of the ČSSR Academy of Sciences, is of some interest for chromatographic methods[1]. This cellulose was tested in liquid chromatography of dextrans and found to have quite satisfactory properties for the separation of water-soluble biopolymers[2]. It was also proposed for use in gas and liquid adsorption chromatography of low-molecular-weight substances[3,4]. Therefore, an evaluation of the interaction parameters of model organic substances with the cellulose surface is important, *e.g.*, in gas chromatography of organic substances on cellulose columns[3,4].

EXPERIMENTAL

Adsorbent

A sample of microspherical macroporous cellulose was kindly provided by Dr. J. Hradil (Institute of Macromolecular Chemistry, Prague, Czechoslovakia). The preparation of samples of cellulose beads has been described in detail in refs. 1 and 2. The specific surface area of the sample determined by means of the BET method by low-temperature adsorption of nitrogen was equal to 110 m^2/g. The average diameter of the pores determined by the method of small-angle scattering of X-rays was 280 Å.

0021-9673/88/$03.50 © 1988 Elsevier Science Publishers B.V.

Apparatus

A Tswett-104 gas chromatograph (NPO Chimavtomatica, U.S.S.R.) with a flame ionization detector was employed. The column (20 cm × 3 mm I.D.) was packed with 0.3 g cellulose. The diameters of the cellulose beads were 0.2–0.25 mm. Helium was used as the carrier gas at a flow-rate of 30 cm^3/min. The sample vapours were introduced into the column by a heated injection port, using a microsyringe (1 μl). Methane was used as the non-adsorbed gas. Prior to chromatographic measurements, the cellulose beads in the column were dried in the carrier gas stream at 110°C for 2 h.

In order to calculate the retention volumes, V, and then the adsorption heats, $-\Delta\bar{U}$, the corrected retention times of the vapours of adsorbed substances were determined from the maxima of chromatographic peaks from series of injections at very low concentration. The values of V were calculated according to

$$V = \frac{t_R w P T_c}{T P_o} \cdot \frac{3}{2} \cdot \frac{(P_i/P_o)^2 - 1}{(P_i/P_o)^3 - 1} \tag{1}$$

where t_R = corrected retention time in min, w = the flow-rate of carrier gas in ml/min, P_i, P_o, P are the pressures at the inlet and outlet of the column and that corrected for the presence of water vapour in the flow-meter, respectively, T_c and T are the temperatures of the column and of the flow-meter, respectively. The absolute retained volume, V_A, was calculated according to[5]

$$V_A = V/ms \tag{2}$$

where m is the mass of cellulose in the column and s its specific surface area. The retention values for each adsorbate were calculated from at least ten chromatographic peaks at each temperature. The accuracy was 5%.

The values of the differential adsorption heats were calculated on the basis of the dependence of the experimental values of the retention volumes on the temperature:

$$-\Delta\bar{U} = R \, \mathrm{d} \ln (V/T)/\mathrm{d}(1/T) \tag{3}$$

RESULTS

Fig. 1 shows chromatograms of n-alkanes (a) and aromatic hydrocarbons (b). The peaks are symmetrical, and the retention times do not depend on the amount of vapour injected over a range of one order of magnitude. Fig. 1c shows examples of the separation of a mixture of three substances: namely, n-heptane, toluene and n-propanol, *i.e.*, substances with similar boiling points (100–110°C). The separation of these substances in a chromatographic column proceeds due to specific interaction of molecules with different chemical structures with the cellulose surface.

Fig. 2 shows the dependences of log V/T on $1/T$ for hydrocarbons and alcohols. These graphs allow us to calculate the values of the differential adsorption heats, and are practically linear over the temperature range of 60–110°C.

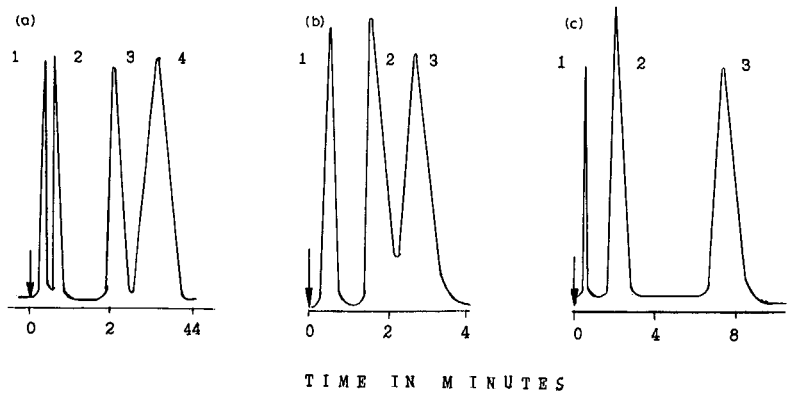

Fig. 1. Gas chromatograms on microspherical cellulose at 100°C. (a) *n*-Alkanes: 1 = *n*-hexane; 2 = *n*-heptane; 3 = *n*-octane; 4 = *n*-nonane. (b) Aromatic hydrocarbons: 1 = benzene; 2 = toluene; 3 = ethylbenzene. (c) 1 = *n*-Heptane; 2 = toluene; 3 = *n*-propanol.

DISCUSSION

Table I gives the values of the retention volumes, V_A, of *n*-alkanes, aromatic hydrocarbons and aliphatic alcohols on microspherical cellulose at 100°C, as well as the differential adsorption heats of these substances calculated from the chromatographic data. For comparison, the Table gives the values $-\Delta\bar{U}$ on C-120 silochrome[6], graphitized carbon black[5] and immobilized polymeric sorbent polyarylate[7]. The V_A

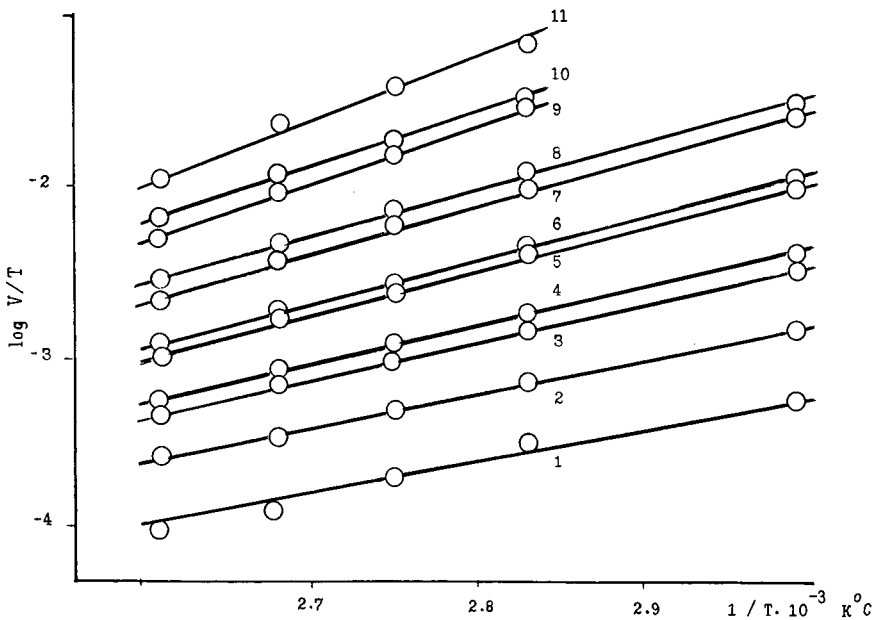

Fig. 2. Dependence of log V/T on $1/T$ for *n*-pentane (1), *n*-hexane (2), benzene (3), *n*-heptane (4), toluene (5), *n*-heptane (6), ethylbenzene (7), *n*-nonane (8), *n*-propanol (9), *n*-decane (10) and *n*-butanol (11).

TABLE I

VALUES OF V_A AT 100°C AND OF $-\Delta\bar{U}$ FOR ORGANIC SUBSTANCES UPON INTERACTION WITH CELLULOSE (MC), C-120 SILOCHROME[6], GRAPHITIZED CARBON BLACK[5] AND POLYARYLATE[7]

Adsorbate	V_A (cm^3/m^2) *MC*	$-\Delta\bar{U}$ *(kJ/mol)*			
		MC	*C-120*	*Carbon black*	*Polyarylate*
n-Pentane	0.067	33.5	–	37.4	–
n-Hexane	0.12	37.1	37.3	43.7	55.4
n-Heptane	0.27	42.4	41.1	52.5	64.0
n-Octane	0.62	48.1	–	56.3	72.8
n-Nonane	1.4	52.4	48.8	62.2	80.4
n-Decane	3.5	57.9	53.1	70.1	–
Benzene	0.21	41.1	41.1	41.2	62.3
Toluene	0.61	46.1	45.5	48.7	71.3
Ethylbenzene	1.3	53.3	49.3	53.3	–
Methanol	1.9	61.9	35.9	–	41.3
Ethanol	1.7	61.7	37.8	29.0	51.7
n-Propanol	3.4	70.3	39.7	34.0	59.1
n-Butanol	7.2	75.5	–	39.5	68.1

values at low concentrations of the adsorbate at equilibrium appear to be the Henry constants which characterize the adsorbent–adsorbate system at a given temperature[5]. Table I shows that, in the interaction of normal hydrocarbon molecules with the surface of microspherical cellulose, the Henry constant $K = V_A$ and $-\Delta\bar{U}$, characterizing the change in the internal energy of adsorption, increase in the homologous series with an increase in the molar volume and average polarizability of the molecules. However, the effect of the molar volume becomes less pronounced due to differences in the geometric and electronic structures of the molecules of the sorbates studied.

The molecules of toluene and ethylbenzene have volumes close to those of *n*-heptane and *n*-octane, respectively, but they are retained in the column 2–2.5 times longer. Alcohol molecules having a free electron pair at the oxygen atom are retained much longer than *n*-alkanes, though their molar volume is smaller.

A comparison of $-\Delta\bar{U}$ values shows that the heats of adsorption of *n*-alkanes on the MC surface are lower than those for graphitized carbon black, approximately equal to $-\Delta\bar{U}$ values for C-120 and considerably less than those for polyarylate. Initial adsorption heats of alcohols on the cellulose surface exceed $-\Delta\bar{U}$ values for all the sorbents, and this appears to be characteristic of the cellulose sorbent.

Fig. 3 shows the dependence of $-\Delta\bar{U}$ for homologous series of *n*-alkanes, alkylbenzenes and *n*-alcohols on the polarizability of the molecules. These dependences are linear to a first approximation. The $-\Delta\bar{U}$ values of aromatic compounds and alcohols capable of specific interaction exceed those of *n*-alkanes having the same numbers of carbon atoms. The values $\Delta(-\Delta\bar{U})$ calculated from these dependences show a contribution of the specific interaction of the molecules of alcohol and alkylbenzenes with the surface hydroxyl groups of cellulose. In the case of aromatic compounds, the $\Delta(-\Delta\bar{U})$ values are on average equal to 7–9 kJ/mol; in the case of

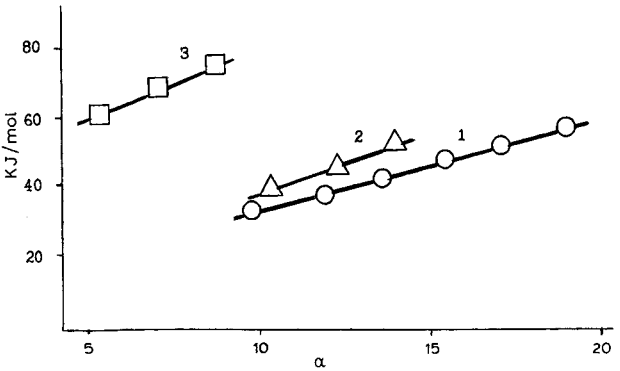

Fig. 3. Dependence of differential adsorption heats, $-\Delta\bar{U}$, of *n*-alkanes (1), alkylbenzenes (2) and *n*-alcohols (3) on the average polarizability of the molecules. α in Å.

alcohols they are equal to 42–45 kJ/mol. The concentrated electron density at the periphery of the π-bonds in aromatic molecules and at the oxygen atom of alcohol molecules is responsible for the specific interaction of these molecules with the partly protonized hydrogen atoms of the hydroxyl groups of the cellulose surface. The specific interaction of the alcohol molecules exhibits an higher energy than that of the alkylbenzene molecules, probably due to the formation of hydrogen bonds between the alcohol molecules and the cellulose hydroxyl groups, the bond strength being equal

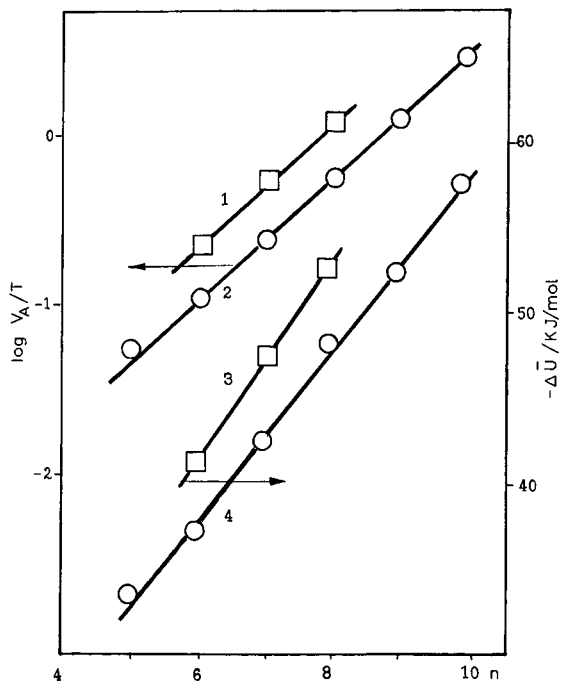

Fig. 4. Dependences of log V_A and $-\Delta\bar{U}$ on the number of carbon atoms, *n*, in *n*-alkanes and aromatic hydrocarbons.

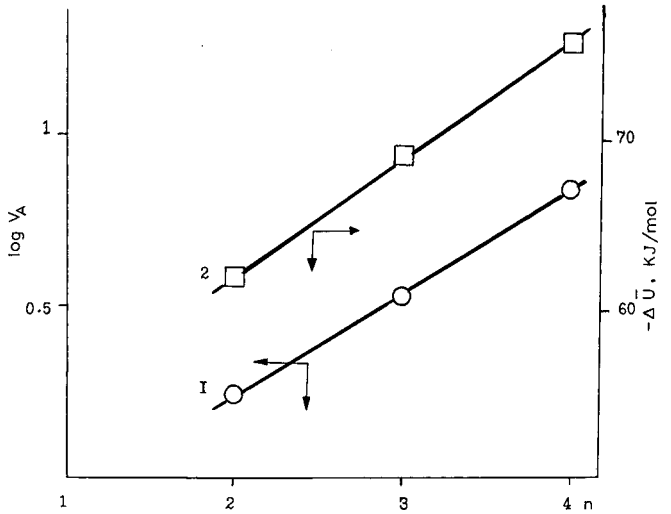

Fig. 5. Dependences of log V_A and $-\Delta\bar{U}$ on the number of carbon atoms, n, in alcohols.

to 40 kJ/mol. The strength of the adsorption interaction of alcohols with the surface of microspherical cellulose particles is determined by the energy of the hydrogen bond formation. The heat of adsorption also depends on the structure of the adsorbent pores.

The dependences of log V_A and $-\Delta\bar{U}$ on the number of carbon atoms, n, in the n-alkanes, aromatic hydrocarbons (Fig. 4) and alcohols (Fig. 5) were plotted on the basis of the chromatographic data. These dependences are satisfactorily described by the equations $\log V_A = a + bn$ and $-\Delta\bar{U} = \bar{a} + \bar{b}n$. This allows one to predict retention and the $-\Delta\bar{U}$ values for individual members of homologous series as well as to evaluate the contributions of the specific interaction of functional groups or bonds and the increments due to CH_2 groups in retention and the heat of adsorption on cellulose. Table II gives the values of the coefficients in these equations for the adsorption of n-alkanes, aromatic hydrocarbons and alcohols with the surface of microspherical cellulose. The increment in $-\Delta\bar{U}$ for non-specific interaction by one CH_2 group is equal to 6.1 kJ/mol for n-alkanes, 6.9 kJ/mol for n-alcohols and 5.2

TABLE II

VALUES OF THE COEFFICIENTS OF a AND b IN THE EQUATIONS FOR ADSORPTION ON CELLULOSE (MC) AND CHROMOSORB 101

Adsorbates	$\log V_A = a + bn$		$-\Delta\bar{U} = \bar{a} + \bar{b}n$			
	MC		*MC*		*Chromosorb 101*	
	a	b	$\bar{a}$	$\bar{b}$	$\bar{a}$	$\bar{b}$
n-Alkanes	−3.14	0.37	7.6	6.1	11.7	6.4
Alkylbenzenes	−2.76	0.37	6.0	5.2	–	
n-Alcohols	−0.09	0.31	54.6	6.9	29.5	6.4

kJ/mol for aromatic hydrocarbons. The data[8] for Chromosorb 101 are given for comparison. The values of the increment are on average similar for these polymers. However, the coefficients a and b seem to change with a change in the type of homologous series and chemical nature of the adsorbent surface.

CONCLUSIONS

The interaction of n-alkanes, aromatic hydrocarbons and alcohols with a sample of microspherical cellulose has been studied by means of gas chromatography. The values of the retention volume, V_A, of these organic substances were determined at 60, 80, 90, 100 and 110°C. Using the temperature dependence of V_A, the differential adsorption heats $-\Delta\bar{U}$, characterizing the adsorption energy of the molecules of the adsorbates studied upon interaction with the surface of microspherical cellulose have been calculated. The contribution of the specific interaction to the total heat of adsorption of aromatic hydrocarbons and alcohols upon interaction with the cellulose surface has been evaluated. It has been shown that microspherical cellulose can be used as an adsorbent in gas chromatography. In accordance with the classification of molecular interactions proposed by Kiselev and Yashin[5], this adsorbent can be classified as Type II, *i.e.*, a specific sorbent.

ACKNOWLEDGEMENTS

The authors thank Dr. Y. Štamberg, Y. Peška and Y. Hradil for supplying samples of macroporous cellulose and for helpful discussion.

REFERENCES

1 J. Peška, J. Štamberg and Z. Blače, *Czech. Pat.*, 172 640 (1976).
2 J. Peška, J. Štamberg, J. Hradil and M. Ivavský, *J. Chromatogr.*, 125 (1976) 455.
3 G. M. Dorris and D. C. Gray, *J. Colloid Interface Sci.*, 71 (1979) 93.
4 G. M. Dorris and D. C. Gray, *J. Colloid Interface Sci.*, 77 (1980) 2.
5 A. V. Kiselev and Ya. I. Yashin, *Gas Adsorption Chromatography* (in Russian), Nauka, Moscow, 1967, p. 83.
6 L. I. Dernovaya and Yu. A. Eltekov, in *IX Vsesoyuznaya konferentsiya po gasovoi khromatografii*, Kuibyshev University (in Russian), 1987, p. 24. (Collection "The IXth All-Union Conference on Gas Chromatography".)
7 A. V. Kiselev, N. V. Kovaleva and Yu. S. Nikitin, *J. Chromatogr.*, 58 (1971) 19.
8 A. V. Kiselev, D. P. Poshkus and Ya. I. Yashin, *Molecular Fundamentals of Adsorption Chromatography* (in Russian), Khimiya, Moscow, 1986, p. 154.

Journal of Chromatography, 455 (1988) 271–277
Elsevier Science Publishers B.V., Amsterdam — Printed in The Netherlands

CHROM. 20 907

LIQUID CHROMATOGRAPHIC DETERMINATION OF ALLIIN IN GARLIC AND GARLIC PRODUCTS

EMIKO MOCHIZUKI* and AKIRA NAKAYAMA
Yamanashi Institute for Public Health, 1-7-31 Fujimi, Kofu 400 (Japan)
YOSHIMI KITADA
Nara Prefectural Institute of Public Health, 57-6 Ohmori, Nara 630 (Japan)
KOICHI SAITO
Saitama Prefectural Institute of Public Health, 639-1, Kamiokubo, Urawa, Saitama 338 (Japan)
and
HIROYUKI NAKAZAWA, SUMIKO SUZUKI and MASAHIKO FUJITA
The National Institute of Public Health, Department of Pharmaceutical Sciences, 4-6-1 Shirokane-dai, Minato-ku, Tokyo 108 (Japan)
(Received August 9th, 1988)

SUMMARY

A liquid chromatographic (LC) method is proposed for the determination of alliin in garlic and garlic products. The method involves heating of the sample with water in a bath of boiling water followed by homogenization and centrifugation. Interfering components are eliminated by use of a Sep-Pak C_{18} cartridge as a clean up step before injection. The LC system with ultraviolet detection at 210 nm consists of a separation on a Zorbax TMS column and isocratic elution with water as a mobile phase. Fluorometric determination by ion-pairing chromatography with tetra-*n*-butylammonium bromide on a Nucleosil 5C_{18} column is also described. The overall recoveries of alliin added to garlic products were greater than 90%. Thin-layer chromatography and enzymatic degradation of alliin were performed for the confirmation of alliin detected in garlic products.

INTRODUCTION

Garlic (*Allium sativum L.*) has been used world-wide as a seasoning, spice and folk medicine. A recent study shows that garlic extracts inhibit platelet aggregation and smooth muscle contractions[1]. In 1981, the platelet aggregation inhibitor was identified as methyl allyl trisulphide by Ariga *et al.*[2]. Cavallito and Bailey[3] found in 1944 that allicin, an enzymatic conversion product of alliin (Fig. 1), is responsible for the antibacterial and antifungal properties of garlic.

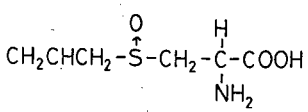

Fig. 1. Structure of alliin.

0021-9673/88/$03.50 © 1988 Elsevier Science Publishers B.V.

In Japan, garlic and garlic products have been popular in recent years as a drug and health food. There is now a need for a simple and rapid method of evaluating the quality of these products. Being a specific amine in garlic, alliin could be used as an indicator.

The current method for estimation of the alliin level in garlic employs allinase in an enzymatic method which rapidly converts alliin into allicin, ammonia and pyruvic acid. The ammonia is then measured by azotometry, pyruvic acid spectrophotometrically at 430 nm as the dinitrophenylhydrazone derivatives[4]. These methods are non-specific and time-consuming. Alliin is a primary amine exhibiting an absorption maximum at 210 nm. Thus a fluorophore derivative with fluorescamine was also investigated. Fluorescamine, a fluorophore labelling reagent, has been used for the determination of primary amines[5,6], and its effectiveness has been reported for the determination of various other compounds. This paper describes a liquid chromatographic (LC) method for the rapid and simple determination of alliin in garlic and garlic products, based on ultraviolet (UV) and fluorometric (FL) detection.

EXPERIMENTAL

Apparatus

A Model LC-2 liquid chromatograph (Shimadzu, Kyoto, Japan) equipped with a Shimadzu SPD-1 spectrophotometer operated at the wavelength of 210 nm and a Shimadzu RF-510 spectrofluorometer with excitation at 405 nm and emission at 480 nm was used.

For UV detection, the separation of alliin was performed on a Zorbax TMS (5 μm, 250 mm × 4.6 mm I.D.; DuPont, Wilmington, DE, U.S.A.) with isocratic elution using water as a mobile phase at a flow-rate of 0.5 ml/min.

For FL detection, the chromatographic column was Nucleosil $5C_{18}$ (5 μm, 250 mm × 4 mm I.D.; Macherey, Nagel & Co., Düren, F.R.G.), thermostatted at 50°C. The mobile phase used was 0.03 *M* sodium acetate (pH 7.0)–acetonitrile (66:34, v/v) with 5 m*M* tetra-*n*-butylammonium bromide, at a flow-rate of 0.5 ml/min.

Materials

Fresh garlic bulbs and garlic products were obtained commercially.

The acetonitrile and distilled water were of high-performance liquid chromatography (HPLC) grade (Wako, Osaka, Japan). Analytical grade chemicals were used unless otherwise specified. The alliin standard was donated by Wakunaga Pharmaceutical, Osaka, Japan. A 10-mg amount was weighed accurately into a 10-ml flask and diluted to volume in distilled water.

Sep-Pak C_{18} cartridges (Millipore, Bedford, MA, U.S.A.) were washed with 10 ml of methanol and then 10 ml of water before use.

Thin-layer chromatographic (TLC) plates (10 cm × 5 cm) were precoated with Silica gel 70 (Wako). The developing solvents were ethanol–25% ammonium hydroxide (63:37), *n*-propanol–25% ammonium hydroxide (67:37), chloroform–methanol–25% ammonium hydroxide (2:2:1) and *n*-butanol–acetic acid–water (3:1:1).

Allinase was prepared from fresh garlic by the method of Tsuno[7] with slight modifications as follows: 10 g of garlic were ground and homogenized with water and diluted to a volume of 100 ml. The homogenate was centrifuged at 3000 *g* for 10 min at

4°C. The supernatant was adjusted to pH 4.0 with phosphoric acid and centrifuged at 12000 *g* for 5 min at 4°C. The supernatant was discarded. The precipitate was dissolved in water, and adjusted to pH 4.0 with phosphoric acid. After centrifugation at 12000 *g* for 5 min at 4°C, the supernatant was discarded. The precipitate was dissolved in 10 ml of phosphate buffer (pH 6.4) and stored in a refrigerator.

Sample preparation

A 10-g sample was weighed in a 100-ml beaker or blender cup with addition of 40 ml hot water. After heating for 15 min in boiling water, the contents were cooled to room temperature and homogenized for 3 min. The homogenate was transferred to a volumetric flask and diluted to 100 ml in distilled water. After centrifugation at 12000 *g* for 10 min at 4°C, the supernatant was filtered through Toyo Roshi No. 5A filter-paper. A 1-ml volume of filtrate was passed through a Sep-Pak C_{18} cartridge and eluted with 8 ml distilled water and brought to a volume of 10.0 ml. The eluate was analysed directly by liquid chromatography with an ultraviolet detector at 210 nm; 10 μl of the solution were injected into the LC system. If necessary, the sample was diluted further in distilled water.

Fluorometric determination of alliin was performed as follows; 50 μl of the eluate from the Sep-Pak C_{18} cartridge were transferred to a 10-ml amber test-tube containing 2 ml of 0.2 *M* sodium borate buffer (pH 8.0), and mixed. A 200-μl volume of a solution of fluorescamine (Roche Diagnostics, Nutley, NJ, U.S.A.) in acetone (3 mg/ml) was then added and mixed well. The LC analysis was carried out with a fluorometric detector (excitation, 405 nm; emission, 480 nm).

Confirmation of alliin by TLC and enzymatic treatment

The sample solution, prepared through use of the Sep-Pak C_{18} cartridge, was evaporated to dryness below 45°C in a vacuum. The residue was dissolved in 0.5 ml of water, and applied to precoated silica gel plates. After development in different media, the plates were sprayed with 0.2% ninhydrin reagent and placed in an oven at 110°C for 10 min. Alliin was identified by comparison with the standard on the same TLC plate.

For further confirmation, enzymatic treatment was employed. A 1-ml volume of allinase solution was added to 1 ml of sample solution which had been previously analysed by LC. The pooled sample was incubated for 15 min at 37°C. The results were confirmed by the disappearance of the alliin peak on the liquid chromatogram.

RESULTS AND DISCUSSION

As alliin shows maximum UV absorption at 210 nm, UV detection was employed. The retention of alliin on different columns was examined using phosphate buffer, pH from 2.5 to 8.0, mixed with acetonitrile. A trimethylsilyl (TMS) column gave symmetrical peaks with more reasonable retention times than those on an ODS column, when water was used as a mobile phase. No significant differences between retention times and peak shapes were observed in the range pH 2.5 to 8.0. Based on preliminary studies of the chromatographic separation including interference from co-existing compounds, a Zorbax TMS column and water as a mobile phase were chosen for the UV method.

The introduction of fluorophore derivatives with fluorescamine was considered because co-existing interfering substances were found with UV detection in some liquid preparations. The optimum LC operating conditions were derived from variation of the column, column temperature and mobile phase composition. The widely used C_{18} reversed-phase column gave better resolution of the alliin–fluorescamine complex than RP-8 and TMS columns. The maximum temperature for a reasonable retention time and resolution was 50°C, when the column temperature was investigated from 25 to 55°C. The effect of the mobile phase composition on the alliin separation was investigated with different contents of acetonitrile and acetate buffer. Ion-pairing chromatography with tetra-*n*-butylammonium bromide was also studied since the alliin–fluorescamine complex possesses a carboxyl group. The effect of the sodium acetate concentration up to 50 m*M* was studied, and 30 m*M* sodium acetate buffer, pH 7.0 was employed to measure the alliin–fluorescamine complex.

As fluorescamine reacts with primary amines at pH ranging from 8.0 to 9.5, and with peptides from pH 8.0 to 8.5[8], the effect of the pH of the borate buffer was studied and a pH of 8.0 was chosen. The excitation and emission maxima for the fluorescamine–alliin reaction product were 405 and 480 nm, respectively. A fluorescamine concentration of $9.6 \cdot 10^{-4}$ *M* resulted in the maximum fluorescence intensity in the range of $1.6 \cdot 10^{-4}$–$1.3 \cdot 10^{-3}$ *M* fluorescamine against 50 μl alliin (0.1 mg/ml). The fluorophore derivatives of alliin were stable for over 9 h when kept in a dark room at room temperature.

Correlation between the two detection methods, UV and FL, for concentrations ranging from 10 to 60 μg/ml was high with a correlation coefficient, *r*, of 0.996. The detection limits with these two methods were 10 μg/ml for UV and 1 μg/ml for FL. The standard graphs were linear throughout the ranges of 10–200 μg/ml for UV and 1–1000 μg/ml for FL.

Effect of heating on alliin

Alliin is readily converted into allicin, ammonia and pyruvic acid by the enzyme in fresh plants during dropping and crushing. Thus, fresh garlic and garlic products were heated in boiling water to inactivate the enzyme. The stability of alliin to heating was studied at 100°C and it was shown to be fairly stable; the amount of alliin remaining was 94.7% after 20 min, 88.3% after 40 min and 79.4% after 60 min.

Clean up

The Sep-Pak C_{18} cartridge was examined as a rapid and easy clean-up for alliin from the extract. A 1-ml volume of alliin solution (0.5 and 2.5 mg/ml) was loaded on the prepared Sep-Pak cartridges and eluted with water. No alliin was retained on the cartridge. Even the larger amount of alliin (2.5 mg) was totally eluted from the reversed-phase cartridge; alliin was totally eluted with 6 ml water, and co-existents such as dyes were retained on the cartridge. The eluent containing tetra-*n*-butylammonium chloride did not completely separate alliin from sample coextractives. Therefore, water was chosen as the eluent for clean up.

Recovery of alliin

The recovery of alliin from selected and spiked samples is shown in Table I. The recovery from four determinations with the UV method ranged from 96.6 to 99.5%

TABLE I

RECOVERY OF ALLIIN FROM COMMERCIAL GARLIC PRODUCTS

Sample	*Added (mg/g)*	*Recovery, % (mean ± S.D.)**	
		UV	*FL*
Garlic bulbs in honey	2.5	97.8 ± 5.1	90.4 ± 3.7
Garlic bulbs in soy sauce	3.0	99.5 ± 2.4	103.3 ± 14.1
Salted bulbs	2.5	96.7 ± 4.6	
Freeze-dried powder	7.5	98.0 ± 1.4	94.9 ± 2.8
Freeze-dried tablet	6.0	99.1 ± 1.2	
Liquid formulation	7.5	96.6 ± 0.9	91.0 ± 1.3

* Average of four determinations.

with excellent precision. The recovery with the FL method ranged from 90.4 to 103.3%. The minimum detection limits for alliin were 0.5 mg/g (UV) and 0.05 mg/g (FL).

Analysis of commercial samples

The alliin contents of fresh garlic and commercial products determined by the methods proposed are shown in Table II. Alliin was found in garlic pellets, freeze-dried samples and salted products. Fresh garlic contained 4.9 mg/g alliin (coefficient of variation, C.V. = 13.8%). Other forms contained little or no alliin. Figs. 2 and 3 show typical chromatograms of commercial garlic products. Alliin was found in freeze-dried garlic powder. UV detection was simple, but susceptible to interference by compounds absorbing at 210 nm. FL detection was 10 times more sensitive and specific than UV detection.

TABLE II

CONTENTS OF ALLIIN IN GARLIC AND GARLIC PRODUCTS

Sample	*n*	*Found (mg/g)*	
		UV	*FL*
Garlic bulbs	8	4.5–6.2	4.0–6.0
Garlic bulbs in honey	5	<0.5	<0.05
Garlic bulbs in miso	1	0.6	
Garlic bulbs in mirin	1	<0.5	
Garlic bulbs in soy sauce	2	0.5–0.6	
Salted bulbs	3	0.6–0.9	
Garlic powder	2	<0.5	<0.05
Grated garlic paste	2	<0.5	<0.05
Garlic pellets	1	6.1	5.4
Freeze-dried powder	1	10.5	9.0
Freeze-dried tablet	1	3.0	2.8
Liquid formulation	2	<0.5	<0.05
Tablet formulation	1	<0.5	<0.05

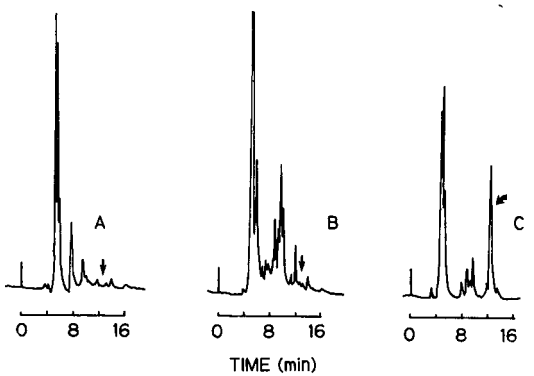

Fig. 2. Liquid chromatograms of commercial garlic products with ultraviolet (UV) detection. Arrow shows alliin peak. (A) Garlic bulbs in honey; (B) liquid formulation; (C) freeze-dried powder. Conditions: column, Zorbax TMS (250 mm × 4.6 mm I.D.); mobile phase, water; flow-rate, 0.5 ml/min.

Confirmation of alliin

TLC with several developing solvents was investigated for confirmation of alliin. Ethanol–25% ammonium hydroxide (63:37), *n*-propanol–25% ammonium hydroxide (67:33), chloroform–methanol–25% ammonium hydroxide (2:2:1) and *n*-butanol–acetic acid–water (3:3:1) gave R_F values of 0.77, 0.64, 0.20 and 0.75, respectively. By comparison of these R_F values with those of an authentic sample, TLC provided a means of confirmation of alliin.

In addition to TLC, enzymatic treatment of alliin by allinase was also studied by Tsuno's method[7]. The extract was incubated with allinase for 15 min at 37°C. This treatment resulted in the disappearance of the peak established as alliin on the LC chromatogram, as shown in Figs. 4 and 5. Alliin degradation by enzymatic treatment provided additional proof of the presence of alliin.

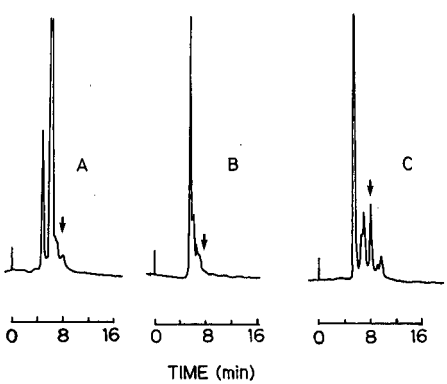

Fig. 3. Liquid chromatograms of commercial garlic products with fluorometric (FL) detection. Arrow shows alliin peak. (A) Garlic bulbs in soy sauce; (B) liquid formulation; (C) freeze-dried powder. Conditions: column, Nucleosil $5C_{18}$ (250 × 4.0 mm I.D.); mobile phase, 0.03 *M* sodium acetate (pH 7.0)–acetonitrile (66:34, v/v) with 5 m*M* tetra-*n*-butylammonium bromide; flow-rate, 0.5 ml/min; column temperature, 50°C.

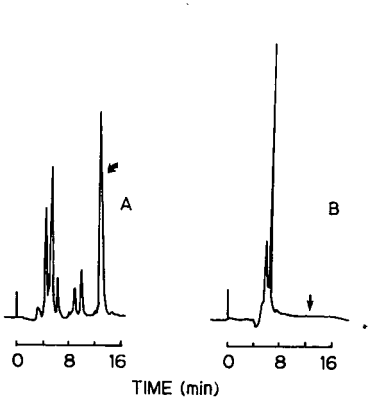

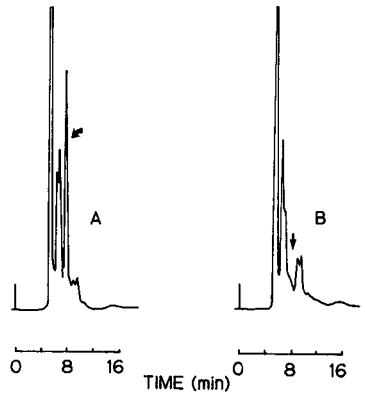

Fig. 4. Disappearance of the alliin peak in a garlic extract upon enzyme treatment (UV detection). (A) Untreated; (B) treated. Arrow shows alliin peak. Conditions: as in Fig. 2.

Fig. 5. Disappearance of the alliin peak in a commercial garlic product upon enzyme treatment (FL detection). (A) Untreated; (B) treated. Arrow shows alliin peak. Conditions: as in Fig. 3.

The data obtained from the present study indicated that the LC method for the determination of alliin was simple, straightforward and accurate. Ultraviolet detection enabled direct determination of alliin, and the FL method, based on a fluorometric derivatization, showed greater specificity and sensitivity. Both the UV and FL methods for the determination of alliin using LC are suitable for the quality assessment of garlic and garlic products. The present LC method can be applied to the other alliin containing plants of *Allium* species.

ACKNOWLEDGEMENTS

The authors thank Wakunaga Pharmaceutical for donating the alliin standard, Kazuya Nakagomi, Fermentation Research Institute for helpful suggestions and Craig Cherrie, General Assembly Library, Parliament of New Zealand for literature searching.

REFERENCES

1 J. D. Gaffen, I. A. Tavares and A. Bennet, *J. Pharm. Pharmacol.*, 36 (1984) 272–274.
2 T. Ariga, S. Oshiba and T. Tamada, *The Lancet*, i (1981) 150–151.
3 C. J. Cavallito and J. H. Bailey, *J. Am. Chem. Soc.*, 66 (1944) 1950–1954.
4 M. A. Mao and E. V. Rao, *Indian Drugs*, 20 (1982) 6–7.
5 K. Tamase, Y. Kitada, M. Mizobuchi and M. Sasaki, *Shokuhin Eiseigaku Zasshi*, 25 (1984) 525–529.
6 K. Tamase, Y. Kitada, M. Sasaki, Y. Ueda and R. Takeshita, *Shokuhin Eiseigaku Zasshi*, 26 (1985) 515–518.
7 S. Tsuno, *Vitamin*, 14 (1958) 659–664.
8 *FLURAM™ (fluorescamine) Roche (package insert)*, Roche Diagnostics, Nutley, NJ, April 1981.

Journal of Chromatography, 455 (1988) 279–289
Elsevier Science Publishers B.V., Amsterdam — Printed in The Netherlands

CHROM. 20 867

SIMULTANEOUS HIGH-PERFORMANCE LIQUID CHROMATOGRAPHIC DETERMINATION OF PROPOXYPHENE AND ACETAMINOPHEN IN PHARMACEUTICAL PREPARATIONS

TRACY L. ASCAH* and BRIAN T. HUNTER
Supelco, Inc., Supelco Park, Bellefonte, PA 16823-0048 (U.S.A.)
(First received May 2nd, 1988; revised manuscript received July 20th, 1988)

SUMMARY

A normal-phase high-performance liquid chromatographic method, using a 3.3 cm × 4.6 mm silica column (3 μm packing) and an ammonium hydroxide–methanol–dichloromethane mobile phase, has been developed to separate propoxyphene and acetaminophen in less than 5 min. Quantitative recovery of both compounds from various pharmaceutical preparations was achieved, following a single dilution scheme. The method is stable, reproducible, and selective.

INTRODUCTION

Propoxyphene (dextropropoxyphene, 1,2-diphenyl-2-propionoxy-3-methyl-4-dimethylaminobutane) is an analgesic commonly prescribed for the treatment of moderate pain. The need to quantify propoxyphene in biological fluids is brought about by its inherent addictability and the frequent occurrence of self-poisoning. The compound exists in two diastereoisomeric forms: α-*d,l* and β-*d,l*. The α-*d* isomer has analgesic properties; the α-*l* isomer has antitussive properties. The β isomers are unwanted, inactive contaminants of pharmacological preparations.

Barkan and Wainer[1] separated the α-*d* and β isomers of propoxyphene on a silica high-performance liquid chromatography (HPLC) column, using a water–isopropanol–hexane mobile phase. The content of β isomers in various commercial formulations was 0 to 0.45%. Angelo *et al.*[2] used a cyano HPLC column and an acetonitrile–methanol–10 m*M* sodium phosphate (pH 7) mobile phase to separate propoxyphene from its major metabolite, nordextropropoxyphene, in serum. The separation followed a relatively simple liquid–liquid extraction procedure. The problems associated with propoxyphene determination by gas chromatography have been discussed elsewhere[3].

Propoxyphene and acetaminophen (APAP, paracetamol, 4-acetamidophenol) are combined in various pain reliever formulations. A reliable simultaneous HPLC method for both compounds would be of interest to the manufacturers of these formulations. Such an analysis has been reported[4], but we could not reproduce the separation in our laboratory. Our goal was to separate propoxyphene and

0021-9673/88/$03.50 © 1988 Elsevier Science Publishers B.V.

acetaminophen by isocratic elution in a short analyis time, while resolving the drugs from impurities and tablet excipients. The method should also yield good recoveries from dosage forms.

EXPERIMENTAL

Chemicals and reagents

All solvents were of HPLC grade and obtained from Accusolv Anachemia (Champlain, NY, U.S.A.). Deionized water was prepared in-house (Milli-Q system, Millipore, Milford, MA, U.S.A.). Reagent-grade concentrated ammonium hydroxide and HPLC-grade potassium dihydrogenphosphate were purchased from Fisher Chemical (Fair Lawn, NJ, U.S.A.). Triethylamine was obtained from Kodak (Rochester, NY, U.S.A.).

The acetaminophen and/or propoxyphene content was determined for the following dosage forms obtained from a local pharmacy: Darvon-N® (100 mg propoxyphene napsylate, Eli Lilly & Co.), Darvocet-N® 100 (100 mg propoxyphene napsylate, 650 mg acetaminophen, Lilly), and generic propoxyphene N 100 APAP (100 mg propoxyphene napsylate, 650 mg acetaminophen).

Propoxyphene hydrochloride standard (United States Pharmacopeia, Rockville, MD, U.S.A.) was dried at 105°C for 3 h prior to use. Acetaminophen standard and the acetaminophen-related compounds, *p*-nitrophenol, *p*-hydroxyacetophenone, and 4-aminophenol, were obtained from Sigma (St. Louis, MO, U.S.A.).

Chromatographic system

The chromatographic system employed an HP-1090 liquid chromatograph (Hewlett-Packard, Avondale, PA, U.S.A.) equipped with an autosampler, column oven, HP-85B system controller, HP-3392A integrator/recorder, and a HP 1040A diode array detector set at 220 or 244 nm UV with a response time of 160 ms. All Supelcosil® HPLC columns (3.3 cm × 4.6 mm I.D., 3-μm packings) were obtained from Supelco, Bellefonte, PA, U.S.A. Analytical columns were protected by guard columns (2 cm × 4.6 mm I.D., 5-μm packings) containing the same phase. In some experiments, small-bore (3.3 cm × 2.1 mm I.D.) columns packed with 3-μm silica were used to conserve mobile phase.

Chromatography

The standard stock solution for construction of the calibration curve was prepared by dissolving 10 mg propoxyphene and 100 mg acetaminophen in 2 ml of methanol in a 50-ml volumetric flask and diluting to the mark with dichloromethane. This stock solution was quantitatively diluted in mobile phase to yield six solutions ranging from 20 to 80 μg/ml propoxyphene and 200 to 800 μg/ml acetaminophen. These solutions bracketed the concentrations of the drugs in the final dilution from the dosage forms. Calibration curves for each compound were generated by making triplicate 10-μl injections of each of the standard solutions. Average peak area or height was plotted versus concentration.

One Darvocet-N 100 tablet, generic propoxyphene N 100 APAP tablet, or Darvon capsule was added to each of six 100-ml volumetric flasks. A 10-ml volume of methanol and 80 ml of dichloromethane were added to each flask. The solutions were

sonicated for 5 min and, after cooling to room temperature, diluted to the mark with dichloromethane. These solutions were quantitatively diluted 2/25 in mobile phase to yield solutions of 520 μg/ml acetaminophen and/or 52 μg/ml propoxyphene.

Average peak area or height was obtained from triplicate 10-μl injections of final tablet or capsule dilutions. Recovery of the active ingredient (percentage of label claim) was obtained by interpolating the calibration curves.

In addition, three acetaminophen decomposition products or synthesis precursors (*p*-nitrophenol, *p*-hydroxyacetophenone and 4-aminophenol) were investigated for possible interference with the drug analysis. Interference from dosage form excipients was also investigated.

The mobile phase for analysis on silica HPLC columns consisted of ammonium hydroxide in methanol (3.33%, v/v)–dichloromethane (1.5:98.5). It is important to store all reagents and solvents at the same temperature, prior to mixing, to prevent volume/temperature effects.

Retention behavior of propoxyphene and acetaminophen was studied on silica, cyano and diol polar phases under various mobile phase conditions. After establishing a suitable HPLC method, changes in retention of propoxyphene and acetaminophen over time, with increasing mobile phase volume, were investigated to evaluate the stability of the system. In some experiments, the mobile phase was recycled by inserting the outlet from the detector into the solvent reservoir, after approximately ten column-volumes had passed through the system. Small-bore columns were used in this portion of the experiment to reduce mobile phase consumption. Reproducibility of the analysis was investigated by using a total of five columns representing three lots of silica.

RESULTS AND DISCUSSION

Assay procedure

Propoxyphene and acetaminophen were separated isocratically in less than 5 min on a 3.3-cm column containing 3-μm silica using ammonium hydroxide in methanol (3.33%, v/v)–dichloromethane (1.5:98.5) as the mobile phase. Typical chromatograms showing the two compounds extracted from commercial tablets are shown in Fig. 1. The sample solvent must contain at least 1.5% methanol to maintain

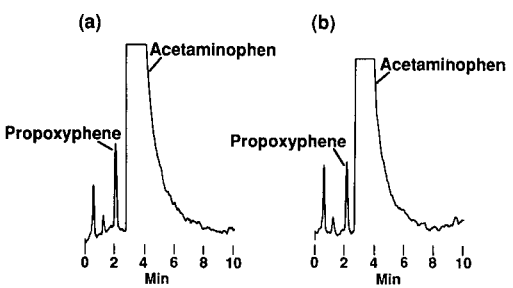

Fig. 1. Drug analysis on silica. Column: 3.3 cm × 4.6 mm Supelcosil LC-Si (3-μm packing) with guard column, mobile phase ammonium hydroxide in methanol (3.33%, v/v)–dichloromethane (1.5:98.5), 2 ml/min, 30°C, detection 244 nm 0.004 a.u.f.s., 10-μl injection volume (52 μg/ml propoxyphene, 520 μg/ml acetaminophen). (a) Darvocet-N 100 extract; (b) generic propoxyphene N 100 APAP extract.

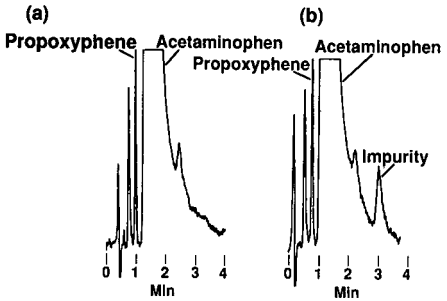

Fig. 2. Drug analysis on silica. Conditions: as in Fig. 1 except mobile phase ammonium hydroxide in methanol (1.67%, v/v)–dichloromethane (3:97). (a) Darvocet-N 100 extract; (b) generic propoxyphene N 100 APAP extract.

solubility of acetaminophen, but no more than 2.5% methanol to prevent interference of the solvent front with the propoxyphene peak. By increasing the amount of methanol in the mobile phase, an unidentified peak was revealed in the generic formulation that was not detected in the Darvocet-N 100 formulation (Fig. 2).

Extraction of propoxyphene and acetaminophen from various commercial formulations was complete and without interference from excipients. Recovery data for both compounds are given in Table I. Propoxyphene and acetaminophen response was linear for both peak height and area *versus* concentration over the investigated concentration ranges. Despite the wide disparity between propoxyphene and acetaminophen concentrations in the dosage forms, the linear acetaminophen response at high levels ensured the drugs could be simultaneously assayed through a single dilution scheme. Calibration curve data for acetaminophen and propoxyphene are given in Table II.

The normal-phase analysis is sensitive. At 244 nm UV the limits of detection were 25 and 1 ng, on-column quantities of propoxyphene and acetaminophen, respectively, with a signal-to-noise ratio of 2:1.

None of the acetaminophen-related compounds interfered with propoxyphene or acetaminophen quantification. *p*-Nitrophenol elutes in 0.71 min, *p*-hydroxyacetophenone in 0.72 min, and 4-aminophenol in 1.03 min. Two unidentified impurities in the acetaminophen preparations elute at 1.05 and 1.85 min. Impurities in acetaminophen preparations have been studied by others[5,6].

TABLE I

RECOVERY OF PROPOXYPHENE AND ACETAMINOPHEN FROM DOSAGE FORMS

Preparation	*Recovery (%)*	
	Propoxyphene	*Acetaminophen*
Darvocet-N 100	96.7 ± 4.8%	102.4 ± 1.7%
Propoxyphene N 100 APAP	92.2 ± 2.2%	102.0 ± 0.9%
Darvon	105.4 ± 4.2%	–

TABLE II

STANDARD PEAK AREA OR PEAK HEIGHT *VS.* CONCENTRATION CURVES FOR PROPOXYPHENE AND ACETAMINOPHEN UNDER VARIOUS CONDITIONS

$y = mx + b$; r = coefficient of correlation.

Compound	*Concentration range (μg/ml)*	*r*	*m*	*b*
Propoxyphene	20–160	0.9988	750 area counts/(μg/ml)	−3137 area counts
	20–80	0.9988	0.03889 cm/(μg/ml)	0.283 cm
Acetaminophen	200–800	0.9992	58083 area counts/(μg/ml)	$-1.29 \cdot 10^6$ area counts

TABLE III

RETENTION OF ACETAMINOPHEN AND PROPOXYPHENE ON NORMAL-PHASE COLUMNS IN VARIOUS MOBILE PHASES

k' = Capacity factor.

Column	*Mobile phase*	$k'_{Propoxyphene}$	$k'_{Acetaminophen}$
Diol	Isopropanol–hexane (60:40)	>20	0.14
	Isopropanol–hexane (72:28)	>20	0.10
	Ethylacetate–hexane (35:65)	>20	>20
	Dichloromethane	>20	3.5
	Dichloromethane–tetrahydrofuran (99:1)	1.1	–
	Water–methanol–dichloromethane (0.1:0.5:99.4)	0.25	1.5
	Water–methanol–dichloromethane (0.1:0.5:99.4) + 0.05% ammonium hydroxide	0	1.4
Cyano	Isopropanol–hexane (60:40)	0	0.1
	Isopropanol–hexane (50:50)	2.7	–
	Isopropanol–hexane (50:50) + 2% tetrahydrofuran	3.4	0.18
	Isopropanol–hexane (20:80) + 0.02% ammonium hydroxide	>20	1.6
	Isopropanol–hexane (20:80) + 0.01 ammonium hydroxide	>20	0.25
	Dichloromethane	>20	>20
	Water–methanol–dichloromethane (0.1:0.5:99.4)	>20	>20
	Methanol–dichloromethane (1.5:98.5) + 0.05% ammonium hydroxide	0	0
	Acetonitrile–dichloromethane (2.5:97.5) + 0.05% ammonium hydroxide	3.7	12.0
Silica	Isopropanol–hexane (25:75)	0	0.1
	Isopropanol–hexane (10:90)	0	5.9
	Dichloromethane	>20	–
	Acetonitrile–dichloromethane (2:98) + 0.05% ammonium hydroxide	>20	>20
	Isopropanol–dichloromethane (2:98) + 0.05% ammonium hydroxide	>20	>20
	Methanol–dichloromethane (2:98) + 0.02% triethylamine	>20	5.1
	Methanol–dichloromethane (2:98) + 0.2% triethylamine	>20	10.8
	Methanol–dichloromethane (2:98) + 0.05% ammonium hydroxide	2.6	7.1
	Methanol–dichloromethane (1.5:98.5) + 0.05% ammonium hydroxide	5.2	10.0

Investigation into retention mechanism

Retention behavior of propoxyphene and acetaminophen on silica, cyano and diol polar phase columns under various mobile phase conditions is summarized in Table III. The mobile phase chosen for separating propoxyphene and acetaminophen on a silica column was too strong for use with a cyano column. Substituting acetonitrile for the methanol, however, resulted in satisfactory separation on the cyano column. Peak shapes obtained on the cyano column, however, were not as good as those obtained on the silica column, and equilibration time was too long. Further experimentation on the cyano column was not pursued. Mobile phase conditions for the simultaneous analysis of both drugs on a diol column could not be found.

The effect of changes in the ammonium hydroxide concentration on retention of the two drugs on silica and cyano columns is shown in Fig. 3. Ammonium hydroxide was needed in the mobile phase to elute propoxyphene, a tertiary amine, from the silica

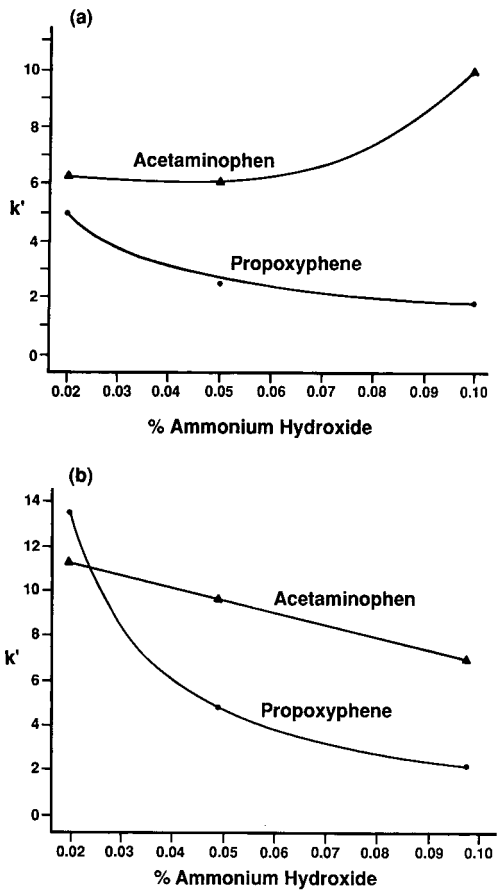

Fig. 3. Retention of propoxyphene and acetaminophen as a function of ammonium hydroxide concentration in mobile phase. (a) Silica column, mobile phase ammonium hydroxide in methanol (1–5%)–dichloromethane (2:100); (b) cyano column, mobile phase ammonium hydroxide in acetonitrile (0.8–4%)–dichloromethane (2.5:97.5).

column. Without ammonium hydroxide, 7% methanol in dichloromethane was required for elution of propoxyphene from a silica column. Acetaminophen, however, was not retained under these conditions. By adding a small amount of ammonium hydroxide to the mobile phase, the percentage of methanol could be decreased and both drugs analyzed simultaneously. Concentrations of 1.5% methanol and 0.05% ammonium hydroxide in dichloromethane produces good k' values and sharp, symmetrical peaks for both drugs.

On the silica column, ammonium hydroxide forms strong hydrogen bonds with surface silanols. Thus, increasing its concentration decreases the number of silanols available for binding of the weakly basic propoxyphene. This decreases the retention of propoxyphene while also improving peak shape.

Acetaminophen, a weak acid, and ammonium hydroxide undergo ion-pair interaction forming a complex that can undergo weak hydrogen bonding with the surface silanols. For a complete treatment of silanol interaction see Unger[7].

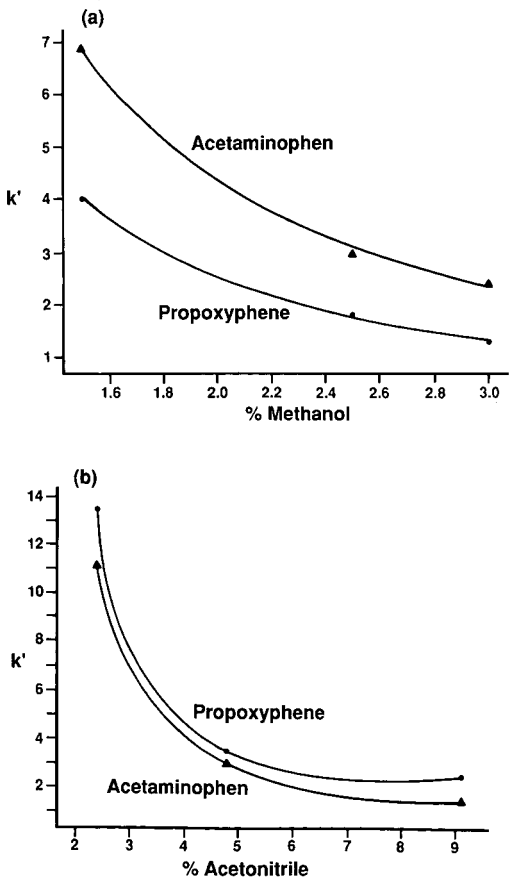

Fig. 4. Retention of propoxyphene and acetaminophen as a function of polar organic modifier concentration in mobile phase. (a) Silica column, mobile phase 1.5–3% methanol in dichloromethane, 0.05% ammonium hydroxide; (b) cyano column, mobile phase 2.4–9.1% acetonitrile in dichloromethane, 0.02% ammonium hydroxide.

We also established that propoxyphene would not elute from a silica column if triethylamine and water (to promote ionization of the triethylamine) replaced the ammonium hydroxide in the mobile phase. The use of ionic eluents as mobile phase additives, for analysis of basic compounds on unmodified silica, has been studied elsewhere[3,8,9].

While hydrogen bonding is the dominant mechanism in retention by unmodified silica, dipole interactions become important with cyano-modified silica in a normal-phase mode of operation (non-aqueous environment). With the cyano-bonded phase, however, interaction with residual silanols can also occur. These silanols have high polarity relative to the nitrile moieties of the bonded phase. It is therefore likely that the change in retention with increasing ammonium hydroxide concentration seen for both drugs is due mostly to the effect of ammonium hydroxide on the activity of the residual silanols.

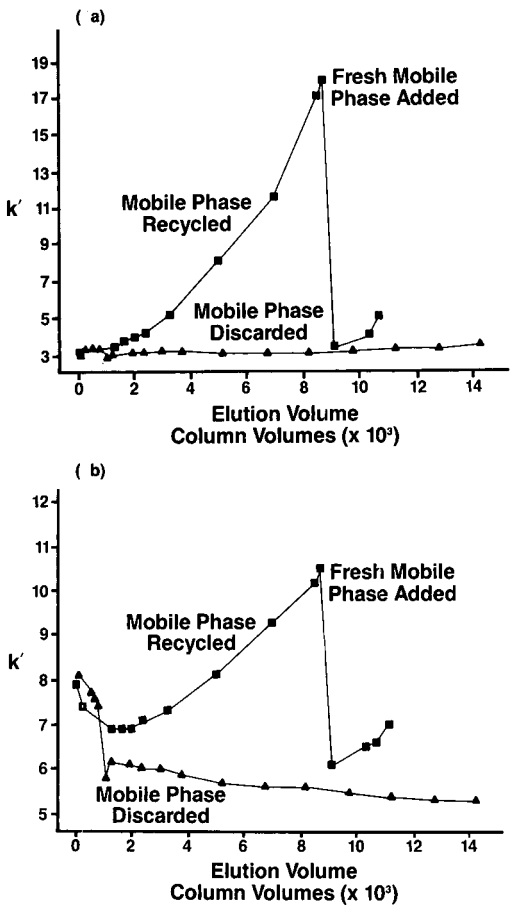

Fig. 5. Effect of mobile phase volume passed through column on retention of (a) propoxyphene and (b) acetaminophen by silica column. Mobile phase: ammonium hydroxide in methanol (3.33%)–dichloromethane (1.5:98.5).

The effect of varying the polar organic modifier (methanol or acetonitrile) concentration is shown in Fig. 4. As expected, both propoxyphene and acetaminophen retention decreased with increasing competing organic modifier concentration. This behavior is consistent with a normal-phase mechanism on both the silica and cyano columns (see ref. 10). Methanol was a stronger polar modifier than isopropanol and acetonitrile for elution of both acetaminophen and propoxyphene from the silica column.

Stability of retention

Changes in retention of acetaminophen and propoxyphene on a 3-μm silica column as a function of number of column volumes of mobile phase passed through the column can be seen in Fig. 5. Mobile phase leaving the column was either discarded (conventional) or recycled. The baseline usually stabilized within ten column volumes (5–10 ml) for a new column.

With mobile phase pumped in the conventional mode, acetaminophen shows a rapid decrease in retention over the first 200 column volumes (100 ml), and a shallow but steady decrease thereafter. Retention of propoxyphene changes only slightly. The drift in retention of acetaminophen does not adversely affect its resolution from propoxyphene for at least 10 000 column volumes (Fig. 6). This represents 48 h of continuous use, or 1000 analyses.

Recycled and conventional mobile phase operation yields similar retention for acetaminophen and propoxyphene over the first 200 column volumes. After this volume of recycled mobile phase, retention for both compounds increases steadily, leading to coelution and peak reversal at about 4000 column volumes. The separation could be returned to normal by pumping fresh mobile phase through the column (Figs. 5 and 6).

An apparent drawback to mobile phase recycling is the gradual loss of transmission of UV light through the detector cell. Flushing the cell with methanol will restore the output, but the baseline may take a great deal of time to restabilize. Flushing the column with methanol does not hasten the stabilization of the baseline.

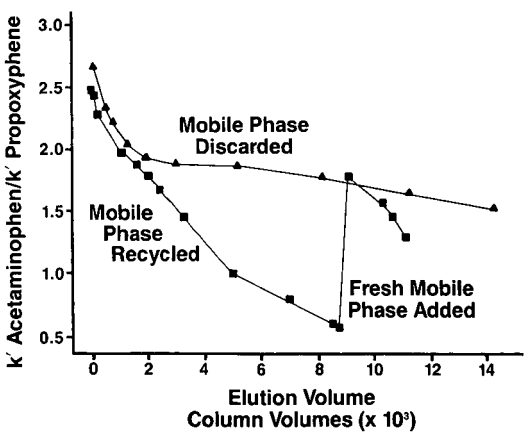

Fig. 6. Effect of mobile phase volume passed through column on separation factor on silica column. Mobile phase: ammonium hydroxide in methanol (3.33%)–dichloromethane (1.5:98.5).

TABLE IV

REPRODUCIBILITY OF NORMAL PHASE ANALYSIS FOR PROPOXYPHENE AND ACETAMINOPHEN

Column: 3.3 cm × 4.6 mm silica, 3-μm packing; mobile phase: ammonium hydroxide in methanol (3.33%, v/v)–dichloromethane (1.5:98.5); flow-rate: 2.0 ml/min.

Silica lot and column number	*k'*					
	Propoxyphene			*Acetaminophen*		
	Initial	*After 0.2 l mobile phase*	*After 1 l mobile phase*	*Initial*	*After 0.2 l mobile phase*	*After 1 l mobile phase*
Lot A, column 1 (recycled mobile phase)	4.0	4.0	4.0	10.2	9.0	7.8
Lot B, column 2	3.7	3.7	3.6	9.8	8.8	7.5
Lot B, column 3	3.8	3.8	3.6	10.4	9.6	6.9
Lot B, column 4 (recycled mobile phase)	3.8	3.7	3.7	9.8	8.6	7.3
Lot C, column 5	5.7	4.0	3.9	11.6	8.4	7.4

Decreased detector output was also seen when stagnant mobile phase was left in the detector cell (in both normal and recycled modes).

Reproducibility

The normal-phase separation we developed was reproduced on five columns, representing three silica lots, without the need for mobile phase adjustment. Table IV shows the k' values obtained initially, after 200 ml, and after 1 l of mobile phase had passed through the column. Capacity factors were consistent from column-to-column and lot-to-lot. Column 5 from Lot C showed initially higher k' values for both compounds, but after a short equilibration time (10 column volumes), became consistent with the other columns.

CONCLUSION

A method to simultaneously quantify propoxyphene and acetaminophen from dosage forms has been developed. The system employs a 3.3 cm × 4.6 mm column containing 3-μm silica, and an ammonium hydroxide in methanol (3.3%, v/v)–dichloromethane mobile phase (1.5:98.5). The method has been shown to be stable, sensitive and reproducible.

REFERENCES

1 S. Barkan and I. W. Wainer, *J. Chromatogr.*, 240 (1982) 547.
2 H. R. Angelo, T. Kranz, J. Strøm, B. Thisted and M. B. Sørensen, *J. Chromatogr.*, 345 (1985) 413.
3 R. K. Gilpin, J. A. Korpi and C. A. Janicki, *J. Chromatogr.*, 107 (1975) 115.
4 S. Sa'sa, A. Rashid and I. Jalal, *Talanta*, 31 (1984) 397.
5 W. R. Sisco, C. T. Rittenhouse and L. A. Everhart, *J. Chromatogr.*, 348 (1985) 253.
6 W. R. Sisco, C. T. Rittenhouse, L. A. Everhart and A. M. McLaughlin, *J. Chromatogr.*, 354 (1986) 355.

7 K. K. Unger, *Porous Silica (Journal of Chromatography Library*, Vol. 16), Elsevier, Amsterdam, 1979, pp. 57–146.
8 R. J. Flanagan and I. Jane, *J. Chromatogr.*, 323 (1985) 173.
9 I. Jane, A. McKinnon and R. J. Flanagan, *J. Chromatogr.*, 323 (1985) 191.
10 L. R. Snyder and J. J. Kirkland, *Introduction to Modern Liquid Chromatography*, Wiley, New York, 2nd ed., 1979, pp. 246–268.

Journal of Chromatography, 455 (1988) 291–296
Elsevier Science Publishers B.V., Amsterdam — Printed in The Netherlands

CHROM. 20 859

PURIFICATION OF PHOSPHOFRUCTOKINASE USING TRANSITION-STATE ANALOGUE AFFINITY CHROMATOGRAPHY

S. P. J. BROOKS and K. B. STOREY*

Institute of Biochemistry and Department of Biology, Carleton University, Ottawa, Ontario K1S 5B6 (Canada)

(First received May 16th, 1988; revised manuscript received August 1st, 1988)

SUMMARY

A novel purification of phosphofructokinase has been achieved in a two step process using ion-exchange affinity chromatography and a transition-state analogue affinity column matrix. The procedure can be performed in one day, and gives a 25% yield of the starting material. The transition-state analogue chromatography is carried out using an ADP-agarose column in the presence of fructose 6-phosphate, magnesium ions and nitrate ions. In the presence of nitrate ion plus substrate, phosphofructokinase binds immobilized ADP while other proteins pass through the column. Previous studies with creatine kinase have shown that the nitrate ion mimics the planar phosphate in the transition state resulting in a complex which is stable under the relatively high ionic strength of the column buffer. This permits the elution of phosphofructokinase in a single peak of high specific activity. This column typically results in a 20–30 fold increase in specific activity with only a small loss of activity.

INTRODUCTION

Phosphofructokinase (PFK) can exist in several different states *in vivo* depending on the degree of enzyme polymerization and subunit phosphorylation. Both these factors regulate the enzyme's kinetic activity with the polymerized enzyme having a higher activity[1–3], and the phosphorylated enzyme having a lower activity, although this has only been unequivocally demonstrated in lower vertebrates and invertebrates[4–7]. In order to investigate the importance of these effects on PFK catalytic activity it is necessary to analyze the purified enzyme under various *in vitro* conditions. Because of the known instability of the enzyme during purification it is important to devise purification schemes which incorporate the least number of steps, and which can be performed in the shortest amount of time. The present paper presents a rapid purification of PFK which requires only two chromatography steps and two polyethylene glycol precipitations. The procedure can be completed in a single day minimizing losses due to inherent enzyme instability. The protocol represents an extension of previous work on kinase transition states which indicated that nitrates could mimic planar phosphate groups in the transition state allowing a stable complex to form between substrate, ADP and nitrate ion[8,9].

0021-9673/88/$03.50 © 1988 Elsevier Science Publishers B.V.

MATERIALS AND METHODS

Animals, tissues and chemicals

Turtles (*Pseudymes scripta*) were obtained from Carolina Biological Supply Company (Burlington, NC, U.S.A.) and kept in dechlorinated water at 10–14°C. Tissues were removed within one minute after decapitation, frozen in liquid nitrogen, and stored at −80°C until use. All chemicals were obtained from Sigma (St. Louis, MO, U.S.A.) or Boehringer-Mannheim (Montreal, Canada) and were of the highest quality available.

Enzyme and protein assays

All enzyme activities were performed at pH 7.0 in 50 m*M* imidazole buffer containing 50 m*M* potassium chloride, 5 m*M* magnesium chloride and 2 m*M* potassium phosphate at 20°C. PFK was assayed in the presence of 0.5 m*M* MgATP, 4 m*M* fructose 6-phosphate, 15 m*M* ammonium chloride, 0.15 m*M* NADH, and 1 IU each of aldolase, triose phosphate isomerase, and α-glycerol phosphate dehydrogenase. Adenylate kinase activity was assayed using 1 m*M* MgATP, 2 m*M* AMP, 5 m*M* phospho(enol)pyruvate, 0.15 m*M* NADH, and 1 IU of lactate dehydrogenase and pyruvate kinase. Phosphoglucose isomerase activity was assayed using 10 m*M* fructose 6-phosphate, 0.15 m*M* NADH, and 1 IU of glucose 6-phosphate dehydrogenase. Reactions were monitored by following NADH disappearance at 340 nm using a Gilford Model 240 spectrophotometer.

Protein concentration was determined by the change in absorbance at 280 nm (DEAE-Sephadex G-25 column chromatography), by the Bio-Rad protein assay kit (Coomassie Blue G-250 dye-binding method[10]), or by measuring the reaction with *o*-phthalaldehyde[11]. Bovine serum albumin was used as the standard for all protein measurements.

Purification of phosphofructokinase

All steps of the purification were performed at 22°C.

Crude homogenate. Approximately 0.4 g of tissue was homogenized with 4 volumes of homogenization buffer [50 m*M* imidazole, pH 7.0, 30 m*M* β-mercaptoethanol, 5 m*M* EDTA, 5 m*M* EGTA, 100 m*M* sodium fluoride, 1 m*M* phenylmethylsulfonyl fluoride (PMSF)], and centrifuged at 16 000 *g* for 10 min.

First polyethylene glycol (PEG) precipitation. The supernatant from the previous step was made up to 11% (w/v) PEG 8000 and mixed at room temperature for 20 min. The suspension was centrifuged at 12 000 *g* and the pellet was resuspended by adding 0.5 ml of buffer A (20 m*M* potassium phosphate, pH 7.2, 1 m*M* EDTA, 5 m*M* β-mercaptoethanol, 1 m*M* fructose 6-phosphate, 30 m*M* sodium fluoride) to the pellet and gently homogenizing.

DEAE Sephadex G-50 chromatography. The resuspended pellet from step 2 was loaded on a 1.5-ml DEAE-Sephadex G-50 column pre-equilibrated with buffer A. The column was washed with 20 ml buffer A, and developed with a 15-ml 0–0.6 *M* phosphate gradient in buffer A (see Fig.1). Fractions of 1 ml were collected, and the tubes with specific activity greater than 2 IU/mg were pooled.

Second PEG precipitation. The pooled fractions from step 3 were made up to 20% (w/v) PEG, mixed 20 min, and centrifuged for 20 min at 16 000 *g*. The supernatant

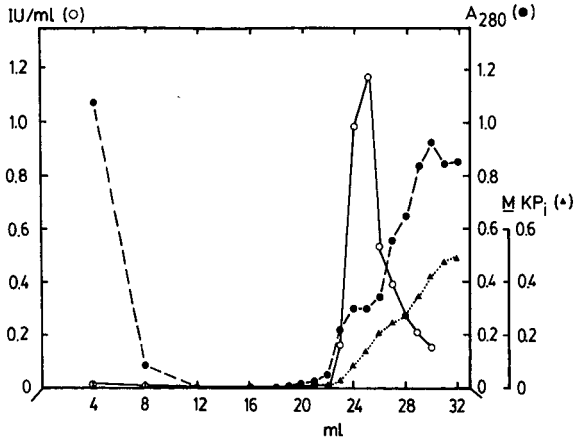

Fig. 1. DEAE Sephadex G-50 column chromatography of turtle white muscle PFK. The resuspended pellet from step 2 was loaded on a 1.5-ml DEAE-Sephadex G-50 column previously equilibrated with buffer A. The column was washed with 20 ml of buffer A to elute non-bound protein. After the column eluent was free of contaminating protein ($A_{280} = 0$), the column was developed with a 15-ml gradient of 0–0.6 *M* potassium phosphate at pH 7.2 in buffer A (▲). Fractions of 1 ml were collected and analysed for protein (A_{280}, ●), and PFK activity (○). Analysis of adenylate kinase and phosphoglucomutase activity indicated that these enzyme activities did not bind to the column matrix (data not shown).

was discarded and the pellet resuspended in 0.5 ml of buffer B [20 m*M* 4-(2-hydroxyethyl)-1-piperazimethanesulphonic acid (HEPES), pH 8, 25 m*M* β-mercaptoethanol, 30 m*M* potassium nitrate, 2 m*M* magnesium chloride, 10 m*M* fructose 6-phosphate].

ADP-agarose affinity chromatography. The enzyme was then loaded on a 1 ml ADP-agarose column (adenosine 5′-diphosphate agarose, Sigma No. 4398, attached through the N^6-amino group) which was pre-equilibrated in buffer B. The column was washed with 15 ml of buffer B and developed with a 15 ml of 0–5 m*M* MgATP gradient. Fractions of 0.5 ml were collected and those with a specific activity greater than 100 IU/mg were pooled.

Concentration and storage of the enzyme. The final enzyme was placed in a dialysis bag, concentrated against solid sucrose and dialyzed against 500 ml of stabilization buffer (SB) (40 m*M* potassium phosphate, pH 7.0, 10 m*M* β-mercaptoethanol, 0.1 m*M* EDTA, 2% (v/v) glcerol). The final enzyme is stored in SB plus 6 m*M* fructose 6-phosphate. Note that the final enzyme is unstable and looses activity quickly, even when stored at 4°C. Consequently, it should not be stored for periods greater than one week.

RESULTS AND DISCUSSION

Table I shows the results of a typical purification of PFK from turtle white muscle. The enzyme was purified approximately 240 fold and the final specific activity is similar to that reported for other PFK enzymes isolated from other animal tissues[12–15].

The procedure presented in this paper can also be used to purify PFK isozymes from other turtle tissues. For example, both turtle heart and turtle brain PFK were

TABLE I

PURIFICATION OF PHOSPHOFRUCTOKINASE FROM TURTLE WHITE MUSCLE

Enzyme was isolated from approximately 0.43 mg white muscle tissue.

Stage	*Total protein (mg)*	*Total activity (IU)*	*Specific activity (IU/mg)*	*Yield (%)*	*Purification (fold)*
Crude	17.5	7.72	0.44	100	1
PEG pellet No. 1	14.7	6.65	0.45	86	1
DEAE-Sepharose G-25 peak fractions	0.85	5.99	7.05	78	16
PEG pellet No. 2	0.40	3.57	8.93	46	21
ADP-Agarose peak fractions	0.012	1.352	112.67	18	256
Concentated enzyme	0.010	1.063	106.30	14	242

purified to similar specific activities (150 and 95 IU/mg respectively) by using the protocol outlined in this paper. It was important to increase the fructose 6-phosphate concentration to 30 m*M* and decrease the potassium nitrate concentration to 25 m*M* when purifying these latter isozymes because a large proportion of these enzymes did not bind to the column when a lower concentration of fructose 6-phosphate was used. The requirement for increased fructose 6-phosphate concentrations reflects the different kinetic constants for these two isozymes; both turtle brain and turtle heart PFK have K_m values which are 5–10 fold higher than that measured for the muscle isozyme. Since the ADP-agarose column functions by binding PFK through the active site, the concentration of fructose 6-phosphate in buffer A must be changed to compensate for this fact.

It was important to include sodium fluoride and EDTA in both the homogenization buffer and buffer A to prevent any changes in the phosphorylation state of the enzyme during the purification procedure. Sodium fluoride is a potent competitive inhibitor of alkaline phosphatase and EDTA removes Mg^{2+}, a necessary component of protein kinase reactions. The rapidity of the procedure helps to minimize the modifications which may occur during isolation, as does the addition of PMSF to the initial homogenization medium.

The graph of Fig. 1 shows the elution profile of PFK from the DEAE-Sephadex G-50 column. This step resulted in an approximately 16-fold purification of the enzyme, with 75% of the enzyme recovered in a single peak (see Table I). Before applying the peak fractions from the DEAE column to the ADP-agarose column, it is necessary to precipitate the enzyme with PEG. This step serves to concentrate the enzyme so that it may be resuspended in a small amount of buffer B at a relatively low phosphate concentration. Thus, if the DEAE peak fractions are simply brought up to 10 m*M* fructose 6-phosphate and 30 m*M* potassium nitrate in buffer A, the enzyme does not bind to the ADP-agarose column.

Elution of PFK from the ADP-agarose column is accomplished with a 0–5 m*M* MgATP gradient (Fig. 2). The enzyme elutes at a MgATP concentration of 0.1 m*M* (a value which reflects the K_m value for MgATP of 30 μM). The specific activity of the enzyme is closely monitored at this point so that only pure enzyme is collected. Note that the first fraction containing activity has contaminating protein and is usually discarded.

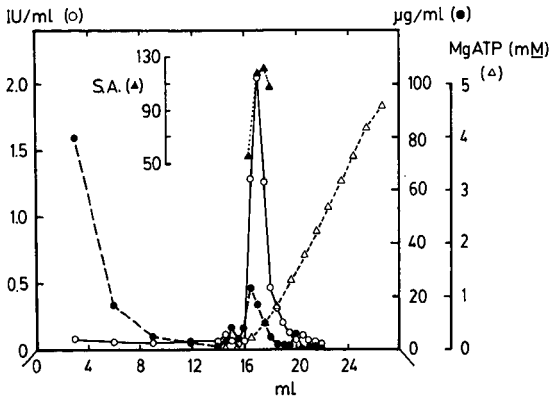

Fig. 2. ADP–agarose column chromatography of turtle white muscle PFK. The second PEG precipitate was resuspended in 0.5 ml buffer B and loaded on a 1-ml ADP-agarose column previously equilibrated in buffer B. The column is washed with buffer B until no further protein is washed from the column (approximately 15 ml). The column is then developed with a 15-ml 0–5 m*M* MgATP gradient in buffer B. Fractions of 0.5 ml are collected and monitored for protein concentration (*o*-phthalaldehyde method) and activity. Only fractions with a high specific activity are collected.

The protocol for the transition state analogue affinity chromatography step can be modified to enable one to purify several different enzymes which have ATP as one of their substrates. The principal of the column procedure was initially developed for creatine kinase[9] and is based on initial work by Milner-White and Watts[8] who demonstrated that a transition state analogue could be formed if ADP, substrate, and potassium nitrate are incubated together at an appropriate pH value. The nitate anion mimics a planar phosphate in the transition state and serves to bridge the ADP and substrate, forming a relatively stable (and highly specific) complex. The specificity of the column allows one to selectively purify different enzymes by adding excess of specific substrates and, as such, can be considered a general tool for purifying a number of different kinase molecules.

ACKNOWLEDGEMENT

This work was supported by an NSERC (Canada) grant to KBS and an NSERC (Canada) post-doctoral fellowship to S.P.J.B.

REFERENCES

1 G. D. Reinhart and H. A. Lardy, *Biochemistry*, 19 (1980) 1477.
2 G. D. Reinhart and H. A. Lardy, *Biochemistry*, 19 (1980) 1491.
3 L. Bosca, J. J. Aragon and A. Sols, *J. Biol. Chem.*, 260 (1985) 2100.
4 M. A. Luther and J. C. Lee, *J. Biol. Chem.*, 261 (1986) 1753.
5 K. B. Storey, *J. Biol. Chem.*, 262 (1987) 1670.
6 M. S. Rahman and K. B. Storey, *J. Comp. Physiol. B*, 157 (1988) 813.
7 K. B. Storey, *Arch. Biochem. Biophys.*, 235 (1984) 665.
8 E. J. Milner-White and D. C. Watts, *Biochem. J.*, 122 (1971) 727.
9 S. P. J. Brooks, V. D. Bennett and C. H. Suelter, *Anal. Biochem.*, 164 (1987) 190.

10 M. M. Bradford, *Anal. Biochem.*, 72 (1976) 248.
11 G. L. Peterson, *Methods Enzymol.*, 91 (1983) 95.
12 K. B. Storey, *Methods Enzymol.*, 90 (1982) 39.
13 E. M. Sale and R. M. Denton, *Biochem. J.*, 232 (1985) 897.
14 C. R. Hussey, P. F. Liddle, D. Ardon and G. L. Kellett, *Eur. J. Biochem.*, 80 (1977) 497.
15 J. A. Starling, B. L. Allen, M. R. Kaeini, D. M. Payne, H. J. Blytt, H. W. Hofer and B. G. Harris, *J. Biol. Chem.*, 257 (1982) 3795.

Journal of Chromatography, 455 (1988) 297–300
Elsevier Science Publishers B.V., Amsterdam — Printed in The Netherlands

CHROM. 20 911

Note

Damage to gas chromatographic columns caused by peroxides in liquid chromatographic eluents for coupled liquid chromatography–gas chromatography

KONRAD GROB*
Kantonales Labor, P.O. Box, CH-8030 Zürich (Switzerland)
and
ZHANGWAN LI
West China University of Medical Sciences, Chengdu, Sichuan (China)
(Received August 18th, 1988)

We wish to report a technical problem encountered when working with coupled liquid chromatography–gas chromatography that considerably hindered us. Using diethyl ether as an LC eluent, we repeatedly observed that apolar, polysiloxane-coated GC capillary columns were ruined after a single or a few transfers of 500 μl volumes of eluent. The general column test[1] showed broadening and tailing of all peaks, as shown in Fig. 1. Removal of the column inlet did not result in any improvement, ruling out that the problem was caused by contamination of the inlet with high boiling or involatile by-products. One of these columns was broken into two, both of

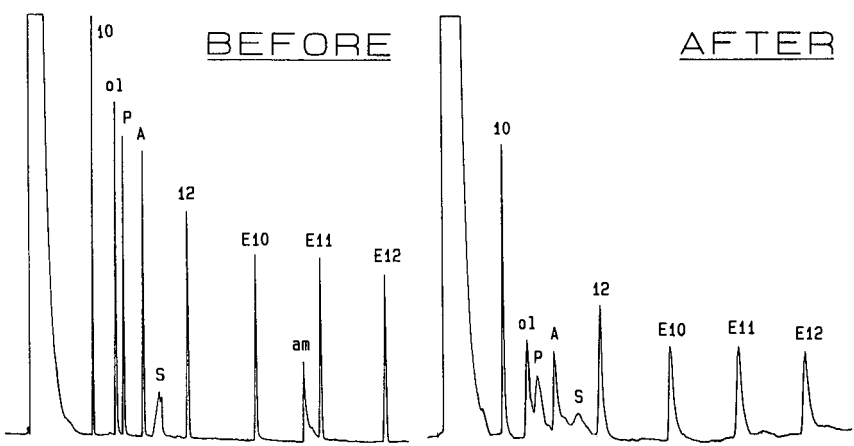

Fig. 1. Test chromatograms of a 5 m × 0.32 mm I.D. glass capillary column coated with PS-255 (a methylsilicone) of film thickness 0.23 μm. Left: column test before passage of ether. Right: column test after introduction of a 500-μl volume of ether containing 200 ppm of peroxides. Peaks: 10 = *n*-decane; ol = 1-octanol; P = 2,6-dimethylphenol; A = 2,6-dimethylaniline; S = 2-ethylhexanoic acid; 12 = *n*-dodecane; E10–E12 = methyl esters of the acids C_{10}–C_{12}; am = dicyclohexylamine.

0021-9673/88/$03.50 © 1988 Elsevier Science Publishers B.V.

which were retested. These tests indicated that the exit half of the column was severely damaged, too, although somewhat less than the first half. We first assumed that the damage was due to contamination of the column with packing material from the LC column. However, experiments described below showed that the damage of the GC column was caused by peroxides present in the ether.

Diethyl ether is an important eluent for LC–GC with concurrent eluent evaporation[2,3] because of its low boiling point, allowing transfer at relatively low temperature. Further, its use is convenient as all mixtures with *n*-pentane have practically the same boiling point[4].

EXPERIMENTAL

Volumes of solvent (500 μl) were introduced into apolar GC columns by concurrent solvent evaporation[5] using an experimental set-up that resembles a loop-type LC–GC interface. The inlet of the test capillary column was drawn out of the GC oven and mounted into a six-port switching valve. This valve was equipped with a 500-μl loop and the two fill ports. The last port was occupied by the carrier gas supply line.

The sample loop was filled with the solvent to be tested by suction through metal capillary tubes into a 10-ml plastic syringe. Diethyl ether was transferred to the GC column at an inlet pressure of 1.5 bar and an oven temperature of 85°C. Columns were tested before and after such treatment, using the standard procedure and test II[6]. Sections (5 m) of long 0.32 mm I.D. GC glass capillary columns were used as test columns. They were coated with PS-255 and SE-54 of film thickness 0.2–0.3 μm.

RESULTS

Peroxides as the source of the problem

Without having passed through an LC column, "HPLC-grade" diethyl ether and ether distilled about 1 year ago (stored in a bottle packed into aluminium foil) produced the same damage to the test columns as described above after a single introduction of a 500-μl volume into the GC column. Peroxide concentrations, determined by the "Perex-Test" (Merck, Darmstadt, F.G.R.), were between 100 and 200 ppm. Ethers stabilized with 2,6-di-*tert.*-butyl-*p*-cresol did not damage the column after ten transfers of 500-μl volumes. These ethers contained up to 2 ppm of peroxides.

The LC column involved in the LC–GC experiments (packed with Nucleosil CN) did not contribute to the problem. This was established from the fact that ether containing 1 ppm of peroxides did not damage the GC test columns after passage through the LC column (10 transfers of 500-μl volumes).

We do not know how peroxides damage methylpolysiloxane stationary phases. However, the damage produced phenomera resembling those observed when using old stationary phase solutions for coating the column[7]. Hydroxy groups might be introduced either by oxidation of methyl groups or by opening of siloxanes. In fact, resilylation of the columns with hexamethyldisilazane (HMDS) improved the column performance, but did not fully restore it. On the other hand, even non-adsorptive compounds such as alkanes were more or less strongly affected (strongly in Fig. 1.).

Excessive cross-linking within the stationary phase ("lacquering"), occurring through the same mechanisms as used for immobilizing the stationary phase, is unlikely to be the cause of the column deterioration as this usually reduces the retention power of the column. However, the elution temperature of the last peak of the test mixture (E12) did not decrease by a single degree.

Removal of peroxides

Ethers stored in an atmosphere of nitrogen and stabilized with copper metal might appear to solve our problem as they are free of organic additives disturbing GC. However, a sample taken from a bottle opened a few months ago rapidly ruined a GC column. In fact, it contained 100 ppm of peroxides (another ether sample from the same source, taken from a new bottle, contained 2 ppm of peroxides and did not damage GC columns). Hence, periodic tests for peroxides are a prerequisite when using such ethers. Organic antioxidants seem to be safer in keeping ether free of peroxides, but must be removed before use because the amounts involved severely disturb GC.

Antioxidants as well as peroxides can be removed from ether using basic aluminium oxide: with 7 g aluminium oxide 90 active, basic (70–230 mesh) (Merck, Darmstadt, F.R.G.) and ether containing some 500 ppm peroxides, a 90-ml volume of ether was freed from peroxides to less than 1 ppm, while the following 10 ml of ether contained 200 ppm of peroxides.

DISCUSSION

Use of ether for coupled LC–GC necessitates previous removal of organic stabilizers as well as of peroxides. In practice, there are various ways of solving this problem. Often ether must be distilled before use because of interfering impurities. This also removes antioxidants, and, if some iron(II) sulphate is added, the peroxides. However, the resulting ether is unprotected, and the peroxide concentration tends to increase rapidly upon storage. Brown bottles or bottles shielded with aliminium foil must be used as solvent reservoirs, and periodic checks on peroxides are important. If the ether is of sufficient purity and distillation is not required, stabilizers and peroxides are most conveniently removed using basic aluminium oxide (see above). This can be done at short intervals, ensuring that the peroxide concentration remains low.

Stabilizers and peroxides can be removed from the eluent by an aluminium oxide column installed between the LC pump and the LC injector. The required size of this column and the frequency of exchanging its content strongly depends on the eluent flow-rate and the eluent composition. Using pure ether, about 8 ml of ether can be cleaned per gram aluminium oxide. The capacity of the aliminium oxide column rapidly increases when using pentane–ether mixtures, as chromatographic retention volumes of stabilizers and peroxides are increased. Such on-line cleaning rules out peroxide formation in the cleaned ether during storage, but care is required to avoid contamination of the LC system after exchanging the aluminium oxide.

Finally, problems concerning peroxides can be avoided by replacing diethyl ether by *tert.*-butyl methyl ether. The latter does not form any peroxides, but its boiling point is 55°C, about 20° above that of diethyl ether.

REFERENCES

1 K. Grob, G. Grob and K. Grob, *J. Chromatogr.*, 156 (1978) 1.
2 K. Grob and J. M. Stoll, *J. High Resolut. Chromatogr. Chromatogr. Commun.*, 9 (1986) 518.
3 E. Munari and K. Grob, *J. High Resolut. Chromatogr. Chromatogr. Commun.*, 11 (1988) 172.
4 K. Grob and Th. Läubli, *J. High Resolut. Chromatogr. Chromatogr. Commun.*, 10 (1987) 435.
5 K. Grob, Ch. Walder and B. Schilling, *J. High Resolut. Chromatogr. Chromatogr. Commun.*, 9 (1986) 95.
6 K. Grob, G. Grob and K. Grob, *J. Chromatogr.*, 219 (1981) 13.
7 K. Grob and G. Grob, *J. High Resolut. Chromatogr. Chromatogr. Commun.*, 1 (1978) 221.

Journal of Chromatography, 455 (1988) 301–309
Elsevier Science Publishers B.V., Amsterdam — Printed in The Netherlands

CHROM. 20 869

Note

Identification of alkylbenzenes up to C_{12} by capillary gas chromatography and combined gas chromatography–mass spectrometry

I. OV-101 as stationary phase

E. MATISOVÁ*, M. RUKRÍGLOVÁ, J. KRUPČÍK, E. KOVAČIČOVÁ and Š. HOLOTÍK
Department of Analytical Chemistry, Faculty of Chemical Technology, Slovak Technical University, 812 37 Bratislava (Czechoslovakia)

(First received May 4th, 1988; revised manuscript received July 14th, 1988)

Aromatic hydrocarbons are particularly important in the petrochemical industry and environment. C_7–C_{15} alkylbenzenes represent the major part of the monoaromatic fraction of natural and synthetic hydrocarbons mixtures.

Alkylbenzenes may be determined by capillary gas chromatography (GC) in multicomponent hydrocarbon mixtures or in aromatic concentrates from fractions obtained by liquid chromatography with the aim of resolving and identifying or at least classifying all the components using non-polar, medium-polar and polar stationary phases in isothermal and temperature-programmed GC[1].

The role of capillary GC and the advantages and the possibilities of combined GC–mass spectrometry (GC–MS) for the identification of alkylbenzenes in multicomponent mixtures have been discussed in a recent review[2]. In that paper much space was devoted to the inter-laboratory reproducibility of retention data. The best reproducibility was achieved on non-polar squalane and silicone stationary phases. However, owing to the low-temperature stability of squalane and therefore the long analysis times for the determination of alkylbenzenes above C_9, non-polar silicones, such as OV-101 and SE-30, are much more preferable.

A few papers have given isothermal retention indices on OV-101[3–5] and SE-30[6,7] for alkylbenzenes up to C_{10}. With increasing number of carbon atoms the number of isomers rapidly increases and only a few retention data for alkylbenzenes over C_{10} are available. There are some published retention indices for hydrocarbons up to C_{18} on squalane[8,9], where the analysis time is hardly acceptable for practical purposes, and on the slightly polar phases Ucon LB 550X[8,10] and Citroflex A-4[9], for which the inter-laboratory reproducibility for alkylbenzenes is generally worse than that on squalane and non-polar silicones[2].

The aim of this work was to compile retention indices of C_{11} and C_{12} alkylbenzenes on capillary columns using OV-101 as the stationary phase. Owing to a lack of standard alkylbenzenes over C_{10}, synthesized samples were prepared for which the identification was performed on the basis of GC–MS measurements, correlation between the molecular structure and retention data[11,12] and by application of quantum chemistry methods[13,14].

0021-9673/88/$03.50 © 1988 Elsevier Science Publishers B.V.

EXPERIMENTAL

Capillary columns of soda-lime glass (Unihost, Teplice, Czechoslovakia) were used. Surface roughening was performed by statically etching the inner surface with hydrogen chloride gas at 330°C for 16 h. The columns were coated with the solutions of OV-101 dynamically (column I, 278 m × 0.25 mm I.D. with 15% OV-101 in chloroform) and statically (column II, 50 m × 0.24 mm I.D. with 0.56% OV-101 in pentane).

GC measurements were performed on a Carlo Erba Model 2350 gas chromatograph equipped with a flame ionization detector and a stream splitter and on OV-101 in glass capillary columns (column I with hydrogen as carrier gas with a linear gas velocity of about 30 cm/s; column II with nitrogen as carrier gas at a linear gas velocity of about 10 cm/s) under isothermal conditions at 100 and 120°C.

Synthesized mixed samples were prepared by alkylation of benzene or alkylbenzenes with alkyl halides in the presence of $AlCl_3$. The following reactions were carried out:

(1) ethylbenzene, isopropylbenzene, a mixture of propylbenzenes, *tert.*-butylbenzene and a mixture of butylbenzenes with methyl iodide[15];

(2) benzene, 1,2-dimethylbenzene, 1,4-dimethylbenzene, technical mixtures of dimethylbenzenes and 1-methyl-4-isopropylbenzene with ethyl bromide[15];

(3) methylbenzene with ethyl and *n*-propyl bromide[15];

(4) benzene, 1,2,4-trimethylbenzene and isopropylbenzene with *n*-propyl bromide[15];

(5) 1,2,4-trimethylbenzene and isopropylbenzene with isopropylbromide[17];

(6) 1,2-dimethylbenzene, 1,4-dimethylbenzene and a technical mixture of dimethylbenzenes with *n*-butyl bromide[16];

(7) benzene, 1,2-dimethylbenzene, a technical mixture of dimethylbenzenes and ethylbenzene with *tert.*-butyl bromide[17]; and

(8) benzene and methylbenzene with *n*-pentyl bromide[15].

Samples after dilution in acetone and addition of C_7–C_{14} *n*-alkanes were injected with 1- and 10-μl Hamilton syringes. Methane was used for the determination of the gas holdup time. Elution times were measured with a Time Calculator RM 4111 digital stop-watch.

GC–MS measurements with electron-impact ionization were performed using an HP 5995 instrument under temperature-programmed conditions (initial temperature 80°C, increased at 1°C/min, final temperature 190°C with an isothermal run).

RESULTS AND DISCUSSION

Owing to the lack of standard materials and retention and mass spectral data for alkylbenzenes over C_{10} ($nC > 10$), synthesized mixed samples were prepared with the aim of preparing C_{12} alkylbenzenes. After sample dilution the mixture components were analysed by GC and GC–MS on OV-101 glass capillary columns. Alkylbenzenes were characterized by retention indices measured at 100°C and their temperature coefficients. From mass spectra obtained by electron-impact ionization the molecular weight and the type and number of substituents present in the benzene ring were obtained. The molecular weight distribution of alkylbenzenes was determined from

molecular ions by selected ion monitoring in the mutiple ion mode. However, the use of GC–MS for the identification of alkylbenzenes is limited by the great similarity of the mass spectra of isomeric compounds (positional isomers).

In capillary GC the synthesized samples often gave more than 20–30 chromatographic peaks. Multicomponent mixtures were obtained owing to the formation of C_{14} and C_{15} alkylbenzenes and impurities in the parent compounds. From the theory of Friedel–Crafts alkylation concerning the entry of further substituents into the benzene ring it follows unambiguously that alkyl substituents present in the ring which repulse electrons direct the introduction of the next substituent into *ortho* and *para* positions[18]. The ratio of *ortho* to *para* isomers in the electrophilic substitution predominantly influences the steric effects. However, in the presence of Friedel–Crafts catalysts and cocatalysts (AlX_3–HX), isomerization, disproportionation and transalkylation reactions take place[18–23], hence considerably increasing the number of components in the synthesized mixtures. Owing to isomerization a large percentage of *meta*-derivatives is formed and *n*-alkyl substituents isomerize to isoalkyl groups. In the disproportionation from two molecules of alkylbenzenes, by the transfer of an alkyl group from one aromatic ring to the other, two molecules of new aromatics are formed.

By transalkylation of alkylaromatics two molecules of different alkylaromatics with distinct numbers of alkyl groups in the aromatic ring react, whereby intermolecular transfer of alkyl groups takes place predominantly from the ring with a higher number of alkyl groups to the ring with a smaller number of alkyl groups or without an alkyl group.

For illustration two chromatograms are given for synthesized products of alkylbenzenes and *n*-alkanes on the OV-101 capillary column at 120°C. Fig. 1a shows the separation of the alkylation products of a technical mixture of dimethylbenzenes with ethyl bromide and Fig. 2a the separation of the alkylation products of 1,2,4-trimethylbenzene with *n*-propyl bromide. After GC–MS, from the mass spectra and by comparison with retention data in the literature (only for alkylbenzenes with $nC \leqslant 10$ and a very few higher alkylbenzenes) the most probable structures were proposed. According to the results obtained, in many samples the number of isomers determined in the synthesized mixtures was lower than the theoretically possible number of isomers. Therefore, concentrated samples (synthesized samples without dilution) were also analysed by GC, (Figs. 1b and 2b) and GC–MS. The number of alkylbenzenes with $nC > 10$ determined increased considerably. However, in many instances the concentration of isomers observed in the synthesized samples was so small that the recorded spectra were of low quality and it was not possible to specify the kind of alkyl substituents in benzene ring, only to determine the number of carbon atoms. The peak designations for Fig. 1a and b are given in Table I and for Fig. 2a and b in Table II, together with measured and published retention indices (I) of alkylbenzenes in the mentioned synthesized samples at 100°C and their temperature coefficients, ΔT per 10°C.

In some samples during synthesis, in addition to an oily mixture also a crystalline portion was formed which was additionally dissolved in benzene. In these samples (alkylation products of *n*-propylbenzene, *n*-butylbenzene with methyl iodide and benzene with *n*-propyl bromide) the concentrations of the components were too low for GC measurements, so retention and MS data were acquired by direct analysis of

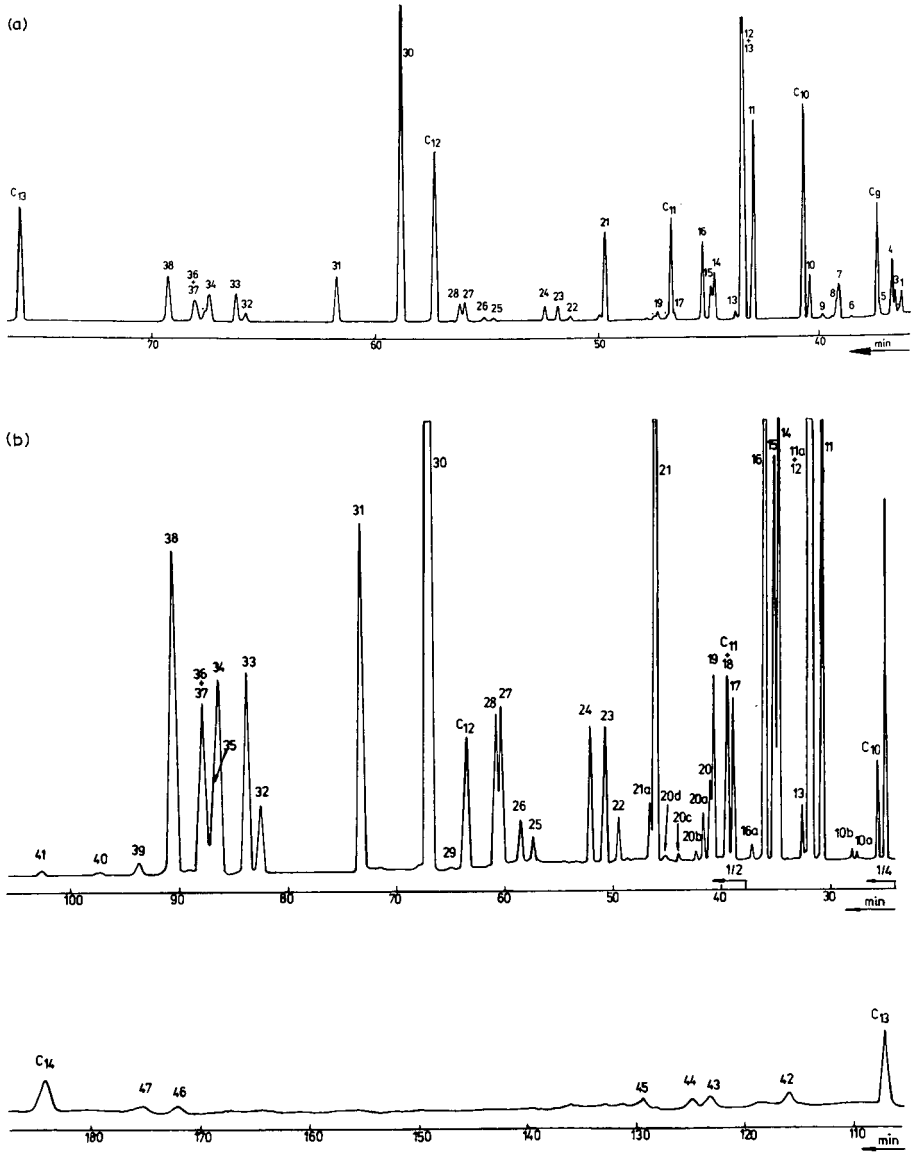

Fig. 1. Chromatograms of the separation of *n*-alkanes and alkylation products of a technical mixture of dimethylbenzenes with ethyl bromide on OV-101 glass capillary column at 120°C. For peak designations, see Table I. (a) Diluted synthesized mixture, column I; (b) concentrated synthesized mixture, column II.

the synthesized mixtures. A chromatogram for the separation of one of these mixtures (alkylation products of *n*-propylbenzene with methyl bromide) is shown in Fig. 3. The mixture composition and retention data are given in Table III.

In alkylbenzenes with $nC > 10$ in 25 synthesized samples for which there are no

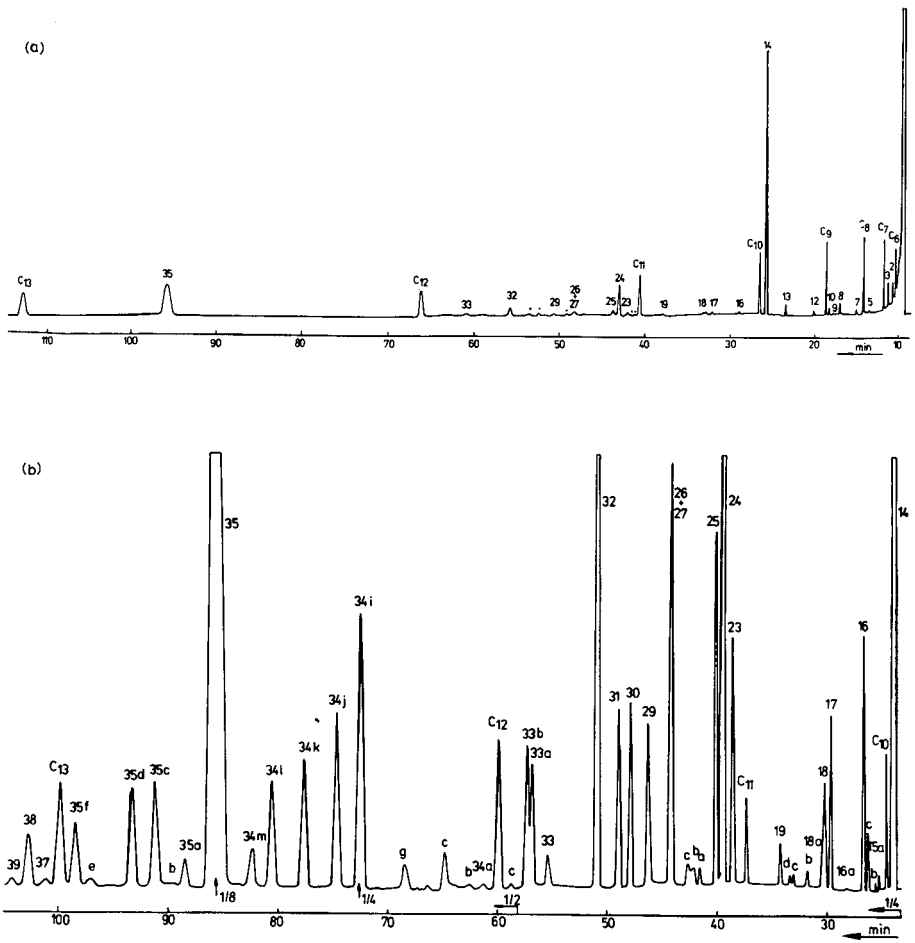

Fig. 2. Chromatograms of the separation of *n*-alkanes and alkylation products of 1,2,4-trimethylbenzene with *n*-propyl bromide on OV-101 glass capillary column II at 120°C. For peak designations see Table II. (a) Diluted synthesized mixture; (b) concentrated synthesized mixture.

published retention data the alkyl substituents were identified by interpretation of the mass spectra. The determination of the position of alkyl substituents was based on the following approach:

(1) Correlation between molecular structure and retention data; for the numbers of homologous series the dependences of the homeomorph factor (*H*) on the number of carbon atoms (*n*C) were constructed[11,12].

(2) Interpretation of retention data by quantum chemistry methods; by the correlation of interaction energies between partitioned substances and the stationary phase with retention characteristics, correlation equations were obtained that enabled structures to be assigned to the individual peaks and elution data to be prediced[13,14].

(3) Probability of the formation of isomers during synthesis; by the application of quantum chemistry for the study of the stability of isomers[14].

TABLE I

RETENTION INDICES (I) OF ALKYLATION PRODUCTS OF A TECHNICAL MIXTURE OF DIMETHYLBENZENES WITH ETHYL BROMIDE AND THEIR TEMPERATURE COEFFICIENTS ($\Delta I/10°C$) ON AN OV-101 CAPILLARY COLUMN

Peak No.	*Compound**	*Measured*		*Published*	
		$I_{100°C}$	$\Delta I/10°C$	$I_{100°C}$	$\Delta I/10°C$
3	EtB	857.7	2.50	857.3	2.38[4]
4	1,3-DiMeB	865.8	2.45	865.2	2.27[4]
	1,4-DiMeB	865.8	–	866.1	2.24[4]
5	1,2-DiMeB	888.8	2.90	888.6	2.75[4]
7	1-Me-3-EtB	954.8	2.55	954.5	2.38[4]
8	1-Me-4-EtB	957.1	2.54	957.1	2.50[4]
8a	1,3,5-TriMeB	962.1	2.30	963.1	2.30[3]
9	1-Me-2-EtB	973.2	3.05	972.5	2.85[4]
10	1,2,4-TriMeB	987.3	3.10	987.1	2.88[4]
11	1,3-DiEtB	1039.5	2.44	1040.4	2.58[3]
11a	1-Me-4-nPrB	1046.2	2.80	1047.1	3.0[7]
12	1,4-DiEtB	1046.0	2.65	1047.8	2.85[3]
13	1,3-DiMe-5-EtB	1048.5	2.40	1050.1	2.50[7]
14	1,4-DiMe-2-EtB	1967.2	3.00	1068.6	3.20[7]
15	1,3-DiMe-4-EtB	1069.0	3.10	1070.3	3.20[7]
16	1,2-DiMe-4-EtB	1074.7	3.18	1075.4	3.10[7]
17	C_{11}-alkylB	1092.6	2.20	–	–
18	1,2-DiMe-3-EtB	1094.1	3.65	1094.6	3.70[7]
19	C_{11}-alkylB	1103.9	1.52	–	–
20	C_{11}-alkylB	1103.9	2.35	–	–
20a	1,2,4,5-TetraMeB	1106.0	3.47	1107.2	3.49[3]
21	1-Me-3,5-DiEtB	1129.8	2.40	–	–
21a	C_{11}-alkylB	1140.6	2.33	–	–
22	4-Me-1,2-DiEtB	1143.7	3.00	–	–
23	2-Me-1,4-DiEtB	1149.1	3.05	–	–
24	1-Me-2,4-DiEtB	1154.2	3.15	–	–
25	1,2,4-TriMe-5-EtB	1173.0	3.55	–	–
26	C_{12}-alkylB	1179.9	1.80	–	–
27	1,3,5-TriMe-2-EtB	1182.8	3.24	–	–
28	1,2,5-TriMe-3-EtB	1184.9	3.25	–	–
29	1,2,3-TriMe-5-EtB	1193.4	3.40	–	–
30	1,3,5-TriEtB	1206.6	1.90	1207.1	1.99[7]
31	1,2,4-TriEtB	1223.2	2.80	–	–
32	1,2,3-TriEtB	1245.7	3.10	–	–
33	C_{13}-alkylB	1251.5	1.45	–	–
34	DiMe-DiEtB	1254.5	3.05	–	–
35	DiMe-DiEtB	1255.7	3.00	–	–
36	DiMe-DiEtB	1257.3	3.25	–	–
37	DiMe-DiEtB	1258.4	2.80	–	–
38	1,2-DiMe-3,5-DiEtB	1263.5	3.15	–	–

* Abbreviations: Me = methyl; Et = ethyl; nPr = *n*-propyl; B = benzene.

TABLE II

RETENTION INDICES (I) OF ALKYLATION PRODUCTS OF 1,2,4-TRIMETHYLBENZENE WITH *n*-PROPYL BROMIDE AND THEIR TEMPERATURE COEFFICIENTS ($\Delta I/10°C$) ON AN OV-101 CAPILLARY COLUMN

Peak No.	*Compound**	*Measured*		*Published*	
		$I_{100°C}$	$\Delta I/10°C$	$I_{100°C}$	$\Delta I/10°C$
8	1,3-DiMeB	865.8	2.50	865.2	2.65[4]
9	1,4-DiMeB	865.8	–	866.1	2.24[4]
10	1,2-DiMeB	888.8	2.90	888.6	2.75[4]
12	iPrB	919.5	2.80	920.4	2.84[3]
13	1,3,5-TriMeB	963.0	2.40	963.1	2.30[3]
14	1,2,4-TriMeB	987.3	3.10	987.1	2.88[4]
15c	1-Me-4-iPrB	1016.5	2.63	1017.0	2.50[7]
16	1,2,3-TriMeB	1015.5	3.70	1015.9	3.83[3]
16a	1-Me-2-iPrB	1029.1	2.92	1028.4	2.60[7]
17	1-Me-3-nPrB	1041.9	2.72	1043.2	2.80[7]
18	1-Me-4-nPrB	1045.6	2.80	1047.1	3.00[7]
18a	1,3-DiMe-5-EtB	1048.4	2.40	1050.1	2.5[7]
18b	1-Me-2-nPrB	1057.0	3.34	1058.2	3.0[7]
18c	1,4-DiMe-2-EtB	1067.0	3.00	1068.6	3.2[7]
18d	1,3-DiMe-4-EtB	1068.8	3.10	1071.3	3.2[7]
19	1,2-DiMe-4-EtB	1074.3	3.18	1075.4	3.1[7]
23	1,3-DiMe-5-iPrB	1103.3	2.17	–	–
24	1,2,4,5-TetraMeB	1106.0	3.47	1107.2	3.49[3]
25	1,2,3,5-TetraMeB	1109.0	3.75	1110.5	3.63[3]
25a	1,4-DiMe-2-iPrB	1118.7	2.61	–	–
25b	1,3-DiMe-4-iPrB	1123.4	2.96	–	–
26	1,2-DiMe-4-iPrB	1130.4	2.87	–	–
27	1,3-DiMe-5-nPrB	1132.6	2.35	–	–
29	1,2,3,4-TetraMeB	1139.0	4.40	–	–
30	1,4-DiMe-2-nPrB	1147.5	2.97	–	–
31	1,3-DiMe-4-nPrB	1152.1	3.02	–	–
32	1,3-DiMe-2-nPrB	1160.5	3.03	–	–
33	1,2-DiMe-3-nPrB + $+C_{12}$-alkylB	1176.6	3.71	–	–
33a	1,3,5-TriMe-2-EtB	1182.8	3.24	–	–
33b	1,2,5-TriMe-3-EtB	1184.3	3.29	–	–
33c	1,2,3-TriMe-5-EtB	1193.2	3.40	–	–
34c	C_{12}-alkylB	1211.7	2.05	–	–
34g	C_{12}- + C_{13}-alkylB	1224.7	–	–	–
34i	1,2,4-TriMe-5-iPrB	1232.7	2.73	–	–
34j	1,3,5-TriMe-2-iPrB	1238.5	2.65	–	–
34k	1,2,3-TriMe-5-iPrB	1245.7	2.95	–	–
34l	1,2,4-TriMe-5-nPrB	1251.7	3.47	–	–
35	1,3,5-TriMe-2-nPrB	1263.2	3.46	–	–
35c	1,2,5-TriMe-3-nPrB	1276.6	3.18	–	–
35d	1,2,3-TriMe-5-nPrB	1278.8	3.97	–	–
35f	Me-DinPrB	1293.1	2.21	–	–
38	1,2,4-TriMe-3-nPrB	1297.0	4.22	–	–

* Abbreviations as in Table I; iPr = isopropyl.

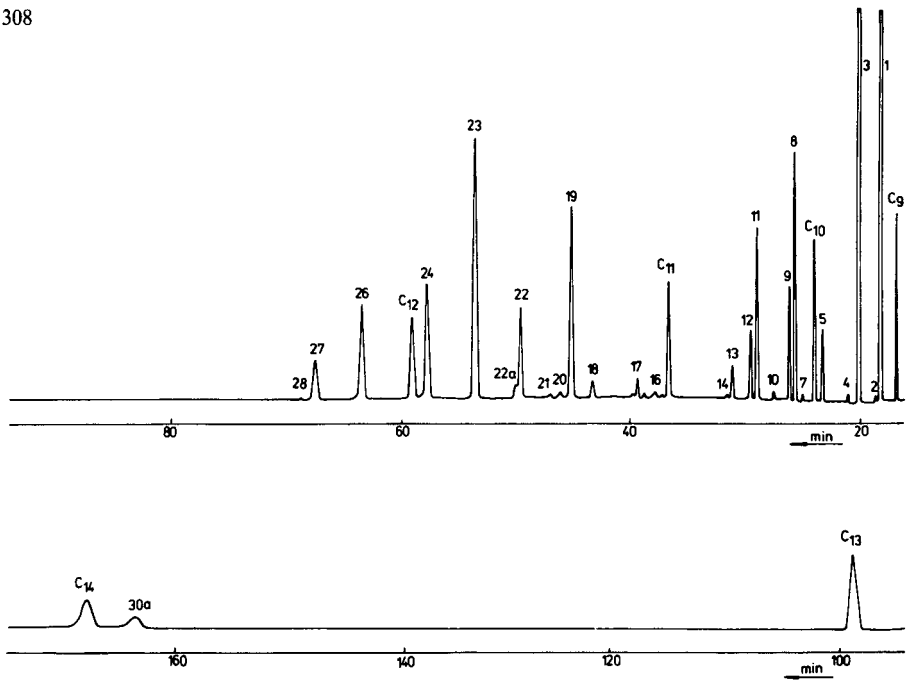

Fig. 3. Chromatogram of the separation of *n*-alkanes and concentrated alkylation products of *n*-propylbenzene with methyl iodide on OV-101 glass capillary column II at 120°C. For peak designations see Table III.

TABLE III

RETENTION INDICES (*I*) OF ALKYLATION PRODUCTS OF *n*-PROPYLBENZENE WITH METHYL IODIDE AND THEIR TEMPERATURE COEFFICIENTS ($\Delta I/10°C$) ON AN OV-101 CAPILLARY COLUMN

Peak No.	*Compound**	*Measured*		*Published*	
		$I_{100°C}$	$\Delta I/10°C$	$I_{100°C}$	$\Delta I/10°C$
1	iPrB	919.5	2.75	920.4	2.84[3]
3	nPrB	949.3	2.65	949.3	2.93[3]
4	1,3,5-TriMeB	963.0	2.40	963.3	2.55[3]
5	1,2,4-TriMeB	987.3	3.10	988.4	3.23[3]
7	sBuB	1005.2	3.10	1005.7	3.38[3]
8	1-Me-3-iPrB	1012.6	2.35	1013.2	2.20[7]
9	1-Me-4-iPrB	1016.6	2.58	1017.0	2.50[7]
10	1-Me-2-iPrB	1029.5	2.77	1028.4	2.60[7]
11	1-Me-3-nPrB	1041.8	2.72	1043.2	2.80[7]
12	1-Me-4-nPrB	1045.8	2.70	1047.1	3.00[7]
13	1-Me-2-nPrB	1057.1	3.16	1058.2	3.00[7]
16	1,3-DiMe-5-iPrB	1102.8	2.14	–	–
17	1,2,4,5-TetraMeB	1106.0	3.44	1107.2	3.49[3]
18	1,2-DiMe-4-iPrB	1130.5	2.81	–	–
19	1,3-DiiPrB	1140.8	2.02	1142.7	2.00[3]
22	1,4-DiiPrB	1159.7	2.44	–	–
23	1-iPr-3-nPrB	1175.7	2.32	–	–
24	1-iPr-4-nPrB	1190.1	2.71	–	–
26	1,3-DinPrB	1209.2	2.60	–	–
27	1,4-DinPrB	1220.7	2.97	–	–
28	Me-DiiPrB	1224.7	3.01	–	–

* Abbreviations as in Tables I and II; sBu = *sec.*-butyl.

The retention data collected for C_7–C_{15} alkylbenzenes determined in synthesized mixtures on OV-101 capillary columns will be pulished in Part II[12].

ACKNOWLEDGEMENTS

The authors thank Dipl. Ing. V. Rattay of the Faculty of Chemical Technology (Bratislava) for the synthesis of alkylbenzenes and Dipl. Ing. P. Čellár and Dipl. Ing. E. Kolek of Slovnaft AV VVZ (Bratislava) for the GC–MS measurements on synthesized mixed samples.

REFERENCES

1 B. Kumar, R. K. Kuchhal, P. Kumar and P. L. Gupta, *J. Chromatogr. Sci.*, 24 (1986) 99.
2 E. Matisová, *J. Chromatogr.*, 438 (1988) 131.
3 V. A. Gerasimenko and V. M. Nabivach, *Zh. Anal. Khim.*, 37 (1982) 110.
4 J. A. Lubeck and D. L. Sutton, *J. High Resolut. Chromatogr. Chromatogr. Commun.*, 6 (1983) 328.
5 W. Engewald, I. Topalova, N. Petsev and Chr. Dimitrov, *Chromatographia*, 23 (1987) 561.
6 V. Švob and D. Deur-Šiftar, *J. Chromatogr.*, 91 (1974) 677.
7 T. Tóth, *J. Chromatogr.*, 279 (1983) 157.
8 W. Engewald and L. Wennrich, *Chromatographia*, 9 (1976) 540.
9 L. Soják and J. A. Rijks, *J. Chromatogr.*, 119 (1976) 505.
10 C. E. Döring, D. Estel and R. Fischer, *J. Prakt. Chem.*, 316 (1974) 1.
11 E. Matisová, J. Krupčík, J. Garaj, P. Čellár and E. Kolek, in *Abstracts, 16th International Symposium on Chromatography, September 21–26, 1986*, GAMS, Paris, 1986, p. 53.
12 E. Matisová, E. Kovačičová, Pham Thi Ha and W. Engewald, *J. Chromatogr.*, in preparation.
13 E. Matisová, S. Miertuš, J. Krupčík, V. Jakuš and J. Garaj, in *Abstracts, 6th Danube Symposium on Chromatography, Varna, Golden Sands, 1987*, p. 3PS-80.
14 E. Matisová, S. Miertuš, V. Jakuš and E. Kovačičová, *J. Chromatogr.*, in preparation.
15 J. F. Norris and D. Rubinstein, *J. Am. Chem. Soc.*, 61 (1939) 1163.
16 D. V. Nightingale and J. M. Shackelford, *J. Am. Chem. Soc.*, 76 (1954) 5767.
17 R. B. Contractor and A. T. Peters, *J. Chem. Soc.*, (1949) 1314.
18 H. G. O. Becker, *Einführung in die Elektronentheorie organisch-chemischer Reaktionen*, VEB Deutscher Verlag der Wissenschaften, Berlin, 1961, p. 387.
19 H. C. Brown and C. R. Smooth, *J. Am. Chem. Soc.*, 78 (1956) 2176.
20 H. C. Brown and C. R. Smooth, *J. Am. Chem. Soc.*, 78 (1956) 2185.
21 H. C. Brown and H. W. Pearshall, *J. Am. Chem. Soc.*, 73 (1951) 4681.
22 H. C. Brown and H. W. Pearshall, *J. Am. Chem. Soc.*, 74 (1952) 191.
23 P. Hudec, J. Novanský and M. Mihálik, *Ropa Uhlie*, 27 (1985) 129.

Journal of Chromatography, 455 (1988) 310–315
Elsevier Science Publishers B.V., Amsterdam — Printed in The Netherlands

CHROM. 20 965

Note

Effect of pH on the reaction of 2,4-dinitrophenylhydrazine with formaldehyde and acetaldehyde*

MERLIN K. L. BICKING*,** and W. MARCUS COOKE
Battelle Columbus Division, 505 King Avenue, Columbus, OH 43201 (U.S.A.)
and
FRED K. KAWAHARA and JAMES E. LONGBOTTOM
U.S. Environmental Protection Agency, 26 West St. Clair Street, Cincinnati, OH 45268 (U.S.A.)
(First received May 25th, 1988; revised manuscript received August 25th, 1988)

The acid-catalyzed condensation reaction of a molecule of 2,4-dinitrophenylhydrazine (DNPH) with a carbonyl compound is a well known reaction for characterizing aldehydes and ketones[1,2]. The DNPH derivatives are used to identify qualitatively the parent carbonyl compound by melting point determination. Gram quantities of the derivatives are easily prepared by well-established procedures. The derivatization is also useful as a quantitative analytical procedure. Numerous applications have been reported using either gas chromatography (GC) with flame ionization[3–6] or electron-capture[7] detection, or high-performance liquid chromatography (HPLC) with absorbance[8–13] or electrochemical[14,15] detection. Detection limits are usually in the low μg/l range for the more sensitive detectors. The GC methods have not found widespread acceptance because of the low volatility of the derivative, the relative insensitivity of the flame ionization detector, and the response variations of the electron capture detector. Similar response variations are common for the electrochemical detector.

The reaction is known to proceed by a multi-step mechanism[16–18], where the rate-limiting step involves the addition of reagent to the protonated carbonyl moiety. Rapid dehydration occurs to yield the hydrazone. The rate of reaction has been shown to be a function of several experimental variables: reaction pH, the concentration of acid used as catalyst, carbonyl compound concentration, and reagent concentration. At low pH, the carbonyl group is activated toward nucleophilic addition by the acid, but the amount of free nucleophile present is reduced because of its basicity. At higher pH values, typically in basic solution, more free reagent is available but the carbonyl group is less reactive. Because of these competing effects, the rate passes through a maximum at a pH which is characteristic of the basicity of the nucleophilic reagent[16].

* Although the research described in this article has been funded wholly or in part by the U.S. Environmental Protection Agency through Contract Number 68-03-1760 (WA 2-16) to Battelle Memorial Institute, it has not been subjected to Agency review and therefore does not necessarily reflect the views of the Agency and no official endorsement should be inferred. Mention of trade names or commercial products does not constitute endorsement or recommendation for use.

** Present address: Twin City Testing Co., 662 Cromwell Avenue, St. Paul, MN 55114, U.S.A.

0021-9673/88/$03.50 © 1988 Elsevier Science Publishers B.V.

Under the conditions commonly employed in conventional analytical derivatization reactions, the reagent and buffer are present in at least ten-fold molar excess. The rate should then be a function only of acidity and carbonyl compound concentration. However, there are no reports in the literature to document these trends under conditions of interest to analytical chemists. Furthermore, the resulting yield of the reaction as a function of pH has not been reported. Based on published procedures[8–10,19]. It appears that most analytical derivatizations with DNPH are performed at a pH in the range 0–2.

The effect of pH on reaction yield was studied here to ascertain whether the derivatization could be performed under less acidic conditions. Derivatizations of environmental samples should be performed under mild acid conditions to minimize generation of formaldehyde from matrix precursors, since numerous environmentally occurring species have been shown to generate formaldehyde under a variety of conditions[20]. In general, mild acid conditions are preferred or a false positive formaldehyde result may be obtained.

The objective of this study was to determine if a quantitative derivatization could be performed at a reasonable rate under mild conditions which minimized the possibility of a matrix false positive. The results of this study indicate that the derivatization can indeed be performed in high yield at a pH as high as 5.

EXPERIMENTAL

Reagents and solutions

The following reagents were reagent grade and used as received: 37% formaldehyde (Baker); 2,4-dinitrophenylhydrazine (Aldrich), containing approximately 30% (w/w) water; acetaldehyde (Aldrich); phosphoric acid (Baker); glacial acetic acid (Baker); and sodium hydroxide (Baker). All solvents were distilled-in-glass or equivalent: methanol, ethanol, methylene chloride, and reagent water. DNPH derivatives of formaldehyde and acetaldehyde were prepared in gram quantities according to published procedures[2].

A 1000 mg/l stock solution of formaldehyde and acetaldehyde in reagent water was prepared from formalin and neat acetaldehyde. The formaldehyde concentration was determined by standard titrimetric procedures using sodium sulfite and hydrochloric acid. Individual 1 mg/l solutions of formaldehyde and acetaldehyde were prepared by dilution of this stock solution with reagent water. A 5 *M* phosphoric acid solution in reagent water was prepared from the concentrated acid. The DNPH reagent was prepared by dissolving 143 mg of the 70% (w/w) solid in absolute ethanol. Gentle warming was required to dissolve the solid. A 5 *M* sodium hydroxide solution was prepared in reagent water from the solid. Solutions of synthesized derivatives were prepared in methanol.

Equipment

Laboratory glassware included 500-ml separatory funnels equipped with PTFE stopcocks, 500-ml erlenmeyer flasks equipped with standard taper joints, and a Kuderna-Danish apparatus, including a 25-ml concentrator tube, evaporating flask, three-ball macro-Snyder column, and a two-ball micro-Snyder column. Volumetric flasks were 25 ml. The pH meter used (Orion Research) was capable of measuring solution pH in increments of 0.02 units.

Chromatographic apparatus and operating conditions

The LC system consisted of an Altex 110A pump, a 250 × 4.6 mm Zorbax ODS column, and an LDC Spectromonitor III detector. The mobile phase was methanol–water (75:25), injection volume was 20 μl, and the detector was run at 360 nm.

Procedure

A 250-ml aliquot of reagent water spiked with 1 mg/l of formaldehyde and acetaldehyde was placed in a 500-ml flask and 5 ml of 5 *M* phosphoric acid was added. This resulted in a solution pH of approximately 1.7. Reaction yields were obtained at solution pH values of 1.7, 3, 4, 5, and 7. Higher pH values were obtained by addition of 5 *M* sodium hydroxide prior to addition of the derivatizing reagent. The method was as follows: a 10-ml aliquot of a DNPH solution (1 mg/ml) was added to the solution. The flask was capped and allowed to react one hour at room temperature on a wrist-action shaker. The solution was placed in a 500-ml separatory funnel and extracted manually with three 20-ml portions of methylene chloride. The combined organic layers were concentrated to 10 ml using the Kuderna-Danish apparatus. A solvent exchange to methanol was performed near the end of the concentration step. The resulting methanol solution was diluted to 25 ml using a volumetric flask. An aliquot of this solution was analyzed by LC with absorbance detection at 360 nm. Yields were calculated based on injection of independently synthesized derivative standards[2]. All values reported were corrected for the presence of a non-zero laboratory blank.

RESULTS AND DISCUSSION

The yield of the reaction between formaldehyde and DNPH as a function of pH is shown in Fig. 1. The reaction yield data for reaction of formaldehyde and acetaldehyde in reagent water are summarized in Table I. Over the pH range of 1.7 to 7.0, a smooth relationship was observed with a maximum at a solution pH of approximately 4. However, reaction yields did not change significantly over the pH range from three to five. The observed yields followed the same trend as the rate of reaction, with the maximum under mild acid conditions and a sharp decrease at either extreme. The excellent yield under mild acid conditions is surprising, considering that most literature procedures used high acid conditions. However, the results reported here clearly indicated that milder conditions provided excellent yield and would be preferred when derivatizing an acid-sensitive matrix.

Yields were generally about 90% under the conditions employed. Standard deviations were less than 5% in each case. At pH 5, the yield appeared to be independent of formaldehyde concentration.

As illustrated in Table I, the yield did not appear to be a function of type of buffer. The value for acetate at pH 5 was not statistically different from the phosphate value. This is important since the buffering capacity of acetate is high in this region and pH 5 acetate buffers are used for extraction of environmental samples[21].

The observed yields for acetaldehyde were significantly lower. This was expected due to steric hindrance of the carbonyl moiety. Yields could be increased by performing the derivatization under more rigorous conditions (*i.e.*, higher temperatures or longer times) but this was not attempted during the present investigation since the primary objective was to evaluate the effect of pH only. Acetaldehyde did not

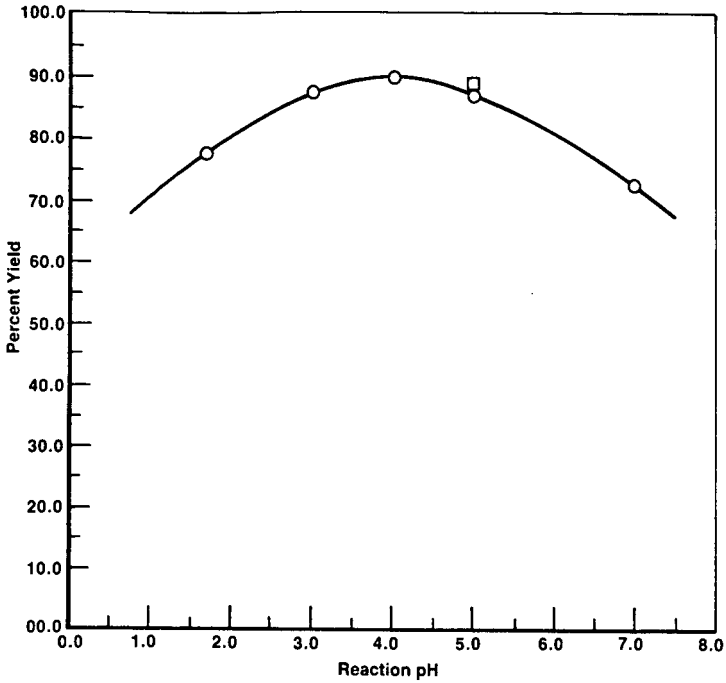

Fig. 1. Effect of reaction pH on percent yield of formaldehyde-DNPH derivative. Symbols: circles, phosphate buffer; square, acetate buffer.

show the same trend in yield as a function of pH, but was relatively constant at 60% in the pH range from 3 to 5. This was probably due to the presence of additional resonance structures in acetaldehyde, which affected the concentration of the reactive form. These additional structures were not present in formaldehyde. Other carbonyl compounds are likely to follow the same trend as acetaldehyde.

TABLE I

RECOVERY OF DNPH DERIVATIVES AS A FUNCTION OF pH

pH	*Recovery (%)**	
	Formaldehyde	*Acetaldehyde*
1.7	77.3 (4.1)	64.2 (1.9)
3	87.3 (4.1)	60.0 (7.5)
4	89.6 (1.6)	58.9 (1.4)
5	86.8 (1.3)	57.1 (1.6)
5**	88.8 (0.23)	63.0 (0.30)
7	72.0 (8.0)	48.1 (16)

* Spiking levels: 1.02 mg/l formaldehyde, 1.00 mg/l acetaldehyde. Standard deviation ($N=3$) is given in parenthesis.

** Acetate buffer, all other experiments used a phosphate buffer.

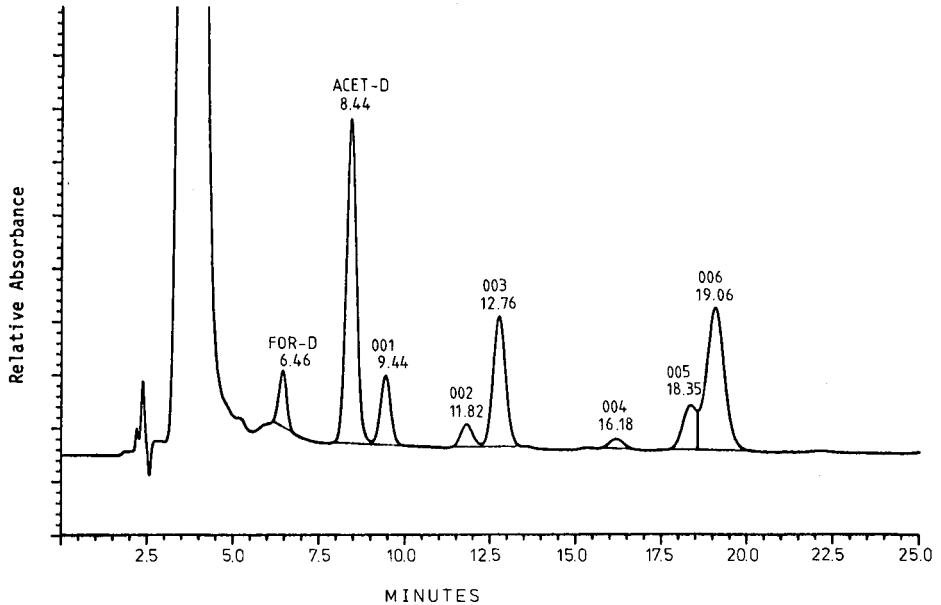

Fig. 2. Representative chromatogram from derivatization of landfill leachate sample using procedure described in Experimental section. Peak identity: FOR-D, formaldehyde derivative; ACET-D, acetaldehyde derivative. Both *syn-* and *anti-*forms are present for acetaldehyde but only the major product is quantified.

This general procedure is readily applicable to direct derivatization and analysis of environmental samples. The result of direct derivatization of an industrial landfill leachate is demonstrated in Fig. 2. A 250 ml aliquot was derivatized using the procedures described in the experimental section, employing a pH 5 acetate buffer in this case. For this matrix, no modifications of the original procedure were necessary. The formaldehyde and acetaldehyde derivatives were readily identified in the chromatogram, based on a comparison of retention times with independently synthesized standards. The identity of the derivatives of formaldehyde and acetaldehyde was confirmed by gas chromatography–mass spectrometry. The formaldehyde derivative peak (6.46 minutes) represented approximately 50 μg/l formaldehyde in the original solution; the larger acetaldehyde derivative peak (8.44 min) represented approximately 120 μg/l acetaldehyde in solution. There were no interferences observed and the derivatives were well separated from the excess DNPH reagent (3.5 min), which eluted near the void volume. Note that two peaks (8.44 min and 9.44 min) were observed for acetaldehyde. These peaks represented two possible isomers, *syn-* and *anti-*, for the derivative product. Geometric isomers were not possible for symmetrical carbonyl compounds, such as formaldehyde, and only a single peak was observed. The remaining peaks in the chromatogram represented low levels of other DNPH derivatives.

CONCLUSIONS

It is possible to achieve high recovery of DNPH derivatives of formaldehyde and acetaldehyde at trace levels under mild derivatization conditions. An acetate buffer at

pH 5 is convenient for this purpose. These data suggest that derivatization of other compounds will also be possible at similar pH values, but some modification of reaction conditions (time, temperature) will be necessary. The combination of solvent extraction followed by absorbance detection at 360 nm provides sufficient selectivity so that no interferences are observed in the chromatogram, even when complex environmental samples are derivatized directly. Additional data regarding the derivatization of other sample types over a range of formaldehyde concentrations will be the subject of a forthcoming manuscript. Subsequent issues to be discussed include the source of non-zero laboratory blanks, emulsion formation, the kinetics of derivatization, and an evaluation of ability of this method to avoid generation of false positives.

ACKNOWLEDGEMENT

The authors acknowledge the guidance of J. S. Warner and the technical assistance of L. Roberts, S. Harsh, and W. Miller.

REFERENCES

1 A. I. Vogel, *Elementary Practical Organic Chemistry*, Part 2, Wiley, New York, 1966, p. 113.
2 L. F. Fieser and M. Fieser, *Reagents for Organic Synthesis*, Vol. 1, Wiley, New York, 1967, p. 330.
3 Y. Hoshika and T. Takata, *J. Chromatogr.*, 120 (1976) 379.
4 R. A. Smith and I. Drummond, *Analyst (London)*, 104 (1979) 875.
5 P. Kalo, *J. Chromatogr.*, 205 (1981) 39.
6 R. R. Linko, H. Kallio and K. Rainio, *J. Chromatogr.*, 155 (1978) 191.
7 H. Kallio, R. R. Linko and J. Kaitaranta, *J. Chromatogr.*, 65 (1972) 355.
8 F. Van Hoof, A. Wittcox, G. Van Buggenbout and J. Jonssens, *Anal. Chim. Acta*, 169 (1985) 419.
9 S. Selim, *J. Chromatogr.*, 136 (1977) 271.
10 K. Kuwata, M. Uebori and Y. Yamasaki, *J. Chromatogr. Sci.*, 17 (1979) 264.
11 H. R. Van Langenhove, M. Van Acker and N. M. Schamp, *Analyst (London)*, 108 (1983) 329.
12 S. Steinberg and I. R. Kaplan, *Int. J. Environ. Anal. Chem.*, 18 (1984) 253.
13 J. O. Levin, K. Andersson, R. Lindahl and C. Nilsson, *Anal. Chem.*, 57 (1985) 1032.
14 W. A. Jacobs and P. T. Kissenger, *J. Liq. Chromatogr.*, 5 (1982) 669.
15 G. Chiavari and C. Bergamini, *J. Chromatogr.*, 318 (1985) 427.
16 J. Hine, *Physical Organic Chemistry*, McGraw-Hill, New York, 1956, Ch. 8 and 11.
17 F. H. Westheimer, *J. Am. Chem. Soc.*, 56 (1934) 1962.
18 P. D. Bartlett and J. B. Conant, *J. Am. Chem. Soc.*, 54 (1932) 2881.
19 E. Sawicki and C. R. Sawicki, *Aldehydes — Photometric Analysis*, Vol. 1, Academic Press, London, 1975.
20 E. Sawicki and C. R. Sawicki, *Aldehydes — Photometric Analysis*, Vol. 5, Academic Press, London, 1978.
21 Anonymous, *Fed. Regist.*, 51 (1986) 21685.

Journal of Chromatography, 455 (1988) 316–322
Elsevier Science Publishers B.V., Amsterdam — Printed in The Netherlands

CHROM. 20 967

Note

Use of mobile phase modifiers to alter retention and stereoselectivity on a bovine serum albumin high-performance liquid chromatographic chiral stationary phase

IRVING W. WAINER* and YA-QIN CHU*
Pharmaceutical Division, St. Jude Children's Research Hospital, Memphis, TN 38101 (U.S.A.)
(First received May 18th, 1988; revised manuscript received August 9th, 1988)

Bovin serum albumin (BSA) is a globular, hydrophobic protein which has been shown to stereoselectively bind small enantiomeric molecules[1]. The enantioselectivity of BSA has been utilized in the development of chiral stationary phases (CSPs) for use in liquid chromatography. For example, in 1973, Stewart and Doherty[2] immobilized BSA on succinoylaminoethyl-Sepharose and used the resulting CSP to stereochemically resolve D,L-tryptophan. In 1983, Allenmark *et al.*[3] reported the covalent immobilization of BSA on 10-μm silica. His latter work was used as the basis for the development of a commercially available high-performance liquid chromatographic (HPLC) CSP (BSA-CSP).

A wide variety of enantiomeric solutes have been stereochemically resolved on the BSA-CSP[4]. However, while the stereoselectivity of the BSA-CSP is impressive, the routine application of this column to large-scale clinical and pharmacological studies is often hampered by the CSP's chromatographic properties, *i.e.* high retention and low efficiency.

Allenmark and co-workers[4–7] have altered the retention (k') and stereoselectivity (α) on the BSA-CSP by manipulating the composition of the mobile phase. The standard mobile phase used with the BSA-CSP is composed of an aqueous solution of phosphate buffer modified with 1-propanol. The parameters which have been studied by Allenmark and co-workers include the concentration of the buffer[4,5], the pH[6,7] and the 1-propanol content[6].

This is not the only possible approach to the alteration of k' and α on the BSA-CSP. Another method has been suggested by the work of Schill *et al.*[8,9] with the HPLC CSP based upon immobilized α_1-acid glycoprotein (AGP-CSP). The retention and stereoselectivity of solutes on the AGP-CSP can be changed through the addition of neutral or ionic compounds to the mobile phase. These mobile phase modifiers affect k' and α through a variety of mechanisms including direct competition with the solute for binding sites on the protein; alteration of the affinity of the protein for the solute; and formation of ion pairs with the solute.

* On leave from the National Institute for the Control of Pharmaceutical and Biological Products, Beijing, China.

0021-9673/88/$03.50 © 1988 Elsevier Science Publishers B.V.

The potential also exists for using mobile phase modifiers with the BSA-CSP. This possibility is suggested by *in vitro* and *in vivo* studies which have demonstrated the competitive displacement from BSA binding of a variety of substances including warfarin[1,10–12]. It was assumed that the compounds which displace warfarin from serum albumin could be used as mobile phase modifiers to reduce the retention of warfarin on the BSA-CSP.

In this study, we have used three compounds (trichloroacetic acid, cyclamic acid and lauric acid) which are known to displace warfarin from serum albumin as mobile phase modifiers and have confirmed that these modifiers alter the retention and stereoselectivity of warfarin on the BSA-CSP. Three compounds (lorazepam, D- and L-tryptophan) which do not displace warfarin from serum albumin in *in vitro* studies were also investigated and their affects on k' and α varied. The effect of trichloroacetic acid and cyclamic acid on k' and α of other solutes was also investigatd. It appears that these modifiers offer a valuable method for improving the chromatographic properties of the BSA-CSP.

EXPERIMENTAL

Apparatus

The chromatography was performed with a modular liquid chromatograph composed of a Beckman 110B solvent module pump (Beckman Instruments, Houston, TX, U.S.A.), a Spectra-Physics Spectraflow 980 or a Spectra-Physics 8480 scanning UV detector (Spectra-Physics, Santa Clara, CA, U.S.A.), a Shimadzu C-R6A Chromatopac integrator (Shimadzu Scientific Instruments, Columbia, MD, U.S.A.) and a commercially packed chiral phase HPLC column composed of bovine serum albumin immobilized on 10-μm spherical silica (Resolvosil, Alltech Assoc., Deerfield, IL, U.S.A.). The column temperature was maintained within ± 0.1°C of the desired setting with a Forma Scientific Model 2006 circulating water bath (VWR Scientific, Chicago, IL, U.S.A.) and an Alltech HPLC column water jacket.

Chemicals

(*R,S*)-Warfarin, (6*R*,6*S*)-leucovorin, N-benzoyl-(*S,R*)-alanine, N-benzoyl-(*R*)-alanine, N-benzoyl-(*S,R*)-phenylalanine, N-benzoyl-(*R*)-phenylalanine and cyclamic acid (sodium salt) were purchased from Sigma (St. Louis, MO, U.S.A.). (*R,S*)-Benzoin and (*S*)-(+)-benzoin were purchased from Aldrich (Milwaukee, WI, U.S.A.). Trichloroacetic acid was purchased from J. T. Baker (Phillipsburg, NJ, U.S.A.) and lorazepam was obtained from Wyeth Labs. (Princeton, NJ, U.S.A.). The remaining chemicals were reagent grade and used as purchased.

Chromatographic conditions

The basic mobile phases were composed of an aqueous solution of sodium phosphate and 1-propanol. The molarity and pH of the phosphate buffer and the 1-propanol content were varied according to the solute. However, once these parameters were set for a particular solute, they remained constant throughout the study. In particular, the pH of the mobile phase was adjusted after the addition of the mobile phase modifier to the phosphate buffer and before the addition of the 1-propanol.

RESULTS AND DISCUSSION

The structures of solutes used in this study are presented in Fig. 1. During the chromatographic studies, the solute concentrations averaged 10^{-6} *M*. The actual concentrations were selected by plotting *k'* *versus* on column solute molarity to determine the binding capacity of the BSA-CSP. This process was repeated for each of the BSA-CSPs used in this study ($n = 5$) and the calculated binding capacities ranged from $2 \cdot 10^{-6}$ *M* to $8 \cdot 10^{-5}$ *M*. A solute molarity which was five-fold lower than the observed saturation concentration was then used. A 10^{-4} *M* lorazepam solution was used because of difficulties in the detection of this compound.

Where possible, the enantiomeric elution order was determined for each of the solutes. The enantiomeric elution orders on the BSA-CSP for warfarin[13] and leucovorin[14] have been previously determined as *S* before *R*. The enantiomeric elution orders for benzoin, N-benzoyl-alanine and N-benzoyl-phenylalanine were determined during the cours of this study using unequal mixtures of the resolved enantiomers. In each case, the isomer with the *S* configuration at the chiral center eluted first. The resolved enantiomers of lorazepam were not available and the enantiomeric elution order was not determined.

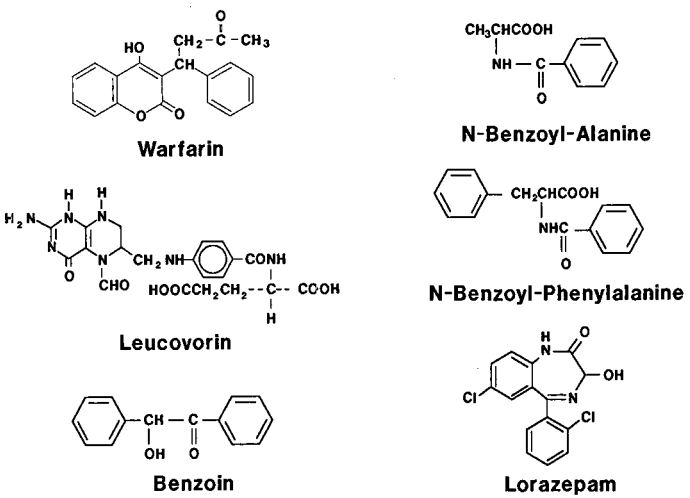

Fig. 1. The structures of the solutes used in this study.

The effect of mobile phase modifiers on retention, stereoselectivity and stereochemical resolution

Warfarin. Table I summarizes the maximum observed effect of the mobile phase modifiers used in this study on the retention (*k'*), stereoselectivity (α) and stereochemical resolution (R_s) of warfarin. Trichloroacetic acid, cyclamic acid and lauric acid were chosen as modifiers based on previous work by Sellers and Koch-Weser[10] in which these compounds were shown to displace warfarin from serum albumin binding. The effect of lorazepam and D- and L-tryptophan on *k'* and α were also examined.

TABLE I

EFFECT OF MOBILE PHASE MODIFIERS ON THE RETENTION AND STEREOCHEMICAL RESOLUTION OF WARFARIN

k'_1 = capacity factor of the first elued enantiomer [(*S*)-warfarin], k'_2 capacity factor of the second eluted enantiomer [(*R*)-warfarin], α = stereoselectivity (k'_2/k'_1), and R_s = stereochemical resolution = $(t_{R2} - t_{R1})/(W_1 + W_2)$ (where t_R = retention time and W = peak width).

Modifier	*Concentration (mM)*	k'_1	k'_2	α	R_s
Trichloroacetic acid	0.0	18.1	21.8	1.20	1.32
	5.0	9.4	10.9	1.16	1.09
Cyclamic acid	0.0	23.9	28.6	1.20	1.23
	7.0	18.3	21.2	1.16	0.79
Lauric acid	0.0	20.7	24.8	1.20	1.18
	0.5	6.1	6.1	1.0	0.0
Lorazepam	0.0	23.6	28.3	1.20	1.29
	0.4	19.4	20.1	1.04	0.45
L-Tryptophan	0.0	19.8	26.0	1.31	1.62
	3.0	18.3	24.0	1.31	1.570
D-Tryptophan	0.0	18.2	23.	1.26	1.48
	3.0	17.3	22.3	1.29	1.39

The consecutive addition of trichloroacetic acid to the mobile phase up to a concentration of 5.0 m*M* resulted in a decrease in the measured parameters (Table I, Fig. 2A). The addition of 5.0 m*M* trichloroacetic acid resulted in a 50% reduction of the k' values of (*S*)- and (*R*)-warfarin while α and R_s were diminished by 3% and 17%, respectively. Similar results were obtained through the addition of cyclamic acid to the mobile phase although the magnitude of the effect on k' was not as large (Table I, Fig. 2B). A 7.0 m*M* concentration of cyclamic acid reduced the k' for both enantiomer by an average of 25%, α was reduced by 3% and R_s was diminished by 36%.

Dramatically different results were obtained with either lauric acid or lorazepam as the mobile phase modifier. The addition of 0.5 m*M* lauric acid to the mobile phase reduced the k' of both enantiomers by more than 70% with an accompanying loss of stereoselectivity (Table I). When 0.4 m*M* lorazepam was added to the mobile phase the effect is similar to the result obtained with lauric acid. There was an 18% reduction in k' for (*S*)-warfarin, a 29% reduction in k' for (*R*)-warfarin, α fell from 1.20 to 1.04 and R_s was reduced from 1.29 to 0.45. Higher concentrations of lorazepam were not studied due to the lack of solubility in the mobile phase.

The effects of D- and L-tryptophan on the measured chromatographic parameters of warfarin on the BSA-CSP were not significant (Table I). A 3.0 m*M* concentration of L-tryptophan in the mobile phase produced an 8% reduction in k' for both warfarin enantiomer and no change in α. With the same concentration of D-tryptophan, the k' of (*S*)-wafarin was reduced by 5%, the k' of (*R*)-warfarin was increased by 2% and α increased from 1.26 to 129. The calculated R_s values also remained essentially constant.

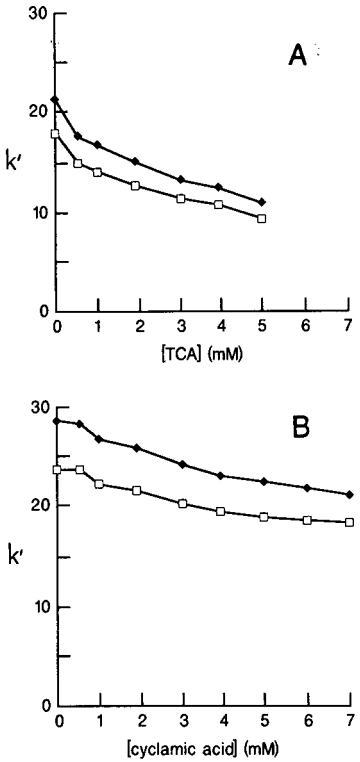

Fig. 2. The effect of (A) trichloroacetic acid and (B) cyclamic acid on the k' of warfarin. Chromatographic conditions: mobile phase, 0.2 *M* phosphate buffer (pH 7.5)–1-propanol (97.3, v/v); temperature, 30°C; flow-rate, 1 ml/min. □ = (*S*)-warfarin; ◆ = (*R*)-warfarin.

Leucovorin, benzoin, N-benzoyl-alanine and N-benzoyl-phenylalanine. In order to assess the general applicability of trichloroacetic acid and cyclamic acid as mobile phase modifier, their effect on the retention and stereoselectivity of the four above-mentioned solutes was investigated. The results of these studies are summarized in Table II. As observed with warfarin, the mobile phase modifiers produced a reduction in k' and α for each solute although the magnitude of the effect varied. The R_s value were also decreased except when N-benzoyl-phenylalanine was chromatographed using 5 m*M* trichloroacetic acid as the mobile phase modifier (Fig. 3).

Lorazepam. The effect of the trichloroacetic acid concentration in the mobile phase on the retention of the two enantiomer of lorazepam is presented in Fig. 4. Since the resolved enantiomer were not available, the elution order is unknown. The addition of up to 3.0 m*M* trichloroacetic acid had very little effect on the k' of the first eluted enantiomer. However, the k' of the second eluted enantiomer passed through a maximum between 0.5 and 1.0 m*M* trichloroacetic acid and then returned to approximately the initial value at 3.0 m*M* trichloroacetic acid. As a result, the stereoselectivity also passed through a maximum rising from α = 1.48 (0 m*M* trichloroacetic acid) to 1.95 (1.0 m*M*) to 1.62 (3.0 m*M*).

When the concentration of trichloroacetic acid in the mobile phase was raised

TABLE II

EFFECT OF TRICHLOROACETIC ACID AND CYCLAMIC ACID ON THE RETENTION AND STEREOCHEMICAL RESOLUTION OF LEUCOVORIN, BENZOIN, N-BENZOYL-ALANINE AND N-BENZOYL-PHENYLALANINE

k_1', k_2' = capacity factors of first and second eluted enantiomer, respectively.

Solute	*Modifier*	*Concentration (mM)*	k_1'	k_2'	α	R_s	*Mobile phase**
Leucovorin	Trichloroacetic acid	0	4.01	5.99	1.49	1.57	A
		5	3.18	3.65	1.15	0.40	A
	Cyclamic acid	0	5.12	7.35	1.44	1.5	A
		7	3.94	5.24	1.33	0.91	A
Benzoin	Trichloroacetic acid	0	4.75	8.0	1.68	2.15	B
		5	3.40	3.60	1.06	0.20	B
	Cyclamic acid	0	4.5	7.50	1.67	2.15	B
		7	3.43	4.75	1.39	1.31	B
N-Benzoyl-alanine	Trichloroacetic acid	0	6.00	15.58	2.55	4.74	C
		5	1.00	1.33	1.33	0.69	C
	Cyclamic acid	0	5.5	15.50	2.45	5.12	C
		7	1.20	1.63	1.36	0.97	C
N-Benzoyl-phenylalanine	Trichloroacetic acid	0	20.25	46.00	2.27	3.96	C
		5	6.50	12.75	1.96	4.29	C
	Cyclamic acid	0	21.00	46.75	2.23	4.00	C
		7	6.25	9.75	1.56	2.71	C

* A = 0.2 *M* phosphate buffer (pH 5.0), B = 0.05 *M* phosphate buffer (pH 7.5)–1-propanol (98:2, v/v), C = 0.05 *M* phosphate buffer (pH 6.5)–1-propanol (99:1).

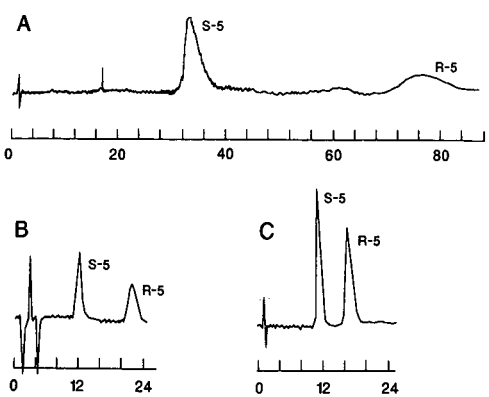

Fig. 3. The effect of mobile phase modifier on the chromatography of N-benzoyl-phenylalanine. Mobile phase, 0.05 *M* phosphate buffer (pH 6.5)–1-propanol (99:1, v/v); temperature, 40°C; flow-rate, 1 ml/min. (A) No mobile phase modifier, (B) 5.0 m*M* trichloroacetic acid added to mobile phase, (C) 7.0 m*M* cyclamic acid added to mobile phase. S-5 = (*S*)-N-benzoyl-phenylalanine; R-5 = (*R*)-N-benzoyl-phenylalanine Injected: 3.7 μM in phosphate buffer (0.05 *M*, pH 7.5). (A + C) 0.02 a.u.f.s. (B) 0.03 a.u.f.s.

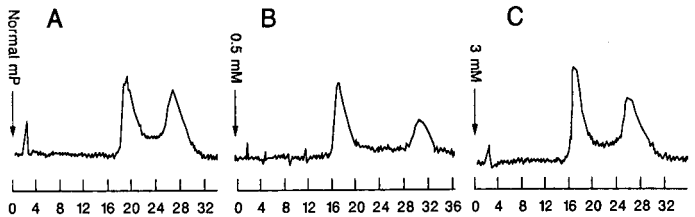

Fig. 4. The effect of trichloroacetic acid on the chromatography of lorazepam. Mobile phase, 0.01 *M* phosphate buffer (pH 6.6)–1-propanol (99:1, v/v); temperature, 40°C; flow-rate, 1 ml/min. (A) No mobile phase modifier, (B) 0.5 m*M* trichloroacetic acid added to mobile phase, (C) 3.0 m*M* trichloroacetic acid added to mobile phase.

from 3.0 m*M* to 5.0 m*M*, the k' of the first eluted enantiomer increased from 9.3 to 15.8 (70% increase) and the stereoselectivity was lost. An additional rise in trichloroacetic acid concentration from 5.0 m*M* resulted in an increase in the k' of both enantiomers to 18.5.

CONCLUSION

This study has demonstrated that mobile phase modifiers can be used to improve the chromatographic performance on the BSA-CSP. Trichloroacetic acid and cyclamic acid are now regularly used as modifiers in this laboratory and have been utilized in the development of assays for large-scale clinical studies[13,14].

The results also suggest that the effect of the modifiers on k' and α is a function of where the solute and the modifier bind to the BSA and the strength of that binding. The results of an investigation of the relationship between HPLC retention on the BSA-CSP and *in vitro* studies of BSA protein binding will be reported elsewhere.

ACKNOWLEDGEMENTS

The authors would like to thank Dr. Philippe Jadaud for his assistance in the preparation of this manuscript. This work was supported in part by the Rockefeller Foundation (Grant No. RF 86068).

REFERENCES

1 W. E. Muller, in I. W. Wainer and D. E. Drayer (Editors), *Drug Stereochemistry, Analytical Methods and Pharmacology*, Marcel Dekker, New York, 1988, pp. 227–244.
2 K. K. Stewart and R. F. Doherty, *Proc. Natl. Acad. Sci. U.S.A.*, 70 (1973) 2850.
3 S. Allenmark, B. Bomgren and H. Borén, *J. Chromatogr.*, 264 (1983) 63.
4 S. Allenmark, *J. Liq. Chromatogr.*, 9 (1986) 425.
5 S. Allenmark, B. Bomgren and H. Borén, *J. Chromatogr.*, 316 (1984) 617.
6 S. Allenmark and S. Anderson, *J. Chromatogr.*, 351 (1986) 231.
7 S. Allenmark and J. Bojarski, *J. Chromatogr.*, 436 (1988) 479.
8 G. Schill, I. W. Wainer and S. A. Barkan, *J. Liq. Chromatogr.*, 9 (1986) 641.
9 G. Schill, I. W. Wainer and S. A. Barkan, *J. Chromatogr.*, 365 (1986) 73.
10 E. M. Seller and J. Koch-Weser, *Ann. N.Y. Acad. Sci.*, 179 (1971) 213.
11 I. Sjoholm, B. Emann, A. Kober, I. Ljungstedt-Pahlma, B. Seiving and T. Sjodin, *Mol. Pharmacol.*, 16 (1979) 767.
12 K. J. Fehske, W. E. Muller and U. Wollert, *Biochem. Pharmacol.*, 30 (1981) 687.
13 Y.-Q. Chu and I. W. Wainer, *Pharm. Res.*, in press.
14 I. W. Wainer and R. M. Stiffin, *J. Chromatogr.*, 424 (1988) 158.

Journal of Chromatography, 455 (1988) 323–326
Elsevier Science Publishers B.V., Amsterdam — Printed in The Netherlands

CHROM. 20 872

Note

Isothiocyanate as a liquid crystalline stationary phase in capillary gas chromatography for the separation of polyaromatic hydrocarbons

J. MAZUR, Z. WITKIEWICZ* and R. DĄBROWSKI
Institute of Chemistry, Military Technical Academy, 01-489 Warsaw 49 (Poland)
(First received April 27th, 1988; revised manuscript received August 2nd, 1988)

Polycyclic aromatic hydrocarbons (PAHs) occur in diverse materials such as atmospheric particulate matter, tobacco smoke, processed food, high-boiling petroleum distillates and other environmental situations. Some of the strongest carcinogens are members of, or directly derived products of, this class of compound. Methods for their separation and determination have been widely studied[1–5]. PAHs can be separated by various methods, *e.g.*, high-performance liquid chromatography, supercritical fluid chromatography and capillary gas chromatography (GC). GC has been used with a considerable number of stationary phases, such as organopolysiloxanes, liquid crystals and mixtures of both. Liquid crystalline stationary phases provide a unique selectivity for the separation of isomers whose molecules have different length-to-breadth ratios. The combination of the high selctivity of liquid crystals and the high efficiency of capillary columns seems to be one of the best methods for PAH separations. The use of polymeric mesomorphic stationary phases is the most efficient method[1,6–8], but low-molecular-weight liquid crystalline phases are still in the use because of the simplier method for the preparation of capillaries[2,3].

This paper deals with a new liquid crystalline stationary phase in GC capillary columns and the possibility of using it for PAH separations.

EXPERIMENTAL

Materials

A new group of rod-like liquid crystalline stationary phases were applied in glass capillary columns. The method for their synthesis and some of their chromatographic applications have been reported[9–11]. The formula of the liquid crystal is

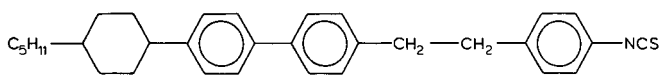

1-[4′-(4-*trans*-Pentylcyclohexyl)biphenylyl]-2-(4-isothiocyanatophenyl)ethane

and the temperatures of the phase transitions are $K \overset{135°C}{\rightleftharpoons} S \overset{163°C}{\rightleftharpoons} N \overset{280°C}{\rightleftharpoons} I$, the phases being the solid crystal (K), smectic mesophase (S), nematic mesophase (N) and

0021-9673/88/$03.50 © 1988 Elsevier Science Publishers B.V.

isotropic liquid (I). The temperatures of phase transitions were measured using a polarizing microscope with a heated stage, type PHMK (Analytik, Dresden, G.D.R.).

The purity of the compound was checked by high-performance liquid and thin-layer chromatography.

Column preparation

The columns (12.5 m × 0.3 mm I.D.) were drawn from soft sodium glass (Glass Factory, Krosno, Poland), prepared according to the carbonate procedure of the Grobs[12,13] and deactivated with Carbowax 1000. The columns were coated with the stationary phase using the static procedure. The film thickness was 0.3 μm. Capillary columns were installed in the chromatograph oven and conditioned by heating from room temperature to the clearing temperature at 1°C/min and maintaining the maximal temperature for 4 h. A Pye Unicam GCV gas chromatograph equipped with a split-stream injector and a flame ionization detector was used. The carrier gas was helium and the make-up gas was nitrogen.

RESULTS AND DISCUSSION

The capillary columns attained about 700 m^{-1} real plates according to Kaiser[14]. The separation of a 3–5-ring PAH mixture was performed (Fig. 1). No special attempts

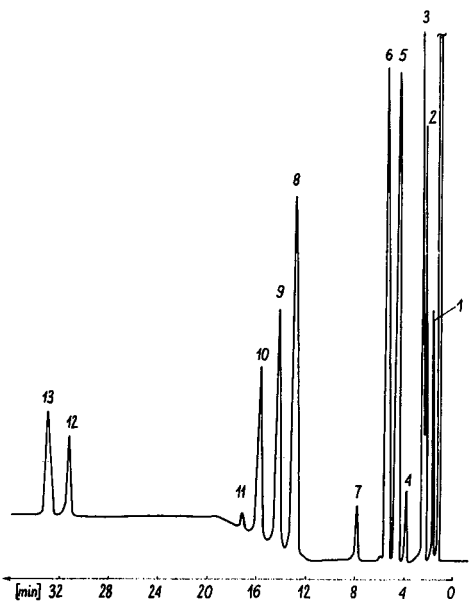

Fig. 1. Separation of selected 3–5-ring PAH isomers. Temperature programme: 9 min at 246°C, heated to 279°C at 3°/min. Injector and detector temperature, 360°C; carrier gas, helium with a linear velocity of 20 cm/s; splitting ratio, 1:100. Peaks: 1 = fluorene; 2 = phenanthrene; 3 = anthracene; 4 = unidentified impurity to fluoranthene; 5 = fluoranthene; 6 = pyrene; 7 = 2,3-benzofluorene; 8 = triphenylene; 9 = benz[*a*]anthracene; 10 = chrysene; 11 = naphthacene; 12 = perylene; 13 = benzo[*a*]pyrene.

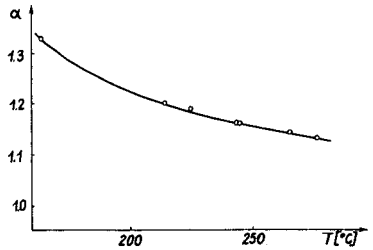

Fig. 2. Relationship between the separation factor (α) for anthracene–phenanthrene and column temperature.

were made to improve this separation. Noteworthy is the resolution of the 4-ring isomers triphenylene, benz[*a*]anthracene, chrysene and naphthacene. The separation factors measured isothermally at 276°C are as follows: benz[*a*]anthracene–triphenylene = 1.14, chrysene–benz[*a*]anthracene = 1.16 and naphthacene–chrysene = 1.34. Under the same conditions the separation factor of benzo[*a*]pyrene and perylene was 1.09.

Anthracene and phenanthrene were not separated to the baseline, but an excellent resolution was obtained by decreasing the column temperature to 200–210°C. Fig. 2 shows the relationship between the separation factor of anthracene–phenanthrene and column temperature.

Many PAHs were identified in the extract of carbon black from a gas stove. The chromatogram is shown in Fig. 3. The peaks were identified by comparison with the retention times of known standards.

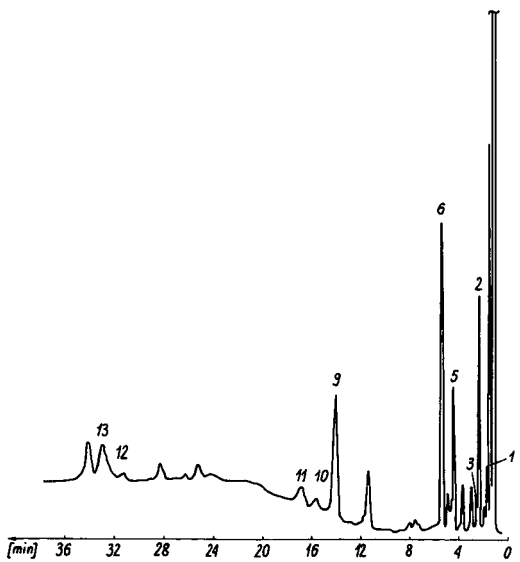

Fig. 3. Chromatogram of PAHs in an extract of carbon black. Conditions and peak identification as in Fig. 1.

Chromatographic separations might be possible only in the nematic region of the mesophase because of the very low column efficiency below the temperature of the smectic–nematic transition (in the smectic region). However, the nematic region from 163 to 280°C is fairly wide and sufficient for using temperature programming. The columns containing the liquid crystalline phase have useful lifetimes of the order of several months without any special operating care.

It has been shown that with short capillary columns coated with the new liquid crystalline stationary phase it is possible to separate mixtures of 3–5-ring PAHs including real samples in a short time.

ACKNOWLEDGEMENT

This work was carried out as a part of the research program RP 1.08.

REFERENCES

1 K. E. Markides, H.-C. Chang, C. N. Schregenberger, B. J. Tarbet, J. S. Bradshaw and M. L. Lee, *J. High Resolut. Chromatogr. Chromatogr. Commun.*, 8 (1985) 516
2 S. Rokushika, K. P. Naikwadi, A. L. Jadhav and H. Hatano, *J. High Resolut. Chromatogr. Chromatogr. Commun.*, 8 (1985) 480.
3 H. Moser and H. Arm, *J. High Resolut. Chromatogr. Chromatogr. Commun.*, 7 (1984) 637.
4 K. P. Naikwadi, A. M. McGovern and F. W. Karasek, *Can. J. Chem.*, 65 (1987) 970.
5 A. Ziółek, Z. Witkiewicz and R. Dąbrowski, *J. Chromatogr.*, 299 (1984) 159.
6 K. E. Markides, M. Nishioka, B. J. Tarbet, J. S. Bradshaw and M. L. Lee, *Anal. Chem.*, 57 (1985) 1296.
7 M. A. Apfel, H. Finkelmann, G. M. Janini, R. J. Laub, B.-H. Luhmann, A. Price, W. L. Roberts, T. J. Shaw and C. A. Smith, *Anal. Chem.*, 57 (1985) 651.
8 A. L. Jadhav, K. P. Naikwadi, S. Rokushika, H. Hatano and M. Ohshima, *J. High. Resolut. Chromatogr. Chromatogr. Commun.*, 10 (1987) 77.
9 R. Dąbrowski, J. Dziaduszek, T. Szczucinski, W. Drzewinski and E. Gołas, *Polish Patent Application*, (1986) P-260393.
10 J. Mazur, Z. Witkiewicz, R. Dąbrowski, *Polish Patent Application*, (1987) P-268841.
11 J. Mazur, Z. Witkiewicz and R. Dąbrowski, *Biul. Wojsk. Akad. Tech.*, 9 (1988) 33–47.
12 K. Grob and G. Grob, *J. Chromatogr.*, 125 (1976) 471.
13 K. Grob, Jr., G. Grob and K. Grob, *J. High Resolut. Chromatogr. Chromatogr. Commun.*, 1 (1978) 149.
14 R. E. Kaiser, *Chromatographia*, 10 (1977) 323.

Journal of Chromatography, 455 (1988) 327–331
Elsevier Science Publishers B.V., Amsterdam — Printed in The Netherlands

CHROM. 20 864

Note

Temperature programming in high-performance liquid chromatography

SANA U. SHEIKH and JOSEPH C. TOUCHSTONE*
Department of Obstetrics and Gynecology, School of Medicine, University of Pennsylvania, Philadelphia, PA 19104 (U.S.A.)
(Received July 22nd, 1988)

Recently there has been renewed interest in temperature as one of the operating parameters in high-performance liquid chromatography (HPLC). Several reports indicate that resolution may be improved by increasing the column temperature, but we found the opposite, particularly with steroids. We have previously reported that resolution improves on cooling the column[1]. The separation of compounds which are difficult to separate at ambient temperature can be improved using either aqueous or non-aqueous mobile phases[2–4].

Temperature programming in HPLC has been largely ignored and there are few reports in the literature[5]. This paper describes the increased resolution in the separation of steroids as a result of temperature programming from ambient to subambient temperatures using both aqueous and non-aqueous mobile phases. The results indicate that an investigation of the successive lowering of the column temperature together with manipulation of the mobile phase composition may increase the ability to separate compounds difficult to resolve.

EXPERIMENTAL

All chemicals were of analytical-reagent grade and all solvents were EM Omnisolve products (EMScience, Cherry Hill, NJ, U.S.A.). Solutions of estrone (E_1), 17β-estradiol (E_2), cortisone (E), cortisol (F) and desoxycorticosterone (D) (Sigma) were prepared in methanol and kept at 4°C.

A modular liquid chromatograph equipped with an LDC pump, a Kratos Spectroflow 773 variable-wavelength detector and a Rheodyne loop injector was used. A Whatman Partisil 10 ODS-3 reversed-phase C_{18} (25 cm × 4.6 mm I.D.) column with methanol–water (65:35, v/v) as the mobile phase was used at a flow-rate of 1.5 ml/min. Acetonitrile–methanol (65:35, v/v) was used as the non-aqueous mobile phase; all conditions were the same as for the aqueous solvent system. All steroids were injected after stabilization of the column temperature. The column temperature was decreased stepwise in each experiment and samples were injected at the selected temperature after stabilization. The temperature range was ambient to −15°C for the aqueous mobile phase and ambient to −50°C for the non-aqueous mobile phase. Liquid nitrogen bled into a glass jacket was used to cool the insulated chamber in

0021-9673/88/$03.50 © 1988 Elsevier Science Publishers B.V.

which the column was suspended. The absorption was recorded at 245 nm for corticoids and 280 nm for estrogens.

For temperature gradients mixtures of model steroids were injected at various stages during cooling the column from ambient to subambient temperatures The column was cooled at the rate of 5°C min^{-1} for E_1–E_2 and 3.5°C min^{-1} of E–F pairs, together with desoxycorticosterone (D). Another experiment followed the same protocol except for elevation of the column temperature, which was increased from −50°C to ambient at the rate of 1.0°C min^{-1}.

Graphs were plotted of retention time (t_R) and resolution (R_s) against temperature. The rate of decrease or increase of column temperature was calculated by using the arithmetic mean value:

$$\text{Rate of temperature decrease/or increase} = \frac{\text{column temperature (initial} - \text{final)}}{\text{retention time}}$$
$$= (T_i - T_f)/t_R$$
$$= \Delta T/t_R$$

RESULTS AND DISCUSSION

The effect of column temperature on resolution is shown in Figs. 1 and 2. It can be seen that the resolution is dependent on temperature, in addition to other HPLC parameters. The straight-lines in Figs. 1 and 2 indicate that the pairs estrone–17β-estradiol (E_1–E_2) and cortisone–cortisol (E–F) were not resolved at ambient temperature (25°C) with either the aqueous or non-aqueous mobile phase. The resolution gradually improved as the column temperature decreased and was maximal at −15°C with the aqueous mobile phase. The column back-pressure was between 1400 and 1500 p.s.i. With the non-aqueous mobile phase, initially E and F appeared as a single peak and D, which was used as an internal standard, was isolated at ambient temperature. Similar and successive improvements in resolution were observed as the temperature decreased from ambient to −50°C, at which the column back-pressure did not exceed practical limits.

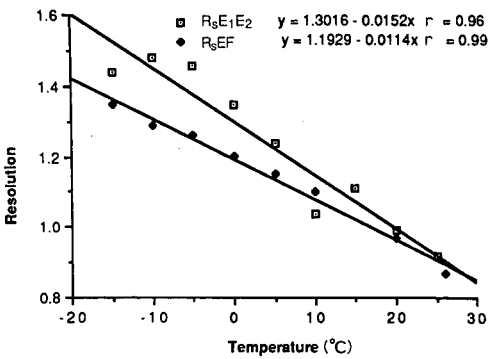

Fig. 1. Resolution–temperature curves for the aqueous mobile phase [methanol–water (65:35,v/v)]. Temperature range = ambient to −20°C. Column = Whatman Partisil 10 ODS-3 C_{18} (25 cm × 4.6 mm I.D.). R_s = Resolution. E_1 = estrone; E_2 = 17β-estradiol; E = cortisone; F = cortisol.

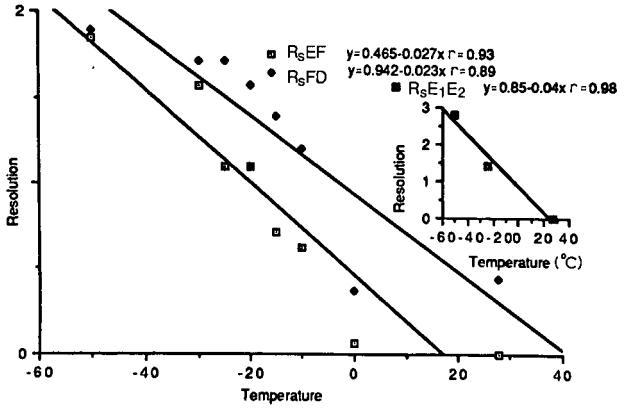

Fig. 2. Resolution–temperature curves for the non-aqueous mobile phase [acetonitrile–methanol (65:35, v/v)]. Temperature range = ambient to −50°C. D = Desoxycorticosterone. Other parameters as in Fig. 1.

With the aqueous mobile phase t_R increases were E_1 34.8, E_2 43.5, E 26, F 34.9 and D 82.9% when the column was cooled from ambient to −15°C, and with the non-aqueous mobile phase 25.28, 39.7, 15.4, 21.3 and 38.3%, respectively, from ambient to −50°C. The increase in t_R was due to an increase in the mobile phase viscosity[6,7].

The temperature gradients shown in Figs. 3 and 4 are plots of R_s and t_R against temperature from ambient to subambient to ambient. These curves indicate that the improvement in R_s increases with decrease in temperature, which is inversely proportional to the column temperature, which is the reverse of the situation in gas chromatography (GC). The situation in GC is different in that there is interaction

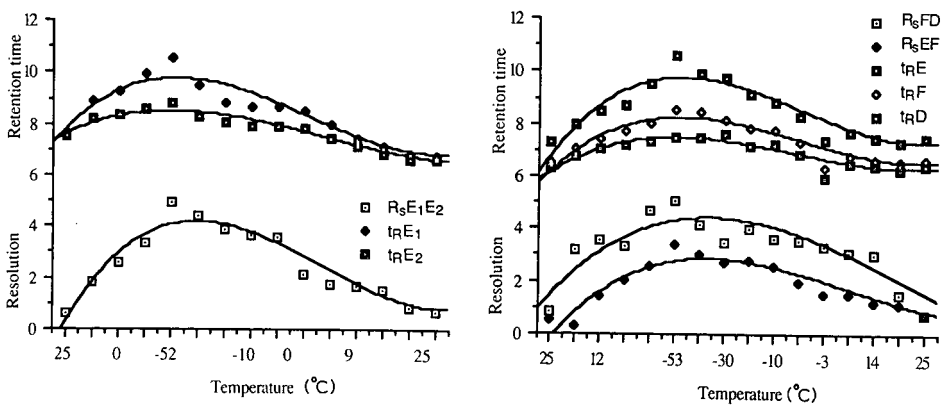

Fig. 3. Resolution, retention and temperature programming for estrogens. Temperature range = 25 to −52 to 25°C; t_R = retention = time difference between injection and appearance of specific peak during development. $R_sE_1E_2$ = resolution of E_1 and E_2. Other parameters as in Figs. 1 and 2.

Fig. 4. Resolution, retention and temperature programming for corticoids. Temperature range = 25 to −52 to 25°C. R_sEF = resolution of E and F; R_sED = resolution of E and D. Other parameters as in Fig. 2.

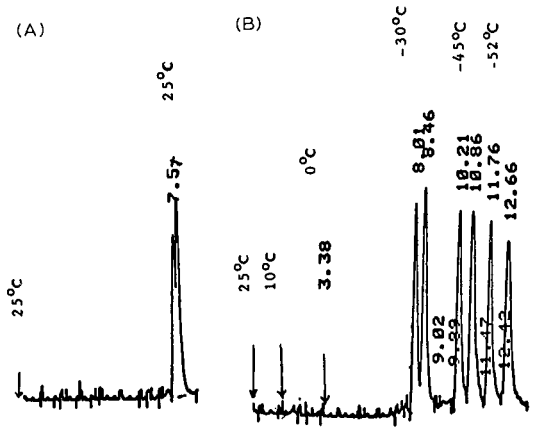

Fig. 5. Temperature programming; (A) sample injected at 25°C and chromatogram developed at 25°C; (B) steroid pair sample E_1–E_2 injected at 25, 10 and 0°C. Peaks were seen at −30, −45 and −52°C. See Fig. 3. See Fig. 1 for key to designations.

between gas and liquid phases and both the solute and mobile phase are in gas form, but in HPLC the interaction is between liquid and liquid phases.

These graphs of retention and resolution *versus* temperature confirmed that the lower the temperature the better is R_s, which reached a maximum at −15 and −50°C with the aqueous and non-aqueous mobile phase, respectively. An interesting feature was that at both ends (ambient temperature) R_s was minimal (no separation achieved).

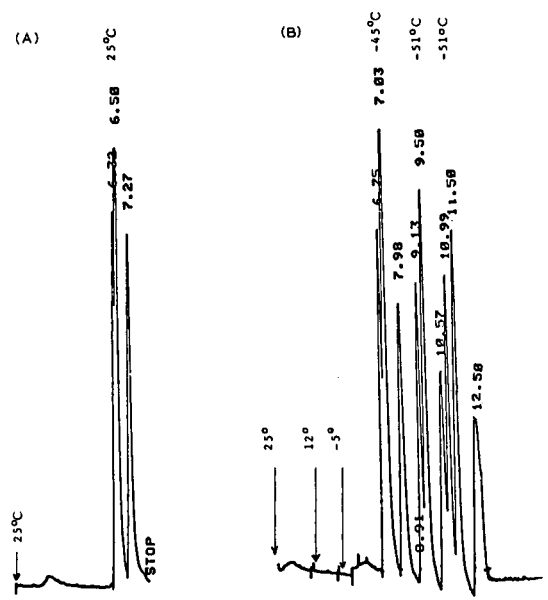

Fig. 6. Temperature programming: (A) sample injected at 25°C and chromatogram developed at 25°C; (B) steroid pair sample E–F and D injected at 25, 12 and −5°C. Peaks were seen at −45 and −51°C. See Fig. 4. See Fig. 1 for key to designations. D = Deoxycorticosterone.

The chromatograms shown in Figs. 5 and 6 summarize the effect of the temperature gradient on R_s. The sample mixture was injected in Fig. 5B at 25, 10 and 0°C. Resolved pairs of E_1–E_2 peaks were seen at −30, −45 and −52°C with t_R = 8.10, 8.46; 10.21, 10.86; and 11.76, 12.66 min. R_s was significantly improved compared with the chromatogram in Fig. 5A for ambient temperature. Similar results were obtained for the corticoid E–F–D mixture. Fig. 6A shows E and F as a shoulder at ambient temperature, but when the column temperature was programmed all components were resolved very clearly at −52°C with t_R = 10.86, 11.76 and 12.66 min, as shown in Fig. 6B.

It was observed that with increase in column temperature the resolution started to decrease and at ambient temperature the compounds were not resolved.

REFERENCES

1 J. C. Touchstone and S. U. Sheikh, *J. High Resolut. Chromatogr. Chromatogr. Commun.*, 9 (1986) 464.
2 S. U. Sheikh and J. C. Touchstone, *Chim. Oggi*, 10 (1987) 25.
3 S. U. Sheikh and J. C. Touchstone, *Anal. Chem.*, 59 (1987) 1472.
4 S. U. Sheikh and J. C. Touchstone, *J. Liq. Chromatogr.*, 11 (1987) 2489.
5 D. E. Henderson and D. J. O'Connor, *Adv. Chromatogr.*, 23 (1984) 65.
6 L. R. Snyder, *J. Chromatogr. Sci.*, 8 (1970) 692.
7 L. R. Snyder and J. J. Kirkland, *Introduction to Modern Liquid Chromatography*, Wiley, New York, 1979, p. 714.

Journal of Chromatography, 455 (1988) 332–335
Elsevier Science Publishers B.V., Amsterdam — Printed in The Netherlands

CHROM. 20 922

Note

High-sensitivity laser-induced fluorescence–high-performance liquid chromatography studies of polyaromatic hydrocarbons using the argon ion laser–Yeung detector cell configuration

MARK C. ROACH* and MARLIN D. HARMONY*
Department of Chemistry, University of Kansas, Lawrence, KS 66045 (U.S.A.)
(First received December 15th, 1987; revised manuscript received August 2nd, 1988)

The outstanding properties of lasers (*e.g.*, monochromaticity, temporal and spatial coherence, high photon flux) have made them increasingly attractive sources for fluorescence detection of low concentrations of high-performance liquid chromatographic (HPLC) effluents[1–10]. In order to take the fullest advantage of laser sources a number of detector cell designs have been developed and reported in the literature[3]. We recently reported[10] excellent laser-induced fluorescence (LIF)–HPLC results for tagged amino acids (at less than femtomole levels) using the detection cell configuration reported by Sepaniak and Yeung[5] in conjunction with the 458-nm line of the CW argon ion laser. In order to demonstrate further the applicability of this LIF detection configuration for other HPLC effluents, we have used an essentially identical system with the UV laser lines from the argon ion laser to detect polyaromatic hydrocarbons (PAHs) at low levels. There is, of course, no universal laser source, but the CW argon ion laser is attractive because it has a number of useful laser lines in both the near UV and visible spectral ranges. Thus the principal goal of this short communicaton is to demonstrate the versatility of the argon ion–Yeung cell configuration by operating with UV excitation. We have also utilized the tripled output of a pulsed Nd-YAG laser to provide a qualitative comparison with another commonly available laboratory laser.

EXPERIMENTAL

Reagents and chemicals

All the polyaromatic hydrocarbons used in this study were purchased from Aldrich (Milwaukee, WI, U.S.A.) and were used without further purification. The PAHs investigated include anthracene (An), fluoranthene (Fl), pyrene (Py), benz[*a*]-anthracene (BaA), chrysene (Chr), benz[*b*]fluoranthene (BbF), benz[*k*]fluoranthene (BkF), benz[*a*]pyrene (BaP), dibenz[*a,h*]anthracene (ah) and benz[*g,h,i*]perylene (ghi). Reagent-grade hexane, toluene and chloroform and HPLC-grade acetonitrile were

* Present address: Syntex Research, 3401 Hillview Avenue, Palo Alto, CA 94304, U.S.A.

0021-9673/88/$03.50 © 1988 Elsevier Science Publishers B.V.

purchased from J. T. Baker (Phillipsburg, NJ, U.S.A.). Deionized, distilled water was used for all experiments. Solvents were degassed using an ultrasonic bath and further degassing was effected by flushing with helium gas throughout the experiment. Stock solutions of the various PAHs were prepared in a solvent mixture of hexane–chloroform–toluene–acetonitrile (81:11:2:6) to ensure solubility of all the PAHs and also compatibility with the mobile phase in the HPLC system.

Apparatus

All separations were performed on a 250 × 2.6 mm I.D. reversed-phase column (Perkin Elmer HC-ODS 0089-0716) using either a Milton Roy Model 396 single piston pump or an LKB 2150 HPLC pump, and a Rheodyne 7125 injector fitted with a 20-μl loop. The detector cell, irradiation configuration and fiber optics for fluorescence collection were identical to the system described in our earlier work[10]. For the argon ion laser (Spectra Physics Model 171-17) experiments the total UV output (334, 351 and 363 nm) was utilized after removing superradiance with a Schott UG-11 filter. Fluorescence from the PAHs was detected by a photomultiplier tube after bandpass (10 nm) filtering at 430 nm, and signals were processed by conventional photon counting methods. The comparison Nd-YAG pulsed laser (Quantel YG-481) experiment used the tripled output at 355 nm after filtering with the same Schott UG-11 filter to remove residual 532-nm radiation. Photomultiplier tube detected fluorescence at 430 nm was processed at the 10-Hz laser repetition rate using a boxcar averager (PARC M162/164). Chromatographic data were either output directly to a strip chart recorder or were processed with a microcomputer data acquisition system before plotting.

RESULTS

Fig. 1 presents a chromatogram obtained under isocratic conditions for a mixture of ten PAHs using the argon ion laser system. Note that all but the two PAHs with the longest retention times are readily identified and distinguished although

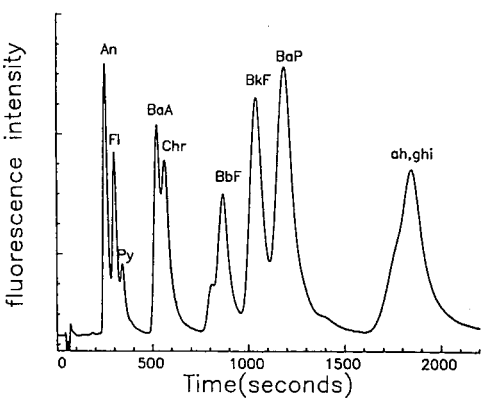

Fig. 1. Chromatogram of a mixture of ten PAHs using isocratic conditions: acetonitrile–water (70:30) at a flow-rate of 1.0 ml/min. A 20-μl injection contained 200 pg of An, Fl, BkF and BaP; 300 pg BbF; 500 pg ghi; 1 ng BaA and ah; 2 ng Py; and 40 ng Chr.

resolution is certainly not complete. From chromatograms of the pure components, detection limits have been determined for several of the PAHs as summarized in Table I. The calibration curves were linear over more than two decades with $r \geqslant 0.997$. Similar data were also collected for the same PAHs using the pulsed Nd-YAG laser system and the detection limits are presented in Table I.

DISCUSSION

The detection limits observed for the CW argon ion experiments vary roughly over the range of 0.2 to 1.3 pg (*ca.* 1–6 femtomol), approximately 100 times lower than obtained with a conventional HPLC system with $\lambda_{ex} = 365$ nm and $\lambda_{em} = 455$ nm[11]. On the other hand, conventional HPLC fluorescence detection limits reported for deuterium lamp excitation at 280 nm are within a factor of five of our argon ion results[12], showing the efficacy of irradiating into the more intense shorter wavelength UV band. In any case, the argon ion–Yeung cell system clearly performs excellently in the UV with detection limits comparable to those reported earlier for tagged amino acids irradiated in the visible spectral region[10]. Again, as in our earlier studies[10], we find the Yeung detector cell design and optical geometry to be trouble free and experimentally reliable for routine studies.

When the tripled pulsed YAG laser output at 355 nm is used in place of the argon ion laser lines, the detection limits as presented in Table I are seen to be generally degraded by approximately one order of magnitude. This poorer performance was not unexpected and arises primarily because the YAG laser used in these studies shows pulse-to-pulse power variations of up to 10%, while the CW argon ion laser output has a stability approaching 1%. In addition, the spatial beam quality of the YAG output is substantially poorer than that of the CW argon ion laser which leads to poorer focusing and an increase in scattered light.

For either laser source, the detection limits vary from one compound to the other depending upon factors such as the absorption coefficient at the exciting line wavelength(s) and the fluorescence yields in the filter bandwidth of the detection system. In the case of the pulsed laser, the detection limits may also be importantly effected by the gated integrator aperture delay and duration if not properly matched to the fluorescence lifetimes, which may vary from one compound to the other.

Overall, it is clear from this work and our earlier studies[10] that the CW argon ion

TABLE I
DETECTION LIMITS FOR FIVE PAHs

Compound	*CW argon laser**	*Pulsed YAG laser**
Anthracene	0.16	0.80
Fluoranthene	0.38	0.38
Benz[*a*]anthracene	1.3	23.0
Benz[*b*]fluoranthene	0.72	15.0
Benz[*a*]pyrene	0.18	0.80

* Detection limits in pg based on a signal-to-noise ratio of 2.

laser used with the detector cell configuration of Sepaniak and Yeung[5] yields highly reliable and sensitive chromatographic determinations for compounds whose excitation bands are accessible to the UV or visible lines of the laser.

ACKNOWLEDGEMENTS

Support of this work by the National Science Foundation (Grant CHE 81-08395), and by the Kansas Commisson on Advanced Technology and Oread Laboratories, Inc., is gratefully acknowledged.

REFERENCES

1 G. Diebold and R. N. Zare, *Science (Washington, D.C.)*, 196 (1977) 1439.
2 M. J. Sepaniak and E. S. Yeung, *Anal. Chem.*, 49 (1977) 1554.
3 E. S. Yeung and M. J. Sepaniak, *Anal. Chem.*, 52 (1980) 1465A.
4 J. H. Richardson, K. M. Larson, G. R. Haugen, D. C. Johnson and J. E. Clarkson, *Anal. Chim. Acta*, 116 (1980) 407.
5 M. J. Sepaniak and E. S. Yeung, *J. Chromatogr.*, 190 (1980) 377.
6 S. Folestad, L. Johnson, B. Josefsson and B. Galle, *Anal. Chem.*, 54 (1982) 925.
7 T. Imasaka, K. Ishibashi and N. Ishibashi, *Anal. Chim. Acta*, 142 (1982) 1.
8 R. N. Zare, *Science (Washington, D.C.)*, 226 (1984) 298.
9 K. Sauda, T. Imasaka and N. Ishibashi, *Anal. Chem.*, 58 (1986) 2649.
10 M. C. Roach and M. D. Harmony, *Anal. Chem.*, 59 (1987) 411.
11 K. Ogan, E. Katz and W. Slavin, *J. Chromatogr. Sci.*, 16 (1978) 517.
12 B. S. Das and G. H. Thomas, *Anal. Chem.*, 50 (1978) 967.

Journal of Chromatography, 455 (1988) 336–343
Elsevier Science Publishers B.V., Amsterdam — Printed in The Netherlands

CHROM. 20 837

Note

Simultaneous determination of thiols and corresponding disulphides in mixtures by high-performance liquid chromatography with polarographic detection using a Dual-Tast Analyser

BARBARA DĘBOWSKA and KRYSTYNA SAMOCHOCKA*
Department of Chemistry, Warsaw University, Pasteura 1, 02-089 Warsaw (Poland)
and
MAREK PRZASNYSKI* and DANUTA SYBILSKA
Institute of Physical Chemistry, Polish Academy of Sciences, Kasprzaka 44, 01-224 Warsaw (Poland)
(First received May 16th, 1988; revised manuscript received July 18th, 1988)

Reduced glutathione (GSH), cysteine (CSH) and the corresponding disulphides, *i.e.*, oxidized glutathione (GSSG) and cystine (CSSC) form important biological systems. Their rôle in living processes has stimulated the interest of analysts and various procedures have recently been reported for their determination; they are mainly chromatographic methods. Due to the scarcity of sensitive detectors for disulphides, the latter are usually determined as thiols after precolumn reaction, thus the most of the elaborated methods do not distinguish thiols from disulphides. Very often, however, such determinations are not sufficient and more specific data are desirable, *i.e.*, describing the equilibria between thiols and disulphides. The following two different approaches have recently been designed to resolve this problem by high-performance liquid chromatography (HPLC) with electrochemical detection.

Allison *et al.*[1,2] used an amperometric detector with dual thin-layer mercury–gold amalgam electrodes. After chromatographic separation of all species, disulphides were converted into the corresponding thiols at an upstream electrode and were then detected as thiols at a downstream electrode via their oxidation of the mercury surface. The upstream electrode serves as a postcolumn reactor so only the downstream electrode current need be monitored.

We have applied polarographic detection with a DC-Tast polarograph at two suitably chosen potentials of the dropping mercury electrode (DME)[3]. Species of interest (cysteine and cystine) were separated on a reversed-phase (RP) column (according to the ion-pair mechanism) and the first cystein eluted was detected at the DME (at +0.25 V *vs.* silver–silver chloride) according to the anodic reaction

$$2CSH + Hg \rightarrow Hg(CS)_2 + 2H^+ + 2e^- \quad (1)$$

* Present address: 40, Powsińska Str., 02-903 Warsaw, Poland.

0021-9673/88/$03.50 © 1988 Elsevier Science Publishers B.V.

while subsequently eluted cystine was reduced after a rapid shift of the potential of the DME to −0850 V *vs.* silver–silver chloride, the reaction:

$$CSSC + 2H^+ + 2e^- \rightleftarrows 2CSH \quad (2)$$

For quantitation of the species, both currents, *i.e.*, oxidation and reduction, should be recorded. Due to the continuously renewed mercury surface, the reproducibility of this simple method is satisfactory and its sensitivity comparable to that attained with chemical derivatization and fluorescence detection[4]. The main disadvantage arises from the change in potential during the chromatogram. Besides the difficulties of automatization, it implies the need for chromatographic separation of both species, which should be better than baseline separation. To avoid this inconvenience, for the present work we applied a specially constructed supplementary apparatus, a Dual-Tast. This enables automatic measurements of both anodic and cathodic currents on each mercury drop.

EXPERIMENTAL

Reagents

L-Cysteine puriss was obtained from Fluka (Buchs, Switzerland) and L-cystine, reduced and oxidized glutathione from Reanal (Budapest, Hungary). All other reagents were of analytical reagent or laboratory grade and were used without further purification.

Apparatus

Chromatographic experiments were performed using a Type 302 liquid chromatograph equipped with a Type PP2 flow-through detector, a Type PPW1 DC-Tast polarograph coupled with a Dual Tast Analyser. All the above instruments were constructed at the Institute of Physical Chemistry of the Polish Academy of Sciences (Warsaw, Poland). The DC-Tast mode presents several advantages as compared with the DC one, particularly with respect to detection in flow-through systems[3,5]. These advantages can sometimes be enlarged by coupling a DC-Tast polarograph with a Dual-Tast Analyser. A more detailed description of the apparatus mentioned above was given previously[5]. In the present work a simplified scheme of measurements is given. Chromatograms were registered with a Type TZ 4200 dual pen recorder (Laboratorni Přistroje, Prague, Czechoslovakia). Stainless-steel columns (250 mm × 4 mm I.D. and 100 mm × 4.6 mm I.D.) slurry packed with 10-μm LiChrosorb RP-8 (Merck, Darmstadt, F.R.G.) were used for separation.

The Dual-Tast Analyser performs automatic measurements of the current on each mercury drop at two different potentials suitably chosen and at the delay times chosen in advance. Detection is performed at the naturally dropping electrode.

The key principles of the measurements are shown in Fig. 1. Fig. 1A shows the changes in potential applied to the DME *versus* time, t. Two different potentials, E_1 and E_2, chosen for tast measurements in this work, correspond to the oxidation and the reduction of thiols and disulphides at the DME, according to eqns. 1–4 and the polarograms exemplified in Fig. 2.

The corresponding changes in current due to the electrode reaction of thiols and

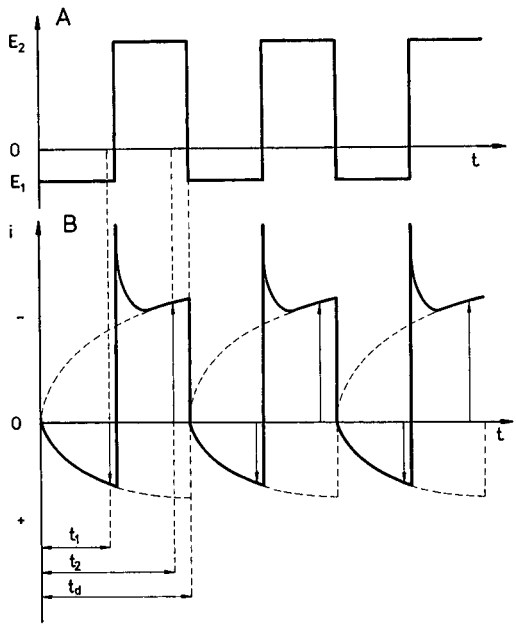

Fig. 1. Measurement scheme using a DC-Tast polarograph equipped with a Dual-Tast Analyser. (A) Changes of potential *versus* time; (B) corresponding changes of the current due to the electrode reaction of thiols and disulphides.

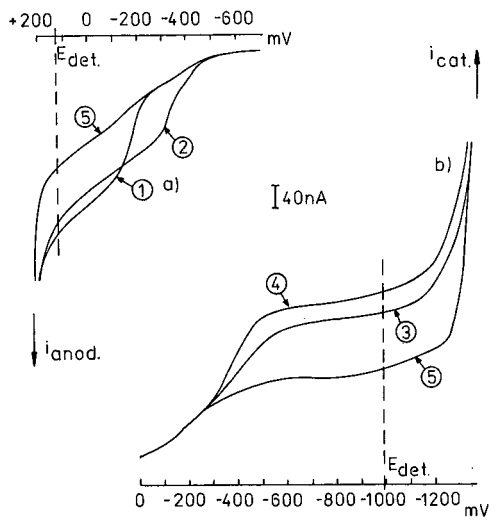

Fig. 2. Polarographic curves of (a) $2 \cdot 10^{-5}$ *M* reduced glutathione (1), $2 \cdot 10^{-5}$ *M* cysteine (2) and supporting electrolyte (5) and (b) 10^{-5} *M* cystine (3), 10^{-5} *M* oxidized glutathione (4) and supporting electrolyte (5) 0.03 *M* phosphate buffer pH 3.5. Reference electrode: SCE.

disulphides are shown in Fig. 1B; t_d is the natural drop lifetime, t_1 and t_2 are the delay times for the first (at E_1) and second (at E_2) measurements respectively counted from the drop fall. The full line corresponds to the current flowing through the detector when potentials E_1 and E_2 are applied successively to each mercury drop. The dotted line represents the current flowing when only one potential, namely E_1 or E_2, is applied. The measured values of the current are marked in Fig. 1B with arrows.

The first tast measurement of the current is performed at the potential E_1 after the delay time t_1. Then the potential of the DME is automatically adjusted to E_2 and after the delay time t_2 (counted from the drop fall) the second measurement is carried out.

The sampling time (*ca.* 5 ms) is not shown in Fig. 1 because this value is very small compared with t_1, t_2 and t_d (*ca.* 2 s). The times t_1 and t_2 should be as long as possible under the following conditions: (a) $t_1 < t_2 < t_d$; (b) $(t_2 - t_1)$ should be longer than the recharging time of the double layer after the change of potential; (c) the time necessary for the detection of the drop fall $(t_d - t_2)$ should be at least 50 ms.

In order to detect the drop fall the sinusoidal voltage ($U_0 \sin\omega t$, $U_0 = 20$ mV, $f = 3.5$ kHz, not shown in Fig. 1) is superimposed just after the second measurement of the current at E_2.

The disappearance of the alternating current with drop fall changes the electrode potential to E_1.

In the case of a reversible polarographic process, a shadow chromatographic peak of the same retention as the main component was detected at the second potential (E_2). This is due to the compound produced at the electrode at the first potential (E_1) if E_2 corresponds to the electrode reaction of the compound produced.

Procedure

All measurements were carried out at 25 ± 0.2°C and at a constant flow-rate of 0.8 or 1.0 ml/min.

The aqueous mobile phase containing 0.03 *M* phosphate buffer of various pH and various concentrations of D-camphor-10-sulphonic acid (CSA) (Merck, Schuchard) as a pairing ion and methanol were deareated with argon. Samples (5 µl) injected on the column contained oxygen or were deoxygenated by the simple procedure described by Lloyd[6]. Chromatograms were obtained by monitoring simultaneously two currents: anodic (at +0.250 V *vs.* silver–silver chloride) and cathodic (at −0.850 V *vs.* silver–silver chloride). In order to avoid the appearance of small additive peaks due to the products of the reversible reactions 2 and 3

$$GSSG + 2H^+ + 2e^- \rightleftarrows 2GSH \tag{3}$$

it was necessary to hold the DME first at a potential of +0.250 V corresponding to the irreversible reactions 1 and 4

$$GSH + Hg \rightarrow GSHg + H^+ + e^- \tag{4}$$

and then change it to −0.85p V. In the case of the opposite sequence (first potential −0.850 V, second +0.250 V) it was possible to detect the trace amounts of the products of the reversible reduction reactions 2 and 3, *i.e.*, CSH and GSH respectively in the second step at +0.25 V.

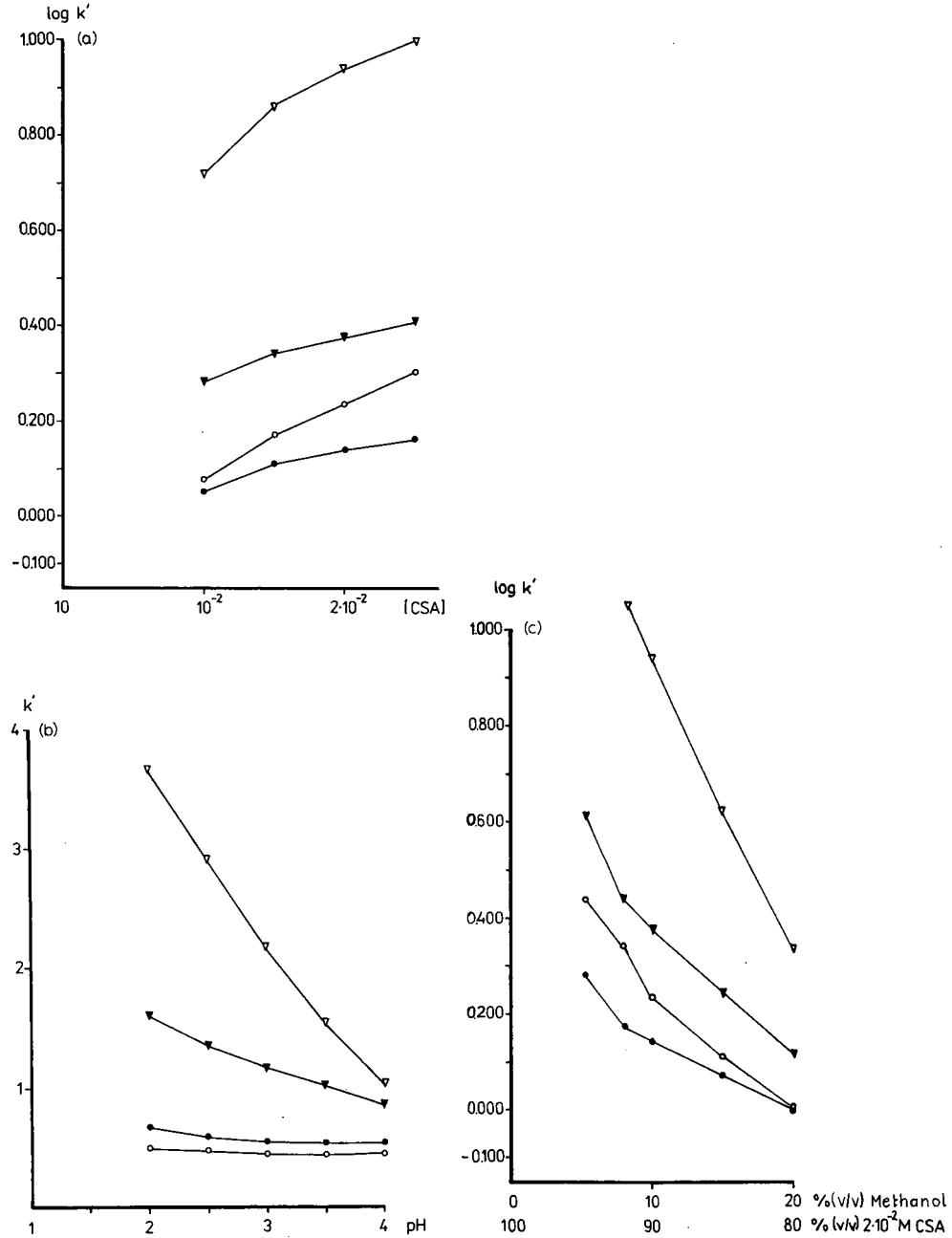

Fig. 3. (a) Plots of the logarithms of capacity factors, k', of cysteine (●), cystine (○), reduced glutathione (▼) and oxidized glutathione (▽), *versus* CSA concentration. Stationary phase: 10-μm LiChrosorb RP-8. Mobile phase: 0.03 *M* phosphate buffer with 10% (v/v) methanol, pH 2. (b) Plots of k' *versus* pH of the mobile phase (0.03 *M* phosphate buffer). Stationary phase: 10-μm LiChrosorb RP-8. (c) Plots of the logarithms of k' *versus* % of methanol in the mobile phase: $2 \cdot 10^{-2}$ *M* CSA in 0.03 *M* phosphate buffer pH 2. Stationary phase: 10-μm LiChrosorb RP-8.

Polarographic curves of pure cysteine, cystine and reduced and oxidized glutathione were obtained with a saturated calomel electrode (SCE) as the reference elctrode, and for the detection in chromatography a silver–silver chloride electrode was used, $V_{Ag/AgCl} - V_{SCE} = 139$ mV.

RESULTS AND DISCUSSION

Fig. 3 shows the changes in capacity factors of investigated solutes with pH and CSA and methanol concentrations. Each k' value was determined with a relative standard deviation of 0.3%.

It has already been stated that better than baseline separation of CSH and CSSC can be achieved at high CSA concentration and at low pH, *i.e.*, at $2 \cdot 10^{-2}$ *M* CSA and pH 2.0[3]. However, as the plots in Fig. 3 demonstrate, under these conditions the retention of GSH and GSSG strongly increases, prolonging the analysis time and worsening the detectability. Small amounts of methanol may suppress this effect to some extent, but the Dual-Tast Analyser was designed to avoid these difficulties. To exemplify how it operates, two chromatographic systems using mobile phases of different compositions (I and II) were chosen: I, $2 \cdot 10^{-2}$ *M* CSA, 0.03 *M* phosphate buffer pH 2 and 10% (v/v) methanol in water; II, 0.03 *M* phosphate buffer pH 3.5–methanol (90:10).

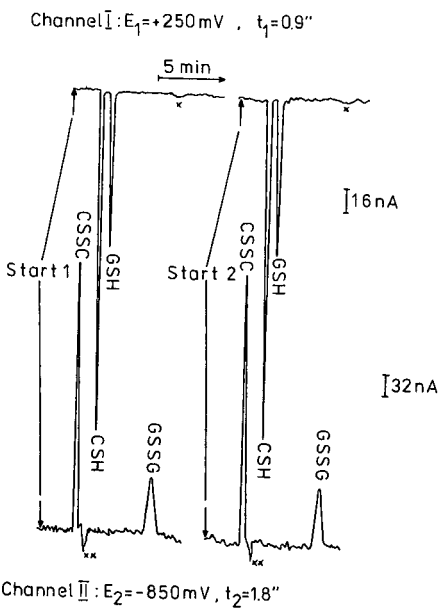

Fig. 4. Two consecutive chromatograms of a mixture of $2 \cdot 10^{-4}$ *M* CSH, $2 \cdot 10^{-4}$ *M* GSH, 10^{-4} *M* CSSC and 10^{-4} *M* GSSG. Mobile phase: $2 \cdot 10^{-2}$ *M* CSA in 0.03 *M* phosphate buffer pH 2 with 10% (v/v) methanol. Column (100 mm × 4.6 mm I.D.): 10-μm LiChrosorb RP-8. Flow-rate: 1 ml/min. Samples deoxygenated. Drop time: $t_d = 2.15$ s. ×, Unidentified peak accompanying oxidized glutathione of retention equal to that of DSSC; × ×, unidentified peak accompanying reduced glutathione of retention equal to that of GSH.

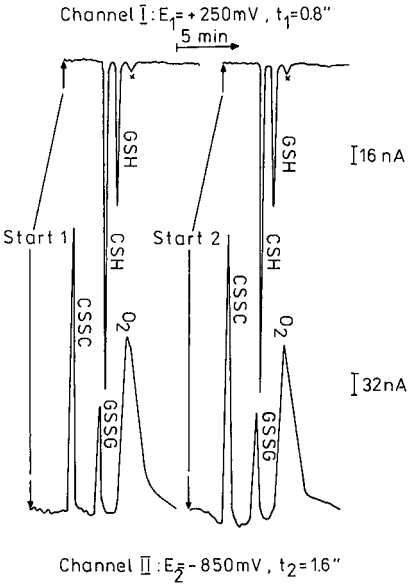

Fig. 5. Two consecutive chromatograms of a mixture of $2 \cdot 10^{-4}$ *M* CSH, $2 \cdot 10^{-4}$ *M* GSH, 10^{-4} *M* CSSC and 10^{-4} *M* GSSG. Mobile phase: 0.03 *M* phosphate buffer pH 3.5 with 10% (v/v) methanol. Column (250 mm × 4 mm I.D.); 10-μm LiChrosorb RP-8. Flow-rate: 0.8 ml/min. Samples containing oxygen. Drop time: t_d = 2.08 s.

The corresponding chromatograms demonstrating different resolutions, different analysis times and also different detectabilities are shown in Figs. 4 and 5. Mobile phase solution I results in almost baseline resolution of CSH and CSSC and complete separation of GSH and GSSG within *ca.* 10 min (Fig. 4). The samples should be deaerated because elution of oxygen is partly superimposed on the cystine peak. With mobile phase II, during *ca.* 6 min baseline separation of GSH and GSSG is observed but the resolution of CSH and CSSC is then poor (Fig. 5). Oxygen forms a separate peak and thus the sample must not be deaerated.

As seen in Figs. 4 and 5, each species can be determined both in the case of complete and poor resolution. The detection limits, defined as the amount of injected substance giving a signal twice that of the baseline noise, are collected in Table I.

TABLE I

DETECTION LIMITS OF INVESTIGATED THIOLS AND DISULPHIDES IN TWO CHROMATOGRAPHIC SYSTEMS

Compound	*Detection limit (pmol)*	
	System I	*System II*
Cysteine	4	4
Cystine	18	17
Reduced glutathione	9	10
Oxidized glutathione	82	43

A linear dependence of the peak height on concentration up to 10^{-3} *M* for CSH, GSH, GSSG and up to $5 \cdot 10^{-4}$ *M* for CSSC was found.

In all, the analysis time in system II presenting the poor resolution is almost half that of system I with complete separation. The detectability achieved for GSSG is also twice as good.

The Dual-Tast Analyser seems to be an efficient tool for rapid determinations of such redox systems as sulphides. It may also be useful in the case of other poorly resolved compounds differing significantly in their polarographic behaviours.

REFERENCES

1 L. A. Allison and R. E. Shoup, *Anal. Chem.*, 55 (1983) 8.
2 L. A. Allison, J. Keddington and R. E. Shoup, *J. Liq. Chromatogr.*, 6 (1983) 1975.
3 D. Sybilska, M. Przasnyski, B. Mysior and K. Samochocka, *J. Chromatogr.*, 283 (1984) 453.
4 J. D. H. Cooper and D. C. Turnell, *J. Chromatogr.*, 227 (1982) 158.
5 M. Przasnyski, J. Piecek and W. Kutner, *Nauch. Apparat., Scientific Instrumentation*, 2 (1987) 21–38.
6 J. B. F. Lloyd, *J. Chromatogr.*, 256 (1983) 323.

Journal of Chromatography, 455 (1988) 344–348
Elsevier Science Publishers B.V., Amsterdam — Printed in The Netherlands

CHROM. 20 878

Note

Separation of thiols on Spheron Ara activated with 2-nitrophenylhydrazonopropandinitrile ligand

D. PODHRADSKÝ*

Department of Special Biology, Faculty of Sciences, P. J. Šafárik University, Moyzesova 11, 041 67 Košice (Czechoslovakia)

M. ANTALÍK

Institute of Experimental Physics, Slovak Academy of Sciences, Solovjevova 47, 040 01 Košice (Czechoslovakia)

and

E. ŠTURDÍK

Department of Biochemical Technology, Slovak Technical University, Radlinského 9, 812 37 Bratislava (Czechoslovakia)

(First received April 26th, 1988; revised manuscript received August 9th, 1988)

As we have shown[1,2], phenylhydrazonopropandinitrile derivatives react reversibly with thiols through the nitrile group. In the previous studies we considered the use of these substances as ligands for the reversible immobilization of SH peptides and proteins. Using the 2-nitrophenyl derivative of hydrazonopropandinitrile it is possible to perform the desorption of thiols in such a way that individual components are well separated from each other.

EXPERIMENTAL

Reagents

3-Mercaptopropionic acid (Sigma), N-acetylcysteine, reduced glutathione, NADPH, coenzyme A (Calbiochem), 5,5′-dithiobis(2-nitrobenzoic) acid (Ellman's reagent) (Koch-Light) and Spheron Ara 1000 (0.04–0.06 mm) (Lachema) were used.

Processing of yeast Saccharomyces cerevisiae

Cells of baker's yeast (1 g) were disintegrated by homogenizaton with glass beads (8 min) followed by sonication (2 min, 22 kHz, 5°C) in 2 ml of Britton–Robinson buffer (pH 2.5) (100 ml of 0.04 mol dm^{-3} orthophosphoric acid, 0.04 mol dm^{-3} acetic acid, 0.04 mol dm^{-3} boric acid and 15 ml of 0.2 mol dm^{-3} sodium hydroxide) containing 1.5 mmol dm^{-3} of EDTA. After deproteination with 0.2 ml of 70% perchloric acid, the pH of the sample was adjusted to 7.55 with 0.35 ml of saturated sodium hydrogencarbonate solution.

Chromatographic procedure

NPHPD-Spheron, which has been used as a sorbent for chromatography, was

0021-9673/88/$03.50 © 1988 Elsevier Science Publishers B.V.

prepared by modificaton of Spheron Ara 1000 with 4-chlorocarbonyl-2-nitrophenylhydrazonopropandinitrile[2]. The column for chromatography (50 × 1.5 cm I.D.) was packed with the swollen sorbent and equilibrated with eluting buffer [Britton–Robinson buffer (pH 7.55) + 1 m*M* EDTA]. The sample containing thiols was dissolved in 2 ml of the eluting buffer. The flow-rate of the mobile phase was 1 ml/min.

The thiols were detected with Ellman's reagent[3]. The peaks in the chromatographic analysis of yeast sample were identified by comparison with the elution volumes of standards obtained previously. In addition, glutathione reductase was used for the determination of glutathione in the enzymatic cycling reaction[4] and coenzyme A was identified spectrophotometrically at 280 nm.

RESULTS AND DISCUSSION

The mechanism of the reactions of phenylhydrazonopropandinitriles with thiols has been published previously[5–7]. It was shown that the 4-nitrophenyl derivative, which is able to act as a ligand within the pH range 4–8, is the most suitable for the reversible immobilization of SH compounds. The interaction of tiols with the carrier may be depicted as shown in Scheme 1.

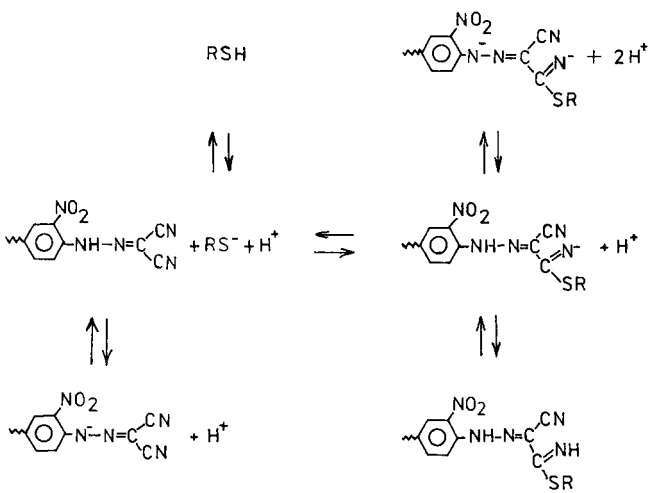

Scheme 1.

Whereas the binding of thiol is dependent on the pK_a values of the hydrazo group of the ligand and the SH group of the separated compound, its release is more complicated because the rate of thiol release is significantly influenced by the imino group present in the addition product. Protonatable nitrogen atoms of the 2-nitrophenylhydrazonopropandinitrile ligand play a decisive role in the binding and release of separated compounds. This is evident from the increasing elution volumes of glutathione with increasing pH of the eluting buffer (Fig. 1). The processes that occur in the column may be characterized by continuous renewal of the equilibrium among the ligand, separated thiols and protons of the eluting medium.

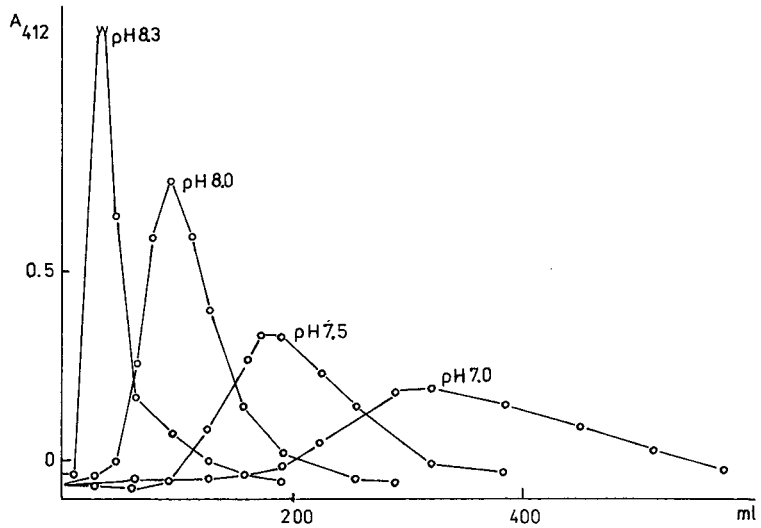

Fig. 1. Elution of glutathione on a 25-cm NPHPD-Spheron column as a function of pH.

The separation of four thiols on a 50-cm column is sown in Fig. 2. The elution volumes are inversely proportional to the pK_a values of the SH groups of thiols (Table I). Whereas the most reactive thiols are eluted at the beginning of the analysis, the biochemically important glutathione (pK_a = 8.56) is the last substance to be eluted from the column.

The quantitative evaluation of a standard mixture of thiols showed a maximal recovery of glutathione and a minimal recovery of coenzyme A. The losses did not exceed 6% and could be explained by oxidation during analysis.

The method of separation has been used to determine the thiols in yeast

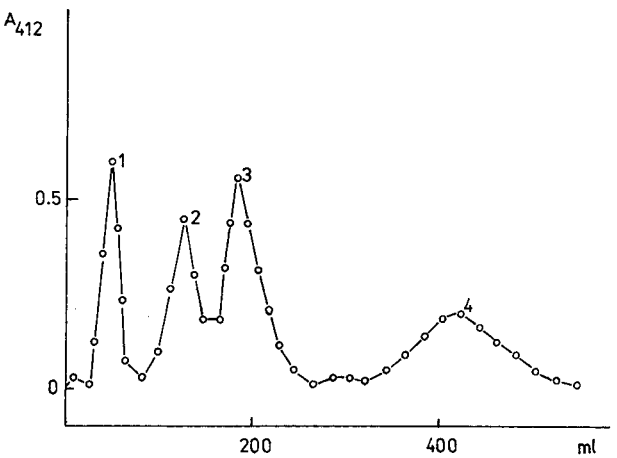

Fig. 2. Separation of a mixture of thiols at pH 7.55. Peaks: 1 = 3-mercaptopropionic acid; 2 = coenzyme A; 3 = N-acetylcysteine; 4 = glutathione.

TABLE I
PARAMETERS OBTAINED FROM THE CHROMATOGRAPHIC ANALYSIS OF THIOLS
Column, NPHPD-Spheron (50 × 1.5 cm I.D.), pH 7.55.

Thiol	pK_a*	*Elution volume (ml)*	*Sample (μmol per 2 ml)*	*Recovery (μmol)*
3-Mercaptopropionic acid	10.61	48	28.3	26.6
Coenzyme A	9.60	128	13.0	12.5
N-Acetylcysteine	9.52	180	30.6	29.7
Glutathione	8.56	408	26.0	25.6

* According to ref. 8.

homogenate. As shown in Fig. 3, glutathione is the main thiol present (0.015 μmol/mg dry matter. Traces amounts of coenzyme A and two unidentified peaks are also present.

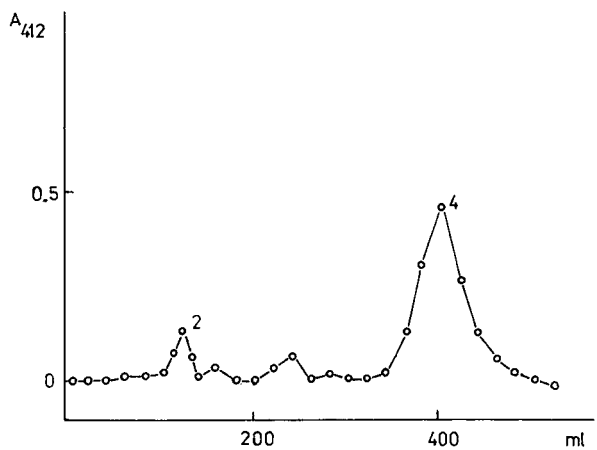

Fig. 3. Analysis of non-protein thiol in a sample from *Saccharomyces cerevisiae*. The conditions are the same as for standards. Peak identification as in Fig. 2.

The method presented for the separation of thiols is of analytical and preparative importance, especially if it is taken into account that regeneration of column can be omitted. The procedure enables carriers to be prepared for the high-performance liquid chromatograhy of thiols, in which the use of a pH gradient is very attractive.

REFERENCES

1 V. Marko, P. Gemeiner, M. Antalík, E. Šturdík, Ľ. Drobnica and P. Kristián, *React. Polym.*, 1 (1983) 91.
2 D. Podhradský, G. Toth, G. Suchár, P. Kristián and M. Antalík, *J. Chromatogr.*, 328 (1985) 402.
3 G.L. Ellman, *Arch. Biochem. Biohys.*, 74 (1958) 443.
4 P. Eyer and D. Podhradský, *Anal. Biochem.*, 153 (1986) 57.

5 Ľ. Drobnica and E. Šturdík, *Biochim. Biophys. Acta*, 585 (1979) 462.
6 M. Antalík, E. Šturdík, O. Pytela, Ľ. Drobnica and P. Sulo, *Collect. Czech. Chem. Commun.*, 49 (1984) 2807.
7 P. Sulo, E. Šturdík, T. Liptay, T. Jakubík and M. Antalík, *Collect. Czech. Chem. Commun.*, 50 (1985) 375.
8 J. P. Danehy and K. N. Parameswaran, *J. Chem. Eng. Data*, 13 (1968) 386.

Journal of Chromatography, 455 (1988) 349–354
Elsevier Science Publishers B.V., Amsterdam — Printed in The Netherlands

CHROM. 20 905

Note

Derivatisation of amines with O-acetylsalicyloyl chloride to enhance electrochemical detection in high-performance liquid chromatography*

ROGER M. SMITH*, ASRI ABDUL GHANI, DECLAN G. HAVERTY, GILLIAN S. BAMENT, A. Y. CHAMSI and ARNOLD G. FOGG

Department of Chemistry, Loughborough University of Technology, Loughborough, Leics. LE11 3TU (U.K.)

(First received April 18th, 1988; revised manuscript received July 25th, 1988)

Many compounds, such as simple aliphatic amines or alcohols, lack a chromophore and cannot be readily directly analysed by high-performance liquid chromatography (HPLC) using spectrophotometric detection. This problem can often be overcome by derivatisation to introduce a chromophore or fluorophore. However, derivatisation to introduce an electrochemically active group into the analyte has rarely been utilised even though electrochemical detection can be both highly sensitive and selective. Suitable electrochemically active groups include nitrophenyls, which can be detected by reductive electrochemical methods, or phenolic and arylamino groups, which can be detected oxidatively. Oxidative detection is usually preferred because it avoids the need to exhaustively remove oxygen from the sample solution and mobile phase.

Compared with the wide versatility of derivatisation reactions which can be used to introduce a chromophore, only a relatively small number of reactions have been reported for the formation of electrochemically active derivatives. The early methods, which were primarily for the formation of reducible derivatives were surveyed by Kissinger et al.[1]. They also tested many of the nitroaromatic derivatives, such as the 3,5-dinitrobenzoates of aliphatic alcohols, which are also frequently formed in order to enhance spectrophotometric detection[2].

Most interest in recent years has been found in compounds which can be detected electrochemically in the oxidative mode. For example aliphatic isocyanates have been derivatised with 1-(2-methoxyphenyl)-piperazine to provide a sensitive method for environmental monitoring[3], and hydrazines can be detected as the corresponding salicylaldehyde derivatives[4]. These and other methods have been summarised in a recent review by Leroy and Nicolas[5]. However, the introduction of a phenolic group into many compounds can be difficult. This is because the most common route for the derivatisation of hydroxyl or amino groups is the use of reagents containing reactive carbonyl or sulphonyl chlorides, which would also react with any phenolic groups.

The present study describes the application of a protected reagent, O-acetylsal-

* Presented at the *11th International Symposium on Column Liquid Chromatography, June 29–July 3, 1987, Amsterdam.*

0021-9673/88/$03.50 © 1988 Elsevier Science Publishers B.V.

icyloyl chloride, as a pre-column derivatisation reagent for aliphatic amines. Initially this compound will react with an amino group to form an O-acetylsalicylamide, which will be hydrolysed spontaneously under the alkaline conditions of the synthesis to give a 2-hydroxybenzamide. This free phenolic group can then be detected electrochemically following separation by HPLC. While this study was in progress, a related reaction was described by Chou *et al.*[6]. They derivatised amines in a solid phase reaction using a polymeric anhydride substituted with O-acetylsalicyl groups. This reagent gave the corresponding O-acetylsalicylamides, which were usually detected spectrophotometrically. However, it was also found that the derivatives responded in an electrochemical detector despite the absence of a free phenolic group.

EXPERIMENTAL

Reagents

O-Acetylsalicyloyl chloride was purchased from Fluka (Buchs, Switzerland) and was used as received. Sample amines, N-methylaniline, benzylamine and piperidine, were laboratory reagent-grade from a range of suppliers. Buffer reagents were AR-grade and methanol was HPLC-grade from FSA Laboratory Supplies (Loughborough, U.K.). Water was distilled.

Equipment

Separations were carried out using a rapid stroke reciprocating pump ACS Model LC 500 (Applied Chromatography Systems; Macclesfield, U.K.), a Cecil 2012 spectrophotometric detector (Cecil Instruments; Cambridge, U.K.) set at 254 nm and Kipp Analytica 9205 electrochemical detector (Emmen, The Netherlands) with a glassy carbon thin film detector cell at a potential of + 0.90 V with respect to an Ag/AgCl reference electrode. The samples (10 μl) were injected using a Model 7125 Rheodyne valve onto an ODS-Hypersil 5-μm column (100 × 5 mm I.D.). The eluent was methanol–0.025 *M* phosphate buffer, pH 8.0 (50:50) containing 0.001 *M* sodium chloride at a flow-rate of 1 ml min^{-1}.

Preparation of standard derivatives

Samples of the derivatives were prepared by condensation of the free amine with O-acetylsalicyloyl chloride in 0.1 *M* aqueous sodium hydroxide (Schotten–Baumann conditions). The product of the reaction was extracted and recrystallised. The structures of the products were confirmed by NMR and IR spectroscopy.

Derivatisation of dilute aqueous solutions of amines

O-Acetylsalicyloyl chloride (20 mg) was mixed with a dilute solution of the amine in 0.1 *M* sodium hydroxide solution (1.0 ml). After shaking and standing for 1 h, samples (10μl) were analysed directly by HPLC.

RESULTS AND DISCUSSION

Amines and amino acids are usually derivatised for HPLC analysis by using either a pre- or post-column reaction. For small numbers of samples the former method is easier and a wide range of reagents to form derivatives with enhanced

spectrophotometric or fluorescence properties have been described. A common derivatisation route is the conversion of the amine into an amide with an acyl or sulphonyl chloride under alkaline conditions. As the products no longer possess basic amino groups they usually suffer less interactions with the stationary phase and the derivatives have better chromatographic properties.

However, the use of acylation to introduce an electrochemically active group, such as an aromatic amine or phenolic group, directly into an aliphatic amine would be difficult. The problem is that the reagent may also react with the electrochemically active group. The present study sets out to demonstrate that if the phenolic group is protected as an ester, the acylation reaction of the amine can proceed. The protecting group could then be easily removed using alkali to reveal the phenolic group. These conditions should have little effect on the amido group.

The present study therefore examined the reaction of the commercially available reagent O-acetylsalicyloyl chloride with amines under alkaline Schotten–Baumann conditions. In trial experiments, even under mild conditions, the reaction was found to give the corresponding 2-hydroxybenzamides directly. The intermediate O-acetylsalicylamide appeared to be spontaneously hydrolysed during the synthesis (Fig. 1).

Pure samples of the derivatives of a series of simple amines, piperidine, benzylamine and N-methylaniline, were therefore prepared. These derivatives were examined by HPLC on an ODS-Hypersil column with a methanol–0.025 *M* aqueous phosphate buffer, pH 8.0 (50:50) eluent and were found to be well retained (capacity factors of piperidine, N-methylaniline and benzylamine were 2.7, 3.5 and 11.5, respectively) and to give good peak shapes. The peaks could be readily detected using spectrophotometric detection at 254 nm. This eluent was selected because at lower pH the phenolic groups gave only a poor electrochemical response.

In order to study the electrochemical properties of these phenolic derivatives and determine the optimum potential for detection, a series of replicate injections of a $1 \cdot 10^{-3}$ *M* solution of the derivative of piperidine was carried out using an electrochemical detector with a thin-film glassy carbon electrode. The peak heights were measured at different applied potentials (Fig. 2). There was no evidence of electrode deterioration or contamination and good reproducibility was obtained, although in previous studies there had been problems with electrode contamination using other phenolic compounds[7]. The results suggested that a working potential of + 0.90 V would be suitable and this was used in all subsequent work. Using these conditions, linear calibration curves were obtained for dilute solutions of each of the derivatives (*e.g.* 2-hydroxybenzamide of piperidine gave a correlation coefficient of 0.9950 from $1 \cdot 10^{-7}$ to $1 \cdot 10^{-6}$ *M*). The derivatives could be detected down to concentrations of

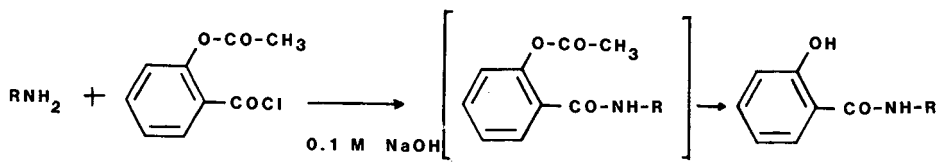

Fig. 1. Reaction of O-acetylsalicyloyl chloride with an amine in alkaline solution.

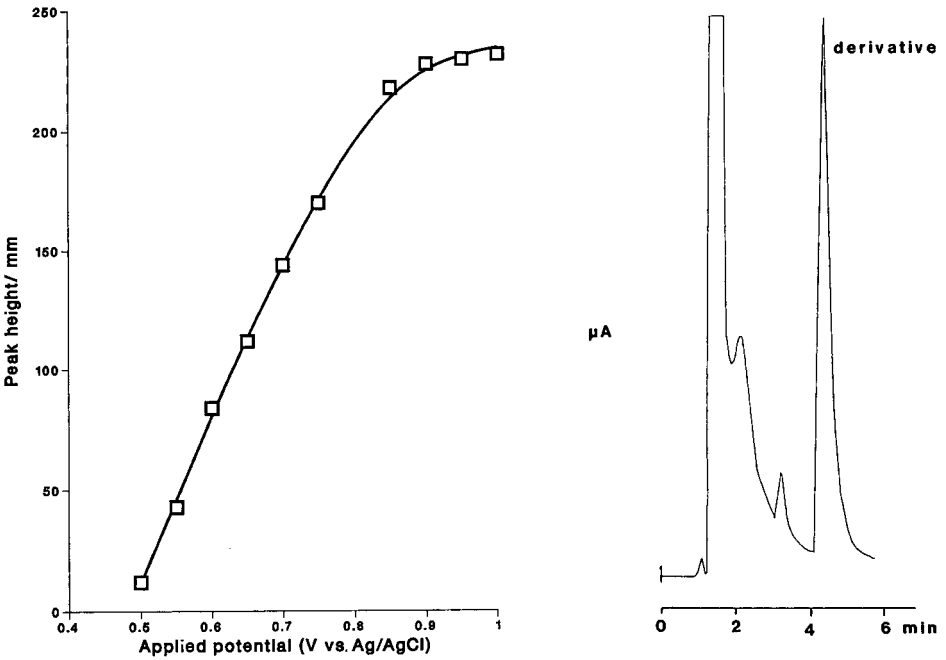

Fig. 2. Effect of measurement potential of the electrochemical detector on peak height on injecting replicate samples of 10 μl of a $1 \cdot 10^{-3}$ *M* solution of the 2-hydroxybenzamide of piperidine.

Fig. 3. Separation of the reaction mixture from the addition of 20 mg of O-acetylsalicyloyl chloride to an aqueous alkaline solution of $1 \cdot 10^{-4}$ *M* piperidine (1.0 ml). Column ODS-Hypersil 100 mm × 5 mm I.D.. Mobile phase methanol–phosphate buffer, pH 8.0 (50:50). Electrochemical detection at +0.90 V, sensitivity range 1 μA.

$1 \cdot 10^{-7}$ *M* in the analyte solution using a 10-μl injection. At these concentrations no reponse was observed using an ultraviolet spectroscopic detector at 254 nm.

The interest in this reaction lay in its ability to be applied to the determination of low concentrations of aliphatic amines in aqueous solution. A series of experiments was therefore carried out to determine the amount of reagent required in order to ensure a high yield of the derivative. A series of dilute solutions of piperidine ($1 \cdot 10^{-4}$ *M*) in 0.1 *M* sodium hydroxide were prepared and different amounts of O-acetylsalicyloyl chloride were added and left for 1 h at room temperature. The derivative was not extracted but an aliquot of the reaction solution was injected directly onto the HPLC column. In the separation the excess of the reagent and its hydrolysis products were well separated from the derivatives of the amines (Fig. 3). It may be possible to use shorter reaction times but this was not investigated. In order to determine the efficiency of the reaction the peak heights of the derivatives were compared with standard solutions of the pure derivative.

The yield of the derivative increased with the amount of reagent added up to about 19 mg/ml of amine solution. Thus to ensure complete reaction a considerable excess of the reagent was required. Apparently at lower levels much of the reagent was being hydrolysed before reaction with the amine was complete. In subsequent studies on more dilute amine solutions a ratio of 20 mg of reagent to 1 ml of dilute amine solution was used as the standard method.

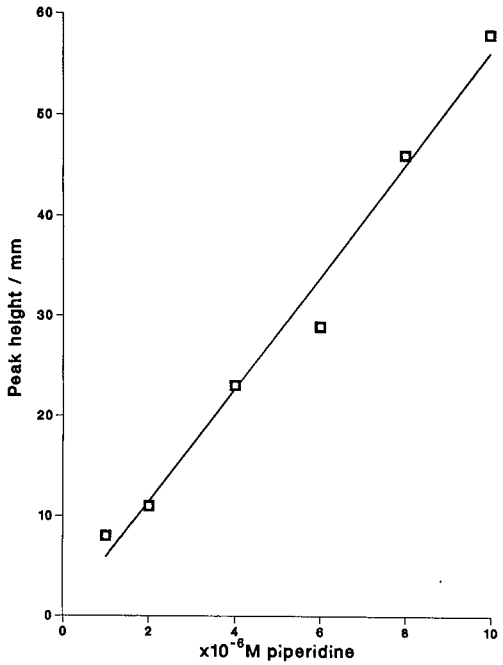

Fig. 4. Calibration graph for peak for 2-hydroxybenzamide of piperidine formed from piperidine in dilute aqueous alkaline solution following addition of O-acetylsalicyloyl chloride.

A series of dilute solutions containing different concentrations of the amines were then analysed. The aliphatic amine, piperidine, gave virtually quantitative yields at the 10^{-4} to 10^{-6} *M* levels, when compared with the separation of a pure derivative. The derivatisation of four samples of a $1 \cdot 10^{-5}$ *M* solution of piperidine showed good reproducibility (relative standard deviation 1.4%). Derivatisation of both piperidine and benzylamine gave a linear response for the amine (*e.g* piperidine from $1 \cdot 10^{-6}$ to $10 \cdot 10^{-6}$ *M* correlation coefficient 0.9915, Fig. 4). The limit of detection (signal-to-noise ratio of 2) of piperidine was about $6 \cdot 10^{-7}$ *M* in the aqueous solution. A lower limit of detection could probably have been reached if the product had been extracted and concentrated before chromatography but this would have been more time consuming.

However, the yield of the derivative of aromatic amine N-methylaniline was much lower, 42% at $1 \cdot 10^{-4}$ *M* and 55% at $1 \cdot 10^{-5}$ *M*. This level of reaction was unaffected by further increasing the amount of reagent added to the solution. It appeared that the reaction was slower because of the lower basicity of the aromatic amino group and as a consequence hydrolysis of the reagent was competing with derivatisation. The separation in this case was also more complicated as unreacted N-methylaniline also gave an electrochemically active peak, which confused the chromatogram. Despite the poor yield the reaction with N-methylaniline still gave a linear response at 10^{-4} *M* levels in the aqueous sample solution. However, direct electrochemical detection would probably be a more suitable method for the detection of the arylamines.

CONCLUSION

Aliphatic amines on reaction with O-acetylsalicyloyl chloride are readily converted into the corresponding 2-hydroxybenzamides, which can be detected at low concentrations in aqueous solution using HPLC with electrochemical detection.

ACKNOWLEDGEMENTS

The authors thank the Malaysian Public Service Department for a studentship to A.A.G.

REFERENCES

1 P. T. Kissinger, K. Bratin, G. C. Davis and L. A. Pachla, *J. Chromatogr. Sci.* 17 (1979) 137.
2 W. A. Jacobs and P. T. Kissinger, *J. Liq. Chromatogr.*, 5 (1982) 881.
3 C. J. Purnell and R. F. Walker, *Analyst (London)*, 110 (1985) 893.
4 P. E. Kester and N. D. Danielson, *Chromatographia*, 18 (1985) 125.
5 P. Leroy and A. Nicolas, *Analusis*, 14 (1986) 263.
6 T.-Y. Chou, S. T. Colgan, D. M. Kao, I. S. Krull, C. Dorschel and B. Bidlingmeyer, *J. Chromatogr.*, 367 (1986) 335.
7 R. M. Smith, *Chromatographia*, 17 (1982) 155.

Journal of Chromatography, 455 (1988) 355–359
Elsevier Science Publishers B.V., Amsterdam — Printed in The Netherlands

CHROM. 20 887

Note

Development of an high-performance liquid chromatographic method for the simultaneous analysis of the species involved in diethyl L-tartrate hydrolysis

DEVENDRA S. KALONIA* and ANTHONY P. SIMONELLI
School of Pharmacy and Institute of Material Sciences, University of Connecticut, Storrs, CT 06268 (U.S.A.)
(First received July 13th, 1988; revised manuscript received August 2nd, 1988)

The hydrolysis kinetics of diesters generally follow a two step reaction that involves rate constants, k_1 and k_2, as shown by the following equations.

$$\mathrm{Di} + \mathrm{R} \xrightarrow{k_1} \mathrm{Mo} + \mathrm{P} \quad (1)$$

$$\mathrm{Mo} + \mathrm{R} \xrightarrow{k_2} \mathrm{Ac} + \mathrm{P} \quad (2)$$

Here, Di, Mo and Ac are starting material, intermediate and final products, respectively. The common co-reactant is R and the common co-product is P. In order to simplify the analysis of data, pseudo-first order conditions, are generally used by maintaining the concentration of the co-reactant, R, at a constant level throughout the course of the reaction. The rate constants can be calculated from the concentrations of

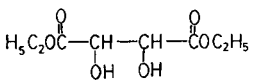

Diethyl Tartrate

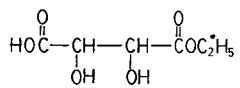

Monoethyl Tartrate

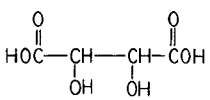

Tartaric Acid

Fig. 1. Different species involved in the diester hydrolysis.

0021-9673/88/$03.50 © 1988 Elsevier Science Publishers B.V.

Di, Mo and Ac as a function of time[1]. Under pseudo-first order conditions, diethyl tartrate hydrolysis involves three major species, starting material (diethyl tartrate), intermediate species (monoethyl tartrate), and the end product (tartaric acid). See Fig. 1.

A reversed-phase high-performance liquid chromatographic (HPLC) assay in which the mobile phase is aqueous, would be best suited to analyze these species. This paper describes an HPLC assay that can analyze all the species simultaneously with the added advantage that no pretreatment of samples is required. This can be important as pretreatment could change the kinetics by altering the amounts of one or more of the three species during the pretreatment process.

EXPERIMENTAL

Materials

The following chemicals were used: diethyl L-tartrate and L-tartaric acid (Aldrich, Milwaukee, WI, U.S.A.) and sodium hydroxide (Primary Standard, J. T. Baker, Phillipsburg, NJ, U.S.A.). Monoethyl tartrate was synthesized in the laboratory (see next section). Both methanol (J. T. Baker) and water were distilled and filtered through a 0.2-nm membrane (Millipore, Bedford, MA, U.S.A.). Tetrabutylammonium phosphate (PIC A, Waters Assoc., Milford, MA, U.S.A.) was used as received.

Sample preparation

Stock solutions of the diester, monoester and tartaric acid were prepared by using 243.53 mg of diester, 111.56 mg of monoester and 140.00 mg of tartaric acid. The volume of each solution was adjusted to 100 ml. The samples for HPLC analysis were prepared by mixing 10 μl of each of the stock solutions of diester, monoester and tartaric acid and; diluting the mixture to 10 ml with water. Other samples were prepared similarly by using 20, 30, 40, 50, 100 and 200 μl of each of the stock solutions and diluting the mixture to 10 ml.

Chromatographic equipment and conditions

The HPLC apparatus (Waters Assoc.) was equipped with the following: HPLC pump 6000A, solvent programmer, U6K injector, 730 data module (to record the chromatogram and to calculate the area under the peak), C_{18} column (μBondapak, 10 μm, 30 cm $\times$ 3.9 mm I.D.). In addition an LC-55 variable-wavelength UV detector (Perkin-Elmer, Instrument Division, Norwalk, CT, U.S.A.) was used to monitor the eluent.

The mobile phase consisted of methanol–water (20:80, v/v) with 0.005 *M* PIC A and the pH adjusted to 3.2. Other conditions were: flow-rate, 1.5 ml/min; wavelength, 210 nm; and sample volume, 10 μl.

Preparation of monoester

The following procedure was developed for the preparation of monoester (sodium monoethyl L-tartrate). An amount of 1 g (0.0025 equiv.) of sodium hydroxide pellets was added to 50 ml of chloroform in an erlenmeyer flask. The mixture was placed in a water bath adjusted to 45°C. Over a period of 5 min 5.15 g (0.0025 equiv.) of

diethyl tartrate was slowly added while the mixture was vigorously stirred. A white precipitate began to form immediately. The mixture was stirred for another 30 min and then filtered through Whatmann filter paper. The precipitates were washed at least five times with 20-ml portions of chloroform (dried overnight with anhydrous calcium chloride). The precipitates were air dried overnight and then tested for purity. The product was identified using HPLC assay and confirmed by mass spectroscopy (MS).

RESULTS AND DISCUSSION

During the optimization of HPLC eluents it was found that the retention times of monoethyl tartrate and tartaric acid were extremely sensitive to pH. As shown in Fig. 2, the monoethyl tartrate and tartaric acid peaks were fused at pH 7.0. The order of elution reversed and retention times were slightly reduced when the pH was changed to 4.2. As the pH of the eluent was further decreased to 3.5, the two peaks showed a better resolution. The resolution was further improved when the pH was changed to 1.5 but the first peak eluted with the solvent front. This suggested that an intermediate pH between 3.5 and 1.5 would yield a better separation. In fact, pH 3.2 yielded the optimum separation and was used for all analysis. A typical chromatogram is shown in Fig. 3.

The first and third peaks were confirmed to be tartaric acid and diester, respectively, by using pure samples. Since, monoethyl tartrate was not available commercially and methods in the literature[2] failed to give a pure compound, a synthetic approach was developed to obtain monoethyl tartrate. The method resulted in relatively pure monoethyl tartrate in very high yields (95%). The

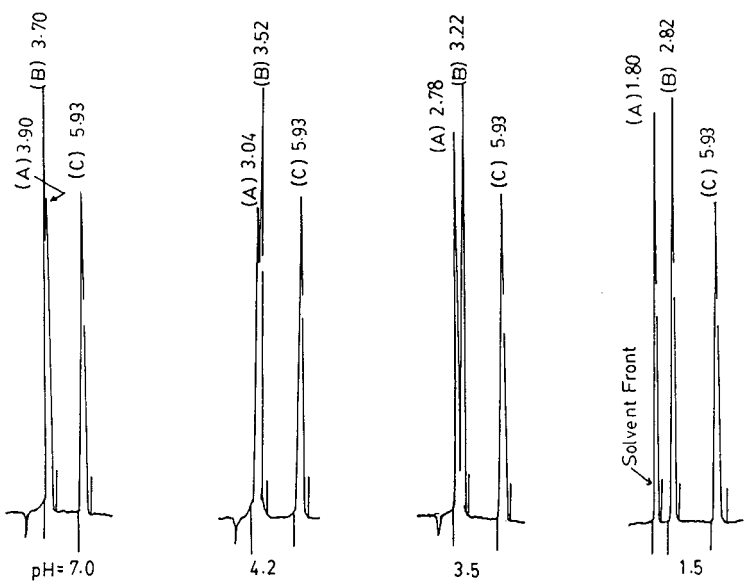

Fig. 2. Effect of the eluent pH on the retention time of diester (C), monoester (B) and tartaric acid (A) using ion-pair chromatography.

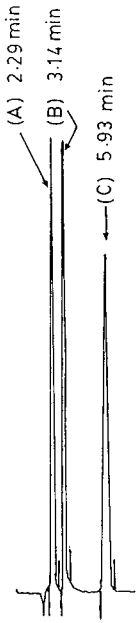

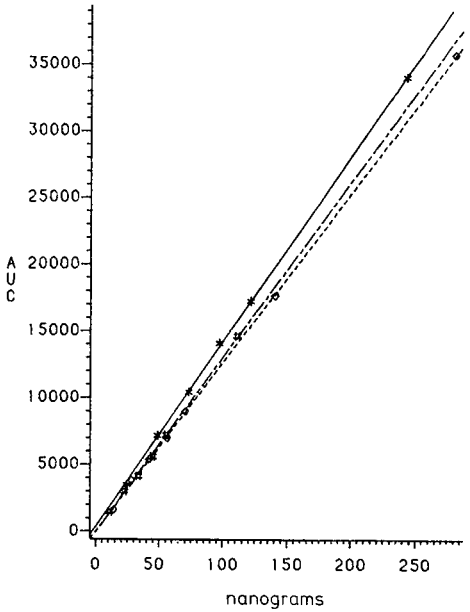

Fig. 3. Separation of diester (C), monoester (B) and tartaric acid (A) using ion-pair chromatography, eluent pH adjusted to 3.2.

Fig. 4. Calibration plot of area under the curve, AUC, *versus* amount injected for all three species. (*) Tartaric acid; (◇) diester; (#) monoester.

synthesized monoester was analyzed by the HPLC procedure described above. The chromatograms of this sample showed only one peak which corresponded to the peak located between the diester and tartaric acid peaks. The eluent corresponding to this peak was collected and analyzed and confirmed by MS.

Fig. 4 shows that a linear relationship was obtained for all three species. The calibration coefficients of the three species were calculated and found to be: diester, 126.4 area units/ng; monoester, 130.7 area units/ng; and tartaric acid, 138.3 area units/ng.

Application to hydrolysis kinetics

The technique was used to follow the hydrolysis kinetics of the diester compound at pH 7.0 and 85°C. Using this assay, the concentrations of all three species as a function of time were determined and the plots of the results are shown in Fig. 5. The figure shows a typical diester to monoester to carboxylic acid plot and indicates that the HPLC assay reported in this communication can differentiate all three species as a function of time and is suitable for kinetic hydrolysis studies.

This assay was used for an extensive investigation of diethyl tartrate hydrolysis kinetics under various conditions. The results of these studies are reported in a subsequent paper[3]. Briefly, the results indicated that only 0.003% diethyl tartrate and 0.0013% monoethyl tartrate will hydrolyze during the chromatographic procedure

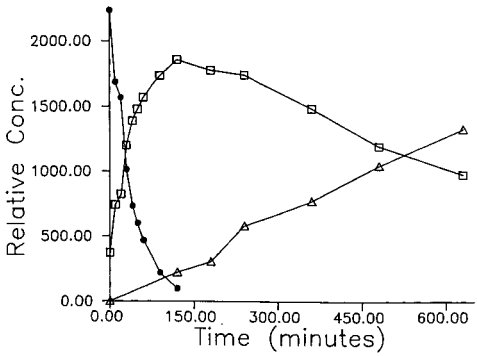

Fig. 5. Experimental kinetic data obtained for diester hydrolysis at pH = 7.0 and temperature = 85°C, (●) Tartaric acid; (□) monoester; (△) diester.

which required 10 min or less. Therefore, for practical purposes, all species were found to be stable during the chromatographic analysis. Further tests also indicated that there were no racemic changes occurring during hydrolysis or analysis. This was expected, since the hydrolysis studies were carried out under acidic and neutral conditions.

REFERENCES

1 R. G. Pearson and J. W. Moore, *Kinetics and Mechanism*, Wiley, New York, 3rd ed., 1981, Ch. 8.
2 T. S. Patterson, *J. Chem. Soc. Trans.*, (1901) 167.
3 D. S. Kalonia and A. P. Simonelli, *Pharm. Res.*, submitted for publication.

Journal of Chromatography, 455 (1988) 360–363
Elsevier Science Publishers B.V., Amsterdam — Printed in The Netherlands

CHROM. 20 862

Note

Simultaneous collection of the eluate from up to twenty liquid chromatographic columns by a minor modification to the fraction collector

FINN MARQUARD and OLE SONNE*
Institute of Physiology, University of Aarhus, Universitetsparken, DK-8000 Aarhus C (Denmark)
(Received July 20th, 1988)

This paper describes a simple modification of an LKB 2070 Ultrorac II fraction collector that allows the simultaneous collection of up to twenty fractions. As the number of fractions, which during unattended operation can be collected from each column, is reduced to ten (twenty if only ten columns are in operation), it is best suited for preparative purposes. We have used the modified fraction collector in connection with a multi-channel pump during a study of the receptor-mediated degradation of insulin in isolated rat adipocytes[1].

APPARATUS

Fraction collector

The LKB 2070 Ultrorac II fraction collector was modified so that the pulse from the timer initiating a step to the next position was changed to a feed command allowing a complete rack of ten tubes to change position. This was achieved by using the AUX(iliary) setting, where the functions are controlled via a 25-pole socket on the rear panel of the fraction collector. This modification does not affect the original operation of the fraction collector under the normal RUN conditions.

Fig. 1 shows the external control unit and its connections to the fraction collector. A minor modification was made inside the LKB 2070 as shown by the asterisk in Fig. 1. For unknown reasons, the AUX pin on the function switch, mounted on the front panel, has no connections. A single wire should be run from this point, all the way back to pin 3 on the 25-pole socket.

In the AUX mode, the external interface will take over the main control of the fraction collector, by introducing "feed" and "run" signals. This continues until the feedback from "rack count" resets collection.

A holder was constructed to space the ends of the outlet tubings from the columns over the ten tubes in the rack.

Pump

We used an Ismatec IPN-12 twelve-channel peristaltic pump. However, it was necessary to insert a small interface between the pump outlet (J2) on the fraction collector and the remote inlet on the pump (Fig. 2).

This interface incorporates an external speed and direction control, because the

0021-9673/88/$03.50 © 1988 Elsevier Science Publishers B.V.

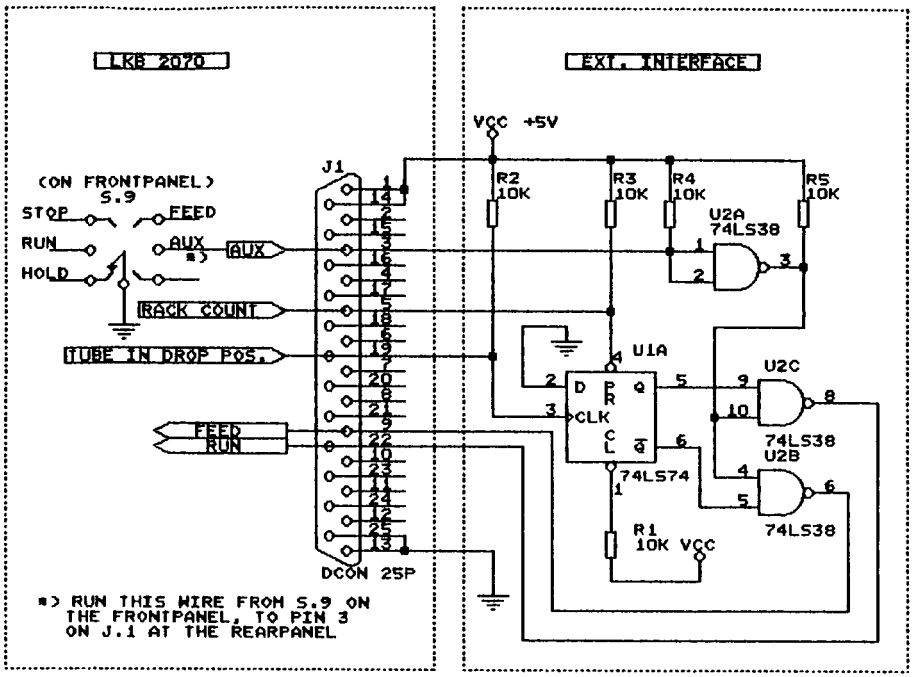

Fig. 1. Diagram of the external interface connected to the LKB 2070 fraction collector through the J1 25-pin socket. When the front panel instrument mode control is in the AUX position, the timer, instead of giving a step command moving the fraction collector one tube forward, will give a feed command changing a complete rack on both sides of the fraction collector. Note that the AUX pin on the front panel should be wired up to pin 3 on J1 on the rear panel as indicated by the asterisk.

internal adjustment in the pump unfortunately is disconnected when the DIN plug is inserted into the pump. The interface is shown in Fig. 2, and described as the follows. When the TTL output at pin 3 from the fraction collector becomes high, the contact on

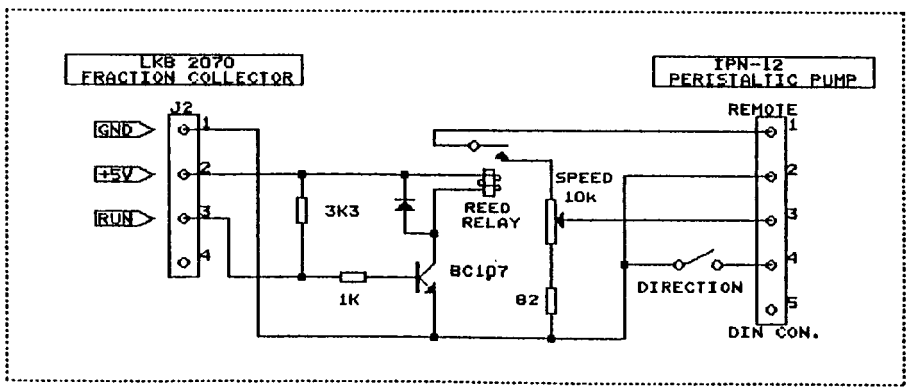

Fig. 2. Diagram of the external interface connecting the LKB 2070 fraction collector through the pump socket with the IPN-12 peristaltic pump through the remote control socket.

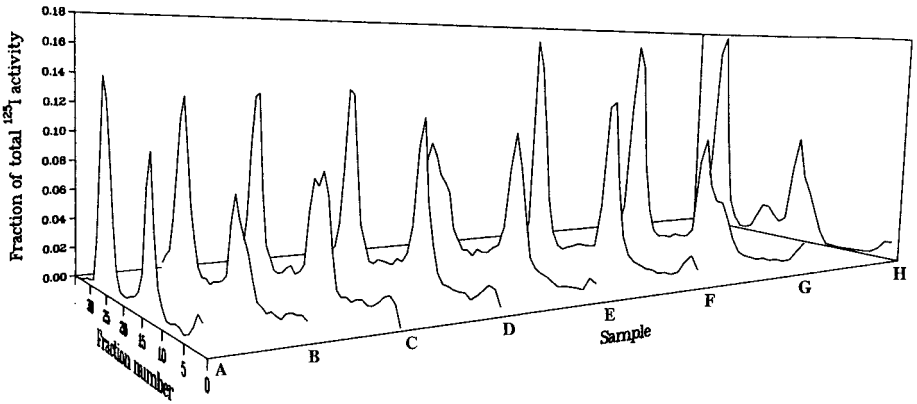

Fig. 3. Preparative liquid chromatography of degraded insulin. Isolated rat adipocytes were incubated at 37°C with either of the four monoiodinated isomers of insulin as previously described in detail[1]. The cells were isolated, reincubated in fresh buffer and the cell-associated iodoinsulin was allowed to dissociate. The medium was isolated, Blue Dextran (Pharmacia) was added, and the mixture was subjected to chromatography on 75 × 1.5 cm I.D. columns of Sephadex G-50 Fine (Pharmacia), eluting with 0.5 *M* acetic acid containing 1 g/l of bovine serum albumin (Sigma). When the blue colour reached the bottom of the column, the collection of the eluate was initiated. As the degradation product monoiodotyrosine is retarded on Sephadex G-50 Fine, eluting at $K_{av} = 1.4$, the size of the fractions were adjusted so that at least 1.5 column volumes were eluted in the 40 fractions collected. Incubation medium isolated from cells previously incubated with the A14 isomer is shown in track A and B, the A19 isomer in tracks C, D and E, the B16 isomer in tracks F and G and the B26 isomer in track H. Iodoinsulin elutes in fraction 15 and monoiodoinsulin in fraction 30. The B26 isomer gave rise to a small degradation product that eluted between the two main peaks. As the different pump heads did not operate with exactly the same flow-rate, the positions differ slightly from track to track.

the reed relay will close. This connects a voltage of 5.8 V to the speed potentiometer, and the adjustable voltage is then led back to pin 3 at the remote connector, which is the analogue input for the pump-motor driver.

RESULTS

The preparative chromatography of radioactive products dissociated from isolated rat adipocytes previously incubated with either of the four monoiodinated isomers of insulin is shown in Fig. 3.

DISCUSSION

We found that the liquid chromatography of the samples from a project on the receptor-mediated degradation of insulin in isolated rat adipocytes was too slow for our purposes. Therefore, we looked for possibilities for speeding up this step. The acquisition of a twelve channel pump combined with the modification of the fraction collector described here allowed the simultaneous operation of up to ten columns.

The LKB 2070 Ultrorac II has a capacity of 20 × 10 tubes. During unattended operation of the fraction collector in the modified mode, the number of fractions per column is restricted to twenty. Therefore, the void was directed to waste, and the first

twenty fractions were collected during the daytime. The racks were changed and the last twenty fractions were collected during the evening.

If one is satisfied with a maximum of ten fractions per column, it is possible to collect fractions on both sides of the fraction collector, and hence collect the eluate from up to twenty columns a time.

ACKNOWLEDGEMENTS

This study was supported in part by grants from the Danish Medical Research Council (12-4423, 12-4144). Dr. Susanne Linde (Hagedorn Research Laboratory, Gentofte, Denmark) is thanked for the generous gift of the four monoiodinated isomers of insulin and Charlotte Bjørnbak Nielsen is thanked for excellent technical assistance.

REFERENCE

1 O. Sonne, *Biochim. Biophys. Acta*, 927 (1987) 106–111.

Journal of Chromatography, 455 (1988) 364–368
Elsevier Science Publishers B.V., Amsterdam — Printed in The Netherlands

CHROM. 20 932

Note

Measurement of methylated DNA purines by reversed-phase high-performance liquid chromatography and fluorimetric detection

ANNA MARIA TACCHI-BEDFORD*
Department of Clinical Pharmacology, University College, London WC1 6JJ (U.K.)
(First received May 2nd, 1988; revised manuscript received August 30th, 1988)

DNA covalent binding is considered one of the critical events in chemically-induced mutagenesis and carcinogenesis[1]. Studies on the mode of action of alkylating agents have stimulated the development of analytical techniques for the measurement of specific DNA adducts in target tissues.

Mainly two column liquid chromatographic methods have emerged in recent years for the quantitative analysis of chemically-modified bases. One involves the use of reversed-phase high-performance liquid chromatography (RP-HPLC) followed by the monitoring of ultraviolet absorption, whereas the other is based on HPLC by cation-exchange columns and peak detection by fluorescence spectrometry[2–10]. Whereas some reversed-phase systems are time-consuming and require the use of complicated gradients or two columns[2,5], others have been simplified so that separation of normal and modified bases is achieved under isocratic conditions[3,4]. However, the detection method based on ultraviolet absorption spectrometry does not provide the adequate sensitivity for the optical determination of adducts at picomol levels, which is desirable in chemical carcinogenesis studies, and radiolabelled carcinogens must be used to overcome this problem.

The introduction by Herron and Shank[6] of fluorimetric detection allowed a 60-fold increase in sensitivity thus offering the advantage that methylated bases could be measured by an entirely optical system, without requiring the use of radiolabelled carcinogens and liquid scintillation counting. Compared to the ion-exchange columns used in those studies, however, reversed-phase columns are easier to equilibrate and offer a higher degree of reproducibility in resolution and retention volumes[11].

An analytical technique is described here, in which reversed-phase separation and fluorimetric detection are combined together. This method was succesfully applied to the measurement of methylated purines in the DNA of rat liver and colon after 1,2-dimethylhydrazine[12].

MATERIALS AND METHODS

Authentic markers for HPLC included adenine, 3-methyladenine, guanine, 7-

* Present address: DHSS Department of Toxicology, St. Bartholomew's Hospital Medical College, 59 Bartholomew Close, London ECI 7ED, U.K.

0021-9673/88/$03.50 © 1988 Elsevier Science Publishers B.V.

methylguanine (7MeG) (Sigma, Poole, U.K.) and 06-methylguanine (06MeG) (kindly supplied by Dr. P. F. Swann, Middlesex Hospital Medical School, London, U.K.). Calf thymus DNA was from Sigma and 1,2-dimethylhydrazine · 2HCl (DMH) was from Aldrich (Gillingham, U.K.). All other reagents were of analytical- or HPLC-grade and were purchased either from Sigma or BDH (Poole, U.K.). The markers were dissolved in 0.1 *M* hydrochloric acid whereas calf-thymus DNA was hydrolysed in 0.1 *M* hydrochloric acid at 70°C for 40 min in order to release free purines. DNA from the livers of rats treated with DMH (20 mg/kg, subcutaneously) was isolated by phenol extraction according to the modified Kirby procedure[13], purified as previously described[12] and hydrolysed in a volume of 0.1 *M* hydrochloric acid to obtain a concentration of 5–6 mg DNA/ml. Approximately 100 μg of DNA were injected onto the column. All samples were filtered through 0.45 μm Millipore filters before use.

The chromatographic system consisted of a Waters model 6000A pump, a Rheodyne injection valve with a 20 μl loop and a Waters μBondapak C_{18} column, 30 cm x 3.9 mm I.D. (10 μm). A pre-column with the same packing was also used.

The detection apparatus included a Perkin Elmer LS-4 fluorescence spectrometer equipped with a 4 μl flow cell. Peaks were integrated by a Perkin Elmer LCI-100 computing integrator.

The purines were eluted with 10 m*M* ammonium formate (pH 3.8) containing 10% of methanol at a flow-rate of 1 ml/min at room temperature and the fluorescence was monitored at 286 nm excitation and 366 nm emission wavelength.

Calibration curves (concentration *versus* peak area) were made with known concentrations of guanine, 7MeG and 06MeG. An external standard method was used for the integration of unknown peaks.

RESULTS AND DISCUSSION

Under the chromatographic conditions used in this study, 3-methyladenine eluted at 4 min, guanine at 5.5–6.1 min, adenine at 7.6–8.3 min, 7MeG at 9.6–10.4 min, and 06MeG at 19–20 min. In this way five bases of different polarity could be eluted in less than 25 min under isocratic conditions. The retention times remained constant after repeated use of the same column over a long period of time, or with different types of C_{18} reversed-phase-columns, such as Spherisorb ODS or Novapak C_{18}. In order to optimise reproducibility of the results, great care had to be taken in the preparation of the mobile phase. In fact, variations in pH (0.1–0.3 units) or in the amount of methanol (1–10%) resulted in a loss of resolution between guanine and adenine or adenine and 7MeG.

Excellent resolution was obtained between guanine, 7MeG and 06MeG as shown in Fig. 1. The standard mixture contained 2.4 nmol of guanine, 1.9 nmol of 7MeG and about 1 nmol of 06MeG. The larger peak corresponding to 06MeG was due to the higher fluorescence of this molecule as compared to the other purines. Although a lower pH increased the fluorescence response of 06MeG, it failed to resolve guanine from adenine.

Limits of detection were 40 pmol for 7MeG and 4 pmol for 06MeG, which are in agreement with those published in a previous work[6]. The fluorescence response was linear for guanine from 0.6 to 60 nmol, for 7MeG from 40 pmol to 4 nmol and for 06MeG from 4 to 700 pmol. This linearity in the fluorescence response together with

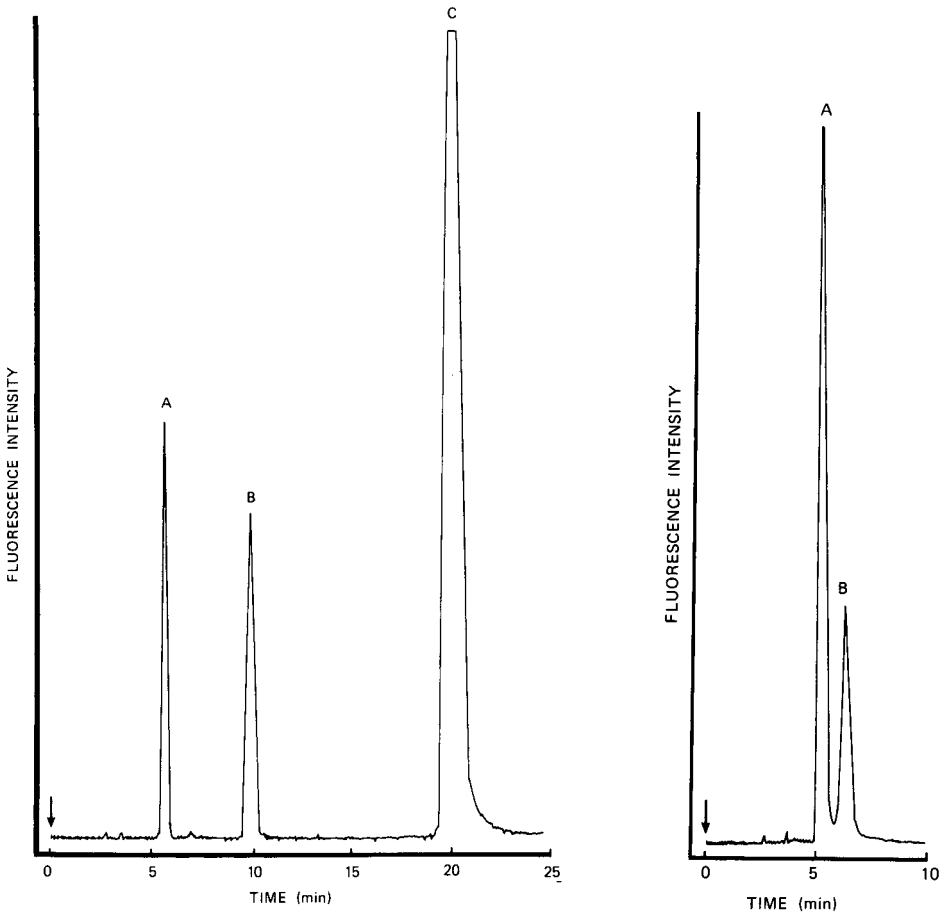

Fig. 1. Elution profile of a standard mixture containing guanine (A), 7MeG (B) and 06MeG (C). Column: 30 cm x 3.9 mm I.D., μBondapak C_{18}. Mobile phase consisted of 10 m*M* ammonium formate (pH 3.8) containing 10% methanol at a flow-rate of 1 ml/min. The peaks were monitored by fluorescence detection with the excitation wavelength set at 286 nm and the emission at 366 nm.

Fig. 2. Elution of a DNA hydrolysate from calf-thymus. DNA was hydrolysed in 0.1 *M* hydrochloric acid at 70°C for 40 min. The two peaks correspond to guanine (A) and adenine (B). For chromatographic conditions see Fig. 1.

good resolution was particularly important for the quantitation of guanine and 06MeG in DNA hydrolysates from animal tissues. With such a system it was actually possible to detect and integrate very low amounts of 06MeG and 1000-fold larger amounts of guanine in the same hydrolysate without any further sample manipulation, re-chromatography or use of two different detection methods, as described by other workers[10,14]. Examples of elution profiles of hydrolysates either from calf-thymus DNA or rat liver DNA after DMH-treatment are given in Figs. 2 and 3 respectively. Normal and methylated bases were completely resolved and retention times were well in agreement with those of the corresponding authentic markers.

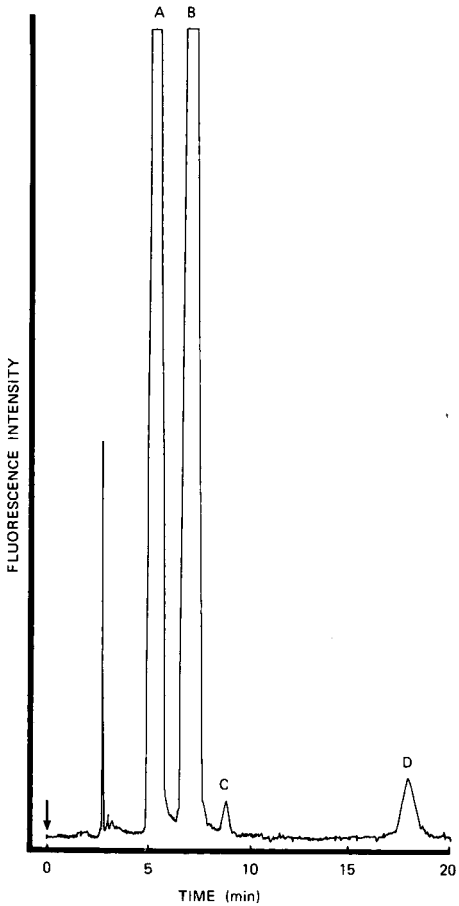

Fig. 3. Elution profile of a liver DNA hydrolysate from a rat treated with DMH (20 mg/kg, subcutaneously) and killed 6 h later. DNA was isolated by phenol extraction[13] and hydrolysed in 0.1 *M* hydrochloric acid at 70°C for 40 min. Peaks: (A) guanine; (B) adenine; (C) 7MeG; (D) 06MeG. Details on the chromatographic conditions are given in Fig. 1.

Peaks A and D in Fig. 3 represent 48 nmol of guanine and 49 pmol of 06MeG respectively. Linear regression analysis of peak area *versus* purine concentration in a series of DNA samples gave a correlation coefficient of 0.989 for guanine ($n=14$), 0.991 for 7MeG ($n=22$) and 0.998 for 06MeG ($n=32$). Because of their weaker polarity as compared to free purines, pyrimidine oligonucleotides did not elute within 25 min under the chromatographic conditions used here and were washed off the column after each run with 90–100% methanol.

In summary, the combination of reversed-phase chromatography and fluorimetric detection described here resulted in a rapid, efficient and sensitive analytical procedure for the determination of chemically-modified DNA purines.

ACKNOWLEDGEMENTS

Thanks are due to Miss R. Lawrence for editorial assistance. This work was part of a project funded by the Ministry of Agriculture, Fisheries and Food.

REFERENCES

1 C. E. Searle (Editor), *Chemical Carcinogens* (*ACS Monograph* 182), American Chemical Society, Washington, DC, 2nd ed. 1984.
2 A. W. Bull, A. D. Burd and N. D. Nigro, *Cancer Res.*, 41 (1981) 4938.
3 A. M. Tacchi, D. E. Jensen and P. N. Magee, *Biochem. Pharmacol*, 36 (1987) 881.
4 D. E. Jensen, G. J. Stelman and A. Spiegel, *Cancer Res.*, 47 (1987) 353.
5 J. F. Lawrence, R. Leduc and J. J. Ryan, *Anal. Biochem.*, 116 (1981) 433.
6 D. C. Herron and R. C. Shank, *Anal. Biochem.*, 100 (1979) 58.
7 D. C. Herron and R. C. Shank, *Cancer Res.*, 41 (1981) 3967.
8 A. E. Pegg, D. Scicchitano and M. E. Dolan, *Cancer Res.*, 44 (1984) 3806.
9 T. A. Ratko and J. M. Pezzuto, *J. Chromatogr.*, 324 (1985) 484.
10 M. A. Bedell, J. G. Lewis, K. C. Billings and J. A. Swenberg, *Cancer Res.*, 42 (1982) 3079.
11 P.R. Brown, *HPLC in Nucleic Acid Research. Methods and Applications* (*Chromatographic Science Series*, Vol 28), Marcel Dekker, New York, 1984.
12 A. M. Tacchi-Bedford, G. D. Whyman and A. E. M. McLean, *Toxicology*, 50 (1988) 181.
13 P. F. Swann and P. N. Magee, *Biochem. J.*, 110 (1968) 39.
14 D. H. Barch and C. C. Fox, *Carcinogenesis*, 8 (1987) 1461.

Journal of Chromatography, 455 (1988) 369–375
Elsevier Science Publishers B.V., Amsterdam — Printed in The Netherlands

CHROM. 20 852

Note

Étude par chromatographie liquide haute performance des métabolites potentiels de la caféine

Comparaison de différentes techniques

M. F. VERGNES, C. GROSSET et J. ALARY*
Service de Chimie Analytique, UFR de Pharmacie, F-38700 La Tronche (France)
(Reçu le 21 juillet 1986; manuscrit modifié reçu le 25 juillet 1988)

Le métabolisme de la caféine chez l'homme est à la fois complexe et quantitativement important. En effet, moins de 1% de la dose absorbée est éliminée dans les urines sous forme inchangée.

La métabolisation est essentiellement hépatique, sous la dépendance du cytochrome P-448. Les nombreux métabolites identifiés sont le résultat d'étapes successives ou compétitives[1].

Les principales voies du catabolisme sont: (i) des déméthylations en position 1, 3 ou 7, qui donnent naissance à des di- ou monométhylxanthines; (ii) des oxydations sur le carbone 8, qui donnent lieu à la formation d'acides méthyluriques; (iii) des ouvertures de cycle, qui ont été récemment mises en évidence[2] et qui conduisent à la formation de dérivés de l'uracile.

Compte-tenu des deux voies métaboliques principales, nous nous sommes intéressés à deux séries de molécules: (a) la xanthine et ses dérivés diversement méthylés (Fig. 1); (b) l'acide urique et quelques dérivés méthylés correspondants (Fig. 2).

Nous avons tenté de séparer l'ensemble de ces molécules par chromatographie en phase liquide haute performance (CLHP), selon diverses techniques (adsorption et partage).

La chromatographie d'adsorption a surtout été utilisée pour le dosage des xanthiques naturels (caféine, théophylline et théobromine[3], éventuellement en présence de monométhylxanthine[4], d'acide urique[5] ou de paraxanthine[6], mais jamais pour l'ensemble des 17 molécules étudiées.

En effet, sur silice, la séparation des trois principaux xanthiques ne présente pas de difficulté particulière et se prête tout à fait à une détermination quantitative. Par contre, parmi les molécules étudiées, certaines sont peu ou pas solubles dans les solvants organiques.

La chromatographie de partage en phase inverse a été beaucoup plus largement utilisée[7–12]. Les auteurs préconisent le plus souvent une silice sur laquelle est greffé un octadécylsilane. Ils utilisent ou non la technique de l'appariement d'ions, mais ici encore, la totalité des molécules retenues n'a jamais été envisagée.

0021-9673/88/$03.50 © 1988 Elsevier Science Publishers B.V.

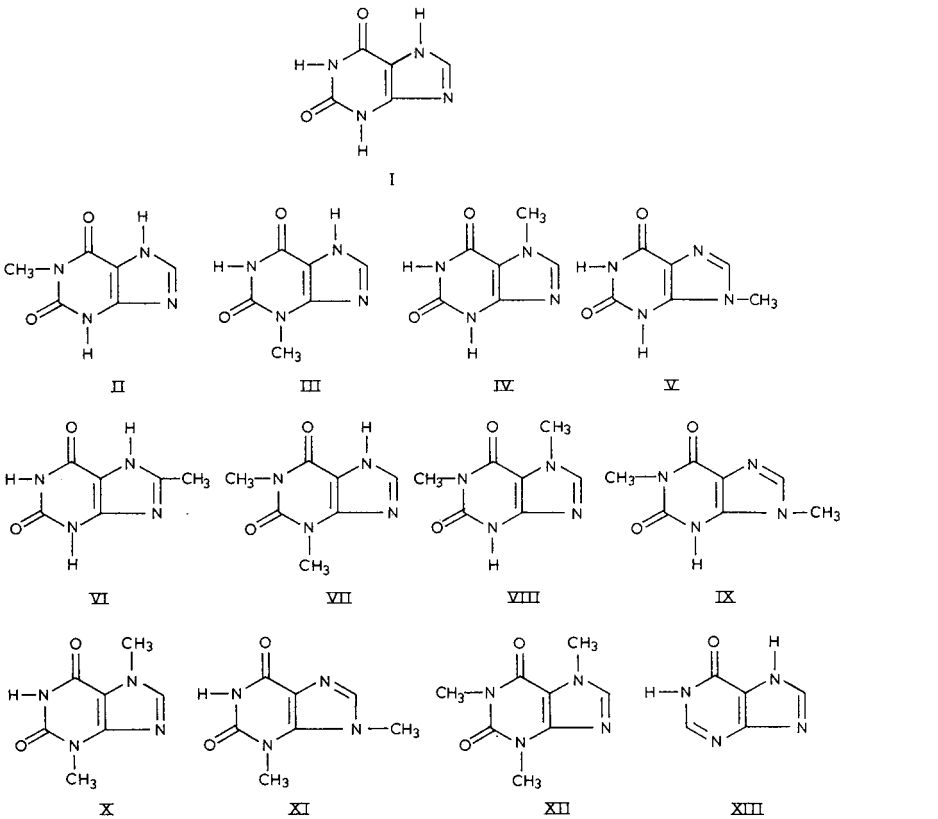

Fig. 1. La xanthine et ses dérivés. I = Xanthine; II = méthyl-1 xanthine; III = méthyl-3 xanthine; IV = méthyl-7 xanthine; V = méthyl-9 xanthine; VI = méthyl-8 xanthine; VII = diméthyl-1,3 xanthine (théophylline); VIII = diméthyl-1,7 xanthine; IX = diméthyl-1,9 xanthine; X = diméthyl-3,7 xanthine (théobromine); XI = diméthyl-3,9 xanthine; XII = triméthyl-1,3,7 xanthine (caféine); XIII = hypoxanthine.

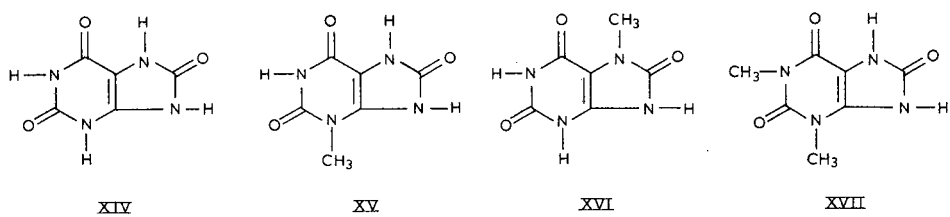

Fig. 2. Acide urique et ses dérivés. XIV = Acide urique; XV = méthyl-3 acide urique; XVI = méthyl-7 acide urique; XVII = diméthyl-1,3 acide urique.

MATÉRIEL ET MÉTHODES

Appareillage

Pompes Waters M 510; vanne d'injection à boucle (20 μl); détecteur UV Philips longueur d'onde de détection: 273 nm (cette longueur d'onde permet la détection de toutes les molécules).

Produits

Les dérivés de la xanthine et l'acide urique proviennent de la firme Fluka, les dérivés de l'acide urique de la firme Sigma. Les solvants utilisés sont de qualité pour CLHP.

Méthodes

Chromatographie d'adsorption. Les produits utilisés sont en solution dans le dioxanne. Colonne: silice Resolve 5 μm (Waters), 15 cm × 3.9 mm I.D.; il s'agit d'une silice poreuse très homogène, de très haute efficacité. Solvant: dichlorométhane–méthanol–ammoniaque concentrée (A:B:1), de manière à ce que les molécules se trouvent exclusivement sous leur forme molaire; gradient obtenu grâce à un programmateur Waters, permettant des gradients non linéaires: gradient retenu No. 7 (Fig. 3); débit 1 ml/min.

Chromatographie de partage. Les produits utilisés sont en solution dans l'eau bidistillée. Colonnes: μBondapak C_{18} (Waters), 30 cm × 3,9 mm I.D.; colonne à compression radiale (Novapak C_{18}, 10 cm × 8 mm I.D.), utilisée avec un système de compression (Z module), qui fournit une compression statique de la cartouche, identique sur toute sa longueur; 10 cm. Solvant: posphate monopotassique 0,05 *M* en solution aqueuse–méthanol; gradient linéaire pour la colonne μBondapak C_{18}; gradient concave No. 5 pour la colonne à compression radiale (Fig. 3); débit 2,5 ou 2 ml/min.

Chromatographie de partage avec appariement d'ions. Les produits utilisés sont en solution dans l'eau bidistillée. Colonne: à compression radiale Nova-Pak C_{18}, 10 cm × 8 mm I.D.; solvant: phosphate de tétrabutylammonium 0,005 *M*–méthanol (le contre-ion utilisé est le seul ammonium quaternaire cité dans les techniques de CLHP. Il s'agit du Pic A commercialisé par Waters); gradient concave No. 7 (Fig. 3); débit 2 ml/min.

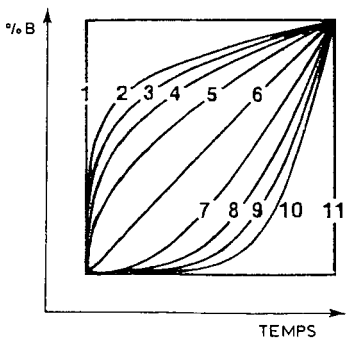

Fig. 3. Courbes de gradients préprogrammés Waters.

RÉSULTATS ET DISCUSSION

Chromatographie d'adsorption (Fig. 4)

Malgré le choix du dioxanne comme solvant et en dépit de l'emploi d'ammoniaque, la mise en solution de toutes les molécules n'a pu être obtenue. Par ailleurs, les dérivés de l'acide urique présentaient des pics dédoublés. Huit molécules seulement ont pu être étudiées, elles sont bien séparées, donc identifiables sans ambiguité. Cependant, la mauvaise dissolution ne permet des applications quantitatives que pour les xanthiques naturels[13].

Chromatographie de partage en phase inverse (Figs. 5 et 6)

Sur colonne classique tous les composés sont séparés à l'exception de la méthyl-9 xanthine et de la xanthine qui forment un pic unique. Sur colonne à compression radiale la séparation est moins efficace, puisqu'en dehors du couple de molécules cité précédemment, le diméthyl-1,3 acide urique et la théobromine ont également des temps de rétention identiques.

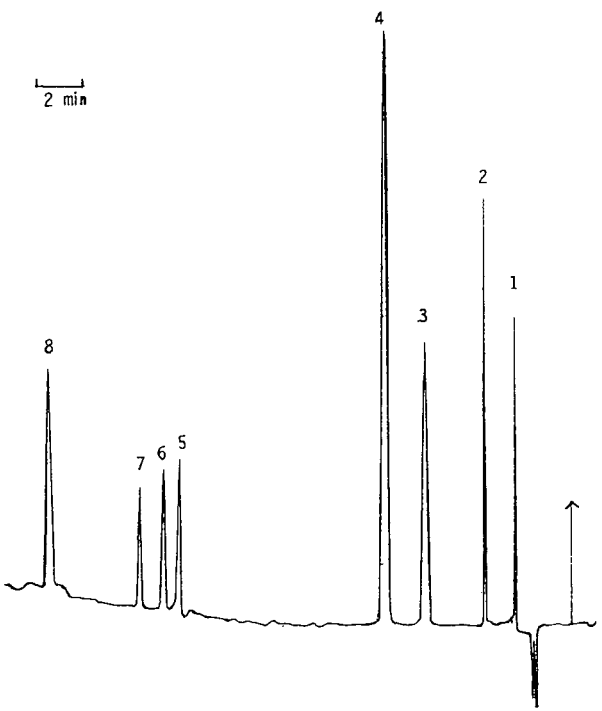

Fig. 4. Séparation de quelques xanthines par CLHP. 1 = Caféine (XII); 2 = théobromine (X); 3 = diméthyl-1,7 xanthine (VIII); 4 = théophylline (VII); 5 = méthyl-7 xanthine (IV); 6 = méthyl-3 xanthine (III); 7 = méthyl-1 xanthine (II); 8 = diméthyl-1,3 acide urique (XVII). Conditions chromatographiques: colonne de silice sphérique Resolve 5 μm. Phase mobile: dichlorométhane (A)–méthanol (B) + 1% d'ammoniaque. Gradient avec 3% de B dans A pendant 8 min, augmentation en 17 min jusqu'à 50% de B dans A selon la courbe 7. Débit 1 ml/min. Détecteur UV à 273 nm.

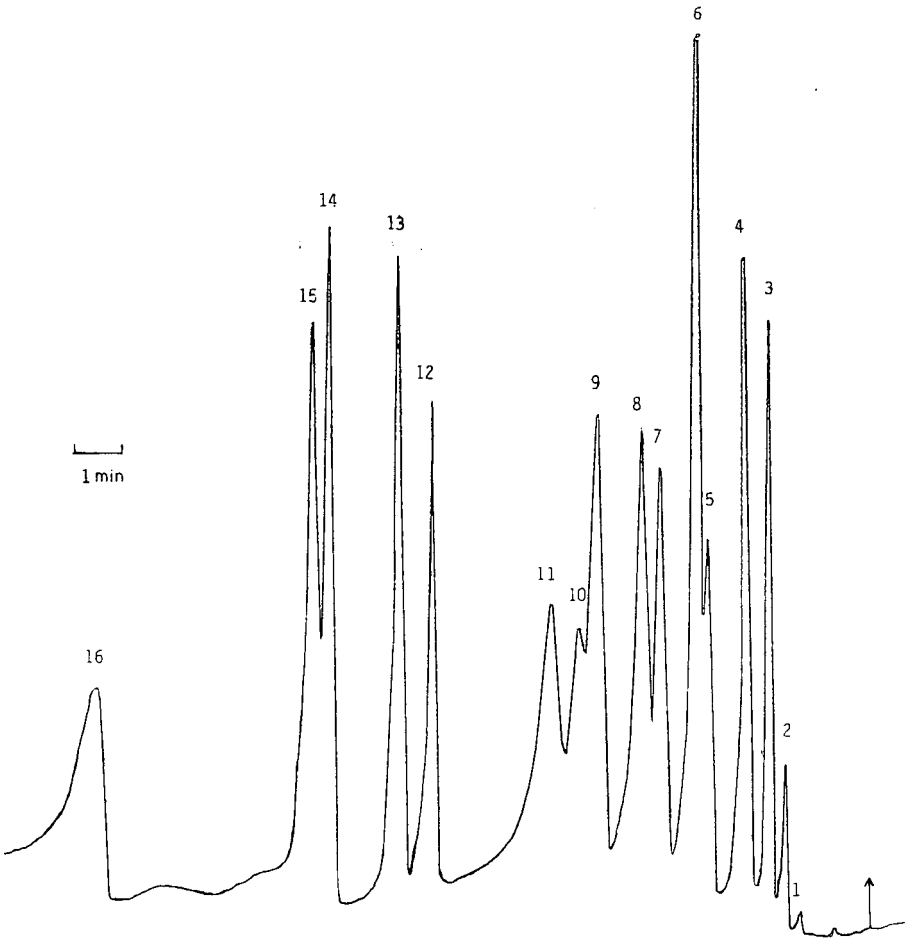

Fig. 5. Séparation de l'ensemble des molécules par CLHP en phase inverse. 1 = acide urique (XIV); 2 = hypoxanthine (XIII); 3 = xanthine (I) + méthyl-9 xanthine (V); 4 = méthyl-3 acide urique (XV); 5 = diméthyl-3,9 xanthine (XI); 6 = méthyl-7 acide urique (XVI); 7 = méthyl-8 xanthine (VI); 8 = méthyl-7 xanthine (IV); 9 = diméthyl-1,9 xanthine (IX); 10 = méthyl-3 xanthine (III); 11 = méthyl-1 xanthine (II); 12 = diméthyl-1,3 acide urique (XVII); 13 = théobromine (X); 14 = diméthyl-1,7 xanthine (VIII); 15 = théophylline (VII); 16 = caféine (XII). Conditions chromatographiques: colonne μBondapak. Phase mobile: solution aqueuse de phosphate monopotassique 0,05 *M* (A) –méthanol–phosphate monopotassiques 0,05 *M* 50/50 (B) (pH 4,5). Gradient de 5 à 30% de B en 4 min. Débit 2,5 ml/min. Détecteur UV à 273 nm.

Chromatographie de partage avec appariement d'ions (Fig. 7)

Dans cette technique, les ordres d'élution sont modifiés par rapport à la même technique sans utilisation de contre-ion. Deux molécules ne sont pas séparées, ce sont dans ce cas les méthyl-8 et méthyl-3 xanthines. Dans toutes les techniques, les temps de rétention sont reproductibles. Le coefficient de variation est compris entre 0,2 et 2,1% selon les molécules.

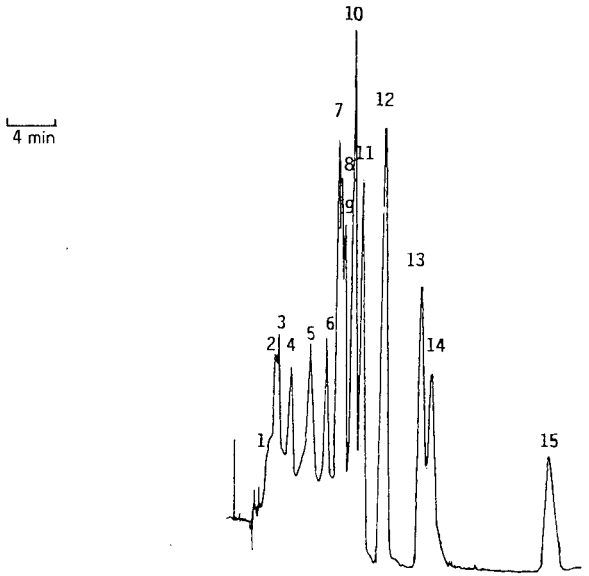

Fig. 6. Séparation de l'ensemble des molécules par CLHP en phase inverse. 1 = Acide urique (XIV); 2 = hypoxanthine (XIII); 3 = xanthine (I) + méthyl-9 xanthine (V); 4 = acide méthyl-3 urique (XV); 5 = diméthyl-3,9 xanthine (XI); 6 = méthyl-7 acide urique (XVI); 7 = méthyl-8 xanthine (VI); 8 = méthyl-7 xanthine (IV); 9 = diméthyl-1,9 xanthine (IX); 10 = méthyl-3 xanthine (III); 11 = méthyl-1 xanthine (II); 12 = diméthyl-1,3 acide urique (XVII) + thébromine (X); 13 = diméthyl-1,7 xanthine (VIII); 14 = théophylline (VII); 15 = caféine (XII). Conditions chromatographiques: cartouche Nova-Pak C_{18} à compression radiale. Phase mobile: solution aqueuse de phosphate monopotassique 0,05 *M* (A)–méthanol (B). Gradient de 3 à 15% de B dans A, selon la courbe 6. Débit 2 ml/min. Détecteur UV à 273 nm.

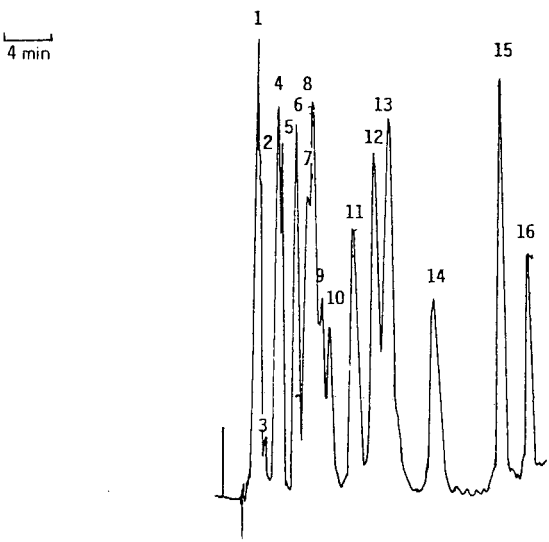

Fig. 7. Séparation de l'ensemble des molécules par CLHP en phase inverse avec appariement d'ions. 1 = Diméthyl-3,9 xanthine (XI); 2 = hypoxanthine (XIII); 3 = xanthine (I); 4 = acide urique (XIV); 5 = méthyl-7 xanthine (IV); 6 = méthyl-3 xanthine (III) + méthyl-8 xanthine (VI); 7 = méthyl-1 xanthine (II); 8 = méthyl-9 xanthine; (V); 9 = méthyl-3 acide urique (XV); 10 = théobromine (X); 11 = méthyl-7 acide urique (XVI); 12 = diméthyl-1,7 xanthine (VIII); 13 = diméthyl-1,9 xanthine (IX); 14 = théophylline (VII); 15 = caféine (XII); 16 = diméthyl-1,3 acide urique (XVII). Conditions chromatographiques: cartouche Nova-Pak C_{18} à compression radiale. Phase mobile: solution aqueuse de phosphate de tétrabutylammonium 0,005 *M* (A)–méthanol (B). Gradient de 8 à 30% de B dans A selon la courbe 7. Débit: 2 ml/min. Détecteur UV à 273.

La chromatographie de partage en phase inverse a permis d'étudier un plus grand nombre de molécules que la chromatographie d'adsorption. L'emploi d'une colonne à compression radiale n'a pas amélioré la résolution des pics, par rapport à l'utilisation d'une colonne classique.

Cependant, la mise en jeu du phénomène d'appariement d'ions a modifié l'ordre d'élution de certains composés et peut donc permettre de confirmer des identifications délicates et tout particulièrement de séparer xanthine et méthyl-9 xanthine qui ont le même temps de rétention dans la technique classique proposée.

BIBLIOGRAPHIE

1 M. M. Callahan, *9th Colloquium on the Science and Technology of Coffee*, London, 1980.
2 J. L. Brazier et B. Ribon, *Med. Nut.*, 18 (1982) 295.
3 W. Wildanger, *Dtsch. Lebensm. Rundsch.*, 72 (1976) 160.
4 S. Sved et D. L. Wilson, *Res. Commun. Chem. Pathol. Pharmacol.*, 17 (1977) 319.
5 O. H. Weddle et W. D. Mason, *J. Pharm. Sci.*, 65 (1976) 865.
6 A. Wahlländer, E. Renner et G. Karlaganis, *J. Chromatogr.*, 338 (1985) 369.
7 J. Blanchard, J. D. Mohammadi et J. M. Trang, *Clin. Chem.*, 27 (1981) 637.
8 C. Bory, P. Baltassat et C. Gonnet, dans A. Frigerio (Rédacteur), *Chromatography and Mass Spectrometry in Biomedical Sciences, 2*, Elsevier, Amsterdam, 1983, p. 105.
9 R. K. Desiraju, E. T. Sugita et R. L. Mayock, *J. Chromatogr. Sci.*, 15 (1977) 563.
10 L. C. Franconi et G. L. Hawk, *Anal. Chem.*, 48 (1976) 372.
11 R. Klassen et B. Stavric, *J. Liq. Chromatogr.*, 6 (1983) 895.
12 B. Stavric, R. Klassen et S. G. Gilbert, *J. Chromatogr.*, 310 (1984) 107.
13 M. F. Vergnes et J. Alary, *Talanta*, 33 (1986) 997.

Journal of Chromatography, 455 (1988) 376–381
Elsevier Science Publishers B.V., Amsterdam — Printed in The Netherlands

CHROM. 20 930

Note

Activity stain for polygalacturonase

THOMAS A. McKEON
U.S. Department of Agriculture, Agricultural Research Service, Western Regional Research Center, Albany, CA 94710 (U.S.A.)

(First received March 29th, 1988; revised manuscript received August 29th, 1988)

Polygalacturonase (E.C. 3.2.1.15) (PG) degrades the polygalacturonate component of pectin and is known to be involved in the breakdown of plant cell walls[1]. Hence, endogenous polygalacturonases influence fruit texture, which is an important quality component of harvested produce. With recent work suggesting roles for oligogalacturonides in plant development[2], the fact that these fragments are generated by the action of PG underlines the importance of detecting the presence of PG during stages of plant development.

As one part of a project to examine factors that influence the texture of ripening-delayed and lightly-processed (sliced) tomatoes we have developed an activity stain for polygalacturonase which provides detection of the activity after sodium dodecyl sulfate, polyacrylamide gel electrophoresis (SDS-PAGE) and is thus based on separation by molecular size. This technique is useful in observing qualitative changes in PG levels and PG isoenzyme patterns during ripening of tomato fruit.

MATERIALS AND METHODS*

Pectinase purified from *Aspergillus niger* was purchased from Cappel-Worthington (Malvern, PA, U.S.A.). Acrylamide, bisacrylamide and SDS were purchased from Bio-Rad Labs. Polygalacturonic acid from orange was purchased from Sigma as the free acid, Sigma grade III. Molecular mass standards and Toluidine Blue O are also from Sigma. Tomato fruit (*Lycopersicon esculentum* Mill. cv. Rutgers) were harvested from plants grown in a greenhouse, graded based on internal (MG 4) or external coloring (as described in ref. 3), and pericarp was cut into pieces, frozen in liquid nitrogen and stored at −30°C. Polygalacturonase was extracted from the frozen pericarp as previously described[4], through the 75% ammonium sulfate precipitation and dialysis step. A unit of polygalacturonase activity generates 1 μmol of reducing sugar per minute from digestion of polygalacturonate. Reducing sugar produced by polygalacturonase action was measured using the 3,5-dinitrosalicylic acid method[5].

The procedure developed for polygalacturonase activity staining uses SDS-PAGE for separation based on molecular mass followed by digestion of endogenous substrate. The separating gel was 12.5% polyacrylamide, 2.7% cross-linked, and in

* Reference to a company or product named by the USDA is only for purposes of information and does not imply recommendation of the product to the exclusion of others.

addition to 0.375 *M* Tris–HCl, pH 8.8, 0.1% SDS[6], contained 0.67 mg/ml polygalacturonate (added as a 1% solution of polygalacturonic acid in water brought to pH 7 by addition of 1 *M* sodium hydroxide) and 100 μg/ml fibrinogen[7]. The stacking gel was 5% polyacrylamide, 2.7% cross-linked, containing 0.125 *M* Tris–HCl, pH 6.7, 0.1% SDS and contained no fibrinogen or polygalacturonate. Gels were run at room temperature with the Laemmli buffer system at 150 V through the stacking gel and 300 V through the separating gel. After electrophoresis, the dye front was marked and gels were shaken for 15 min with 250 ml of 0.01 *M* Tris–HCl, pH 8.3, in 20% isopropanol two times, twice for 15 min each in 250 ml of 0.01 *M* sodium acetate, pH 4.5 and finally incubated for 16 h at room temperature in 0.05 *M* sodium acetate, 0.20*M* sodium chloride, pH 4.5. After incubation, gels were washed briefly (30 min) with 0.01 *M* Tris–HCl, pH 8.3, stained for 5 min with 0.1% Toluidine Blue O in the same buffer and destained for approximately 1 h with three changes of Tris–HCl buffer. Use of 0.05% Ruthenium Red provides similar sensitivity to Toluidine Blue O, albeit with less intense background staining.

For quantitation, gels were scanned using a Bio-Med Model SL-TRFF densitometer. The light soure was a tungsten lamp with a 525-nm filter, and scans were carried out in the logarithmic range and inverse mode. The densitometer was equipped with an integrator which provided peak areas.

RESULTS AND DISCUSSION

The basis of the activity stain is the removal of SDS after electrophoresis, renaturation of enzyme in situ, digestion of substrate trapped in the gel matrix, removal of fragmented substrate from the gel by diffusion, and staining of the gel with Toluidine Blue O which binds to the polygalacturonate, leaving clear zones where PG has digested away the substrate. It is conceptually similar to the procedure developed by Blank *et al.*[8] for ribonuclease activity-staining. Fig. 1 illustrates the sensitivity of the staining technique, using purified *A. niger* pectinase. Lane a contains 50 ng of the purified protein. A clear, sharp band corresponding to a molecular mass of $57 \cdot 10^3$ appears in the gel. Lanes b and c contain 5 and 0.5 ng of the pectinase, and the band apparent in lane b demonstrates the detection of 5 ng of pectinase, corresponding to $8 \cdot 10^{-5}$ units of enzyme.

Fig. 2 is a comparison of detectable polygalacturonases present in tomato pericarp during ripening. Lanes a through d contain extracts from tomatoes of increasing ripeness. As previously reported[3,4,9] there is no detectable PG activity in the MG 4 stage (lane a) which represents the late mature green fruit. There is also no detectable PG in the turning stage (lane b) in agreement with levels of PG based on assay[3,4,9]. The pink (lane c) and ripe (lane d) samples illustrate the dramatic appearance and rise in PG activity during ripening and also give an indication of the isozyme distribution[9–11]. The high molecular mass PG 1 in lane d appears to be composed of two bands, the higher molecular mass of the two predominating. In the PG 2 pair the lower molecular mass band represents the major species. Previous workers have purified the PG 1 and PG 2[4,11–13] and demonstrated that they are immunologically related and, under stringent denaturing conditions (100°C, 2% SDS), PG 1 is converted to a subunit that is immunologically related and similar in size to PG 2 and a protein subunit that is not related to PG 2[10,12,13]. Relative molecular

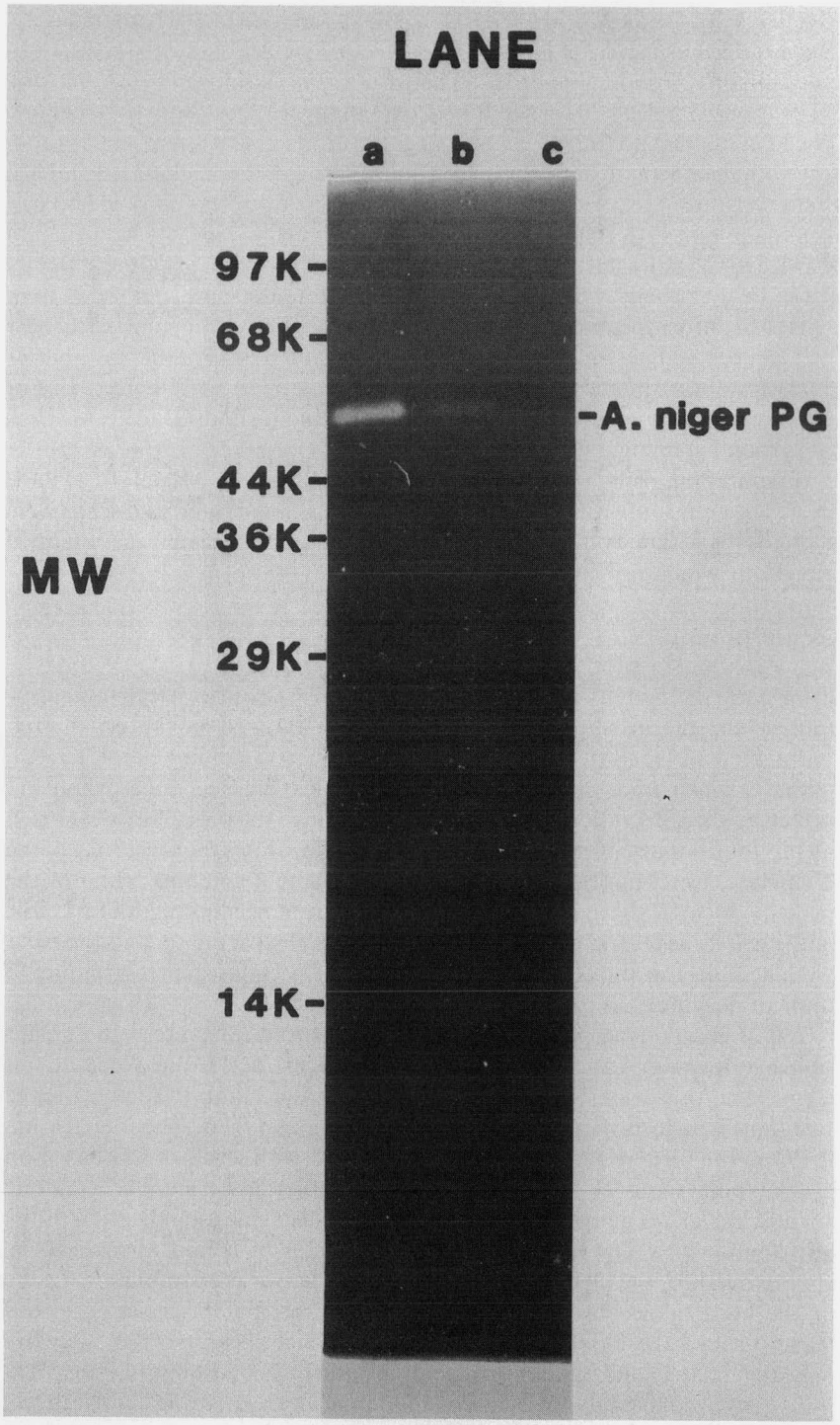

Fig. 1. Pectinase from *Aspergillus niger*. Samples were denatured in 2% SDS at 37°C and loaded on the gels. Loading buffer contained 0.02% fibrinogen to prevent losses due to surface binding. Each lane contained the specified number of units: (a) $8 \cdot 10^{-4}$; (b) $8 \cdot 10^{-5}$; (c) $8 \cdot 10^{-6}$.

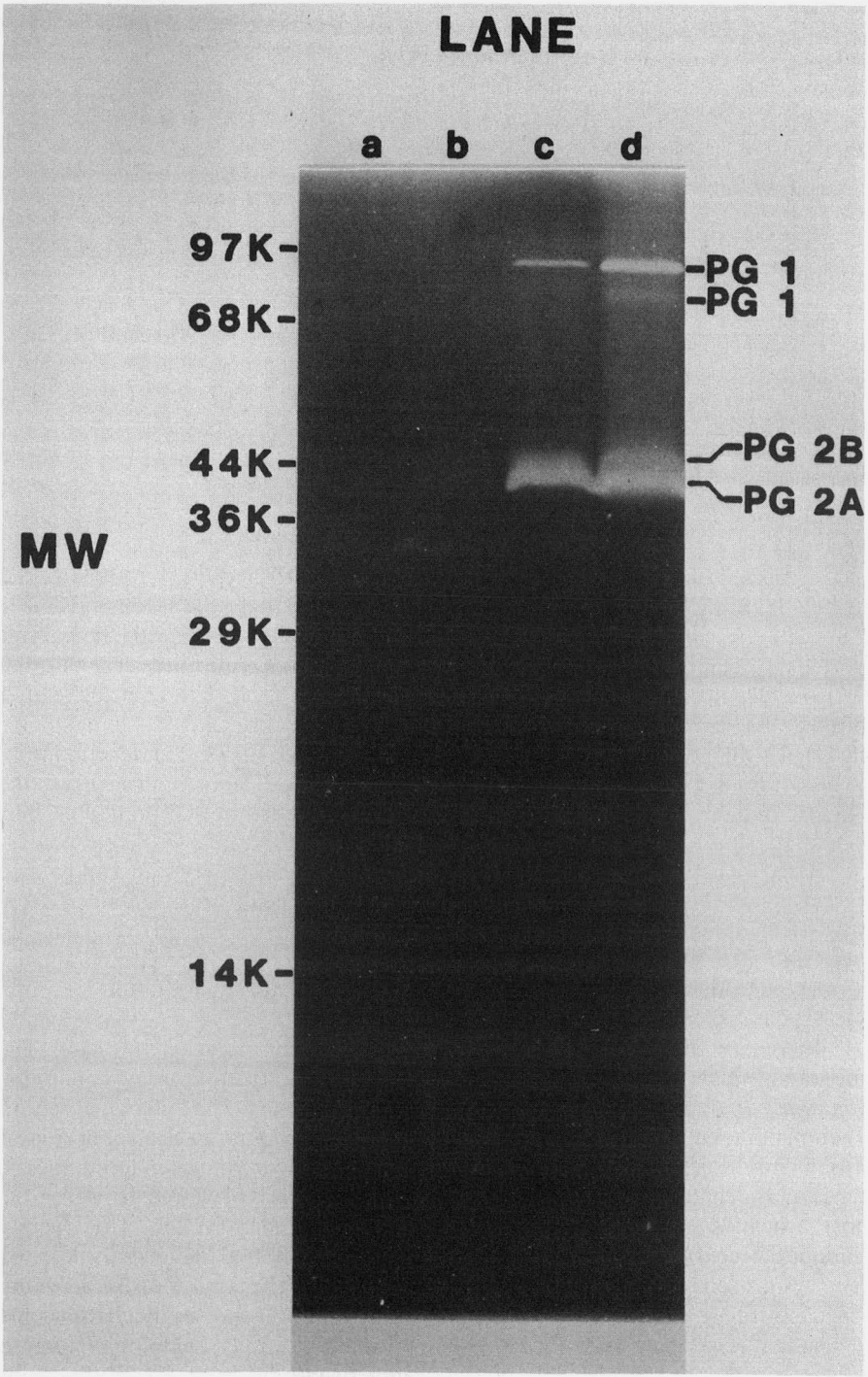

Fig. 2. Samples of tomato extracts were loaded on gels after denaturation at 37°C in 2% SDS. The developmental stage of the extracted tomato and the units loaded are: lane (a), MG4, no activity detected by assay; lane (b), turning, no activity detected by assay; lane (c), pink, 0.018 units; lane (d), ripe, 0.07 units.

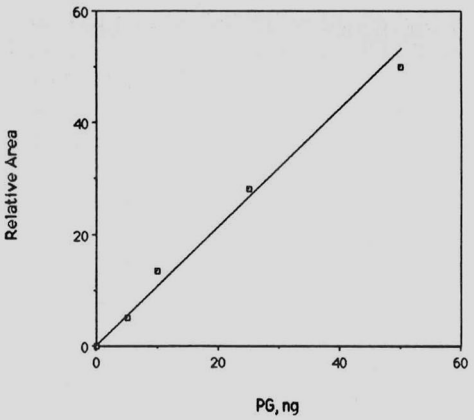

Fig. 3. A gel loaded with varying levels of *A. niger* pectinase was activity-stained after electrophoresis (gel not shown) and scanned as described in the Methods section. The units for relative peak area are directly proportional to absorbance and have been normalized to 50 for 50 ng pectinase.

masses reported for PG 1 include $84 \cdot 10^3$ (ref. 11), $100 \cdot 10^3$ (ref. 4), $115 \cdot 10^3$ (ref. 12) and $199 \cdot 1^3$ (ref. 13). The relative molecular masses found in the SDS, activity-stained gel are $89 \cdot 10^3$ and $79 \cdot 10^3$ (Fig. 2), and suggest, in accordance with the varying reported molecular weights for PG1, that PG1 exists in isoenzyme forms. The PG2 has been isolated and consists of two isoenzymes, PG2A and PG2B, with reported relative molecular masses of $43 \cdot 10^3$ and $46 \cdot 10^3$, respectively[12]). Molecular masses of $44 \cdot 10^3$ (ref. 11), $42 \cdot 10^3$ (ref. 4) and $47 \cdot 10^3$ (ref. 13) were reported for PG2 under conditions that do not resolve the two forms. The bands shown in Fig. 2, lanes c and d correspond to $43 \cdot 10^3$ and $47 \cdot 10^3$, indicating the resolution and detection of PG2A and PG2B by this activity stain.

Based on activity patterns shown in Figs. 1 and 2, the activity stain can be used for semi-quantitative purposes. As shown in Fig. 3, peak areas obtained from densitometry are linearly proportional to the amount of enzyme loaded over a ten-fold range from 5 to 50 ng. This linear relation of enzyme loaded to renatured activity indicates that the activity stain can reliably be used for quantitation of polygalacturonase isoenzymes.

There are three general types of activity-stain for polygalacturonase. The zymogram, which relies on diffusion of the enzyme into an overlay containing polygalacturonate followed by digestion and negative staining. The other types rely on the action of the enzyme *in situ* upon substrate incorporated prior to electrophoresis or diffused into the gel after electrophoresis[14]. Of two reported zymogram techniques[15], one uses non-denaturing conditions and separates on the basis of charge. However, the report[15] includes a zymogram technique used after SDS-PAGE. The overlay technique detected 0.1 units or more while the technique reported in this study detected $8 \cdot 10^{-5}$ units of enzyme activity. The reduced sensitivity of the zymogram for detecting polygalacturonase is due to incomplete enzyme diffusion, a shorter incubation time and harsher denaturing (100°C, 2% SDS, 2 min) conditions; samples of tomato polygalacturonase are not readily detected after denaturation at 100°C (data not

shown). The general disadvantage of overlay techniques is their reliance on diffusion which results in reduced sensitivity and loss of resolution of narrowly-resolved isoenzymes. One advantage of incorporating substrate in the gel is that a large, essentially non-diffusible substrate can be cast in the gel, providing a fixed uniform background after staining. Additionally, it has been suggested[16] that incorporated substrate may aid refolding of the enzyme to its native form after SDS denaturation.

Other activity stains incorporate polygalacturonate[17] or pectin[18] in the gel, both using non-denaturing conditions for sample treatment and electrophoresis. The advantage of the SDS activity stain is that separation is based on molecular mass. The use of a discontinuous gel buffer system provides stacking, resulting in a generally sharp banding pattern capable of resolving isoenzymes. These factors, coupled with the sensitivity of detection, make the SDS-PAGE activity stain for polygalacturonase a simple and effective means for detecting activity and for observing isoenzyme patterns during plant development.

ACKNOWLEDGEMENT

I would like to thank Ms. Rose de Lemos for typing this manuscript.

REFERENCES

1 J. M. Labavitch, *Ann. Rev. Plant Physiol.*, 32 (1981) 385–406.
2 M. McNeil, A. G. Darvill, S. C. Fry and P. Albersheim, *Ann. Rev. Biochem.*, 53 (1984) 625–663.
3 L. Y. Su, T. McKeon, D. Grierson, M. Cantwell and S F. Yang, *Hort. Science*, 19 (1984) 576–578.
4 G. A. Tucker, N. G. Robertson and D. Grierson, *Eur. J. Biochem.*, 112 (1980) 119–124.
5 W. W. Luchsinger and R. A. Cornesky, *Anal. Biochem.*, 4 (1962) 346–347.
6 U. K. Laemmli, *Nature (London)*, 227 (1970) 680–685.
7 A. Blank, J. R. Silber, M. P. Thelen and C. A. Dekker, *Anal. Biochem.*, 135 (1983) 423–430.
8 A. Blank, R. H. Sugiyama and C. A. Dekker, *Anal. Biochem.*, 120 (1982) 267–275.
9 C. J. Brady, G. MacAlpine, W. B. McGlasson and Y. Ueda, *Aust. J. Plant Physiol.*, 9 (1982) 171–178.
10 G. A. Tucker, N. G. Robertson and D. Grierson, *Eur. J. Biochem.*, 115 (1981) 87–90.
11 R. Pressey and J. K. Avants, *Biochim. Biophys. Acta*, 309 (1973) 363–369.
12 Z. M. Ali and C. J. Brady, *Aust. J. Plant Physiol.*, 9 (1982) 155–169.
13 M. Moshrefi and B. S. Luh, *Eur. J. Biochem.*, 135 (1983) 511–514.
14 N. Lisker and N. Retig, *J. Chromatogr.*, 96 (1974) 245–249.
15 J. L. Ried and A. Collmer, *Appl. Environ. Microbiol.*, 52 (1985) 305–310.
16 S. A. Lacks and S. S. Springhorn, *J. Biol. Chem.*, 255 (1980) 7467–7473.
17 H. Stegemann, *Hoppe-Seyler's Z. Physiol. Chem.*, 348 (1967) 951–952.
18 R. H. Cruickshank and G. C. Wade, *Anal. Biochem.*, 107 (1980) 177–181.

Journal of Chromatography, 455 (1988) 382–390
Elsevier Science Publishers B.V., Amsterdam — Printed in The Netherlands

CHROM. 20 910

Note

Indirect fluorimetric detection of non-electrolytes in thin-layer chromatography

YINFA MA and EDWARD S. YEUNG*
Ames Laboratory-USDOE and Department of Chemistry, Iowa State University, Ames, IA 50011 (U.S.A.)
(First received March 14th, 1988; revised manuscript received June 15th, 1988)

Thin-layer chromatography (TLC) is one of the oldest and perhaps the simplest chromatographic separation techniques still in widespread use. In recent years, emphasis has been on high-performance liquid chromatography (HPLC) to separate complicated samples because of its high separation efficiency and advanced instrumental detection system. Therefore, TLC is far behind HPLC, even though a lot of developments in sorbent materials, particle sizes and detection instruments have been achieved[1–5]. However, TLC has certain advantages because it is an open bed while HPLC is a closed bed systems. Since each plate is used only once, there is no possibility of poisoning a TLC plate, which is far too easy to do with an HPLC column. This may result in permanent damage to the column if samples cannot be removed. TLC plates, however, are free from this problem and highly retained components can still be detected. Simultaneous sample separation and detection[6] and two-dimensional separation[7–9] can be used. TLC is also quick, simple, convenient, inexpensive and disposable. TLC can complement HPLC as a pilot technique for the optimization of separation conditions[10] and can be used as a sample preparation technique for further separation[11–12].

Detection in TLC, unlike HPLC, is a static process, being completely separated from chromatographic development. So, a detector that works well for HPLC may not work for TLC. Detection of colored compounds, in general, causes no problem. The same holds true of compounds which exhibit fluorescence or phosphorescence under UV light. For colorless compounds, one usually adopts densitometry[13], directly if the compounds are UV-absorbing, or after color reaction[14] for which a specific spray reagent is required. Even though these methods are sometimes quite sensitive, they cannot be used to detect analytes which do not absorb in the UV region or have no appropriate spray reagents. The use of fluorescence layers[15–17] has been successfully demonstrated for detecting colorless compounds. However, this still requires that the analytes absorb either at the absorption or the emission wavelength of the fluorophore on the plate.

Recently, indirect fluorimetric detection of anions and non-electrolytes in HPLC has been demonstated[18–21]. Briefly, a fluorophore in the mobile phase generates a large uniform background fluorescence. When the analytes elute, displacement of the fluorophore causes a change in the fluorescence intensity to allow detection. Following the same principles, the indirect fluorimetric detection of anions in TLC has also been achieved[22]. This article will present an indirect fluorimetric detection method for

0021-9673/88/$03.50 © 1988 Elsevier Science Publishers B.V.

non-electrolytes (alkanols, bile acids and digoxin series) in TLC. Not only are detection limits improved, but the method is also much simpler and analysis time is much shorter compared with other detection methods in TLC for the same compounds[23,24].

EXPERIMENTAL

Reagents

HPLC grade acetonitrile and methanol, and certified grade methyl ethyl ketone were obtained from Fisher Scientific (Fairlawn, NJ, U.S.A.). HPLC grade chloroform was obtained from Burdick & Jackson Labs. (Muskegon, MI, U.S.A.). HPLC grade tetrahydrofuran and analytical grade salicylic acid were obtained from Baker (Phillipsburg, NJ, U.S.A.). Alkanols, digoxin, digitoxin, taurocholic acid and taurodeoxycholic acid were purchased from Aldrich (Milwaukee, WI, U.S.A.). Digoxigenin, glycocholic acid and glycodeoxycholic acid were purchased from Sigma (St. Louis, MO, U.S.A.). 2-(1,1'-Biphenyl)-4-yl-5-phenyl-1,3,4-oxadiazole (PBD) was purchased from Eastman-Kodak (Rochester, NY, U.S.A.). 2-(1-Naphthalenyl)-5-phenyloxazale from Lambda Physik (Acton, MA, U.S.A.). Deionized water further purified on a Milli-Q system (Millipore, Bedford, MA, U.S.A.) was used to prepare pretreating solutions or eluents.

Materials

K_6 silica gel plates and KC_{18} reversed-phase plates were purchased from Whatman Chemical Separation (Clifton, NJ, U.S.A.). Adsorbosil RP-HPTLC plates were obtained from Alltech Assoc. (Deerfield, IL, U.S.A.). UV lamps (312 nm, 254 nm) were purchased from Cole Palmer (Chicago, IL, U.S.A.). A microsyringe calibrated to 0.1 μl units was purchased from Hamilton (Reno, NV, U.S.A.).

Sample preparations

Alcohol mixtures were prepared by dissolving decanol, dodecanol, tetradecanol and hexadecanol in acetonitrile–toluene (90:10). Bile acids mixtures were prepared by dissolving taurocholic acid (TC), taurodeoxycholic acid (TCD), glycocholic acid (GC), glycodeoxycholic acid (GDC) in methanol. Digoxin series mixtures were prepared by dissolving digoxin, digitoxin and digoxigenin in chloroform–methanol (2:1).

Chromatography and detection

Alcohols. (a) The Adsorbosil RP-HPTLC plate is immersed in acetonitrile–water (40:60) containing $2 \cdot 10^{-5}$ *M* PBD for 2 h. The plate is then dried with a heat-gun. Samples are spotted by a micro-syringe. The plate was developed by acetonitrile–water (98:2) containing $4 \cdot 10^{-3}$ *M* PBD for 6 min. After drying the plate again, the plate was placed under a UV lamp (312 nm). A series of negative spots can be observed.

(b) The samples were spotted on a KC_{18} reversed-phase plate directly (no pretreatment) by a microsyringe and the plate was developed by acetonitrile–water (98:2) containing $4 \cdot 10^{-5}$ *M* α-NPO for 6 min. The plate is then dried and visualized under the UV lamp (312 nm). A series of positive spots can be observed.

Bile acids. A K_6 silica gel plate was treated by chloroform–acetonitrile (50:50)

containing $1 \cdot 10^{-4}$ *M* salicylic acid for 1 h and was then dried. After spotting the bile acid mixture on the plate by a microsyringe, the plate is developed with chloroform–methanol–methyl ethyl ketone (46:46:8) containing $3 \cdot 10^{-3}$ *M* salicylic acid for 24 min. The plate was then dried and visualized under a UV lamp (312 nm). A series of positive spots can be observed.

Digoxin series. (a) An Adsorbosil RP-HPTLC plate was pretreated with acetonitrile–water (40:60) containing $1 \cdot 10^{-5}$ *M* α-NPO for 1 h and was dried with a heat-gun. Samples were spotted with a micro syringe, and the plate was developed by methanol–water (7:3) containing $4 \cdot 10^{-5}$ *M* α-NPO for 8 min. The plate was then dried and visualized under a UV lamp (254 nm). A series of negative spots can be observed.

(b) After spotting the samples on a KC_{18} RP-TLC plate directly (no pre-

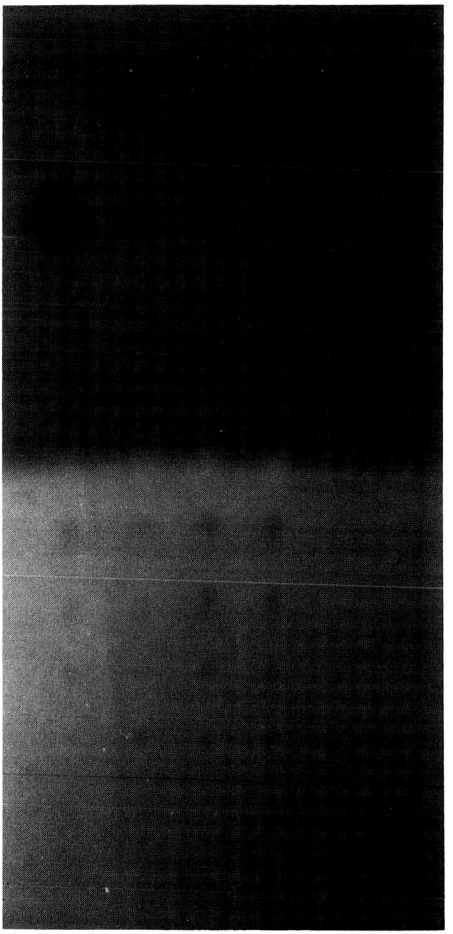

Fig. 1. Indirect fluorometric detection of alkanols on an Adsorbosil RP-HPTLC plate using procedure (a) in the text. Development is from bottom to top, with the front midway up the plate. The sample at the right contains 20 nmol each of decanol (C_{10}), dodecanol (C_{12}), tetradecanol (C_{14}) and hexadecanol (C_{16}), showing as lower intensity spots from top to bottom of the picture. The other three samples contain the same components as the right one but at concentrations of 1/3, 1/10 and 1/30 of that at the right.

treatment) by a microsyringe, the plate is developed by methanol–water (7:3) containing $2 \cdot 10^{-3}$ *M* salicylic acid for 8 min. Then, the plate is dried and visualized under a UV lamp (312 nm). A series of positive spots can be observed.

RESULTS AND DISCUSSION

Figs. 1 and 2 demonstrate the indirect fluorometric detection of alkanols by reversed-phase TLC. Nanomole levels of each alkanol can be detected by our eyes. The dark spots in Fig. 1 are not due to the presence of an absorbing species. Rather, less of the fluorophore exists locally because it has been transferred out of the stationary phase by the analyte. It should be mentioned that the positive (higher intensity) spots observed in Fig. 2 are not due to the fluorescence of alkanols. The reason for this

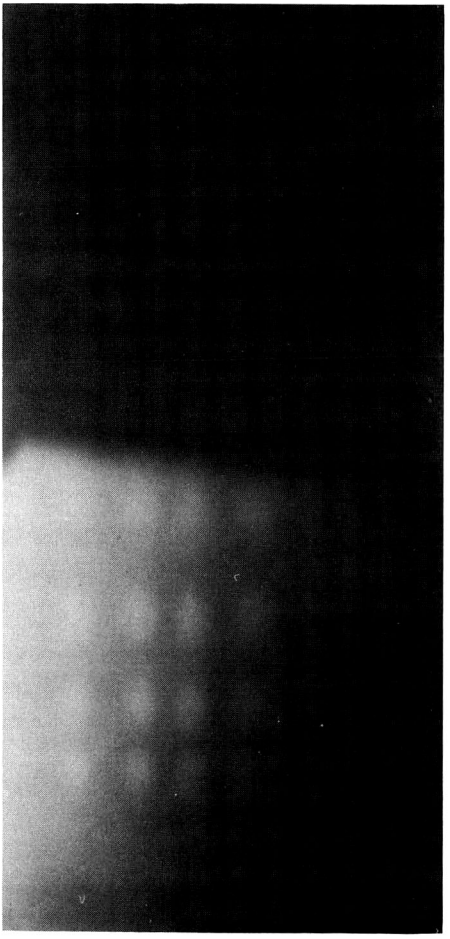

Fig. 2. Indirect fluorometric detection of alkanols on a KC_{18} reversed-phase TLC plate using procedure (b) in the text. Development is from bottom to top, with the front midway up the plate. The analytes show up as higher intensity spots. The sample components and concentration range are the same as those of Fig. 1.

phenomenon is that alkanols transfer visualizing reagent (α-NPO here) from the mobile phase to the stationary phase. So, where the sample spot is, more of the fluorophor exists, and a stronger fluorescence signal is observed. An earlier paper[25] had a detailed discussion on this. The choice of fluorophore determines whether positive or negative (lower intensity) spots are observed, even though the same developing solution is used. This clearly shows that differences in partition into the stationary phase between the fluorophore and the analytes is responsible for the signal.

Fig. 3 shows the indirect fluorometric detection of bile acids. Subnanomoles of each can be detected. The reason for the presence of positive spots is the same as that for alkanols. Touchstone *et al.*[24] had previously demonstrated the separation of

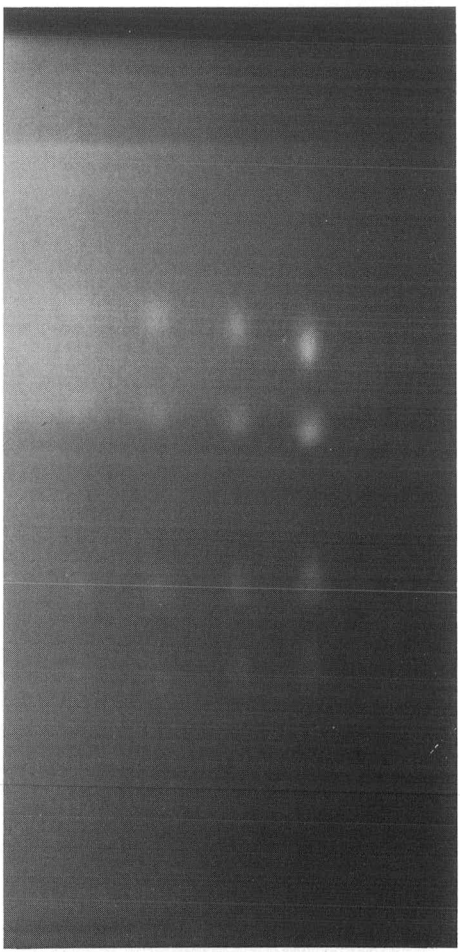

Fig. 3. Indirect fluorometric detection of bile acids on a K_6 silica gel plate. Development is from bottom to top, with the front near the top edge of the plate. The sample at the right contains 10 nmol each of taurodeoxycholic acid (TDC), taurocholic acid (TC), glycodeoxycholic acid (GDC) and glycocholic acid (GC), showing up from top to bottom of the picture as higher intensity spots. The other three samples contain the same components as the right one but at concentrations of 1/3, 1/10 and 1/30 of that at the right.

conjugated bile acids on reversed-phase TLC and detection by a spectrodensitometer in the transmission mode. But the method is time consuming and one needs to search for a specific spray reagent. By our approach, separation is faster and detection is simpler. Similar detection limits can be achieved even by our naked eyes. With a scanning laser beam for excitation, one would expect even better detection due to signal averaging and intensity enhancement.

The indirect fluorometric detection of digoxin series is shown in Figs. 4 and 5. The positive spots in Fig. 5 occur for the same reasons as the alkanols in Fig. 2. Comparing the results from a previous paper[23], the detection limits for digoxin,

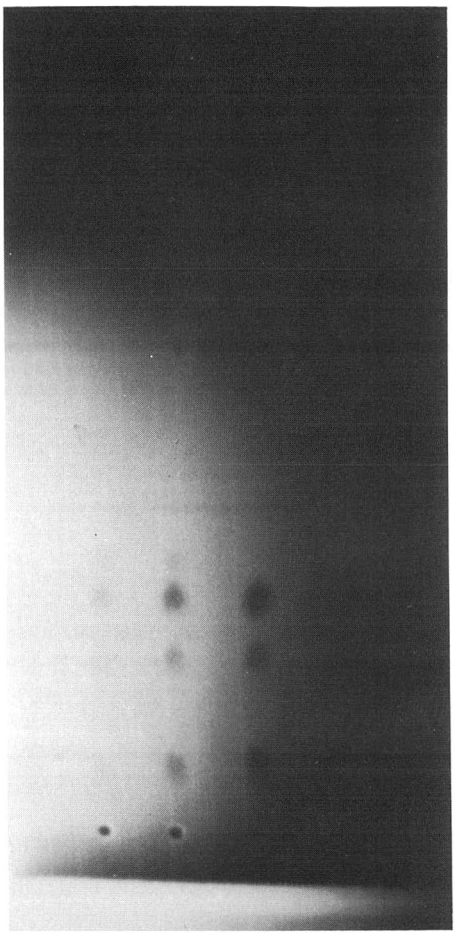

Fig. 4. Indirect fluorometric detection of digoxin series on an Adsorbosil RP-HPTLC plate using procedure (a) in the text. Development is from bottom to top, with the front midway up the plate. The sample at the right (barely illuminated) contains 15 nmol of digoxigenin and 7.7 nmol each of digoxin and digitoxin, showing up from top to bottom of the picture as lower intensity spots. The other three samples contain the same components as the right one but at concentrations of 1/3, 1/10 and 1/30 of that at the right. Two impurities are present, one above and one below the set of three analytes.

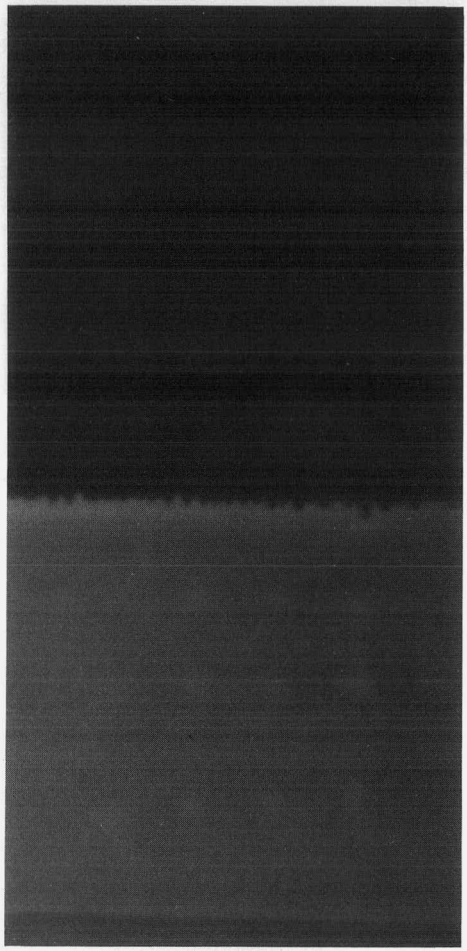

Fig. 5. Indirect fluorometric detection of digoxin series on a KC_{18} reversed-phase TLC plate using procedure (b) in the text. Development is from bottom to top, with the front midway up the plate. The sample components and concentration range are the same as those of Fig. 4.

digitoxin and digoxigenin are at least two orders of magnitude lower by our approach. Also, spray reagents are omitted in our method.

In indirect fluorimetric detection methods, the following equation can be used to estimate the limit of detection of non-electrolytes[26]

$$C_s > \frac{1}{D_R(R/C_m + V_s)} \tag{1}$$

where C_s is the molar concentration of the analyte detected, D_R is the dynamic reserve (which is defined as the ratio of the background signal to the noise level), R is the displacement ratio (which is defined as the number of visualizing molecules transferred

by one analyte molecule), C_m is the molar concentration of visualization reagent and V_s is the volume of 1 mol of the analyte. The equation tells us that the dynamic reserve, concentration of the visualization reagent and the displacement ratio all play important roles in the sensitivity of indirect fluorometric detection.

In order to improve the detection limit or sensitivity of indirect fluorometric detection further in TLC, the background signal should be decreased as much as possible. This can be achieved by decreasing the concentration of the visualization reagent in the pretreating solution or in the developing solution. However, if the background signal is too low, the displacement ratio may also decrease and contrast will be lost.

The visual (or photographic) observation in this work is obviously poor compared to instrumental detection methods with respect to D_R in eqn. 1. Therefore, further improvements in detectability should be possible. Fluorescence with high-frequency modulation should allow D_R to increase by 2 to 3 orders of magnitude[18]. The high sensitivity of laser-excited fluorescence should make it compatible with much lower fluorophore concentrations, if the natural fluorescence of the TLC substrate can be discriminated against.

CONCLUSION

Indirect fluorometric detection of non-electrolytes (alkanols, bile acids and digoxin series) has been presented. Nanomolar detection limits were achieved. The selection of the visualization reagent and the chromatographic conditions is important because of the dependence of displacement ratio and spot character (negative spot or positive spot) on it. With minor modifications of the recipes given in this work, one can now essentially combine indirect fluorometric detection with any TLC separation.

ACKNOWLEDGEMENTS

The Ames Laboratory is operated for the U.S. Department of Energy by Iowa State University under contract No. W-7405-Eng-82. This work was supported by the Office of Basic Energy Sciences, Division of Chemical Sciences.

REFERENCES

1 R. M. Belchamber, H. Read and J. D. M. Roberts, *J. Chromatogr.*, 395 (1987) 47.
2 D. H. Burns, J. B. Callis and G. D. Christian, *Trends Anal. Chem.*, 5 (1986) 50.
3 B. Fried and J. Sherma, *Thin Layer Chromatography*, Dekker, New York, 2nd ed., 1986.
4 J. Donovan, M. Gould and R. Majors, *LC · GC Mag. Liq. Gas Chromatogr.*, 5 (1987) 1024.
5 B. G. Belenkii, E. S. Gankina, T. B. Adamovich, A. P. Lobazov, S. V. Nechaev and M. G. Solonento, *J. Chromatogr.*, 365 (1986) 315.
6 D. G. Gelderloos, K. L. Rowlen, J. W. Birks, J. P. Avery and C. G. Enke, *Anal. Chem.*, 58 (1986) 900.
7 B. DeSpiegeleer, W. Van den Bossche, P. DeMoerloose and D. Massart, *Chromatographia*, 23 (1987) 407.
8 G. Matysik and E. Soczewiński, *J. Chromatogr.*, 369 (1986) 19.
9 J. C. Giddings, *Anal. Chem.*, 56 (1984) 1258A.
10 W. Jost, H. E. Hauck and F. Eisenbeiss, *Kontakte (Darmstadt)*, 3 (1984) 45.
11 R. L. White, *Anal. Chem.*, 57 (1985) 1819.
12 K. H. Shafer, J. A. Herman and H. Bui, *Am. Lab. (Fairfield, Conn.)*, (1988) 142.
13 J. C. Touchstone and J. Sherma, *Densitometry in Thin Layer Chromatography*, Wiley, New York, 1979.

14 J. G. Kirchner, *Thin-Layer Chromatography*, Wiley, New York, 1978, 2nd ed., p. 193.
15 J. W. Sease, *J. Am. Chem. Soc.*, 69 (1947) 2242.
16 J. G. Kirchner, J. M. Miller and G. J. Keller, *Anal. Chem.*, 23 (1951) 420.
17 J. M. Miller and J. G. Kirchner, *Anal. Chem.*, 26 (1954) 2002.
18 S. Mho and E. S. Yeung, *Anal. Chem.*, 57 (1985) 2253.
19 T. Takeuchi and E. S. Yeung, *J. Chromatogr.*, 370 (1986) 83.
20 T. Takeuchi and E. S. Yeung, *J. Chromatogr.*, 366 (1986) 145.
21 W. Pfeffer, T. Takeuchi and E. S. Yeung, *Chromatographia*, 24 (1987) 123.
22 Y. Ma and E. S. Yeung, *Anal. Chem.*, 60 (1988) 722.
23 D. E. Bloch, *J. Assoc. Off. Anal. Chem.*, 63 (1980) 707.
24 J. C. Touchstone, R. E. Levitt, S. S. Levin and R. D. Soloway, *Lipids*, 15 (1980) 386.
25 J. J. Stranahan and S. N. Deming, *Anal. Chem.*, 54 (1982) 1540.
26 T. Takeuchi and D. Ishii, *J. Chromatogr.*, 396 (1987) 149.

Journal of Chromatography, 455 (1988) 391–395
Elsevier Science Publishers B.V., Amsterdam — Printed in The Netherlands

CHROM. 20 902

Note

Gas chromatographic determination of chloroacetamide herbicides in plants and soil*

ANNA BALINOVA
Institute for Plant Protection, Kostinbrod 2230, P.O.B. 238, Sofia (Bulgaria)
(First received October 12th, 1987; revised manuscript received June 15th, 1988)

Alachlor [2-chloro-N-(2,6-diethylphenyl)-N-(methoxymethyl)acetamide], acetochlor [2-chloro-N-(2-ethyl-6-methylphenyl)-N-(ethoxymethyl)acetamide], metolachlor [2-chloro-N-(2-ethyl-6-methylphenyl)-N-(2-methoxy-1-methylethyl)acetamide] and propachlor [2-chloro-N-(1-methylethyl)-N-phenylacetamide] are some of the currently most widely used herbicides.

The methods of analysis of alachlor, propachlor and metolachlor in the literature are based mainly on gas chromatography (GC) with flame ionization detection (FID)[1–6]. With a non-specific detector, the sensitivity of the determination is relatively low (0.05 mg/kg), and laborious purification of samples is needed. GC determination with nitrogen–phosphorus detection (NPD) has been applied to the analysis of acetochlor residues after hydrolysis to the corresponding aniline (sensitivity of the method 0.02–0.05 mg/kg)[7], as well as in the analysis of alachlor, propachlor and butachlor in water[8].

Electron-capture detection (ECD) is a highly sensitive method for these compounds. I have used it in the analysis of alachlor and propachlor residues[9]. Ammann *et al.*[10] also determined alachlor by ECD. Other authors have used ECD in the analysis of alachlor after derivatization to the heptafluorobutyryl derivative[11]. This method is highly sensitive, but chemical derivatization complicates the analysis.

The method offered here is comparatively easy and less time-consuming than derivatization. It is highly sensitive and accurate, providing the separation, identification and quantitation of four of the most common chloroacetamide herbicides.

EXPERIMENTAL

The clean-up column was a 300 mm × 10 mm I.D. glass column. The gas chromatograph was a Model Sigma 300 (Perkin-Elmer, Norwalk, CT, U.S.A.), equipped with a ^{63}Ni electron-capture detector and glass columns (183 cm × 2 mm I.D.) packed with 5% QF-1 + 2.5% DC-200 or 10% Apiezon L on Chromosorb W AW DMCS 80–100 mesh. The operating conditions were: injector, 220°C; column, 200°; detector, 300°; carrier gas (nitrogen) flow-rate 30 ml/min when a column with

* Presented at the *6th Danube Symposium on Chromatography, Varna, October 12–17, 1987*. The majority of the papers presented at this symposium has been published in *J. Chromatogr.*, 446 (1988).

0021-9673/88/$03.50 © 1988 Elsevier Science Publishers B.V.

5% QF-1 + 2.5% DC-200 was used and 60 ml/min when a column with 10% Apiezon L was used.

All reagents and solvents were of reagent grade. Chloroform, *n*-hexane and benzene were also distilled in glass. Florisil (Fluka, Buchs, Switzerland), 60–100 mesh, was heated at 135°C for 24 h, and deactivated with 10% (w/v) water. Since Florisil is not a perfectly standardized product, the elution characteristics of each batch should be determined before use.

All reagents were tested for impurities by GC–ECD.

The sample (50 g) was weighed out in the cup of a blender and then thoroughly homogenized with 100 ml acetonitrile for 2–3 min at high speed. Wet samples (fruit, vegetables) were filtered with suction through a buchner funnel or centrifuged. The blender jar and the cake were washed with 2 × 25 ml acetonitrile. The volume of the filtrates was measured. The extract was mixed thoroughly and an aliquot, corresponding to 25 g of sample, was taken. Dry samples (less than 10% water content) were blended with 100 ml acetonitrile–water (9:1) and filtered or centrifuged. A 50-ml volume of the filtrate (corresponding to 25 g of sample) was taken for analysis.

For clean-up, the extract was transferred to a 250-ml separatory funnel and extracted with two 20-ml portions of *n*-hexane. The hexane layers were discarded and the acetonitrile layer was transferred to a vacuum evaporator. The acetonitrile was removed at 50°C under vacuum. In the case of dry samples the extracts were evaporated to about 5 ml. The watery remainder was transferred to a 250-ml separatory funnel, using 20 ml of chloroform and 50 ml of saturated sodium chloride solution for rinsing, shaken for 2 min and the phases allowed to separate. The chloroform layer was collected and the extraction was repeated with two 20-ml portions of chloroform. The chloroform layers were pooled and dried over anhydrous sodium sulphate. After evaporation of the chloroform under vacuum at 40°C, the residue was dissolved in 1 ml hexane–diethyl ether (1:1).

The clean-up column was packed with 1 g Florisil in hexane–diethyl ether (1:1) and a 1-cm layer of anhydrous sodium sulphate on top. The residue was transferred to the column using four 1-ml portions of hexane–diethyl ether (1:1) and the column was eluted with the same solvent. The first 1-ml portion of the eluate was discarded, the following 7 ml were collected and evaporated under a gentle stream of air or nitrogen, about to dryness. The volume of the residue was adjusted to 2.0 ml with benzene. When necessary the samples were diluted to an higher volume.

For the GC determination, samples were injected with a 1-μl syringe and interspersed with standards, prepared by dissolving the analytical standards alachlor, acetochlor, propachlor (obtainable from Monsanto) and metolachlor (from Ciba-Geigy) in benzene to suitable concentrations. For quantitation, the detector response (peak height) was plotted against the amount of each standard compound. The samples were identified by comparing the retention times of the chromatographic peaks of the sample and standard compounds.

RESULTS AND DISCUSSION

The minimum detectable amounts of the compounds tested were between 0.02 and 0.05 ng (Table I). The relative retention times on two GC columns are presented in Table II. The chromatographic separation of the four compounds is complete

TABLE I

MINIMUM DETECTABLE AMOUNTS

Compound	*Amount (ng)*
Propachlor	0.05
Acetochlor	0.02
Alachlor	0.02
Metolachlor	0.05

TABLE II

RELATIVE RETENTION TIMES (RRT), BASED ON ALDRIN, FOR FOUR CHLOROACETAMIDE HERBICIDES ON TWO GC COLUMNS

Compound	*RRT*	
	5% QF-1 + 2.5% DC-200	*10% Apiezon L*
Propachlor	0.54	0.20
Acetochlor	1.06	0.53
Alachlor	1.13	0.57
Metolachlor	1.44	0.77
Aldrin	1.00	1.00

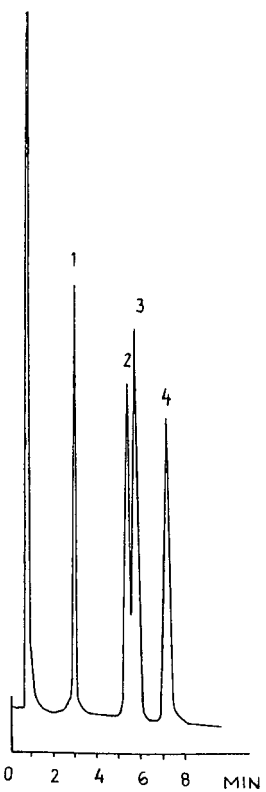

Fig. 1. Gas chromatogram of 0.4 ng propachlor (1), 0.2 ng acetochlor (2), 0.2 ng alachlor (3) and 0.4 ng metolachlor (4). A 183-cm column packed with 5% QF-1 + 2.5 % DC-200 on Chromosorb W AW DMCS (80–100 mesh) operated at 200°C and ECD were used.

TABLE III

RECOVERIES OF THE HERBICIDES TESTED FROM SPIKED SOIL AND POTATO SAMPLES

(Average of 11 fortifications).

Compound	*Spiking levels (mg/kg)*	*Recovery (%) and coefficient of variation (%)*	
		Soil	*Potatoes*
Propachlor	0.1	85.1 ± 9.3	82.5 ± 6.1
	0.02	69.5 ± 8.1	64.8 ± 7.4
Acetochlor	0.1	80.6 ± 7.1	84.0 ± 5.2
	0.02	71.3 ± 6.9	73.2 ± 8.6
Alachlor	0.1	83.2 ± 6.5	84.3 ± 4.9
	0.02	70.7 ± 7.3	68.2 ± 6.1
Metolachlor	0.1	86.7 ± 8.8	85.3 ± 7.4
	0.02	66.2 ± 5.8	65.6 ± 6.5

(Table II, Fig. 1), except for acetochlor and alachlor, which are isomeric. Their chromatographic separation proved to be difficult. Among the numerous columns tested, two (10% Apiezon L and 5% QF-1 + 2.5% DC-200) gave the best results.

The accuracy of the method developed is given in Table III. Since derivatization is avoided, a higher precentage recovery is obtained. The application of ECD, distinguished by an higher sensitivity than that of NPD and a greater specificity than that of FID, makes the method highly sensitive (Tables I and IV).

The method was applied to the determination of residues of the four herbicides in soil and plants (potatoes, tomatoes, grains and leaves of maize). Impurities in the extracts did not interfere with the determination of the compounds.

TABLE IV

LIMIT OF DETERMINATION OF THE METHOD

Compound	*Limit (mg/kg)*	
	Soil	*Potatoes*
Propachlor	0.005	0.01
Acetochlor	0.002	0.004
Alachlor	0.002	0.004
Metolachlor	0.005	0.01

REFERENCES

1 K. D. Wenzel, M. Monke and R. Grahl, *Fresenius' Z. Anal. Chem.*, 322 (1985) 423.
2 A. Krause, W. G. Hancock, R. D. Minard, A. J. Freyer, R. C. Honeycutt, H.M. LeBaron, D. L. Paulson, S. Y. Lin and J. M. Bollag, *J. Agric. Food Chem.*, 22 (1985) 584.
3 G. T. Gale and A. H. Hofberg, *J. Assoc. Off. Anal. Chem.*, 68 (1985) 570.
4 *Pesticide Analytical Manual*, Vol. II, U.S. Dept. of Health, Education and Welfare, Food and Drug Administration, 1974.

5 *Information to Support Label Registration Request*, Lasso, Book 2, Monsanto, St. Louis, MO, 1971.
6 *Information to Support Label Registration Request*, Analytical Section, 2-chloro-N-isopropylacetanilide, Monsanto, St. Louis, MO, 1968.
7 *Analytical Residue Method for Acetochlor*, Lab 7127, Monsanto, St. Louis, MO, 1982.
8 J. W. Worley, M. L. Rueppel and F. L. Rupel, *Anal. Chem.*, 52 (1980) 1845.
9 A. Balinova, *Materiali Symposiuma "Ostatochnie Kolichestva Gerbicidov v Rastenijach i v Pochve", Wroclaw, 1973*, SEV, Poznan, 1975, 111.
10 B. D. Ammann, D. J. Call and H. A. Draayer, *J. Assoc. Off. Anal. Chem.*, 859 (1976) 859.
11 W. H. Newsome, P. Collins and D. Lewis, *J. Assoc. Off. Anal. Chem.*, 69 (1986) 591.

Journal of Chromatography, 455 (1988) 396–400
Elsevier Science Publishers B.V., Amsterdam — Printed in The Netherlands

CHROM. 20 962

Note

Simultaneous separation and identification of carotenoids and chlorophylls in turf bermudagrass by high-performance liquid chromatography

C. A. BAILEY* and B. H. CHEN

Department of Poultry Science, Texas Agricultural Experiment Station, The Texas A&M University System, College Station, TX 77843 (U.S.A.)

(First received June 22nd, 1988; revised manuscript received September 8th, 1988)

Both carotenoids and chlorophylls are important biological compounds that are present in green tissues of higher plants. It has been well established[1,2] that the primary function of carotenoids in plant tissue is to prevent photosensitization by endogenous photosensitizers such as chlorophylls. Due to the different polar characteristics of carotenoids and chlorophylls, the separation of these pigments has been difficult. Therefore, a simple, rapid method for the simultaneous separation of carotenoids and chlorophylls is important in order to learn more about the role of these pigments in photosynthesis.

The separation of carotenoids and chlorophylls by high-performance liquid chromatography (HPLC) has been well documented[3–9]. However, these methods are lengthy and time-consuming. Some methods[3,4] even require 75 min or longer for complete elution of these pigments. In a previous study[10] we reported the separation of major carotenoids in turf bermudagrass. By using a 15-cm, reversed-phase column we have since been able to resolve 19 peaks within 10 min, of which 10 pigments were identified. These pigments included xanthophylls, chlorophylls and β-carotene.

EXPERIMENTAL

Instrumentation

The HPLC instrument consisted of an IBM (Danbury, CT, U.S.A.) LC 9533 ternary gradient liquid chromatography with an IBM UV–VIS fixed-wavelength detector employing a 440 nm filter and a Water Nova-Pak C_{18} stainless-steel column (15 cm × 3.9 mm I.D.). A Sargent-Welch recorder (Skokie, IL, U.S.A.) was used for recording the chromatographs at 0.05 a.u.f.s. Spectrophotometric determinations were made with a Beckman (Irvine, CA, U.S.A.) DU-6 spectrophotometer. Water–acetonitrile–chloroform (2:83:15)[10], pumped at a flow-rate of 1.0 ml/min, was used as the solvent system.

Materials

Trans-β-carotene, chlorophyll *a* and chlorophyll *b* standards were purchased from Sigma (St. Louis, MO, U.S.A.). Neoxanthin and violaxanthin standards were prepared from saponified turf bermudagrass extract by thin-layer chromatograpy

0021-9673/88/$03.50 © 1988 Elsevier Science Publishers B.V.

(TLC) as described by Chen and Bailey[10]. Lutein and zeaxanthin standards were prepared from corn by open-column chromatography using a method[11] similar to that described by Quackenbush *et al.*[12]. Lutein monoester was prepared from unsaponified turf bermudagrass extract by TLC. Pheophytins *a* and *b* were prepared by adding a few drops of 0.01 *N* ethanolic HCl to chlorophylls *a* and *b*, respectively[9]. The silica gel G TLC plates were purchased from Whatman (Clifton, NJ, U.S.A.). All solvents were purchased from Fisher Scientific (Pittsburgh, PA, U.S.A.). Acetonitrile, water and chloroform were HPLC grade. Acetone, hexane, toluene, ethanol, methanol, ethyl acetate, light petroleum (b.p. 37.9–55.4°C) and benzene were ACS grade. HPLC-grade solvents were filtered through a 0.2-μm membrane filter and degassed under vacuum prior to use.

Turf bermudagrass was fresh-cut from Maxim Productions in South Central Texas. The grass was stored in a dark, ventilated room to dry for 1 week before grinding into fine materials with a hammer mill fitted with a 3.2 mm screen.

Preparation of lutein monoester from unsaponified turf bermudagrass extract

A solvent system of methanol–ethyl acetate–benzene (5:20:75)[13] was used to separate the major carotenoids, lutein monoester and chlorophylls in concentrated turf bermudagrass extracts on silica gel G TLC plates. Individual carotenoids, lutein monoester and chlorophylls were characterized by determining their R_F values and absorption spectra. For co-chromatographic test, β-carotene, chlorophyll *a*, chlorophyll *b*, pheophytin *a*, pheophytin *b*, lutein, violaxanthin and neoxanthin were used as reference standards.

Extraction and HPLC analysis of unsaponified turf bermudagrass extract

A 1-g amount of ground turf bermudagrass was extracted with 30 ml hexane–acetone–ethanol–toluene (10:7:6:7) in a 100-ml volumetric flask under nitrogen overnight. A 30-ml volume of hexane was added to each flask which was then diluted to volume with 10% sodium sulfate and mixed. After 1 h, 10 ml of the upper phase were evaporated to dryness and dissolved in 10 ml chloroform and filtered through a 0.2-μm membrane filter. A 10-μl volume of extract was injected onto the HPLC column and developed with water–acetonitrile–chloroform (2:83:15) at a flow-rate of 1.0 ml/min. Samples were monitored at 4.40 nm with a sensitivity of 0.05 a.u.f.s. All the sample preparations were conducted under diffused light and samples were kept under nitrogen whenever possible during the procedure. Identification of the various carotenoids and chlorophylls in turf bermudagrass was verified by comparison of retention time with standards and co-chromatography with added standards.

RESULTS AND DISCUSSION

Fig. 1 presents the chromatogram of carotenoid and chlorophyll standards. Although the water–acetonitrile–chloroform (2:83:15)[10] solvent system provides a clear separation of these standards, there were minor peaks present. These were probably lutein and zeaxanthin isomers originally present in corn extract.

Fig. 2 presents the chromatogram of unsaponified turf bermudagrass extract. The major peaks were identified by comparison of retention time with standards and

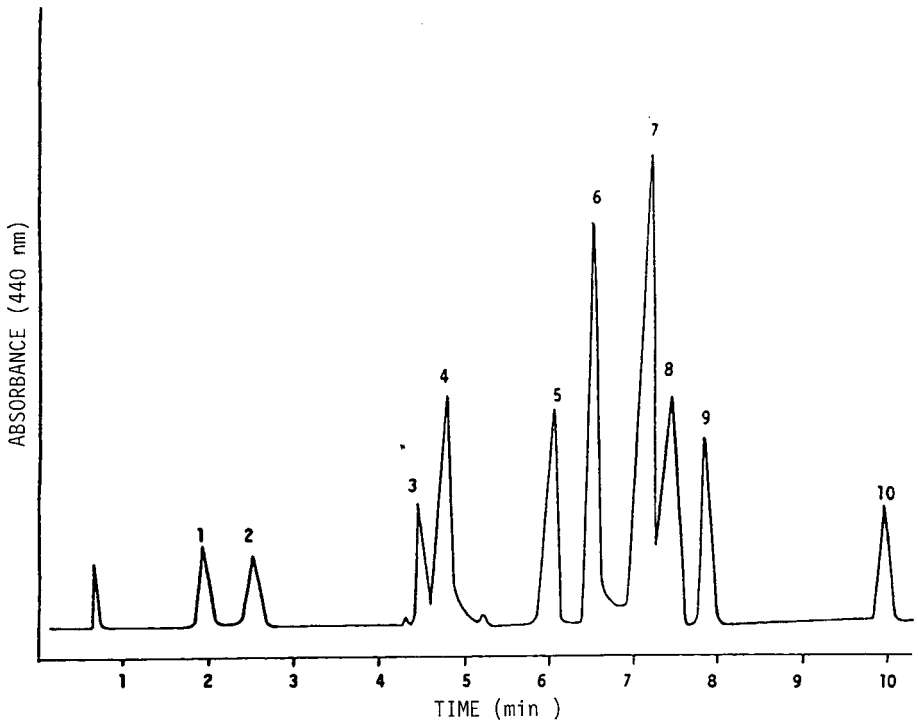

Fig. 1. A chromatogram of carotenoid and chlorophyll standards by employing an isocratic solvent system of water–acetonitrile–chloroform (2:83:15). Peaks: 1 = neoxanthin; 2 = violaxanthin; 3 = zeaxanthin; 4 = lutein; 5 = lutein monoester; 6 = chlorophyll *b*; 7 = chlorophyll *a*; 8 = pheophytin *b*; 9 = pheophytin *a*; 10 = β-carotene.

co-chromatography with added standards. Some minor peaks were not identified but may be due to the artifacts formed during storage of turf bermudagrass[10]. Peak 5 was identified as lutein monoester based on visible spectra and R_F value. It has been reported that xanthophylls normally occur unesterified in the chloroplast but during senescence, when chloroplasts disintegrate, the xanthophylls released into the cytoplasm are esterified[14]. Therefore, most xanthophylls in ripe or aged plants occur naturally acylated with fatty acids[15–19]. Lutein and lutein monoester have identical visible spectra, indicating that no color change occurs as a result of esterification. The presence of only small amounts of lutein monoester indicated that most xanthophylls in green turf bermudagrass remain unesterified.

Table I shows the identification data of various pigments from unsaponified turf bermudagrass extract by TLC. Compared to carotenoids, chlorophyll *a* and chlorophyll *b* were present in large amounts of turf bermudagrass extract as shown by the presence of two large peaks on the HPLC chromatogram (Fig. 2). Pheophytins *a* and *b*, the most common derivatives of chlorophylls *a* and *b*, were also present in turf bermudagrass. The absorption spectra of each pigment were compared with those reported in the literature[3–9]. A hypsochromic shift upon acidification with HCl was used to identify 5,6-epoxycarotenoids such as neoxanthin and violaxanthin[13].

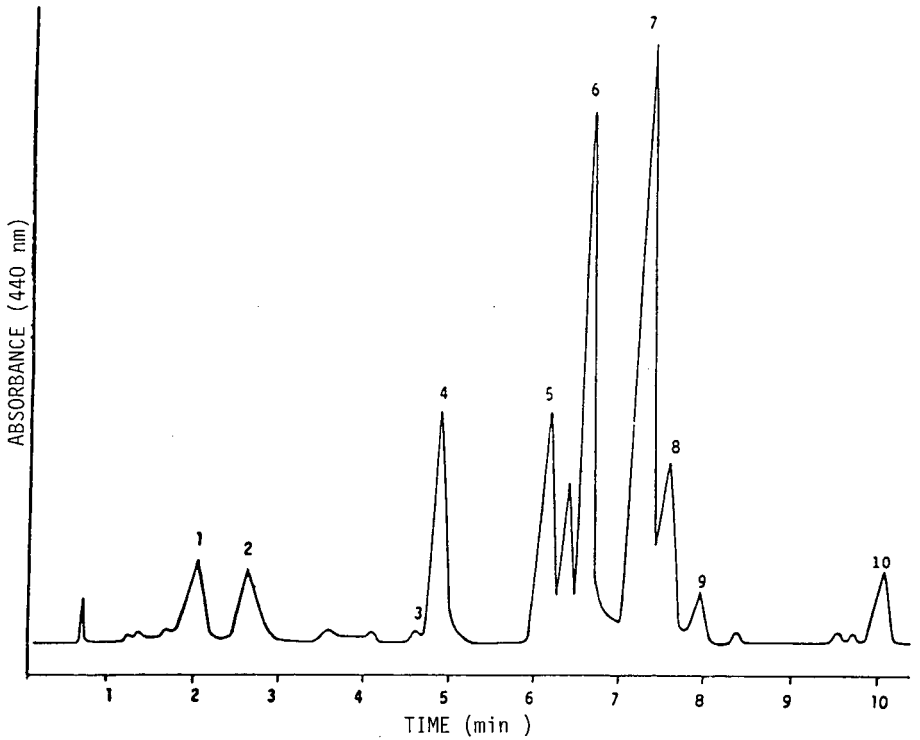

Fig. 2. A chromatogram of unsaponified turf bermudagrass extract. Peaks: 1 = neoxanthin; 2 = violaxanthin; 3 = zeaxanthin; 4 = lutein; 5 = lutein monoester; 6 = chlorophyll *b*; 7 = chlorophyll *a*; 8 = pheophytin *b*; 9 = pheophytin *a*; 10 = β-carotene.

TABLE I

TLC IDENTIFICATION OF VARIOUS PIGMENTS FROM UNSAPONIFIED TURF BERMUDAGRASS EXTRACTS

Pigment	*Visible spectra*		R_F	*Epoxide test*	
	Maxima found (nm)	*Solvent*		*Hypsochromic shift (nm)*	*Color*
β-Carotene	434, 460, 483	Chloroform	0.95	–	–
Chlorophyll *a*	660, 432	Acetone	0.74	–	–
Chlorophyll *b*	645, 454	Acetone	0.65	–	–
Lutein monester	423, 444, 475	Ethanol	0.61	–	–
Lutein	423, 445, 473	Ethanol	0.52	–	–
Violaxanthin	417, 440, 468	Ethanol	0.35	378, 400, 427,	Blue
Neoxanthin	416, 437, 465	Ethanol	0.14	400, 420, 448	Blue
Pheophytin *a**	670, 410	Acetone	0.78	–	–
Pheophytin *b*	658, 430	Acetone	0.75	–	–

* Pheophytin *a* and *b* were prepared from chlorophyll *a* and *b* standards, respectively. They were purified by TLC to determine visible spectra and R_F value.

Reproducibility and precision were checked by making a series of 10 injections of lutein, chlorophyll *a* and β-carotene standards with an IBM Instrument LC/9505 auto sampler. Coefficients of variation in regard to peak area were 2.0, 2.0 and 8.3%, respectively. Coefficients of variation with respect to retention time were 0.4, 0.4 and 0.5%, respectively.

REFERENCES

1 N. I. Krinsky, *Pure Appl. Chem.*, 51 (1979) 649.
2 M. M. Mathews-Roth, *Pure Appl. Chem.*, 57 (1985) 717.
3 K. Eskins, C. R. Scholfield and H. J. Dutton, *J. Chromatogr.*, 135 (1977) 217.
4 K. Iriyama, M. Yoshiura and M. Shiraki, *J. Chromatogr.*, 154 (1978) 302.
5 T. Braumann and L. H. Grimme, *J. Chromatogr.*, 170 (1979) 264.
6 D. Davies and E. S. Holsworth, *J. Liq. Chromatogr.*, 3 (1980) 123.
7 T. Braumann and L. H. Grimme, *Biochim. Biophys. Acta*, 637 (1981) 8.
8 S. W. Wright and J.D. Shearer, *J. Chromatogr.*, 294 (1984) 281.
9 F. Khachik, G. R. Beecher and N. F. Whittaker, *J. Agric. Food Chem.*, 34 (1986) 603.
10 B. H. Chen and C. A. Bailey, *J. Chromatogr.*, 393 (1987) 297.
11 B. H. Chen and C. A. Bailey, *Poultry Sci.*, 66 Suppl. 1 (1987) 62.
12 F. W. Quackenbush, J. G. Firch, W. J. Rabourn, M. Mcquistan, E. M. Petzold and T. E. Karl, *J. Agric. Food Chem.*, 9 (1961) 132.
13 B. H. Davies, in . W. Goodwin (Editor), *Chemistry and Biochemistry of Plant Pigments*, Vol. II, Academic Press, London, 1976, pp. 38–165.
14 K. L. Simpson, T. C. Lee, D. B. Rodriquez and C. O. Chihster, in T. W. Goodwin (Editor), *Chemistry and Biochemistry of Plant Pigments*, Vol. I, Academic Press, London, 1976, pp. 798–812.
15 A. U. Alem, J. R. Couch and C. R. Creger, *Lipids*, 3 (1968) 183.
16 T. Philip, W. W. Nawar and F. J Francis, *J. Food Sci.*, 36 (1971) 98.
17 F. W. Quackenbush and S. Miller, *J. Assoc. Off. Anal. Chem.*, 55 (1972) 617.
18 T. Philip, *J. Agric. Food Chem.*, 21 (1973) 964.
19 T. Philip and J. W. Berry, *J. Food Sci.*, 40 (1975) 1089.

Journal of Chromatography, 455 (1988) 401–405
Elsevier Science Publishers B.V., Amsterdam — Printed in The Netherlands

CHROM. 20 943

Note

Separation of RNA and DNA by histone affinity high-performance liquid chromatography

CHRISTOPHER P. HOLSTEGE, MICHAEL J. PICKAART and LARRY L. LOUTERS*
Chemistry Department, Calvin College, Grand Rapids, MI 49506 (U.S.A.)
(Received June 22nd, 1988)

The nature of the histones, H1, H2a, H2b, H3, and H4, and their biological association with DNA within the nucleosome structure of chromatin have been well characterized[1–6]. These interactions consist of more than simple electrostatic bonding between the lysine/arginine-rich histones and the phosphate backbone of DNA. We have taken advantage of these specific interactions between histones and DNA by using histone affinity chromatography to separate the polyanions, RNA and DNA.

Currently, the separation of DNA and RNA can be achieved by several standard techniques. For example, one can take advantage of differences in density to separate these polymers by centrifugation techniques. Also, one can separate DNA and RNA by a selective enzymatic degradation of one or the other of the polymers. Or, because of differences in size and shape, separation can be achieved by standard electrophoretic techniques. More recently the technology of high-performance liquid chromatography (HPLC) has also been applied to the separation of these polynuleotides. For example, reversed-phase HPLC[7], size-exclusion[8], and ion-exchange chromatography[9] have all been used to separate RNAs and DNAs. However, most of these studies demonstrated separation of RNA from RNA or DNA from DNA. In the present study we demonstrate a new HPLC method to separate a mixture of RNA and DNA; one based on differential affinities for histones. A histone-silica affinity column was developed for HPLC. This column was shown to bind both RNA and DNA. However, the binding of DNA is, as expected, stronger and it requires a higher salt concentration to elude it from the column. This method has several advantages over other methods in that it can be used both preparatively and analytically to achieve a rapid, non-degradative separation of RNA and DNA.

MATERIALS AND METHODS

Histone-silica preparation

Porous silica (60 Å, 230–400 mesh from Aldrich) was activated and histones covalently attached by methods adapted from those previously described[10–12]. Briefly, 10.0 g of silica was dried by heating the silica to 150°C under vacuum. The dried silica was converted to epoxy-silica by refluxing the silica for 16 h in 150 ml of anhydrous toluene containing 10 ml of 3-glycidoxypropyltrimethoxysilane and 0.25 ml of triethylamine. The epoxy-silica was then converted to the diol by treatment with

0021-9673/88/$03.50 © 1988 Elsevier Science Publishers B.V.

10 m*M* sulfuric acid at 90°C for 1 h. The diol-silica was washed sequentially with water, ethanol and ether and dried under vacuum. The dry diol-silica can be stored in this form. To activate the diol-silica, 10.0 g were washed with anhydrous acetone, resuspended in 25 ml of the acetone containing 1.0 ml of anhydrous pyridine and 0.45 ml of trifyl chloride (1,1,1-trifluoromethanesulfonyl chloride). The reaction mixture was stirred for 15 min in an ice bath and quenched by washing with water. The activated silica can be washed with acetone, dried and stored if desired.

In order to covalently attach histones to the silica, 3.0 g of activated trifyl-silica were added to 20 ml of a solution containing 1.0 mg/ml histones (Sigma) and 0.1 *M* sodium bicarbonate, pH 7.5. The reaction mixture was stirred overnight in an ice bath and allowed to warm to room temperature over 5 h to complete the reaction. A 50.0-ml solution of 2 m*M* 2-mercaptoethanol in Tris buffer, pH 6.8, was then added to react with the remaining trifyl functional groups and the histone-silica was extensively washed with and stored in 20 m*M* Tris, pH 7.4.

HPLC histone-affinity chromatography

An HPLC column was prepared by packing a stainless steel tube, 200 mm × 0.46 mm I.D., with approximately 1.0–1.5 g of the histone-silica. Calf thymus DNA was purchased from Sigma and yeast RNA from U.S. Biochemical Co. RNA and DNA were dissolved in 20 m*M* Tris, pH 7.0, at a concentration of 1.0 ml/ml. An RNA, DNA or an RNA/DNA mixture was loaded onto the column and the column was washed with 20 m*M* Tris, pH 7.0, followed by elution of the RNA and DNA with a 0.0–2.0 *M* sodium chloride gradient in 2 m*M* Tris, pH 7.0. The HPLC pump was from LDC, Model 2396 and the detector was LDC UV III (wavelength of 254 nm). The flow-rate in each experiment was 1.3 ml/min and the pressure was about 1900 p.s.i.

Isolation and electrophoresis of RNA and DNA

The fractions from the HPLC column which had a positive absorbance were collected, adjusted to 0.3 *M* sodium bicarbonate and precipitated with cold isopropanol. The dried pellets were redissolved in a standard Tris-acetate buffer (40 m*M* Tris-acetate, 1.0 m*M* ethylenediaminetetraacetate (EDTA), pH 7.8, containing 30% glycerol, 0.25% bromophenol blue, and 0.25% xylene cyanol. Electrophoresis was performed using 1.0% agarose gels dissolved in Tris-acetate buffer. The gels were stained with ethidium bromide.

RESULTS AND DISCUSSION

To test if HPLC histone affinity chromatography could be used to separate RNA and DNA, three separate samples, 50 μg of RNA, 50 μg of DNA, or a mixture containing 50 μg RNA and 50 μg DNA, were loaded onto a histone affinity column. Each was washed with 7–10 ml of 20 m*M* Tris, pH 7.0, and the material that bound to the column was then eluted by a 0.0–2.0 *M* sodium chloride gradient containing 20 m*M* Tris, pH 7.0. The results are summarized in Fig. 1. As shown in panel A of Fig. 1, the RNA sample was separated into three peaks. About a third of the material did not bind to the column while the remaining material bound and was eluted as a double peak between 0.4 and 0.7 *M* sodium chloride. All of the DNA bound to the column and was eluted as a single peak at about 1.0–1.2 *M* sodium chloride (Fig 1, panel B). The

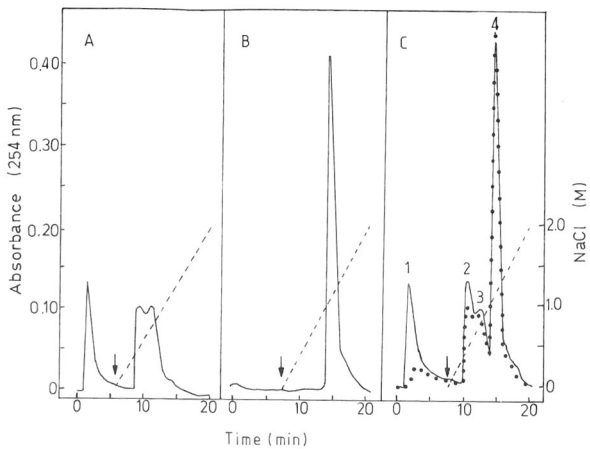

Fig. 1. Binding of RNA and DNA to a histone affinity HPLC column. RNA, DNA, or a mixture were loaded onto the column, the column was washed with 20 m*M* Tris, pH 7.0, and the nucleic acids were removed by addition of a 0.0–2.0 *M* sodium chloride gradient (designated by dashed line and arrow indicating the start). (A) 50 μg RNA; (B) 50 μg DNA; and (C) 50 μg RNA plus 50 μg DNA (solid line) and 50 μg RNA plus 50 μg DNA precipitated with isopropanol and resuspended just prior to loading (dotted line). Elution was monitored by UV absorbance at 254 nm; flow-rate was 1.3 ml/min.

RNA/DNA mixture was separated as shown in panel C with the absorbance pattern essentially being the results shown in panel A superimposed on those in panel B. The capacity of the column to bind DNA was at least 1–1.5 mg as shown by a multiple loading experiment (data not shown).

We confirmed the complete separation of RNA and DNA by precipitating the material eluted at each peak and analyzing the contents by electrophoresis. The results are shown in Fig. 2. No material could be isolated from peaks 1 and 2 suggesting that this material is either too small to precipitate and/or too small to be isolated on a 1% agarose gel. Peak 3 contains only RNA and peak 4 contains only DNA. The DNA isolated from the histone affinity column was somewhat smaller in size than the DNA that had been loaded. This was not entirely surprising as the high pressure (1900 p.s.i.) may have caused some shearing of the large DNA molecules. It would be expected that

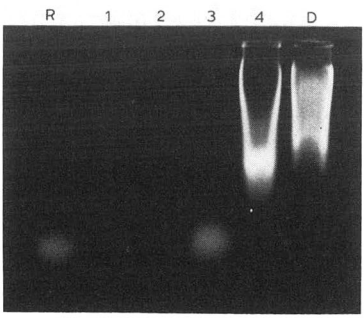

Fig. 2. 1% Agarose gel electrophoresis of fractions 1–4 from the separation described in Fig. 1, panel C, solid line. Material from each fraction was collected by isopropanol precipitation. Samples of RNA and DNA that were loaded onto the column are shown in lanes R and D, respectively.

synthesizing the affinity matrix using silica of larger particle size and larger pores (300–1000 Å) would reduce both the pressure and the shearing.

The three peaks of RNA shown in Fig. 1 most likely represent different sizes of RNA generated by RNA degradation. We would suggest that the first peak is extensively degraded RNA consisting of nucleotides and fragments too small to effectively bind to the column. The second peak may be partially degraded RNA and the third peak represents intact RNA. This conclusion is based on several observations. First, the sensitivity of RNA to nucleases is well known and no special precautions were taken to prevent RNA degradation. Second, when the RNA was purposely digested with RNase A prior to loading, the third peak disappeared completely while the first peak of nonbinding material was greatly increased (data not shown). Third, when an RNA/DNA mixture (50 μg of each) was precipitated with isopropanol and redissolved prior to loading, the first peak was the most significantly reduced, the second was somewhat reduced, the third of RNA was only slightly reduced, and the DNA peak was not affected (see dotted line in Fig. 1, panel C). These data are consistent with the expected precipitation efficiencies of the RNAs and DNAs relative to their size. Finally, the inability to isolate material from the first two peaks of RNA, as shown in Fig. 2, is consistent with these two absorbance peaks representing small RNA fragments.

One possible explanation for the separation of RNA and DNA is an argument based on differences in size, similar to the reason for the three peaks of RNA. We tested this possibility by sonicating DNA and thereby reducing the size of the DNA to resemble that of the RNA. DNA sheared in this fashion can still be separated from RNA and the DNA shows no shift in retention time (data not shown). Thus, the result that DNA binds more tightly than RNA indicates that the predominate reason RNA and DNA can be separated is that histones attached to a silica matrix can still exhibit some of the specific associations that it has with DNA. Therefore, the histone affinity column is functioning as a bona-fide affinity column, and not simply acting as an ion-exchange column. This specificity likely does not require an intact histone octamer since the reaction linking the histone to the activated silica was done under ionic conditions where the histones exist as H2a/H2b dimers and H3/H4 tetramers[13]. Interestingly, the ionic conditions required to remove the DNA from the column (1.0–1.2 *M* sodium chloride) are similar to that required to remove histones H2a and H2b from chromatin[14].

The results reported here suggest a new way to separate DNA and RNA. The separation of DNA and RNA by HPLC histone affinity chromatography can be done either preparatively or analytically. It also has the added advantages over other techniques in that it is both very rapid (20 min) and it does not require the enzymatic or chemical destruction of one of the two biopolymers. For example, it could be conveniently used for a rapid determination of both the quantity and quality of the polynuclotides in a DNA/RNA mixture.

ACKNOWLEDGEMENTS

This work was supported by a Cottrell College Science Grant from The Research Corporation.

REFERENCES

1 I. Isenberg, *Ann. Rev. Biochem.*, 48 (1979) 159.
2 J. D. McGhee and G. Felsenfeld, *Ann. Rev. Biochem.*, 49 (1980) 1115.
3 R. D. Kornberg and A. Klug, *Sci. Am.*, 244 (1981) 52.
4 J. C. Wang, *Cell*, 29 (1982) 724.
5 R. W. Burlingame, W. E. Love, B.-C. Wan, R. Hamlin, N.-H. Xuong and E. N. Moudrianakis, *Science*, 228 (1985) 546.
6 A. Klug, J. T. Finch and T. J. Richmond, *Science*, 229 (1985) 1109.
7 R. D. Wells, *J. Chromatogr.*, 336 (1983) 3.
8 R. Dornburg, P. Földi and P. H. Hofschneuder, *J. Chromatogr.*, 296 (1984) 379.
9 R. Dornburg, J. Kruppa and P. Földi, *LC, Liq. Chromatogr. HPLC Mag.*, 4 (1986) 22.
10 P.-O. Larsson, *Methods Enzymol.*, 104 1984) 212.
11 K. Nilsson and K. Mosbach, *Methods Enzymol.*, 104 (1984) 56.
12 J. D. Saffer and J. E. Coleman, *Biochemistry*, 19 (1980) 5874.
13 R. C. Benedit, E. N. Mourianakis and G. K. Ackers, *Biochemistry*, 23 (1984) 1214.
14 J. Bartley and R. Chalkley, *J. Biol. Chem.*, 247 (1972) 3647.

Journal of Chromatography, 455 (1988) 406–409
Elsevier Science Publishers B.V., Amsterdam — Printed in The Netherlands

CHROM. 20 908

Note

Procyanidines galloylées du sarment de vigne (*Vitis vinifera*)

Séparation et identification par chromatographie liquide haute performance et chromatographie en phase gazeuse

M. BOUKHARTA, M. GIRARDIN* et M. METCHE
Laboratoire de Biochimie Appliquée, École Nationale Supérieure d'Agronomie et des Industries Alimentaires, 2, avenue de la Forêt de Haye, 54500 Vandoeuvre (France)
(Reçu le 11 août 1988)

La plupart des proanthocyanidines acylées rencontrées dans la nature sont des esters de l'acide gallique et l'estérification porte le plus souvent sur la position 3 de l'hétérocycle oxygéné. C'est ainsi qu'ont été identifiés non seulement plusieurs dérivés galloylés des flavanes 3 ol[1–4] mais aussi des proanthocyanidines dimères, trimères et polymères mono et poly galloyées. Les végétaux dans lesquels elles ont été mises en évidence, sont pour l'instant peu nombreux et il s'agit principalement du thé[1], de la rhubarbe[2] et du raisin[5]. Ces proanthocyanidines acylées présentent pourtant des propriétés pharmacologiques intéressantes, nettement supérieures à celles des tanins non galloylés. Elles ont notamment des effets anti-inflammatoire et anti-allergique[6] et semblent utilisables pour traiter l'hypertension[7].

Lors d'une étude plus générale portant sur la caractérisation des tanins condensés de *Vitis vinifera*, nous avons observé chez le sarment de vigne, la présence de différentes procyanidines galloylées et nous décrivons ici les méthodes de séparation et d'identification de ces composés.

PARTIE EXPÉRIMENTALE

Extraction

Les sarments de vigne (cépage Carignan) sont broyés dans un mixeur en présence d'un mélange acétone–eau (7:3, v/v). Après filtration, la solution est saturée en chlorure de sodium de façon à provoquer sa séparation en deux phases. La phase supérieure est recueillie puis évaporée sous pression réduite à une température inférieure à 30°C pour en éliminer l'acétone; la solution aqueuse résultante est alors soumise à des extractions répétées à l'acétate d'éthyle. Les différents extraits acétate d'éthyle sont évaporés à sec et le résidu obtenu est repris dans un minimum de butanol tertiaire puis lyophilisé. On recueille ainsi les proanthocyanidines de faible masse moléculaire. Les proanthocyanidines polymères sont, elles, obtenues par lyophilisation de la phase aqueuse préalablement dialysée 24 h contre de l'eau distillée.

Séparation

Les proanthocyanidines sont fractionnées sur colonne de Sephadex LH-20 (150

0021-9673/88/$03.50 © 1988 Elsevier Science Publishers B.V.

× 3,8 cm I.D.) en utilisant soit l'éthanol (60 ml h^{-1}) soit le mélange acétone–eau (7:3, v/v) comme solvants d'élution. Les fractions absorbant à 280 nm sont recueillies puis rechromatographiées individuellement sur colonne de Fractogel TSK HW 40 (45 × 2,5 cm I.D.) avec du méthanol comme éluant (30 ml h^{-1}).

Hydrolyses

Hydrolyse enzymatique. Elle est effectuée à l'aide d'une galloyle estérase fongique, la tannase AJ (Sankyo) dans un tampon acétate (0,05 *M*, pH 5) à 30°C. L'acide gallique libéré est identifié et dosé par chromatographie liquide haute performance (HPLC).

Hydrolyse acide. Les proanthocyanidines sont hydrolysées par une solution éthanolique d'acide chlorhydrique 4 *M* dans des tubes scellés placés 10 min dans une étuve à 100°C. Les pigments anthocyaniques formés sont identifiés par chromatographie sur couches minces de cellulose par comparaison avec des témoins commerciaux en utilisant le mélange de développement: acide acétique–acide chlorhydrique–eau (30:3:10, v/v).

Dans le cas d'une hydrolyse ménagée, on utilise l'acide chlorhydrique 0,1 *M* en plaçant les tubes scellés seulement 2 min au bain marie bouillant.

Hydrolyse en présence de toluène α-thiol. Cette hydrolyse est effectuée dans des tubes scellés en milieu éthanolique contenant 4% (v/v) de toluène α-thiol et 10% (v/v) d'acide acétique. Après 20 h à l'étuve à 105°C, les hydrolysats sont chromatographiés sur colonne de silice (6 × 4 cm I.D.). L'excès de toluène α-thiol est entraîné par l'hexane et les thiodérivés formés sont élués au méthanol.

Analyses chromatographiques

Les proanthocyanidines et leurs produits d'hydrolyse sont identifiés comparativement à des témoins par HPLC et, après silylation, par chromatographie en phase gazeuse (GC) dans les conditions définies ci-après.

HPLC. Colonne (250 × 4 mm I.D.), Merck Lichrospher RP-18, 5 μm, détecteur UV (280 nm), gradient d'acide acétique de 2 à 10% (v/v) en 99 min, avec un débit 0,5 ml/min.

GC. Colonne SP 2100 (200 × 0,4 cm I.D.) à 3% sur Chromosorb WAW 100–120 mesh, température de l'injecteur et du détecteur à ionisation de flamme 330°C, température de la colonne 180°C à 320°C à raison de 2°C/min, débit d'azote 25 ml/min, silylation des composés par le bis-(triméthylsilyl)acétamide (BSA) dans la pyridine anhydre.

RÉSULTATS

Le traitement des sarments de vigne par une solution aqueuse d'acétone comme décrit par Jones *et al.*[8] conduit à l'isolement de l'ensemble des proanthocyanidines. Les flavanes de faibles masses moléculaires sont séparés des tanins les plus condensés par extraction à l'acétate d'éthyle avant d'être fractionnés sur Séphadex LH-20. La Fig. 1 représente le diagramme d'élution obtenu avec l'éthanol. L'hydrolyse par la tannase de chaque fraction puis la recherche d'acide gallique dans les hydrolysates montrent que seuls les pics numérotés 1 et 2 sur cette figure incorporent des flavanes galloylés. Après purification par passage de ces deux fractions sur colonne de Fractogel, on isole deux composés.

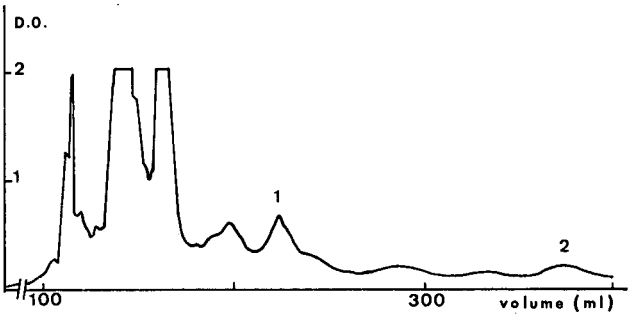

Fig. 1. Diagramme d'élution de l'extrait acétate d'éthyle des sarments de vigne sur colonne de Séphadex LH-20; éluant: éthanol, débit 60 ml h^{-1}; absorption 280 nm. D.O. = Densité optique.

Le premier (issu du pic No. 1) ne donne pas de pigments anthocyaniques par hydrolyse acide mais par contre il est coupé par la tannase en acide gallique et en (−)épicatéchine ce qui conduit à lui attribuer une structure de (−)épicatéchine-O-gallate.

Le second (pic No. 2) est hydrolysé par l'acide chlorhydrique concentré, en cyanidine. Il s'agit donc d'une procyanidine dont la sous-unité supérieure est de type catéchique. Une hydrolyse plus douce par l'acide chlorhydrique 0,1 *M* permet d'identifier la sous-unité inférieure au composé 1 c'est-à-dire à la (−)épicatéchine-O-gallate. Ce résultat fait ressortir la grande fragilité de la liaison C–C interflavane qui est rompue avant la liaison ester.

Par ailleurs, le clivage en présence de toluène α-thiol conduit à deux produits qui en GC ont des temps de rétention identiques à ceux de la (−)épicatéchine gallate et du thiodérivé 2*R*,3*S*,4*R* de la (−)épicatéchine.

Ces résultats indiquent que le composé 2 est une procyanidine dimère dont les sous-unités supérieure et inférieure sont respectivement la (−)épicatéchine et la (−)épicatéchine-O-gallate.

Cette structure de procyanidine B_2-*O*-gallate est d'ailleurs confirmée par l'action de la tannase qui libère deux produits identifiés par HPLC à l'acide gallique et à la procyanidine B_2.

Le spectre de résonance magnétique nucléaire du ^1H permet, d'autre part, de déterminer que le groupement galloyle est porté par le carbone 3′ de la sous-unité inférieure; on remarque, en effet, que par rapport au tétraméthylsilane, le signal dû au proton du $C_{3'}$ se situe à 5,57 ppm alors que celui du proton du $C_{3'}$ de la procyanidine B_2 est à 4,00 ppm. Ces résultats sont conformes à ceux de la littérature[1,9].

Parmi les flavanes de faibles masses moléculaires du sarment de vigne, on identifie donc deux dérivés galloylés qui sont la (−)-épicatéchine-3-O-gallate et la procyanidine B_2-3′-O-gallate (Fig. 2). Il est intéressant de noter que ces composés ont été signalés par Czochanska *et al.*[5] dans les baies de raisin de différents cépages.

Pour vérifier si la galloylation concerne également les flavanes polymères (fraction insoluble dans l'acétate d'éthyle), ceux-ci ont été purifiés globalement par passage sur colonne de Séphadex LH-20 avec le mélange acétone–eau (7:3, v/v) pour l'élution avant d'être hydrolysés comme précédemment.

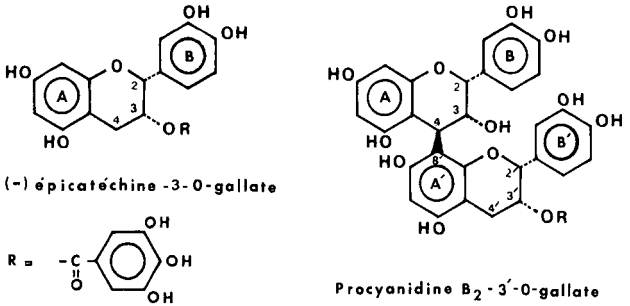

Fig. 2. Structure des flavanes galloylés du sarment de vigne.

Dans ces conditions, on constate qu'il y a libération d'acide gallique par la tannase et formation de cyanidine au cours de l'hydrolyse acide.

Ces résultats montrent que ces polymères sont constitués uniquement de procyanidines plus ou moins galloylées. Par dosage de l'acide gallique, on détermine en fait qu'une unité flavane sur dix en moyenne est estérifiée.

Le sarment de vigne s'avère donc un matériau riche en procyanidines galloylées: d'après des résultats récents[7,10,11], ces proanthocyanidines devraient manifester des propriétés pharmacologiques et tannantes supérieures à celles de tanins non galloylés.

BIBLIOGRAPHIE

1 G. I. Nonaka, O. Kanahara et I. Nishioka, *Chem. Pharm. Bull.*, 31 (1983) 3906.
2 Y. Kashiwada, G. I. Nonaka et I. Nishioka, *Chem. Pharm. Bull.*, 34 (1986) 4083.
3 M. V. Piretti, R. Pistore et C. Razzoboni, *Ann. Chim. (Rome)*, 75 (1985) 137.
4 E. Malan et D. H. Pienaar, *Phytochemistry*, 26 (1987) 2049.
5 Z. Czochanska, L. Y. Foo et L. J. Porter, *Phytochemistry*, 18 (1979) 1819.
6 H. Kakegawa, H. Matsumoto, K. Endo, T. Satoh, G. I. Nonaka et I. Nishioka, *Chem. Pharm. Bull.*, 33 (1985) 5079.
7 S. Uchida, N. Ikari, H. Ohta, M. Niwa, G. I. Nonaka, I. Nishioka et M. Ozaki, *Jpn. J. Pharmacol.*, 43 (1987) 242.
8 W. T. Jones, R. B. Broadhurst et J. W. Lyttleton, *Phytochemistry*, 15 (1976) 1407.
9 G. I. Nonaka, I. Nishioka, T. Nagasawa et H. Oura, *Chem. Pharm. Bull.*, 29 (1981) 2862.
10 T. Yokozawa, N. Suzuki, H. Oura, G. I. Nonaka et I. Nishioka, *Chem. Pharm. Bull.*, 34 (1986) 4718.
11 T. Okuda, K. Mori et T. Hatano, *Chem. Pharm. Bull.*, 33 (1985) 1424.

Journal of Chromatography, 455 (1988) 410–414
Elsevier Science Publishers B.V., Amsterdam — Printed in The Netherlands

CHROM. 20 863

Note

Determination of geniposide, gardenoside, geniposidic acid and genipin-1-β-gentiobioside in *Gardenia jasminoides* by high-performance liquid chromatography

TOSHIYUKI OSHIMA*, KAZUHIKO SAGARA and TSUGUCHIKA YOSHIDA
Research Centre, Taisho Pharmaceutical Co., Ltd., 1-403, Yoshino-cho, Ohmiya-shi, Saitama 330 (Japan)
and
YO-YI TONG, GUANDE ZHANG and YU-HENG CHEN
Institute of Materia Medica, Chinese Academy of Medical Sciences, 1 Xing Nong Tan Street, Beijing (China)
(Received July 21st, 1988)

The crude drug Gardenia Fructus (Chinese name zhi-zi[1]), which is the fruit of *Gardenia jasminoides*, is well known and frequently used as an important component of Chinese traditional medicine. It contains a large amount of iridoids[2–8], including geniposide, gardenoside, geniposidic acid, genipin-1-β-gentiobioside, schanzhiside and deacetylasperuloside methyl ester, in addition to a few components such as croin-like pigments, nonacosane, β-sitosterol and mannitol[9,10]. The content of geniposide, which is the main component of the crude drug, ranges from 4 to 6%. It has been reported that Gardenia Fructus has purging[11–13] and choleretic[14–18] effects, and that the active component is geniposide, which exibits these effects after its hydrolysis to genipin[19–22]. As genipin-1-β-gentiobioside is also one of the glycosides of genipin, it seemed important to determine genipin-1-β-gentiobioside together with geniposide from the pharmacological point of view.

Biological[23], ultraviolet (UV)[23], paper-partition chromatographic (PPC)[23] and thin-layer chromatographic (TLC)[23] methods for the determination of geniposide in this crude drug have been reported. In addition, high-performance liquid chromatographic (HPLC)[24–26] methods have been applied to detect geniposide as an indicator compound for checking whether gardenia fruit has been used as a natural yellow dye in food, but these are not suitable methods for the analysis of Gardenia Fructus. Hatakawa *et al.*[27] reported an HPLC method using ODS silica gel for the determination of geniposide in Gardenia Fructus and its application to some preparations. Akada and Kanematsu[28] determined geniposide, gardenoside and geniposidic acid simultaneously by HPLC using a C_8 silica gel column. However, genipin-1-β-gentiobioside, which seems to have the same effects as geniposide after hydrolysis, has not been determined.

In this paper, we report an HPLC method using an ODS silica gel column for the determination of geniposide, gardenoside, geniposidic acid and genipin-1-β-gentiobioside in Gardenia Fructus. We also discuss the distribution of these compounds in various parts of the fruit.

0021-9673/88/$03.50 © 1988 Elsevier Science Publishers B.V.

EXPERIMENTAL

Plant materials

Gardenia jasminoides samples were collected in Shichuan, Guizhou and Hainandao, China.

Apparatus

A Shimadzu Model LC-6A liquid chromatographic system and a stainless-steel column (150 × 4 mm I.D.) packed with chemically bonded ODS silica gel (TSK gel LS-410, 5 μm; Toyo Soda) were used. The peak area was measured with a Chromatocoder 11 (System Instruments) integrator.

Reagents

Geniposide, gardenoside and geniposidic acid were purchased from Wako. Genipin-1-β-gentiobioside was isolated from gardenia fruit. Methanol of chromatographic grade was used.

HPLC conditions

Water–methanol–phosphoric acid (870:130:1) was used as the mobile phase. The column temperature was maintained at 50°C and the flow-rate was 1.0 ml/min. The substances eluted were detected by a UV detector at 238 nm.

Assay procedure

Dry fruit powder (0.2 g) of *Gardenia jasminoides* was placed in 15 ml of water–methanol (1:1), then heated under reflux on a water-bath at 85°C. After cooling, it was centrifuged at 1600 *g* and decanted. The residue was refluxed with 15 ml of water–methanol (1:1) twice more in the same manner. The extracts were placed in a 50-ml volumetric flask and diluted to 50 ml with water–methanol (1:1). A 10-μl volume of this solution was injected for HPLC. The contents of geniposide, gardenoside, geniposidic acid and genipin-1-β-gentiobioside in the whole fruit and in the peel and seed of the fruit of *Gardenia jasminoides* were calculated from the relevant peak areas.

Calibration graphs and detection limits

The calibration graphs for geniposide, gardenoside, geniposidic acid and genipin-1-β-gentiobioside were obtained over the concentration ranges 1.0–500, 0.25–100, 0.2–100 and 1.0–500 μg/ml, respectively. The corresponding regression equations were as follows: $y = 102200x - 22800$ ($r = 0.999$), $y = 84900x - 900$ ($r = 0.999$), $y = 108100x - 5300$ ($r = 0.999$) and $y = 63800x - 12600$ ($r = 0.999$). The detection limits were 30, 8, 5 and 30 ng, respectively, at a signal-to-noise ratio of 3:1 for the peak heights.

RESULTS AND DISCUSSION

Acetonitrile has been used previously in mobile phases on an ODS column to detect geniposide in food as an indicator compound for checking the use of gardenia fruit as a natural yellow dye. However, regarding the crude drug, Gardenia Fructus,

TABLE I

IRIDOID CONTENTS (%) IN *GARDENIA JASMINOIDES* SAMPLES

Source of sample	*Part of fruit*	*Geniposidic acid*	*Gardenoside*	*Genipin-1-β-gentiobioside*	*Geniposide*
Shichuan	Whole	0.25	0.34	0.60	4.11
	Peel	0.18	0.51	Trace	1.74
	Seed	0.29	0.25	0.93	5.41
Guizhou	Whole	0.27	0.71	1.24	4.22
	Peel	0.22	1.21	Trace	2.36
	Seed	0.29	0.43	1.91	5.24
Hainandao	Whole	0.49	0.20	2.29	3.91
	Peel	0.42	0.21	0.03	1.74
	Seed	0.52	0.20	3.01	5.41

methanol was a better modifier than acetonitrile because of the separation and shape of each peak.

Geniposidic acid is the most polar of these four compounds and was eluted at an earlier position on the chromatogram when the ODS silica gel column was used. The ion-pair technique was applied to control the retention time of geniposidic acid, because geniposidic acid has a carboxylic acid moiety. Unexpectedly, when a counter ion was added to the mobile phase, the elution time of the other components in addition to that of geniposidic acid became much shorter than when the counter ion was absent from the mobile phase. Therefore, neutral and acidic conditions were examined. The ion-suppression effect under acidic consitions delays the retention of geniposidic acid slightly and has no influence on the other components. Ion-suppression conditions were therefore selected for the analysis of the fruit of *Gardenia jasminoides*, and water–methanol–phosphoric acid (870:130:1) was selected on the basis of the separation and analysis time.

The extraction conditions were also examined using Soxhlet extraction and direct extraction. Soxhlet extraction was not efficient and, although direct extraction by both methanol and water–methanol (1:1) showed the best extraction efficiency, the latter was selected because it was more similar to the mobile phase for injection. The reliability of this determination method was examined by repeating the analysis five times, and the coefficient of variation was 1.8%.

Three samples produced in different provinces were examined and the results are shown in Table I and Fig. 1. The geniposide content of the whole fruit was about 4%. The content of genipin-1-β-gentiobioside was the second highest in the whole fruit as analysed in this study, and the sample from Hainandao contained 2.29%. The geniposide content in the seed was 5.24, 4.16 and 5.41% higher than in the peels, which contained 2.36, 3.15 and 1.74% per respective fruit sample. The geniposidic acid content showed the same tendency as geniposide. On the other hand, the peels contained more gardenoside than the seeds. Genipin-1-β-gentiobioside, which was determined for the first time, was hardly present in the peel. Judging from the fact that the aglycone of genipin-1-β-gentiobioside, genipin, is the same as that of geniposide, it

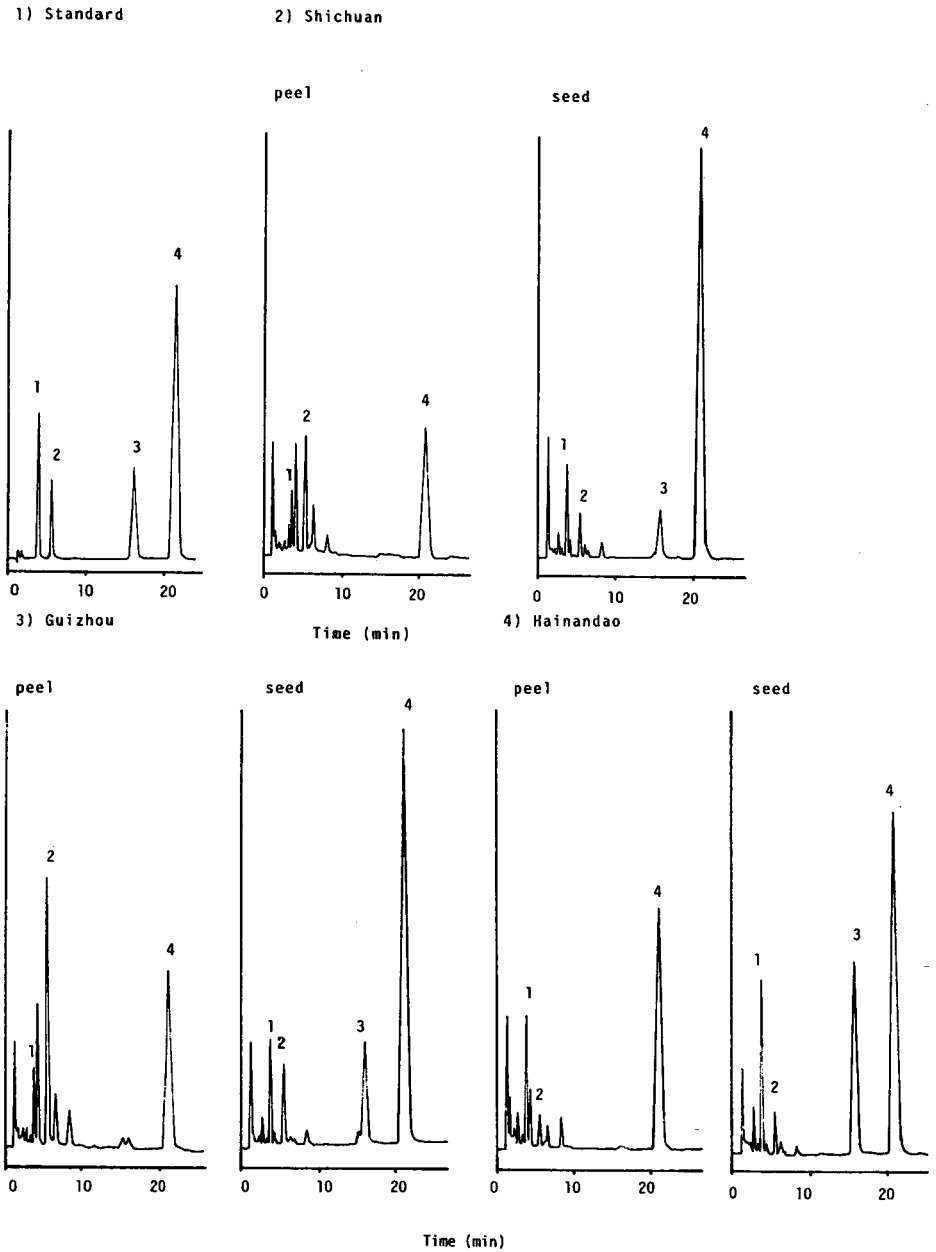

Fig. 1. Chromatograms of standard and *gardenia jasminoides* samples. Peaks: 1 = geniposidic acid; 2 = gardenoside; 3 = genipin-1-β-gentiobioside; 4 = geniposide. Mobile phase: water–methanol–phosphoric acid (870:130:1). Flow-rate: 1 ml/min. Temperature: 50°C.

is interesting from the pharmacological point of view that the genipin-1-β-gentiobioside content was second to geniposide among these four components.

This method was developed for the quality control of Gardenia Fructus, and this is the first determination of the four individual components, especially genipin-1-β-gentiobioside. Various Gardenia Fructus samples on the market can now be analysed using this method.

REFERENCES

1 Juangsu New Medical College, *Zhong Yao Da Ci Dian (Dictionary of Chinese Materia Medica)*, Shanghai Scientific and Technological Publishers, Shanghai, 1977, p. 1049.
2 H. Inouye and S. Saito, *Tetrahedron Lett.*, (1969) 2347.
3 H. Inouye, S. Saito and T. Shingu, *Tetrahedron Lett.*, (1970) 3581.
4 T. Endo and H. Taguchi, *Chem. Pharm. Bull.*, 18 (1970) 1066.
5 T. Endo and H. Taguchi, *Chem. Pharm. Bull.*, 21 (1973) 2684.
6 H. Inouye, Y. Takeda, S. Saito, H. Nishimura and R. Sakuragi, *Yakugaku Zasshi*, 94 (1974) 577.
7 H. Inouye, Y. Takeda and H. Nishimura, *Phytochemistry*, 13 (1974) 2219.
8 Y. Takeda, H. Nishimura, O. Kadota and H. Inouye, *Chem. Pharm. Bull.*, 24 (1976) 2644.
9 T. Munesada, *Yakugaku Zasshi*, 42 (1922) 666.
10 R. Kuhn, A. Winterstein and W. Wiegand, *Helv. Chim. Acta*, 11 (1928) 716.
11 K. Yamauchi, R. Sakuragi, S. Kuwano and H. Inouye, *Planta Med.*, 25 (1974) 219.
12 H. Inouye, Y. Takeda, K. Uobe, K. Yamauchi, N. Yabuuchi and S. Kuwano, *Planta Med.*, 25 (1974) 285.
13 K. Yamauchi, N. Fujimoto, S. Kuwano, H. Inouye and K. Inoue, *Planta Med.*, 30 (1976) 39.
14 T. Miwa, *Jpn. J. Pharmacol.*, 2 (1953) 102.
15 T. Miwa, *Jpn. J. Pharmacol.*, 2 (1953) 139.
16 T. Miwa, *Jpn. J. Pharmacol.*, 3 (1953) 1.
17 T. Miwa, *Jpn. J. Pharmacol.*, 4 (1953) 69.
18 Che, C. T., T. T. Yip, K. H. Ng and Y. C. Kong, *Planta Med.*, 32 (1977) 18.
19 M. Harada, N. Tenmyo, M. Aburada and T. Endo, *Yakugaku Zasshi*, 94 (1974) 157.
20 M. Abrada, S. Takeda, Y. Shibata and M. Harada, *J. Pharm. Dyn.*, 1 (1978) 81.
21 M. Aburada, S. Takeda, M. Sakurai and M. Harada, *J. Pharm. Dyn.*, 3 (1980) 423.
22 S. Takeda, T. Endo and M. Aburada, *J. Pharm. Dyn.*, 4 (1981) 612.
23 K. Yamaguchi, R. Sakuragi, S. Kuwano and H. Inouye, *Planta Med.*, 25 (1974) 219.
24 M. Nishizawa, T. Chonan, I. Sekijo and T. Sugii, *Hokkaidoritsu Eisei Kenkyushoho*, 33 (1983) 28.
25 N. Noda, S. Yamada, J. Hayakawa and K. Uno, *Eisei Kagaku*, 29 (1983) 7.
26 M. Kamikura and K. Nakazato, *Shokuhin Eiseigaku Zasshi*, 25 (1984) 517.
27 J. Hayakawa, N. Noda, S. Yamada, E. Mikami and K. Uno, *Yakugaku Zasshi*, 105 (1985) 996.
28 Y. Akada and Y. Kanematsu, *Bunseki Kagaku*, 35 (1986) 215.

Journal of Chromatography, 455 (1988) 415–419
Elsevier Science Publishers B.V., Amsterdam — Printed in The Netherlands

CHROM. 20 856

Note

Quantitative high-performance liquid chromatographic determination of ampicillin embonate and amoxycillin embonate

TARJA SAESMAA

Department of Pharmaceutical Chemistry, School of Pharmacy, University of Helsinki, Fabianinkatu 35, SF-00170 Helsinki (Finland)

(Received June 13th, 1988)

In order to improve the taste and the stability of ampicillin and amoxycillin, nearly water-insoluble embonic acid salts of these semi-synthetic penicillins (1:2) were prepared (Fig. 1)[1]. Owing to the amphoteric character of amoxycillin and ampicillin, it is not possible to extract the components of the salts quantitatively for separate chemical analysis. Moreover, the solubilities of embonic acid and its antibiotic salts are very low in all common solvents.

The quantitation of some sparingly soluble salts formed between organic bases and penicillin G and V has been achieved by assaying the anionic and cationic portions of the salts separately following isolation, and also simultaneously using high-performance liquid chromatography (HPLC)[2–5]. Embonic acid salts of hydroxyzine and noscapine have been quantitated using silica and cyano phase HPLC columns, respectively[6,7]. The retention times of embonic acid on these columns are approximately 13 and 4 min, respectively.

This paper describes a rapid and simple reversed-phase HPLC method for the determination of ampicillin embonate and amoxycillin embonate. The method permits the simultaneous quantitation of the components of amoxycillin embonate. In contrast, the analysis of components of ampicillin embonate require separate assays. By using internal standard methods a good linear range of detection at 240 nm was obtained for all the substances investigated.

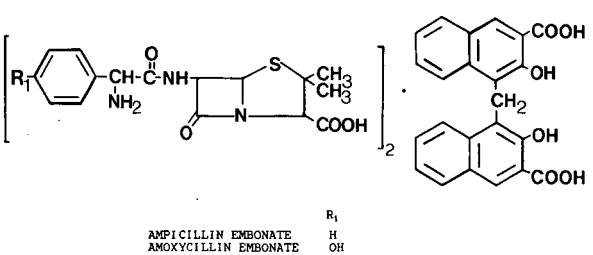

Fig 1. Structure of ampicillin embonate (2:1) and amoxycillin embonate (2:1).

0021-9673/88/$03.50 © 1988 Elsevier Science Publishers B.V.

EXPERIMENTAL

Chemicals

Amoxycillin trihydrate (Amphar, Amsterdam, The Netherlands), ampicillin trihydrate (Fermion, Helsinki, Finland) and phenoxymethylpenicillin potassium (Biochemie, Kundel-Tirol, Austria) were kindly supplied by Orion Pharmaceutica. Embonic acid (99%) was obtained from Ega-Chemie (Steinheim, F.R.G.). All other chemicals were of commercial analytical-reagent grade. The identification of the compounds and the preparation methods for ampicillin embonate (2:1) and amoxycillin embonate (2:1) have been described elsewhere[1]. The water contents of ampicillin embonate and amoxycillin embonate were 8.15 and 8.80%, respectively.

Chromatographic conditions

A Hewlett-Packard (HP) 1090 liquid chromatograph, equipped with an HP 85 B computer, a Pye Unicam 4020 UV detector, an HP 3380 A computing integrator and a 5-μl injection loop was used during the study. A reversed-phase column (RP-8, 200 mm $\times$ 4.6 mm I.D., particle size 10 μm, HP 79915 MO) was used at 40°C with a flow-rate of 1.5 ml/min. Detection was carried out at 240 nm. The mobile phase consisted of 1/15 *M* Sörensen phosphate buffer (pH 7.0)[8]–methanol (62:38).

Preparation of calibration graphs

Stock solutions of ampicillin trihydrate (1 mg/ml), embonic acid (30 μg/ml) and amoxycillin trihydrate (600 μg/ml) used as an internal standard were prepared in 1/15 *M* Sörensen phosphate buffer (pH 7.0)–methanol (3:7, v/v) (solvent I) in an ultrasonic bath at room temperature. Dilutions were made using solvent I: the concentration ranges were 50–500 μg/ml for ampicillin trihydrate and 1.5–21 μg/ml for embonic acid. The concentration of the internal standard was 60 μg/ml.

Stock solutions of amoxycillin trihydrate (200 μg/ml), embonic acid (30 μg/ml) and penicillin V potassium (10 mg/ml) used as an internal standard were prepared in solvent I in an ultrasoni bath at room temperature. Dilutions were made using solvent I; the concentration ranges were 10–110 μg/ml for amoxycillin trihydrate and 1.5–21 μg/ml for embonic acid. The concentration of the internal standard was 1 mg/ml.

Sample preparation

The samples of ampicillin embonate and amoxycillin embonate were prepared using solvent I. Dissolution was performed rapidly (about 5 min) in an ultrasonic bath at room temperature. The ampicillin content of the embonate salt was assayed in solutions containing accurately measured amounts of ampicillin embonate (about 350 μg/ml) and 60 μg/ml of amoxycillin trihydrate as an internal standard. The embonic acid content of ampicillin embonate was determined using solutions containing accurately measured amount of ampicillin embonate (about 23 μg/ml) and 60 μg/ml of amoxycillin trihydrate as an internal standard.

The amoxycillin and embonic acid contents of amoxycillin embonate were determined using solutions containing accurately measured amount of amoxycillin embonate (about 42 μg/ml) and 1 mg/ml of penicillin V potassium as an internal standard.

RESULTS AND DISCUSSION

The most recent HPLC methods for β-lactam antibotic anlysis have employed reversed-phase or ion-pair reversed-phase techniques[9,10]. Penicillins containing a side-chain amino group have mostly been analysed with or without a pairing ion using methanol–phosphate buffer mixtures or gradients, or acetonitrile–phospate buffer mixtures over the pH range 4.5–7.5.

Embonic acid and the prepared ampicillin embonate and amoxycillin embonate were poorly soluble in mixtures of acetonitrile and phosphate buffers. The embonates dissolved easily in the mixtures of methanol and 1/15 *M* Sörensen phosphate buffer (pH 7.0) (at pH <7.0 the solubilities decreased rapidly). The latter mixtures gave baseline resolution for the penicillins and embonic acid on an RP-8 column within a few minutes (Fig. 2). Increasing the methanol content in the mobile phase accelerated the passage of embonic acid through the column. Ampicillin and amoxycillin had very short retention times; the methanol content of the eluent had very little influence on the retenton times of the penicillins.

The lack of intrinsic absorption is the major problem in the HPLC of penicillins[10]. Further, the absorption of embonic acid at all UV wavelengths is much higher than that of ampicillin and amoxycillin. At 240 nm the molar absorptivity ratios of embonic acid and amoxycillin trihydrate and embonic acid and ampicillin

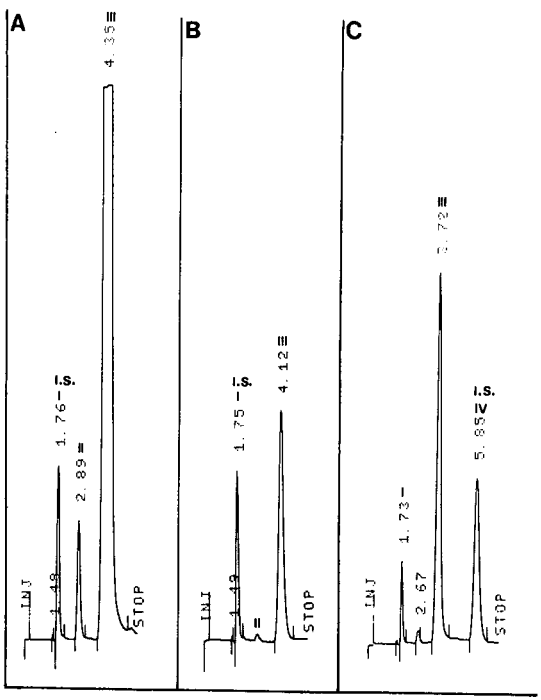

Fig. 2. HPLC traces of ampicillin embonate (A, 350 μg/ml; B, 23 μg/ml) and amoxycillin embonate (C, 42 μg/ml). Peaks: I = amoxycillin; II = ampicillin; III = embonic acid; IV = penicillin V (I.S. = internal standard). For chromatographic conditions see Experimental. Time scale in minutes.

trihydrate were about 10 and 45, respectively. However, UV detection gave a sensitivity that was adequate for the determination of the contents of the salt components and for evaluating the salt syntheses. The analysis of the components of ampicillin embonate required separate assays owing to the tailing peaks of embonic acid and the low detector response to ampicillin (Fig. 2A and B).

The reference standards and salts were dissolved rapidly in solvent I in order to avoid degradation of the penicillins. It has been concluded that solvent I reduces the degradation of penicillin G and V salts[3]. No degradation was detected when ampicillin trihydrate, amoxycillin trihydrate or embonate salts were dissolved in solvent I in thin-layer chromatographic experiments[11]. The internal standard method was used owing to its better linearity compared with the external standard method.

Linearity of the HPLC metod for the salt components

A linear response was obtained for both components of embonates; the equations of the calibration graph for six solutions were $y = 0.0065x + 0.0225$ ($r = 0.998$) for amoxycillin trihydrate, $y = 0.0048x - 0.0514$ ($r = 0.999$) for ampicillin trihydrate and $y = 0.1336x - 0.0441$ ($r = 0.999$) (penicillin V potassium as internal standard) and $y = 0.3543x - 0.1436$ ($r = 0.998$) (amoxycillin trihydrate as internal standard) for embonic acid, where x is the concentration of salt component injected (μg/ml) and y the corresponding peak-area ratio. The precision at the lowest and highest levels were, on average, 1.8 and 1.4%, respectively.

Determination of ampicillin embonate and amoxycillin embonate

The penicillin and embonic acid contents were determined by assaying six samples of the salts *versus* the standards. The mean recoveries (anhydrous) of ampicillin embonate and amoxycillin embonate were 101.6 and 103.1%, respectively (Table I). The ampicillin and amoxycillin contents of the salts are close to the theoretical values (64.3 and 65.3%, respectively). The results suggest that both of the

TABLE I

DETERMINATION OF AMPICILLIN EMBONATE (I) AND AMOXYCILLIN EMBONATE (II) IN BULK

S.D. = Standard deviation.

Sample No.	*Recovery of salt components (%)**			
	I		*II*	
	Ampicillin	*Embonic acid*	*Amoxycillin*	*Embonic acid*
1	65.1	37.8	66.1	34.5
2	63.6	38.9	64.9	39.8
3	62.7	37.4	65.5	36.1
4	64.5	38.3	64.6	38.3
5	64.3	38.1	65.0	38.9
6	63.5	36.0	67.1	38.2
Mean ± S.D.	63.9 ± 0.85	37.7 ± 0.99	65.5 ± 0.93	37.6 ± 1.9

* Calculated from anhydrous salts.

prepared salts may contain some unreacted embonic acid. A suitable washing system must be found in order to obtain exact stoichiometry of 2:1 for these embonates.

The applicaton of these HPLC methods is not limited to the quality control of the pure penicillin salts; the methods can also be used for pre-formulation studies, *e.g.*, studies on *in vitro* solubility and dissolution behaviour of ampicillin embonate and amoxycillin embonate as a function of pH[12].

REFERENCES

1 T. Saesmaa and J. Halmekoski, *Acta Pharm. Fenn.*, 97 (1988) 59.
2 M. LeBelle, K. Graham and W. L. Wilson, *J. Pharm. Sci.*, 68 (1979) 555.
3 F. Nachtmann and K. Gstrein, *J. Chromatogr.*, 236 (1982) 461.
4 B. Stuber, *Pharm. Acta Helv.*, 57 (1982) 293.
5 M. Puttemans, M. Lippens, L. Dryon and D. L. Massart, *J. Pharm. Biomed. Anal.*, 1 (1983) 99.
6 *The United States Pharmacopeia*, XXI Revision, Pharmacopeial Convention, Rockvile, MD, 1985, p. 521.
7 V. Haikala, *J. Chromatogr.*, 389 (1987) 299.
8 H. M. Rauen, *Biochemisches Taschenbuch*, II Teil, Springer-Verlag, Berlin, 1964, p. 96.
9 J. O. Miners, *J. Liq. Chromatogr.*, 8 (1985) 2827.
10 P. C. Van Krimpen, W. P. Van Bennekom and A. Bult, *Pharm. Weekbl. Sci. Ed.*, 9 (1987) 1.
11 T. Saesmaa, *J. Chromatogr.*, submitted for publication.
12 T. Saesmaa and A. M. Tötterman, in preparation.

Journal of Chromatography, 455 (1988) 420–424
Elsevier Science Publishers B.V., Amsterdam — Printed in The Netherlands

CHROM. 20 853

Note

Application of amperometric detection to the high-performance liquid chromatographic determination of antipyrine and 4-aminoantipyrine in urine

ANDREA BURCINOVÁ and MILOŇ TICHÝ
Institute of Hygiene and Epidemiology, Šrobárova 48, Prague 10 (Czechoslovakia)
and
VĚRA PACÁKOVÁ and KAREL ŠTULÍK*
Department of Analytical Chemistry, Charles University, Albertov 2030, 128 40 Prague 2 (Czechoslovakia)
(Received July 25th, 1988)

Antipyrine and aminopyrine are routinely used as model compounds in the study of hepatic microsomal mixed-function oxidase activity *in vitro* and *in vivo*[1–3] and 4-aminoantipyrine is one of the metabolites of aminopyrine. Antipyrine, aminopyrine and their metabolites can be determined in biological fluids using various chromatographic methods. Thin-layer chromatographic procedures[4,5] have poor sensitivity and yield only semi-quantitative results. Gas chromatography[6,7] and gas chromatography–mass spectrometry[2,8] exhibit sufficient sensitivity and selectivity, but require derivatization. High-performance liquid chromatography (HPLC) with spectrophotometric detection has found wide use in assaying these compounds in plasma, urine and liver microsomes[9–14].

However, biological fluids contain many components that interfere in photometric detection and thus a sample purification step is required prior to the analysis, especially with urine samples. One of the advantages of voltammetric detection is its high selectivity, which often considerably simplifies the sample pre-treatment[15]. This paper describes a simple HPLC method with amperometric detection for determining antipyrine and 4-aminoantipyrine in human urine, which does not require a pre-purification step.

EXPERIMENTAL

Reagents

All the chemicals, including standard antipyrine (AP) and 4-aminoantipyrine (4-AAP), were of analytical-reagent grade from Lachema (Brno, Czechoslovakia) and Merck (Darmstadt, F.R.G.) and were used as received.

Apparatus

The chromatographic apparatus consisted of a Model 2150 HPLC pump, 2151 variable-wavelength UV–VIS detector (both from LKB, Bromma, Sweden), a Rheodyne sampling valve with a 20-μl loop and an EDLC electrochemical detector

0021-9673/88/$03.50 © 1988 Elsevier Science Publishers B.V.

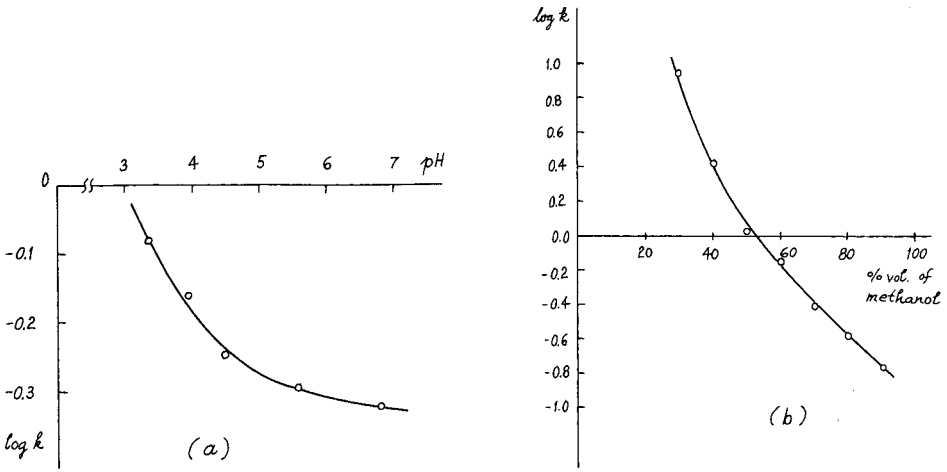

Fig. 1. Depencence of the capacity factor for 4-AAP on (a) mobile phase pH and (b) methanol content. Mobile phase in (a), methanol–0.01 *M* NaH_2PO_4 (75:25); pH adjusted by addition of sodium hydroxide and phosphoric acid solutions; flow-rate, 0.3 ml min^{-1}; UV detection, 254 nm.

(Laboratorní Přístroje, Prague, Czechoslovakia) with a detector cell containing a carbon fibre array working electrode[16], a stainless-steel counter electrode and a silver–silver chloride reference electrode. The photometric and electrochemical detectors were connected in series and their signals were recorded using a TZ 4200 dual-trace chart recorder (Laboratorní Přístroje). The glass analytical column (Separon SGX C_{18}, 7 μm, 150 × 3 mm I.D.) was preceded by a glass pre-column (Separon SGX C_{18}, 7 μm, 50 × 3 mm I.D.), both from Tessek (Prague, Czechoslovakia).

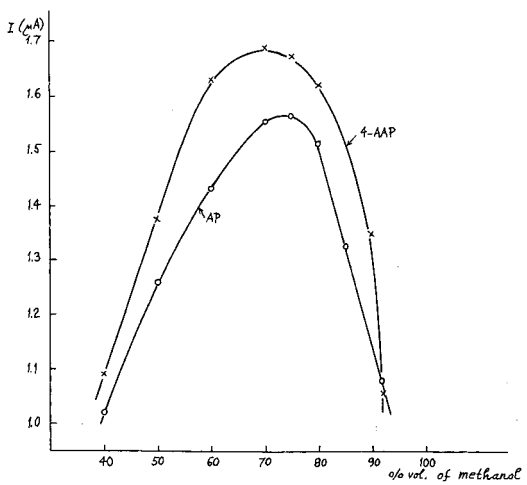

Fig. 2. Dependence of the amperometric signal for 4-AAP and AP on the methanol content in the mobile phase. Mobile phase, methanol–0.01 *M* NaH_2PO_4 (pH 3.0); flow-rate, 0.3 ml min^{-1}. Potentials: 4-AAP, +1.4 V; AP, +1.8 V.

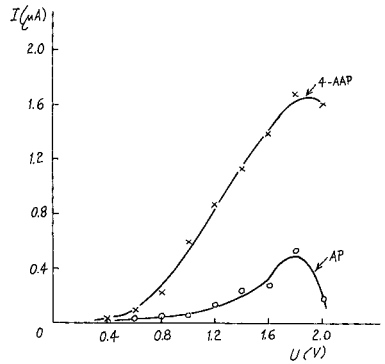

Fig. 3. Hydrodynamic voltammograms of AP and 4-AAP. Mobile phase, methanol–0.01 *M* NaH_2PO_4 (pH 3.0) (75:25); flow-rate, 0.3 ml min^{-1}. The background current was subtracted.

The mobile phase was degassed in an ultrasonic bath and by passage of helium. All the measurements were carried out at laboratory temperature (20 ± 2°C). The electrode potentials are referred to the saturated silver–silver chloride reference electrode.

RESULTS AND DISCUSSION

For separation on the C_{18} chemically bonded reversed phase, aqueous sodium dihydrogenphosphate–methanol was selected as the mobile phase on the basis of our previous experience. The conditions were optimized from the point of view of the capacity factors and the sensitivity of UV photometric and amperometric detection. It was found that the capacity factors decrease with increasing methanol content and increasing pH. The dependences for the two substances are very similar and the curves for 4-AAP are shown in Fig. 1a and b. The sensitivity of detection was maximal at

TABLE I

DETERMINATION OF ANTIPYRINE AND 4-AMINOANTIPYRINE IN URINE

For experimental conditions, see text. R.S.D = Relative standard deviation.

Parameter	*Antipyrine*		*4-Aminoantipyrine*	
	UV (254 nm)	*Amperometric (+1.8 V)*	*UV (254 nm)*	*Amperometric (+1.4 V)*
Correlation coefficient	0.9999	0.9992	0.9998	0.9993
Limit of detection (ng)	0.3	8.6	0.2	5.0
Minimal detectable concentration (mol/l)	$8.0 \cdot 10^{-8}$	$2.3 \cdot 10^{-6}$	$4.9 \cdot 10^{-8}$	$1.2 \cdot 10^{-6}$
Linear dynamic range (ng)	0.3–2500	9–1000	0.2–2500	5.0–1000
R.S.D. (%):				
1.3 ng	10.6	–	5.2	–
6.0 ng	2.7	–	2.6	15.0
260 ng	1.2	1.9	1.0	1.5

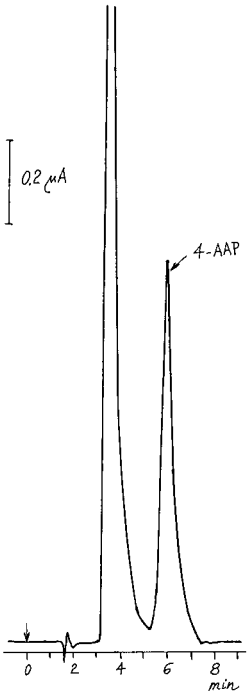

Fig. 4. Chromatogram of a urine sample containing 167 μg of 4-AAP in 1 ml. Experimental conditions as in Fig. 3; amperometric detection at +1.4 V.

a methanol content of *ca.* 70–75% (v/v) (Fig. 2). The optimal mobile phase thus consisted of methanol–aqueous 0.01 *M* NaH_2PO_4 (pH 3.0) (75:25, v/v).

The hydrodynamic voltammograms of AP and 4-AAP obtained in the detection cell under flow conditions and corrected for the background current are given in Fig. 3. The highest signal-to-noise ratio was obtained at potentials of +1.4 and +1.8 V for 4-AAP and AP, respctively. The measurement of 4-aminoantipyrine is more sensitive owing to the presence of the amino group, which is readily oxidized electrochemically. The parameters of the calibration graphs and the limits of detection for photometric detection at 254 nm and amperometric detection at +1.4 V for 4-AAP and +1.8 V for AP are given in Table I.

It can be seen that photometric detection is more sensitive than amperometric detection. However, photometric detection requires pre-purification of urine samples, usually by extraction. On the other hand, urine can be analysed directly with amperometric detection, employing only a short pre-column. The chromatogram of a urine sample containing 4-AAP is shown in Fig. 4.

REFERENCES

1 M. W. E. Teunissen, L. G. J. DeLeede, J. K. Boeijinga and D. D. Breimer, *J. Pharmacol. Exp. Ther.*, 223 (1985) 770.
2 J. Goromaru, A. Noda, K. Matsuyama and S. Iguchi, *Chem. Pharm. Bull.*, 24 (1976) 1376.
3 K. O. Haustein, G. Hüller and H. Sensing, *Eur. J. Clin. Invest.*, 12 (1982) 157.

4 R. Gradnik and L. Fleischman, *Pharm. Acta Helv.*, 48 (1973) 181.
5 E. Lohse, *Pharmazie*, 40 (1985) 358.
6 D. R. Abernathy, D. J. Greenblatt and A. W. Zumbo, *J. Chromatogr.*, 223 (1981) 432.
7 A. Sioufi and F. Marfil, *J. Chromatogr.*, 146 (1978) 508.
8 J. D. Baty and D. A. Price-Evans, *J. Pharm. Pharmacol.*, 25 (1973) 83.
9 K. Shimada and Y. Nagase, *J. Chromatogr.*, 181 (1980) 51.
10 K. Inoue, K. Fujimori, K. Mizokami, M. Sunouchi, A. Takanaka and Y. Omori, *J. Chromatogr.*, 274 (1983) 201.
11 N. Miyagi, N. Hikichi and H. Niwa, *J. Chromatogr.*, 375 (1986) 91.
12 M. W. E. Teunissen, J. E. Meerburg-van der Torren, N. P. E. Vermeulen and D. D. Breimer, *J. Chromatogr.*, 278 (1983) 367.
13 M. Eichelbaum and N. Spannbrucker, *J. Chromatogr.*, 140 (1977) 288.
14 S. Itoh, K. Tanabe, Y. Furuichi, T. Suzuki, K. Kubo, M. Yamazaki and A. Kamada, *Chem. Pharm. Bull.*, 32 (1984) 3194.
15 K. Štulík and V. Pacáková, *Electroanalytical Measurements in Flowing Liquids*, Ellis Horwood, Chichester, 1987.
16 K. Štulík, V. Pacáková and M. Podolák, *J. Chromatogr.*, 298 (1984) 225.

Journal of Chromatography, 455 (1988) 425–429
Elsevier Science Publishers B.V., Amsterdam — Printed in The Netherlands

CHROM. 20 848

Note

Liquid chromatographic determination of trace amounts of low-molecular-weight fatty acid vapours in industrial emissions

KAZUHIRO KUWATA* and SEIJI TANAKA
Environmental Pollution Control Centre, 1-3-62 Nakamichi, Higashinari-ku, Osaka City 537 (Japan)
(First received April 28th, 1988; revised manuscript received July 4th, 1988)

Low-molecular-weight fatty acids have received much attention as odorous substances around painting workshops and dairy establishments. As they generate odour at parts per trillion (ppt) (v/v) levels, specific techniques are required in order to determine trace amounts of these vapours.

Such fatty acid vapours have been sampled in alkaline solution[1] and on solid particles[2]. However, a large volume of sample needs to be sampled in order to compensate for the detector response in chromatographic analysis. High analytical accuracy is difficult to achieve in trace determinations because of their reactivity and/or adsorption on solid surfaces.

Fatty acids reacts with phenacyl bromides under the catalytic effect of crown ethers to produce ultraviolet-absorbing[3–5] or fluorescent[5] derivatives that can be detected by liquid chromatography (LC)[6,7]. Trace amounts of fatty acids such as are present in air are difficult to determine, however, because of the limited response.

Several convenient methods have been developed for the determination of trace amounts of aldehydes[8], amines[9,10], alkanethiols[11] and phenols[12] in air by using a Sep-Pak C_{18} (SP-18) cartridge. Recently, the application of LC for introducing a large volume of sample has been used to compensate for the detector response in determining ultra-trace levels of phenols in environmental samples[12,13].

In this paper, a convenient method is presented for the determination of trace levels of gaseous and aerosol-adsorbed C_3–C_6 fatty acids in industrial emissions. The fatty acids were sampled by the use of an SP-18 cartridge impregnated with sodium hydroxide and derivatized with *p*-bromophenacyl bromide (PBPB). The derivatives were introduced into a liquid chromatograph on a large scale through an ODS mini-column sampling loop. The method may be useful for determining fatty acids at parts per billion (ppb) (v/v) or ppt levels, such as those found in industrial emissions or ambient air, especially in field research.

EXPERIMENTAL

Reagents and materials

Propionic acid, *n*-butyric acid, *n*-valeric acid and *n*-caproic acid were of special grade and methanol and acetonitrile were of chromatographic grade from Wako (Osaka, Japan). PBPB and 18-crown-6-(1,4,7,10,13,16-hexaoxacyclooctadecane)

0021-9673/88/$03.50 © 1988 Elsevier Science Publishers B.V.

(18-crown-6-ether) were of special grade from Dojindo Labs. (Kumamoto, Japan) and Tokyo Kasei (Tokyo, Japan), respectively.

A standard solution was prepared to contain 1 mg/ml of the individual fatty acids in methanol. PBPB solution was prepared by dissolving 0.4 g of PBPB and 0.04 g of 18-crown-6-ether in 100 ml of acetonitrile. The Sep-Pak C_{18} cartridge was obtained from Waters Assoc. (Milford, Ma, U.S.A.).

Apparatus

A Waters Assoc. ALC/GPC 244 liquid chromatograph was employed, equipped with a mini-column sampling loop system and an M440 UV absorbance detector adjusted to 245 nm. The mini-column, attached to a Rheodyne (Cotati, CA, U.S.A.) 7125 six-way switching valve, was a 10.0 mm × 4.0 mm I.D. stainless-steel tube packed with 15–30 μm ODS silica particles (Nomura Kagaku, Aichi, Japan). The loop was washed with 5 ml of methanol prior to use. The analytical column used was a 15 cm × 4.6 mm I.D. tube packed with Develosil ODS-3 (3 μm) (Nomura Kagaku). The mobile phase was acetonitrile–methanol–water (55:10:35) at a flow-rate of 1.0 ml/min.

Preparation of sampling cartridge

An SP-18 cartridge was washed with 2 ml of methanol prior to use. A 2-ml volume of 0.1% sodium hydroxide in methanol was forced through the cartridge, which was then dried for 1 h under reduced pressure in a stream of nitrogen and subsequently dried further by passing nitrogen (99.999%) at 70–100 ml/min for 30 min. The cartridge was closed with glass plugs, sealed in a vial and stored in a cool place in the dark until use.

Analytical procedure

A 1–100-l volume of air sampled was sampled at 0.5–1.5 l/min through a coated SP-18 cartridge. The absorbed substances in the cartridge were eluted with 2 ml of acetonitrile in the opposite direction to that used in sampling. The eluate was mixed with 0.1 ml of 1% sodium hydroxide solution in distilled water and 0.1 ml of the PBPB solution and allowed to stand for 15 min at 80–90°C. The sample volume was then adjusted to 6 ml with distilled water. A 0.1–1.5-ml aliquot of the sample was injected into the mini-column sampling loop. The adsorbed substances were introduced into the liquid chromatograph with the carrier in the opposite direction to that used in the injection and determined by LC. Identification was made on the basis of capacity factors (k') and the quantitation was performed by measuring the peak heights. The cartridges could be used repeatedly at least five times by washing them with 3–5 ml of methanol each time.

RESULTS AND DISCUSSION

Adsorption and desorption of fatty acids on and from the cartridge

A 100-l volume of air sample containing 0.2–5.0 μg of the fatty acids, prepared by using a Yuasa (Osaka, Japan) KS-04C standard-gas generation apparatus[12], was passed at 1.5 ml/min through two coated SP-18 cartridges in series. The fatty acids were detected only on the first cartridge and none was found on the second at any relative humidity (20–80%) of the air samples. The adsorbed substances were

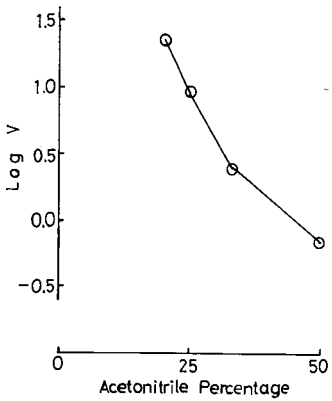

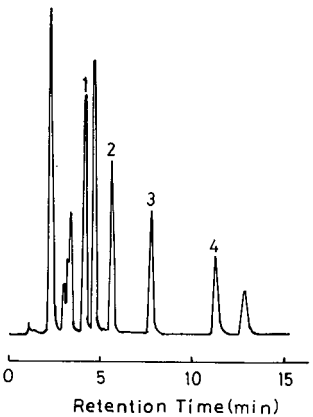

Fig. 1. Retention volume of propionic acid–PBP derivative *vs.* percentage of acetonitrile in acetonitrile–water eluent. V = retention volume (ml).

Fig. 2. Liquid chromatogram of fatty acid–PBP derivatives: (1) propionic acid; (2) *n*-butyric acid; (3) *n*-valeric acid; (4) *n*-caproic acid. Amount of the individual fatty acids introduced, 200 ng; sample volume introduced, 1.5 ml.

completely eluted with 1.0 ml of acetonitrile. As a result, the maximum sampling volume of air and the elution volume of methanol were set to 100 l and 2.0 ml, respectively.

Derivatization of fatty acids with PBPB in the organic medium

The fatty acids couple with PBPB to form a *p*-bromophenacyl (PBP) derivatives in the presence of the crown ether in a weakly alkaline medium[3–5]. In the reaction medium, the absorbance of the PBP derivatives reached a maximum within 10 min at 80–90°C, as reported earlier[3–5].

Sample introduction by the mini-column loop system

The reversed-phase mini-column was used in order to concentrate the sample and to introduce it on a large scale into the liquid chromatograph to compensate for

TABLE I

RECOVERY OF LOW-MOLECULAR-WEIGHT FATTY ACID VAPOURS IN AIR SAMPLES

*Fatty acid vaporized (μg)**	*Average recovery ± S.D. (%)***			
	C_3***	C_4***	C_5***	C_6***
0.2	101.5 ± 1.5	97.7 ± 2.5	98.6 ± 2.9	101.2 ± 3.1
1.0	99.1 ± 2.2	99.3 ± 2.2	96.3 ± 2.8	98.3 ± 4.4
5.0	98.0 ± 2.3	97.6 ± 2.6	99.3 ± 3.0	97.2 ± 5.0

* Fatty acids were vaporized at 180°C in an air stream and introduced into an air stream at 1.0 l/min.

** Average of six runs.

*** C_3, propionic acid; C_4, *n*-butyric acid; C_5, *n*-valeric acid; C_6, *n*-caproic acid.

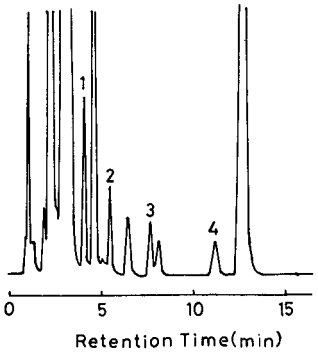

Fig. 3. Fatty acids in emission from a baking finish in painting work: (1) propionic acid, 3.6 ppb; (2) *n*-butyric acid, 2.6 ppb; (3) *n*-valeric acid, 0.3 ppb; (4) *n*-caproic acid, 0.2 ppb. Air sample volume, 60 l; sample volume introduced after the derivatization procedures, 1.5 ml.

the low response of detector. The breakthrough behaviour of the propionic acid–PBP derivative, which eluted first among the C_3–C_6 fatty acid–PBP derivatives, was investigated on the mini-column by varying the acetonitrile content in the acetonitrile–water eluent. Fig. 1 shows the retention volume of the derivative *versus* percentage of acetonitrile in the eluent. The acetonitrile concentration in the sample after the derivatization procedure was adjusted to 25% in order to give a large breakthrough volume and to minimize the effects of the eluent on the analysis. The retention volume of the derivative could be more than 10 ml under the conditions used. The sampling volume was 0.1–1.5 ml in order to suppress the effects of coexisting substances that appeared with larger sampling volume. In calibration, excellent linearity was obtained for the fatty acids in the range 0.2–1.6 μg in 0.1–1.5 ml of sample. Fig. 2 shows a typical chromatogram for the fatty acid–PBP derivatives with mini-column introduction.

Analytical accuracy and detection limits for fatty acid vapours

To investigate the analytical accuracy for fatty acid vapours, a 100-l volume of air sampling containing 0.2–5.0 μg of the fatty acids was generated by using the standard-vapour generation apparatus. The air sample was sampled with a coated SP-18 cartridge and analysed for the individual fatty acids. Table I indicates that the recovery of the fatty acids was 96.3–101.5% with standard deviations of 1.5–5.0% at these levels. The detection limit of the fatty acids was defined as the amount or concentration corresponding to a response of three times of noise level on a chromatogram. The estimated detection limits of the acid vapours were 2–3 ppt for 100 l of air sample.

Stability of the sample

The fatty acids placed on the cartridge were recovered without loss after the cartridge had been stored for 7 days at room temperature. The PBP derivatives were stable for at least 2 weeks in the sample solution.

Application

The method was applied to the determination of low-molecular-weight fatty acids in an emission sample from painting work. Fig. 3 shows a typical chromatogram of fatty acids in the emission from a baking finish, which is one of the most complex samples, containing solvent vapours, synthetic resins and their decomposition products. Low-molecular-weight fatty acids were easily determined at the levels involved without any effects from coexisting substances.

REFERENCES

1 Y. Hoshika, *Bunseki Kagaku*, 27 (1978) 381.
2 M. Okabayashi, T. Ishiguro, T. Hasegawa and Y. Shigeta, *Bunseki Kagaku*, 25 (1976) 436.
3 A. Darbre, in K. Blau and G. S. King (Editors), *Handbook of Derivatives for Chromatography*, Heyden, London, 1978, p. 79.
4 K. Kihara, S. Rokushika and H. Hatano, *Bunseki Kagaku*, 33 (1985) 647.
5 E. Mentasti, M. C. Gennaro, C. Sarzanini, C. Baiocchi and M. Savigliano, *J. Chromatogr.*, 322 (1985) 177.
6 E. Vioque, M. P. Maza and F. Millán, *J. Chromatogr.*, 331 (1985) 187)
7 W. Voelter, R. Huber and K. Zech, *J. Chromatogr.*, 217 (1981) 491.
8 K. Kuwata, M. Uebori, H. Yamasaki, Y. Kuge and Y. Kiso, *Anal. Chem.*, 55 (1983) 2013.
9 K. Kuwata, E. Akiyama, Y. Yamasaki, Y. Kuge and Y. Kiso, *Anal. Chem.*, 55 (1983) 2199.
10 Y. Nishikawa and K. Kuwata, *Anal. Chem.*, 56 (1984) 1790.
11 Y. Nishikawa and K. Kuwata, *Anal. Chem.*, 57 (1985) 1864.
12 K. Kuwata and S. Tanaka, *J. Chromatogr.*, 442 (1988) 407.
13 K. Takami, K. Mochizuki, T. Kamo, A. Sugimae and M. Nakamoto, *Bunseki Kagaku*, 36 (1987) 601.

Journal of Chromatography, 455 (1988) 430–433
Elsevier Science Publishers B.V., Amsterdam — Printed in The Netherlands

CHROM. 20 847

Note

High-performance liquid chromatographic determination of hinokitiol in cosmetics by the formation of difluoroborane compounds

MASARU ENDO, TETSUO MIZUTANI and MITSURU MATSUMURA
Quality Control Department, NOEVIR Co., Ltd., Enmyo-cho, Kashihara 582, Osaka (Japan)
and
MASATAKA MORIYASU*, MOMOYO ICHIMARU, ATUSHI KATO and YOHEI HASHIMOTO
Kobe Women's College of Pharmacy, Motoyamakita-machi, Higashinada-ku, Kobe 658, Hyogo (Japan)
(First received May 3rd, 1988; revised manuscript received June 23rd, 1988)

Hinokitiol (β-thujaplicin, 4-isopropyl-2-hydroxycyclopenta-2,4,6-triene-1-one) is a naturally occurring aromatic seven-membered tropolone compound found in the heartwood of several cupressaceous plants such as western red cedar (*Thuja plicata*), eastern white cedar (*Thuja occidentalis*) and hinoki cypress (*Chamaecyprais obtusa*). Hinokitiol has potent bactericidal activity and thus finds wide use in cosmetics such as hair lotions and hair tonics. It is also added to other preparations such as eye drops, toothpastes and sunscreen preparations.

Hinokitiol has been determined by photometry on the basis that it is a β-diketone and therefore forms a red iron chelate[1]. This method, however, cannot be applied to complex mixtures and a chromatographic method is required. Little work has been described on the gas chromatography (GC) and high-performance liquid chromatography (HPLC) of hinokitiol, because the tropolone ring is unstable towards heat and inconsistent results are obtained by GC and hinokitiol is acidic and often irreversibly adsorbed on the stationary phase, resulting in broad and tailing peaks in HPLC. Further, especially with reversed-phase systems, a minute amount of contaminant iron ions in the eluent, which stems from the stainless-steel part of the HPLC apparatus, reacts with hinokitiol partially to form an iron chelate. Hence the reproducibility is poor and derivatization is needed.

Metal chelate formation has been used but many of them dissociate during chromatography owing to their labile properties. The copper chelate is relatively stable and HPLC is possible[2], but it is still necessary to add a large amount of copper ion to the eluent in order to prevent dissociation. HPLC of hinokitiol metal chelates has also been investigated for the determination of metal ions[3]. Because two or more hinokitiol molecules may coordinate to the central metal ions unsymmetrically, it is probable that two or more isomeric chelates may be formed and separated, which complicates the chromatograms.

In this work we found that a difluoroborane compound of hinokitiol, which was a sort of chelate produced by the reaction of hinokitiol with boron trifluoride[4,5] (see Scheme 1), was applicable to the microdetermination of hinokitiol by HPLC. Because the boron–fluorine bond is strong, only a 1:1 complex is formed quantitatively.

0021-9673/88/$03.50 © 1988 Elsevier Science Publishers B.V.

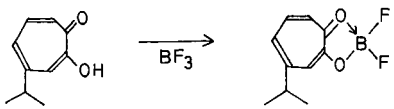

Scheme 1.

EXPERIMENTAL

A Shimadzu LC 6A HPLC apparatus equipped with an SPD 6AV variable-wavelength UV detector was used. The normal- and reversed-phase column packings listed in Table I were slurry packed into stainless-steel columns (15 cm × 4.6 mm I.D.). The mobile phase was hexane–1-propanol (10:1) (normal phase) or water–acetonitrile (3:2) (reversed-phase) was used. The column temperature was kept at 40°C because the column efficiency was slightly better at 40°C than at 25°C.

A standard sample of hinokitiol difluoroborane [difluoro-(3-isopropyl-7-oxo-1,3,5-cycloheptatrienyloxy)borane (A)] was prepared as follows. To 1.0 g of hinokitiol, 1.9 g of 50% boron trifluoride–methanol complex solution was added. Hinokitiol dissolved immediately and white crystals gradually precipitated. The crude reaction product (1.2 g), which was found to be almost pure, was recrystallized from methanol. The spectral data as shown below agreed with those previously reported[4,5] for A: m.p., 178°C (methanol); ^{1}H NMR (C^2HCl_3), 1.36 (s, 3H, $-CH_3$), 1.39 (s, 3H, $-CH_3$), 3.17 [sept., 1H, J = 7 Hz, $-CH(CH_3)_2$], 7.65-8.09 (4H, arom. H); high-resolution mass spectrum, m/z, M^+ $C_{10}H_{11}O_2BF_2$, 212.0819 (calc. 212.0819). The product was stable for a long period on storage. Its UV absorption is so high (log ε = 4.64, 246 nm in methanol) that microdetermination by HPLC is promising. A methanol solution of A is also stable in the presence of about a 1000-fold excess of BF_3, but it decomposes gradually in the absence of BF_3. Using similar procedures, a standard sample of tropolone difluoroborane (B) as an internal standard was obtained[6].

The sample treatment procedure for hair tonics was as follows. A 5-g sample of hair tonic containing about 0.04% of hinokitiol placed in a round-bottomed flask was evaporated and 10 cm^3 of BF_3 in diethyl ether (or methanol) was added. The mixture was heated at 50°C for 10 min and, after cooling, a definite amount of a methanol solution of the internal standard (B) was added if necessary, and the volume adjusted to exactly 50 cm^3 with methanol. An aliquot of the sample was analysed by HPLC. The method for toothpaste, for which the treatment was the most tedious, was as follows. A 1-g amount of the sample was suspended in 30 cm^3 of dilute ethanol (50 vol.-%) and the mixture was centrifuged at 10 000 rpm (8900 g) for 10 min. The supernatant was decanted off and the procedure was repeated three times. The combined ethanol extract was evaporated and the procedure for hair tonic was then followed.

RESULTS AND DISCUSSION

The retention times of A and B on different normal- and reversed-phase column packings are listed in Table I. Typical chromatograms are shown in Fig. 1a and b. Very sharp and symmetrical peaks were obtained with both systems. Determination in the subnanogram range were easy using the linear calibration graph shown in Fig. 2. The

TABLE I

RETENTION TIMES OF DIFLUOROBORANE COMPOUNDS OF HINOKITIOL AND TROPOLONE ON DIFFERENT COLUMNS

Eluent: normal phase, hexane–1-propanol (10:1) at 3.5 cm^3/min; reversed phase, acetonitrile–water (2:3) at 1.5 cm^3/min.

Column	*Retention time (min)*	
	Hinokitiol–BF_2 (A)	*Tropolone–BF_2 (B)*
Normal phase		
LiChrosorb Si 60 (10 μm)	2.3	8.6
Polygosil 60-10	1.9	6.4
Nucleosil 7-OH	3.2	11.3
Polygosil 10-CN	3.2	5.2
Polygosil 5-NO_2	2.1	6.0
Nucleosil 10-NH_2	2.9	11.0
LiChrosorb Alox (5 μm)	0.8	1.4
Reversed phase		
Nucleosil 10-C_{18}	4.7	2.2
LiChrosorb RP-18 (10 μm)	7.3	2.7
LiChrosorb RP-8 (5 μm)	4.3	2.1
Nucleosil 7-Ph	3.0	2.0

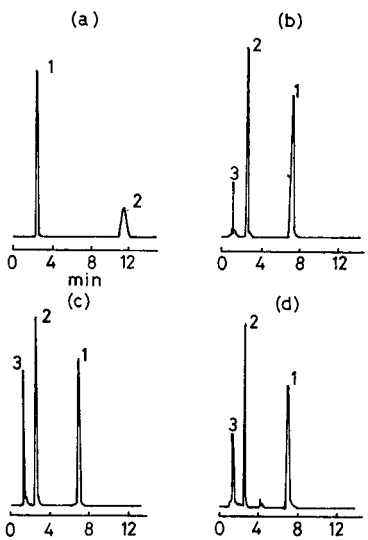

Fig. 1. Chromatograms of difluoroborane compound of hinokitiol. Column: (a) LiChrosorb Si 100 (10 μm); (b)–(d) LiChrosorb RP-18 (10 μm). Other HPLC conditions as described under Experimental. (a) Standard (normal phase); (b) standard (reversed-phase); (c) hair tonics (reversed phase); (d) toothpastes (reversed phase). Peaks: 1 = hinokitiol–BF_2; 2 = tropolone–BF_2 (internal standard); 3 = BF_3.

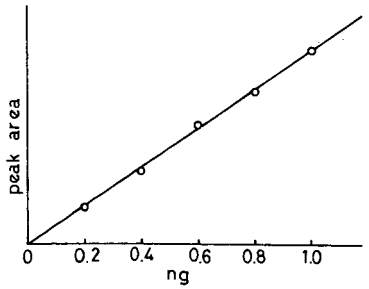

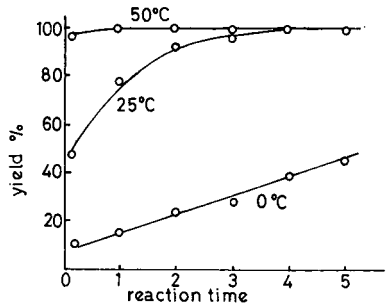

Fig. 2. Calibration graph for hinokitiol.

Fig. 3. Effect of reaction temperature and time on the reaction yield. Reaction time in hours.

detection limit of hinokitiol was 40 pg (with a signal-to-noise ratio of 3) under the conditions shown in Fig. 1b.

The optimum reaction conditions for derivatization were examined. To 10 cm^3 of a methanol solution containing 0.0002% of hinokitiol, 5 cm^3 of BF_3–methanol complex (or diethyl ether complex) solution was added. The mixture diluted to exactly 50 cm^3 with methanol, allowed to stand for 10 min to 5 h at different temperatures (0, 25 and 50°C) and then submitted to HPLC. The reaction yield was calculated from the HPLC peak areas. As shown in Fig. 3, the reaction was not so rapid at room temperature or below, but at 50°C it proceeded quantitatively in about 10 min.

The hinokitiol contents of some preparations were determined and chromatograms of hair tonics and toothpastes are shown in Fig. 1c and d, respectively. The total recovery during the overall procedure was examined for both products.

As the hair tonic sample tested was a NOEVIR product, its hinokitiol content was known. The recovery was 99.6, 101.2, 97.2, 100.2 and 97.4% (average = 98.9%, $n = 5$, $\sigma = 1.73\%$).

For toothpastes obtained commercially, the hinokitiol contents of which were unknown, a measured amount of hinokitiol was added and the recovery of the added hinokitiol was then measured. The results were 100.7, 99.7, 101.0 and 96.1% ($n = 4$, $\sigma = 2.29\%$).

Using the procedures described here, the determination of hinokitiol in hair tonics and toothpastes was successfully carried out without interference from coexisting foreign substances.

REFERENCES

1 H. MacLean and J. A. F. Gardner, *Anal. Chem.*, 28 (1956) 509.
2 F. Hanabusa, O. Nakata and S. Tsugano, *Abstracts of Papers, 107th Annual Meeting of the Pharmaceutical Society of Japan, Kyoto, April 1987*, p. 725.
3 B. Maiti and S. R. Desai, *Analyst (London)*, 111 (1986) 809.
4 S. Seto, S. Matsumura and K. Ro, *Chem. Pharm. Bull.*, 10 (1962) 901.
5 H. Yamamoto, A. Hara, A. Noguchi, H. Kawamoto, S. Inokawa and T. Nozoe, *Bull. Chem. Soc. Jpn.*, 55 (1982) 1594.
6 J. W. Cook, R. A. Rasphael and A. I. Scott, *J. Chem. Soc.*, (1952) 4416.

Journal of Chromatography, 455 (1988) 434–438
Elsevier Science Publishers B.V., Amsterdam — Printed in The Netherlands

CHROM. 20 934

Note

High-performance affinity chromatography of human progesterone receptor

DENIS M. BOYLE* and L. ANDRÉ VAN DER WALT

Endocrinology Unit, Department of Chemical Pathology of the South African Institute for Medical Research and the University of the Witwatersrand, P.O. Box 1038, Johannesburg 2000 (South Africa)

(First received January 5th, 1988; revised manuscript received July 2nd, 1988)

Obtaining a pure protein molecule can be a difficult task, yet it is often the only way in which new structural or regulatory information may be obtained. Affinity chromatography has proven to be a powerful tool in obtaining highly purified proteins in a single step with minimal elution volume while retaining the biological activity of the molecule[1].

High-performance liquid chromatography (HPLC) is a means of separating biological components rapidly and reproducibly due to the sophisticated technology and the availability of different stationary phases for specific separations. This technique has gained wide acceptance in many fields of study by providing data of high resolution while retaining small sample volumes. A thorough characterization and/or purification of a particular protein may now be carried out by HPLC alone.

One particular HPLC separation mode that has only recently found extensive application has been high-performance affinity chromatography (HPAC). We present here the first use of a commercially-available epoxide-reactive column matrix to purify high affinity (K_d = 0.1 n*M*) steroid-binding progesterone receptors by HPAC. This method takes advantage of the availability of the 21-hydroxy group contained in the synthetic progestin steroid 16-α-ethyl-21-hydroxy-19-norpregn-4-ene-3,20-dione. The final product resulted in a functional affinity matrix which may be utilized for the affinity separation of progestin receptors with the retention of biological activity.

EXPERIMENTAL

Unlabeled and tritiated 16-α-ethyl-21-hydroxy-19-nor[6,7-^{3}H]-pregn-4-ene-3,20-dione (Organon 2058, 52 Ci/mmol) [2,4,6,7-^{3}H]estradiol and [^{35}S]methionine (1280 Ci/mmol) were purchased from Amersham. The Ultraffinity-EP column was obtained from Beckman. All other chemicals were analytical-grade or better.

HPAC separations were performed using an LKB GTi 2150 HPLC system attached to a Model 2152 controller. All solvents were filtered trough 0.45-μm HA Millipore filters prior to use.

Incubation with saturating amounts of tritiated steroid plus or minus a 200-fold excess of unlabeled steroid to assess non-specific binding was performed at 4°C as previously described[2]. Specific receptor binding is defined as the total minus non-specific binding after adsorption of excess, non-protein bound steroid with dextran-coated charcoal and expressed as fmol/mg protein.

0021-9673/88/$03.50 © 1988 Elsevier Science Publishers B.V.

Human breast cancer cells or human uterine tissue were the two sources of tissue used for progesterone receptor purification. T47D human breast cancer cells[3] were cultured at 37°C in Earle's minimal essential medium (MEM) with 10% fetal calf serum and containing 2 m*M* glutamine, 100 U/ml penicillin, 100 μg/ml streptomycin and 0.25 μg/ml fungizone. Incorporation of [^{35}S]methionine into proteins was as described in ref. 4.

Human uteri obtained at surgery from hysterectomies were used as alternative starting material and these were stored under liquid nitrogen until use. All purification procedures were performed at 4°C unless otherwise indicated. A standard cytosol fraction in 10 m*M* Tris, 2 m*M* EDTA, and 1 m*M* dithiothreitol, pH 7.6 (buffer A) was prepared by homogenization and ultracentrifugation (100 000 *g*) as previously described[2]. This was either used directly or more commonly, receptors from uterine tissue were prefractionated and concentrated from DEAE-Sephacel (0.1 ml bed volume per mg protein) in a batchwise fashion. After pouring into a column and washing thoroughly with buffer A containing 80 m*M* sodium chloride, receptors were collected in a solution of buffer A containing 0.5 *M* sodium chloride. The yield of receptor at this stage was 70% and progesterone receptor concentrations were five-fold enriched. Cytosol fractions from the cultured cells were used directly.

A 50 × 4.6 mm I.D. Ultraffinity-EP column (0.5 ml volume) was used for all separations. The epoxide-activated silica is supplied ready to use. The affinity matrix was prepared by recycling 100 nmol Organon 2058 (7 μl of a 5 mg/ml acetonitrile solution) in 10 ml acetonitrile–water (50:50) at a flow-rate of 0.2 ml/min for 24 h at 25°C according to the manufacturer's instructions. Any remaining reactive groups were blocked overnight (25°C) with 0.5 *M* β-mercaptoethanol in 0.1 *M* potassium phosphate, pH 6.5. Following extensive washing with buffer A the column was ready for use.

Protein solutions were filtered through a 0.45-μm membrane filter before pumping onto the affinity column. The mixture was pumped through the solvent inlet line at 0.05 ml/min.

The column was then washed at 1 ml/min with buffer A for 2 h. Elution was performed by injecting 1.0 ml of a solution containing 10% N,N-dimethylformamide, 0.5 *M* sodium thiocyanate, 20 μ*M* [^{3}H]Organon 2058 (diluted to 1 Ci/mmol) in buffer A, stopping the flow, and warming the column to 25°C for 1.5 h.

The column temperature was then decreased to 4°C when the flow was started and 0.5 ml fractions of eluate were collected. The column was subsequently cleaned with ten column volumes of 0.2 *M* glycine, 10% N,N-dimethylformamide, 0.5 *M* sodium thiocyanate, pH 3.5, followed by washing with distilled water overnight. The column was re-equilibrated for 1 h with buffer A just prior to re-use.

Denaturing sodium dodecyl sulfate polyacrylamide gel electrophoresis was performed according to Laemmli[5] and protein content determined by the Bradford dye-binding assay[6].

RESULTS

The binding of the progesterone receptor to the column matrix was rapid: only one pass of sample through the column was required to bind 90–100% of receptor (Table I). Under the same conditions, the estradiol-17β receptor, possessing little

TABLE I

HIGH-PERFORMANCE AFFINITY CHROMATOGRAPHY OF HUMAN UTERINE PROGESTERONE RECEPTOR

Experiments 1 and 2 refer to data generated from two separate attempts at receptor purification.

Sample	*Experiment*	*Volume (ml)*	*Progesterone receptor**	*Recovery (%)*	*Estrogen receptor**	*Recovery (%)*
DEAE-Sephacel	1	75	15 763	(100)**	10 852	(100)
eluted fraction	2	100	33 170	(100)	4463	(100)
Affinity column	1	75	953	8	7784	91
flow through	2	100	0	0	5044	113
Affinity column	1	0.5	6678	43	–	–
eluted fraction	2	0.5	16 702	50	–	–

* Determined by association with saturating concentrations of radioactive ligand according to ref. 2 and expressed as total number of femtomol of receptor protein.

** 100% Recovery is taken here to indicate the first step in the affinity purification procedure.

affinity for progestins, was unable to compete with progesterone receptor for the matrix. Once progesterone receptor was bound, exhaustive washing was continued and elution of receptor could only be accomplished in the presence of free steroid. Recoveries were consistently in the range of 40 to 50% as long as the chaotropes thiocyanate and N,N-dimethylformamide were included in the elution buffer and to less than 10% in their absence. The 116 000-dalton polypeptide thus observed after sodium dodecyl sulfate gel electrophoresis from affinity column eluates (Fig. 1) agrees with reported values[7] for the mass of the intact progesterone receptor and was not present if unlabeled Organon 2058 was incubated with the sample prior to HPAC. The

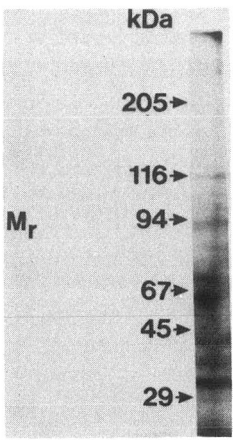

Fig. 1. Autoradiography of affinity purified ^{35}S-labeled progesterone receptor from T47D human breast cancer cells. [^{35}S]methionine (200 μCi/ml) was incorporated into total cellular proteins over 6 h in culture as described in ref. 4. Affinity-eluted proteins were separated by gel electrophoresis using a 7.5 to 15% polyacrylamide gradient. The gel was fixed and impregnated with fluor, dried down, and exposed to an X-ray film at −70°C. Lane 1 shows the elution pattern of proteins obtained from the HPAC column. Progesterone receptor migrates as a 116 000-dalton polypeptide. kDa = kilodalton.

degree of purification obtained through one affinity step from the crude protein mixture used as starting material was satisfactory although at least a dozen other bands were also present in the sample shown in Fig. 1. Although the absolute capacity of the column was not measured, in one experiment 234 pmol of progestin receptor as determined by ligand binding was purified from human uterus with 45% recovery (data not shown).

DISCUSSION

The recent availability of this epoxide reactive silica has allowed the efficient coupling of small molecules or proteins to the solid matrix under very mild conditions[8]. The only requirement is that the molecule contains a free sulphydryl, primary or possibly secondary amino, or hydroxyl group. In cases where affinity interactions are high, *i.e.* $K_d \leq 1.0$ nM, reduced ligand concentrations as used here (100-fold less concentration than manufacturer's recommendation) for column derivatization have proved to be beneficial since high ligand concentrations on the support dictate that high concentrations of eluting ligand must be used to elute the binding protein. In the present application, a desirably small elution volume was possible with the affinity column. Greater utility in a preparative sense might be obtained if the 100 × 10 mm I.D. column is employed although the larger derivatizable column and amount of radioactive steroid needed for elution may prove considerably more expensive.

As presented here, attachment via the 21-hydroxyl of Organon 2058 to the solid silica support maintained the activity of the steroid for successful binding of the progesterone receptor. Although an affinity constant was not measured, this retention of steroid binding ability by the receptor protein and the harsh conditions required for elution indicate that biological activity was maintained although the receptor was probably recovered in the smaller dissociated form instead of the native, hetero-oligomeric form[9]. There also did not appear to be any proteolytic degradation of the receptor protein. The potential affinity interaction of the column with other steroid receptors, however, remains a possibility although the gluco-corticoid receptor's affinity for progestational agents is 10–100 fold lower than for gluco-corticoids[10]. Interaction of the androgen receptor with progesterone is similarly inefficient[11]. Inclusion of the appropriate unlabeled steroid to samples just before affinity purification could also be used to block any potentially interfering binding sites.

In conclusion, affinity isolations of progesterone receptor on both large and small samples have been performed with ease and completed in 3–4 h. This HPAC method has found particular application in this laboratory in the analysis of post-translational modifications (phosporylation) related to receptor function[12].

ACKNOWLEDGEMENT

This work was supported in part by a grant from the S. A. Medical Research Council.

REFERENCES

1 O. Hoffman-Ostenhof, *Affinity Chromatography*, Pergamon Press, Oxford, 1978.
2 D. M. Boyle, R. D. Wiehle, N. A. Shahabi and J. L. Wittliff, *J. Chromatogr.*, 327 (1985) 369.
3 I. Keyder, L. Chen, S. Karby, F. R. Weiss, J. Delarea, M. Rudu, S. Chaitcik and H. J. Breeners, *Eur. J. Cancer*, 15 (1979) 659.
4 B. Westley and H. Rochefort, *Cell*, 20 (1980) 353.
5 U. K. Laemmli, *Nature (London)*, 277 (1970) 680.
6 M. M. Bradford, *Anal. Biochem.*, 72 (1976) 248.
7 W. T. Schrader, R. W. Kuhn and B. W. O'Malley, *J Biol. Chem.*, 252 (1977) 299.
8 P. Formstecher, H. Hammadi, N. Bouzerna and M. Dautrevaux, *J. Chromatogr.*, 369 (1986) 379.
9 J. J. Dougherty, R. K. Puri and D. O. Toft, *J. Biol. Chem.*, 259 (1984) 8004.
10 M. Lippman, K. Huff, G. Bolan and J. P. Neifeld, in W. L. McGuire (Editor), *Progesterone Receptor in Normal and Neoplastic Tissues*, Raven Press, New York, 1977, p. 200.
11 E. A. Wilson, O. A. Lea and F. S. French, in B. W. O'Malley and L. Birnbaumer (Editors), *Receptors and Hormone Action II*, Academic Press, New York, 1978, p. 519.
12 D. M. Boyle and L. A. van der Walt, *J. Steroid Biochem.*, 30 (1988) 239.

Journal of Chromatography, 455 (1988) 439–443
Elsevier Science Publishers B.V., Amsterdam — Printed in The Netherlands

CHROM. 20 944

Note

Separation of some rodenticides and related compounds by thin-layer chromatography

KOFI OPONG-MENSAH*,*
ICI Americas, Inc., Agricultural Division, 1200S 47th St., Richmond, CA 94804 (U.S.A.)
and
WILLIAM R. PORTER
Abbott Laboratories, North Chicago, IL 60064 (U.S.A.)
(First received July 5th, 1988; revised manuscript received August 24th, 1988)

Coumarins, indandiones, vitamin D_3 and halogenated analogues of vitamin K in various formulations are used as rodenticides. It is important to separate and identify the acyl indandiones, coumarins and related compounds in quality control analysis of bait formulations. Paper chromatography (PC) and thin-layer chromatography (TLC) of coumarins have been described[1–4]. However, no satisfactory separation by unidimensional TLC has so far been reported for diphenadione, pindone, valone, warfarin, bromadiolone, vitamin K_1 and vitamin D_3.

EXPERIMENTAL

Materials

Thin-layer plates (5 × 20 cm) were obtained from Whatman (Clifton, NJ, U.S.A.). They were coated with LK6DF Linear-K silica gel. The layer thickness was 250 μm. Drummond Microcap micropipets were obtained from Drummond Scientific (Broomall, PA, U.S.A.). All solvents were analytical-grade unless otherwise indicated and mixtures were on a v/v basis. The chemicals used were: 1,2-dichloroethane, purity 99+% (Aldrich, Milwaukee, WI, U.S.A.); acetic acid (glacial) (Mallinckrodt, St. Louis, MO, U.S.A.); methanol (anhydrous), absolute and acetone-free (Mallinckrodt); chloroform (stabilized with 0.75% ethanol) and ferric chloride (MCB, Cincinnati, OH, U.S.A.); antimony trichloride (22% w/v solution) (Allied Chemical, Morristown, NJ, U.S.A.); hydrochloric acid (electronic grade) (HI-PURE Chemicals, Nazereth, PA, U.S.A.); ethanol and sulfuric acid (0.5 *M* solution) (Fisher Scientific, Fairlawn, NJ, U.S.A.). Potassium chloroplatinate 0.15%, potassium iodide 3.0% in 0.01 *M* hydrochloric acid and phosphomolybdic acid (10% phosphomolybdic acid in ethanol) were obtained from Sigma, St. Louis, MO, U.S.A. The following eluting solvents were used for the normal-phase (silica gel) chromatography: (a) 1,2-dichlo-

* Part of the research was done at the University of Wisconsin-Madison, WI, U.S.A.

0021-9673/88/$03.50 © 1988 Elsevier Science Publishers B.V.

roethane–methanol–acetic acid (glacial) (90:8:2); (b) chloroform–methanol (97:3); and (c) cyclohexane–1,2-dichloroethane–acetic acid (glacial) (75:25:0.6).

Chromatography

A smooth sheet of filter paper, *ca.* 20 × 50 cm, was laid in the form of a U in the glass rectangular TLC tank (30 × 26 × 10 cm) and soaked in the mobile phase which was already placed in the tank and covered with the lid for the TLC tank. The paper ensures the saturation of the chamber. About 25 μg of alcoholic solutions containing 1 mg/ml of the compounds listed in Table I were applied to the TLC plates to form spots[2,3]. Drummond Microcap micropipets were used for sample application. Spot size was minimized by applying the sample volume in small increments on top of each other, with complete drying of the solvent after each application. A stream of nitrogen was used to dry the sample solvent. The plate was placed in the TLC tank filled with solvent to a depth of about 0.7 cm. The breadth of the TLC plate dipped into the solvent to the same depth, *i.e. ca.* 0.7 cm, but not so as to cover the spots at the start. The tank with the TLC plates were then covered with the lid. The plates were left in the tank at ambient conditions (23°C) for 30 min. Vitamin D_3 and Vitamin K_1 spots were dried in a nitrogen atmosphere. The experiments were carried out in dim light or darkness.

Visualization. Six color reagents were used: antimony trichloride [22% (w/v) in chloroform], ferric chloride [2.7% (w/v) in 2 *M* hydrochloric acid], sulfuric acid [5% (w/v) in ethanol], sodium hydroxide (8% in methanol), potassium iodoplatinate (potassium chloroplatinate 0.15%, potassium iodide 3.0% in 0.01 *M* hydrochloric acid). Phosphomolybdic acid (10% phosphomolybdic acid in ethanol). All spots were examined in visible light as well as under a UV lamp at 254 nm. Intensification of the color of the spots was obtained by drying in an oven at 115°C for 5 min.

RESULTS AND DISCUSSION

R_F values and comments on the chromatographic conditions are given in Tables II and III. Iron is known to interfere in the chromatographic separations of phenolic compounds. This might be the reason for tailings observed for vitamin K_3, vitamin D_3, valone and bromadiolone. However, prewashing the silica gel G with hydrochloric acid in order to remove existing traces of iron did not make any difference. Three potentially useful mobile phases using silica gel as stationary phase were examined. None of the mobile phases used alone could separate all seven compounds. However, by repeating the separation in all three systems, each compound could be uniquely identified. Of six visualization reagents experimented with, phosphomolybdic acid was the most useful. The limit of detection for the compounds with individual reagents was 1–8 μg based on visual inspection of areas with unaided eyes.

ACKNOWLEDGEMENTS

Special thanks to Dr. Ronald H. Laessig for valuable advice and to Bell Laboratories, Inc. Madison, WI, U.S.A. and Dr. Richard Petterson for their financial support.

TABLE I

COMPOUNDS FOR TLC ANALYSIS

General formula	*Derivative*	*Chemical name*
Derivatives of 4-OH coumarin	R_1 =	3-(α-Acetonylbenzyl)-4-hydroxycoumarin (Warfarin*)
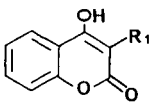	R_1 = 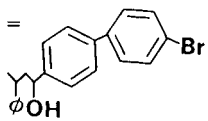	3-{3-[4'-Bromo(1,1'-biphenyl)-4-yl]-3-hydroxy-1-phenylpropyl}-4-hydroxy-2H-1-benzopyran-2-one (Bromadiolone*)
Derivatives of 2-acyl-1,3-indandione	R_2 =	2-Diphenylacetyl-1,3-indandione (Diphacinone*)
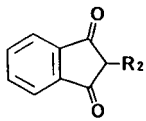	R_2 =	2-Pivalyl-1,3-indandione (Pindone*)
	R_2 =	2-Isovaleryl-1,3-indandione (Valone*, PMP*)
Others		
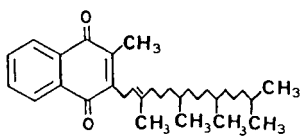		2-Methyl-3-phytyl-1,4-naphtoquinone (Vitamin K_1*)
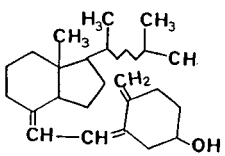		9,10-Seocholesta-5,7,10 (19)-trein-3-ol (Vitamin D_3, cholecalciferol*)

* Trade name.

TABLE II

R_F VALUES OF SELECTED COUMARINS, INDANDIONES AND VITAMINS

Compound	*R_F value × 100* for solvent*		
	*a***	*b***	*c***
Diphacinone 1	42	24	9
Pindone 2	88	91	48
Valone 3	47	50	13
Warfarin 4	53	59	4
Bromadiolone 5	41	51	5
Vitamin K_1 6	75	92	6
Vitamin D_3 7	59	68	12

* R_F values are the average of several chromatograms.

** See text for mobile phase composition.

TABLE III

COLOR FORMATION WITH SPRAY REAGENTS

*Compound**	*Color formed*											
	$SbCl_3$		*$FeCl_3$*		*H_2SO_4*		*NaOH*		*Iodoplatinate (brownish red background)*		*Phosphomolybdate (yellow background)*	
	Visible	*UV*	*Visible*	*UV*	*Visible*	*UV*	*Visible*	*UV*	*Visible*	*UV*	*Visible*	*UV*
1	Yellowish brown	Pink	Dark brown	Brown	Yellow	Black	–	–	–	Orange	Brown	Orange
2	Brown	Light brown	Light brown	Brown	Brownish yellow	Orange	Yellow	–	Brown	Brown	Brown	–
3	–	–	White on yellow	–	–	–	–	Blue	Brown	–	Brown	–
4	Light brown	Brown	Yellowish brown	Orange	Yellow	–	Brown	Black	–	–	Black	Black
5	Pink	–	–	–	–	–	–	Blue	–	–	Black	Black
6	Brown	Black	Blue	–	Greenish brown	–	–	–	Yellow	Brown	Black	–
7	Pink	–	Brownish red	–	–	–	Yellow	Orange	Black	Brown	Pinkish brown	–

* See Table II.

REFERENCES

1 H. Mitsuhaski, U. Nagai, T. Muraamatsu and H. Tashior, *Chem. Pharm. Bull.*, 8 (1960) 243.
2 E. Stahl, *Thin-layer Chromatography*, Academic Press, New York, 2nd ed., 1969.
3 B. Fried and J. Sherma, *Thin-Layer Chromatography*, Marcel Dekker, New York, 2nd ed., 1986.
4 P. G. Willing, K. P. Lee, U. Khanna and J. G. Wagner, *J. Pharm. Sci.*, 59 (1970) 1621.

Journal of Chromatography, 455 (1988) 444
Elsevier Science Publishers B.V., Amsterdam — Printed in The Netherlands

CHROM. 20 909

Book Review

Introduction to microscale high-performance liquid chromatography, edited by D. Ishii, VCH, Weinheim, 1988, XIII + 208 pp., price DM 118.00, £41.45, ISBN 3-527-26636-4.

The first book on microcolumn high-performance liquid chromatography (HPLC) was edited by Paul Kucera[1], and contained contributions by Guiochon, Hartwick and a long chapter by Novotny. It appeared in 1984 and covered the literature up to 1983. In 1985 the book Microcolumn Separations, edited by Milos V. Novotny and Daidō Ishii[2], was published, containing updated chapters from a meeting in Honolulu, which covered similar topics to the book edited by Kucera and also covering the literature up to and including 1983.

Now we have a book on microscale HPLC edited by D. Ishii. More or less the same topics are covered as in the first two books with coverage up to 1984, with a very few papers from 1985. Hence similar and overlapping fields are covered in all three volumes, two of which have the same Editor and another Editor wrote chapters in the other two books.

Microcolumn HPLC is an interesting topic and many workers will be glad to have books which collect the literature. However, it is difficult to see why three books were needed, nor is it clear why the latest volume appeared only in 1988, when it is evidently 3 years out of date.

The book is attractively produced and this reviewer found no obvious printer's errors.

1 P. Kucera (Editor), *Microcolumn High-Performance Liquid Chromatography* (*Journal of Chromatography Library*, Vol. 28), Elsevier, Amsterdam, 1984.
2 M. V. Novotny and D. Ishii (Editors), *Microcolumn Separations —Columns, Instrumentation and Ancillary Techniques* (*Journal of Chromatography Library*, Vol. 30), Elsevier, Amsterdam, 1985.

Journal of Chromatography, 455 (1988) 445
Elsevier Science Publishers B.V., Amsterdam — Printed in The Netherlands

CHROM. 20 895

Book Review

Quantitative gas chromatography for laboratory analyses and on-line process control, by G. Guiochon and C. L. Guillemin, Elsevier, Amsterdam, Oxford, New York, Tokyo, 1988, XII + 793 pp., price Dfl. 315.00, US$ 165.75, ISBN 0-444-42857-7.

This, the largest book on gas chromatography, has appeared as Volume 42 of the *Journal of Chromatography Library*. In 17 chapters, it covers almost al aspects of gas chromatography in such a way as to be useful for the quantitative interpretation of results.

The book begins with a short but concise and clear chapter with definitions (4%), then a description of the fundamentals of the gas chromatographic process (three chapters explaining flow phenomena, retention, peak broadening and column overloading) (15%), methodology (five chapters dealing with optimization, packed and capillary columns, instrumentation and detectors) (41%), qualitative analysis (two chapters on retention data and hyphenated techniques) (10%), quantitative analysis (four chapters covering basic relationships, response, peak area, source of errors) (16%) and the last chapter presents an outline of process control analysis (6.5%). Each chapter is followed by a list of strictly selected references on each topic. A "Chromatography Lexicon" and a subject index make the terms and matter quickly available.

The concept of this book is to present the subject of gas chromatography in a form suitable both for practice and education. There are currently a large number of comprehensive and specialized books on gas chromatography on the market and/or in libraries, but the authors are right when they state that there is a lack of books that also discuss the theoretical premises of the separation process and the practical parameters of the key parts of the instrumental line which influence the quantitative results to be used in practice. The great experience in basic research and the knowledge of practical needs of the senior author can be clearly seen. This is the reason why the authors entitled their book *Quantitative gas chromatography*, although *Gas chromatography* would have been sufficient. The book represents an up-to-date continuation of Purnell's book on gas chromatography published in 1962, with a contemporary level of knowledge and with the aim of making this mature method useful for modern quantitative analysis.

It is certainly possible to take a standpoint slightly different in detail to that of the authors, *e.g.*, the selection of references. For instance, one would have liked to find more about Novák's ideas as outlined in Chapters 13–15 in his book *Quantitative Analysis by Gas Chromatography* (Marcel Dekker, 1975, 1988). In my opinion, some criticism by the first author of Novák's book probably played a rôle in his decision to cover this topic on a broader basis. Further, a length of 800 pages is not commonly accepted as the optimal size of a book; however, this book reads well and, in practice, one can, if desired, use only the chapters dealing with particular problems of interest. Unfortunately, the price of the book is high for individuals.

In conclusion, the book is a good piece of work and it can be recommended both for practitioners and for teachers as a very good source of concentrated knowledge.

Brno (Czechoslovakia) JAROSLAV JANÁK

Author Index

Abdul Ghani, A., see Smith, R. M. 349
Alary, J., see Vergnes, M. F. 369
Antalík, M., see Podhradský, D. 344
Ascah, T. L.
—— and Hunter, B. T.
Simultaneous high-performance liquid chromatographic determination of propoxyphene and acetaminophen in pharmaceutical preparations 279
Bailey, C. A.
—— and Chen, B. H.
Simultaneous separation and identification of carotenoids and chlorophylls in turf bermudagrass by high-performance liquid chromatography 396
Balinova, A.
Gas chromatographic determination of chloroacetamide herbicides in plants and soil 391
Bament, G. S., see Smith, R. M. 349
Barceló, D., see Farran, A. 163
Barman, B. N., see Jones, H. K. 1
Barnes, K. W., see Sentell, K. B. 95
Bicking, M. K. L.
——, Cooke, W. M., Kawahara, F. K. and Longbottom, J. E.
Effect of pH on the reaction of 2,4-dinitrophenylhydrazine with formaldehyde and acetaldehyde 310
Bier, M., see Wenger, P. 225
Boukharta, M.
——, Girardin, M. and Metche, M.
Procyanidines galloylées du sarment de vigne (*Vitis vinifera*). Séparation et identification par chromatographie liquide haute performance et chromatographie en phase gazeuse 406
Boyle, D. M.
—— and Van der Walt, L. A.
High-performance affinity chromatography of human progesterone receptor 434
Brooks, S. P. J.
—— and Storey, K. B.
Purification of phosphofructokinase using transition-state analogue affinity chromatography 291
Brunet, P.
——, Sarrobert, B. and Paris-Pireyre, N.
Adaptation d'une méthode d'analyse des acides aminés, par chromatographie liquide haute performance, dans les sèves xylémiques 173
Burcinová, A.
——, Tichý, M., Pacáková, V. and Štulík, K.
Application of amperometric detection to the high-performance liquid chromatographic determination of antipyrine and 4-aminoantipyrine in urine 420
Burkholder, H. R., see Sawyer, D. J. 193
Burton, S. J.
——, Stead, C. V. and Lowe, C. R.
Design and applications of biomimetic anthraquinone dyes. II. The interaction of C.I. Reactive Blue 2 analogues bearing terminal ring modifications with horse liver alcohol dehydrogenase 201
Carroll, D. L., see Robinson, R. S. 143
Chamsi, A. Y., see Smith, R. M. 349
Chen, B. H., see Bailey, C. A. 396
Chen, Y.-H., see Oshima, T. 410
Chu, Y.-Q., see Wainer, I. W. 316
Cooke, W. M., see Bicking, M. K. L. 310
Cribbes, R. L., see Smillie, R. H. 253
Dąbrowski, R., see Mazur, J. 323
Dębowska, B.
——, Samochocka, K., Przasnyski, M. and Sybilska, D.
Simultaneous determination of thiols and corresponding disulphides in mixtures by high-performance liquid chromatography with polarographic detection using a Dual-Tast analyser 336
Dellamonica, E. S., see Jones, W. J. 45
De Pablo, J., see Farran, A. 163
Dernovaya, L. I.
—— and Eltekov, Yu. A.
Retention and heats of adsorption of hydrocarbons and aliphatic alcohols on cellulose 263
Dorsey, J. G., see Sentell, K. B. 95
Dunphy, M. J., see Fulton, J. A. 183
Dziwiński, E., see Szymanowski, J. 119, 131
Egen, N. B., see Wenger, P. 225
Egoville, M. J., see Jones, W. J. 45
Eltekov, Yu. A., see Dernovaya, L. I. 263
Endo, M.
——, Mizutani, T., Matsumura, M., Moriyasu, M., Ichimaru, M., Kato, A. and Hashimoto, Y.
High-performance liquid chromatographic determination of hinokitiol in cosmetics by the formation of difluoroborane compounds 430

Farran, A.
——, De Pablo, J. and Barceló, D.
Identification of organophosphorus insecticides and their hydrolysis products by liquid chromatography in combination with UV and thermospray–mass spectrometric detection 163
Fogg, A. G., see Smith, R. M. 349
Fujita, M., see Mochizuki, E. 271
Fulton, J. A.
——, Pokharna, H. K., Dunphy, M. J. and Smith, D. J.
Resolution of diastereomers of N,N,N′,N′-tetrakis(2-hydroxypropyl)ethylenediamine (Quadrol) by reversed-phase high-performance liquid chromatography 183
Gemmel, B.
——, Schmitz, F. P. and Klesper, E.
Consecutive gradients in chromatography. Gradients under sub- and supercritical conditions including composition gradients and multiple gradients 17
Giddings, J. C., see Jones, H. K. 1
Gill, R., see Smith, R. M. 77
Girardin, M., see Boukharta, M. 406
Grant, B., see Smillie, R. H. 253
Grob, K.
—— and Li, Z.
Damage to gas chromatographic columns caused by peroxides in liquid chromatographic eluents for coupled liquid chromatography–gas chromatography 297
Grosset, C., see Vergnes, M. F. 369
Hards, R. G.
—— and Patterson, D.
Resolution of the intermediates of *de novo* purine biosynthesis by ion-pair reversed-phase high-performance liquid chromatography 217
Harmony, M. D., see Roach, M. C. 332
Hashimoto, Y., see Endo, M. 430
Haverty, D. G., see Smith, R. M. 349
Heydt, A., see Wenger, P. 225
Holstege, C. P.
——, Pickaart, M. J. and Louters, L. L.
Separation of RNA and DNA by histone affinity high-performance liquid chromatography 401
Holotík, Š., see Matisová, E. 301
Hunter, B. T., see Ascah, T. L. 279
Hurdley, T. G., see Smith, R. M. 77
Ichimaru, M., see Endo, M. 430
Ito, Y.
—— and Zhang, T.-Y.
Cross-axis synchronous flow-through coil planet centrifuge for large-scale preparative counter-current chromatography. III. Performance of large-bore coils in slow planetary motion 151
Jinno, K.
—— and Niimi, S.
Retention behaviour of polycyclic aromatic hydrocarbons in supercritical fluid chromatography on various chemically bonded stationary phases with carbon dioxide as a mobile phase 29
Jones, H. K.
——, Barman, B. N. and Giddings, J. C.
Resolution of colloidal latex aggregates by sedimentation field-flow fractionation 1
Jones, W. J.
——, Egoville, M. J., Strolle, E. O. and Dellamonica, E. S.
Determination of partition coefficients by headspace gas chromatography 45
Kalonia, D. S.
—— and Simonelli, A. P.
Development of an high-performance liquid chromatographic method for the simultaneous analysis of the species involved in diethyl L-tartrate hydrolysis 355
Kato, A., see Endo, M. 430
Kawahara, F. K., see Bicking, M. K. L. 310
Kemp, M. W., see Li, C.-Y. 241
Kitada, Y., see Mochizuki, E. 271
Klesper, E., see Gemmel, B. 17
König, A., see Schoene, K. 67
Kovačičová, E., see Matisová, E. 301
Krupčík, J., see Matisová, E. 301
Kusz, P., see Szymanowski, J. 119, 131
Kuwata, K.
—— and Tanaka, S.
Liquid chromatographic determination of trace amounts of low-molecular-weight fatty acid vapours in industrial emissions 425
Larsson, P.-O., see Wikström, P. 105
Latocha, Cz., see Szymanowski, J. 119
Li, C.-Y.
—— and Kemp, M. W.
Determination of phenols by liquid chromatography using reductive electrochemical detection via precolumn derivatization 241
Li, Z., see Grob, K. 297
Long, T. D., see Wenger, P. 225
Longbottom, J. E., see Bicking, M. K. L. 310
Louters, L. L., see Holstege, C. P. 401
Lowe, C. R., see Burton, S. J. 201

Ma, Y.
—— and Yeung, E. S.
Indirect fluorimetric detection of non-electrolytes in thin-layer chromatography 382
McKeon, T. A.
Activity stain for polygalacturonase 376
Mandenius, C. F., see Wikström, P. 105
Marquard, F.
—— and Sonne, O.
Simultaneous collection of the eluate from up to twenty liquid chromatographic columns by a minor modification to the fraction collector 360
Matisová, E.
——, Rukríglová, M., Krupčík, J., Kovačičová, E. and Holotík, Š.
Identification of alkylbenzenes up to C_{12} by capillary gas chromatography and combined gas chromatography–mass spectrometry. I. OV-101 as stationary phase 301
Matsumura, M., see Endo, M. 430
Mazur, J.
——, Witkiewicz, Z. and Dąbrowski, R.
Isothiocyanate as a liquid crystalline stationary phase in capillary gas chromatography for the separation of polyaromatic hydrocarbons 323
Metche, M., see Boukharta, M. 406
Mizutani, T., see Endo, M. 430
Mochizuki, E.
——, Nakayama, A., Kitada, Y., Saito, K., Nakazawa, H., Suzuki, S. and Fujita, M.
Liquid chromatographic determination of alliin in garlic and garlic products 271
Moriyasu, M., see Endo, M. 430
Nakayama, A., see Mochizuki, E. 271
Nakazawa, H., see Mochizuki, E. 271
Niimi, S., see Jinno, K. 29
Opong-Mensah, K.
—— and Porter, W. R.
Separation of some rodenticides and related compounds by thin-layer chromatography 439
Oshima, T.
——, Sagara, K., Yoshida, T., Tong, Y.-Y., Zhang, G. and Chen, Y.-H.
Determination of geniposide, gardenoside, geniposidic acid and genipin-1-β-gentiobioside in *Gardenia jasminoides* by high-performance liquid chromatography 410
Osselton, M. D., see Smith, R. M. 77
Pablo, J. De, see Farran, A. 163
Pacáková, V., see Burcinová, A. 420
Paris-Pireyre, N., see Brunet, P. 173
Patterson, D., see Hards, R. G. 217
Pickaart, M. J., see Holstege, C. P. 401
Podhradský, D.
——, Antalík, M. and Šturdík, E.
Separation of thiols on Spheron Ara activated with 2-nitrophenylhydrazonopropandinitrile ligand 344
Pokharna, H. K., see Fulton, J. A. 183
Porter, W. R., see Opong-Mensah, K. 439
Powell, J. E., see Sawyer, D. J. 193
Przasnyski, M., see Dębowska, B. 336
Roach, M. C.
—— and Harmony, M. D.
High-sensitivity laser-induced fluorescence–high-performance liquid chromatography studies of polyaromatic hydrocarbons using the argon ion laser–Yeung detector cell configuration 332
Robinson, R. S.
——, Tavss, E. A., Santalucia, J. and Carroll, D. L.
Flavor characterization of dentifrices using equilibrium headspace gas chromatography 143
Rukríglová, M., see Matisová, E. 301
Saesmaa, T.
Quantitative high-performance liquid chromatographic determination of ampicillin embonate and amoxycillin embonate 415
Sagara, K., see Oshima, T. 410
Saito, K., see Mochizuki, E. 271
Samochocka, K., see Dębowska, B. 336
Santalucia, J., see Robinson, R. S. 143
Sarrobert, B., see Brunet, P. 173
Sawyer, D. J.
——, Powell, J. E. and Burkholder, H. R.
Purification of diethylenetriamine-N,N,N′,-N″-tetraacetic acid-N″-propionic acid using anion-exchange displacement chromatography 193
Schmitz, F. P., see Gemmel, B. 17
Schoene, K.
——, Steinhanses, J. and König, A.
Determination of the solubility of vapours in polymers by automated headspace gas chromatography 67
Seiber, J. N., see Woodrow, J. E. 53
Sentell, K. B.
——, Barnes, K. W. and Dorsey, J. G.
Ultrasound driven synthesis of reversed-phase stationary phases for liquid chromatography using 4-dimethylaminopyridine as acid-acceptor 95
Sheikh, S. U.
—— and Touchstone, J. C.
Temperature programming in high-performance liquid chromatography 327
Simonelli, A. P., see Kalonia, D. S. 355

Smillie, R. H.
——, Grant, B. and Cribbes, R. L.
Determination of phosphate and phosphite in plant material by gas chromatography–mass spectrometry and ion chromatography 253
Smith, D. J., see Fulton, J. A. 183
Smith, R. M.
——, Abdul Ghani, A., Haverty, D. G., Bament, G. S., Chamsi, A. Y. and Fogg, A. G.
Derivatisation of amines with O-acetylsalicyloyl chloride to enhance electrochemical detection in high-performance liquid chromatography 349
——, Hurdley, T. G., Westlake, J. P., Gill, R. and Osselton, M. D.
Retention reproducibility of basic drugs in high-performance liquid chromatography on a silica column with a methanol–ammonium nitrate eluent. Batch-to-batch reproducibility of the stationary phase 77
Sonne, O., see Marquard, F. 360
Stead, C. V., see Burton, S. J. 201
Steinhanses, J., see Schoene, K. 67
Storey, K. B., see Brooks, S. P. J. 291
Strolle, E. O., see Jones, W. J. 45
Štulík, K., see Burcinová, A. 420
Šturdík, E., see Podhradský, D. 344
Suzuki, S., see Mochizuki, E. 271
Sybilska, D., see Dębowska, B. 336
Szymanowski, J.
——, Kusz, P. and Dziwiński, E.
Chemical degradation and analysis of polyoxyethylene glycols and ethylene oxide–α-butylene oxide block copolymers 131
——, Kusz, P., Dziwiński, E. and Latocha, Cz.
Degradation and analysis of polyoxyethylene monoalkyl ethers in the presence of acetyl chloride 119
Tacchi-Bedford, A. M.
Measurement of methylated DNA purines by reversed-phase high-performance liquid chromatography and fluorimetric detection 364
Tanaka, S., see Kuwata, K. 425
Tavss, E. A., see Robinson, R. S. 143
Tichý, M., see Burcinová, A. 420
Tong, Y.-Y., see Oshima, T. 410
Touchstone, J. C., see Sheikh, S. U. 327
Van der Walt, L. A., see Boyle, D. M. 434
Vergnes, M. F.
——, Grosset, C. and Alary, J.
Étude par chromatographie liquide haute performance des metabolites potentiels de la caféine. Comparaison de différentes techniques 369
Wainer, I. W.
—— and Chu, Y.-Q.
Use of mobile phase modifiers to alter retention and stereoselectivity on a bovine serum albumin high-performance liquid chromatographic chiral stationary phase 316
Walt, L. A. van der, see Boyle, D. M. 434
Wenger, P.
——, Heydt, A., Egen, N. B., Long, T. D. and Bier, M.
Purification of lentil lectins using preparative electrophoresis 225
Westlake, J. P., see Smith, R. M. 77
Wikström, P.
——, Mandenius, C. F. and Larsson, P.-O.
Gas phase silylation, a rapid method for preparation of high-performance liquid chromatography supports 105
Witkiewicz, Z., see Mazur, J. 323
Woodrow, J. E.
—— and Seiber, J. N.
Vapor-pressure measurement of complex hydrocarbon mixtures by headspace gas chromatography 53
Yeung, E. S., see Ma, Y. 382
Yoshida, T., see Oshima, T. 410
Zhang, G., see Oshima, T. 410
Zhang, T.-Y., see Ito, Y. 151

PUBLICATION SCHEDULE FOR 1988

Journal of Chromatography and Journal of Chromatography, Biomedical Applications

MONTH	J	F	M	A	M	J	J	A	S	O	N	D
Journal of Chromatography	435/1 435/2 435/3 436/1	436/2 436/3	437/1 437/2	438/1 438/2	439/1 439/2 440 441/1	441/2 442 443	444 445/1 445/2 446	447/1 447/2 448/1	448/2 448/3 449/1	449/2 450/1 450/2 450/3 452	453 454 455	456/1 456/2 457 458 459
Bibliography Section		460/1		460/2		460/3		460/4		460/5		460/6
Cumulative Indexes, Vols. 401–450												451
Biomedical Applications	424/1	424/2	425/1 425/2	426/1 426/2	427/1	427/2 428/1	428/2 429	430/1	430/2 431/1	431/2	432	433 434/1 434/2

INFORMATION FOR AUTHORS

(Detailed *Instructions to Authors* were published in Vol. 445, pp. 453–456. A free reprint can be obtained by application to the publisher, Elsevier Science Publishers B.V., P.O. Box 330, 1000 AH Amsterdam, The Netherlands.)

Types of Contributions. The following types of papers are published in the *Journal of Chromatography* and the section on *Biomedical Applications*: Regular research papers (Full-length papers), Notes, Review articles and Letters to the Editor. Notes are usually descriptions of short investigations and reflect the same quality of research as Full-length papers, but should preferably not exceed six printed pages. Letters to the Editor can comment on (parts of) previously published articles, or they can report minor technical improvements of previously published procedures; they should preferably not exceed two printed pages. For review articles, see inside front cover under Submission of Papers.

Submission. Every paper must be accompanied by a letter from the senior author, stating that he is submitting the paper for publication in the *Journal of Chromatography*. Please do not send a letter signed by the director of the institute or the professor unless he is one of the authors.

Manuscripts. Manuscripts should be typed in double spacing on consecutively numbered pages of uniform size. The manuscript should be preceded by a sheet of manuscript paper carrying the title of the paper and the name and full postal address of the person to whom the proofs are to be sent. Authors of papers in French or German are requested to supply an English translation of the title of the paper. As a rule, papers should be divided into sections, headed by a caption (*e.g.*, Summary, Introduction, Experimental, Results, Discussion, etc.). All illustrations, photographs, tables, etc., should be on separate sheets.

Introduction. Every paper must have a concise introduction mentioning what has been done before on the topic described, and stating clearly what is new in the paper now submitted.

Summary. Full-length papers and Review articles should have a summary of 50–100 words which clearly and briefly indicates what is new, different and significant. In the case of French or German articles an additional summary in English, headed by an English translation of the title, should also be provided. (Notes and Letters to the Editor are published without a summary.)

Illustrations. The figures should be submitted in a form suitable for reproduction, drawn in Indian ink on drawing or tracing paper. Each illustration should have a legend, all the *legends* being typed (with double spacing) together on a *separate sheet*. If structures are given in the text, the original drawings should be supplied. Coloured illustrations are reproduced at the author's expense, the cost being determined by the number of pages and by the number of colours needed. The written permission of the author and publisher must be obtained for the use of any figure already published. Its source must be indicated in the legend.

References. References should be numbered in the order in which they are cited in the text, and listed in numerical sequence on a separate sheet at the end of the article. Please check a recent issue for the layout of the reference list. Abbreviations for the titles of journals should follow the system used by *Chemical Abstracts*. Articles not yet published should be given as "in press" (journal should be specified), "submitted for publication" (journal should be specified), "in preparation" or "personal communication".

Dispatch. Before sending the manuscript to the Editor please check that the envelope contains three copies of the paper complete with references, legends and figures. One of the sets of figures must be the originals suitable for direct reproduction. Please also ensure that permission to publish has been obtained from your institute.

Proofs. One set of proofs will be sent to the author to be carefully checked for printer's errors. Corrections must be restricted to instances in which the proof is at variance with the manuscript. "Extra corrections" will be inserted at the author's expense.

Reprints. Fifty reprints of Full-length papers, Notes and Letters to the Editor will be supplied free of charge. Additional reprints can be ordered by the authors. An order form containing price quotations will be sent to the authors together with the proofs of their article.

Advertisements. Advertisement rates are available from the publisher on request. The Editors of the journal accept no responsibility for the contents of the advertisements.

Also available in a paperback student edition

Contemporary Practice of Chromatography

by **C.F. Poole** *and* **S.A. Schuette,** *Dept. of Chemistry, Wayne State University, Detroit, MI, USA*

"A tremendous amount of work has gone into the writing of this book, and it may be considered to be one of the few volumes of its kind that could be used both as a text by senior students in the field and by analysts in many industries. All academic, research association and appropriate industrial laboratories should buy at least one copy (preferably more, as borrowers will probably wish to keep it on loan for some time)." (The Analyst)

Written for everyone who uses chromatography as an analytical tool, this book covers all areas of gas, liquid, and thin-layer chromatography; **no other book offers the same scope.** The authors have had considerable experience in teaching graduate-level courses and the material presented here has been tried and tested, having formed the basis for short courses taught to groups of industrial chemists. Emphasis is on the practice of chromatographic methods, including "how to" sections and numerous examples of calculation methods. Extensively illustrated, the book contains numerous tables of all useful constants, materials and formulas frequently used by chromatographers. Valuable features are the chapters on sample preparation for chromatographic analysis, on instrumental methods for sample identification, and the comprehensive literature review.

Contents: 1. Fundamental Relationships of Chromatography. 2. The Column in GC. 3. Instrumental Requirements for GC. 4. The Column in LC. 5. Instrumental Requirements for HPLC. 6. Preparative-Scale Chromatography. 7. Sample Preparation for Chromatographic Analysis. 8. Hyphenated Methods for Identification after Chromatographic Separation. 9. High Performance Thin-Layer Chromatography. Subject Index.

1984. 2nd repr. 1986 x + 708 pages

Hardcover edition:	*Paperback edition:*
US$92.00/Dfl.175.00	US$37.50/Dfl.110.00
ISBN 0-444-42410-5	ISBN 0-444-42506-3

ELSEVIER SCIENCE PUBLISHERS

P.O. Box 211, 1000 AE Amsterdam, The Netherlands
P.O. Box 882, Madison Square Station, New York, NY 10159, USA